Evaluating the potential of non-pathogenic *Magnaporthaceae* species for the control of take-all disease in wheat

Submitted by

Tania Chancellor

Thesis submitted to the University of Nottingham for the degree of Doctor of Philosophy, March 2022

ABSTRACT

Take-all disease, caused by the soil-borne ascomycete fungus *Gaeumannomyces tritici*, is one of the most important root diseases of wheat in the UK and worldwide. The fungus invades the roots and destroys the vascular tissue, hindering the uptake of water and nutrients from the soil. Current control methods include crop rotation, later sowing of crops at risk and the use of partially effective fungicide seed dressings. Closely related species in the *Magnaporthaceae* family, such as *Gaeumannomyces hyphopodioides,* occur naturally in arable and grassland soils and have considerable potential to suppress take-all disease. *In vitro* assays revealed that the direct interaction between *G. tritici* and *G. hyphopodioides* is unlikely to play a significant role in take-all control. Co-inoculation bioassays demonstrated that effective take-all control is achieved when *G. hyphopodioides* colonises the root system before *G. tritici.* Detailed microscopy analyses revealed that *G. hyphopodioides* produces chlamydospore-like structures in the root cortex, which could also play a role in the infection cycle. Furthermore, the analyses confirmed previous findings that *G. hyphopodioides* induces physical plant defence responses such as cell-wall lignification. A dual RNA sequencing experiment of *G. tritici* infected and *G. hyphopodioides* colonised roots further highlighted this defence induction and revealed extensive transcriptional reprogramming in wheat following *G. hyphopodioides* colonisation. Taken together, these findings indicate that induced plant resistance is responsible for take-all control by *G. hyphopodioides*. Despite the clear upregulation of several defence pathways, plant bioassays revealed that *G. hyphopodioides* colonisation alone does not adversely affect wheat health. Finally, an improved protocol for virus-induced gene silencing (VIGS) in wheat roots was developed, which could facilitate the functional validation of candidate *G. tritici* resistance/susceptibility genes in wheat. This PhD project provides novel information regarding wheat responses to *G. hyphopodioides* and *G. tritici* infection, and provides vital data which could inform future biocontrol strategies against take-all disease in wheat.

ACKNOWLEDGEMENTS

This PhD project would not have been possible without help and support from a great number of people. Firstly, I would like to thank my previous supervisor Vanessa McMillan, for introducing me to take-all research and inspiring me with her work ethic. A huge thank you to my supervisor Javier, for his constant support and guidance over the last two years. Thank you for giving me the freedom to run with my ideas, for reigning me in when needed and for inspiring me to keep going. Thank you to my supervisor Kim, for sharing her vast wealth of knowledge and for steering the take-all team through some choppy waters and an international pandemic! Thank you to Kostya for his valuable guidance with the VIGS experiments and for always being willing to help. Thank you to Wanxin Chen for sharing her VIGS expertise and for helping me with many hours of root processing! Thanks also to my Nottingham supervisor Matthew Dickinson for his helpful feedback. To Gail and Jess, thank you for your hard work, friendship and support over the last 4 and half years. I'll never forget all the laughs (and tears) we shared up at the mud hut!

Thank you to the members of the Wheat Pathogenomics Group for providing support in the lab and for valuable feedback during lab meetings. A special thank you to Claire Kanja, Alina Igna and Chris Stephens for helping to solve many VIGS related issues. Thank you also to Blyth for being the best DTP and thesis writing buddy! Thank you to Kirstie Halsey, Eudri Venter and Hannah Walpole for all their help in bioimaging and for the pep talks. Thank you to Suzanne Clark for answering my many stats related questions and to Dan Smith, for guiding me through the world of bioinformatics. Thank you to my BSPP undergraduate student Kallie Botha and summer student Jade Smith, for working incredibly hard and helping to generate data which has contributed to this thesis.

Thank you to Oxford University Innovation for hosting me for my 3-month Professional Internship for PhD Students (PIP) and to the BBSRC for providing the funding for my PhD project. I am also very grateful to have received additional COVID-19 related funding from the BSPP.

I would like to thank all the incredible friends and colleagues that I have met at Rothamsted, particularly the original manor clan for all the fun nights at the pav, and to my amazing housemates Emily and Maiara, for being the ultimate female role models and for making these last 4 and a half years some of the best of my life. A heartfelt thank you to my mum, dad and brother for their unconditional love and support. Finally, a very special thank you to Harry, for being my biggest cheerleader and motivator. I am eternally grateful that you have been a part of this journey, and I can’t wait to see what the future holds.

TABLE OF CONTENTS

ABSTRACT i
ACKNOWLEDGEMENTS iii
TABLE OF CONTENTS v
LIST OF FIGURES x
LIST OF TABLES xiv
LIST OF ABBREVIATIONS xix
1 General Introduction 21
1.1 Global food security and wheat production 21
1.2 The importance of root health 24
1.3 The root microbiome 25
1.4 The impact of crop pathogens on global food security 29
1.5 Plant pathogens and climate change 33
1.6 Genetic and genomic resources for improved disease resistance in wheat 35
1.7 The potential of biocontrol strategies against plant pathogens 39
1.8 Take-all disease of wheat: a global problem 42
1.8.1 Introduction 43
1.8.2 Taxonomy of the *Magnaporthaceae* family 44
1.8.3 Take-all infection cycle 45
1.8.4 Detection and quantification of take-all disease 47
1.8.5 Take-all build up (TAB), decline (TAD) and the soil microbiome 49
1.8.6 Molecular understanding of the wheat-*G. tritici* interaction 52
1.8.7 Control of take-all disease 57
1.9 The disease control potential of closely related *Magnaporthaceae* fungi 63
1.9.1 Introduction 63
1.9.2 Taxonomy 63
1.9.3 Genome resources 67
1.10 Research objectives 68
2 General materials and methods 69
2.1 Media preparation 69
2.2 Maintenance and storage of *Magnaporthaceae* isolates 69
2.3 Isolation of *Magnaporthaceae* fungi from root material 69
2.4 Seedling pot bioassays 70
2.5 Seedling root assessments 70
2.6 Plant biomass measurements 72
2.7 Microscopy and imaging 73
2.7.1 Light microscopy 73
2.7.2 Photographic documentation 73
2.8 DNA extractions from plant and fungal material 73

2.9 RNA extractions from plant and fungal material 74
2.10 Quantification of nucleic acid concentration 74
2.11 Polymerase Chain Reaction (PCR) 74
2.12 Gel Electrophoresis 76
2.13 Sanger sequencing of PCR products 76
2.14 Quantification of *G. tritici* fungal biomass by TaqMan qPCR 76
2.15 Statistical analyses 78
3 Investigating the mechanism of take-all control by non-pathogenic *Magnaporthaceae* species 81
3.1 Introduction 81
3.2 Aims and hypotheses 82
3.3 Methods: 83
3.3.1 Fungal confrontation assays 88
3.3.2 Multiple interaction confrontation assays 90
3.3.3 Seedling co-inoculation assays: 91
3.3.4 Disease assessments 94
3.3.5 Quantification of *G. tritici* fungal biomass by qPCR 94
3.3.6 Plant biomass measurements 94
3.4 Results 94
3.4.1 Fungal confrontation assays 94
3.4.2 Seedling co-inoculation assay: experiment 1 101
3.4.3 Seedling co-inoculation assay: experiments 2 and 3 103
3.5 Discussion 110
3.6 Future work 116
3.7 Summary 117
3.8 Acknowledgement of contributions 117
4 Investigating the infection biology and lignification response to non-pathogenic *Magnaporthaceae* species 119
4.1 Introduction 119
4.2 Aims and hypotheses 124
4.3 Methods 124
4.3.1 Eppendorf seedling infection assay 125
4.3.2 Fixation and embedding protocol 126
4.3.3 Semi-thin sectioning and staining of roots for light microscopy 127
4.3.4 Preparation of roots containing *G. hyphopodioides* SEVs for transmission electron microscopy 127
4.3.5 Preparation and staining of ultrathin sections for transmission electron microscopy 128
4.3.6 Transmission electron microscopy and image analysis 129
4.4 Results: 129
4.4.1 Eppendorf seedling infection assay 129

4.4.2 Transmission electron microscopy of *G. hyphopodioides* sub-epidermal vesicles 143
4.5 Discussion 145
4.6 Future work 151
4.7 Summary 152
4.8 Acknowledgement of contributions 152
5 Investigating wheat transcriptional responses to *G. hyphopodioides* colonisation and *G. tritici* infection 153
5.1 Introduction 153
5.2 Methods 157
5.2.1 Co-inoculation experiment 157
5.2.2 Seedling infection protocol 158
5.2.3 *In vitro* fungal samples 159
5.2.4 Root sampling 160
5.2.5 RNA extractions 160
5.2.6 Confocal microscopy of infected root pieces 161
5.2.7 Library preparation and sequencing 161
5.2.8 Transcriptome annotation and analysis 162
5.2.9 Quantification of hormones from root samples 163
5.2.10 Lignin staining of root samples 164
5.2.11 Validation of gene expression by RT-qPCR 164
5.3 Results 165
5.3.1 Control of take-all disease by *G. hyphopodioides* 165
5.3.2 Characterising fungal colonisation across time points 166
5.3.3 RNA sequencing and read mapping 172
5.3.4 Identification of DEGs in wheat roots during the response to *G. tritici* infection and *G. hyphopodioides* colonisation 174
5.3.5 Gene Ontology (GO) enrichment analysis 176
5.3.6 Core response to *G. tritici* infection and *G. hyphopodioides* colonisation. 185
5.3.7 Plant lignification response 186
5.3.8 Expression of genes relating to cell wall organisation and biogenesis in *G. hyphopodioides* colonised roots 191
5.3.9 Expression of genes associated with plant defence responses 192
5.3.10 Role of phytohormones 192
5.4 Discussion 200
5.5 Acknowledgement of contributions 206
6 A Virus-induced gene silencing (VIGS) system to study wheat interactions with root-infecting fungi 208
6.1 Abstract 208
6.2 Introduction 208
6.3 Materials and methods 211

6.3.1 Gene target choice 211
6.3.2 VIGS construct preparation and *Nicotiana benthamiana* infiltration 212
6.3.3 *G. tritici*-wheat VIGS infection protocol 212
6.3.4 Harvesting and imaging root material 214
6.3.5 Take-all disease root assessments 215
6.3.6 RT-qPCR analysis of gene expression 216
6.4 Results and discussion 217
6.4.1 Development of a positive silencing control for wheat roots 217
6.4.2 Investigating the impact of BSMV infection on *G. tritici* virulence ... 220
6.5 Conclusions 222
6.6 Acknowledgement of contributions 223
7 Investigating the effect of non-pathogenic *Magnaporthaceae* species on plant health and evaluating their field applicability 223
7.1 Introduction 223
7.2 Aims and hypotheses 226
7.3 Methods 227
7.3.1 Seedling health experiments 227
7.3.2 Adult plant health experiment 228
7.3.3 Latitude® sensitivity experiments 233
7.3.4 Seedling bioassay to assess the susceptibility of elite winter wheat varieties to colonisation by *G. hyphopodioides* 235
7.4 Results 237
7.4.1 The effect of non-pathogenic *Magnaporthaceae* species on seedling health 237
7.4.2 The effect of *G. hyphopodioides* on adult health 241
7.4.3 Sensitivity of non-pathogenic *Magnaporthaceae* species to Latitude® fungicide 248
7.4.4 Susceptibility of elite winter wheat cultivars to colonisation by *G. hyphopodioides* 252
7.5 Discussion 254
7.6 Future work 257
7.7 Summary 258
7.8 Acknowledgement of contributions 259
8 General discussion 260
8.1 Summary and main findings 260
8.2 How does *G. hyphopodioides* control take-all disease? 261
8.3 Should *G. hyphopodioides* be applied as a commercial biocontrol agent? 263
8.4 The importance of investigating fungal endophytes in arable settings .. 266
8.5 Potential implications of this work for the wider research and farming communities 267
Appendices 270

References 323

LIST OF FIGURES

Figure 1.1 The top 10 wheat producing countries worldwide..... 23

Figure 1.2 Direct and indirect selection of root traits by root and shoot phenotyping methods. 25

Figure 1.3 The importance of root system functions on plant health and the associated soil microbiome..... 27

Figure 1.4 The tripartite disease triangle. 30

Figure 1.5 Characteristic take-all disease symptoms. 44

Figure 1.6 *G. tritici* life cycle within a crop season..... 45

Figure 1.7 Scanning electron micrograph of a developing *G. tritici* perithecium on an infected wheat root. See previous page..... 47

Figure 1.8 The 2-year, synergistic genetic traits concept to reduce take-all root disease in wheat crops. 50

Figure 1.9 Take-all levels during successive years of wheat cropping. 51

Figure 1.10 Phylogenetic tree based on ITS5-ITS4 rDNA regions of the *Magnaporthaceae* isolates used in this PhD project..... 67

Figure 2.1 Key symptoms for visual root assessments. 71

Figure 2.2 Disease severity assessments based on the percentage of black lesion coverage in the first 10 cm of each root..... 72

Figure 2.3 PCR and gel electrophoresis confirming species-specific detection of *G. tritici* using EF1-α primers (Keenan et al., 2015)..... 78

Figure 3.1 Representative images of fungal confrontation assays between non-pathogenic *Magnaporthaceae* species and *G. tritici.* 97

Figure 3.2 *G. hyphopodioides* and *G. tritici* intra-species confrontation assays on 100% PDA..... 98

Figure 3.3 Representative images demonstrating that colony separation distance and nutrient content of growth media affect the melanisation response between *G. hyphopodioides* (NZ.129.2C.17) and *G. tritici* (Gt 16.NZ.1d).. 99

Figure 3.4 *G. hyphopodioides* and *G. tritici* inter-species assays with *I. crassa, T. hamatum, S. sclerotiorum, F. graminearum* and *F. culmorum.*..... 100

Figure 3.5 Take-all disease levels and plant biomass in **co-inoculation experiment 1**. 102

Figure 3.6 Take-all disease levels and plant biomass in **co-inoculation experiment 2**. 105

Figure 3.7 Representative images of wheat seedlings in **co-inoculation experiment 2.** 107

Figure 3.8 Take-all disease levels, *G. tritici* fungal biomass and plant biomass in **co-inoculation experiment 3.** 109

Figure 3.9 Take-all disease severity in **co-inoculation experiment 3.**..... 110

Figure 4.1 Production of *G. hyphopodioides* sclerotia *in vitro*. 119

Figure 4.2 Colonisation structures produced by non-pathogenic *Magnaporthaceae* sp. 121

Figure 4.3 Sub-epidermal vesicles (SEVs) produced by diverse fungi in the roots of a range of plant hosts. 123

Figure 4.4 Image of Eppendorf seedling infection set-up (3 dpi). 126

Figure 4.5 Wheat roots imaged at 3 dpi. 130

Figure 4.6 Wheat roots imaged at 6 dpi. 131

Figure 4.7 Wheat roots imaged at 9 dpi. 131

Figure 4.8 Seedling infection assay micrographs at 3 dpi. 133

Figure 4.9 Seedling infection assay micrographs at 6 dpi. 135

Figure 4.10 Micrographs of transversal sections at 9 dpi. 137

Figure 4.11 Seedling infection assay micrographs at 9 dpi. 139

Figure 4.12 Sub epidermal vesicles (SEVs) produced by *S. cylindrosporus* and the unnamed *Magnaporthaceae* species at 9 dpi. 140

Figure 4.13 Sub epidermal vesicles (SEVs) with penetration pegs, produced by *S. cylindrosporus* in field samples of wheat. 141

Figure 4.14 Confocal micrograph of a *G. hyphopodioides* sub-epidermal vesicle with penetration peg. 142

Figure 4.15 Transmission electron micrographs of a *G. hyphopodioides* hypha (A, B) and a sub-epidermal vesicle (C, D). 144

Figure 4.16 Transmission electron micrograph *G. hyphopodioides* SEV with a penetration peg traversing the plant cell wall. 145

Figure 5.1 Schematic showing the root infection protocol and root areas sampled. 160

Figure 5.2 A. The percentage of roots with take-all lesions and amount of *G. tritici* fungal biomass 166

Figure 5.3 Fluorescence images obtained by confocal microscopy showing runner hyphae on the root surface at key time points selected for RNA sequencing. 168

Figure 5.4 Fluorescence images obtained by confocal microscopy showing infection hyphae in different root cell layers at key time points selected for RNA sequencing..... 169

Figure 5.5 Fluorescence images obtained by confocal microscopy of transversal root sections showing the stage of fungal colonisation at key time points selected for RNA sequencing. 170

Figure 5.6 Confocal micrographs of transversal root sections at 6 dpi 171

Figure 5.7 The percentage of reads mapped to the *T. aestivum* (A) and *G. tritici* (B) genome..... 173

Figure 5.8 Principal Component Analysis (PCA) plot of sample distances..... 174

Figure 5.9 A. The number of differentially expressed genes (DEGs) in wheat colonised by *G. hyphopodioides* or *G. tritici* across three key time points. 176

Figure 5.10 The top 10 most enriched biological process gene ontology (GO) terms unique to each time point in *G. hyphopodioides* colonised roots. .. 178

Figure 5.11 The top 10 most enriched biological process gene ontology (GO) terms unique to each time point in *G. tritici* infected roots. 180

Figure 5.12 Most representative enriched Gene Ontology (GO) terms in *G. tritici* infected and *G. hyphopodioides* colonised wheat at 5 dpi. 185

Figure 5.13 Top 10 GO enriched biological process terms among core DEGs in *G. hyphopodioides* and *G. tritici* infected plants at 5 dpi. 186

Figure 5.14 The role of lignin biosynthesis in the plant response to *G. hyphopodioides* (Gh) and *G. tritici* (Gt). 188

Figure 5.15 Micrographs of transversal root sections stained with potassium permanganate for the visualisation of cell wall lignification..... 190

Figure 5.16 The expression of JA and ET related genes in response to *G. hyphopodioides* (Gh) colonisation and *G. tritici* (Gt) infection. 195

Figure 5.17 Hormone quantifications of GA1, GA4, SA and JA in roots harvested at 5 dpi..... 199

Figure 6.1 Protocol for virus-induced gene silencing (VIGS) for functional studies of candidate *G. tritici* resistance/susceptibility genes in wheat. 214

Figure 6.2 Image analysis of root architecture traits..... 215

Figure 6.3 Root system images of BSMV:TaDGL1 and BSMV:TaRTH3 infected wheat plants compared to the BSMV:mcs4D control..... 219

Figure 6.4 Gene expression and winRHIZO root architecture analyses. 220

Figure 6.5 The effect of BSMV:mcs4D inoculation on take-all disease incidence and severity. 222

Figure 6.6 A. Root system images of *G. tritici* infected roots +/- BSMV:mcs4D. 222

Figure 7.1 The adult plant health experiment in a caged sand bed area. 230

Figure 7.2 The percentage of roots with fungal runner hyphae. 238

Figure 7.3 The average shoot and root biomass per plant (mg) in the seedling health experiments. 239

Figure 7.4 Representative images of wheat seedlings cv. Hereward colonised by different *Magnaporthaceae* species. 240

Figure 7.5 The average root volume (cm^3), total root length (cm) (A) and number of tips and forks (B) as determined by WinRHIZO software. 241

Figure 7.6 Representative images of *G. hyphopodioides*-inoculated and uninoculated wheat plants. 243

Figure 7.7 Foliar measurements of *G. hyphopodioides* inoculated and uninoculated adult wheat plants. 244

Figure 7.8 The average root biomass (g) of *G. hyphopodioides*-inoculated and uninoculated plants. 245

Figure 7.9 Representative images of *G. hyphopodioides*-inoculated and uninoculated wheat roots. 245

Figure 7.10 Micrographs of adult wheat roots exhibiting characteristic sub-epidermal vesicles (SEVs) of the non-pathogenic *Magnaporthaceae* species. 247

Figure 7.11 Representative images of *Magnaporthaceae* colonies growing in an *in vitro* fungicide sensitivity test. 249

Figure 7.12 The average colony diameter of *Magnaporthaceae* species grown on PDA in the presence and absence of the fungicide Latitude®. Error bars represent standard error. Asterisks indicate significant differences as calculated by Tukey's multiple-comparisons test ($p<0.05$). See appendix A.12 (table A.12.1) for full summary statistics. 250

Figure 7.13 The percentage of roots with runner hyphae in the presence and absence of the fungicide Latitude®. 251

Figure 7.14 Colonisation severity in the *in planta* Latitude® sensitivity test. .. 252

Figure 7.15 The percentage of roots colonised with *G. hyphopodioides* in a two-year soil-core baiting study by Osborne et al., (2018) (A, B) and in follow-up seedling susceptibility studies (C, D). 254

Figure A.1.1 Image of sandwich plate bioassay set-up 271

Figure A.3.1 Split-pot assays in sand using liquid inoculum. 280

Figure A.3.2 Split-root hydroponics set-up 281

Figure A.3.3 Take-all disease incidence (A) and severity (B) in a split root hydroponics pilot study. 282

Figure A.6.1 Wheat root stained with WGA and PI, demonstrating severe infection with *G. tritici* hyaline hyphae despite hyphae being invisible by eye. 286

Figure A.7.1 Confocal and transmitted light overlays showing SEVs and melanised runner hyphae with and without WGA staining. 289

Figure A.8.1 Vector map of pCa- γbLIC. 303

Figure A.8.2 Colony PCR to screen colonies for the presence of TaRTH3 or TaDGL1 gene fragments. 304

Figure A.8.3 Investigation of BSMV viral load and wheat root volume. 306

LIST OF TABLES

Table 1.1 New taxonomic classification of the species within the *Gaeumannomyces* family according to Hernández-Restrepo et al. (2016). 44

Table 1.2 Differing techniques used to discriminate between two corresponding genetic groups within the *G. tritici* species 48

Table 1.3 Protein overexpression studies demonstrating enhanced resistance to take-all disease 56

Table 1.4 Bacterial and fungal biocontrol agents implicated in the control of take-all disease 61

Table 1.5 Key characteristics of the non-pathogenic *Magnaporthaceae* species according to Hernández-Restrepo et al. (2016) 64

Table 1.6 Genome summary statistics 67

Table 2.1 Reaction mix for PCR analyses with DreamTaq Green PCR Master Mix (2X). 75

Table 2.2 Reaction mix for PCR analyses with Phusion® High-Fidelity DNA Polymerase 75

Table 2.3 Thermocycling conditions for PCR reactions with DreamTaq Green PCR Master Mix (2X). 75

Table 2.4 Thermocycling conditions for PCR reactions with Phusion® High-Fidelity DNA Polymerase. 75

Table 2.5 Reaction mix for *G. tritici* TaqMan qPCR assays 77

Table 2.6 Thermocycling conditions for *G. tritici* TaqMan qPCR assays 77

Table 3.1 Details of the *Magnaporthaceae* isolates used in chapter 3. 84

Table 3.2 Summary of pathogenic and endophytic species used in confrontation assays with *G. tritici* and *G. hyphopodioides*. 86

Table 3.3 Treatment details of fungal confrontation assays between non-pathogenic *Magnaporthaceae* species and *G. tritici.* 88

Table 3.4 Fungal confrontation assays between *G. hyphopodioides*, *G. tritici* and different endophytic and pathogenic species. 89

Table 3.5 List of fungal isolates used in *G. hyphopodioides* and *G. tritici* intra-species confrontation assays. 91

Table 3.6 Fungal isolates used in the co-inoculation experiments. 92

Table 3.7 Treatment details for co-inoculation experiment 1. 93

Table 3.8 Treatment details for co-inoculation experiments 2 and 3*. 93

Table 3.9 Hyphal melanisation in confrontation assays between *G. tritici* and different non-pathogenic *Magnaporthaceae* species. 97

Table 3.10 Melanisation response at different nutrient contents 99

Table 4.1 Treatment conditions for the Eppendorf seedling infection experiment 125

Table 5.1 Summary of *in planta* treatments explored for RNA sequencing 159

Table 5.2 Summary of *in vitro* treatments for RNA sequencing 159

Table 5.3 List of genes to be validated by RT-qPCR. 164

Table 5.4 Average read counts and percentage mapping statistics to the *T. aestivum* and *G. tritici* genome. 172

Table 5.5 The top 30 most differentially expressed genes relating to cell wall organisation and biogenesis in *G. hyphopodioides* colonised plants. 191

Table 5.6 Expression of genes involved in salicylic acid (SA) biosynthesis and SA mediated signalling. 196

Table 5.7 Expression of key genes involved in the biosynthesis of gibberellic acid (GA). 197

Table 6.1 Root expressed genes selected for VIGS in wheat. 211

Table 6.2 Primer sequences for RT-qPCR analyses. 217

Table 7.1 Treatment details for the seedling biomass experiments 1, 2 and 3*. 227

Table 7.2 Treatment details for the adult plant health experiment. 230

Table 7.3 Chemical inputs applied during the adult plant heath experiment .. 230

Table 7.4 Key adult wheat growth stages as described by the Agriculture and Horticulture Development Board (AHDB) 231

Table 7.5 Treatment details for the *in vitro* Latitude® sensitivity tests. 234

Table 7.6 Treatment details for *in planta* Latitude® sensitivity tests. 234

Table 7.7 UK winter wheat cultivars chosen for inclusion in a *G. hyphopodioides* susceptibility experiment. 236

Table 7.8 Fungal species isolated from root pieces containing sub-epidermal vesicles. 248

Table A.1.1 Summary statistics and ANOVA analysis of the average colony diameter of *G. hyphopodioides* and *G. tritici* after 4 days of growth 270

Table A.1.2 Summary statistics and ANOVA analysis of the average colony diameter of *G. tritici* after 6 days of growth in a sandwich plate bioassay. 271

Table A.2.1 Predicted mean proportions of roots with take-all lesions and accumulated analysis of deviance in co-inoculation experiment 1. 272

Table A.2.2 Summary statistics and ANOVA analysis of the average shoot and root biomass per plant (mg) in co-inoculation experiment 1. 273

Table A.2.3 Predicted mean proportions of roots with take-all lesions and accumulated analysis of deviance in co-inoculation experiment 2. 274

Table A.2.4 Summary statistics and ANOVA analysis of the average shoot and root biomass per plant (mg) in co-inoculation experiment 2. 275

Table A.2.5 Predicted mean proportions of roots with take-all lesions and accumulated analysis of deviance in co-inoculation experiment 3. 276

Table A.2.6 Summary statistics and ANOVA analysis of the mean *G. tritici* fungal biomass (indicated by pg *G. tritici*/ng total DNA) in root samples from co-inoculation experiment 3. 277

Table A.2.7 Summary statistics and ANOVA analysis of the average shoot and root biomass per plant (mg) in co-inoculation experiment 3. 278

Table A.2.8 Statistical analysis of take-all severity in co-inoculation experiment 3. 279

Table A.4.1 Summary of pilot experiments for the optimisation of root infection and sample preparation 282

Table A.4.2 Summary of histochemical stains tested. 283

Table A.5.1 ANOVA analysis of the cell wall width of sub-epidermal vesicles (SEVs) and infection hyphae in TEM micrographs. 283

Table A.6.1 Treatments details for RNAseq pilot study 1 285

Table A.6.2 Nanodrop analysis of RNA extracted using the PicoPure™, RNeasy® or E.Z.N.A kits. 287

Table A.7.1 Predicted mean proportions of roots with take-all lesions and accumulated analysis of deviance 288

Table A.7.2 ANOVA analysis of *G. tritici* fungal biomass as measured in a TaqMan qPCR assay..... 288

Table A.7.3 RNA and RNA sequencing quality control measures. 290

Table A.7.4 Mapping statistics for all RNA sequencing samples. 291

Table A.7.5 Full list of genes involved in the GO term “stomatal movement” . 293

Table A.7.6 Full list of genes involved in the GO term “response to biotic stimulus” 294

Table A.7.7 Differential expression of TIP and PIP aquaporin genes in *G. hyphopodioides* colonised roots compared to the uninoculated control... 296

Table A.7.8 Genes of interest associated with plant defence responses against fungal pathogens 297

Table A.7.9 ANOVA analysis of SA, JA, GA1, GA4 levels (ng/g) in wheat roots at 5 dpi. 299

Table A.8.1 Candidate genes for virus-induced gene silencing (VIGS) in wheat roots..... 302

Table A.8.2 Primer sequences for the amplification of TaDGL1 and TaRTH3 gene fragments..... 303

Table A.8.3 Summary statistics and unbalanced ANOVA analysis of LOG transformed root architecture data. 304

Table A.8.4 Pearson’s correlation coefficient analysis of BSMV viral load and root architecture traits. 307

Table A.8.5 Predicted mean proportions of roots with take-all lesions and accumulated analysis of deviance 307

Table A.8.6 Ordinal regression analysis of take-all disease severity 308

Table A.9.1 Cropping history details for field soils used in experiments in chapter 7. 308

Table A.10.1 Predicted mean proportions of roots with runner hyphae in the seedling health experiments. 309

Table A.10.2 Summary statistics and ANOVA analysis of the average shoot and root biomass per plant (mg) in the seedling health experiments. 310

Table A.10.3 Summary statistics and ANOVA analysis of the total root length (cm) and root volume (cm^3) in seedling health experiment 3. 311

Table A.10.4 Summary statistics and ANOVA analysis of the number of roots tips and forks in the seedling health experiment 3. 312

Table A.11.1 List of winter wheat cultivars investigated for their ability to host *G. hyphopodioides* 313

Table A.11.2 Summary of two-sample t-tests for the analysis of plant health parameters in *G. hyphopodioides* inoculated (Skyfall + Gh) and uninoculated plants (Skyfall). 313

Table A.11.3 Summary statistics and ANOVA analysis of the average Chlorophyll Content Index (CCI) of the main flag leaf at different stages of adult plant growth. 314

Table A.11.4 ITS sequencing and species identification of fungal colonies isolated from wheat roots in the adult health experiment 315

Table A.12.1 Average colony diameter of *Magnaporthaceae* fungi in the presence and absence of Latitude®. 319

Table A.12.2 Proportion of roots with runner hyphae in an *in planta* Latitude® sensitivity test. 319

Table A.12.3 Ordinal logistic regression analysis of colonisation severity in the *in planta* Latitude® sensitivity test. 320

Table A.13.1 The proportion of roots with *G. hyphopodioides* runner hyphae in the first cultivar susceptibility test 321

Table A.13.2 The proportion of roots with *G. hyphopodioides* runner hyphae in a repeat cultivar susceptibility test with reduced inoculum levels. 322

LIST OF ABBREVIATIONS

2,4-DAPG	2,4-diacetylphloroglucinol
ANOVA	analysis of variance
AB	aniline blue
bp	base pair
BLAST	Basic Local Alignment Search Tool
BSPP	British Society for Plant Pathology
CWDEs	cell wall degrading enzymes
cm	centimetre
cDNA	complementary DNA
cv.	cultivar
DAMP	damage associated molecular pattern
dpi	days post infection
d.f.	degrees of freedom
DNA	deoxyribonucleic acid
DEFRA	Department for Environment, Food and Rural Affairs
DEG	differentially expressed gene
DSE	dark septate endophyte
ETI	effector-triggered immunity
ET	ethylene
FAO	Food and Agriculture Organisation of the United Nations
Gh	*Gaeumannomyces hyphopodioides*
Gt	*Gaeumannomyces tritici*
GLM	generalised linear regression model
GA	gibberellic acid
ISR	induced systemic resistance
ITS	internal transcribed spacer
JA	jasmonic acid
m.s.	mean squares
MAMP	microbe associated molecular pattern
µg	microgram
µl	microlitre
µm	micrometre

µM	micromolar
ml	millilitre
mm	millimetre
mM	millimolar
ng	nanogram
PAMP	pathogen-associated molecular pattern
PRR	pattern-recognition receptor
PTI	pattern-triggered immunity
PCR	polymerase chain reaction
PP	potassium permanganate
qPCR	real time quantitative PCR
RNA	ribonucleic acid
SA	salicylic acid
Sc	*Slopeiomyces cylindrosporus*
sp.	species
spp.	species plural
SEV	sub-epidermal vesicle
s.s.	sums of squares
SAR	systemic acquired resistance
TAB	take-all build up
TAD	take-all decline
TEM	transmission electron microscopy
Um	unknown *Magnaporthaceae* species
VOCs	volatile organic compounds
WGIN	Wheat Genetic Improvement Network

1 General Introduction

1.1 Global food security and wheat production

Maintaining global food security while preserving the environment and protecting biodiversity is one of the greatest challenges facing humankind. With the global population estimated to reach over 9 billion by 2050, food production will need to increase by 70% and cereal production will need to reach 3 billion tonnes a year in order to feed a larger, more affluent population (FAO, 2009). Recent statistics released by the Food and Agriculture Organization of the United Nations (FAO) indicate that the COVID-19 pandemic has also had devastating impacts on food security and malnutrition, with the prevalence of undernourishment increasing by 1.5% in just one year, despite having remained unchanged for five years previously. The report projects that between 720 and 810 million people in the world faced hunger in 2020 (FAO et al., 2021) and though complex socioeconomic factors greatly contribute to overall food security, the take-home message is still clear. We are not on track to meet our global commitment to end world hunger and malnutrition by 2030, and COVID-19 has made achieving this goal even more challenging. Furthermore, global food production is at increasing risk from emerging crop diseases (Fones et al., 2020), climate change, soil exhaustion, the plateauing of crop yields and diminishing natural resources (Mc Carthy et al., 2018).

Wheat (*Triticum* species) is considered as one of the most important cereal crops worldwide, second only to rice. Wheat is the most important source of protein and provides around 20% of human caloric intake globally. As a result, wheat is of significant social and economic importance. At present, around 95% of the wheat grown worldwide is hexaploid bread wheat, the remaining 5% being made up mostly of tetraploid durum wheat used in the production of pasta. The domestication of wheat approximately 10,000 years ago is seen as the single most important step towards modern civilisation by allowing a departure from the hunter-gatherer lifestyle. The first cultivated wheats were tetraploid (AABB) emmer and diploid (AA) einkorn grasses which were grown by farmers in the Fertile Crescent, also referred to as the “cradle of civilization” (Shewry, 2009). Genome sequence analysis has revealed that tetraploid emmer is derived from a cross between *Triticum urartu* (AA) and an unknown close

relative of *Aegilops speltoides* (BB). The resulting polyploid species subsequently hybridised repeatedly with *A. tauschii* (DD), the diploid D genome donor. Many centuries of domestication and selection have since resulted in modern allohexaploid bread wheat which consists of three sub-genomes (*Triticum aestivum*, 2*n*=6*x*=42 chromosomes; genomic code AABBDD) (Marcussen et al., 2014).

Wheat is now the most widely cultivated cereal in the world with over 730 million tonnes harvested over an area of approximately 216 million hectares (ha). In comparison, rice is cultivated over an area of 162 million ha, producing 780 million tonnes a year. Maize, a cereal crop now produced primarily for feedstock, is grown over an area of 197 million ha, producing 115 million tonnes a year (FAOSTAT, 2018) However, differences in yield per hectare exist among the wheat producing countries of the world, with average wheat yields in the UK reaching approximately 7.7 t/ha, while many African countries such as Somalia produce as little as 0.4 t/ha, compared to the global average of 3.18 t/ha in 2018 (FAOSTAT, 2018). Asia now accounts for the majority of wheat production, with China ranking as the top wheat producing country worldwide, followed by India (see figure 1.1). The wide distribution of wheat cultivation and high levels of production were made possible by significant technological achievements during the “Green Revolution” of the 50s and 60s. Specifically, the development of semi-dwarfing, high yielding cultivars responsive to fertilizer applications earnt wheat the title “the miracle crop” (Shiferaw et al., 2013). However, many regions have since seen wheat yields levelling off, with the UK experiencing little yield improvements since 1984 (FAOSTAT, 2018).

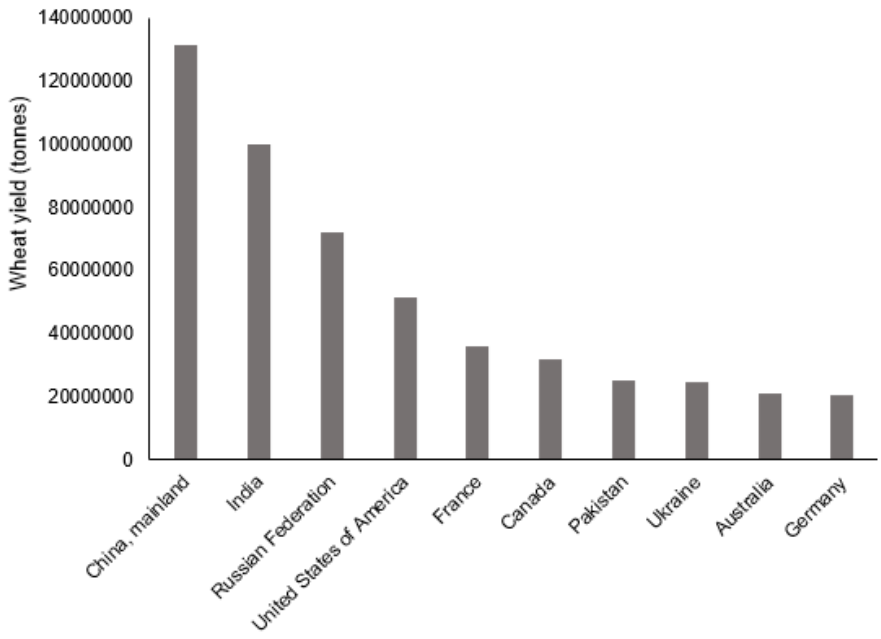


Figure 1.1 The top 10 wheat producing countries worldwide. Data obtained from the FAOSTAT 2018 database (http://www.fao.org/faostat). The UK ranked 15th in 2018.

The yield plateau, along with the growing demand for wheat in developing countries and the increasing global consumption *per capita,* has prompted serious efforts to further increase wheat production. To address productivity, researchers have focused their attention on the hypothetical "yield gap" which represents the difference between theoretical and actual yield levels. The yield gap is affected by a diverse range of factors, including environmental factors such as climate change (Asseng et al., 2015), biotic factors such as disease (Fisher et al., 2012) and genetic factors associated with cultivar genotype (Senapati & Semenov, 2020).

These factors are often interrelated. For example, the ancestral hybridisation events that gave rise to modern cultivated wheat have meant that only a small sample of genetic diversity has been retained, resulting in genetic bottlenecking and the loss of key genes responsible for important traits such as disease resistance and drought tolerance. Therefore, despite tremendous yield increases, modern wheat is more vulnerable to biotic stresses caused by pests and pathogens compared to its progenitor species (Pour-Aboughadareh et al., 2021). Thus, to meet the soaring demand for wheat, cultivars should be bred not only for yield, but also for resilience to biotic and abiotic stresses.

1.2 The importance of root health

Though the importance of plant health on overall productivity is well-recognised, root health is an area which until recently has been neglected. Roots are the organs of the plant responsible for acquiring water and essential nutrients as well as anchoring the plant to the ground. These functions are particularly important for annual cereal crops, which must obtain enough resources to maximise yield, whilst also dealing with the physical weight of increased grain loads (Voss-Fels et al., 2018). Roots are also major soil architects, increasing aeration whilst protecting against erosion (Wong & Plett., 2019). Monocotyledonous cereal root systems are complex; comprising of primary and seminal roots which are formed during embryogenesis, and roots that emerge during later stages of crop development either from existing roots as in the case of lateral roots, or from the shoot as in the case of crown roots (Hochholdinger & Zimmermann, 2018). Root hairs, the cellular outgrowths of epidermal cells which extend from the root surface into the soil, also play an important role in nutrient and water uptake and the interaction with soil microbes (Dolan, 2017).

Root architecture is now a major target for crop improvement (see figure 1.2), though root traits still remain largely unexploited (Tracy et al., 2020). This is partly due to the inaccessibility of roots, making field-scale phenotyping extremely challenging and time-consuming. However, new technologies using artificial growth systems such as soil chambers (Joshi et al., 2017) or direct, deep phenotyping under field conditions (Wasson et al., 2016) allow for high-throughput, non-destructive phenotyping of crop root systems. Sophisticated 3-D imaging of root systems in high definition is now possible through magnetic resonance imaging (MRI) (van Dusschoten et al., 2016) and X-ray computed tomography (CT) (Hou et al., 2022), allowing crop roots to be monitored throughout their development. As a result, plant phenomics is a growing field. Root length, a key trait in determining root distribution and therefore the efficiency of water-uptake has been successfully targeted in rice (Kitomi et al., 2018). DEEPER ROOTING 1 (DRO1), a rice quantitative trait locus controlling root growth angle was the first cloned major gene demonstrating improved yield under water-limited conditions (*ibid*.). More recently, Placido et al. (2020) used RNAi technology to demonstrate that the suppression of the LATERAL ROOT DENSITY (LRD) gene in wheat results in improved root growth under water-limitation and also increased grain size under optimal growth conditions, making this trait a potential candidate for crop

improvement. Interestingly, there is evidence that root architecture is linked to above-ground traits. For instance, VERNALIZATION1 (VRN1), a key gene which regulates flowering in cereals, was also found to modulate root architecture in wheat and barley (Voss-Fels et al., 2018). Therefore, the possible pleiotropic effects of key genes must be fully investigated before being targeted for the genetic improvement of crops. Furthermore, the possible detrimental effects of prior breeding targets should be explored.

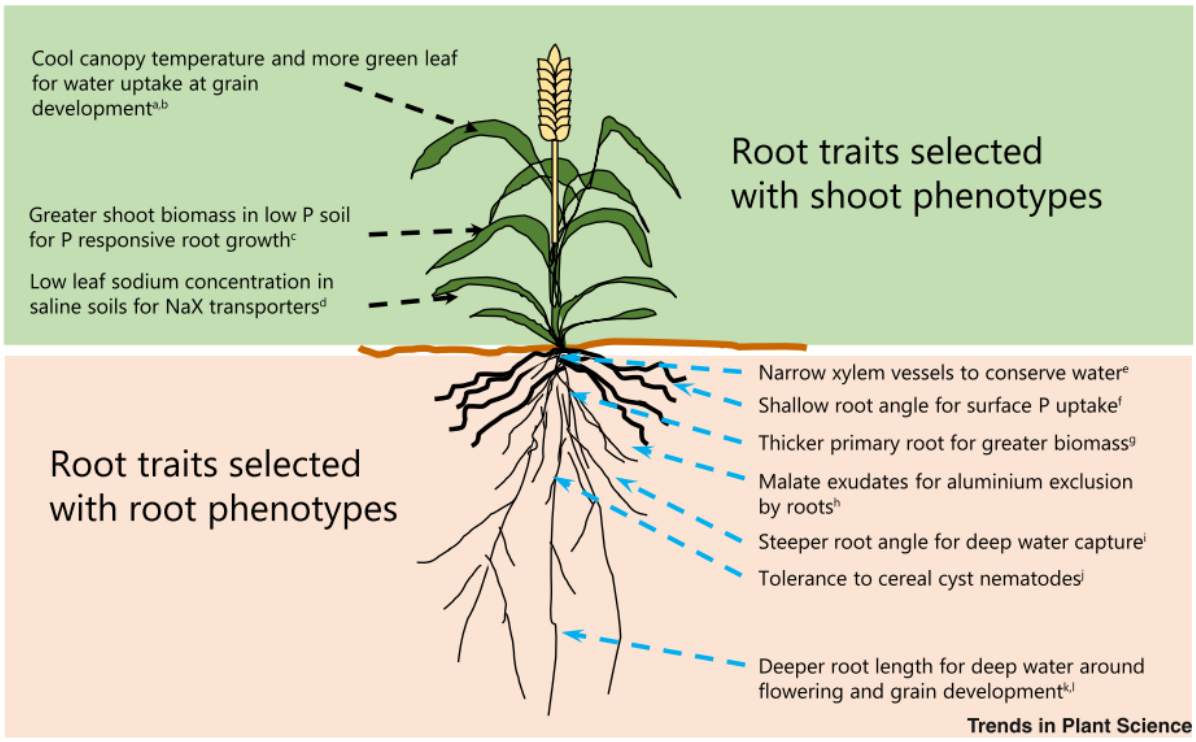


Figure 1.2 Direct and indirect selection of root traits by root and shoot phenotyping methods. Reproduced from Tracy et al., (2020) https://doi.org/10.1016/j.tplants.2019.10.015 under the Creative Commons Attribution License (Creative Commons 4.0).

1.3 The root microbiome

Crops grown in the field do not exist in sterile conditions and must interact with a vast range of organisms, including microbes. The term “plant microbiome” describes the microbial genomes present in the phyllosphere, endosphere and rhizosphere (Compant et al., 2019). The phyllosphere can be described as the above-ground surface of the plant and its associated microorganisms, while the endosphere is described as the internal tissues that are colonised by microbes which must spend at least part of their lifecycle within the plant tissues, and are thus termed endophytes.

Conversely, the rhizosphere refers to the narrow region of substrate surrounding the roots that is directly influenced by root exudates, and its associated microorganisms (de la Fuente Cantó et al., 2020). The root microbiome therefore consists of the rhizosphere and endosphere microbiota, both of which can be recruited from the bulk soil. Microbial lifestyles exist on a dynamic continuum ranging from beneficial, to benign, to pathogenic. Microbes may have a neutral or commensal effect on the plant by recycling plant derived carbohydrates or nutrients back into the soil. On the other hand, beneficial microbes can provide a wide range of plant services such as access to nutrients like phosphorous and nitrogen, as in mycorrhizal and rhizobial associations (Goyal et al., 2021), or by enhancing plant growth as in the plant growth promoting (PGPR) rhizobacteria and fungi (Mishra et al., 2017) (see figure 1.3). Furthermore, some beneficial microbes are also able to provide protection against biotic stresses such as phytopathogen attack (Panda et al., 2019), or buffer against abiotic stresses such as extreme drought (Chareesri et al., 2020; Jiang et al., 2021). However, microbes may also be deleterious to plant health, these being pathogenic or parasitic fungi, bacteria and oomycetes. Roots, being the first barrier to pathogen attack in microbe-rich soil, are therefore tasked with the important role of distinguishing friend from foe (Oldroyd, 2013).

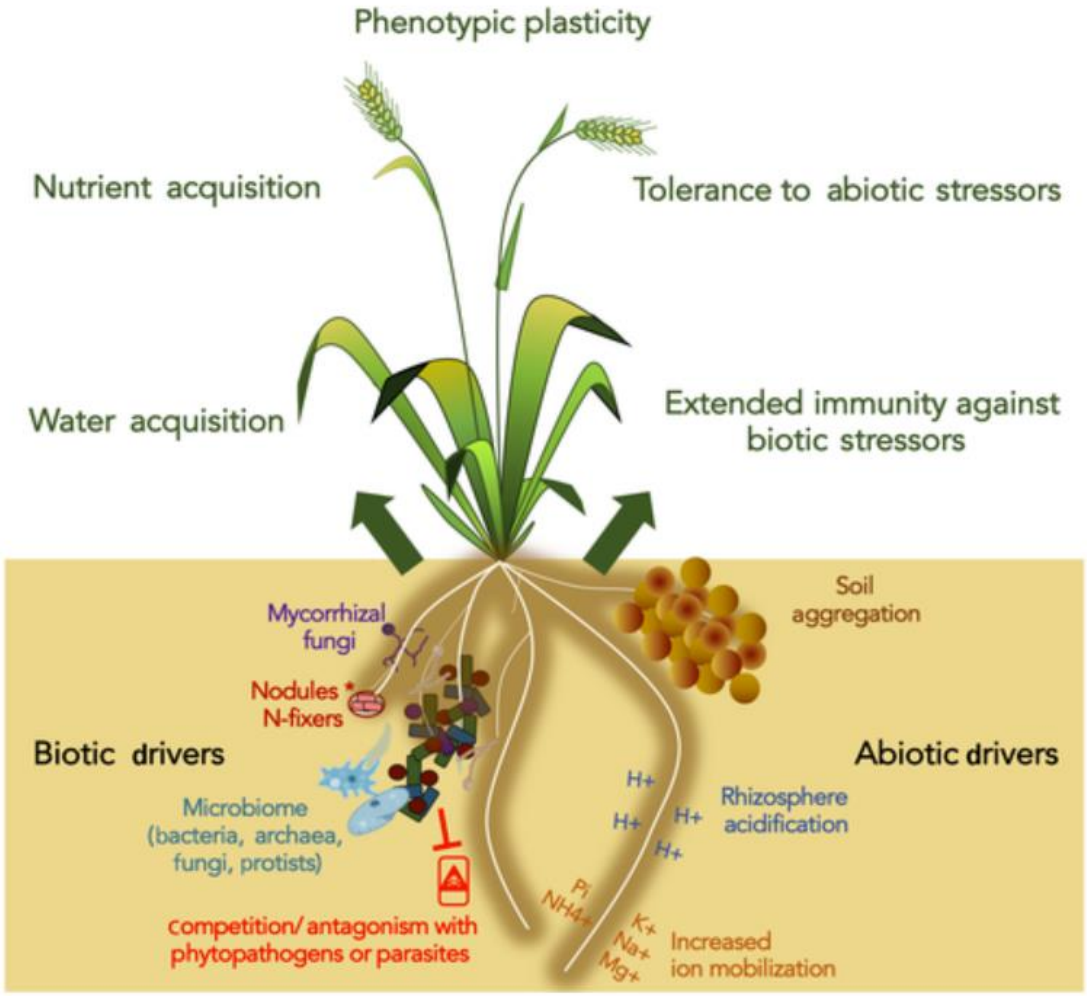


Figure 1.3 The importance of root system functions on plant health and the associated soil microbiome. Reproduced from de la Fuente Cantó et al., (2020) https://doi.org/10.1111/tpj.14781 with publisher permission (License no. 5254161134773).

The root apex is made up of the division zone (otherwise known as the root apical meristem), the transition zone and the elongation zone. The detection of microbe-associated molecular patterns (MAMPs) in the vulnerable root division zone is sufficient to trigger an immune response (Zhou et al., 2020). However, in differentiated cells away from the division zone, an additional damage-associated molecular pattern (DAMP) signal is needed to trigger the plant immune response in Arabidopsis (*ibid.*). (see section 1.1.4 for further detail regarding MAMPs and DAMPs). These findings suggest that cellular damage can activate local immune responses in the root, which could explain why MAMP perception is effective in roots, despite existing in a microbe rich environment.

We are beginning to understand how plants communicate with and differentiate between beneficial and pathogenic microbes. Roots release exudates (e.g., primary metabolites such as monosaccharides, oligosaccharides and organic acids), the changing composition and concentration of which may be responsible for shaping the microbiome (Canarini et al., 2019; Rolfe et al., 2019; Sasse et al., 2018). For example, foliar infection of Arabidopsis by *Pseudomonas syringae* resulted in the selective secretion of L-malic acid, resulting in increased recruitment and colonisation by *Bacillus subtilis*, known to induce plant resistance against several pathogens (Rudrappa et al., 2008). Thus, plants can use exudates as a "cry for help" by recruiting beneficial microbes during stressful conditions. The production of secondary metabolites may be just as important in shaping the root microbiome due to their antimicrobial properties and roles in signalling (Rolfe et al., 2019). Particularly relevant is the production of the antifungal triterpene avenacin which is produced by oat roots and provides protection against the root pathogen *Gaeumannomyces tritici,* the causal agent of take-all disease and the focus of this PhD project. Efforts are currently being made to engineer the avenacin pathway into wheat (Leveau et al., 2018; Li et al., 2021).

There is growing evidence of a bidirectional crosstalk between plants and microbes, for example through the release of phytohormones and microbial signalling molecules. In *Petunia hybrida*, strigalactones (phytohormones with diverse roles in plant signalling and architecture), are exuded by the ABC transporter PDR1 and sensed by mycorrhizal *Glomeromycota* fungi which consequently produce lipochitooligosaccharide (LCO) signalling molecules required for root colonisation (Oldroyd, 2013; Sasse et al., 2018). There is evidence that microbial LCO signals such as *myc* factors produced by mycorrhiza, and *nod* factors produced by rhizobia, are detected by LysM receptor-like kinase complexes in a shared symbiotic pathway. However, some pathogens may be able to hack specific components of such pathways to facilitate infection, hence symbiotic and immune signalling may share certain nodes (Zipfel & Oldroyd, 2017). Some fungal pathogens can deliver small RNAs (sRNAs) into host cells to target defence pathways and suppress immunity in a process known as cross-kingdom RNA interference (RNAi) (Huang et al., 2019). However, plants are also capable of delivering sRNAs, which are transported within extracellular vesicles to pathogen infection sites and can target key pathogenicity

factors to prevent infection (Cai et al., 2018, 2021). Extracellular vesicles have also been implicated in plant-mycorrhizal interactions (Roth et al., 2019), hence RNAi mechanisms may be involved in both symbiotic and pathogenic relationships. Thus, cross-kingdom RNAi is an exciting and rapidly growing area of research and may have future applications for crop improvement (Niu et al., 2021).

Numerous root microbes are now known to play a significant role in determining the overall health status and productivity of the host plant. However, identifying the importance of individual species is difficult given the many multipartite interactions occurring at any one time (Lareen et al., 2016). Multipartite interactions may be influenced by changing soil properties and chemistries, as well as different host plant genotypes (Mauchline & Malone, 2017; Osborne et al., 2018) and even different root architectures (Saleem et al., 2018). Therefore, to improve the overall root health of crop plants, a deeper understanding of root architecture traits and the complex interaction with root microbes and the environment is needed.

1.4 The impact of crop pathogens on global food security

Pests and pathogens significantly reduce the yield and quality of crops. In a recent study, pests and pathogens were estimated to cause average global wheat yield losses of 21.5%, with the highest losses associated with areas of rapid population growth. Such areas often suffer from food deficits and emerging or recurring pests and diseases (Savary et al., 2019). Though both bacterial and fungal pathogens exist, fungal plant pathogens cause more damage than bacterial pathogens and alone can destroy up to 30% of crop products. Even low-level disease can cause losses that, if mitigated, would be able to feed 8.5% of the world population (Fisher et al., 2012). Mycotoxin producing fungi further limit food safety and availability through food spoilage (Avery et al., 2019; Fisher et al., 2012). Adding to the problem is the growing resistance to antifungal chemistries and the emergence of new and devastating pathogens as a result of changing climates, globalisation and an increase in crop monocultures (Fones et al., 2020).

Fungal pathogens interact with their host(s) through a range of different lifestyles, from biotrophic; requiring live plants as a source of nutrients, to necrotrophic; actively killing host plant cells and using the contents to support fungal growth. Fungi which switch from biotrophy to necrotrophy are known as hemibiotrophs. Fungal pathogens also

differ in the range of hosts, as well as the types of tissue that they can infect. For example, fungal pathogens are capable of infecting root tissue, stem base tissue, leaf tissue, floral tissue or a combination of these tissues. The success of a pathogen can therefore be determined by a range of factors relating to the environment, the host and the pathogen itself (figure 1.4).

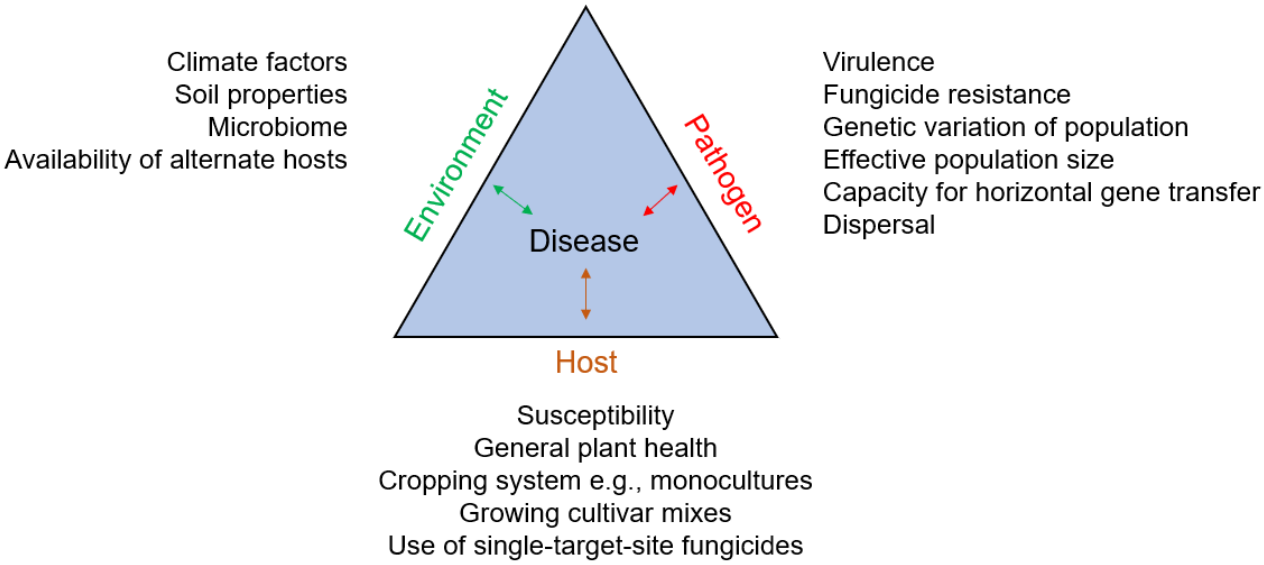


Figure 1.4 The tripartite disease triangle. Many factors affect the different aspects of the disease triangle, and they themselves may be interconnected.

Plants can detect the presence of fungal pathogens through the recognition of conserved molecular patterns known as pathogen-associated molecular patterns (PAMPS) or microbe-associated molecular patterns (MAMPS). PAMPs, such as chitin, the major component of fungal cell walls, are recognised by membrane-localised pattern recognition receptors (PRRs), which trigger PAMP-triggered immunity (PTI), the plants first line of defence (Boller & Felix, 2009). PRRs can also indirectly detect pathogen attack through the recognition of host-derived damage-associated molecular patterns (DAMPs) (Li et al., 2020). PRR signalling results in the accumulation of antimicrobial compounds through a range of processes including the rapid accumulation of reactive oxygen intermediates, defence-related mitogen-activated protein kinase cascades and transcriptional reprogramming of the host. Therefore, a successful pathogen must avoid PTI or find a way to suppress it. Pathogens secrete fungal effectors, secondary metabolites or proteins that kill the host plant, protect the

fungus or suppress the plant immune response (Lo Presti et al., 2015). However, effectors can be detected by plant resistance proteins (R-proteins), some of which are conserved intracellular receptors of the nucleotide-binding leucine-rich receptor (NB-LRR) class. Activation of R-proteins by effectors, often referred to as avirulence (avr) proteins, triggers the second layer of defence known as effector-triggered immunity (ETI). ETI results in disease resistance and usually, a hypersensitive (HR) cell death response at the site of pathogen attack (Jones & Dangl, 2006).

Several foliar wheat pathogens have threatened global production since the domestication of wheat and continue to cause significant yield losses. The wheat rust fungi *Puccinia graminis* f. sp. *tritici* (wheat stem rust), *P. striiformis* Westend. f. sp. *tritici* (*Pst*) (wheat stripe/yellow rust) and *Puccinia triticina* Eriks. (*Pt*) (wheat leaf rust) are obligate biotrophic pathogens which have been predicted to cause global annual yield losses of between US$ 4.3 to 5.0 billion. These basidiomycete rust fungi attack the leaves or stems of wheat producing characteristic masses of yellow to red asexual urediniospores. The airborne nature of the rust fungi along with the rapid evolution of new races make the rust fungi particularly successful (Figueroa et al., 2018). Wheat blotch diseases caused by the ascomycete fungi *Zymoseptoria tritici* (septoria tritici blotch), *Parastagonospora nodorum* (septoria nodorum blotch) and *Pyrenophora tritici-repentis* (tan spot) are also particularly damaging. Septoria tritici blotch disease is regarded as the primary threat to European winter wheat production. Infection is characterised by an initial asymptomatic phase where the fungus remains in the apoplast and fungal growth rates are slow, followed by a symptomatic phase resulting in necrotic black lesions which are visible on leaf surfaces and which drastically reduce the photosynthetic leaf area (Brennan et al., 2019). Chemical control by succinate dehydrogenase inhibitor (SDHIs) and demethylation inhibitor (DMI) fungicides are the primary method of disease prevention, though the efficacy and availability of these chemistries is being limited by growing fungal resistance to SDHIs and more stringent EU regulations (Dooley et al., 2016).

Floral diseases such as fusarium head blight (FHB) cause significant yield losses through reduced grain production and toxin contamination of grain. FHB is caused by several members of the FHB complex, though the primary species responsible globally is *Fusarium graminearum.* The production of various mycotoxins such as deoxynivalenol (DON) is a major risk to human and animal health. As such, many

countries have set legal limits for mycotoxin levels, meaning that affected grain cannot be sold for human or animal consumption (Figueroa et al., 2018).

Soil-borne pathogens, though often less easily spread than foliar pathogens with air-borne spores, are also responsible for major crop losses worldwide. Soil-borne pathogens infect the root system and, in some cases, can grow through the vascular tissue to the aerial parts of the plant. Root-infecting fungal pathogens are notoriously hard to control due to the difficulties in applying chemistries to the root system. Furthermore, many soil-borne pathogens can persist in the soil for long periods of time, even in the absence of the host. Resistant structures such as melanised mycelium, chlamydospores and sclerotia increase the persistence of soil-borne fungal pathogens and make them difficult to control (Hornby, 1988). Despite the significant economic losses caused by root infecting pathogens, the molecular mechanisms mediating infection are less well studied than in foliar diseases.

Rhizoctonia solani is a species complex of basidiomycete fungi that cause “sheath blight”, “root rot” and “leaf blight” in several plant species including cereals, pasture crops, vegetable crops and oil crops (Anderson, 1982). *R. solani* AG8 is the most economically important root disease affecting wheat and barley in southern Australia’s dryland growing regions, causing annual yield losses of up to $77 million (Barnett et al., 2019). *R. solani* root rot results in a reduced ability for water and nutrient uptake in the plant, resulting in stunting of seedlings and bare-patches under high disease pressures (Schillinger & Paulitz, 2006). Pythium species also cause significant damage to wheat and barley. At least 10 *Pythium* species cause *Pythium* root rot and dampening off disease, often occurring in a complex (Paulitz & Adams, 2003). Limited control strategies exist for root diseases caused by *Pythium* and *R. solani*, with no resistant commercial wheat cultivars available and limited efficacy of commercial fungicides. Together with other root-infecting fungi and nematode pests, *R. solani* and *Pythium* damage results yield losses of wheat and barley amounting to $100 million annually in Washington, USA, and billions of dollars worldwide (Mavrodi et al., 2012; Paulitz et al., 2002).

Wheat and barley are also particularly susceptible to the soil-borne pathogen *Fusarium culmorum*, one of the several *Fusarium* species responsible for Fusarium foot and root rot disease (also known as Fusarium crown rot), and a causal agent of

FHB. Fusarium-derived root and stem diseases result in yield losses of around 25% in Australia and 31-65% in North America, with warmer temperatures resulting in greater levels of foot and root rot (Kim et al., 2016; Scherm et al., 2013). In addition, the soil-borne pathogen *G. tritici*, the causal agent of take-all disease, can infect several cereal crops though is primarily a problem in wheat, resulting in devastating yield losses of up to 60% in high disease years (McMillan et al., 2011). Take-all disease is the focus of this PhD project, hence a review of take-all disease is provided in section 1.8.

Emerging plant pathogens also pose significant threats to global wheat production. One of the greatest fungal threats to global wheat production is the recently emerging wheat blast disease. Disease symptoms are characterised by partially bleached spikes with shrivelled grain or no grain at all. The disease is caused by a wheat infecting pathotype of the *Magnaporthe oryzae* fungus (previously *Magnaporthe grisea*), the causal agent of devastating rice blast disease. In 2016, wheat blast disease was found in Bangladesh, the first Asian country to experience the disease. The epidemic covered a total of 15,000 hectares and resulted in yield losses of up to 100% as farmers were forced to burn their fields to contain the disease (Islam et al., 2016). Phylogenetic analysis revealed that the wheat blast fungus in Bangladesh was closely related to the pathotype in South America, indicating that it was likely imported to Bangladesh in infected grain. The disease was likely able to spread due to the similar climatic conditions in the two regions (Islam et al., 2019). Though Bangladesh is not a major producer of wheat, there are concerns that the disease could or has already spread to key wheat producing areas in Asia, such as China, India and Pakistan (Sadat & Choi, 2017). According to Carvajal-Yepes et al. (2020), ten countries with no previous history of wheat blast are still importing infected grain from South America, highlighting the need for a global surveillance system for crop diseases.

1.5 Plant pathogens and climate change

Human activities are now widely recognised to have significant impacts on global climate trends. Anthropogenic greenhouse gas emissions have increased since the pre-industrial era and have driven increased atmospheric concentrations of carbon dioxide, methane and nitrous oxide that are unparalleled in the last 800,000 years. The effects of these increases have been detected throughout the climate system and

are considered to be the dominant cause of global warming. According to the International Panel for Climate Change (IPCC), human-induced warming has reached approximately 1°C above pre-industrial levels (IPCC, 2021). At the same time, changes in extreme weather events have been observed since 1950. Many of these trends, including reduced cold temperature extremes, increased warm temperature extremes, an increase in high sea levels and heavy precipitation events have been linked to human activities. These trends are set to continue, with a “greater than 50% likelihood that global warming will reach or exceed 1.5°C in the near-term, even for the very low greenhouse gas emissions scenario” (IPCC, 2021).

Climatic changes have significant downstream effects in arable landscapes, though the effects can be difficult to predict. Crop plants may show improved growth under high CO_2 conditions, possibly leading to improved yields (Long et al., 2004). Conversely, increased temperatures and water-limitations significantly reduce yields in important crops, with wheat yields expected to decrease by 6% for every °C of temperature increase (Asseng et al., 2015). Furthermore, increased temperatures, particularly at night, along with higher CO_2 levels may result in reduced grain quality and protein content in wheat (Asseng et al., 2015; Impa et al., 2020). Climate change also has significant effects on plant pathogens both directly through environmental changes and indirectly through climate induced changes in the host. Direct impacts include changes in water quality and availability, changes in farming practices, soil properties, nutrient cycling and atmospheric CO_2 levels (Chakraborty & Newton, 2011). Indirectly, increased plant growth could lead to denser canopies, providing humid conditions for pathogens to thrive. In some cases, increased CO_2 levels may also result in increased pathogen fecundity and population size, which in combination with a humid microclimate could accelerate pathogen evolution (Chakraborty & Datta, 2003).

CO_2 levels can also affect the ability of the host to respond to pathogen attack. Generally, plant defences against foliar biotrophs are regulated by salicylic acid (SA) signalling, whereas defence against foliar necrotrophs is mediated by jasmonic acid (JA) signalling. In a study investigating *Arabidopsis thaliana* responses to pathogen attack under current and future CO_2 conditions, Zhou et al. (2019) demonstrated that CO_2 levels affect the balance between SA and JA dependent defences. The SA-responsive marker genes ICS1 and FRK1 showed lower expression under high CO_2

conditions, resulting in reduced resistance to the hemibiotrophic leaf pathogen *Pseudomonas syringae* pv. tomato, but increased resistance to the necrotrophic leaf pathogen *Botrytis cinerea*. The opposite was found when *Arabidopsis* was grown under low CO_2 (Zhou et al., 2019). The availability of nutrients such as potassium is key for the functioning of the jasmonate pathway and therefore potassium availability is also likely to influence plant responses to necrotrophic pathogens under climate change (Chakraborty & Newton, 2011).

Delgado-Baquerizo et al. (2020) conducted a global field survey spanning 235 natural ecosystems from six continents and a 9-year warming field experiment to evaluate how temperature regulates the relative abundance of potential soil-borne plant pathogens. The study found that mean annual temperature had the strongest and most significant association with the relative abundance of soil pathogens globally. The findings indicate that the proportion of potential soil-borne pathogens will likely increase regardless of other climatic factors or changes in land-use. In a study of *Fusarium oxysporum* infected rocket plants (*Eruca sativa*) under simulated conditions, elevated CO_2 levels and higher temperatures resulted in a significant increase in disease incidence, which was also associated with altered root exudate profiles (Chitarra et al., 2015). You et al. (2017) used a comprehensive modelling approach to demonstrate that temperature, soil type, moisture, nutrients and host cultivar had a significant and complex effect on the severity of *Pythium* damping-off and root disease in the subterranean clover (*Trifolium subterraneum)*, a critical pasture legume. However, the accurate modelling of plant pathogens under various climate change scenarios presents serious challenges. For instance, the effects of climate change on host resistance against pathogens, pathogen insensitivity to fungicides and the genetic adaptation of pathogens to changing climates has received little attention, making future trends difficult to predict (Newbery et al., 2016). Nevertheless, despite the mounting evidence, the impact of climate change on plant pathogens has largely been ignored in climatic models (Ireland & Kriticos, 2019).

1.6 Genetic and genomic resources for improved disease resistance in wheat

Crop disease management has largely been achieved through cultural practices, fungicide applications and traditional resistance breeding (Sánchez-Martín & Keller,

2019). Historic seed collections, such as those held at the John Innes Centre Germplasm Resources Unit (https://www.jic.ac.uk/research-impact/germplasm-resource-unit/) have preserved vital biodiversity. By allowing researchers to access these collections, germplasm can be screened for many traits, allowing the identification of new sources of disease resistance as well as abiotic stresses such as drought and salinity. For example, the Watkins collection of bread wheat which was assembled in 1928 contains 1200 wheat cultivars from 32 countries and has proven to be a valuable source of diversity for resistance breeding (Ajaz et al., 2021). Improved breeding technologies such as genomic selection, marker-assisted selection, and speed breeding are helping to unlock the diversity in these wheat collections (Tadesse et al., 2019). Hybrid wheats, generated by a cross between two pure lines, are becoming increasingly attractive for many UK growers due to the better developed root system, increased tillering, good disease resistance and early maturity of hybrids. These superior traits can be attributed to hybrid vigour or heterosis which is expressed as the plant grows. Hybrid breeding programmes are therefore likely to play an important role in future disease resistance (Gupta et al., 2019).

Recent advances in next generation sequencing have allowed for complete genome sequencing and genome annotation of key crops such as rice (Ren et al., 2019), maize (Jiao et al., 2017) and barley (Mascher et al., 2017), paving the way for new functional genomics approaches directed towards crop improvement. However, the genome sequencing of wheat lagged behind due to the challenges associated with assembling a hexaploid genome that is five times as large as the human genome, containing >85% repetitive DNA (Appels et al., 2018). The International Wheat Genome Sequencing Consortium (IWGSC) was set up in 2005 to tackle this challenge. Due to the polyploid nature of wheat, all 21 chromosomes of the cultivar Chinese Spring were separated by flow cytometry for subsequent preparation of bacterial artificial chromosome (BAC) libraries and physical maps. This was a painstaking task but resulted in the successful sequencing of chromosome 3B in 2014, despite its large size (1 Gbp). The resulting assembly was a huge improvement on the whole-genome shotgun assemblies that had previously been made available (Choulet et al., 2014).

Since then, dramatic improvements to genome sequencing technologies have been made through the integration of long-read sequencing technologies, chromosome contact maps (Hi-C), and improved computational biology methods for chromosome

assembly in the presence of a high frequency of repetitive DNA. As a result, the IWGSC released a fully annotated reference genome sequence in 2018 for the cultivar Chinese Spring (Appels et al., 2018). The quality of this genome was superior to previous attempts, with 90% of the assembly represented in scaffolds of at least 4.1 Mb, providing breeders with a valuable resource for crop improvement (Keller et al., 2018). A further ten wheat cultivars are currently being sequenced by IWGSC to the same standard as Chinese Spring. The combined genomes will form the wheat pangenome, allowing for key comparative analysis between genotypes and the characterisation of core and dispensable regions of the genome (http://www.10wheatgenomes.com).

Whole-genome sequences are an important step towards the development of disease-resistant cultivars. The cultivars could provide multiple benefits through the direct reduction of yield losses, by providing an environmentally friendly alternative to fungicide use and by allowing the growth of crops in areas previously limited by high disease pressures. Furthermore, disease-resistant cultivars are unlikely to result in additional costs for farmers which could be especially important in regions where low-income farmers cannot afford chemical controls (Sánchez-Martín & Keller, 2019). The availability of high-quality chromosome sequences allows for faster and more straightforward map-based cloning of disease-resistance genes. In addition, the identification of new resistance genes can be rapidly sped up by comparing sequences with already known disease-resistance genes. Many resistance (R) genes that are effective against biotrophic fungal species encode proteins that contain a nucleotide-binding site (NBS) and leucine-rich repeats (LRRs) (NLRs) type. NLR sequences may be easily detected based on the presence of conserved motifs. Using this technique, 3,400 NLR loci in the Chinese Spring genome were identified, providing potential candidates for new disease-resistance genes (Steuernagel et al., 2016). Finally, orthologous genes can have a conserved function in disease resistance across different species. Thus, the availability of reference genomes greatly simplifies the identification of resistance genes already known in other cereal crops. An example of this is the identification of the mildew A (*Mla*) locus from barley that confers resistance to barley powdery mildew disease caused by the fungal pathogen *Blumeria graminis* f. sp*. hordei.* Following its identification, orthologous genes of *Mla* were found in wheat, conferring resistance to powdery mildew (*B. graminis* f. sp. *tritici)* and stem rust (*P.*

graminis f. sp. *tritici*) (Jordan et al., 2011; Lu et al., 2016; Periyannan et al., 2013; Steuernagel et al., 2017).

However, many resistance genes may be specific to certain cultivars or landraces and therefore may be absent from reference genomes such as Chinese Spring. Therefore, breeders must take advantage of the genetic diversity in gene banks such as those held at the International Wheat and Maize Improvement Center (CIMMYT), where more than 1,000 synthetic wheat lines have been produced from diverse accessions of *Aegilops tauschii,* the D genome donor species (Dreisigacker et al., 2008). To enable genotyping of cultivars in large collections such as this, single nucleotide polymorphism (SNP) arrays have been developed. For example, the wheat breeders array based at Bristol University contains over 35, 000 SNP markers which are publicly available online for use by the global wheat community at 'CerealsDB' (https://www.cerealsdb.uk.net/cerealgenomics/CerealsDB/indexNEW.php) (Allen et al., 2017).

The increasing pace of disease-resistance gene identification in the host, when combined with improved genetic understanding of key crop pathogens, allows for targeted manipulation of wheat-pathogen interactions. The complete genomes of several major fungal wheat pathogens such as *Zymoseptoria tritici* (Goodwin et al., 2011), wheat stem rust (*Puccinia graminis* f. sp. *tritici*) (Duplessis et al., 2011), powdery mildew (*Blumeria graminis* f. sp. *tritici*) (Wicker et al., 2013) and wheat leaf rust (*Puccinia triticina*) (Kiran et al., 2016) have been sequenced. Whole genome analysis has resulted in the identification of pathogenicity factors such as the avirulence (*Avr*) genes *AvrSr35* and *AvrSr50* in wheat stem rust (Chen et al., 2017; Salcedo et al., 2017), and *Avrstb6* in *Zymoseptoria* which complemented the identification of the corresponding resistance gene Stb6 (Saintenac et al., 2018; Zhong et al., 2017). The identification of genes encoding pathogenicity factors allows for the development of specific markers which could determine the presence and evolution of pathogenicity factors in specific pathogen populations in different geographical locations (Keller et al., 2018).

Pathogen-informed breeding strategies will play an increasing role in future disease control. Although only approximately 6% of known disease resistance genes in wheat have currently been cloned, the cloning of disease resistance genes, which would

require a global effort, could allow the development of molecular markers for breeding (Keller et al., 2018). Breeders could then stack the appropriate resistance genes based on the pathogen species and strain/race (with already identified pathogenicity factors) known to be problematic in the area. However, plant pathogens have haploid genomes and can produce multiple generations in a single growing season. As a result, plant pathogens are fast evolving and therefore the application of a single resistant gene may only provide a transient solution. Gene cassettes, where several disease-resistance genes are cloned into the same vector and transformed together into the chosen cultivar, could be used to provide longer-lasting resistance. In addition, genome editing by CRISPR/CAS9 could be used to achieve targeted knock-outs of susceptibility genes (Zhang et al., 2019). However, the downstream effects of many of these proposed/completed gene modification projects remains unknown. Developing resistance to one pathogen may negatively impact other associations with the microbiome by increasing general plant immunity (Plett et al., 2016), or reducing the ability for plants to communicate using root exudates (Pérez-Jaramillo et al., 2016; Wong & Plett, 2019).

1.7 The potential of biocontrol strategies against plant pathogens

The application of synthetic fungicides is one of the most common strategies used to control plant pathogens. As such, modern farming systems are heavily reliant on fungicide additions and chemical usage is set to increase as the demand for food continues to grow. However, the long-term use of fungicides has severe consequences for the environment, with fungicide usage implicated in decreasing soil health, increasing water pollution and causing damage to non-target organisms (Zubrod et al., 2019). Consequently, tougher EU restrictions have resulted in the ongoing banning of fungicides with different modes of action. Furthermore, the increased prevalence of fungicide resistance in fungal pathogens threatens food security and in some cases has severe clinical implications as naturally occurring pathogens have acquired resistance to a wide range of chemistries (Fisher et al., 2018). These problems significantly influence public perceptions, as highlighted by the growing consumer demand for eco-friendly, sustainable, and safe commodities. As a result, efforts are being made to find alternative control strategies against plant pathogens.

Biological control, or biocontrol, is the suppression of plant pests or diseases by other living organisms. The use of biocontrol agents to protect important crop plants dates back centuries, with the earliest reports (c.304 AD) attributed to the biocontrol of citrus fruit insect pests in China. Disease control was achieved by hanging the nests of arboreal ants (*Oecophylla smaragdina)* onto the affected trees (Peng, 1983). However, the most common biocontrol agents against plant pathogens are fungal or bacterial species, which can inhibit plant pathogens in a range of different ways. Biocontrol agents can function by direct antagonism, for example through the production of antimicrobial compounds, by the production of antimicrobial peptides (Fathima Mirza et al., 2018; Tong et al., 2020), killer toxins (De Souza Cabral et al., 2009; Ferraz et al., 2019) or killer toxin-like chitinases produced by filamentous fungi (Tzelepis & Karlsson, 2019). Some fungal biocontrol agents can also inhibit fungal plant pathogens by direct hyphal interference or mycoparasitism. *Trichoderma* species are among the most studied mycoparasites. These biocontrol agents, often used commercially, have a wide range of fungal hosts including several important plant pathogens. The hyphae of antagonistic *Trichoderma* species grow chemotrophically towards their fungal prey and produce specialised structures for hyphal attachment and infection. Following successful attachment by hyphal coiling, the fungus produces an armoury of cell wall degrading enzymes (CWDEs) and antimicrobial secondary metabolites (Karlsson et al., 2017).

Fungal and bacterial biocontrol agents are also known to produce volatile organic compounds (VOCs) capable of inhibiting various plant pathogens. Some, but not all *Trichoderma* species are able to produce the linoleic acid derived VOC 6-pentyl-α-pyrone, (6-PP), which possesses both antifungal and growth-promoting abilities (Karlsson et al., 2017). The VOC 6-PP is also able to inhibit mycotoxin production in Fusarium species, through an unknown mechanism (Cooney et al., 2001). The bacteria *Burkholderia gladioli* pv. *agaricicola* was shown to produce the VOC limonene which was capable of inhibiting the fungal growth of *Fusarium oxysporum* and *Rhizoctonia solani* (Elshafie et al., 2012). In addition to pathogen inhibition and plant growth promotion, microbial VOCs have been shown to induce resistance mechanisms in plants, protecting them against infection by pathogens (Tilocca et al., 2020). The growing potential of microbial and plant VOCs in agriculture has been reviewed by Brilli et al. (2019).

Certain bacteria and fungi can protect distal regions of the plant from a broad range of plant diseases via induced plant resistance. Similarly, local plant infection by pathogens can result in uninfected regions becoming more resistant to disease. Both scenarios are forms of induced resistance, a phenomenon which is characterised by the activation of latent defence pathways which are subsequently expressed upon future challenge by a pathogen. Induced resistance can also lead to the priming of defence related genes or pathways, resulting in stronger elicitation of defences following pathogen attack (Goellner & Conrath, 2008).

The two main forms of induced resistance, induced systemic resistance (ISR) and systemic acquired resistance (SAR), can be distinguished by the type of elicitors involved and signalling pathways which are induced. SAR is generally triggered by pathogen infection via the plant detection of both MAMPs and DAMPs. However, SAR can also be triggered by exposing the plant to avirulent and non-pathogenic microbes (Choudhary et al., 2007). The key characteristic of SAR is the dependence on salicylic acid (SA) signalling, requiring crucial interaction with the NPR1 protein. The onset of SAR in systemic tissues may also be dependent on flavin-dependent-monooxygenase 1 (FMO1), which is proposed to play a role in long-distance signalling (Pieterse et al., 2014).

Conversely, ISR is generally induced by beneficial microbes via the plant detection of MAMPs and results in the priming of jasmonic acid (JA) and ethylene (ET) responsive genes. In Arabidopsis, the root-specific transcription factor MYB72 has been implicated during the onset of ISR and is also associated with the iron-deficiency (Pescador et al., 2022; Segarra et al., 2009). Additionally, biocontrol species may enhance plant defence against pathogens through cytological changes such as the increased deposition of cutin and suberin in the plant apoplast, or the lignification of plant cell walls, which act as physical barriers against future pathogen attack (Pollard et al., 2008). However, there is a trade-off between plant immunity and plant growth, posing the risk that ISR by biocontrol agents could compromise normal plant growth (Eichmann & Schäfer, 2015).

Successful biocontrol agents such as *Trichoderma* often employ more than one mechanism to inhibit plant pathogens. The root endophytic fungi *Serendipita indica* and *Serendipita vermifera* from the order Sebacinales are receiving growing scientific

attention as potential biocontrol agents due to their diverse mechanisms of disease control. In a unique multipartite study, split-root systems were used to investigate the transcriptomes of *S. vermifera*, the plant host barley, and the root and foliar pathogen *Bipolaris sorokiniana.* Sarkar et al. (2019) demonstrated that *S. vermifera* successfully controlled the pathogen even prior to host colonisation. Control was attributed to mycoparasitism, the direct induction of stress related genes and the repression of effector genes in the pathogen. *S. vermifera* could therefore be a powerful biocontrol agent of both root and foliar diseases.

Several hurdles have prevented the widespread use of biocontrol against plant pathogens. The successful application of live microbial agents is often prevented by the longevity of seed dressings (Rocha et al., 2019), the viability of artificially introduced inoculum, the impact on the existing microbial community, and their cost-use efficiency (Mauch-Mani et al., 2019). EU registration procedures exist for microorganisms, semiochemicals and botanicals, which prevent their immediate market introduction. Consequently, biocontrol makes up 1% of agricultural chemical sales in the US, and even less in the EU. According to Ravensberg (2015), the Access and Benefit Sharing (ABS) of genetic resources and the "Nagoya Protocol" (Convention of Biological Diversity 1992) makes exploration for new beneficial microbes an administrative burden and therefore threatens new product development. Nevertheless, the development of biocontrol agents remains a highly promising and environmentally friendly solution for the control of plant pathogens in agroecosystems.

1.8 Take-all disease of wheat: a global problem

A detailed review of take-all disease was written as a team and was published in Trends in Plant Science in 2021. The following introduction highlights several key themes of the review which are relevant for this PhD thesis. For further details please see:

Palma-Guerrero, J., Chancellor, T., Spong, J., Canning, G., Hammond, J., McMillan, V. E., & Hammond-Kosack, K. E. (2021). Take-All Disease: New Insights into an Important Wheat Root Pathogen. Trends in Plant Science, 26(8), 836–848. https://doi.org/10.1016/j.tplants.2021.02.009

1.8.1 Introduction

Take-all disease, caused by the soil-borne ascomycete fungus *Gaeumannomyces tritici* (previously named *Ophiolobus graminis*) (Walker, 1981), was first reported in Australia in the nineteenth century and is now thought to be one of the important root diseases of wheat worldwide (Freeman & Ward, 2004). The ascomycete fungus invades the roots of wheat and several other cereals such as barley, rye, triticale, and other related grasses, resulting in characteristic patches of disease in field settings (Cook, 2003) (figure 1.5). Take-all disease has been documented in all temperate wheat growing regions around the world, as well as several sub-tropical and even arid areas, where the disease is referred to as “dryland take-all” (Hornby, 1998). Despite the importance of take-all disease, a global (or even regional) monitoring system does not exist, hence accurate and up-to-date disease statistics are sorely lacking. Nevertheless, yield losses of up to 60% have been reported in the UK (McMillan et al., 2011), but are typically in the range of 5-20% (https://ahdb.org.uk/take-all). The disease is estimated to cost UK farmers £60 million a year (Bateman et al., 2006), however this figure is outdated and as discussed previously, may increase given recent modelling predictions (Delgado-Baquerizo et al., 2020).



Figure 1.5 Characteristic take-all disease symptoms. A. Take-all disease patch in the field. B. Adult wheat plant with severely infected roots. Image credits: Rothamsted Research Visual Communications Unit. C: Grain harvested from healthy and take-all diseased plants. Reproduced from Bateman et al., (2006). See previous page.

1.8.2 Taxonomy of the *Magnaporthaceae* family

G. tritici belongs to the family *Magnaporthaceae* in the order Magnaporthales. The *Magnaporthaceae* family contains several other important pathogens of economic significance. For example, *Magnaporthe poae* infects the roots and crowns of several turfgrasses used in golf courses and sports fields, while *Magnaporthe oryzae* causes devastating rice blast disease and is an important model organism for the study of fungal disease in plants (Illana et al., 2013). Previously, the *Gaeumannomyces* genus was reported to contain seven known species: *G. graminis, G. caricis, G. cylindrosporus, G. incrustans, G. medullaris, G. amomi* and *G. wongoonoo* (Freeman & Ward, 2004). Within the *G. graminis* species, there were four different varieties: var. *tritici*, var. *avenae*, var. *graminis* and var. *maydis*, which have since been assigned species status. Hernández-Restrepo et al. (2016) used multi-gene analysis from ITS, LSU, rbp1 and tef1 sequences with morphological analysis to delimit 19 species in the *Gaeumannomyces*, 12 of which were proposed as new species, and two as new combinations. The *Gaeumannomyces* genus is now split into four main clades, the tritici clade, the graminis clade, the oryzinus clade and the radicicola clade (table 1.1).

Species	Previous classifications	Host range	Clade
Gaeumannomyces tritici	*Gaeumannomyces graminis var tritici*	Mostly wheat but can also infect rye, triticale, and barley, as well as other cereals and grasses	Tritici clade
Gaeumannomyces avenae	*Gaeumannomyces graminis var avenae*	Mostly oats but can also infect turfgrasses, wheat, rye, and barley	Tritici clade
Gaeumannomyces oryzinus	*Gaeumannomyces graminis var maydis*	Mostly maize, but also *Sorghum* and other cereals	Oryzinus clade
Gaeumannomyces graminis	*Gaeumannomyces graminis var graminis*	Rice and turfgrasses, as well as a weak pathogen on cereals, grasses, and soybean	Graminis clade

Table 1.1 New taxonomic classification of the species within the *Gaeumannomyces* family according to Hernández-Restrepo et al. (2016). Reproduced from Palma-Guerrero et al. (2021) https://doi.org/10.1016/j.tplants.2021.02.009 under the Creative Commons Attribution License (Creative Commons 4.0).

1.8.3 Take-all infection cycle

During the period between crops, *G. tritici* mycelium survive on decaying plant debris in the soil and may also persist by infecting the roots of volunteer species such as grass weeds (figure 1.6; stage 1). Take-all infection typically occurs in two phases. The primary infection phase occurs in autumn from residual inoculum present in crop debris in the soil. Inoculum levels are usually low during this stage and depend largely on the previous crop grown and on the soil type, with lighter soils being more conducive to hyphal growth (Garrett, 1936). However, this inoculum is sufficient to initiate seedling infection of a susceptible crop when roots come into direct contact with the mycelium (figure 1.6; stage 2).

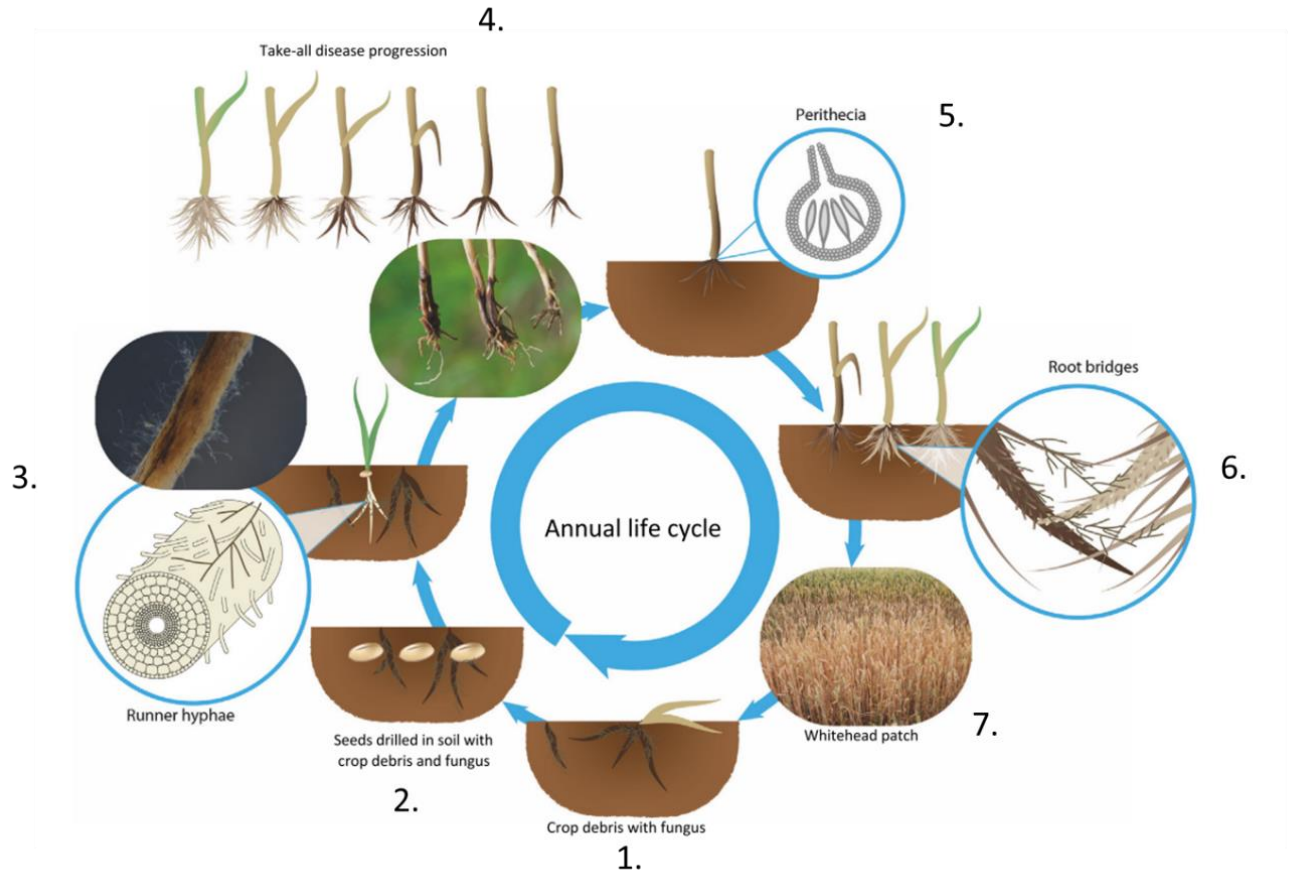


Figure 1.6 *G. tritici* life cycle within a crop season. Adapted from Palma-Guerrero et al., (2021) https://doi.org/10.1016/j.tplants.2021.02.009 under the Creative Commons Attribution License (Creative Commons 4.0).

G. tritici mycelium consists of thick-walled melanised macrohyphae and hyaline, thin-walled hyphae. The hyaline hyphae grow longitudinally across the root surface (figure

1.6; stage 3) and penetrate the epidermal cell wall at various positions in the root via the formation of appressorium-like swellings known as hyphopodia (Asher & Shipton, 1981). The fungus proceeds from cell to cell in its hyaline form through the production of penetration pegs which are thought to exude an armoury of cell wall degrading enzymes. In response to penetration, the plant host produces lignitubers which enclose the infection hyphae. However, the fungus is able to overcome this physiological defence, possibly through the production of 1,3-β -glucanases (Yu et al., 2010). *G. tritici* can successfully penetrate the endodermis and infect the central stele, where the fungus causes significant and irreversible damage to the vascular tissue, resulting in the formation of characteristic black necrotic lesions (figure 1.6; stage 4).

The fungus also has a sexual cycle, producing sexual structures known as perithecia on stem bases, plant stubble and even on roots under high disease pressures (figure 1.7). Perithecia contain unitunicate asci and ascospores which are released from the ostiole when conditions are favourable (figure 1.6; stage 5). However, the importance of the sexual cycle and the role of ascopores on take-all disease incidence and severity remains unknown. *G. tritici* is referred to in the literature as homothallic, although the specific mating type loci have not yet been identified. Laboratory experiments have revealed that the fungus is also capable of outcrossing (Pilgeram & Henson, 1992), though it is not clear to what extent outcrossing affects the genetic diversity of *G. tritici* populations in the field.

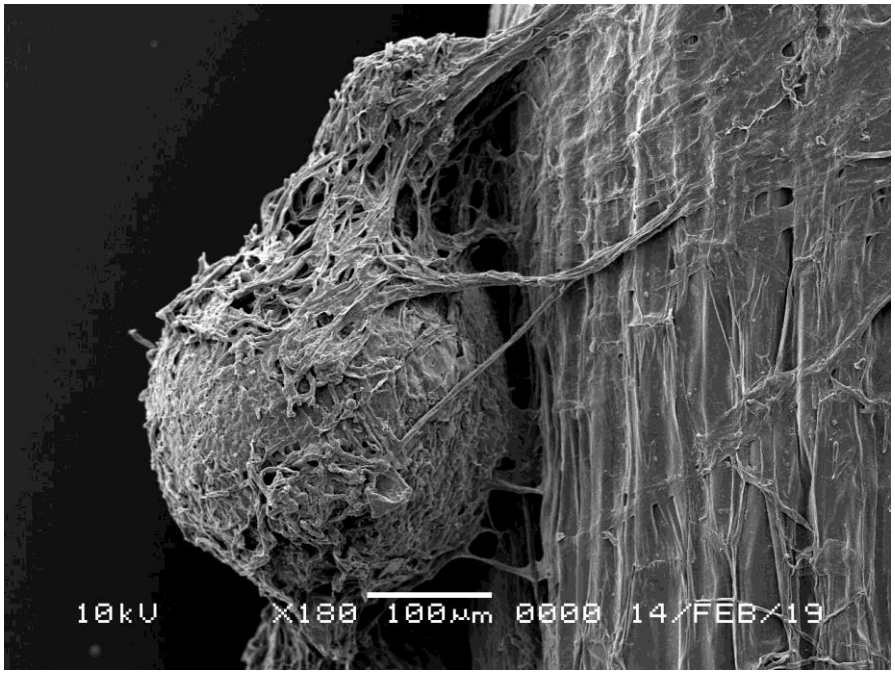


Figure 1.7 Scanning electron micrograph of a developing *G. tritici* perithecium on an infected wheat root. See previous page.

Secondary infection occurs during the spring and summer when the disease spreads from infected seedling roots to developing crown roots. The fungus is then able to infect neighbouring plants through root-to-root contact (figure 1.6; stage 6). The host root system is no longer able to acquire water and nutrients efficiently, resulting in reductions in plant stature, reduced tillering, premature ripening of the crop, and significant reductions in grain yield and quality (figure 1.6; stage 7). In addition, large amounts of unused nitrogen fertiliser are left in the soil, resulting in nitrate residues which can cause further environmental damage through leaching (Macdonald & Gutteridge, 2012). Increased levels of nitrogen in the soil may be converted to nitrous oxide by microbes, potentially contributing to greenhouse gas emissions (Hughes et al., 2011).

1.8.4 Detection and quantification of take-all disease

Various semi-selective media have proven useful for the identification of *G. tritici*, however these methods are not effective when other *Magnaporthaceae* fungi are present (Duffy & Weller, 1994). Molecular methods for the identification and quantification of *G. tritici* in the soil and plant tissues have since been developed and involve the use of polymerase chain reaction (PCR) targeting Mitochondrial DNA and nuclear rDNA (ITS) sequences (Bithell et al., 2012; McCartney et al., 2003). These tests can be helpful when trying to forecast future disease risk. A study by Keenan et al. (2015) successfully used quantitative PCR (qPCR) to detect *G. tritici* in symptomatic and non-symptomatic wheat roots. However, molecular methods such as qPCR are often time-consuming, laborious and do not distinguish dead mycelium from infective inoculum. Molecular techniques are therefore not appropriate for screening large numbers of field-derived plant samples (Sankaran et al., 2010).

Molecular methods and rye infectivity tests have been used for the identification of different groups within the *G. tritici* species. Two distinct genetic groups have been consistently identified by several teams. Interestingly, phylogenetic analysis demonstrated that the molecular markers used by different teams were highly congruent, confirming that two genetically distinct groups of *G. tritici* exist globally and this distinction may be associated with the ability to infect rye (Daval et al., 2010) (table

1.2). Some tentative associations between genetic type and disease severity in wheat have been made (Bateman et al., 1997; Lebreton et al., 2004), however this relationship was not consistent in field trials (Freeman et al., 2005).

Table 1.2 Differing techniques used to discriminate between two corresponding genetic groups within the *G. tritici* species, as identified by Daval et al. (2010). RAPD=Random Amplified Polymorphic DNA, AFLP=Amplified Fragment Length Polymorphism, rDNA=ribosomal DNA.

G. tritici genetic group		Discrimination method	Origin of isolates	Reference
A	B	PCR assay based on polymorphisms in nuclear rDNA	UK	Freeman et al. (2005)
G_2	G_1	RAPD and AFLP fingerprinting	France	Lebreton et al. (2004)
T1	T2	RFLP analysis using mitochondrial rDNA probe	UK	Bateman et al. (1997)
N	R	Ability of isolate to infect rye	Worldwide	Bryan et al. (1995)

Take-all disease severity is commonly assessed by eye, an often time-consuming and subjective process. Non-destructive, high-throughput screening using imaging technology could prove a useful alternative. For such methods to be successful, tests should be rapid, pathogen specific, and sensitive enough to allow early detection of disease symptoms (Sankaran et al., 2010). Graeff et al (2006) used a digital analyser to measure the leaf reflectance of plants that had been inoculated either with the powdery mildew fungus or the take-all fungus. The authors concluded that of the spectra evaluated, the range 490_{780}NM showed the most sensitive response to damage caused by these pathogenic fungi. Such imaging techniques could be applied to precision farming methods to allow targeted fungicide application. However, further tests are needed to discriminate between damage caused by the fungi, and damage caused by other abiotic and biotic stresses. So far, no published studies have attempted to quantify take-all disease by imaging the roots of infected plants.

1.8.5 Take-all build up (TAB), decline (TAD) and the soil microbiome

Take-all disease levels in the roots are generally low during the first wheat crop, though cultivar genotype plays a major role in defining levels of *G. tritici* in the soil, subsequently influencing disease levels and grain yields in the following wheat crop (McMillan et al., 2011). This genetic characteristic is known as the take-all build-up (TAB) trait and has been explored in 71 modern UK elite wheat cultivars under a first wheat scenario (McMillan et al., 2018). Soil cores taken from the field plots revealed a significant cultivar x site interaction which suggests that other environmental, microbial or agronomic factors can influence the TAB trait. However, several cultivars demonstrated a consistent reduction in TAB across all field sites, highlighting that some cultivars can limit *G. tritici* levels in the soil despite large variations in environmental conditions. These so-called lowTAB cultivars are already being exploited by farmers, despite the mechanism(s) of TAB being unknown (figure 1.8).

Several studies have also highlighted the importance of wheat genotype on the microbial populations associated with *G. tritici* (Mauchline & Malone, 2017). Analysis of the genetic and phenotypic diversity of *Pseudomonas fluorescens* (a bacterial antagonist of *G. tritici*) in two consecutive wheat crops revealed that much like *G. tritici,* there was a significant effect of the first wheat genotype on *Pseudomonas* populations in the rhizosphere. Wheat cultivars which supported high *Pseudomonas* genotypic richness were associated with increased take-all disease severity and lower yields in the following year (Mauchline et al., 2015). Synthetic community studies revealed that an increase in *Pseudomonas* diversity resulted in reduced *G. tritici* control due to increased antagonism between different *Pseudomonas* genotypes (Mehrabi et al., 2016). Furthermore, previous studies have shown that *Pseudomonas* root colonisation and production of the antifungal metabolite 2,4-Diacetylephloroglucinol (DAPG) is strongly influenced by host genotype, adding further complexity to this tripartite interaction (Okubara et al., 2004; Okubara & Bonsall, 2008).

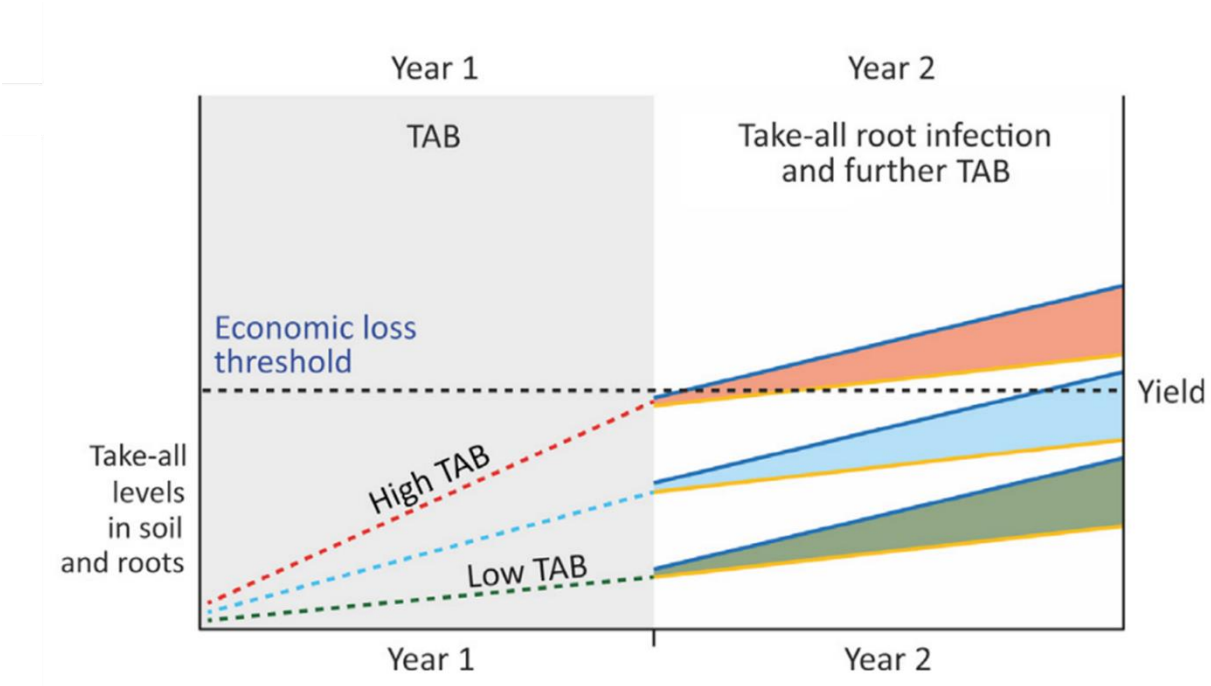


Figure 1.8 The 2-year, synergistic genetic traits concept to reduce take-all root disease in wheat crops. In year 1, the growing of low, intermediate or high take-all inoculum build-up (TAB) cultivars (respectively, green, blue, and red broken lines) leads to different levels post-harvest of take-all fungal mycelium left in the rhizosphere, even though the roots of the first wheat crop remain take-all disease free. In year 2, when a partially resistant wheat cultivar is grown (orange solid line), the disease incidence and severity is lower than when a fully susceptible wheat cultivar is grown (blue solid line). In fields where a high TAB situation has developed in year 1, the economic threshold for severe yield losses is likely to be reached irrespective of second wheat choice. Figure and figure legend reproduced from Palma-Guerrero et al., (2021) https://doi.org/10.1016/j.tplants.2021.02.009 under the Creative Commons Attribution License (Creative Commons 4.0).

Disease severity is also influenced by a natural phenomenon known as take-all decline (TAD) (figure 1.9). TAD is the spontaneous reduction in the incidence and severity of take-all disease and the subsequent increase in wheat yield following continuous monoculture, but only after suffering from severe take-all disease levels in the early years (Weller et al., 2002). Interestingly, despite a decline in disease symptoms in the host, pathogen inoculum levels in the soil can remain unchanged (Durán et al., 2018). TAD is a worldwide phenomenon and farmers can exploit TAD to reduce take-all in crop monocultures. For example, TAD is estimated to protect around 0.8 million ha of wheat in the Pacific Northwest of the USA. As a result, wheat crops in this area suffer

little take-all damage (Lugtenberg, 2014). However, TAD is heavily influenced by environmental factors and as a result is often field-specific (Kwak & Weller, 2013).

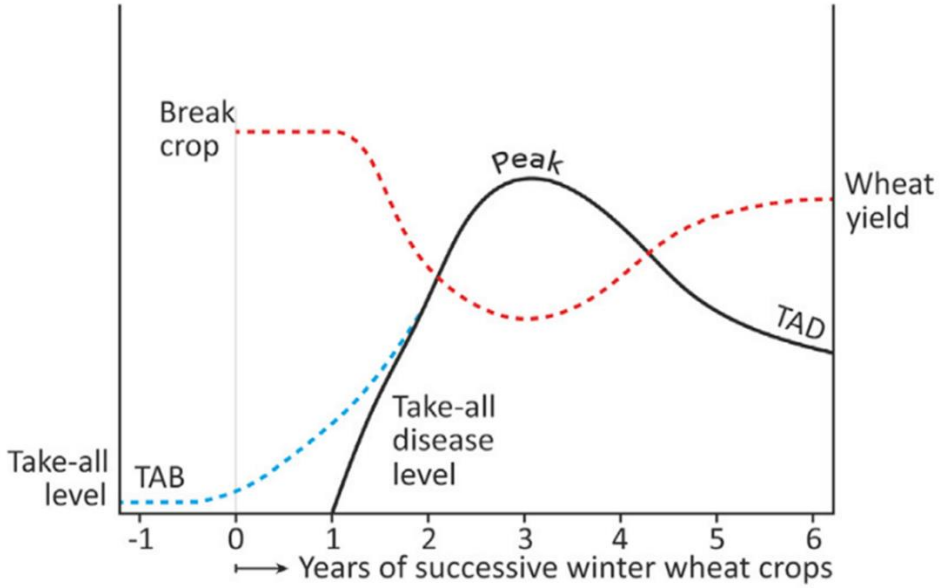


Figure 1.9 Take-all levels during successive years of wheat cropping. The first wheat crop after a rotation break (i.e., non-cereal crop or oats) has low levels of take-all inoculum build-up (TAB) in the rhizosphere and has low take-all disease levels. In subsequent years, take-all disease in the wheat roots increases and peaks during years 2–4 (depending on local conditions) and then declines. Figure and figure legend reproduced from Palma-Guerrero et al., (2021) https://doi.org/10.1016/j.tplants.2021.02.009 under the Creative Commons Attribution License (Creative Commons 4.0).

The majority of TAD studies have focused on the investigation of antagonistic *Pseudomonas* spp., many of which produce antimicrobial compounds which are thought to play a significant role in TAD (Kwak & Weller, 2013). The metabolite 2,4-Diacetylephloroglucinol (DAPG) is a broad-spectrum antimicrobial which has antibacterial, antifungal, antiviral and antihelminthic activity. Genetic and physiological studies in yeast (*Saccharomyces cerevisiae*) revealed that DAPG alters the proton gradient across the mitochondrial membrane, uncoupling respiration and ATP synthesis and resulting in growth inhibition (Troppens et al., 2013). Accordlingly, DAPG treatment of *G. tritici* leads to upregulated V-type proton ATPase activity. DAPG significantly reduces *G. tritici* mycelial growth at concentrations above 5 µg/ml, with complete inhibition achieved at 20 µg/ml (Kwon et al., 2018). However, such

concentrations are unlikely to be achieved in the rhizosphere, especially considering that the half-life of 2,4-DAPG in the rhizosphere is estimated to be 0.25 days (Kwak et al., 2012). Furthermore, natural variation in isolate sensitivity to DAPG exists, though insensitivity is unlikely to increase during extended wheat cropping (Kwak et al., 2009). The role of other bacterial species is less well known, though it is clear other species could play an important part in TAD (Weller et al., 2002).

Recent studies have suggested that endophytic bacteria may be as important as rhizobacterial communities in TAD soils. In a comparative study of suppressive and conducive soils, Durán et al. (2018) found that rhizosphere communities showed little variation between soil types. In contrast, endosphere populations differed significantly between conducive and suppressive soils. The functional importance of microbial endosphere communities was further highlighted by Carrión et al., (2019), who suggested that endosphere bacteria may act as a second line-of defence to pathogen invasion. This additional barrier could perhaps explain why pathogen biomass can remain unchanged in suppressive soils, despite reduced disease symptoms. There is also some evidence that wheat cultivars differ in their ability to support the suppression of take-all when grown in a TAD soil (Yang et al., 2018), highlighting that TAD likely involves complex interactions between the take-all fungus, wheat host genotype, and endosphere and rhizosphere microbes.

The studies discussed here highlight the important role of the soil microbiome for the control of root infecting pathogens, both directly through microbial antagonism and indirectly through changes in microbial community structures. Take-all disease represents an important system for the study of the soil microbiome, the careful manipulation of which, could have significant impacts on pathogen populations.

1.8.6 Molecular understanding of the wheat-*G. tritici* interaction

The molecular understanding of below-ground plant-microbe interactions has lagged behind that of above-ground interactions. This is largely due to the inaccessibility of the rhizosphere and in the case of *G. tritici*, the difficulties in generating and maintaining stable transformants. Despite these challenges, our understanding of the *G. tritici* pathosystem has drastically improved in recent years due to advances in sequencing technologies (Palma-Guerrero et al., 2021).

The first analysis of the *G. tritici* transcriptome was conducted in 2004 and relied on suppression subtractive hybridisation (SSH) and expressed sequence tag analysis (EST) of an unsubtracted cDNA library to analyse gene expression in early stages of wheat infection (Guilleroux & Osbourn, 2004). The SSH approach failed to pick up sequences of fungal origin, but EST analysis of cDNA clones successfully identified fungal sequences implicated in host colonisation. These included several proteases such as polyketide synthases, G proteins and β-1,3-glucanases, all of which have been linked with pathogenicity in other fungi. *G. tritici* gene expression was also analysed by RT-qPCR in a tripartite system with the *Pseudomonas fluorescens* Pf29Arp biocontrol strain and the wheat host (Daval et al., 2011). The study revealed that during the early stages of infection, several fungal genes were down-regulated by Pf29Arp, including two laccases, a β-1,3-exoglucanase and a mitogen-activated protein kinase. The study represents the first evidence of a biocontrol agent altering pathogenesis-related gene expression in *G. tritici.*

In 2011, the Broad Institute released the Magnaporthe comparative genomics database, which included a draft *G. tritici* genome, paving the way for the first genomic studies of the fungus (https://www.broadinstitute.org). Li et al. (2014) used simple sequence repeat (SSR) markers to analyse the pattern of SSRs in the *G. tritici* genome compared with other Magnaporthe species. The analysis revealed that the genome was rich in SSRs, with mononucleotides representing the most common motifs. Primers designed to target 8 polymorphic SSR regions were subsequently used to analyse 116 *G. tritici* isolates in China, revealing a high level of genetic diversity. An improved *G. tritici* genome was published by Okagaki et al. in 2015 along with two other species from the *Magnaportheae* family; *M. oryzae* and *M. poae*. The *G. tritici* genome was assembled by combining sequences generated with Sanger, Illumina, and 454 sequence technologies. The resulting genome was 43.62Mb, making it larger than the genomes of *M. oryzae* and *M. poae.* Analysis of repetitive elements revealed that the *G. tritici* genome consists of 6.71% repetitive DNA, compared to 10.13% in *M. oryzae* and just 1.1% in *M. poae.* The authors conclude that the larger genome of *G. tritici* is not a result of repetitive element DNA but perhaps instead due to a high abundance of paralogs and novel genes compared to the other species. However, only 25x coverage was achieved for *G. tritici*, compared to 40x for *M. poae*, with *M. oryzae* complete to seven chromosomes. Despite this limited coverage, the

sequenced genome remains a valuable resource which has allowed further in-depth transcriptomic analyses.

The first RNAseq study comparing *G. tritici* growing in axenic cultures and on wheat roots was carried out by Yang et al. (2015). RNAseq was performed using Illumina paired-end sequencing, identifying a total of 3,258 differentially expressed genes (DEGs). Many annotated DEGs were associated with putative pathogenicity factors, notably genes for "guanine nucleotide-binding protein alpha-2 sub- unit, cellulase, pectinase, xylanase, glucosidase, aspartic protease and gentisate 1, 2- dioxygenase." Laccases are involved in lignin depolymerisation, lignin being a common defence response to pathogen attack. In this study, two out of three laccase genes were upregulated, suggesting that *G. tritici* is capable of degrading lignin.

In a recent study by Zhang et al., (2020) early *G. tritici* infection resulted in the induction of several pathways involved in pathogen resistance in wheat, including oxidation-reduction processes, tryptophan biosynthesis and phenylpropanoid biosynthesis. Differential gene analyses suggested that the plant hormones jasmonic acid (JA), ethylene (ET), and lipoxygenase (LOX) were likely to be involved, though comparatively fewer genes were associated with SA biosynthesis. Conversely, hormonal quantifications performed by Kang et al., (2019) revealed that both JA and SA levels increase during *G. tritici* infection. The same study also found a significant upregulation of phenylalanine ammonia lyase (PAL) genes which likely reflects the involvement of both SA and lignin biosynthesis in the wheat defence response to *G. tritici.*

Despite the growing knowledge provided by these transcriptomic studies, further investigation is required to validate the function(s) of the candidate genes of interest identified. Few studies have reported the transformation of *G. tritici* and transformation has been reported to be extremely unreliable, as is the case for several other Magnaporthe species tested (Guilleroux & Osbourn, 2004). This is because *G. tritici* cannot be easily induced to form perithecia in culture, and fertile strains do not produce enough ascospores for mutagenesis. However, it is possible to regenerate large numbers of protoplasts and Bowyer et al. (1992) have previously reported successful transformation by 4-nitroquinolene oxide (NQO) treatment of fungal protoplasts. Resistance to the fungicide benomyl and the antibiotic phleomycin has also been

achieved through plasmid mediated transformation of protoplasts (Henson et al., 1988; Pilgeram & Henson, 1990). The targeted mutation of the avenacinase gene in *G. avenae* was later achieved by transformation-mediated homologous recombination. Successfully transformed isolates were sensitive to the oat saponin avenacin A-1 and consequently were unable to infect oat plants, though their ability to infect wheat plants was unchanged (Bowyer et al., 1995). More recently, Wang et al. (2018) reported an optimised protocol for polyethylene glycol (PEG)-mediated protoplast transformation of *G. tritici,* making the prospect of successful transformation more promising.

Several studies have focused on the host side of the interaction by overexpressing heterologous proteins to enhance resistance to take-all disease (table 1.3). Snakin-1 (SN1) is a peptide from potato (*Solanum tuberosum* cv*. desireé*) which exhibits broad-spectrum antimicrobial activity *in vitro.* SN1 gene transformation of wheat by biolistic bombardment resulted in the production of five transgenic wheat lines displaying significantly enhancing resistance to take-all disease (Rong et al., 2013). MYB transcription factors have been implicated in plant defence responses to pathogens and are thus a target for crop improvement (Ambawat et al., 2013). The MYB transcription factor (TF) TiMYB2R-1 was cloned from *Thinopyrum intermedium,* a wild relative of wheat with natural resistance to a broad range of pathogens. TiMYB2R-1 expressing wheat lines had enhanced resistance to take-all disease and exhibited increased expression of several defence-related genes including *pathogenesis-related 1* (PR1). The authors suggest that the increased expression of these wheat-defence related genes were regulated by TiMYB2R-1 expression and led to enhanced take-all resistance (Liu et al., 2013). Endopolygalacturonases are CWDEs produced by several fungi and are important for successful plant colonisation. Wang et al. (2015) demonstrated that the introduction of GmPGIP3, a polygalacturonase-inhibiting protein from soybean *(Glycine max),* resulted in significantly enhanced resistance to *G. tritici* and *B. sorokiniana.*

Table 1.3 Protein overexpression studies demonstrating enhanced resistance to take-all disease.

Protein	Function	Transformation method	Take-all disease reduction	Method of disease assessment	Reference
GmPGIP3	Inhibits fungal endopolygalacturonases (PGs) *in vitro*	Biolistic bombardment of GmPGIP3 expression vector into immature wheat embryos (cv. Yangmai 18)	Average disease index in WT plants was 66.7, compared to 11.4-35.6 across five transgenic lines at T_1-T_3	Average disease index of common root rot	Wang et al. (2015)
Snakin-1 (SN1)	Diverse roles in several biological processes, including defence	Biolistic bombardment of SN1 expression vector into immature wheat embryos (cv. Yangmai 18)	15-34% reduction in disease severity across the five transgenic lines compared to the null segregant control at T_3	Percentage area of take-all lesions covering the roots	Rong et al. (2013)
TiMYB2R-1	MYB TF involved in a diverse range of biological processes, including defence	Biolistic bombardment of TiMYB2R-1 expression vector into immature wheat embryos (cv. Yangmai 12)	21-34% reduction in disease severity across three transgenic lines compared to the null segregant control at T_4	Percentage area of take-all lesions covering the roots	Liu et al. (2013)

1.8.7 Control of take-all disease

Current take-all control methods are limited to cultural practices such as crop rotation and reduced tillage. By rotating different crop species, farmers can reduce the levels of fungal inoculum in the soil and hence lower the risk of severe disease in the following crop. For instance, take-all infections can be minimised by growing wheat after an oat crop, which as mentioned previously, produces the antifungal triterpene avenacin. However, crop rotations do not eliminate the fungus and low levels of inoculum may persist in the soil. Clearing cereal volunteers and grass carriers is an effective way to maximise the benefit of the break crop. An alternative control method adopted by farmers is to delay the autumn sowing of second year winter wheats. This is because take-all inoculum levels start to decrease soon after harvest, hence the risk to the next crop decreases as the interval between the harvest of the first wheat and drilling of the second wheat lengthens (Bateman et al., 2006). A more drastic solution is to drill the following cereal crop in the spring. Such methods cannot completely control the disease, rather their use helps to manage severity.

Chemical control is available although its effect is often inconsistent. Latitude® (common name Silthiofam; previously Mon65500; 4,5-dimethyl-*N*-(2-propen-1-yl)-2-(trimethylsilyl)thiophene-3-carboxamide; CHEBI:83393) is a fungicide seed dressing which has been widely used by farmers for take-all control since the early 2000's. Latitude® treatment is specific to *G. tritici* and is thought to inhibit the transport of the adenine nucleotide ATP from the mitochondrial matrix (Joseph-Horne et al., 2000). However, the precise mechanism of action is unknown. In a study by Huang et al. (2001), treatment with Latitude® resulted in cytological alterations in the fungus including the degeneration of the hyphal cytoplasm and the formation of "daughter hyphae" within the damaged hyphae. Surprisingly, changes were also noted in the root cells, which produced thick cell wall appositions and papillae close to infection sites. The fungus was rarely able to overcome these physical barriers and as a result, hyphae were not found in the endodermis or stele. The results demonstrate that Latitude® is also able to indirectly affect host defences, perhaps through improved detection of the pathogen following hyphal damage.

However, a UK field study found that up to 30% of *G. tritici* isolates were insensitive to Latitude®, even in fields where the treatment had never been applied (Freeman et al.,

2005). According to Yun et al. (2012), the efficacy of Latitude® has also declined in Chinese fields, and the risk of developing resistance is high. Nevertheless, Latitude® has been shown to increase the yield of take-all infected plants and can be effective at controlling primary infection of the roots (Bailey et al., 2005). However, the same authors point out that the rate of secondary infection, which can be greatly affected by environmental conditions, is the principal factor in determining final disease levels. This perhaps explains the often patchy levels of disease control within fields and the inconsistencies found between experiments.

Although seed treatments such as Latitude® allow chemicals to be used in small amounts, thus limiting their risk to the environment, seed treatments do not allow for the flexible timing of applications (Jenkyn et al., 2000). The application of foliar sprays containing active ingredients such as azoxystrobin (CHEBI:40909) and fluoxastrobin (CHEBI:83253) which inhibit mitochondrial respiration, allow for more flexibility and have been shown to decrease the severity of the disease, but environmental conditions also affect their ability to target the roots (Jenkyn et al., 2000). Nevertheless, when used in conjunction with other control methods discussed above, chemical control can contribute to a decrease in disease severity and an increase in yield (Gutteridge & Hammond-Kosack, 2008).

The identification of genetic resistance in wheat relatives could provide a sustainable alternative to chemical applications. Oats are naturally immune to take-all disease due to the production of the antifungal triterpene compound avenacin A-1 (Papadopoulou et al., 1999). As mentioned previously, efforts are currently being made to characterise the avenacin pathway with the aim to engineer the pathway into wheat (Leveau et al., 2018; Li et al., 2021). However, oats are not immune to the pathogenic fungus *G. avenae,* which is able to detoxify avenacin through the production of the enzyme avenacinase. Therefore, resistance may not be durable if avenacin producing wheat leads to the selection of avenacin insensitive *G. tritici* isolates. Equally, increased populations of *G. avenae* could present a risk. Several lines of *Triticum monococcum* have demonstrated increased take-all resistance under field conditions (McMillan et al., 2014). In particular, lines MDR031 and MDR046 showed the greatest and most consistent levels of resistance. Though the genetic and mechanistic basis of resistance has not yet been characterised, there is significant potential for future introgression of *T. monococcum* resistance genes in wheat.

1.8.7.1 Biological control of take-all disease

Efforts are now being made to develop an environmentally safe and sustainable control method against take-all disease. Mining the soil microbiome for natural antagonists has yielded several microbial agents with biocontrol potential. In particular, there has been considerable investigation into the use of DAPG producing pseudomonads which are commonly found in TAD soils (Daval et al., 2011; Kwak & Weller, 2013; Kwon et al., 2018). However, opportunities also exist for other bacterial species (Jasem et al., 2018). Although several fungal species have shown biocontrol potential against take-all disease (Ghanbari & Mohammadi, 2015; Gholami et al., 2019), fungal agents are understudied compared to bacterial agents and their modes of action are less understood (see table 1.4).

Several bacterial *Bacillus* species have shown considerable biocontrol potential due to their ability to produce broad spectrum diffusible and volatile antifungal compounds effective against various phytopathogens (Gao et al., 2017; Lim et al., 2017; Stein, 2005). In addition, *Bacillus* species have been shown to induce plant systemic resistance (Kang, Guo, et al., 2019; Kloepper et al., 2004) and promote plant growth (Asari et al., 2016; Kloepper et al., 2004; Kumar et al., 2011). Some *Bacillus* spp. are also able to extensively colonise the root and migrate to the aerial tissue, providing whole plant protection (Kang et al., 2018). Furthermore, members of the *Bacillus* genus such as the well-studied *Bacillus subtilis* form heat and desiccation resistant endospores (Mckenney et al., 2013), improving the prospect of commercialisation.

Certain *B. subtilis* strains have been found to be as effective (Yang et al., 2018) or more effective (Yang et al., 2015) than Latitude® seed treatments. The endophytic *B. subtilis* strain E1R-j isolated from wheat roots significantly reduced take-all disease in greenhouse experiments from concentrations of 10^6 CFU ml^{-1}. TEM analysis of colonised roots indicated that the suppression of *G. tritici* was accompanied by increased plant defence responses such as the formation of cell wall appositions and papillae. Furthermore, colonisation by E1R-j resulted in the disintegration of *G. tritici* hyphal cytoplasm (Liu et al., 2009).

In a study by Zhang et al. (2017), 128 *Bacillus* strains isolated from rhizosphere and bulk soil samples showed *in vitro* antifungal activity against *G. tritici.* Strain Pnf-12, putatively characterised as *B. subtilis*, showed the greatest biocontrol effect in

greenhouse experiments, as well as displaying some evidence of plant growth promotion. The authors attribute this biocontrol effect to the production of antifungal lipopeptides surfactin, iturin and fengycin. Antifungal lipopeptides are widely reported in *Bacillus* spp. and play an important role in fungal antagonism due to their ability to interact with and disrupt the cell membrane of target organisms. For instance, lipopeptides from the surfactin family can interact with the lipid bilayer and cause irreversible pore formation, or complete solubilisation (Fira et al., 2018). More recently, comparative transcriptomic and proteomic analysis of *Bacillus velezensis* and *G. tritici* colonised wheat roots demonstrated that pre-colonisation by *B. velezensis* strain CC09 increased both pattern-triggered immunity (PTI) and effector triggered immunity (ETI), enhancing plant defences against *G. tritici* (Kang et al., 2019).

Table 1.4 Bacterial and fungal biocontrol agents implicated in the control of take-all disease. Rows with grey shading indicate fungal species.

Biocontrol agent	Strain	Mechanism of control	Control efficiency	References
Bacillus subtilis	Pnf-12	Production of antifungal lipopeptides surfactin, iturin and fengycin	69 % disease reduction when applied as a soil drench in pot tests	Zhang et al. (2017)
Bacillus subtilis	GB03	Induced plant resistance and putative direct antagonism	58% disease reduction when applied in a foliar spray treatment and 92% disease reduction when applied as a seed treatment in pot tests	Jasem et al. (2018)
Bacillus velezensis	CC09	Direct inhibition and/or damage of fungal cells *Sensitisation of plant immunity	67 % disease reduction when applied to wheat seeds in a pot test	Kang et al. (2018) *Kang et al. (2019)
Pseudomonas fluorescens	Pf29Arp	Altered expression of plant pathogenesis related genes	35% disease reduction when bacterial inoculum was added directly to the root in a gnobiotic system	Daval et al. (2011)
Pseudomonas protogens	ChB7, Ca10	Putative production of secondary antimicrobial metabolites	Significant disease reduction and yield increases in field trials, but only when applied as a seed coating with fluquinconazole at 10^6 CFU ml^{-1}	Vera Palma et al. (2019)

Coprinopsis urticola	M2	Suppression of mycelial growth and altered hyphal morphology	89.8% disease reduction when applied to soil in pot tests	Gholami et al. (2019)
*Slopeiomyces cylindrosporus (*previously *Gaeumannomyces cylindrosporus)*	Various	Putative induced plant resistance	Significant disease inhibition in field trials when introduced before the wheat cropping season	Gutteridge et al. (2007)
Talaromyces flavus	60, 136	Penetration and fragmentation of hyphae	60% and 58% in vitro growth inhibition of *G. tritici*	Ghanbari & Mohammadi, (2015)
Trichoderma harzianum	Isolate S	Penetration and fragmentation of hyphae	49 % in vitro growth inhibition of *G. tritici*	Ghanbari & Mohammadi, (2015)

1.9 The disease control potential of closely related *Magnaporthaceae* fungi

1.9.1 Introduction

There has been considerable interest in the use of weakly pathogenic or non-pathogenic species within the *Magnaporthaceae* family as biological control agents against take-all disease. *Slopeiomyces cylindrosporus, Gaeumannomyces radicicola* and *Gaeumannomyces hyphopodioides* occur naturally in UK grasslands and have also been isolated from a range of arable field sites. An unnamed *Magnaporthaceae* species, frequently isolated at the Rothamsted Research field sites and at a site in Germany, has also been identified as a promising candidate (Osborne et al., 2018; Ulrich et al., 2000; Ward & Bateman, 1999). For ease, these species will be referred to collectively as the non-pathogenic *Magnaporthaceae* species.

Several field studies have investigated the use of non-pathogenic species as a control mechanism against take-all. However, results have been largely inconsistent. Wong et al. (1996) demonstrated that certain cold tolerant *G. hyphopodioides* isolates gave effective control of take all disease when artificial inoculum was applied in Australian fields. As a result, patent applications were submitted in the UK, France, Australia and the US (Wong, 1995), but were later withdrawn. Various studies have highlighted the need for a greater proportion of beneficial fungi compared to *G. tritici* inoculum in the soil in order for suppression to be successful. Wong & Southwell (1980) reported that a 3:1 ratio of *G. hyphopodioides* to *G. tritici* was required to protect wheat roots, while Mathre et al. (1998) reported that additions of 54 kg/ha were needed to provide effective control in wheat grown in Montana, USA. Furthermore, several studies have suggested that the non-pathogenic *Magnaporthaceae* species must colonise the root system first to provide effective protection from *G. tritici* (Deacon, 1976b; Gutteridge et al., 2007; Wong & Southwell, 1980)

1.9.2 Taxonomy

Non-pathogenic *Magnaporthaceae* fungi have been subject to multiple taxonomic re-classifications which were largely based on hyphal morphology and colony characteristics (see table 1.5). Previously, the non-pathogenic species were considered to belong to the Gaeumannomyces-Phialophora complex which formerly

consisted of the *Gaeumannomyces* fungi and their asexual anamorphs, the *Phialophora* fungi. However, as mentioned previously, a recent reclassification based on multi-gene analysis of ITS, LSU, rbp1 and tef1 sequences resulted in the reclassification of several fungi in the *Gaeumannomyces* (Hernández-Restrepo et al., 2016). The non-pathogenic species *Phialophora radicicola* and *Phialophora* sp. lobed hyphopodia were assigned to the *Gaeumannomyces* genus (now *Gaeumannomyces radicicola* and *Gaeumannomyces hyphopodioides,* respectively). The classification of the non-pathogenic species *Phialophora graminicola* is unclear. *P. graminicola* is probably the asexual anamorph of *Gaeumannomyces cylindrosporus* (Hornby et al.,1977), which has been re-classified to the *Slopeiomyces* genus (now *Slopeiomyces cylindrosporus*). The unnamed *Magnaporthaceae* sp. formed a separate lineage which was distinct from other genera in the *Magnaporthaceae.* A phylogenetic tree indicating the relationship between the different *Magnaporthaceae* isolates used in this PhD project is shown in figure 1.10.

Table 1.5 Key characteristics of the non-pathogenic *Magnaporthaceae* species according to Hernández-Restrepo et al. (2016), including previous nomenclature.

Current name	Previous names	Characteristics	Evidence for biocontrol of take-all
Gaeumannomyces hyphopodioides	*Phialophora* sp. *lobed hyphopodia*	Hyphae are septate, branched, 1-4 µm in diameter, hyaline to red brown in colour. Produces lobed hyphopodia and lunate conidia. Not reported to produce perithecia. Previously isolated from cereals and wild grasses such as *Pennisetum*. Isolates found mainly in the UK, but also Poland, Germany and Australia.	Wong et al. (1996)
Gaeumannomyces radicicola	*Phialophora radicicola* var*. radicicola, Gaeumannomyces graminis* var. *maydis, Harpophora radicicola, Phialophora zeicola*	Characterised by perithecia, asci and ascospores typical for the *Gaeumannomyces* fungi. Colonises cereal and wild grass roots but has also been described as a corn-root rot pathogen in Canada. Isolated from maize in China and wheat in the UK.	Balis (1970); Deacon, (1973, 1974a, 1974b, 1976b)

Slopeiomyces cylindrosporus	*Gaeumannomyces cylindrosporus,* *Phialophora graminicola,* *Phialophora radicicola* var. *graminicola*	Colonises cereal and wild grass roots. Assigned to the *Slopeiomyces* clade of the *Magnaporthaceae.*	Gutteridge et al. (2007); Holden (1976); Speakman & Lewis (1978)
Unnamed Magnaporthaceae sp.	*N/A*	Produces lobed hyphopodia and curved phialospores. Colonises cereal and wild grass roots. Forms a distinct lineage within the *Magnaporthaceae.*	Ulrich et al. (2000)

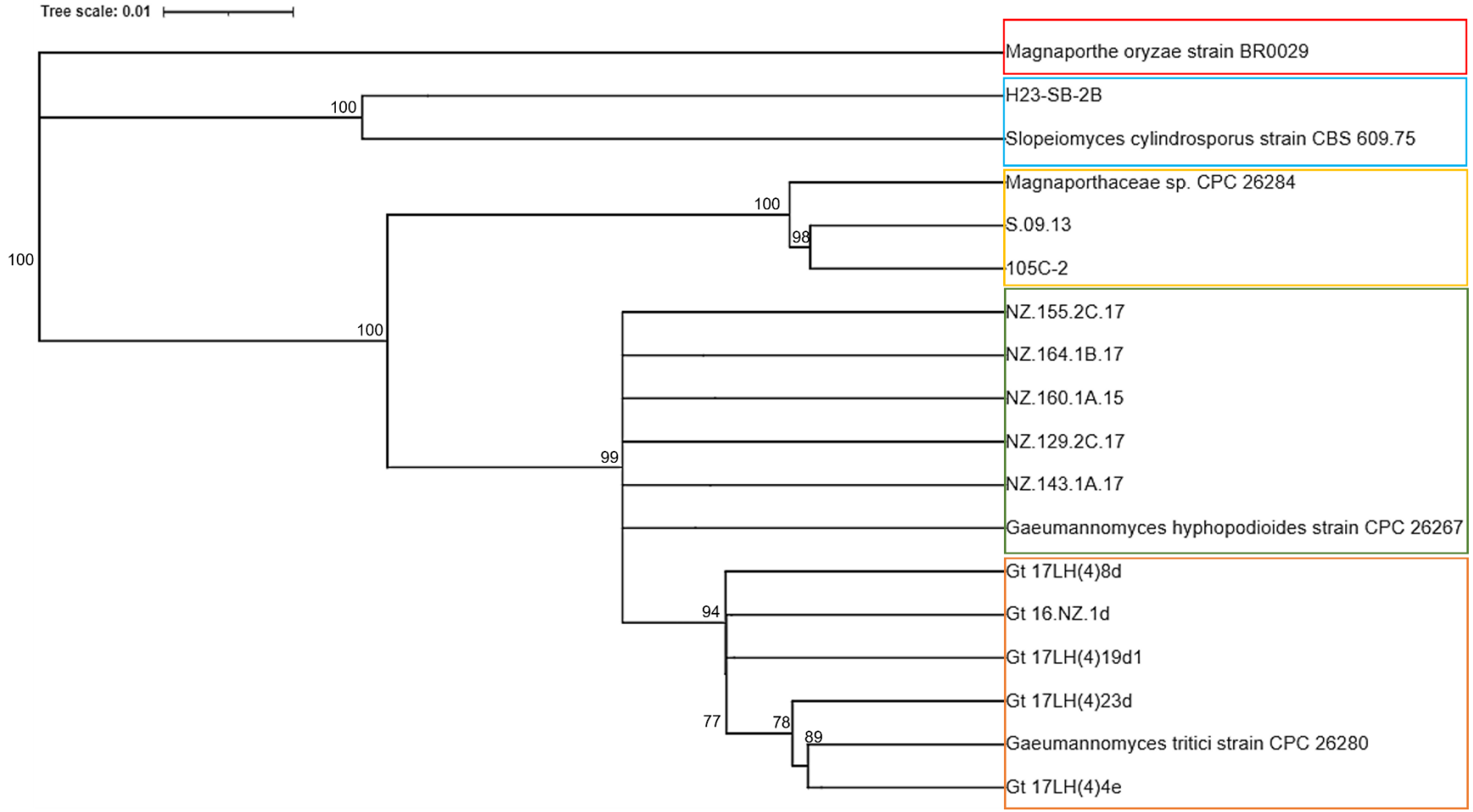

Tree scale: 0.01
Magnaporthe oryzae strain BR0029
H23-SB-2B
Slopeiomyces cylindrosporus strain CBS 609.75
Magnaporthaceae sp. CPC 26284
S.09.13
105C-2
NZ.155.2C.17
NZ.164.1B.17
NZ.160.1A.15
NZ.129.2C.17
NZ.143.1A.17
Gaeumannomyces hyphopodioides strain CPC 26267
Gt 17LH(4)8d
Gt 16.NZ.1d
Gt 17LH(4)19d1
Gt 17LH(4)23d
Gaeumannomyces tritici strain CPC 26280
Gt 17LH(4)4e
100
100
100
98
100
99
94
77
78
89

Figure 1.10 Phylogenetic tree based on ITS5-ITS4 rDNA regions of the *Magnaporthaceae* isolates used in this PhD project. The sequenced ITS5-ITS4 rDNA regions of all isolates were trimmed to 500 bp and aligned in the software package Geneious. Reference ITS regions for each species were obtained from the NCBI nucleotide database and included in the alignment, *Magnaporthe oryzae* was used as the outlier group. The alignment was used to construct a phylogenetic tree based on the genetic distance model of Tamura-Nei, the tree-build method of neighbour-joining with 100 bootstrap replicates and a support threshold set at 75% in Geneious. Values at nodes represent bootstrap support. The Interactive Tree of Life (ITOL) (http://itol.embl.de/) was used to illustrate the tree. See previous page.

1.9.3 Genome resources

Draft genomes currently exist for *G. hyphopodioides*, *S. cylindrosporus* and the unnamed *Magnaporthaceae* species (Osborne, 2016). Sequencing was carried out at the Earlham Institute using the Illumina HiSeq 2500 sequencing platform to generate 125 bp paired-end reads. However, genome comparisons using Benchmarking Universal Single-Copy Orthologs (BUSCO) analysis revealed a lack of completeness across the three genomes when compared to the published *G. tritici* genome (see table 1.6). A collaborative study by Rothamsted Research and the Earlham Institute is currently underway to sequence the genomes of several non-pathogenic *Magnaporthaceae* fungi isolated from Rothamsted arable and grassland field sites (PacBio and Illumina 150 bp paired-end reads). The genomes will facilitate the development of species specific primers for accurate species identification and enable future genomic and transcriptomic analyses. Genome sequencing of *G. radicicola* is not planned because isolates of these species are rarely detected at Rothamsted field sites.

Table 1.6 Genome summary statistics and BUSCO analysis of the non-pathogenic *Magnaporthaceae* draft genomes compared to the *Gaeumannomyces tritici* R3-111a-1 annotated genome. Adapted from Osborne (2016) PhD thesis.

	Fungal species			
	G. hyphopodioides **Isolate:** N.14.13	**Unnamed *Magnaporthaceae* sp.** **Isolate:** S.09.13	***S. cylindrosporus*** **Isolate:** 74/1736-2	***G. tritici*** **Isolate:** R3-111a-1
Reads	13,197,250	14,670,529	25,719,585	43,768,664
G + C (%) content	55.1%	56.0%	55.0%	56.85%
Coverage	39 x	43 x	75 x	25 x

Complete BUSCOs (complete duplicated BUSCOs)	28% (1.3%)	52% (2.9%)	30% (1.8%)	97% (7%)
Fragmented BUSCOs	39%	34%	42%	2%
Missing BUSCOs	31%	13%	27%	0.4%
Total BUSCO groups searched	1438	1438	1438	1438

1.10 Research objectives

Given the significant impacts of take-all disease on root health and wheat yield, and the growing need for new and sustainable control methods, the overall research aim of this PhD project was to evaluate the potential of non-pathogenic *Magnaporthaceae* species as biocontrol agents against take-all disease of wheat. To achieve this overall aim, the following objectives were set out.

Objective 1: To determine the mechanism(s) of control by non-pathogenic *Magnaporthaceae* species against the take-all fungus.

Objective 2: To characterise and inter-compare the infection mechanisms of non-pathogenic *Magnaporthaceae* species.

Objective 3: To investigate wheat transcriptional responses to *G. hyphopodioides* colonisation and *G. tritici* infection.

Objective 4: To develop an effective delivery system to permit BSMV-mediated virus induced gene silencing (VIGS) in wheat roots.

Objective 5: To investigate the effects of colonisation by non-pathogenic *Magnaporthaceae* species on overall plant health and performance.

Objective 6: To further characterise the ability of elite winter wheat cultivars to support *G. hyphopodioides* under controlled environment conditions.

The results of this PhD project were anticipated to provide crucial data to enhance our understanding of wheat responses to *G. tritici* and closely related non-pathogenic relatives, thus helping to inform future strategies for take-all control.

2 General materials and methods

In this chapter, the general methods used in this PhD project are outlined. Details of methods used in specific studies can be found in subsequent chapters.

2.1 Media preparation

Potato dextrose agar (PDA) was prepared by dissolving 16.4 g PDA powder (Formedium^{TM}, UK) in 400 ml distilled water. Potato dextrose broth (PDB) was prepared by dissolving 9.6 g PDB powder (Formedium^{TM}, UK) in 400 ml distilled water. Media was sterilised in a steam autoclave.

2.2 Maintenance and storage of *Magnaporthaceae* isolates

Magnaporthaceae isolates were stored on PDA plates at 4 °C in the dark. A single master plate was set up for each isolate, from which an agar plug was taken each time a fresh culture was required. All plates were sealed with Parafilm M® film (Bemis company Inc, USA). Long-term water stocks were established by placing four agar plugs in a 2 ml screw cap tube containing sterile distilled water. Tubes were stored in the dark at 4 °C. Additional long-term glycerol stocks were established as above and plugs were stored in 50% sterile glycerol at -80 °C. Fresh cultures for use as inoculum in seedling pot experiments or for *in vitro* assays were grown for 14 days at 21 °C in the dark. Fungal plugs were always taken from the growing edge of the colony using a sterile cork-borer. Different sized plugs were taken depending on the experiment (cork-borer no.2 = 5 mm, no.3 = 6 mm, no.4= 7 mm).

2.3 Isolation of *Magnaporthaceae* fungi from root material

Isolation of *Magnaporthaceae* isolates from infected root samples was required when re-passaging take-all isolates which had lost virulence as a result of long-term cold storage, or to remove stubborn bacterial contaminants present in existing long-term water stocks. Isolation of fungi from infected root material was also conducted in chapter 7 to confirm *G. hyphopodioides* colonisation.

Root samples containing visible symptoms of infection or colonisation (presence of lesions, runner hyphae or sub-epidermal vesicles) were cut from the root

system using a sterile scalpel blade. Root samples (2 cm long) were surface sterilised in 4 % w/v sodium hypochlorite for 3-5 minutes, followed by 3x 1 minute washes in sterile distilled water. Sterilised root samples were plated onto PDA supplemented with kanamycin (50 µg/ml) and incubated at 21 °C in the dark for approximately 4 days, at which point fungal cultures were visible. Hyphal tips from individual colonies were carefully cut using a fine scalpel blade, and tips were plated onto fresh PDA plates to ensure pure cultures.

2.4 Seedling pot bioassays

Seedling pot bioassays were required when re-passaging fungal isolates. Several seedling bioassays were also conducted in chapter 7. Bioassays were set up using plastic drinking cups (7.5 cm wide x 11 cm tall) as pots. Pots were drilled with four drainage holes 3 mm in diameter. A 50 cm^3 layer of damp sand was added to each pot, followed by a 275 g layer of dry sand. Inoculum was prepared as per section 2.2 and one sixth of a PDA plate containing a fungal colony was macerated and mixed with sand to make up a 25 g inoculum layer. A final 150 g layer of dry sand was added on top of the inoculum layer. Ten wheat seeds were sown evenly on the surface of the sand and covered with a 50 cm^3 layer of grit to aid germination and create a humid environment for fungal colonisation. Pots were watered well and placed in a controlled environment room (16 hr day, light intensity 250 µmols, 15 °C day, 10 °C night, watered twice a week from above). A randomised block design was generated in GenStat 20th Edition, taking into account potential environmental differences across the growth room. Plants were left to grow for 5 weeks before harvesting. Pots were washed out with water carefully and thoroughly using a hose gun. A sieve was used to prevent loss of material.

2.5 Seedling root assessments

Roots were assessed visually by immersing seedlings in a white tray containing water. An LED lamp was placed above the tray to aid visualisation. Roots were assessed for *G. hyphopodioides* colonisation based on the presence of melanised macrohyphae on the root surface, which could be detected by eye

(figure 2.1 A). In co-inoculation experiments, *G hyphopodioides* colonisation was confirmed by examining roots under a stereomicroscope for the presence of sub-epidermal vesicles. Take-all disease incidence was assessed based on the presence of black necrotic lesions originating from the root stele (figure 2.1 B). Areas of root browning were not classed as take-all lesions. The total number of plants, number of roots, number of colonised/diseased plants, number of colonised/diseased roots was noted down for each pot.

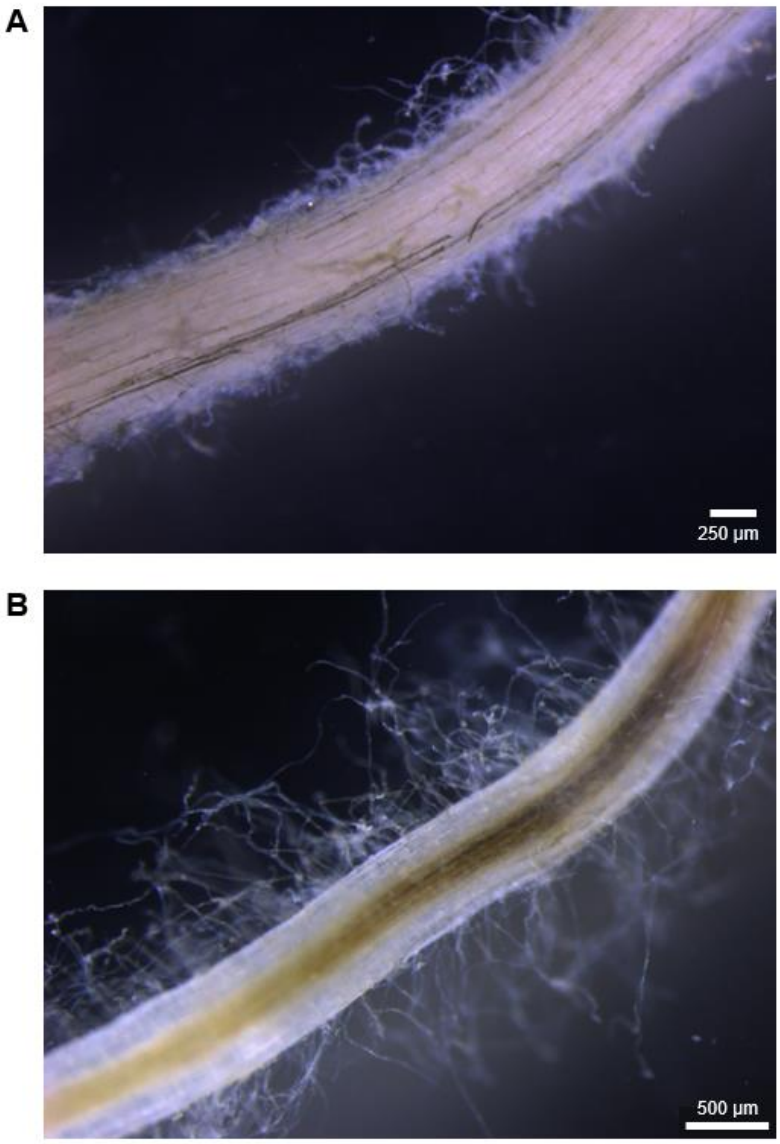


Figure 2.1 Key symptoms for visual root assessments. A. Melanised *G. hyphopodioides* macrohyphae on the surface of a wheat root. B. Black necrotic take-all lesion originating from the stele. Images were taken with a stereomicroscope.

Additional severity measurements were taken in certain experiments. Take-all disease severity was assessed by calculating the percentage of roots with no disease (0% lesion coverage), light disease (1-25 % lesion coverage), moderate disease (26-50% lesion coverage) or severe disease (51-75% disease coverage), based on visual assessments of the first 10 cm of each root (see figure 2.2). Severity was not assessed further down the root as these regions seldom exhibit lesions in seedling bioassays.

Similarly, colonisation severity was assessed by estimating the percentage of roots with no colonisation (0% runner hyphae), light colonisation (1-25% runner hyphae), moderate colonisation (26-50% runner hyphae), high colonisation (51-75% runner hyphae) or extreme colonisation (76-100% runner hyphae), based on visual assessments of the first 10 cm of each root.

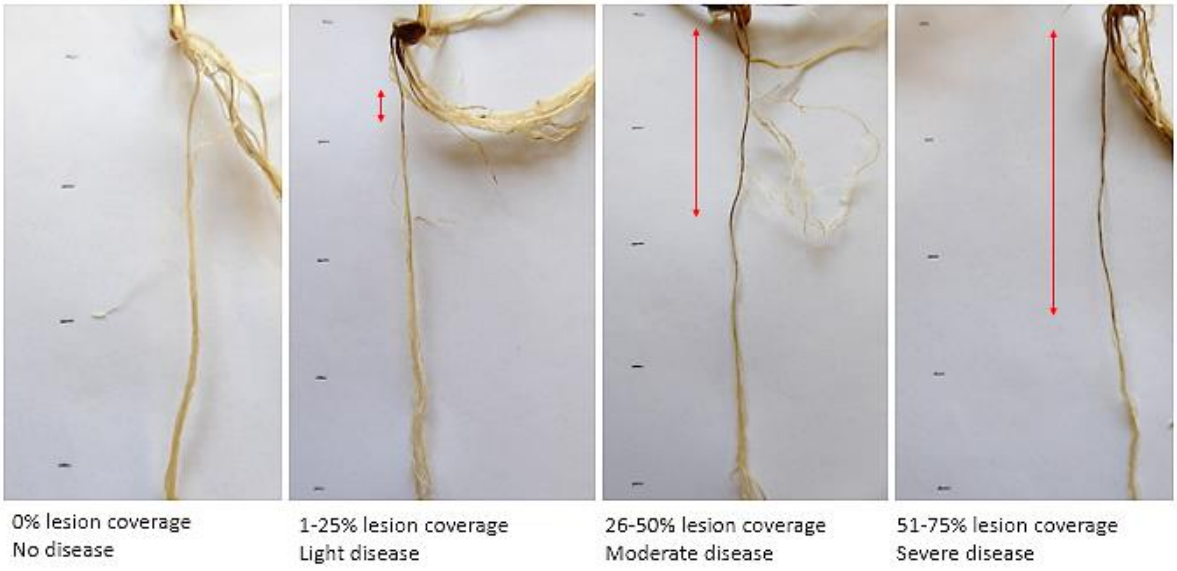


Figure 2.2 Disease severity assessments based on the percentage of black lesion coverage in the first 10 cm of each root. Red arrows indicate the area of each root exhibiting take-all lesions.

2.6 Plant biomass measurements

Plant samples were processed by separating the shoot from the roots with scissors and discarding the seed coat (if still present). Roots/shoots from the same pot were placed in a cardboard weighing boat. Samples were oven dried

for 16 hours at 80 °C before weighing with a pair of scales accurate to 3 decimal places.

2.7 Microscopy and imaging

2.7.1 Light microscopy

A ZEISS Axiophot microscope (ZEISS, Germany) equipped with a Q-Imaging Retiga EXi CCD mono digital camera with RGB filter wheel (QImaging, USA) was used for the analysis of semi-thin sections. Images were acquired using the associated Metamorph software (Molecular Devices, USA).

A Leica M205 Stereomicroscope (Leica Microsystems©, Germany) was used for the imaging of whole plant tissue specimens.

2.7.2 Photographic documentation

A Nikon D80 digital SLR camera (Nikon, Japan) was used for image capture throughout the thesis.

2.8 DNA extractions from plant and fungal material

Fungal material was prepared by growing fungal isolates on PDA plates covered with a cellophane disc (325P cellulose, 80 mm diameter; A.A. Packaging Ltd, UK). Fresh mycelium was scraped off the cellophane disc and taken immediately for DNA extraction. Plant root samples were lyophilised in the LyoDry Compact Benchtop Freeze Dryer (Mechatech systems, UK) for 48 hours. Plant/fungal material was ground with a mortar and pestle until a fine powder was formed. The DNeasy® Plant Mini Kit (Qiagen, Germany) was used to extract DNA from finely ground material (~100 mg fresh material or ~30 mg lyophilised material) as per the manufacturer's instructions. However, the following alterations were made:

- Step 9: Add 500 µl Buffer AW2. Centrifuge for 1 min at 20,000 x g. Discard flow-through and place column back in collection tube. Centrifuge for an additional minute to thoroughly dry the column.
- Step 11: Add 50 µl Buffer AE for elution. Incubate for 5 min at room temperature (15–25°C). Centrifuge for 1 min at ≥6000 x g.

2.9 RNA extractions from plant and fungal material

RNA extractions were performed on fresh material only. All surfaces and pipettes were wiped down with RNase*Zap*™ (Thermo Scientific™, USA) and extractions were carried at room temperature quickly and carefully. Samples were ground to a fine powder using a pre-cooled sterile mortar and pestle under liquid nitrogen. Samples were not allowed to thaw prior to RNA extraction. When the amount of tissue was limited (as in chapter 5), samples were ground in an RNAse-free 1.5 ml Eppendorf tube containing liquid nitrogen, using a pre-cooled RNAse-free disposable pestle (Thermo Scientific™, USA). RNA extractions were carried out using the E.Z.N.A.® Plant RNA Kit with the associated RNase-free DNase I Set (Omega-Biotek, USA) following the standard protocol provided. RNA was eluted in 30 µl RNAse free water and stored at -80 °C.

2.10 Quantification of nucleic acid concentration

A NanoDrop™ 2000c Spectrophotometer (Thermo Scientific™, USA) was used to determine the concentration of DNA and RNA samples. The pedestal was cleaned with non-abrasive tissue paper (Kimtech™, USA) prior to each use and between samples. A blank standard was established using 1 µL of elution buffer or sterile deionised water, and the concentration of each sample (ng/µl), the 260/280 nm ratio and the 260/230 nm ratio was recorded to assess sample purity.

2.11 Polymerase Chain Reaction (PCR)

Routine Polymerase Chain Reactions (PCRs) were performed using DreamTaq Green PCR Master Mix (2X) (Thermo Scientific™, USA). For colony PCRs, individual bacterial colonies picked from selective agar plates were used as a template for amplification and nucleic acid-free sterile water was added to adjust the final reaction volume. For high-fidelity PCR amplification, Phusion® High-Fidelity DNA Polymerase (New England BioLabs®, USA) was used. The reactions were prepared and performed as detailed in tables 2.1 - 2.4 using a Bio-Rad T100™ Thermal Cycler (Bio-Rad, USA).

For fungal species identification, PCR of the internal transcribed spacer regions ITS5 and ITS4 was performed using primers ITS5.F

(GGAAGTAAAAGTCGTAACAAGG) and ITS4.R (TCCTCCGCTTATTGATATGC), respectively. Primer annealing temperature with DreamTaq Master Mix was 55 °C.

Table 2.1 Reaction mix for PCR analyses with DreamTaq Green PCR Master Mix (2X).

Reagent	Volume (µl)	Final concentration
DreamTaq Green Master Mix 2X	10	1X
10 µM forward primer	0.8-1	0.4 µM - 0.5 µM
10 µM reverse primer	0.8-1	0.4 µM - 0.5 µM
DNA template / blank	Variable	10 pg-1 µg
Nuclease-free water	To 20 µl	

Table 2.2 Reaction mix for PCR analyses with Phusion® High-Fidelity DNA Polymerase.

Reagent	Volume (µl)	Final concentration
5 x Phusion HF Buffer	4 µl	1X
Phusion Polymerase	0.2 µl	1.0 units
10 mM dNTPs	0.4 µl	200 µM
10 µM forward primer	1 µl	0.5 µM
10 µM reverse primer	1 µl	0.5 µM
DNA template / blank	Variable	< 250 ng
Nuclease-free water	To 20 µl	

Table 2.3 Thermocycling conditions for PCR reactions with DreamTaq Green PCR Master Mix (2X).

Step	Temperature °C	Duration	Cycles
Initial denaturation	95	3 mins	1
Denaturation	95	30 secs	35
Annealing	54-63	30 secs	
Extension	72	60 secs	
Final extension	72	10 mins	1

Table 2.4 Thermocycling conditions for PCR reactions with Phusion® High-Fidelity DNA Polymerase.

Step	Temperature °C	Duration	Cycles
Initial denaturation	98	30 secs	1

Denaturation	98	30 secs	34
Annealing	61-65	30 secs	
Extension	72	30 secs	
Final extension	72	10 mins	1

2.12 Gel Electrophoresis

DNA/cDNA PCR products and all RNA samples were resolved by gel electrophoresis on a 1-2% agarose gel (containing 0.5 µg/ml ethidium bromide) in 1x Tris-borate-EDTA (TBE) buffer (Thermo Scientific™, USA)**.** Aliquots of nucleic acid samples were mixed with DNA Gel Loading Dye 6X (Thermo Scientific™, USA) to a 1x final concentration in 0.2 ml PCR tubes and the samples were individually pipetted into wells. The GeneRuler 1 Kb plus DNA ladder (Thermo Scientific™, USA) was used as a molecular weight standard. Electrophoresis was performed at 80-150 V for 20 – 45 minutes (PowerPac™ Basic 300V Power Supply; Bio-Rad, USA) depending on the type of nucleic acid being analysed, and nucleic acid bands were visualised using the GeneGenius Bioimaging System (Syngene, UK).

2.13 Sanger sequencing of PCR products

PCR products were purified using the QIAquick® PCR Purification Kit (Qiagen, Germany) as per the manufacturer's instructions and purified products were sent for Sanger sequencing via the TubeSeq service at Eurofins Genomics (Eurofins Genomics, Wolverhampton, UK). Sequence trimming and analyses were performed using the Geneious bioinformatics software. The NCBI Basic Local Alignment Search Tool (BLAST) (https://blast.ncbi.nlm.nih.gov/Blast.cgi) was used to identify regions of similarity between sequences for fungal species verification of ITS PCR products.

2.14 Quantification of *G. tritici* fungal biomass by TaqMan qPCR

TaqMan qPCR assays were carried out by targeting a 105-bp partial DNA sequence of the translation elongation factor 1-alpha (EF1-α) gene in *G. tritici*, using primers GtEFF1 (5'-CCCTGCAAGCTCTTCCTCTTAG-3') and GtEFR1 (5'-

GCATGCGAGGTCCCAAAA-3') with the TaqMan probe (5'-6FAM-ACTGCACAGACCATC-MGB-3') (Thermo Scientific™, USA) (Keenan et al., 2015). The assays were carried out using the KAPA PROBE FORCE qPCR Master Mix (2X) (KAPA Biosystems Inc., USA) on a ThermoFisher QuantStudio™ 6 Pro Real-Time PCR System. Amplification efficiency was confirmed to be between 95 and 100% in all qPCR runs. *G. tritici* fungal biomass (reported as pg *G. tritici* DNA/ng total DNA) was calculated by absolute quantification using the standard curve method. The reactions were prepared and performed as detailed in tables 2.5-2.6.

Table 2.5 Reaction mix for *G. tritici* TaqMan qPCR assays

Reagent	Volume	Final concentration
KAPA PROBE FORCE qPCR Master Mix (2X)	10 µl	1X
EFPR1Probe (100 µM)	0.03 µl	0.15 µM
EFF1 Primer (100 µM)	0.06 µl	0.3 µM
EFR1 Primer (100 µM)	0.06 µl	0.3 µM
Template/NTC/Standard	2 µl	Template: 10 ng/µl Standard: variable
dH_2O	7.85 µl	

Table 2.6 Thermocycling conditions for *G. tritici* TaqMan qPCR assays

Step	Temperature °C	Duration	Cycles
Initial denaturation	95	3 mins	1
Denaturation	94	15 secs	40
Annealing	52	20 secs	
Extension	72	20 secs	

To rule out amplification of non-pathogenic *Magnaporthaceae* species in co-inoculated samples (not previously tested by Keenan et al., (2015)), a routine PCR amplification of *G. tritici*, *G. hyphopodioides*, *S. cylindrosporus* and the unnamed *Magnaporthaceae* sp. DNA was carried out with the EF1-α primers as described above, using DreamTaq Green PCR Master Mix (2X). Amplification of the internal transcribed spacer (ITS) region (as described in section 2.11) was

carried out as a positive control (figure 2.3). Gel electrophoresis was carried out as described in section 2.12.

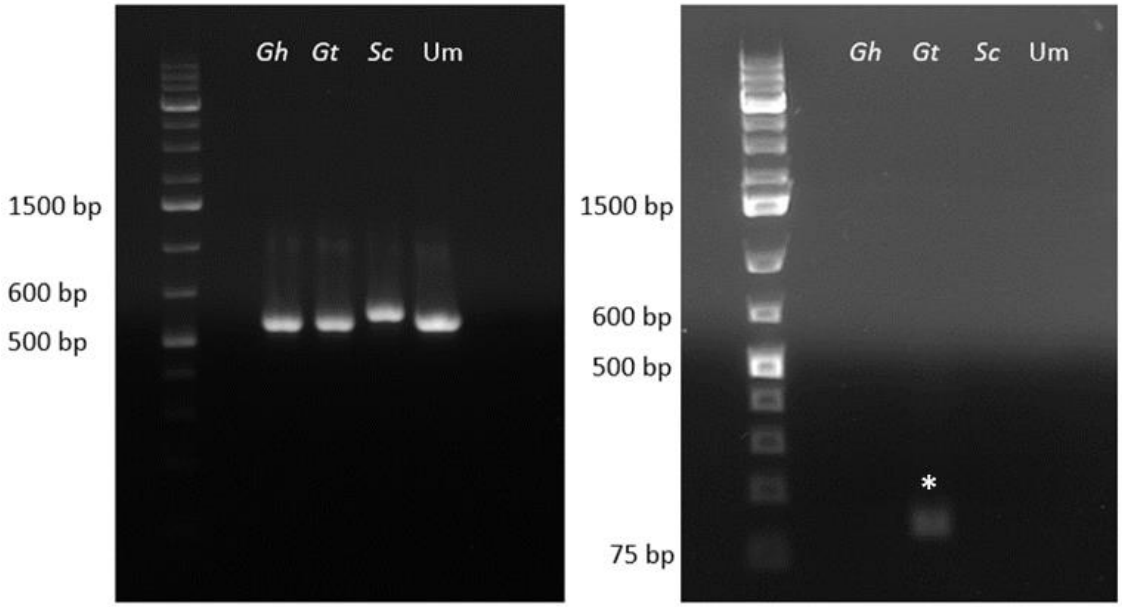


Figure 2.3 PCR and gel electrophoresis confirming species-specific detection of *G. tritici* using EF1-α primers (Keenan et al., 2015). Left: Positive control; PCR amplification of fungal ITS region. Right: PCR amplification of a 105-bp region of the EF1-α gene in *G. tritici*. *Gh= G. hyphopodioides, Gt= G. tritici, Sc= S.cylindrosporus,* Um= Unnamed *Magnaporthaceae sp.*

2.15 Statistical analyses

Statistical analyses were performed in Genstat 20th Edition (VSN International Ltd, Hemel Hempstead, UK) with guidance from Suzanne Clark (Applied Statistician, Computational and Analytical Sciences, Rothamsted Research, UK).

Root assessment data are limited by the total number of roots per pot. Therefore, root colonisation and take-all disease incidence count data were analysed using a Generalized Linear Regression Model (GLM) with a binomial distribution and LOGIT link function. Analyses were adjusted for over-dispersion when the residual of the mean deviance was greater than 1. Predictions of means (proportion of roots with runner hyphae/ lesions) were back-transformed from the LOGIT scale (using the equation exp(x)/(1+exp(x))) and converted to percentages for graphical presentation. Error bars represent back-transformed

95% confidence intervals. Colonisation severity and take-all disease severity were analysed by ordinal logistic regression based on the original count data.

For continuous outcome variables such as plant biomass, data were analysed by Analysis of Variance (ANOVA). Prior to analysis, data were checked for normality by examining residual plots. Data transformations were carried out as appropriate and data were back-transformed for graphical presentation. Errors bars represent standard deviation or standard error for untransformed data, and 95% confidence intervals for back-transformed data.

Post-hoc multiple comparisons tests were carried out when more than one interaction was of interest. For multiple comparisons to a single control treatment, Dunnett's post-hoc test was carried out (Dunnett, 1955). For multiple comparisons to more than one control treatment or between multiple treatments, Tukey's multiple comparisons test or Fishers Least Significant Difference Test (l.s.d.) was carried out. The output summaries of all statistical tests can be found in the appendices.

3 Investigating the mechanism of take-all control by non-pathogenic *Magnaporthaceae* species

3.1 Introduction

The mechanism by which non-pathogenic *Magnaporthaceae* species inhibit *G. tritici* is currently unknown. However, previous studies have suggested that induced plant resistance may be responsible for the reduction in take-all disease. This hypothesis is based on several observations. Firstly, studies by Deacon (1976) reported that *G. tritici* hyphal morphology was not affected by contact with non-pathogenic *Magnaporthaceae* species (although evidence supporting this report is not available). As a result, direct inhibition has been ruled out as a mechanism of control by many authors.

Secondly, non-pathogenic *G. radicicola* and *S. cylindrosporus* (previously *Phialophora graminicola*) have been reported to cause lignification of the root stele and enforcement of the endodermal layer with both lignin and suberin (Speakman and Lewis, 1978), potentially limiting the longitudinal growth of *G. tritici* along the root. Furthermore, ultrastructural and cytochemical studies by Huang et al. (2001) demonstrated that colonisation by *S. cylindrosporus* results in the formation of cell wall appositions and papillae, perhaps acting as a physical barrier to future infection by *G. tritici*. Also common to the non-pathogenic *Magnaporthaceae* is the production of so-called “sub-epidermal vesicles” in the root cortex, hypothesised to be growth cessation structures formed in response to hyphal stress or nutritional limitation, and possibly indicative of plant defence induction (Deacon, 1974b). Detailed investigations into the infection mechanism of *Magnaporthaceae* species and the subsequent plant host responses have been conducted in the chapters 4 and 5, respectively.

Finally, a number of field studies have reported that colonisation by non-pathogenic *Magnaporthaceae* species must occur before *G. tritici* infection for control to be effective (Wong 1981, Gutteridge et al., 2007, Deacon, 1976, Wong and Southwell 1980), again indicating that colonisation by these non-pathogenic species results in the upregulation of plant defence responses. However, co-

inoculation experiments investigating the reduction of take-all disease by non-pathogenic *Magnaporthaceae* species have not been carried out under controlled conditions to validate previous field observations. Therefore, crucial information such as the duration of putative resistance, whether the effects are local or systemic, or how putative resistance may affect plant growth parameters, is still lacking. Nevertheless, induced resistance by non-pathogenic microbes in the rhizosphere is well documented in the literature and several examples already exist for the control of take-all disease. A plant growth promoting sterile red fungus was shown to systemically reduce take-all disease in split-pot wheat assays (Aberra et al., 1998). Using a similar set-up, Khaosaad et al. (2007) demonstrated that high levels of colonisation by arbuscular mycorrhizal fungi (AMF) on barley plants resulted in systemic protection against take-all disease. Furthermore, probiotic rhizobacteria species applied as a foliar spray or as a root drench to wheat plants resulted in similar levels of take-all reduction, revealing induced resistance to be the main control mechanism (Jasem et al., 2018).

Despite strong evidence for induced plant resistance by non-pathogenic *Magnaporthaceae* species, other direct fungal control mechanisms cannot be ruled out. As mentioned in chapter 1.7, endophytic fungi can target their opponents in the rhizosphere through a myriad of strategies such as the production of antifungal compounds, fungal volatile organic compounds (VOCs) or even by mycoparasitism (De Silva et al., 2019, Pieterse et al., 2014, Raaijmakers et al., 2009). Therefore, a comprehensive investigation into the mechanism of take-all control by non-pathogenic *Magnaporthaceae* species was required.

3.2 Aims and hypotheses

Aim 1: To investigate the direct interaction between non-pathogenic *Magnaporthaceae* species and pathogenic *G. tritici.*

Hypothesis: Direct fungal contact does not lead to *G. tritici* inhibition *in vitro.*

Aim 2: To investigate whether non-pathogenic *Magnaporthaceae* species trigger induced plant resistance against take-all disease.

Hypothesis: *G. hyphopodioides* must colonise wheat plants prior to *G. tritici* in order to provide effective take-all control.

3.3 Methods:

A range of *Magnaporthaceae* isolates were included in the following experiments. The isolates were obtained from soil cores or plant samples from several different Rothamsted field trials previously carried out by members of the take-all team. Several isolates were chosen for *de novo* genome sequencing in collaboration with the Earlham Institute. Full details of these isolates can be found in table 3.1. A further selection of fungal pathogens and endophyte species were tested in confrontation assays with *G. hyphopodioides* and *G. tritici*. Full details of these isolates can be found in table 3.2.

Table 3.1 Details of the *Magnaporthaceae* isolates used in chapter 3. Isolates highlighted in grey have been chosen for *de novo* genome sequencing in collaboration with the Earlham Institute. *G. hyphopodioides* building cultivars were characterised by Osborne et al., (2018). Take-all building cultivars were characterised by McMillan et al., (2011). *G. tritici* genetic type identification was performed by Gail Canning and Jessica Hammond (Rothamsted Research), according to Freeman et al., (2005).

Isolate code	Rothamsted field name	Year collected and isolated	Plot-crop species, cultivar	ITS species identification	*G. tritici* genetic "type"	Genome sequencing interest
NZ.184.1C.16	New Zealand	2015	*T. aestivum*, Monterey	*G. hyphopodioides*	-	-
NZ.160.1A.15	New Zealand	2015	*T. aestivum*, KWS Sterling	*G. hyphopodioides*	-	-
NZ.198.1A.17	New Zealand	2016	*T. aestivum*, Invicta	*G. hyphopodioides*	-	-
NZ.155.2C.17	New Zealand	2016	*T. aestivum*, Cordiale	*G. hyphopodioides*	-	-
NZ.143.1A.17	New Zealand	2016	*T. aestivum*, KWS Croft	*G. hyphopodioides*	-	-
NZ.3.2A.17	New Zealand	2016	*T. aestivum*, Scout	*G. hyphopodioides*	-	-
NZ.136.1A.15	New Zealand	2015	*T. aestivum*, Tuxedo	*G. hyphopodioides*	-	-
NZ.164.1B.17	New Zealand	2016	*T. aestivum*, Monterey	*G. hyphopodioides*	-	Isolated from a low *G. hyphopodioides* building plot (cv. Monterey)

NZ.129.2C.17	New Zealand	2016	*T. aestivum*, Scout	*G. hyphopodioides*	-	Isolated from a high *G. hyphopodioides* building plot (cv. Scout)
NZ.24.2A.15	New Zealand	2015	*T. aestivum*, KWS Kielder	*G. hyphopodioides*	-	-
63B-1	Delafield	2018	*T. aestivum*, Avalon	*G. hyphopodioides*	-	-
S.03.13	Summerdells I	2013	*T. aestivum,* Conqueror	*G. hyphopodioides*	-	-
P.09.13	Pastures	2013	*T. aestivum,* Conqueror	*G. hyphopodioides*	-	-
P.10.13	Pastures	2013	*T. aestivum,* Conqueror	*G. hyphopodioides*	-	-
105C-1	Delafield	2018	*T. aestivum*, Cadenza	*G. hyphopodioides*	-	-
105C-2	Delafield	2018	*T. aestivum*, Cadenza	Unnamed *Magnaporthaceae* sp.	-	An unnamed species in the *Magnaporthaceae* family
H23-SB-2B	Highfield	2018	Grassland, Soft Brome (*Bromus hordeaceus*)	*Slopeiomyces cylindrosporus*	-	Isolated from a long-term grassland experiment
17LH(4)9d2	Long Hoos	2017	*T. aestivum*, unknown	*G. tritici*	A	-
16.NZ.1d	New Zealand	2016	*T. aestivum*, unknown	*G. tritici*	A	-
17LH(4)19d1	Long Hoos	2017	*T. aestivum*, Cadenza	*G. tritici*	A	Isolated from a low take-all building plot (cv. Cadenza)

17LH(4)8d	Long Hoos	2017	*T. aestivum*, Hereward	*G. tritici*	A	Isolated from a high take-all building plot (cv. Hereward)
17LH(4)23d	Long Hoos	2017	*T. aestivum*, Cadenza	*G. tritici*	B	Isolated from a low take-all building plot (cv. Cadenza)
17LH(4)4e	Long Hoos	2017	*T. aestivum*, Hereward	*G. tritici*	B	Isolated from a high take-all building plot (cv. Hereward)

Table 3.2 Summary of pathogenic and endophytic species used in confrontation assays with *G. tritici* and *G. hyphopodioides*. [1].Isolates provided by Dr Gareth Thomas, Rothamsted Research. [2].Isolates provided by Dr Martin Urban, Rothamsted Research.

Fungal species	Isolate code	Host	Reason for choice	References
Trichoderma hamatum	GD12[1]	Beneficial plant endophyte residing in soil, colonises roots and foliar tissues of a wide range of host plants	Abundant plant growth promoting fungus, used as biological control against various plant diseases.	(Martínez-Medina et al., 2017; Studholme et al., 2013)
Sclerotinia sclerotiorum	GT18[1]	Necrotrophic broad-spectrum pathogen of dicots capable of infecting wide range of tissue types including stems, fruits, roots and foliage.	Sclerotia reside in the soil and the fungus grows endophytically in cereal crops, exhibiting biocontrol abilities in some non-host species such as wheat	(Tian et al., 2020)

Fusarium graminearum	10FG131[2]	Crop pathogen causing Fusarium Head Blight (FHB) on wheat, barley, rice and oats.	Significant phytopathogen of cereals capable of infecting young wheat roots	(Ding et al., 2022)
Fusarium culmorum	UK99[2]	Important pathogen of cereals causing seedling blight, foot rot and FHB.	Soil-borne fungal pathogen of wheat	(Wagacha and Muthomi, 2007)
Ilyonectria crassa	16LH14d	Wound pathogen reported to cause Cylindrocarpon root rot in a range of hosts including potato	Soil borne root endophyte of wheat with potential biocontrol abilities (based on unpublished data)	(Cabral et al., 2012; Chudinova et al., 2019)

3.3.1 Fungal confrontation assays

Fungal confrontation assays were performed between a range of *G. hyphopodioides, S. cylindrosporus,* unnamed *Magnaporthaceae* sp. and *G. tritici* isolates (see table 3.3 for treatment details). In addition, a subset of *G. hyphopodioides* vs. *G. tritici* assays were conducted on 50% and 10% PDA to investigate the effect of nutrient content on hyphal interaction. The isolates used in these experiments have been marked with an asterisk in table 3.3. As mentioned above, *G. hyphopodioides* and *G. tritici* were also tested against a range of endophytic and pathogenic fungi (see table 3.4 for treatment details). All confrontation assays were set up on PDA plates. PDA media was made up as described in section 2.1. For assays on 50% and 10% PDA, the PDA concentration was reduced accordingly and media was supplemented with agar-agar powder (Formedium^{TM}) as required. Petri dish plates were filled with 25 ml media. Plates were inoculated by removing two PDA plugs either 4 cm or 2 cm apart with a number 3 cork-borer (6 mm diameter) and replacing them with fungal plugs taken from the growing edge of fungal colonies. All isolates were maintained as outlined in section 2.2. Plates were sealed with parafilm and stored at 21°C for up to 18 days in the dark. Four replicates were set up for each treatment and the experiments were carried out twice. Time-course images of confrontation assays were taken every 3 days using a Nikon Digital Camera D80.

Table 3.3 Treatment details of fungal confrontation assays between non-pathogenic *Magnaporthaceae* species and *G. tritici.* Control treatments are highlighted in grey. Confrontations marked with an asterisk were also performed on 50% and 10% PDA.

Side A		Side B	
Fungal species	Isolate	Fungal species	Isolate
S. cylindrosporus	H23-SB-2B	*G. tritici*	Gt 16.NZ.1d
S. cylindrosporus	H23-SB-2B	*G. tritici*	Gt 17LH(4)8d
S. cylindrosporus	H23-SB-2B	*G. tritici*	Gt 17LH(4)23d
S. cylindrosporus	H23-SB-2B	*G. tritici*	Gt 17LH(4)4e
S. cylindrosporus	H23-SB-2B	*G. tritici*	Gt 17LH(4)19d1
S. cylindrosporus	H23-SB-2B	*S. cylindrosporus*	H23-SB-2B
Unnamed *Magnaporthaceae* sp.	105C-2	*G. tritici*	Gt 16.NZ.1d

Unnamed *Magnaporthaceae* sp.	105C-2	*G. tritici*	Gt 17LH(4)8d
Unnamed *Magnaporthaceae* sp.	105C-2	*G. tritici*	Gt 17LH(4)23d
Unnamed *Magnaporthaceae* sp.	105C-2	*G. tritici*	Gt 17LH(4)4e
Unnamed *Magnaporthaceae* sp.	105C-2	*G. tritici*	Gt 17LH(4)19d1
Unnamed *Magnaporthaceae* sp.	105C-2	Unnamed *Magnaporthaceae* sp.	105C-2
G. hyphopodioides	NZ.129.2C.17*	*G. tritici*	Gt 16.NZ.1d*
G. hyphopodioides	NZ.129.2C.17	*G. tritici*	Gt 17LH(4)8d
G. hyphopodioides	NZ.129.2C.17	*G. tritici*	Gt 17LH(4)23d
G. hyphopodioides	NZ.129.2C.17	*G. tritici*	Gt 17LH(4)4e
G. hyphopodioides	NZ.129.2C.17	*G. tritici*	Gt 17LH(4)19d1
G. hyphopodioides	NZ.129.2C.17*	*G. hyphopodioides*	NZ.129.2C.17*
G. hyphopodioides	NZ.164.1B.17	*G. tritici*	Gt 16.NZ.1d
G. hyphopodioides	NZ.164.1B.17	*G. tritici*	Gt 17LH(4)8d
G. hyphopodioides	NZ.164.1B.17	*G. tritici*	Gt 17LH(4)23d
G. hyphopodioides	NZ.164.1B.17	*G. tritici*	Gt 17LH(4)4e
G. hyphopodioides	NZ.164.1B.17	*G. tritici*	NZ.129.2C.17
G. hyphopodioides	NZ.164.1B.17	*G. hyphopodioides*	NZ.164.1B.17
G. hyphopodioides	NZ.160.1A.15*	*G. tritici*	Gt 16.NZ.1d*
G. hyphopodioides	NZ.155.2C.17*	*G. tritici*	Gt 16.NZ.1d*
G. hyphopodioides	NZ.143.1A.17*	*G. tritici*	Gt 16.NZ.1d*
G. hyphopodioides	NZ.160.1A.15*	*G. hyphopodioides*	NZ.160.1A.15*
G. hyphopodioides	NZ.155.2C.17*	*G. hyphopodioides*	NZ.155.2C.17*
G. hyphopodioides	NZ.143.1A.17*	*G. hyphopodioides*	NZ.143.1A.17*
G. tritici	Gt 16.NZ.1d*	*G. tritici*	Gt 16.NZ.1d*
G. tritici	Gt 17LH(4)8d	*G. tritici*	Gt 17LH(4)8d
G. tritici	Gt 17LH(4)23d	*G. tritici*	Gt 17LH(4)23d
G. tritici	Gt 17LH(4)4e	*G. tritici*	Gt 17LH(4)4e
G. tritici	Gt 17LH(4)19d1	*G. tritici*	Gt 17LH(4)19d1

Table 3.4 Fungal confrontation assays between *G. hyphopodioides*, *G. tritici* and different endophytic and pathogenic species. Control treatments are highlighted in grey.

Side A		Side B	
Fungal species	Isolate	Fungal species	Isolate
G. hyphopodioides	NZ.129.2C.17	*I. crassa*	16LH14d
G. hyphopodioides	NZ.129.2C.17	*T. hamatum*	GD12
G. hyphopodioides	NZ.129.2C.17	*S. sclerotiorum*	GT18
G. hyphopodioides	NZ.129.2C.17	*F. graminearum*	10FG131
G. hyphopodioides	NZ.129.2C.17	*F. culmorum*	UK99

G. tritici	16.NZ.1d	*I. crassa*	16LH14d
G. tritici	16.NZ.1d	*T. hamatum*	GD12
G. tritici	16.NZ.1d	*S. sclerotiorum*	GT18
G. tritici	16.NZ.1d	*F. graminearum*	10FG131
G. tritici	16.NZ.1d	*F. culmorum*	UK99
I. crassa	16LH14d	*I. crassa*	16LH14d
T. hamatum	GD12	*T. hamatum*	GD12
S. sclerotiorum	GT18	*S. sclerotiorum*	GT18
F. graminearum	10FG131	*F. graminearum*	10FG131
F. culmorum	UK99	*F. culmorum*	UK99
G. hyphopodioides	NZ.129.2C.17	*G. hyphopodioides*	NZ.129.2C.17
G. tritici	16.NZ.1d	G. tritici	16.NZ.1d

3.3.2 Multiple interaction confrontation assays

Multiple interaction confrontation assays were used to investigate intra-species interactions between different *G. hyphopodioides* isolates and different *G. tritici* isolates. PDA plates were set up in the same manner as above, with the exception that four fungal plugs were added per plate at equal distances. In assays A and B, *G. hyphopodioides* isolates obtained from different Rothamsted field sites were plated together. In assays C and D, *G. tritici* isolates of different genetic “types” were plated together (see table 3.5). Plates were sealed with parafilm and stored at 21 °C for 14 days in the dark. Four replicates were set up for each treatment and the experiment was carried out twice. Time-course images of confrontation assays were taken as above.

Table 3.5 List of fungal isolates used in *G. hyphopodioides* and *G. tritici* intra-species confrontation assays.

Assay	Isolate order	Isolate name	ITS Sequence Confirmation
A	1	63B-1	*G. hyphopodioides*
	2	NZ.24.2A.15	*G. hyphopodioides*
	3	S.03.13	*G. hyphopodioides*
	4	P.09.13	*G. hyphopodioides*
B	1	105C-1	*G. hyphopodioides*
	2	NZ.129.2C.17	*G. hyphopodioides*
	3	S.03.13	*G. hyphopodioides*
	4	P.10.13	*G. hyphopodioides*
C	1	Gt 17LH(4)8d	*G. tritici*
	2	Gt 17LH(4)9d2	*G. tritici*
	3	Gt 17LH(4)23d	*G. tritici*
	4	Gt 17LH(4)4e	*G. tritici*
D	1	16.NZ.1d	*G. tritici*
	2	Gt 17LH(4)8d	*G. tritici*
	3	Gt 17LH(4)23d	*G. tritici*
	4	Gt 17LH(4)9d2	*G. tritici*

3.3.3 Seedling co-inoculation assays:

Plastic drinking cups (7.5 cm wide x 11 cm tall) were used as plant pots. Pots were filled with 9 cm of damp horticultural sand and ten wheat seeds cv. Hereward were sown on the surface. Seeds were covered with a layer of grit to retain moisture and increase humidity for germination and fungal colonisation. Pots were placed in a controlled environment growth room (16 hr day, light intensity 250 µmols, 15 °C day, 10 °C night, watered twice a week) using a randomised block design generated in Genstat 20th Edition.

Liquid inoculum was prepared by adding ten fungal plugs (taken from the leading edge of a 2-week old fungal colony using a number 4 cork-borer) to 400 ml potato dextrose broth (PDB) in a conical flask. The fungal isolates used in these experiments are detailed in table 3.6. Flasks were covered and placed in an orbital incubator for 7 days at 25 °C, 120 RPM. Liquid cultures were homogenised by passing through a 2.8 mm sieve. A 20 ml aliquot of the homogenised fungal culture was mixed with 30 ml water and added to each pot. For treatments where

two fungal species were added at the same time, 20 ml of each fungal culture was combined and mixed with 10 ml distilled water, to make up 50 ml mixed liquid inoculum.

Table 3.6 Fungal isolates used in the co-inoculation experiments.

Fungal species	Isolate
G. tritici	Gt 16.NZ.1d
G. hyphopodioides	NZ.129.2C.17
Unnamed *Magnaporthaceae* sp.	105C-2
S. cylindrosporus	H23-SB-2B

In experiment 1, *G. hyphopodioides*, *S. cylindrosporus* and the unnamed *Magnaporthaceae* species were added to pots containing wheat plants either 2 weeks before, at the same time, or 2 weeks after *G. tritici* (see table 3.7). Inoculum was poured directly into the pots at the stem base. However, this method led to some inoculum becoming trapped in the upper grit layer, resulting in variable amounts of viable inoculum in each pot. In experiments 2 and 3, plants were inoculated with *G. hyphopodioides* or the unnamed *Magnaporthaceae* species 2 weeks before, one week before, at the same time, or two weeks after *G. tritici* (see table 3.8). *S. cylindrosporus* was not included. An improved inoculation method was adopted whereby liquid inoculum was poured through a funnel placed 1 inch into the sand, allowing the inoculum to be delivered directly to the root system.

The first inoculum treatment was applied after 2 weeks of growth, with the exception of treatments 4 and 8 in experiments 2 and 3 (table 3.8), where the first inoculum treatment was applied at week 3. In the PDB control treatment (treatment 1), PDB was applied at week 2 and 4. In the *G. tritici* control treatment (treatment 2), PDB was applied at week 2 and *G. tritici* was applied at week 4. All plants were harvested 3 weeks after the final inoculum addition (at week 7), to allow fungi to colonise and take-all disease symptoms to develop.

Table 3.7 Treatment details for co-inoculation experiment 1.

	Treatment	Replicates
1	PDB control	A, B, C, D, E
2	*G. tritici* control	A, B, C, D, E
3	*G. hyphopodioides* 2-weeks prior to *G. tritici*	A, B, C, D, E
4	*G. hyphopodioides* + *G. tritici* co-inoculation	A, B, C, D, E
5	*G. hyphopodioides* 2-weeks after *G. tritici*	A, B, C, D, E
6	*S. cylindrosporus* 2-weeks prior to *G. tritici*	A, B, C, D, E
7	*S. cylindrosporus* + *G. tritici* co-inoculation	A, B, C, D, E
8	*S. cylindrosporus* 2-weeks after *G. tritici*	A, B, C, D, E
9	Unnamed *Magnaporthaceae* sp. 2-weeks prior to *G. tritici*	A, B, C, D, E
10	Unnamed *Magnaporthaceae* sp. + *G. tritici* co-inoculation	A, B, C, D, E
11	Unnamed *Magnaporthaceae* sp. 2-weeks after *G. tritici*	A, B, C, D, E

Table 3.8 Treatment details for co-inoculation experiments 2 and 3*.

	Treatment	Replicates
1	PDB control	A, B, C, D, E, F*
2	*G. tritici* control	A, B, C, D, E, F*
3	*G. hyphopodioides* 2-weeks prior to *G. tritici*	A, B, C, D, E, F*
4	*G. hyphopodioides* 1-week prior to *G. tritici*	A, B, C, D, E, F*
5	*G. hyphopodioides* + *G. tritici* co-inoculation	A, B, C, D, E, F*
6	*G. hyphopodioides* 2-weeks after *G. tritici*	A, B, C, D, E, F*
7	Unnamed *Magnaporthaceae* sp. 2-weeks prior to *G. tritici*	A, B, C, D, E, F*
8	Unnamed *Magnaporthaceae* sp. 1-week prior to *G. tritici*	A, B, C, D, E, F*
9	Unnamed *Magnaporthaceae* sp. + *G. tritici* co-inoculation	A, B, C, D, E, F*
10	Unnamed *Magnaporthaceae* sp. 2-weeks after *G. tritici*	A, B, C, D, E, F*

3.3.4 Disease assessments

Due to the visual similarity between hyphae of *G. tritici* and the non-pathogenic *Magnaporthaceae* species, the percentage of roots with runner hyphae was not assessed in these experiments. Instead, colonisation by the non-pathogenic species was confirmed by examining root samples under a stereomicroscope for the presence of sub-epidermal vesicles, which are characteristic structures produced by these species in wheat. All plants were assessed for take-all disease using the method outlined in chapter 2.5. In experiment 3, additional disease severity measurements were taken from three out of six replicates using the method outlined in chapter 2.5.

3.3.5 Quantification of *G. tritici* fungal biomass by qPCR

Quantification of *G. tritici* fungal biomass was carried out in experiment 3 only. Following visual assessments, the first 10 cm of root material in replicates A, B and C was removed from each seedling and flash frozen in liquid nitrogen. DNA extractions were performed as described in chapter 2.8. qPCRs were carried out as described in chapter 2.14. Three technical replicates were analysed from each DNA sample.

3.3.6 Plant biomass measurements

Seedling root and shoot biomass measurements were carried out following visual assessments, as described in chapter 2.6. In experiments 1 and 2, plant samples from all five replicates were taken for biomass measurements. In experiment 3, biomass measurements were taken from plant samples in replicates D, E and F only.

3.4 Results

3.4.1 Fungal confrontation assays

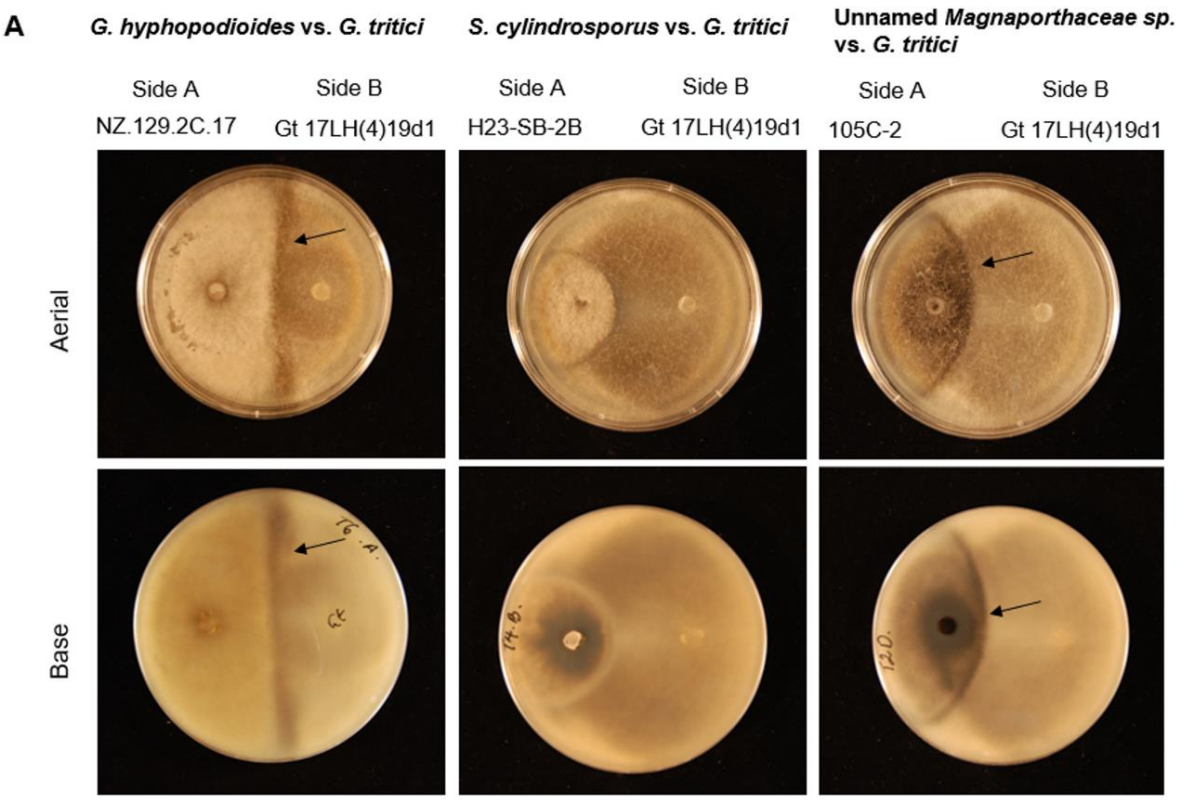
To investigate the role of direct hyphal interaction in the control of take-all disease by non-pathogenic *Magnaporthaceae* species, a series of fungal confrontation assays were conducted on potato dextrose agar (PDA). *G. hyphopodioides* was the main non-pathogenic species of interest due to its frequent isolation from

several arable field sites at Rothamsted Research. The *G. hyphopodioides* isolate NZ.129.2C.17 was a key focus due to its isolation from a field plot containing the high *G. hyphopodioides*-building wheat cultivar Scout (Osborne et al., 2018). In addition, the *G. tritici* isolate Gt17LH(4)19d1 was of particular interest because it was chosen for *de novo* genome sequencing in a collaboration with the Earlham Institute and has also been investigated in subsequent chapters. Though not selected for genome sequencing, the *G. tritici* isolate Gt16.NZ.1d was also of interest in this chapter due to its high level of pathogenicity.

Prior to hyphal contact, the individual growth rates of *G. tritici* and *G. hyphopodioides* colonies did not significantly differ from the dual colony controls (ANOVA: $F=0.39$, d.f. 5, 18, $p=0.85$, see appendix A.1). Furthermore, no obvious inhibition zone was produced and hyphae did not show signs of increased melanisation, suggesting that neither species produce diffusible antifungal compounds or VOCs *in vitro*. Additional studies using “sandwich” plate assays further confirmed that *G. hyphopodioides* fungal volatiles do not contribute to *G. tritici* inhibition *in vitro* (see appendix A.1). In confrontation assays, fungal colonies met after 5 days of growth and surprisingly, darkly coloured hyphae were observed in the hyphal interaction zone after 6-7 days of growth (figure 3.1). This response was not observed when colonies were grown in “sandwich” plate assays, further confirming that direct hyphal interaction is required for the response (see appendix A.1). Based on the crucial role of melanin in fungal stress responses (Cordero & Casadevall, 2017), the darkly coloured hyphae were hypothesised to be highly melanised. This melanisation response occurred when *G. hyphopodioides* isolates were confronted with both genetic type A and type B *G. tritici* isolates (table 3.9). However, it was not clear whether the melanised hyphae belonged to *G. hyphopodioides, G. tritici,* or both species.

The melanisation response was also observed in confrontations between the unnamed *Magnaporthaceae* species and *G. tritici.* Conversely, the melanisation response was not observed when *S. cylindrosporus* was confronted with *G. tritici*; this was true for all *G. tritici* isolates tested (table 3.9). Hyphal melanisation was not observed in the dual colony control assays which comprised two colonies of

the same isolate and species (figure 3.1). Furthermore, melanisation was not observed when several different *G. hyphopodioides* or *G. tritici* isolates were plated together in intra-species confrontation assays (figure 3.2).



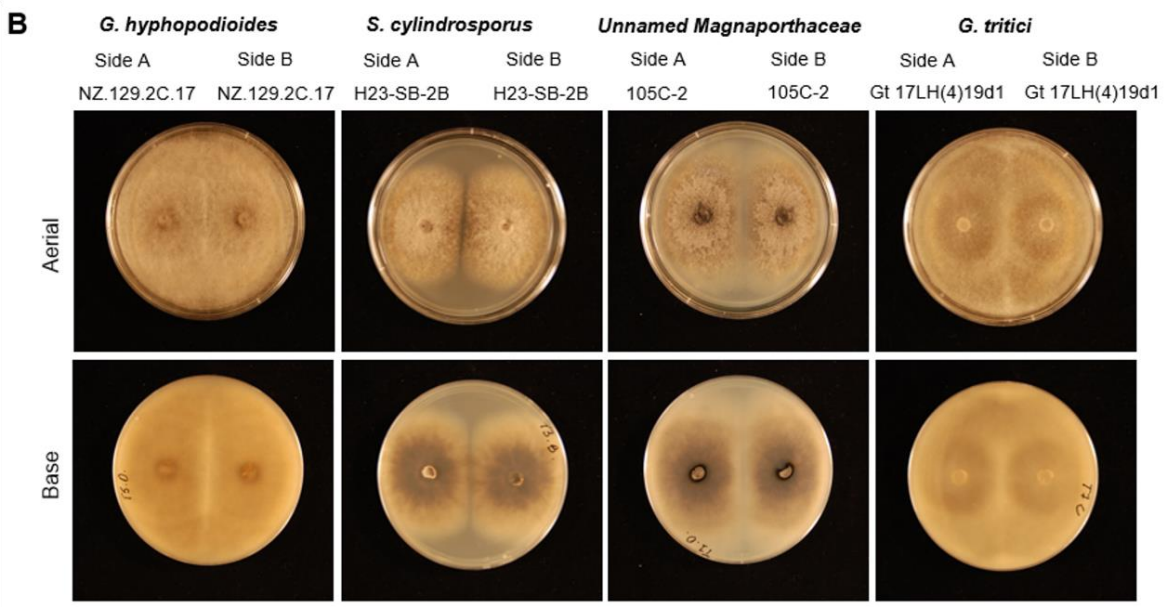


Figure 3.1 Representative images of fungal confrontation assays between non-pathogenic *Magnaporthaceae* species and *G. tritici.* A. Confrontation assays carried out on 100% PDA plates. B. Dual colony control assays. Black arrows indicate a melanised hyphal interaction zone. Images were taken after 11 days of growth, assays containing *S. cylindrosporus* colonies were imaged after 18 days due to the slow growth rate of this species. See previous page.

Table 3.9 Hyphal melanisation in confrontation assays between *G. tritici* and different non-pathogenic *Magnaporthaceae* species.

Non-pathogenic *Magnaporthaceae* species	Isolate	*G. tritici* isolate	*G. tritici* genetic "type"	Melanisation in the interaction zone? (Y/N)
S. cylindrosporus	H23-SB-2B	Gt 16.NZ.1d	A	N
	H23-SB-2B	Gt 17LH(4)8d	A	N
	H23-SB-2B	Gt 17LH(4)19d1	A	N
	H23-SB-2B	Gt 17LH(4)23d	B	N
	H23-SB-2B	Gt 17LH(4)4e	B	N
Unnamed *Magnaporthaceae* sp.	105C-2	Gt 16.NZ.1d	A	Y
	105C-2	Gt 17LH(4)8d	A	Y
	105C-2	Gt 17LH(4)19d1	A	Y
	105C-2	Gt 17LH(4)23d	B	Y
	105C-2	Gt 17LH(4)4e	B	Y
G. hyphopodioides	NZ.129.2C.17	Gt 16.NZ.1d	A	Y
	NZ.129.2C.17	Gt 17LH(4)8d	A	Y
	NZ.129.2C.17	Gt 17LH(4)19d1	A	Y
	NZ.129.2C.17	Gt 17LH(4)23d	B	Y
	NZ.129.2C.17	Gt 17LH(4)4e	B	Y
	NZ.164.1B.17	Gt 16.NZ.1d	A	Y
	NZ.164.1B.17	Gt 17LH(4)8d	A	Y
	NZ.164.1B.17	Gt 17LH(4)19d1	A	Y
	NZ.164.1B.17	Gt 17LH(4)23d	B	Y
	NZ.164.1B.17	Gt 17LH(4)4e	B	Y
	NZ.160.1A.15	Gt 16.NZ.1d	A	Y
	NZ.155.2C.17	Gt 16.NZ.1d	A	Y
	NZ.143.1A.17	Gt 16.NZ.1d	A	Y

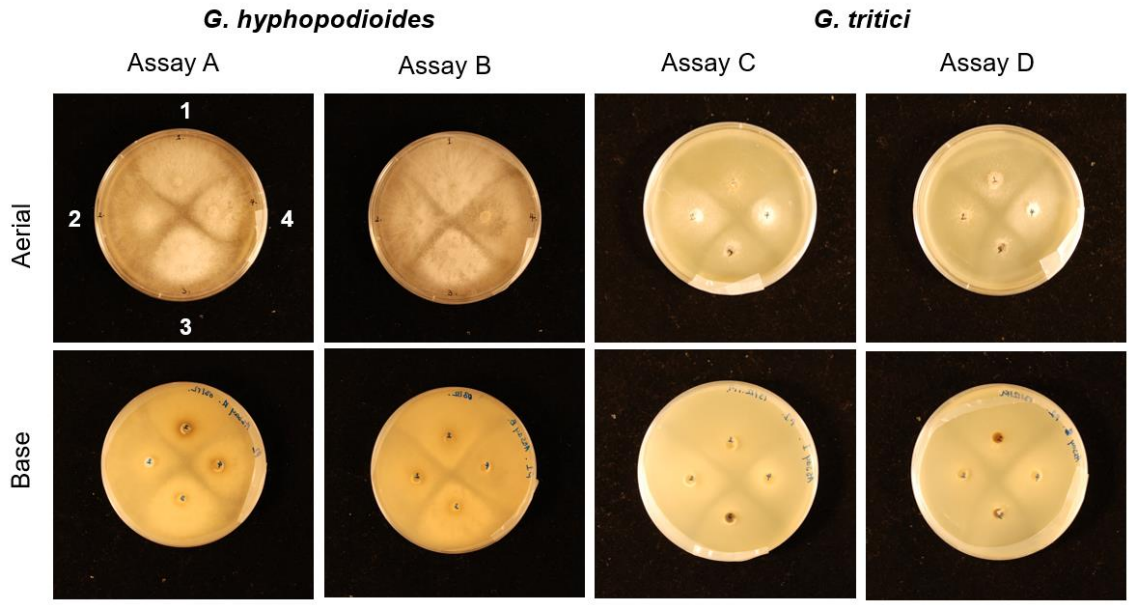


Figure 3.2 *G. hyphopodioides* and *G. tritici* intra-species confrontation assays on 100% PDA. Imaged at 11 days of fungal growth. See table 3.5 for isolate details.

To determine whether the melanisation response was altered at different nutrient levels, a subset of *G. hyphopodioides* vs. *G. tritici* confrontation assays were also conducted on 50% and 10% PDA. Interestingly, the melanisation response was absent when grown on 50% PDA, but not 10% PDA (table 3.10, figure 3.3). Plating the two fungal colonies at a separation distance of 2 cm rather than 4 cm also altered the interaction, favouring the growth of *G. hyphopodioides* over *G. tritici* (figure 3.3). Thus, *in vitro* studies of this nature are highly variable and are unlikely to be representative of *in planta* interactions. Nevertheless, the assays demonstrate that direct contact between *G. tritici* and *G. hyphopodioides* often results in hyphal melanisation, which is likely indicative of hyphal stress.

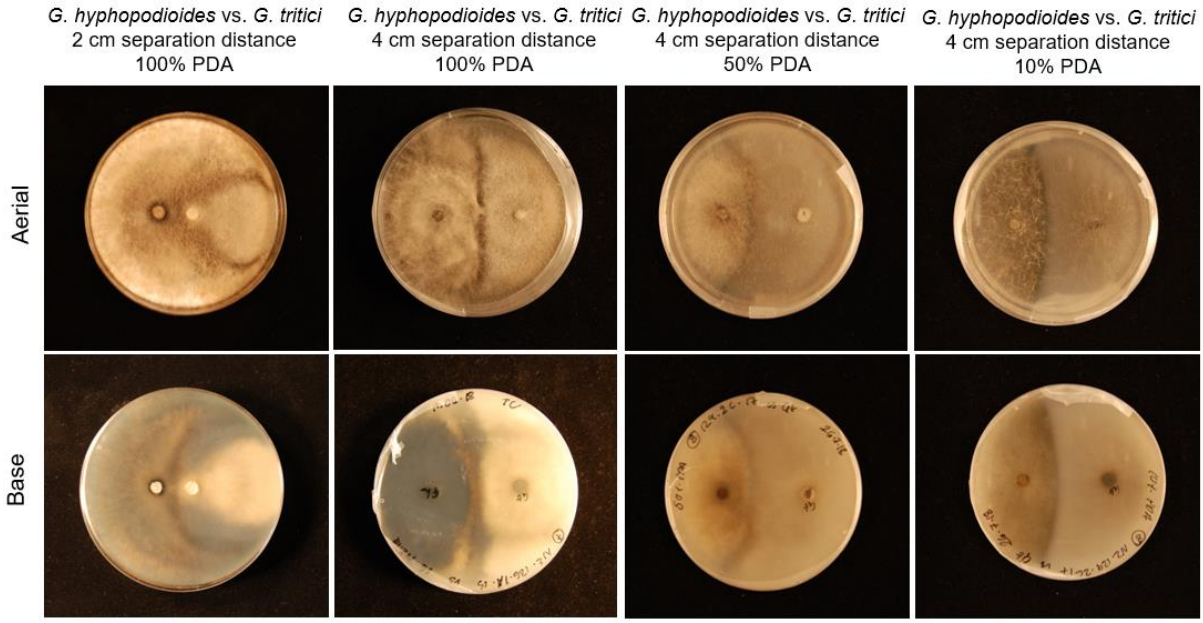


Figure 3.3 Representative images demonstrating that colony separation distance and nutrient content of growth media affect the melanisation response between *G. hyphopodioides* (NZ.129.2C.17) and *G. tritici* (Gt 16.NZ.1d). Imaged at 11 days of growth.

Table 3.10 Melanisation response at different nutrient contents

PDA concentration	*G. hyphopodioides* isolate	*G. tritici* isolate	Melanisation in the interaction zone? (Y/N)
100%	NZ.129.2C.17	Gt 16.NZ.1d	Y
	NZ.160.1A.15	Gt 16.NZ.1d	Y
	NZ.155.2C.17	Gt 16.NZ.1d	Y
	NZ.143.1A.17	Gt 16.NZ.1d	Y
50%	NZ.129.2C.17	Gt 16.NZ.1d	N
	NZ.160.1A.15	Gt 16.NZ.1d	N
	NZ.155.2C.17	Gt 16.NZ.1d	Y
	NZ.143.1A.17	Gt 16.NZ.1d	N
10%	NZ.129.2C.17	Gt 16.NZ.1d	Y
	NZ.160.1A.15	Gt 16.NZ.1d	Y
	NZ.155.2C.17	Gt 16.NZ.1d	Y
	NZ.143.1A.17	Gt 16.NZ.1d	Y

To investigate the specificity of the melanisation response, *G. hyphopodioides* (isolate NZ.129.2C.17) and *G. tritici* (isolate 16.NZ.1d) were confronted with five different fungal species on 100% PDA (figure 3.4). Details of these species can

be found in table 3.2. *G. hyphopodioides* had a slower growth rate than *T. hamatum* and *S. sclerotium,* and was subsequently outcompeted. Hyphal melanisation did not increase in *G. hyphopodioides* or *G. tritici* colonies when confronted with any of the species tested. However, *F. graminearum* and *F. culmorum* produced a red pigment when confronted with *G. hyphopodioides*. A red pigment was also produced by *F. culmorum* when confronted with *G. tritici,* though in comparatively lower amounts. Taken together, the findings described here suggest that the melanisation response is likely specific to interactions between certain *Magnaporthaceae* species.

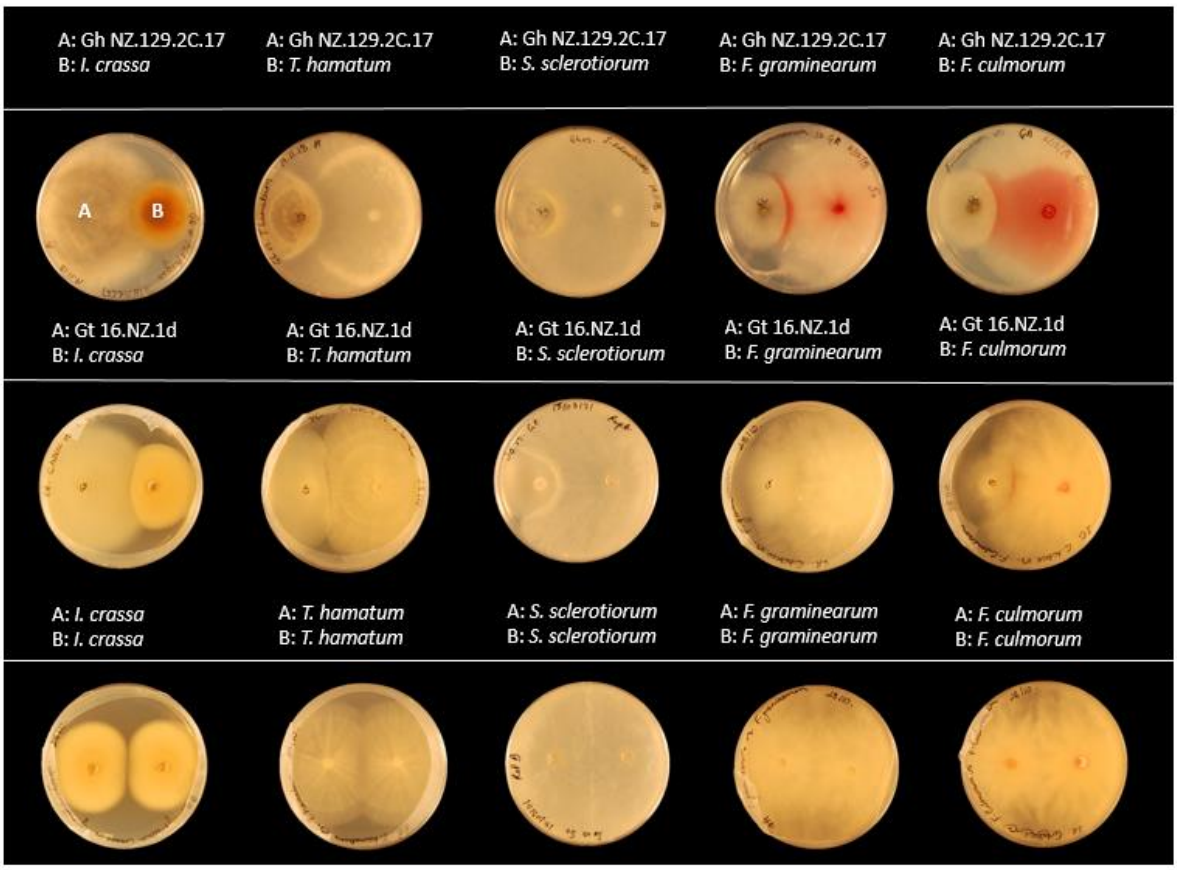


Figure 3.4 *G. hyphopodioides* and *G. tritici* inter-species assays with *I. crassa, T. hamatum, S. sclerotiorum, F. graminearum* and *F. culmorum.* Images have been taken of the base of the plate to aid visualisation of the hyphal interaction zone. Gh= *G. hyphopodioides*, Gt= *G. tritici.* Imaged at 11 days of fungal growth.

3.4.2 Seedling co-inoculation assay: experiment 1

Despite evidence of hyphal stress, the *in vitro* data reported above implies that direct interaction alone is unlikely to be sufficient for effective take-all control. To investigate the hypothesis that non-pathogenic *Magnaporthacea*e species provide protection against take-all disease by induced plant resistance, and therefore must colonise the root first to provide effective disease control, several co-inoculation assays were designed and optimised.

G. hyphopodioides, *S. cylindrosporus* and the unnamed *Magnaporthaceae* species were added to pots containing wheat plants either 2 weeks before, at the same time, or 2 weeks after *G. tritici.* Seedlings were assessed for disease symptoms and plant biomass measurements were taken. Take-all disease control by *G. hyphopodioides* and the unnamed *Magnaporthaceae* species was most effective when inoculum was added 2 weeks prior to *G. tritici* (figure 3.5 A). However, unlike *G. hyphopodioides*, the unnamed *Magnaporthaceae* species did not significantly reduce take-all disease when added at the same time as *G. tritici.* This may suggest that *G. hyphopodioides* is able to infect the root quicker than *G. tritici*, or that direct hyphal interaction provided some level of take-all control at this time point. In contrast, *S. cylindrosporus* did not significantly reduce take-all disease and disease levels were not significantly affected by the timing of inoculum additions.

Despite disease levels being significantly reduced in several treatments, plant biomass never fully recovered to un-inoculated levels (figure 3.5 B, appendix A.2; table A.2.2). This suggests that disease reduction by non-pathogenic species may not translate to improved plant health or grain yield, perhaps indicating a trade-off between induced resistance and plant growth (see chapter 7 for further investigation). In all cases, adding the non-pathogenic species two weeks after *G. tritici* resulted in a significant reduction in shoot biomass compared to the *G. tritici* control treatment, even though the observed disease levels were not significantly altered (figure 3.5 A, B).

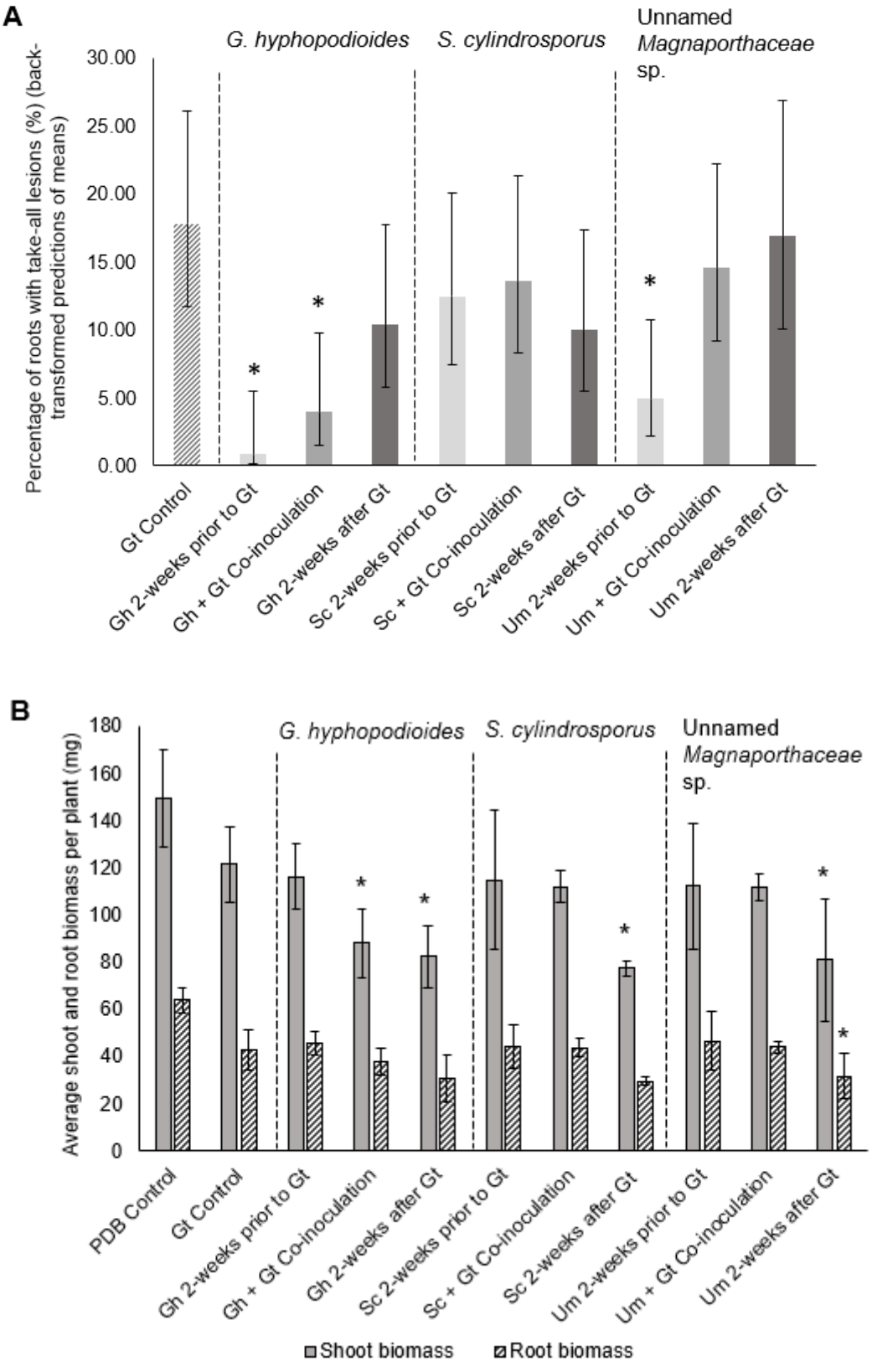


Figure 3.5 Take-all disease levels and plant biomass in **co-inoculation experiment 1**. A. The percentage of roots with take-all lesions. Data represent back-transformed

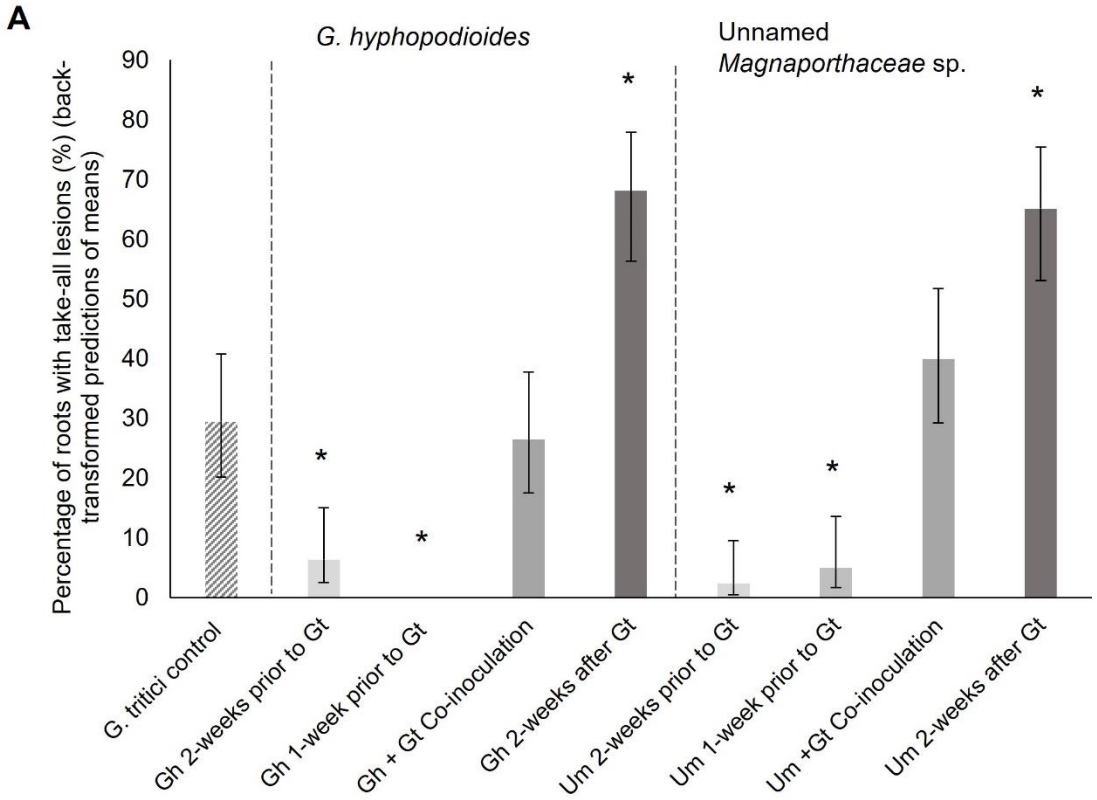
predictions of means calculated using a Generalised Linear Regression Model (GLM). Error bars represent 95% confidence intervals. Asterisks indicate significant differences to the *G. tritici* control as calculated by Dunnett's post-hoc test ($p<0.05$). B. Average dry biomass of roots and shoots per plant (mg). Error bars indicate standard deviation. Asterisks indicate significant differences to the *G. tritici* control as calculated by Tukey's multiple comparisons test ($p<0.05$). Gt = *G. tritici*, Gh = *G. hyphopodioides*, Sc = *S. cylindrosporus*, Um = Unnamed *Magnaporthaceae* sp. See previous page.

Although common in artificially inoculated take-all experiments (Puga-Freitas et al., 2016), take-all disease levels were highly variable among replicates of the same treatment. Therefore, the experiment was repeated twice more (see below) using an altered inoculation protocol. Specifically, a funnel was used to deliver inoculum to the root system, preventing inoculum from being trapped in the upper grit layer of the pot and thereby reducing variation between pots. The method also aimed to increase take-all disease levels, which were lower than expected. As *S. cylindrosporus* did not achieve effective disease control, the species was not included in the following experiments. An additional treatment was added 1-week prior to *G. tritici,* allowing further investigation into the effective period of induced resistance.

3.4.3 Seedling co-inoculation assay: experiments 2 and 3

Adopting an alternative inoculation method resulted in increased baseline levels of take-all disease in both experiments. However, there were still large differences between the two experiments, with the percentage of roots with lesions in the *G. tritici* control treatment being around 30% higher in experiment 3 than experiment 2 (see figures 3.6 A and 3.8 A). In experiment 3, the unnamed *Magnaporthaceae* species significantly reduced take-all disease when inoculated at the same time as *G. tritici,* however this was not the case in experiment 2. Furthermore, adding the non-pathogenic species 2 weeks after *G. tritici* resulted in a significant increase in disease levels and as a result, both root and shoot biomass were significantly reduced in these treatments in experiment 2 (figures 3.6 and 3.7). Conversely, although there was a trend for increased disease levels in these treatments in experiment 3, the differences were not significant and plant biomass was also unaffected (figure 3.8 A, B).

qPCR analysis of *G. tritici* fungal biomass (indicated by ng *G. tritici* DNA/ng total DNA) taken from three replicates in experiment 3 showed mixed support of visual assessments. Though *G. tritici* fungal biomass was significantly reduced in plants pre-treated with *G. hyphopodioides*, the same was not true for plants pre-treated with the unnamed *Magnaporthaceae* species (figure 3.8 A). This discrepancy may be explained by the amplification of *G. tritici* DNA from non-infective or dead mycelium, and hence qPCR data should not be interpreted in isolation.



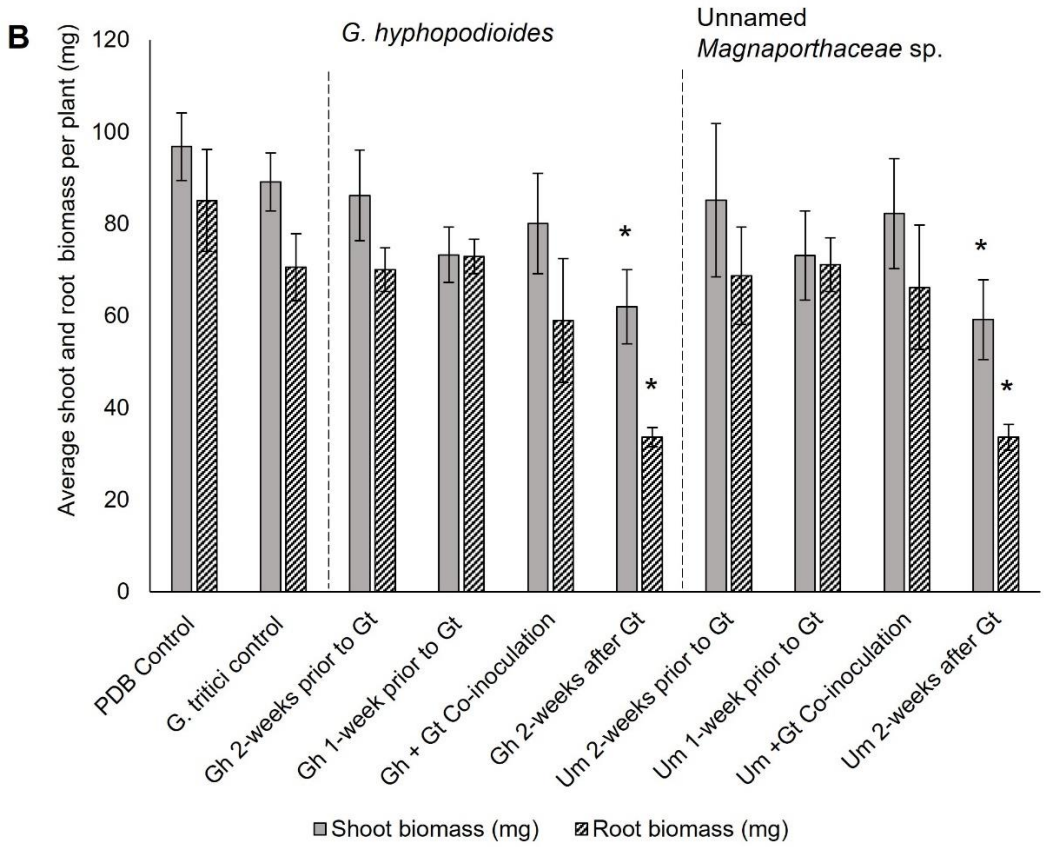


Figure 3.6 Take-all disease levels and plant biomass in **co-inoculation experiment 2**. A. The percentage of roots with take-all lesions. Data represent back-transformed predictions of means calculated using a Generalised Linear Regression Model (GLM). Error bars represent 95% confidence intervals. Asterisks indicate significant differences to the *G. tritici* control as calculated by Dunnett's post-hoc test ($p<0.05$). B. Average dry biomass of roots and shoots per plant (mg). Error bars indicate standard deviation. Asterisks indicate significant differences to the *G. tritici* control as calculated by Tukey's multiple comparisons test ($p<0.05$). Gt = *G. tritici*, Gh = *G. hyphopodioides*, Sc = *S. cylindrosporus*, Um = Unnamed *Magnaporthaceae* sp.

A

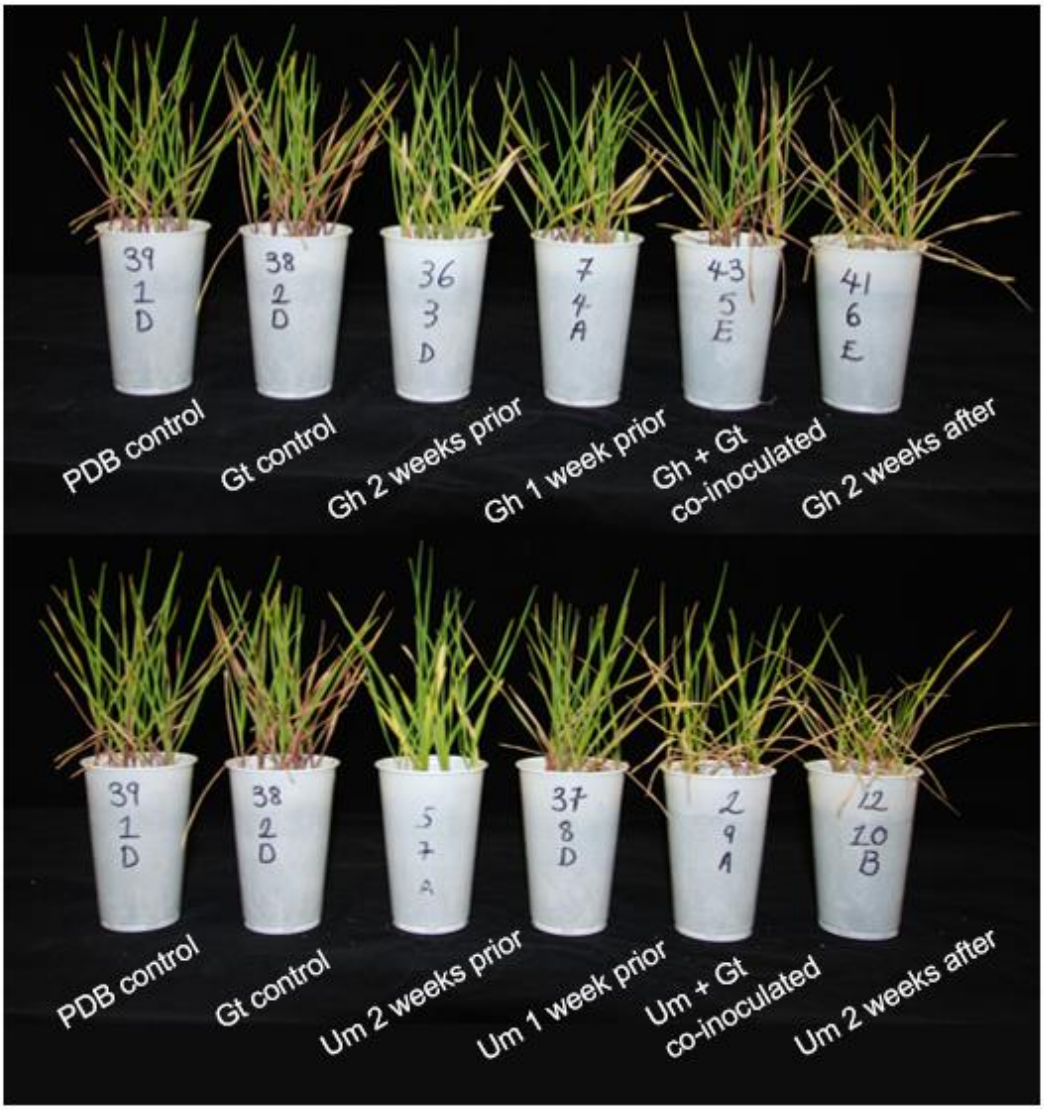

PDB control
Gt control
Gh 2 weeks prior
Gh 1 week prior
Gh + Gt co-inoculated
Gh 2 weeks after
PDB control
Gt control
Um 2 weeks prior
Um 1 week prior
Um + Gt co-inoculated
Um 2 weeks after



Figure 3.7 Representative images of wheat seedlings in **co-inoculation experiment 2.** A. Images of foliar tissues. B. Images of root systems. Images taken after 7 weeks of growth. Gt = *G. tritici*, Gh= *G. hyphopodioides*, Um= Unnamed *Magnaporthaceae* sp.

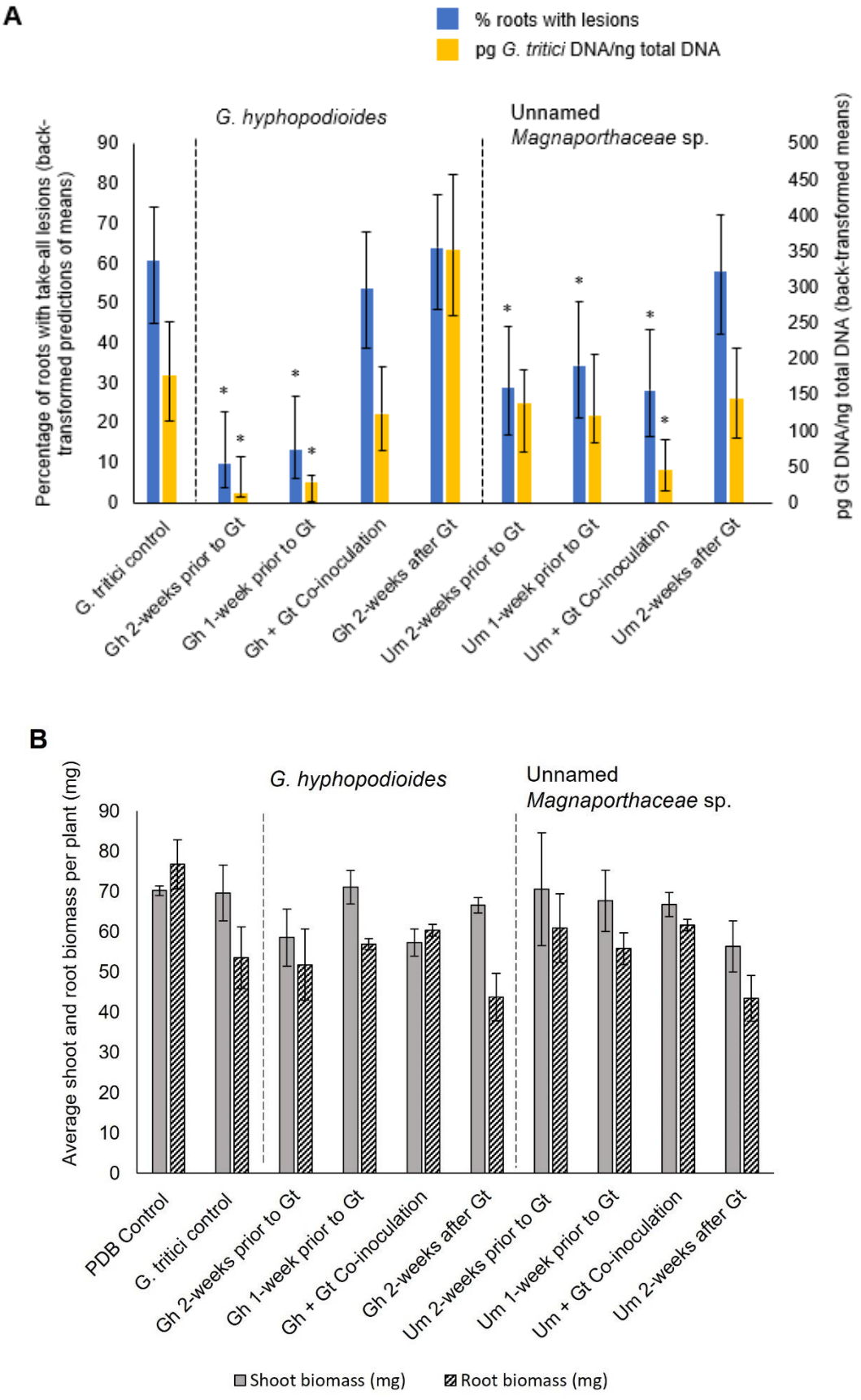

A
% roots with lesions
pg G. tritici DNA/ng total DNA
G. hyphopodioides
Unnamed Magnaporthaceae sp.
Percentage of roots with take-all lesions (back-transformed predictions of means)
pg Gt DNA/ng total DNA (back-transformed means)
0
10
20
30
40
50
60
70
80
90
0
50
100
150
200
250
300
350
400
450
500
G. tritici control
Gh 2-weeks prior to Gt
Gh 1-week prior to Gt
Gh + Gt Co-inoculation
Gh 2-weeks after Gt
Um 2-weeks prior to Gt
Um 1-week prior to Gt
Um + Gt Co-inoculation
Um 2-weeks after Gt
B
G. hyphopodioides
Unnamed Magnaporthaceae sp.
Average shoot and root biomass per plant (mg)
0
10
20
30
40
50
60
70
80
90
PDB Control
G. tritici control
Gh 2-weeks prior to Gt
Gh 1-week prior to Gt
Gh + Gt Co-inoculation
Gh 2-weeks after Gt
Um 2-weeks prior to Gt
Um 1-week prior to Gt
Um + Gt Co-inoculation
Um 2-weeks after Gt
Shoot biomass (mg)
Root biomass (mg)

Figure 3.8 Take-all disease levels, *G. tritici* fungal biomass and plant biomass in **co-inoculation experiment 3.** A. The percentage of roots with take-all lesions and *G. tritici* fungal biomass levels (pg *G.tritici* DNA/ng total DNA). Data represent back-transformed means. Lesion data was analysed using a Generalised Linear Regression Model (GLM), fungal biomass data was analysed by ANOVA. Error bars represent 95% confidence intervals. Asterisks indicate significant differences to the *G. tritici* control as calculated by Dunnett's post-hoc test ($p<0.05$). B. The average shoot and root biomass per plant (mg) in a co-inoculation bioassay. Error bars indicate standard deviation. See previous page.

Despite the inconsistencies described above, both experiments highlight the ability of *G. hyphopodioides* and the unnamed *Magnaporthaceae* species to provide effective disease control when added either one or two weeks prior to *G. tritici,* supporting the hypothesis that take-all control by these species is a result of induced resistance in the plant. Disease severity measurements taken from three replicates in experiment 3 further highlight this finding. Severity data was analysed by ordinal logistic regression and analysis was adjusted for over dispersion (see appendix A.2; table A.2.8). The analysis indicated that *G. hyphopodioides* and the unnamed *Magnaporthaceae* species not only reduced take-all disease incidence, but also take-all disease severity when inoculated two weeks prior, one week prior, and in the case of the unnamed *Magnaporthaceae* species, at the same time as *G. tritici* (figure 3.9).

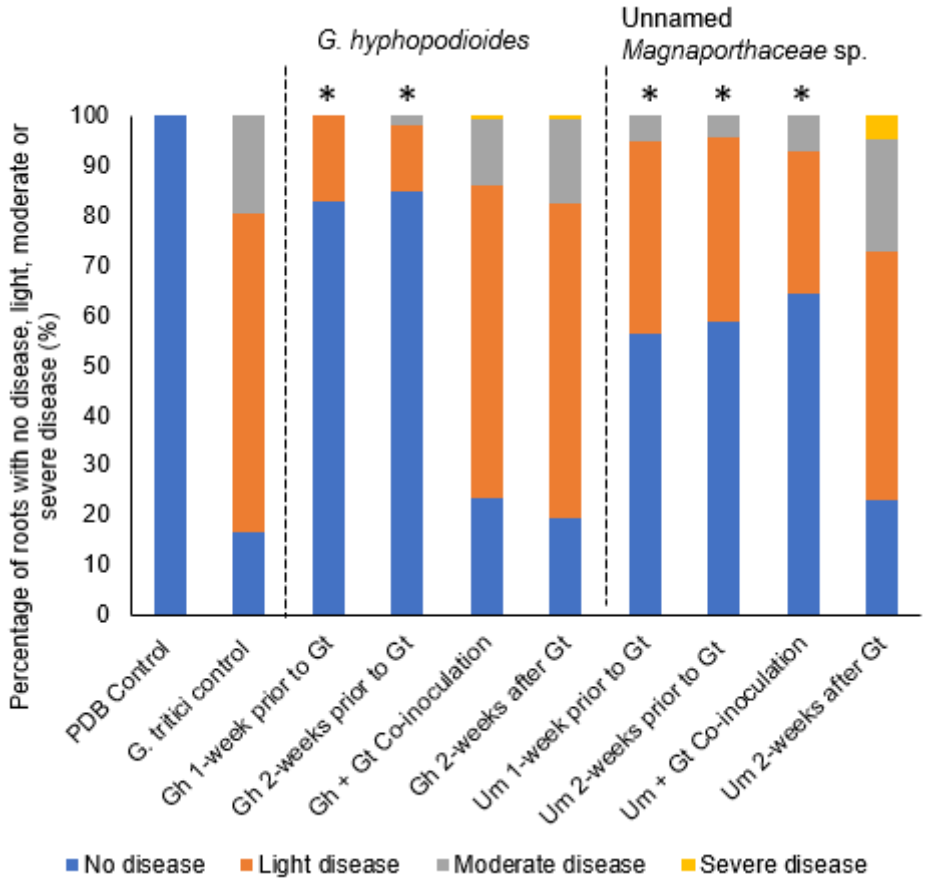


Figure 3.9 Take-all disease severity in **co-inoculation experiment 3.** Severity is represented by the percentage of roots with no disease (0% lesion coverage), light disease (1-25 % lesion coverage), moderate disease (26-50% lesion coverage) or severe disease (51-75% disease coverage), based on assessments of the first 10 cm of root material. Asterisks indicate significant differences to the *G. tritici* control as calculated by logistic ordinal regression analysis ($p<0.05$).

3.5 Discussion

Fungal endophytes are known to provide protection against pathogen attack through a range of strategies including the production of antifungal metabolites (Stracquadanio et al., 2020), the release of VOCs capable of pathogen inhibition (Studholme et al., 2013; Tilocca et al., 2020), direct hyphal interference through mycoparasitism (Rajani et al., 2021; Sarkar et al., 2019), the induction of physical barriers (e.g. lignification and suberisation of plant tissues) (Basińska-Barczak et al., 2020) and the priming of plant defence pathways (Martínez-Medina et al., 2017). Fungal endophytes may rely on a single strategy or a combination of

strategies to provide effective control. To investigate the mechanism(s) by which non-pathogenic *Magnaporthaceae* species control take-all disease, several *in vitro* hyphal assays and *in vivo* plant inoculation assays were carried out.

Fungal confrontation assays aimed to investigate the direct interaction between non-pathogenic *Magnaporthaceae* species and pathogenic *G. tritici.* The main species of interest was *G. hyphopodioides* (previously *Phialophora* sp. lobed hyphopodia), a non-pathogenic species frequently isolated in arable fields at Rothamsted and previously noted for its biocontrol potential (Wong et al., 1996). In addition, *S. cylindrosporus* (previously *Phialophora graminicola*), a species often isolated from plant samples and soil cores at Rothamsted grassland sites and also previously investigated as a potential biocontrol agent of take-all (Speakman & Lewis, 1978) was included in the investigation. Finally, an unnamed *Magnaporthaceae* species isolated from arable sites in the UK and Germany was investigated (Ulrich et al., 2000). Fungal growth was not inhibited prior to hyphal contact when *G. hyphopodioides, S. cylindrosporus* or the unnamed *Magnaporthaceae* species were confronted with *G. tritici*, indicating that diffusible fungal exudates or VOCs are unlikely to be involved in the control of take-all disease. Alternatively, hyphal contact may be required to trigger the production of non-diffusible bioactive compounds by these non-pathogenic species. Unfortunately, it was not possible to investigate the latter scenario in this project, due to the difficulties associated with identifying species specific compounds in mixed samples (samples would need to be taken from the interaction zone, and agar would need to be filtered out without lysing the fungal hyphae).

Colony growth was restricted and putative hyphal melanisation was observed in the interaction zone when *G. hyphopodioides* and the unknown *Magnaporthaceae* species were confronted with *G. tritici.* In both cases, melanisation occurred shortly after the colonies met, suggesting that direct hyphal interaction causes hyphal stress in at least one of the interacting species. This assumption is based on previous findings that the production of melanin can enhance the survival of fungi in stressful environments (Cordero & Casadevall, 2017; Eisenman & Casadevall, 2012). Within the *Magnaporthaceae,* melanin

deficient mutants of *Gaeumannomyces graminis,* a weak pathogen of cereals and grasses, were more sensitive to heavy metals than melanised strains. Furthermore, a constitutively melanised mutant was more resistant to lytic enzymes compared to the melanin deficient mutant (Frederick et al., 1999). Hyphal stress in the interaction zone may be a result of increased competition for nutrients and therefore nutrient deficiency, or as explored in chapter 1.7, due to the production of non-diffusible antifungal compounds, peptides or chitinases.

To determine the specificity of the melanisation response, *G. tritici* and *G. hyphopodioides* were confronted with several different fungal pathogens and endophytes. Neither *G. tritici* nor *G. hyphopodioides* became melanised when plated against the different species, suggesting that the melanisation response could be specific to interactions between certain *Magnaporthaceae* species. Interestingly, a pink/red pigment was localised to the interaction zone in *G. hyphopodioides* vs. *F. graminearum* and *G. hyphopodioides*/*G. tritici* vs. *F. culmorum* assays, though the amount of pigmentation was greater in response to *G. hyphopodioides.* Fusarium species are known to produce a range of secondary metabolites, often with characteristic pigmentation. One such example is aurofusarin, a red-coloured mycotoxin with antibiotic properties, produced by both *F. graminearum* and *F. culmorum* (Cambaza, 2018). Thus, perhaps both *G. tritici* and *G. hyphopodioides* can elicit defence responses in other fungal species.

Despite the valuable information provided by the studies described here, the *in vitro* experiments have significant limitations. For example, the level of melanisation observed in *G. hyphopodioides* vs. *G. tritici* assays was altered when colonies were separated at different distances and when assays were performed at different nutrient levels, highlighting the plasticity of fungal interactions and reinforcing the risk that *in vitro* interactions may not represent those occurring *in planta.*

Interestingly, nutrient content has also been found to alter melanised “barrage” formation between genetically different isolates of the same species (Micali & Smith, 2003). Vegetative incompatibility (VI) is a ubiquitous process amongst fungal ascomycetes and results in the programmed cell death of heterokaryotic

cells formed following anastomosis of genetically incompatible hyphae carrying different heterokaryon incompatibility (*het*) loci (Paoletti, 2016). However, the VI phenomenon describes interactions between genetically incompatible isolates of the same species, rather than between different fungal species. In this study, the melanisation response was not observed when different *G. hyphopodioides* or *G. tritici* isolates were plated together, however the number of interactions tested was limited and hence additional assays should be performed. Curiously, Novotný (1979) reported that multiple hyphal fusions were observed between *G. tritici* and *G. radicicola* during *in vitro* growth, resulting in the halted growth of both species. Therefore, an alternative explanation for the melanisation response described in this study could be that hyphal fusion between *G. tritici* and *G. hyphopodioides*/the unnamed *Magnaporthaceae* sp. results in an incompatibility response, hyphal melanisation and subsequent cell death. Thus, further investigations are now required to determine if hyphal fusion occurs in the interaction zone. The findings of these studies may have important implications for the safety of non-pathogenic *Magnaporthaceae* species as commercial biocontrol agents.

To investigate whether induced plant resistance plays a more significant role in the control of take-all disease by non-pathogenic *Magnaporthaceae* species, several co-inoculation seedling pot assays were carried out. Due to the difficulties in obtaining viable spores from *G. tritici*, inoculum was applied as mycelium in liquid media. However, despite the controlled conditions used to grow the mycelium, the current methodology is prone to variability. For instance, the amount of mycelium applied is likely to have differed between fungal species and between experiments. Furthermore, the nutrient content of the different PDB inoculum treatments is unlikely to have been consistent. To improve the current methodology, the following changes are proposed: after 5 days growth in liquid broth, homogenise the cultures using a blender and allow the mycelium to grow and recover for a further 2 days. Harvest mycelium by filtering the culture through sterile Miracloth (Merck, USA) by vacuum filtration. Weigh out a specific amount of mycelium and resuspend in 50 ml sterile distilled water (thereby removing any possible effects of the nutrient broth on plant growth) before applying to the roots

via a funnel inserted into the growth medium. This method is now being used successfully by members of take-all team at Rothamsted to investigate other potential biocontrol agents against take-all disease.

In the first experiment, non-pathogenic *G. hyphopodioides*, *S. cylindrosporus* and the unnamed *Magnaporthaceae* species were added either 2 weeks before, at the same time, or 2 weeks after *G. tritici*. Despite previous evidence in the literature demonstrating its biocontrol ability (Deacon, 1976b) *S. cylindrosporus* did not provide effective take-all control in any treatment. It is noteworthy that the same isolate did not induce a melanisation response in the *in vitro* hyphal interaction assays, and showed slower growth compared to *G. hyphopodioides* and the unnamed *Magnaporthaceae* species. The biocontrol ability of the *S. cylindrosporus* isolate investigated here may therefore have been reduced by the inability to colonise the root system before *G. tritici*, the inability to cause hyphal melanisation during direct interaction, or both. The species was therefore removed from subsequent experiments, though future investigation of other *S. cylindrosporus* isolates could be worthwhile.

Conversely, *G. hyphopodioides* and the unnamed *Magnaporthaceae* species successfully reduced both take-all disease incidence and severity when added to plants two weeks before or one week before *G. tritici*. This suggests that even very early colonisation is sufficient to induce plant resistance. Adding the species at the same time as *G. tritici* had mixed results, with the unnamed *Magnaporthaceae* species providing a significant reduction in disease levels in experiment 3 only, and *G. hyphopodioides* providing a significant reduction in experiment 1 only. The findings suggest that prior colonisation by the non-pathogenic species is required for effective disease reduction, supporting the hypothesis that take-all control is caused by induced plant resistance. This would explain the inconsistent results when the fungi were inoculated at the same time; if *G. tritici* is able to infect the roots first and reach the vasculature, then subsequent colonisation by the non-pathogenic species would not be sufficient to prevent further damage by *G. tritici* hyphae already present in the root stele. Therefore, if non-pathogenic species are to be developed as biocontrol agents,

care should be taken to select fast-growing isolates which could be applied as a seed coating.

Importantly, adding *G. hyphopodioides* or the unnamed *Magnaporthaceae* species after *G. tritici* resulted in increased levels of disease and reduced shoot and root biomass in experiment 2. Though the average number of roots with lesions did not significantly differ from the *G. tritici* control in experiment 1 or 3, the average shoot biomass was also significantly reduced compared to the *G. tritici* control in experiment 1. It is proposed that heavy infection by *G. tritici* prior to colonisation by the non-pathogenic species compromises plant growth and plant resistance mechanisms. Cellular damage caused by *G. tritici* infection may also lead to nutrient release, thus resulting in greater filamentous growth by *G. hyphopodioides* and the unnamed *Magnaporthaceae* sp. The cellular damage caused by *G. tritici* may also enable the non-pathogenic to penetrate further into the root tissues. This may drive greater competition between *G. hyphopodioides*/the unnamed *Magnaporthaceae* sp. and *G. tritici*, potentially leading to more widespread infection by *G. tritici* in an attempt to acquire more nutrients.

The findings described here have significant implications for the use of *G. hyphopodioides* and the unnamed *Magnaporthaceae* species as biocontrol agents and are vital to inform future control strategies. When added prior to *G. tritici*, *G. hyphopodioides* provided the most consistent disease control across the three experiments and based on severity measurements taken in experiment 3, resulted in the largest reduction in disease severity. However, the corresponding plant biomass measurements were largely inconsistent and require further investigation to allow meaningful interpretation. To reduce variability in future studies, seeds could be weighed and pre-germinated before planting. In addition, seedlings could be grown to the adult stage, enabling further investigation of plant health parameters and grain yield (see chapter 7). To ensure that *G. hyphopodioides* provides effective plant resistance against *G. tritici*, mycelium could be applied as a seed coating, a method that has proved effective for several other endophyte biocontrol agents (Rocha et al., 2019). Alternatively, farmers

could build *G. hyphopodioides* populations in the soil by growing 1st wheat cultivars known to promote the species, thereby providing protection against take-all disease when *G. tritici* levels increase in the following years (Osborne et al., 2018) (see chapter 7 for further investigation of this trait).

3.6 Future work

Differential fungal staining is not currently possible for the *Magnaporthaceae* species investigated here. Hence, it was not possible to determine which species were melanised in the fungal confrontation assays described above. Nevertheless, microscopy studies of hyphae in the interaction zone were not performed in this study and should be a priority for future studies. Samples of hyphae could be taken from the interaction zone and compared with distal regions of the fungal colony to determine whether interacting hyphae are capable of fusing or whether hyphae exhibit stress related phenotypes. For instance, samples could be assessed for hyphal swelling and cell viability stains such as trypan blue could be used to determine whether cell death occurs in the interaction zone. Improved genetic transformation techniques could enable the generation of fluorescently tagged isolates, facilitating future investigations into the role of direct hyphal interaction *in planta.*

The co-inoculation studies carried out in this chapter demonstrate that induced plant resistance plays a vital role in the control of take-all disease by certain non-pathogenic *Magnaporthaceae* species. However, the duration of effective resistance is unknown, as are the molecular mechanisms underpinning this resistance. To address these questions, co-inoculation studies could be repeated with an improved inoculation and seedling growth method as described earlier. *G. hyphopodioides* could be applied several weeks or even months before *G. tritici* to determine the effective length of the resistance. Long-lasting resistance would ensure that protection is provided throughout the growing season. Further studies should be carried out to determine if *G. hyphopodioides*-induced resistance provides effective take-all control in other wheat cultivars, and against other *G. tritici* isolates.

Studies are currently underway to confirm whether the induced resistance is local or systemic. Early pilot data generated in a split-root hydroponic system has indicated that *G. hyphopodioides*-induced resistance provides both local and systemic protection against *G. tritici*, however further replications and method optimisations are required to confirm this finding (see appendix A.3).

Finally, to understand the molecular mechanisms driving induced plant resistance, an RNA sequencing experiment investigating the wheat response to *G. hyphopodioides* colonisation and *G. tritici* infection was carried out at key stages of fungal infection (see chapter 5).

3.7 Summary

In summary, *in vitro* hyphal assays have demonstrated that diffusible antifungal metabolites or VOCs are unlikely to play a significant role in the control of take-all disease by non-pathogenic *Magnaporthaceae* species. Direct hyphal interaction between *G. hyphopodioides*/ the unnamed *Magnaporthaceae* species and *G. tritici* resulted in the melanisation of hyphae in the interaction zone, though this response alone is unlikely to be the only factor involved in take-all control. Co-inoculation of wheat seedlings have clearly demonstrated that *G. hyphopodioides* and the unnamed *Magnaporthaceae* sp., but not *S. cylindrosporus*, provides effective control against take-all disease. However, these species must colonise the root system before *G. tritici* in order to provide effective control. In fact, adding the species after *G. tritici* may exacerbate *G. tritici* infection. Therefore, the studies discussed here have important implications for the future development of biocontrol strategies by non-pathogenic *Magnaporthaceae* species.

3.8 Acknowledgement of contributions

All *Magnaporthaceae* isolates were collected and characterised by current and previous members of the take-all team at Rothamsted, including Dr Sarah-Jane Osborne, Gail Canning and Jessica Hammond. Thank you to undergraduate summer student Kallie Botha (University of Bristol) for helping with the co-inoculation experiments. Kallie was funded by an undergraduate vacation bursary

provided by the British Society for Plant Pathology (BSPP). Thank you also to Dr David Withall who helped with supervision during the summer project.

4 Investigating the infection biology and lignification response to non-pathogenic *Magnaporthaceae* species

4.1 Introduction

Non-pathogenic *Magnaporthaceae* species can colonise a variety of agriculturally important grasses, as well as several cereal species including maize, barley, rye, oats, and wheat. Much like pathogenic *G. tritici*, the fungi can survive saprophytically on rotting plant debris, enabling fungal populations to be maintained across cropping seasons. Unlike *G. tritici,* non-pathogenic species such as *G. hyphopodioides* are not reported to produce perithecia (sexual fruiting structures). However, they are known to produce asexual conidiophores and conidia on solid and liquid media, though with differing reports of viability (Asher & Shipton, 1981). Therefore, the roots of young plants are likely colonised following direct contact with infected plant debris. As previously documented by Deacon (1976a), *G. hyphopodioides* (but not *G. tritici*) produced black sclerotia on solid media, much like the characteristic sclerotia of *Sclerotinia sclerotiorum* (Li et al., 2018), though smaller in size (0.25-1 mm diameter) (figure 4.1). Though the presence of sclerotia in the soil has not yet been documented (likely due to their small size) this finding lends the possibility that inoculum may also be maintained in the soil via the production of these survival structures.

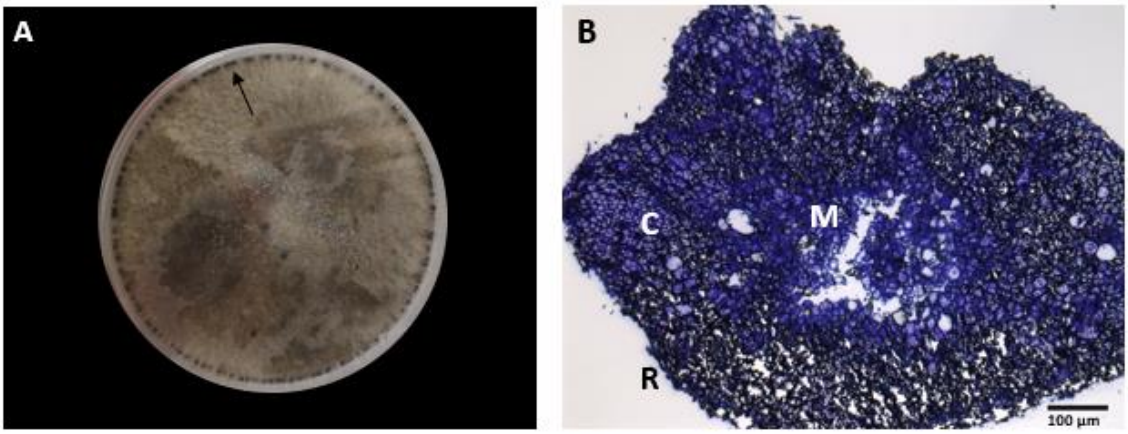


Figure 4.1 Production of *G. hyphopodioides* sclerotia *in vitro*. A. Sclerotia produced at the colony periphery after 30 days growth on PDA. B. Sclerotia contain a characteristic central medulla (M), cortical region (C) and rind (R), distinguished by toluidine blue staining of semi-thin resin sections.

During the active infection of wheat, the fungi produce dark melanised macrohyphae which grow longitudinally across the surface of the root and are often visible by eye (figure 4.2 A). Thinner hyaline hyphae are also produced, from which appressorium-like penetration structures known as hyphopodia are reported to be formed (Asher & Shipton, 1981). Hyphopodia produced in culture may be simple or lobed in structure depending on the individual species and vary from hyaline to brown in colour as they mature (figure 4.2 B). Hyphopodia produced on the root surface are reported to develop penetration pegs which enable the fungus to penetrate the stem base and root epidermal cells (Hernández-Restrepo et al., 2016). Crucially, and much unlike *G. tritici*, non-pathogenic species do not colonise the root stele and fail to penetrate the endodermal barrier, possibly due to increased lignification and suberisation of the endodermal cells (Speakman and Lewis, 1978). Using nuclear staining techniques, Holden (1976) reported that non-pathogenic species colonise only dead or dying cells in the cortex, and though cortical cell death occurs surprisingly rapidly in cereals, colonisation itself does not enhance the rate of cell death (Deacon & Henry, 1981). This finding contrasts that of other root endophytes such as *Serendipita indica* and *Harpophora oryzae,* which are known to trigger localised cell death upon root colonisation (Dunken et al., 2022; Su et al., 2013), suggesting that non-pathogenic *Magnaporthaceae* species may be spatially restricted to senescing cells.

Fungal hyphae remain in the root cortical and epidermal cells, where characteristic structures known as sub-epidermal vesicles (SEVs) are produced. SEVs are highly melanised spherical structures containing one or more pores, and are formed intraradically from melanised macrohyphae. The size and distribution of SEVs within the root varies among non-pathogenic species, being large and often solitary in *G. hyphopodioides* (figure 4.2 C), while small and tightly clustered in *S. cylindrosporus* and the unnamed *Magnaporthaceae* species, (figure 4.2 D). Although frequently referred to in the literature as “growth-cessation structures” (Ulrich et al. 2000; Sesma and Osbourn, 2004; Freeman and Ward, 2004; Osborne et al. 2018) detailed microscopy investigations into the production of SEVs have been hindered by difficulties in generating stable

transformants (see chapter 1.2.6), hence the lack of flourescently tagged isolates. However, Deacon (1976a) reported the production of SEV-like structures when non-pathogenic species were inoculated onto cellophane discs *in vitro*, suggesting that halted growth could be responsible for their formation.

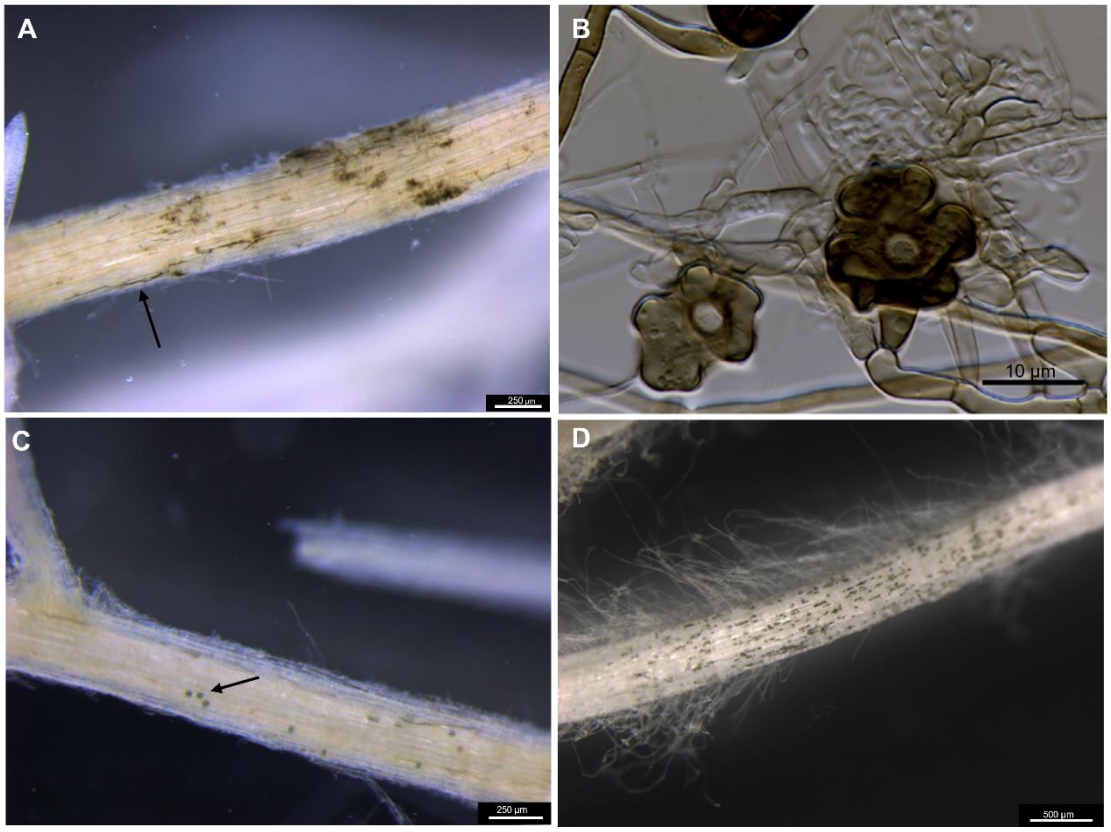


Figure 4.2 Colonisation structures produced by non-pathogenic *Magnaporthaceae* sp. A. *G. hyphopodioides* colonised wheat roots with melanised macrohyphae. Magnification x48. B. *G. hyphopodioides* hyphopodia produced in culture. Reproduced from Hernández-Restrepo et al., (2016) with author permission. C. *G. hyphopodioides* SEVs. Magnification x57. D. Small and tightly clustered *S. cylindrosporus* SEVs. Magnification x32. Images taken using a stereomicroscope.

The production of “growth-cessation structures” has also been described for the closely related rice leaf blast pathogen *Magnaporthe oryzae.* Although a foliar and floral pathogen, *M. oryzae* can cause lesions when inoculated onto cereal roots and shares common features of classical root pathogens such as *G. tritici* (Dufresne & Osbourn, 2001; Sesma & Osbourn, 2004). Green fluorescent protein (GFP)-tagged *M. oryzae* strains and chlorazole black E staining was used to

investigate the developmental events associated with root infection of rice and barley. Rather than producing melanised appressoria, structures normally associated with leaf infection, the fungus produced hyphal swellings resembling hyphopodia. Brown spherical structures were found on the root surface and inside epidermal and cortical cells of rice; resembling the SEVs formed by non-pathogenic *Magnaporthaceae* fungi (figure 4.3 A-C). However, the authors do not go on the speculate what the role of these structures could be.

Interestingly, a literature search revealed that SEV-like structures are also common among dark septate endophytes (DSE), a diverse group of root colonising ascomycete fungi with elusive functions, often found inhabiting stressful environments. The DSE are morphologically characterised by the production of highly melanised septate hyphae which grow intraradically, producing what are (perhaps incorrectly) referred to as “microsclerotia”, but which bear striking similarities to the SEVs of the *Magnaporthaceae* species (figure 4.3 E-F). Again, the function of these “microsclerotia” in the fungal life cycle of the DSE remains unknown and their ultrastructure has yet to be investigated (Ban et al., 2012; Knapp et al., 2018). Based on these morphological characteristics, the non-pathogenic *Magnaporthaceae* species could also be classified as DSE fungi. Evidently, SEVs are a shared but mysterious structure produced by a range of ascomycete root colonising pathogens and endophytes. Further investigation is needed to characterise the ultrastructure of SEVs and to understand their role in the fungal life cycle.

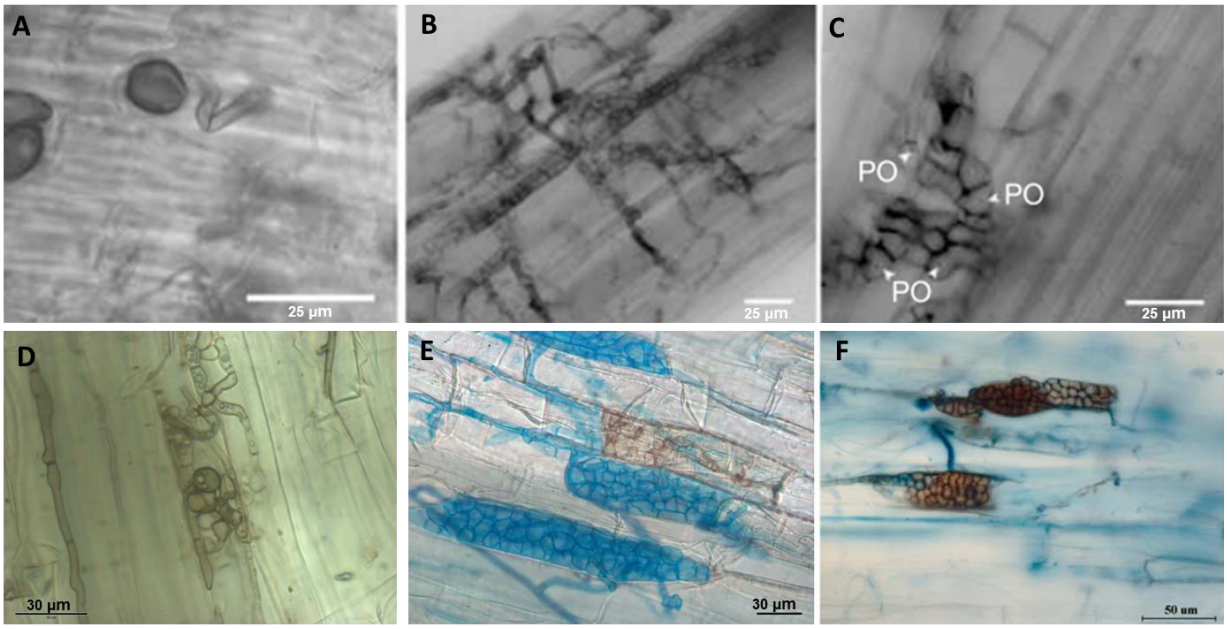


Figure 4.3 Sub-epidermal vesicles (SEVs) produced by diverse fungi in the roots of a range of plant hosts. *M. oryzae* SEVs in rice (A) and barley (B, C) stained with chlorazol black E. Reproduced from Sesma & Osbourn (2004) with permission (License no. 5266500596822). Melanised macrohyphae and SEVs produced by *S. cylindrosporus* in wheat (D). Melanised macrohyphae and SEVs of *Cadophora* sp. in maize after staining with aniline blue (E). Reproduced from Knapp et al. (2018) under the Creative Commons Attribution licence (https://creativecommons.org/licenses/by/4.0/). Melanised macrohyphae and SEVs of *Paraphoma chrysanthemicola* in *Astragalus adsurgens* (milk vetch) stained with trypan blue (F). Reproduced from Ban et al. (2012) under the Creative Commons Attribution Licence.

Non-pathogenic *Magnaporthaceae* species cause significant lignification of the stele and endodermis, well in advance of the infecting hyphae (Speakman & Lewis 1978). Furthermore, colonisation by non-pathogenic species can result in considerably higher lignin levels in cell walls compared to uninoculated and *G. tritici* infected roots (Huang et al., 2001). Lignin is a phenolic polymer synthesised by the polymerisation of p-coumaryl, coniferyl and sinapyl alcohols via the phenylpropanoid pathway. These monolignols are then polymerised into the p-hydroxyphenyl (H), guaiacyl (G) and syringyl (S) subunits, respectively. In roots, lignin deposition in xylem vessels and endodermal cells surrounding vascular tissues enables the critical uptake and transport of water and nutrients, as well

as providing protection from pathogen attack (Reyt et al., 2021). Hence, the deposition of lignin in root tissues has previously been hypothesised to play a key role in the control of *G. tritici* by non-pathogenic species by creating a physical barrier to infection (Holden, 1976; Speakman and Lewis, 1978). A number of analytical methods exist for the qualitative and quantitative assessment of lignin in plant materials (Lupoi et al., 2015). However, in this chapter, the analysis of root lignification was carried out using the histochemical stain potassium permanganate ($KMnO_4$), enabling simple and straightforward comparisons of lignin distribution across different root cell layers.

4.2 Aims and hypotheses

Aim 1: To compare the general infection biology of non-pathogenic *Magnaporthaceae* species (*G. hyphopodioides, S. cylindrosporus,* unnamed *Magnaporthaceae* species) with pathogenic *G. tritici*.

Hypothesis: Unlike G. tritici, non-pathogenic Magnaporthaceae species are unable to colonise the root stele, instead remaining in the cortical cells.

Aim 2: To investigate the ultrastructure of *G. hyphopodioides* SEVs using transmission electron microscopy (TEM).

Hypothesis: SEVs are fungal resting structures with thickened cell walls.

Aim 3: To compare the lignification response to colonisation by non-pathogenic *Magnaporthaceae* species and pathogenic *G. tritici*.

Hypothesis: Root colonisation by non-pathogenic Magnaporthaceae species results in greater lignification of the stele and endodermal cells compared to G. tritici.

4.3 Methods

Several pilot experiments were carried out to optimise root colonisation, sample preparation and sample staining methodologies prior to the final experiment, the results of which are summarised in appendix A.4.

4.3.1 Eppendorf seedling infection assay

A 2 ml Eppendorf tube was filled to the 1.5 ml mark with sterile autoclaved sand. A single agar plug was taken from the leading edge of a 2-week old fungal colony growing on potato dextrose (PDA) using a no. 4 cork-borer (8 mm diameter) and placed in the sand-filled tube. The tube was then topped up with sand to the 2 ml mark. Wheat seeds of the cultivar Hereward were surface sterilised with 1% sodium hypochlorite for 10 minutes and pre-germinated for 24 hours on sterile filter paper in a Petri dish. At this point, the radicle had just emerged. One pre-germinated seed was placed on the sand surface and the tube was covered with parafilm (to increase humidity) for the first 2 days of growth, after which the parafilm was removed (figure 4.4). Three replicates per treatment were set up and a randomised block design was generated in Genstat 20th Edition (see table 4.1 for treatment details). Plants were placed in a growth chamber (20 °C day, 16 °C night, 16hr light cycle, light intensity 5) and were watered daily with sterile distilled water. Seedlings were harvested at 3, 6 or 9 dpi and roots were analysed for symptoms of colonisation using a stereomicroscope (see chapter 2.7.1).

Table 4.1 Treatment conditions for the Eppendorf seedling infection experiment

Treatments	ITS species identification	Isolate	Time points (dpi)	Replicates
1	*G. hyphopodioides*	NZ.129.2C.17	3, 6, 9	A, B, C
2	*S. cylindrosporus*	H23A-SB-2b	3, 6, 9	A, B, C
3	Unnamed *Magnaporthaceae* sp.	105C-2	3, 6, 9	A, B, C
4	*G. tritici*	16.NZ.1d	3, 6, 9	A, B, C
5	PDA Control	N/A	3, 6, 9	A, B, C

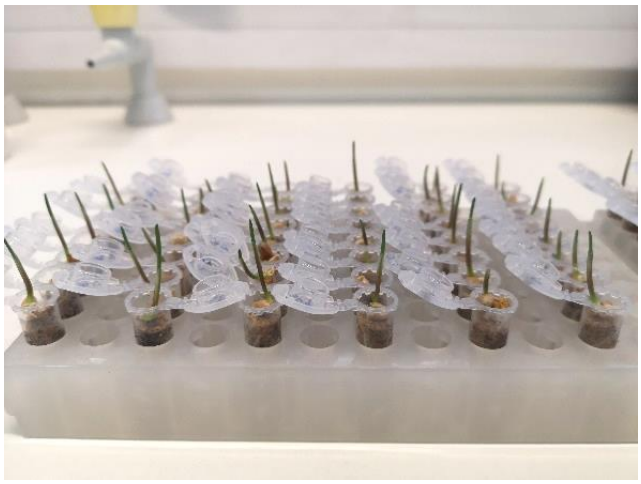


Figure 4.4 Image of Eppendorf seedling infection set-up (3 dpi).

4.3.2 Fixation and embedding protocol

Following imaging by stereomicroscope, one root per plant was prepared for fixation. Roots from treatment replicates A and C were used for transversal sectioning and roots from replicate B were used for longitudinal sectioning. Root sections (1 cm and 2 cm in length for longitudinal and transversal samples, respectively) were cut from the infection zone and placed in glass vials (Rolled Rim Vials, G100, 7mL; TAAB Laboratories Equipment, UK) containing 5 ml fixative (4% paraformaldehyde, 2.5% glutaraldehyde in 0.05M phosphate buffer, pH 7.2). Samples were incubated in fixative for two hours at room temperature on a tube rotator, followed by incubation at 4 °C overnight. Three washing steps of 30 minutes each were performed with 5 ml of 0.05M phosphate buffer. Roots were dehydrated in a graded ethanol series, starting at 10% ethanol and ending at 100% ethanol in 10 % increments for an hour at a time. Roots were infiltrated and embedded in glycol methacrylate resin using the Agar GMA HEMA kit (Agar Scientific, UK). Roots were infiltrated in solution A for 45 minutes, with three changes. Each change was aided by vacuum infiltration for 30 seconds. Roots were embedded in 50 parts solution A to 1 part solution B, using 0.5 ml Eppendorf tubes (Sigma Aldrich®, USA) for roots sectioned transversally and flat bottomed 1.5 ml capsules (C094 TAAB capsule 8mm flat, polyethylene 500; TAAB) for roots sectioned longitudinally. Polymerisation occurred at room temperature under anaerobic conditions and took approximately 2 hours.

4.3.3 Semi-thin sectioning and staining of roots for light microscopy

Resin blocks containing root material were dry sectioned (4 µm thickness) using a glass knife (TAAB superglass 400mm x 25.4mm x 6.4mm) attached to the Reichert-Jung UltraCut Microtome. Individual sections were transferred to drops of distilled water on de-greased glass slides (Menzel- Glaser; Thermo Scientific™, USA) using a pair of ultra-fine forceps. Sections were left to expand in the water droplets before drying at 50 °C on a hot plate. To visualise fungal structures, sections were stained with 1% w/v aniline blue in lactophenol for 30 seconds, followed by three 1-minute washes in distilled water. To visualise lignin, sections were stained in 1% w/v potassium permanganate for 10 minutes, followed by three 1-minute washes in distilled water. The slides were mounted with DPX mounting fluid (Sigma Aldrich®) and glass cover slips (0.17 mm thick, 22 x 50mm, 1½ thickness; Agar Scientific). Sections were imaged using a light microscope (see chapter 2.7.1).

4.3.4 Preparation of roots containing *G. hyphopodioides* SEVs for transmission electron microscopy

Due to the low abundance of *G. hyphopodioides* sub epidermal vesicles in the Eppendorf experiment, root samples were cut from colonised plants grown in a 5-week seedling infection assay (see chapter 2.4). Wheat root samples (cv. Hereward) containing *G. hyphopodioides* sub-epidermal vesicles were prepared for transmission electron microscopy (TEM) by cryofixation. Samples were subject to High Pressure Freezing (HPF) followed by freeze substitution. Each root was transferred to an aluminium sample carrier (6.0 x 0.5mm Type B; Leica Microsystems, Germany) coated with hexadecane (catalogue number H6703, Sigma-Aldrich®). The sample carrier was mounted onto a specimen cartridge. A drop of 0.1 M sucrose was added to the root and another carrier was used to enclose the sample. Each cartridge was then inserted into an EM HPM100 High Pressure Freezing System (Leica Microsystems), and HPF was performed at 2100 bar pressure. The cartridges were dispensed into a container with liquid nitrogen and each HPF sample carrier was carefully opened with fine tweezers. The root samples were transferred to 2 ml screw cap tubes containing 100%

ethanol. Freeze substitution was carried out by Dr Eudri Venter (Electron Microscopist, Department of Computational and Analytical Sciences, Rothamsted Research, UK), using a Reichert AFS instrument (Leica Microsystems) as follows:

Step 1: -85 °C, 26 hours;

Step 2: ramping stage, + 2 °C/hour, 12.5 hours;

Step 3: -60 °C, 8 hours;

Step 4: ramping stage, + 2 °C/hour, 15 hours;

Step 5: -30 °C, 24 hours.

Root samples were transferred to glass vials as described in section 4.3.2 and samples were infiltrated in increasing concentrations (10 %, 20%, 40%, 60%, 80%, 100%) of resin (LR White Resin Medium Catalysed, Agar Scientific). A light vacuum was applied for 20 seconds and samples were rotated for an hour at each stage (glycol methacrylate is not compatible with TEM preparations, hence LR White Resin was used). Samples were placed in 1.5 ml flat-bottomed capsules (C094 TAAB capsule 8mm flat, polyethylene 500; TAAB) containing fresh resin and embedded in a nitrogen oven for 16 hours at 50 °C.

4.3.5 Preparation and staining of ultrathin sections for transmission electron microscopy

Due to COVID-19 restrictions, ultrathin sectioning and staining was carried out by Dr. Eudri Venter (Electron Microscopist, Department of Computational and Analytical Sciences, Rothamsted Research, UK). Ultrathin sections (90 nm thickness) were cut using a UC7 Ultramicrotome (Leica Microsystems) and sections were collected onto formvar/carbon-coated copper grids (Hexagonal Pattern 200 Mesh TEM support grids, Catalogue number AGG2450C; Agar Scientific). A petri dish lined with a layer of dental wax and wrapped in aluminium foil was used as container for the staining steps. Drops of 2.5% uranyl acetate were dispensed onto the wax surface, and copper grids containing ultrathin sections were placed onto the drops for 20 minutes in the dark. The grids were

individually picked with a pair of fine tweezers and rinsed by dipping in deionised water multiple times. Drops of Reynolds lead citrate were dispensed onto the wax surface and the grids were placed onto the stain (Reynolds, 1963). Pellets of sodium hydroxide were scattered onto the dish to prevent the precipitation of lead by exposure to CO_2, and the petri dish was covered for three minutes. The grids were washed again by dipping in deionised water and grids were quickly dried at 60 °C for 30 seconds.

4.3.6 Transmission electron microscopy and image analysis

Ultra-thin sections were imaged using a JEOL-2100Plus Transmission Electron Microscope (JEOL, Japan) equipped with a Gatan OneView IS Camera (Gatan, USA). Micrographs were acquired using the Gatan 89 Microscopy Suite software (Gatan, USA).

ImageJ software was used to measure the cell wall diameter of fungal SEVs and hyphae. Ten measurements were taken from three SEVs and three hyphae per sample and this was repeated across three independent biological replicates. The data were analysed by ANOVA in Genstat 20th Edition.

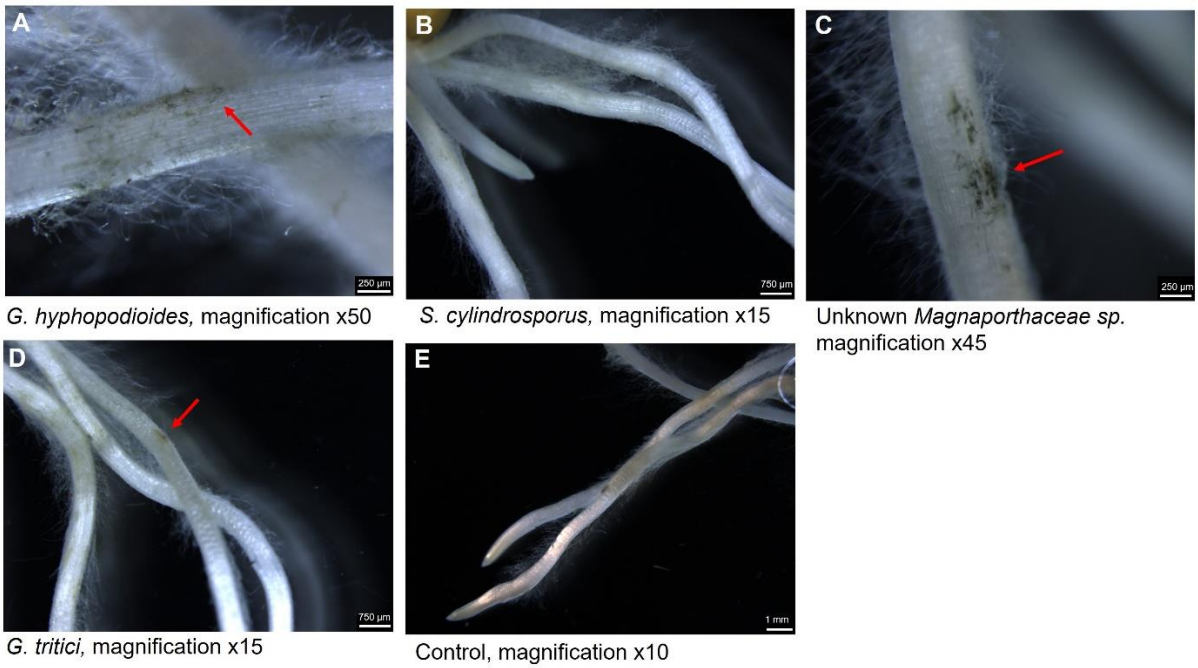
4.4 Results:

4.4.1 Eppendorf seedling infection assay

A miniaturised time-course seedling infection assay was designed for the rapid production of colonised root material, enabling the infection mechanisms of three non-pathogenic *Magnaporthaceae* species (*G. hyphopodioides, S. cylindrosporus,* unnamed *Magnaporthaceae* species) to be compared with pathogenic *G. tritici.*

At 3 dpi, melanised macrohyphae were detected on the surface of roots inoculated with *G. tritici*, *G. hyphopodioides* and the unnamed *Magnaporthaceae* sp. (figure 4.5). However, at the time of the study, the finding that hyaline hyphae (which cannot be visualised without staining) are produced before melanised macrohyphae (which are visible by eye), had not yet been made. This discovery was only made in chapter 5 following fluorescent staining of root material with

Wheat Germ Agglutinin, Alexa Fluor™ 488 Conjugate (WGA). Therefore, although this time-point represents the early stages of root colonisation, the stereomicroscope images presented here probably do not show the full extent of fungal colonisation, as hyaline hyphae were likely growing on the surface of the root undetected.



G. hyphopodioides, magnification x50

S. cylindrosporus, magnification x15

Unknown *Magnaporthaceae sp.* magnification x45

G. tritici, magnification x15

Control, magnification x10

Figure 4.5 Wheat roots imaged at 3 dpi. Red arrows indicate the presence of melanised macrohyphae.

By 6 dpi, melanised macrohyphae were produced by all species and *G. tritici* infection led to visible root browning (figure 4.6 D). *S. cylindrosporus* and the unnamed *Magnaporthaceae* species produced clusters of SEVs which were clearly visible in the epidermal cells (figure 4.6 B, C). By 9 dpi, root browning occurred across all fungal treatments (figure 4.7). This finding suggests that colonisation levels in the present study were higher than natural levels in field-grown wheat, where colonisation by non-pathogenic species does not result in visible plant symptoms. This finding should be kept in mind when interpreting the results of the study. Furthermore, the visible root symptoms described here highlight the potential for non-pathogenic species to cause root damage under extreme inoculum levels.

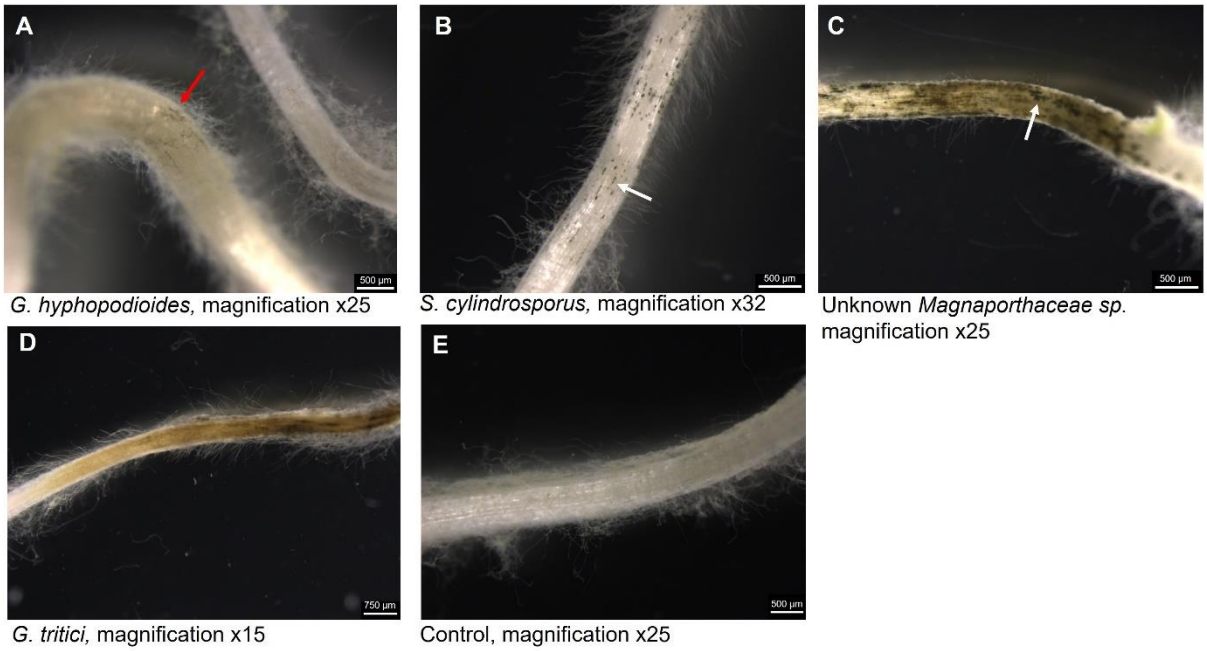


Figure 4.6 Wheat roots imaged at 6 dpi. Red arrow indicates *G. hyphopodioides* runner hyphae, white arrows indicate sub-epidermal vesicles produced by *S. cylindrosporus* and the unnamed *Magnaporthaceae* species.

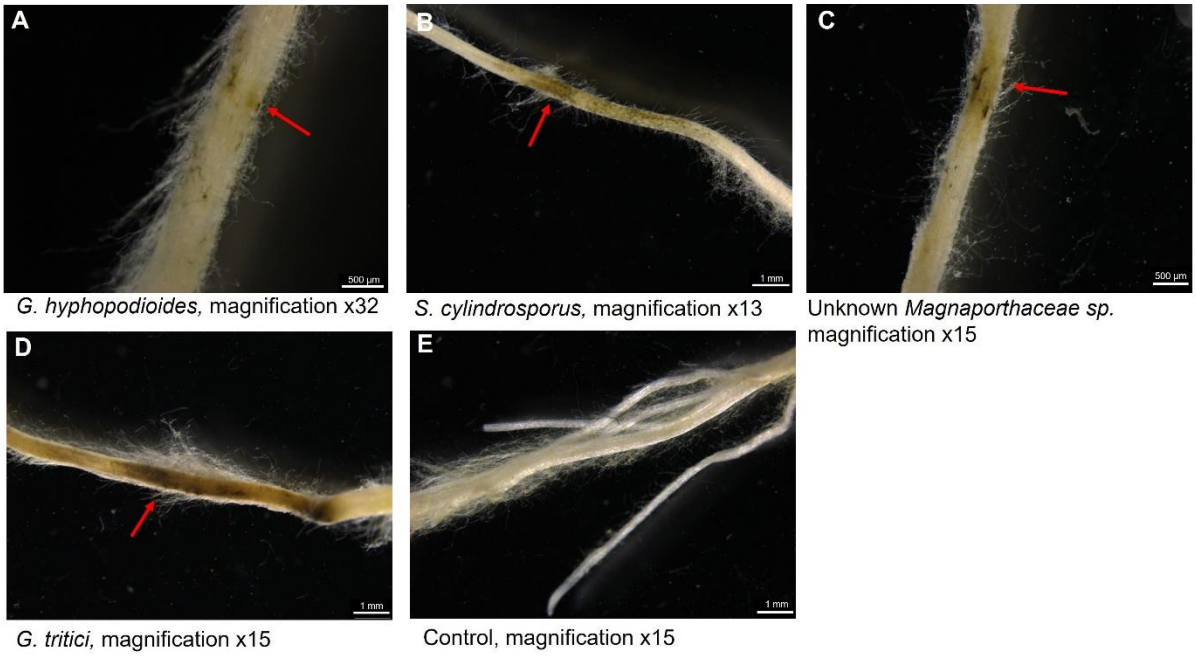


Figure 4.7 Wheat roots imaged at 9 dpi. Red arrows indicate areas of root browning.

Semi-thin sections of root samples were taken both longitudinally and transversally. Longitudinal sections enabled the detailed investigation of colonisation and subsequent cell wall changes in individual cells, while transversal sections offered an insight into the penetration of hyphae across different cell layers and the associated deposition patterns of lignin. Aniline blue (AB) fungal staining revealed that at 3 dpi, very small amounts of fungal hyphae were present in the epidermal and outer cortical cells of roots inoculated with *G. tritici,* though hyphae were difficult to distinguish from plant cell contents (figure 4.8 D). Potassium permanganate (PP) staining revealed increased lignification of cell walls in cells infected by *G. tritici*, with papillae already present close to penetration sites (figure 4.8 I). However, PP also stained fungal hyphae due to the oxidation of fungal cell wall components. Fungal hyphae of the non-pathogenic species could not be detected in AB or PP stained root samples and lignification levels were unchanged compared to the uninoculated control.

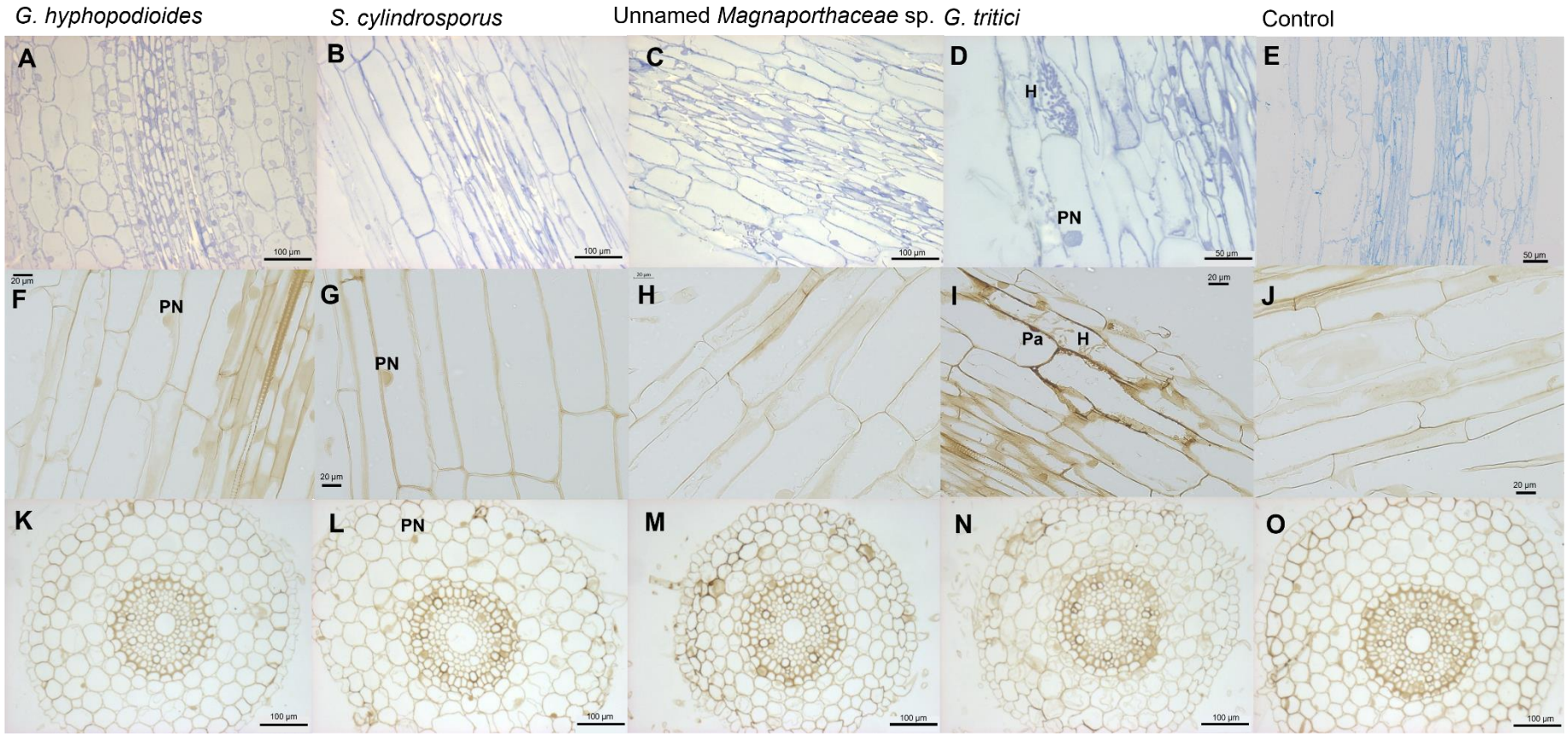


Figure 4.8 Seedling infection assay micrographs at 3 dpi. A-E: Aniline blue staining of longitudinal sections. F-J: Potassium permanganate staining of lignin in longitudinal sections. K-O: Potassium permanganate staining of lignin in transversal sections. H= hyphae, PN= plant nucleus, Pa= papilla.

By 6 dpi, hyphae were detected in the epidermal and cortical cells of all fungal treatments. *G. tritici* and *G. hyphopodioides* showed similar levels of colonisation in the cortex. Both fungi were able to colonise the inner cortex, though were not detected in the stele. However, AB staining of some plant cell contents made identification of hyphae in the stele challenging. Papillae were observed close to infection sites (figure 4.9 F) and lignitubers were formed around highly colonised cells (figure 4.9 A, I). Hyphae of *S. cylindrosporus* and the unnamed *Magnaporthaceae* species were detected in the epidermal cells only, with the unnamed *Magnaporthaceae* species also found in the outer cortical cells (figure 4.9 B-C). Both species produced large clusters of SEVs in the epidermal cells and papillae were associated with the cell walls of colonised cells (figure 4.9 G, H). Curiously, *G. hyphopodioides* SEVs were not identified at this stage. PP staining of transversal sections revealed increased lignification of all cell layers in response to *G. tritici* infection (figure 4.9 N), whereas *G. hyphopodioides* and the unnamed *Magnaporthaceae* species resulted in lignification of the stele and outer cortex only (figure 4.9 K, M). Conversely, though papillae were observed in cells colonised by *S. cylindrosporus*, overall lignin levels were almost indistinguishable from the uninoculated control (figure 4.9 L).

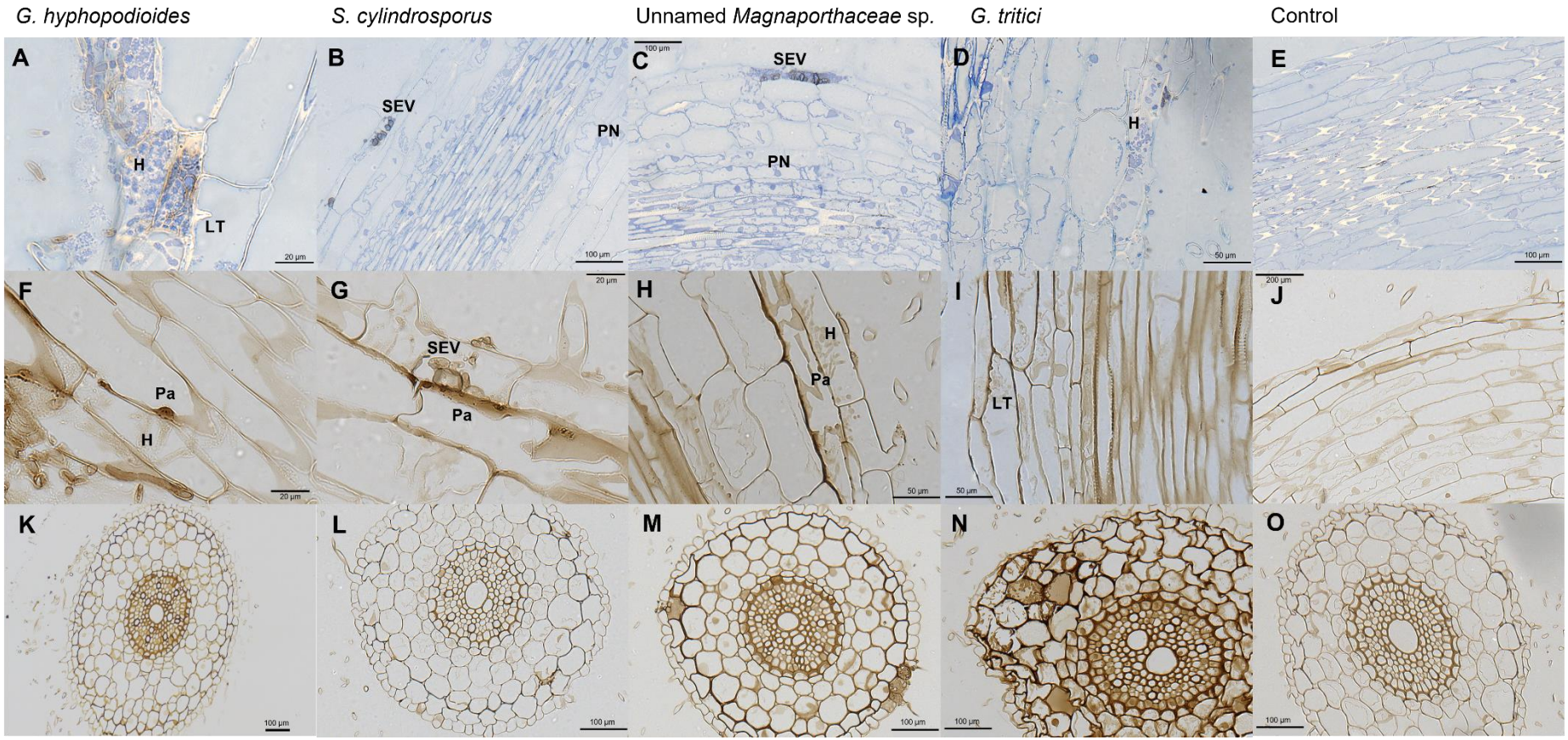


Figure 4.9 Seedling infection assay micrographs at 6 dpi. A-E: Aniline blue staining of fungal hyphae in longitudinal sections. F-J: Potassium permanganate staining of lignin in longitudinal sections. K-O: Potassium permanganate staining of lignin in transversal sections. H= hyphae, CW= cell wall, SEV=sub epidermal vesicle, LT=lignituber, Pa=papilla, PN= plant nucleus.

At 9 dpi, *G. hyphopodioides* and *G. tritici* extensively colonised the cortex and hyphae grew both inter-cellularly and intra-cellularly. Unlike *G. hyphopodioides*, *G. tritici* hyphae colonised the endodermal cells (figure 4.10 A, B). Conversely, colonisation by *S. cylindrosporus* and the unnamed *Magnaporthaceae* species remained limited to the outer cortex and epidermal cells (figure 4.10 C, D). However, as mentioned previously, AB staining of cell contents made it difficult to distinguish fungal hyphae and cell content staining was particularly pronounced in root sections containing the unnamed *Magnaporthaceae* sp. PP staining revealed the presence of unknown circular lignin structures close to *G. tritici* and *G. hyphopodioides* penetration sites, suggesting that the structures were produced in response to infection (figure 4.11 F, I). Hyphae of both species penetrated plant lignitubers, allowing the fungi to proceed from cell to cell. However, *G. tritici* hyphae were also observed directly penetrating the plant cell wall without the formation of lignitubers (figure 4.11 D). *G. hyphopodioides, G. tritici* and the unnamed *Magnaporthaceae* species resulted in extensive lignification of the root, while *S. cylindrosporus* resulted in very slight lignification of the outer cortex only (figure 4.11 K-O).

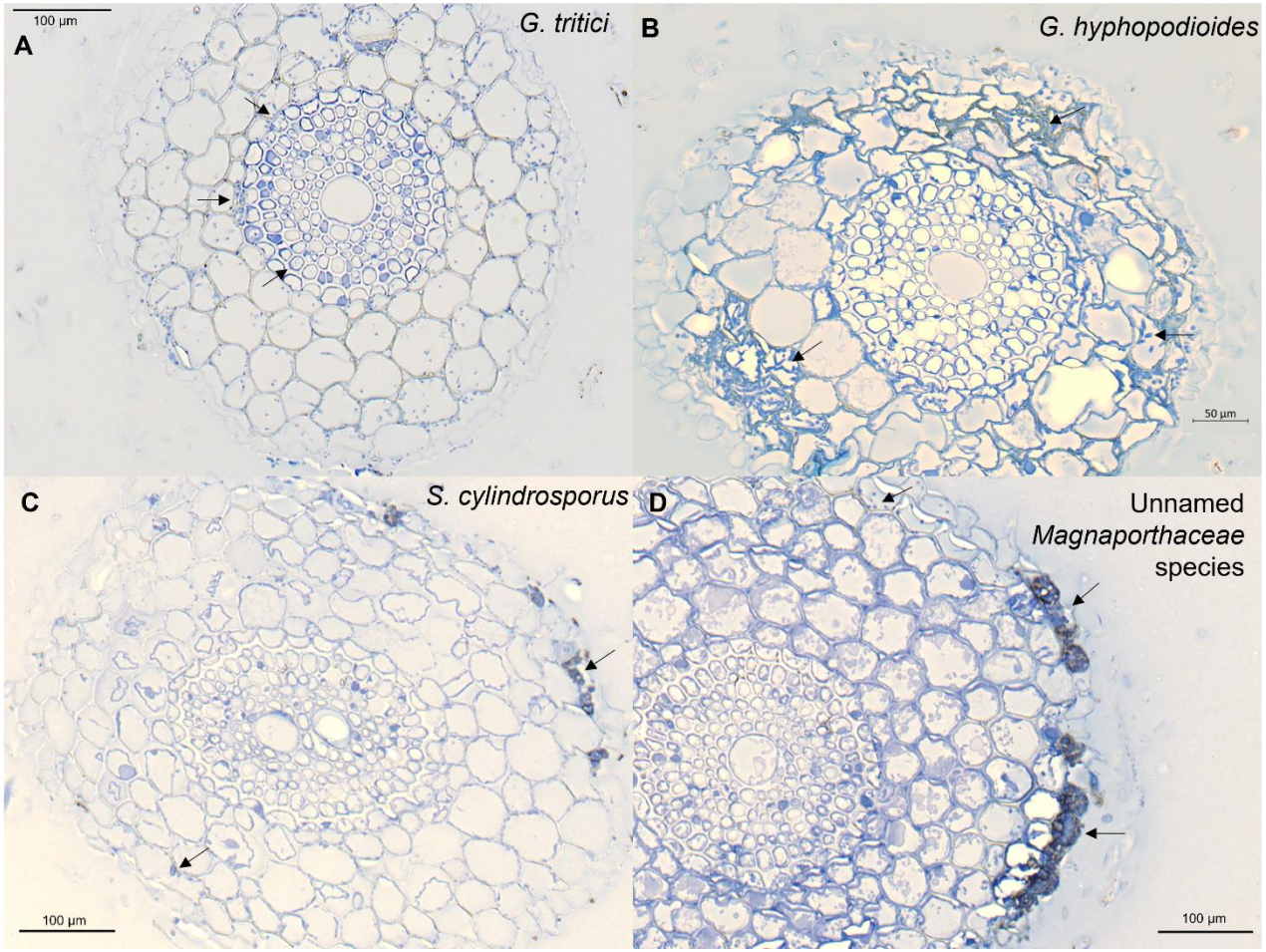


Figure 4.10 Micrographs of transversal sections at 9 dpi. Stained with aniline blue. Arrows indicate fungal hyphae.

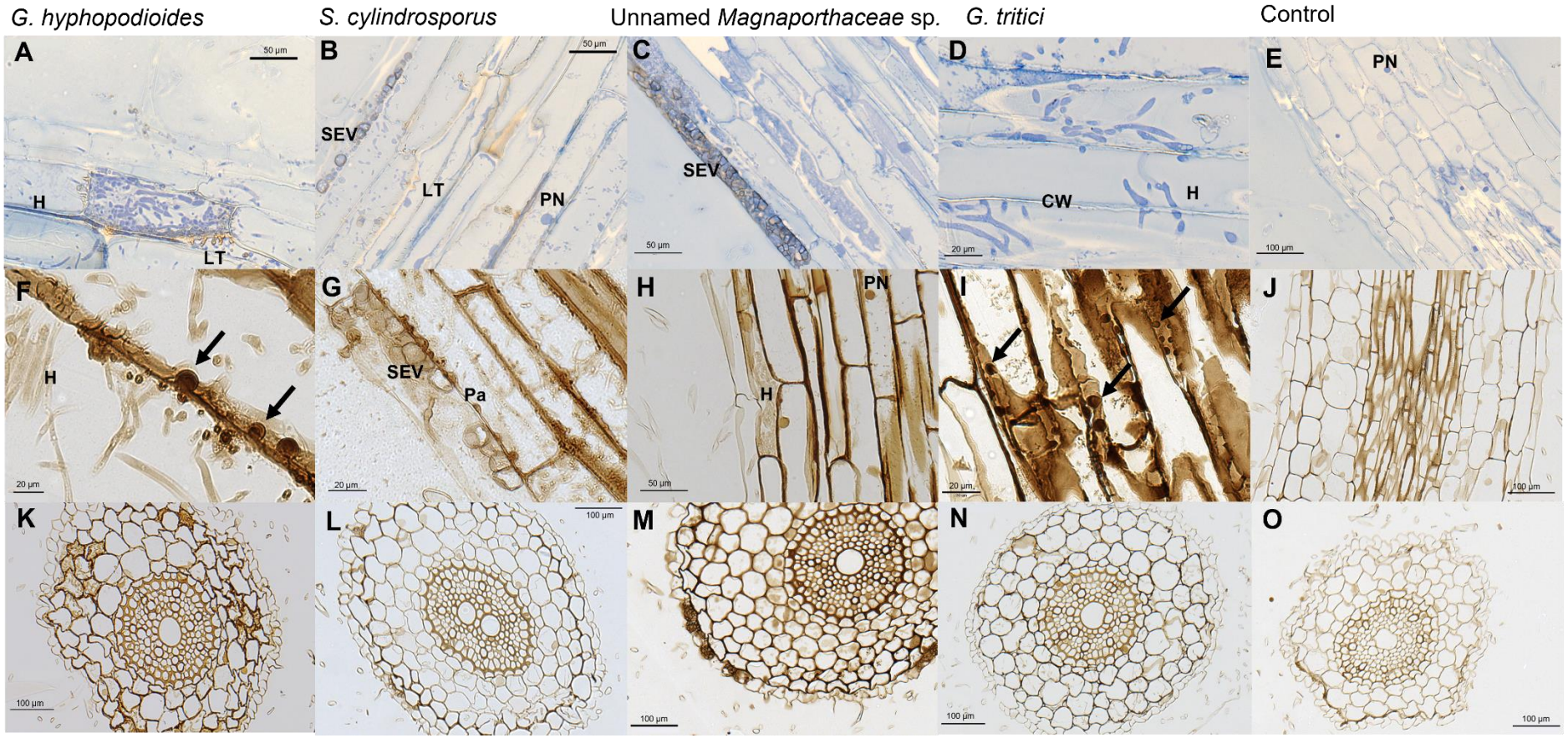

G. hyphopodioides
S. cylindrosporus
Unnamed Magnaporthaceae sp.
G. tritici
Control
A
B
C
D
E
F
G
H
I
J
K
L
M
N
O
H
LT
SEV
LT
PN
SEV
CW
H
PN
H
SEV
Pa
PN
H

Figure 4.11 Seedling infection assay micrographs at 9 dpi. A-E: Aniline blue staining of fungal hyphae in longitudinal sections. F-J: Potassium Permanganate staining of lignin in longitudinal sections. K-O: Potassium Permanganate staining of lignin in transversal sections. H= hyphae, CW= cell wall, SEV=sub epidermal vesicle, LT=lignituber, Pa=papilla, PN= plant nucleus, black arrows= unknown round lignin structures. See previous page.

S. cylindrosporus and the unnamed *Magnaporthaceae* species produced large clusters of small SEVs, whereas *G. hyphopodioides* SEVs were not observed. Consistent with previous findings, SEVs were made up of fungal biomass enclosed by a thick cell wall containing one or more pores (figure 4.12 A). SEVs were found exclusively in epidermal cells or the first layer of the outer cortex (figure 4.12 D). An unexpected finding was the detection of putative penetration pegs which emerged from many SEVs and were found to penetrate the adjacent plant cell wall (figure 4.12 B, D). Also noteworthy was the detection of seemingly empty SEVs devoid of fungal biomass, suggesting that SEVs could be transient structures (figure 4.12 C). Personal communication with Dr Richard Gutteridge revealed that long penetration pegs emerging from SEVs have previously been detected in field samples colonised by *S. cylindrosporus* (unpublished data; figure 4.13). Furthermore, *G. hyphopodioides* penetration pegs were also detected in artificially inoculated samples generated during the RNA sequencing experiment outlined in chapter 5 (figure 4.14).

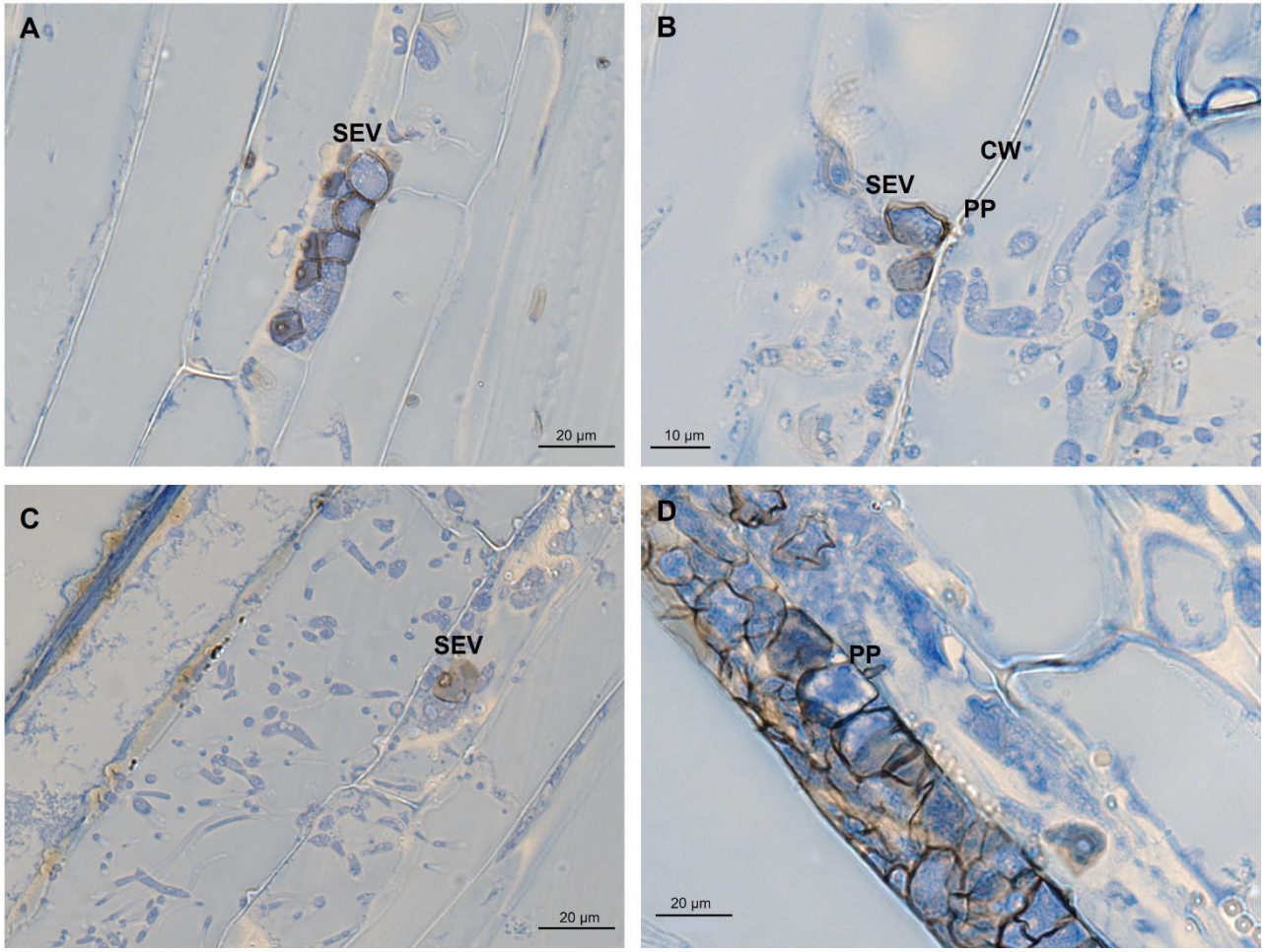


Figure 4.12 Sub epidermal vesicles (SEVs) produced by *S. cylindrosporus* and the unnamed *Magnaporthaceae* species at 9 dpi. A. *S. cylindrosporus* SEVs with pores B. *S. cylindrosporus* SEV with penetration peg. C. Empty *S. cylindrosporus* SEV with pore. D. Clustered SEVs with penetration peg, produced by the unnamed *Magnaporthaceae* species. All samples stained with aniline blue. CW= cell wall, SEV=sub-epidermal vesicle, PP= penetration peg.

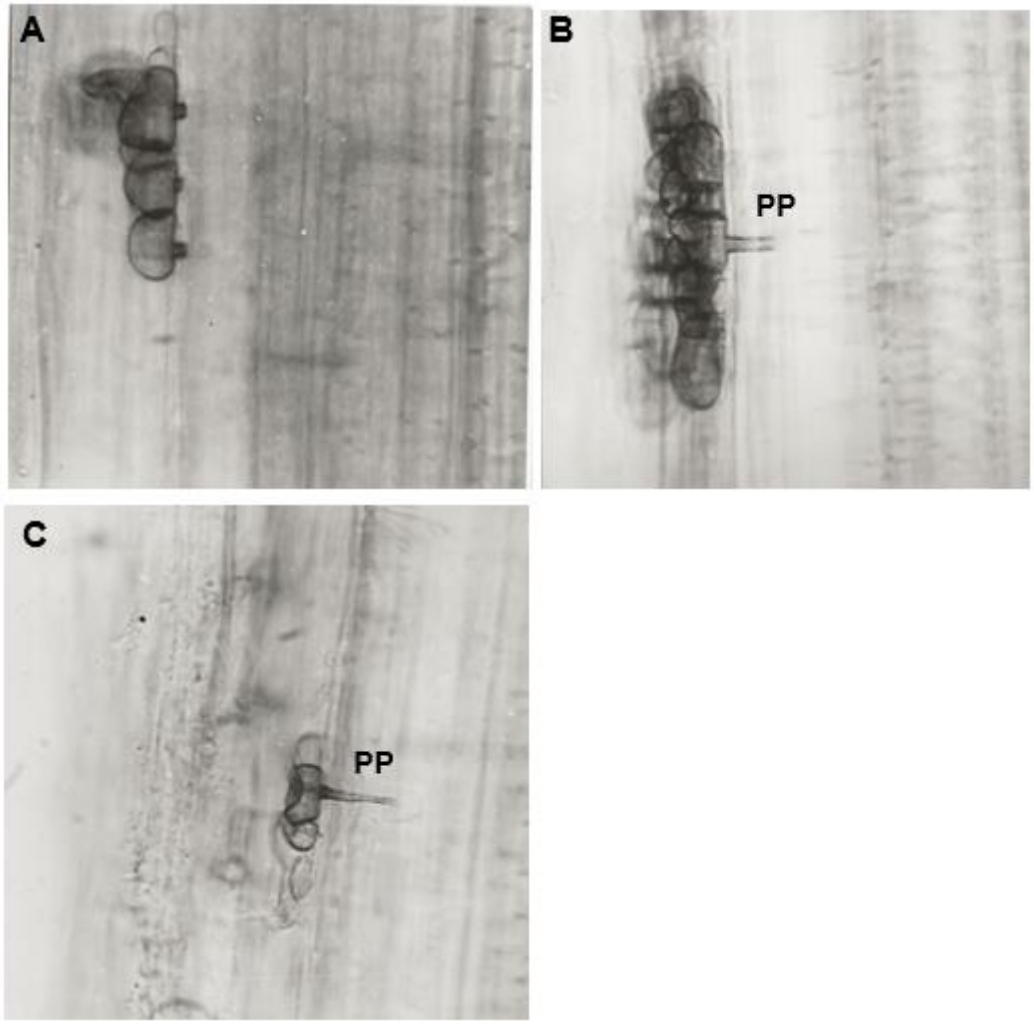


Figure 4.13 Sub epidermal vesicles (SEVs) with penetration pegs, produced by *S. cylindrosporus* in field samples of wheat. PP= penetration peg. Image credits: Dr Richard Gutteridge. Scale bars are not available.

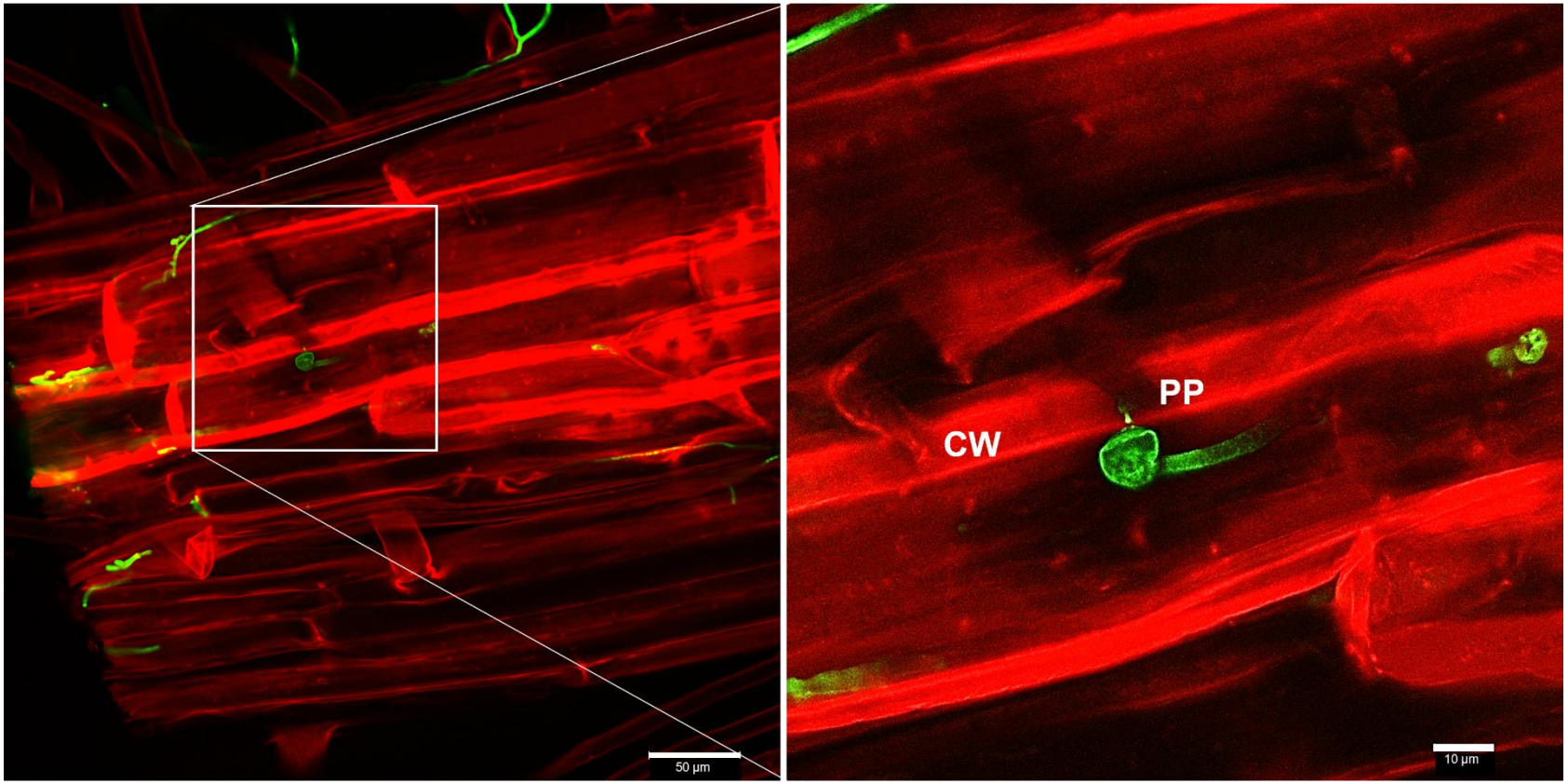


Figure 4.14 Confocal micrograph of a *G. hyphopodioides* sub-epidermal vesicle with penetration peg. Imaged at 5 dpi. Samples have been stained with WGA and PI as described in chapter 5. CW= cell wall, PP= penetration peg.

4.4.2 Transmission electron microscopy of *G. hyphopodioides* sub-epidermal vesicles

G. hyphopodioides appears to be the most promising species for biocontrol (see chapter 3). However, very few SEVs were detected using the present experimental set-up. To further investigate *G. hyphopodioides* SEVs, colonised wheat roots from a 5-week seedling pot assay were sampled and analysed by transmission electron microscopy (TEM). TEM micrographs demonstrate that SEVs contain a multi-layer cell wall of differing densities (figure 4.15). Comparative measurements of fungal hypha and SEVs revealed that the cell wall diameter of SEVs was significantly greater than that of hyphae (d.f. 1, 170, $F= 1798.54$, $p<.001$), with average diameters of 0.66 µm (s.d.= 0.16) and 0.09 µm (s.d = 0.04), respectively (appendix A.5; table A.5.1). In addition, SEVs contained large numbers of putative lipid bodies, potentially providing a nutrient store. The characteristics described here share striking similarities with fungal chlamydospores (Bemena et al., 2021), supporting the initial hypothesis that SEVs are a form of fungal resting/resistance structure. However, as described previously, an SEV with a penetration peg was also detected. Unfortunately, due to poor quality and positioning of this sample on the copper grid, TEM micrographs were not optimal (figure 4.16). Thus, further replications are required before drawing accurate conclusions.

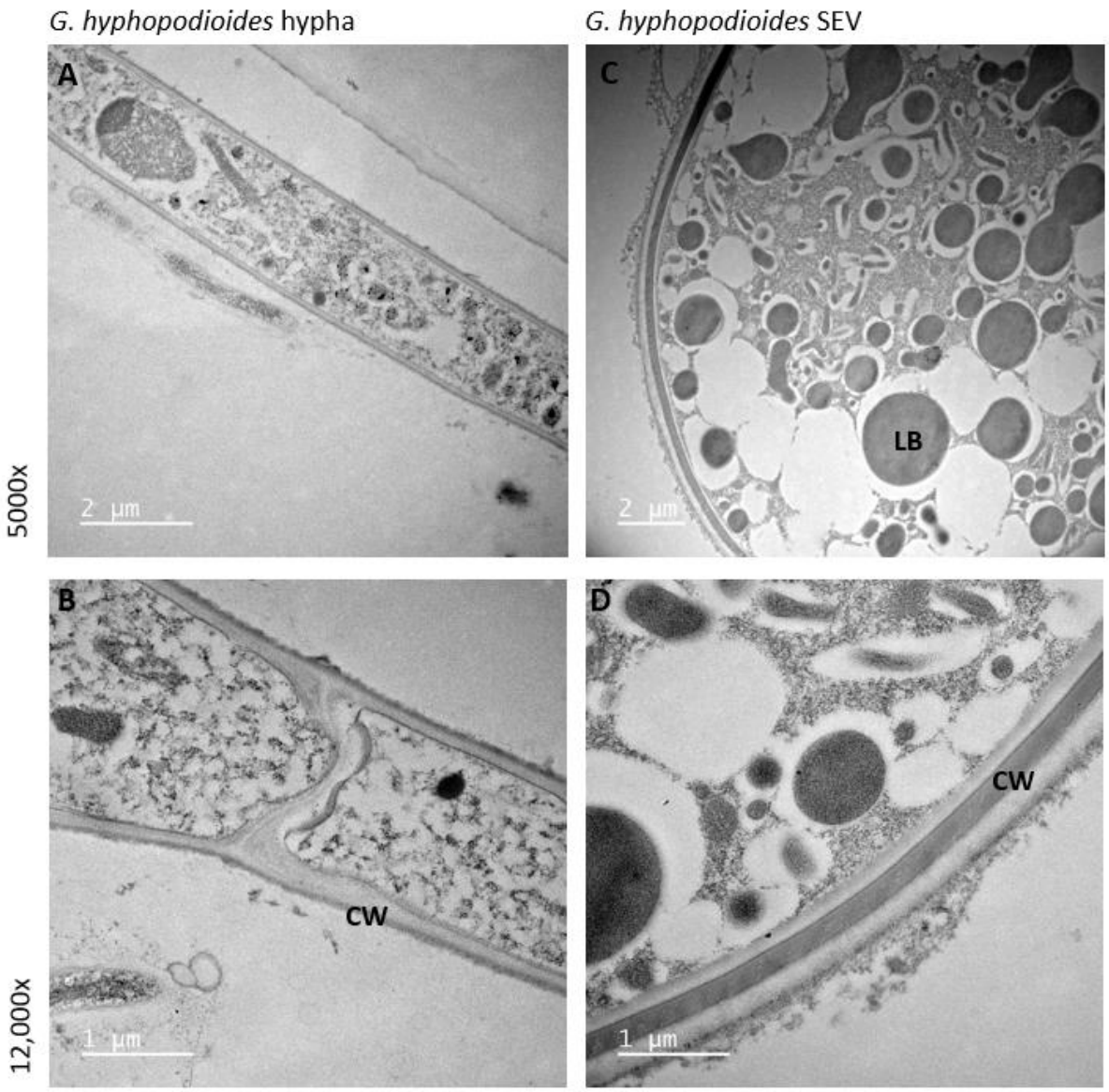


Figure 4.15 Transmission electron micrographs of a *G. hyphopodioides* hypha (A, B) and a sub-epidermal vesicle (C, D). CW= cell wall, LB= putative lipid body.

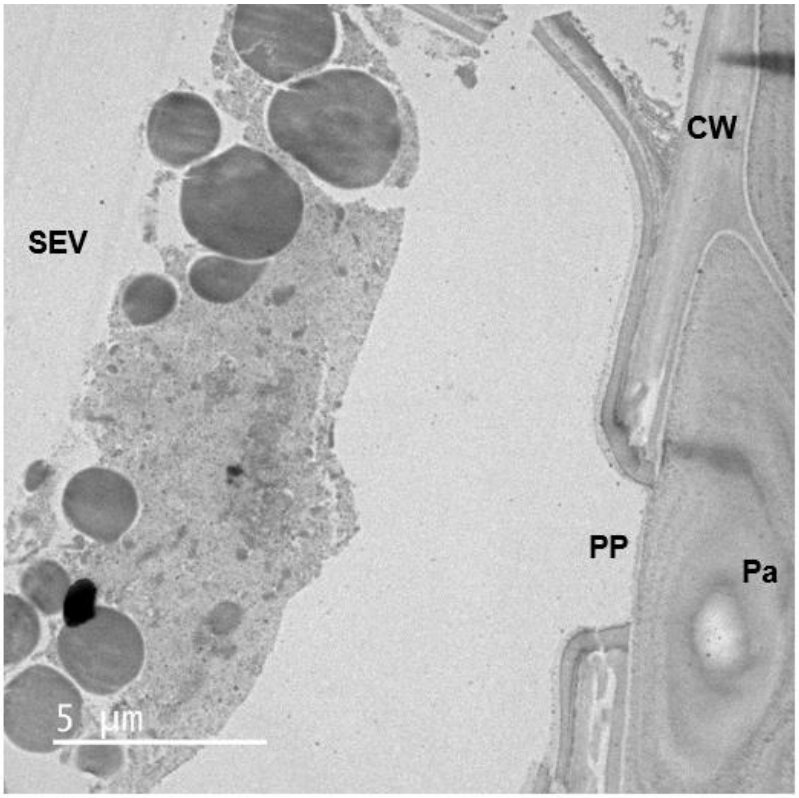


Figure 4.16 Transmission electron micrograph *G. hyphopodioides* SEV with a penetration peg traversing the plant cell wall. SEV= sub-epidermal vesicle, PP= penetration peg, CW= cell wall, Pa= papillae.

4.5 Discussion

In this chapter, a miniaturised seedling infection assay was designed to improve our understanding of the infection biology and physical host responses to three non-pathogenic *Magnaporthaceae* species. The study has offered key information regarding the ability of several *Magnaporthaceae* species to penetrate different cell layers in wheat roots. Consistent with previous reports (Holden, 1976; Speakman and Lewis, 1978), *S. cylindrosporus* hyphae were limited to the epidermal and outer cortical cells, as was true for the unnamed *Magnaporthaceae* species. Conversely, *G. hyphopodioides* was found to penetrate further into the cortex, though hyphae were not detected in the stele. As expected, *G. tritici* was able to penetrate the endodermal cells and proliferate in the stele, resulting in the early formation of characteristic dark lesions. As the depth at which fungi can colonise the root is related to virulence (Asher & Shipton,

1981), the results of this study have important implications for the potential application of these species as biocontrol agents. Though referred to as “non-pathogenic”, there is an obvious risk that *G. hyphopodioides,* able to penetrate further into the root than its other non-pathogenic relatives, could become virulent given optimum conditions.

Plant cell wall appositions are a ubiquitous plant response to pathogen attack, forming one of the first layers of plant immunity. One such example are papillae, complex structures made up of callose, lignin, reactive oxygen species (ROS), and cell wall proteins such as peroxidases and antimicrobial thionins. Papillae are formed at the infection site between the plasma membrane and the inside of the plant cell wall, providing a physical barrier to invading pathogens (Voigt, 2014). Lignitubers are also a common defence strategy against fungal infection and are comprised of highly lignified callose deposits which surround hyphal tips, slowing down fungal growth. Both papillae and lignitubers were observed in response to the fungal species investigated, strengthening the consensus that they are non-specific plant responses to fungal colonisation (Łaźniewska et al., 2012). Large numbers of lignitubers were found surrounding cells colonised by *G. hyphopodioides*, though hyphae were able to overcome them in many cases, presumably by the exudation of cell wall degrading enzymes (CWDEs).

In contrast, far fewer lignitubers were produced in response to *G. tritici* infection and hyphae were observed penetrating the cell wall without the production of lignitubers or cell wall appositions. The finding supports previous reports that *G. tritici* produces highly effective CWDEs (Dori et al., 1995; Huang et al., 2001; Yu et al., 2010) and suggests that some hyphae may be able to avoid host detection. Alternatively, the lack of cell wall modifications in some plant cells could simply be because the cells in question were senescing, or already dead at the time of infection. It would be interesting to determine whether *G. tritici* targets the plasmodesmata to facilitate cell penetration, as is the case for several pathogens including *Fusarium* spp. and *M. oryzae* (Jia et al., 2019; Sakulkoo et al., 2018). Unidentified circular structures (2-8 µm in diameter) were detected in cells colonised by *G. hyphopodioides* and *G. tritici* at 9 dpi and were often deposited

at or associated with the cell wall. The structures were heavily stained by potassium permanganate ($KMnO_4$) in longitudinal sections, indicating a high lignin content. Given these characteristics, a possible role in plant defence seems likely, however further investigation is required.

To compare the distribution of lignin in different root cell layers, potassium permanganate staining of transversal root sections was also carried out. Root colonisation by *G. hyphopodioides* and the unnamed *Magnaporthaceae* species resulted in a marked increase in root lignification in advance of the infecting hyphae. Lignin deposition was localised in the stele and outer cortex during early colonisation, with deposition subsequently spreading to the inner cortex. Interestingly, root lignification was far less pronounced in response to *S. cylindrosporus*, a species more commonly isolated from grassland sites (Asher & Shipton, 1981). This finding is contrary to an early report by Speakman and Lewis (1978), in which significant lignification of the stele and endodermal wall was observed in response to *S. cylindrosporus* (previously *P. radicicola var. graminicola*), highlighting variability between isolates.

As mentioned in previously, lignin polymers are a major component of the secondary cell wall of vascular plants and lignin biosynthesis is known to be upregulated in response to pathogen attack (Bi et al., 2011) by functioning as a physical barrier to microbial invasion (Łaźniewska et al., 2012; Miedes et al., 2014). Increased lignification has also been documented in response to colonisation by beneficial species such as *Trichoderma* (Basińska-Barczak et al., 2020), potentially playing a role in induced resistance against plant pathogens. If lignification is involved in induced resistance against take-all disease, the findings described above could explain why the *S. cylindrosporus* isolate provided poor protection against take-all in co-inoculation bioassays (see chapter 3). However, given that *G. tritici* infection also resulted in extensive root lignification, the lignification response alone is unlikely to play a key role in induced resistance, unless lignin levels are sufficiently high at the point of *G. tritici* infection. Furthermore, Daval et al., (2011) demonstrated that *G. tritici* expresses laccase genes in planta, suggesting that *G. tritici* can degrade lignin.

Also noteworthy was the occurrence of root browning in all fungal treatments at 9 dpi. This finding highlights an important risk when considering species for biocontrol. As mentioned previously, fungal-plant interactions can range from mutualism through commensalism to parasitism in a continuous manner and endophytic relationships could become pathogenic (and vice versa) given the right conditions (Kogel et al., 2006). Nevertheless, the conditions in the present experiment are not representative of the field environment and the associated soil microbiome, where colonisation levels are markedly lower. Therefore, although the Eppendorf protocol allows for rapid colonisation and processing of samples, a system which uses lower inoculum levels may be of greater value when attempting to draw accurate comparisons to a field scenario.

Finally, the studies presented here allowed further investigation into poorly characterised fungal structures previously described in the literature as “sub-epidermal vesicles” (SEVs) or “growth cessation structures”. In the present study, large numbers of clustered SEVs were produced by *S. cylindrosporus* and the unnamed *Magnaporthaceae* species. Light microscopy and histochemical staining by aniline blue confirmed previous findings that SEVs have a thick cell wall with one or more pores. Curiously, SEVs were not produced by *G. hyphopodioides* in this set up. An alternative protocol was therefore used to generate *G. hyphopodioides* SEVs for further analysis. TEM micrographs revealed that SEVs had significantly thickened cell walls made up of two to three cell-wall layers, always comprising an electron dense layer. SEVs also contained large numbers of putative lipid bodies, the presence of which is currently being validated by nile red fluorescent staining. In comparison, hyphal cell walls were made up of a single layer and hyphae contained very few or no lipid bodies. The spherical shape of the SEVs, together with the thickened cell walls and increased lipid content, is highly indicative of a fungal chlamydospore (Bemena et al., 2021).

Chlamydospores are a form of fungal resting structure which are well characterised in many fungal species, including several root infecting fungi (Couteaudier & Alabouvette, 1990; Peškan-Berghöfer et al., 2004; Son et al., 2012). They are known to function as long-term survival structures and can resist

a wide range of environmental stresses (Francisco et al., 2019). Therefore, the SEVs produced in roots by several *Magnaporthaceae* species, including *M. oryzae* (Sesma & Osbourn, 2004), could be fungal chlamydospores, perhaps produced in response to halted growth as a result of physical barriers, nutrient deficiency, upregulated plant defences, or a combination of these factors. As mentioned previously, *G. hyphopodioides* SEVs were not detected in root sections generated in the Eppendorf infection assay. However, the structures are frequently detected in field samples and in samples generated in other plant bioassay experiments. One explanation may be that *G. hyphopodioides* could overcome host defences due to the high inoculum potential in the Eppendorf system, hence hyphal growth was not halted and SEVs were not produced.

Given that *G. tritici* has not been documented to produce SEVs in wheat roots, but is reported to produce SEVs (though perhaps incorrectly referred to as hyphopodia) in perennial ryegrass (*Lolium perenne*) (Umar et al., 2019), it is tempting to suggest that SEV formation is a result of local non-host resistance mechanisms. However, this would not explain why non-pathogenic *Magnaporthaceae* species produce SEVs in their “natural” grass hosts, or why non-pathogenic species can be induced to form SEVs *in vitro* (Deacon, 1976a). Taken together, it is hypothesised that SEV formation occurs as a result of halted hyphal growth, which is in turn governed by a range of factors including inoculum potential and local defence responses in the host plant.

Surprisingly, SEVs produced by *S. cylindrosporus* and the unnamed *Magnaporthaceae* species were often found to produce penetration pegs which traversed the plant cell wall, potentially enabling hyphae to invade adjacent cells. Though *G. hyphopodioides* did not produce SEVs in this system, SEVs with penetration pegs were observed in other systems, including in the TEM samples presented in this chapter, which were generated in a 5-week seedling bioassay, and in samples generated in a water agar system in chapter 5, which were analysed by confocal microscopy (appendix 1.7; figure A.7.3). The role of the penetration pegs is unknown, though the structures have been previously documented in field samples colonised by *S. cylindrosporus* (R. Gutteridge,

personal communication). Furthermore, other DSE fungi such as *Harpophora oryzae*, an endophytic symbiont of rice which shows biocontrol potential against rice blast disease, also produce SEVs/chlamydospores (referred to as intracellular microsclerotia) which seem to play a role in root infection (Su et al., 2013). These observations suggest that SEVs may have an additional function and are not purely resistance structures. Further investigation is needed to determine whether SEVs may in fact play a more active role in the infection biology of DSE fungi. Perhaps, by acting as a root specific, appressoria-like structure within the root, enabling hyphae to traverse the cell wall. Indeed, *G. hyphopodioides* SEVs share certain characteristics of *M. oryzae* appressoria, such as a thick cell wall with an distinct electron dense layer (Wang et al., 2007). In *M. oryzae*, this layer is known to comprise fungal melanin, which is crucial for turgor generation within the appressorium *(ibid.)*. Further investigation is needed to elucidate the molecular pathways involved in fungal SEV production, and the plant defence responses which may trigger SEV formation.

Based on the data presented in this chapter and information drawn from the literature, a basic model for SEV production and functioning is tentatively hypothesised:

1. Hyphal growth of melanised macrohyphae is halted in cortical or epidermal cells as a result of induced plant defences (e.g. antifungals, lignin/callose/suberin deposition, chitinases, ROS), resulting in hyphal swelling and increased cell-wall melanisation, eventually resulting in the development of a mature SEV which can exist independently of the parent macrohypha.
2. SEVs may enable the fungi to survive for extended periods when conditions are suboptimal. For example by providing an important lipid source and a thick protective layer against antifungal compounds or abiotic stresses such as cold soil temperatures.
3. If/when conditions become more favourable (for instance in plant cells which are dying, have lower levels of antifungal defence compounds or when environmental conditions improve), SEVs produce a penetration peg which enable hyphae to invade adjacent cells.

However, numerous inconsistencies remain. For instance, why is *M. oryzae* reported to produce SEVs on the root surface, whereas the non-pathogenic *Magnaporthaceae* species only produce these structures inside the root? Furthermore, why does *G. hyphopodioides* produce large solitary SEVs whereas *S. cylindrosporus* and the unnamed *Magnaporthaceae* sp. produce smaller and clustered SEVs? Is the size and distribution of SEVs related to virulence? Why doesn't *G. tritici* produce SEVs in wheat, is it a better pathogen and hence hyphal growth is not halted? Why then did *M. oryzae* produce SEVs in wheat but was still able to cause significant disease? Is SEV formation a response to a transient defence mechanism that *G. tritici* can overcome immediately, whereas *M. oryzae* cannot? Despite these outstanding questions, the findings presented in this chapter have provided several exciting avenues for future research.

4.6 Future work

Though the Eppendorf infection protocol successfully produced colonised root material, the experimental methods require further optimisation to achieve colonisation levels which better represent those of field samples. Reducing the size of the inoculum plug could produce more representative colonisation levels.

Further optimisation is also needed to improve the specificity of fungal staining. Aniline blue gave superior results compared to other commonly used fungal stains such as trypan blue and toluidine blue (see appendix A.4). However, aniline blue often resulted in unwanted staining of plant cell contents. To avoid this in future experiments, samples could be cleared in KOH for several minutes prior to fixation. Alternatively, the pH of the lactophenol aniline blue solution could be altered to improve the distinction between fungal and plant material. If fluorescent microscopy is appropriate, the staining method utilised in the following chapter could provide an alternative solution.

Potassium permanganate staining revealed a strong lignification response following colonisation by *G. hyphopodioides* and the unnamed *Magnaporthaceae* species. As both species resulted in significant take-all disease reduction when applied before *G. tritici*, future studies could investigate whether root lignification alone is sufficient to prevent disease. This could be achieved by testing wheat

varieties with naturally higher lignin levels (Rengel et al., 1993), or by overexpressing lignin biosynthesis genes using virus-mediated overexpression (VOX) (Bouton et al., 2018).

Though SEVs share key characteristics with fungal chlamydospores, the importance of SEVs in the fungal infection process is unknown. Future studies could investigate the fungal molecular pathways involved in SEV formation in the root, as well as the putative plant defence responses which may trigger SEV production in the plant. However, these analyses are likely to be complex, potentially requiring single-cell RNA sequencing (scRNA-seq) by laser ablation (Roux et al., 2014).

4.7 Summary

The present study has offered important insights into the infection mechanism and physical plant responses to three non-pathogenic *Magnaporthaceae* species. Root infection by *G. tritici*, *G. hyphopodioides* and the unnamed *Magnaporthaceae* species resulted in significant lignification of root tissue, whereas *S. cylindrosporus* colonisation resulted in comparatively low levels of lignification. Colonisation by all non-pathogenic species resulted in cell-wall modifications such as papillae and lignitubers, which restricted the growth of *S. cylindrosporus* and the unnamed *Magnaporthaceae* species, but not *G. hyphopodioides,* which was able to colonise the inner cortex. Light microscopy and TEM analyses of sub-epidermal vesicles (SEVs) revealed that these fungal structures share key characteristics with chlamydospores, perhaps produced in response to upregulated plant defences. However, the presence of penetration pegs supports a role in the infection cycle, hence further investigations are required to determine the true function(s) of fungal SEVs.

4.8 Acknowledgement of contributions

Thank you to Dr Eudri Venter for preparing and sectioning root samples for TEM analysis. Thank you also to Kirstie Halsey for helping to troubleshoot various issues with section quality and to Hannah Walpole for help testing different histochemical stains.

5 Investigating wheat transcriptional responses to *G. hyphopodioides* colonisation and *G. tritici* infection

NB: The present chapter has been written in a manuscript format to facilitate future publication of this work. Hence, the introduction may contain some information which is repeated in other chapters of this thesis.

5.1 Introduction

Root health is essential for overall plant productivity; roots being the organs of the plant responsible for acquiring water and essential nutrients, as well as anchoring the plant to the ground. These functions are particularly important for annual cereal crops, which must obtain enough resources to maximise yield, whilst also dealing with the physical weight of increased grain loads (Voss-Fels, et al., 2018). Roots must constantly interact with the diverse soil microbiome and are tasked with the challenge of distinguishing pathogenic microbes from non-pathogenic or beneficial microbes. However, as global temperatures continue to rise, root health is predicted to face increasing threat from a growing number of potential soil-borne fungal pathogens which could jeopardise future food production (Delgado-Baquerizo et al., 2020).

Plants can detect the presence of fungal pathogens through the recognition of conserved molecular patterns known as pathogen-associated molecular patterns (PAMPS) or microbe-associated molecular patterns (MAMPS). PAMPs, such as chitin, the major component of fungal cell walls, are recognised by membrane-localised pattern recognition receptors (PRRs), which trigger PAMP-triggered immunity (PTI), the plants first line of defence (Boller & Felix, 2009). PRRs can also indirectly detect pathogen attack through the recognition of host-derived damage-associated molecular patterns (DAMPs) (Li et al., 2020). PRR signalling results in the accumulation of antimicrobial compounds through a range of processes including the rapid accumulation of reactive oxygen intermediates, defence-related mitogen-activated protein kinase cascades and transcriptional reprogramming of the host.

Therefore, a successful pathogen must avoid PTI or find a way to suppress it. Pathogens secrete fungal effectors, secondary metabolites or proteins that kill the host plant, protect the fungus or suppress the plant immune response. However, effectors can be detected by plant resistance proteins (R proteins), some of which are conserved intracellular receptors of the nucleotide-binding leucine-rich receptor (NB-LRR) class. Activation of R proteins by effectors, often referred to as avirulence (avr) proteins, triggers the second layer of defence known as effector-triggered immunity (ETI). ETI results in disease resistance and usually, a hypersensitive (HR) cell death response at the site of pathogen attack (Jones & Dangl, 2006; Lo Presti et al., 2015).

The classical model of plant immunity described above is largely based on research into foliar pathogens. However, there is growing evidence that root defence strategies may differ from aboveground strategies. The root apex is made up of the division zone (otherwise known as the root apical meristem), the transition zone and the elongation zone. The detection of microbe-associated molecular patterns (MAMPs) in the vulnerable root division zone is sufficient to trigger an immune response. However, in differentiated cells away from the division zone, an additional damage-associated molecular pattern (DAMP) signal is needed to trigger the plant immune response in Arabidopsis (Zhou et al., 2020). These findings suggest that local responses play an important role in root immunity.

Take-all root disease of wheat, caused by the necrotrophic fungal pathogen *Gaeumannomyces tritici,* is amongst the most important root diseases of wheat worldwide (Jacqueline Freeman & Ward, 2004). The fungus produces runner hyphae which grow across the surface of the root before penetrating the epidermal cells and infecting the cortex and stele, causing irreparable damage to the vascular tissue (Asher & Shipton, 1981; Huang et al., 2001). Necrotic lesions develop from the stele and result in disrupted water and nutrient uptake, with subsequent early ripening of the crop and reduced grain yield and quality. Though mainly a problem for 2nd and 3rd year wheats, take-all disease also affects other cereal species such as rye and barley (Cook, 2003). Currently, there are no

commercial wheat varieties with take-all resistance and chemical control is limited, with approximately 30% of *G. tritici* isolates exhibiting natural insensitivity to the *G. tritici* specific fungicide Latitude® (common name Silthiofam; previously Mon65500; CHEBI:83393) (Freeman et al., 2005).

However, compared to other important foliar pathogens of wheat, relatively little is known about specific wheat defence responses against *G. tritici.* In a recent study by Zhang et al. (2020), early *G. tritici* infection resulted in the induction of several pathways involved in pathogen resistance in wheat, including oxidation-reduction processes, tryptophan biosynthesis and phenylpropanoid biosynthesis. Differential gene analyses suggested that the plant hormones jasmonic acid (JA), ethylene (ET), and lipoxygenase (LOX) were likely to be involved, though comparatively fewer genes were associated with SA biosynthesis. Conversely, hormonal quantifications performed by Kang et al. (2019) revealed that both JA and SA levels increase during *G. tritici* infection. The same study also found a significant upregulation of phenylalanine ammonia lyase (PAL) genes which are involved in the biosynthesis of lignin and SA, suggesting that both are likely to be involved in wheat defence responses against *G. tritici.*

Within the *Magnaporthaceae* family are several non-pathogenic species which also colonise wheat. A number of these species, including *Gaeumannomyces hyphopodioides,* have been shown to provide some protection against take-all disease in field studies. Furthermore, certain elite winter wheat varieties have an improved ability to promote *G. hyphopodioides* in field soils (Osborne et al., 2018), making the species a promising candidate for biocontrol. Early field studies suggested that non-pathogenic *Magnaporthaceae* species must colonise the root system first to provide effective protection from *G. tritici* (Balis, 1970; Deacon, 1976b; Wong & Southwell, 1980). Co-inoculation seedling bioassays carried out in chapter 3 further validated this finding. Additionally, fungal confrontation assays suggested that direct hyphal interaction is unlikely to play a significant role in disease reduction, thus demonstrating that induced plant resistance is responsible for take-all control. Furthermore, initial pilot data from a split-root

hydroponic system suggested that *G. hyphopodioides*-induced resistance is effective in both local and systemic tissues (appendix A.3).

Beneficial microbes, including bacteria and fungi, are known to protect distal regions of the plant from disease. Similarly, local plant infection by pathogens can result in uninfected regions becoming more resistant to disease. Both scenarios are forms of induced resistance, a phenomenon which is characterised by the activation of latent defence pathways which are subsequently expressed upon future challenge by a pathogen. Induced resistance can also lead to the priming of defence related genes or pathways, resulting in stronger elicitation of defences following pathogen attack (Goellner & Conrath, 2008).

The two main forms of induced resistance, induced systemic resistance (ISR) and systemic acquired resistance (SAR), can be distinguished by the type of elicitors involved and signalling pathways which are induced. SAR is generally triggered by pathogen infection via the plant detection of both MAMPs and DAMPs. However, SAR can also be triggered by exposing the plant to avirulent and non-pathogenic microbes (Choudhary et al., 2007). The key characteristic of SAR is the dependence on salicylic acid (SA) signalling. Conversely, ISR is generally induced by beneficial microbes via the plant detection of MAMPs and results in the priming of jasmonic acid (JA)/ethylene (ET) responsive genes. In Arabidopsis, the root-specific transcription factor MYB72 is a node of convergence between different ISR inducing microbes (Segarra et al., 2009). However, specific ISR and SAR mechanisms are likely to differ depending on the microbe and the host in question.

The specific mechanisms mediating *G.* hyphopodioides-induced resistance (ISR/SAR) are unknown and the molecular pathways underpinning the wheat- *G. hyphopodioides* interaction have not been investigated until now. RNA sequencing (RNAseq) is a powerful technology for the study of plant transcriptomic changes during pathogen infection. Comparative transcriptomic investigation of *G. hyphopodioides* colonised and *G. tritici* infected wheat by dual RNAseq offers the unique opportunity to study molecular plant responses to two closely related fungal species with differing levels of pathogenicity. Furthermore,

such analyses will facilitate an improved understanding of the biocontrol mechanism(s) of *G. hyphopodioides* against take-all disease.

In this study, we carried out a time-resolved dual RNAseq experiment to identify wheat differentially expressed genes (DEGs) in response to *G. hyphopodioides* and *G. tritici* at key stages of fungal infection. Our findings contribute to an improved understanding of take-all resistance mechanisms, which will guide future research into this important pathogen system.

5.2 Methods

5.2.1 Co-inoculation experiment

Previous co-inoculation experiments demonstrated that prior colonisation by *G. hyphopodioides* isolate NZ.129.2C.17 in wheat cv. Hereward results in a significant reduction in take-all disease caused by *G. tritici* isolate Gt16.NZ.1d (type A, Latitude® sensitive) (see chapter 3). Since these experiments were carried out, the *G. tritici* isolate GtLH(4)19d1 (type A, Latitude® insensitive) was selected for de *novo* genome sequencing due to its high level of virulence, and was subsequently chosen for inclusion in the present RNAseq experiment. The wheat cv. Chinese Spring was selected due to the availability of an annotated genome (Zhu et al., 2021). Consequently, a further co-inoculation pot test was carried out to confirm that *G. hyphopodioides* isolate NZ.129.2C.17 can also successfully reduce take-all disease caused by GtLH(4)19d1 in wheat cv. Chinese Spring.

The experiment was set up using the methods outlined in chapter 3.3.3, with the exception that *G. hyphopodioides* was added one week prior to *G. tritici* only. The experiment was carried out twice and data were pooled prior to statistical analysis. Visual disease assessments and qPCR analysis of *G. tritici* fungal biomass were carried out as outlined in chapter 2.5 and 2.14, respectively. Statistical analyses were carried out in Genstat 20th Edition (VSN International, UK), as described in chapter 2.15.

5.2.2 Seedling infection protocol

Wheat seeds cv. Chinese Spring were surface sterilised in 1 % w/v sodium hypochlorite for 10 minutes with occasional mixing, followed by 3 x 1 min washes in sterile distilled water. Seeds were placed in Petri dishes lined with sterile filter paper and were watered with 5 ml sterile distilled water, before placing in a growth chamber for 2 days (20 °C day, 16 °C night, 16 hr light cycle, light intensity 5). After 2 days the radicle had emerged and roots were approximately 1 cm long.

Water agar was prepared by diluting agar-agar powder (Pure Granular Powder, Fisher Chemical, 10548030) in distilled water to make a 1.5 % w/v agar solution. The water agar was sterilised in an autoclave before supplementing with kanamycin to a final concentration of 50 µg/ml. Square Petri dishes (12 cm x 12 cm; Greiner Bio-one, UK) were filled with 35 ml water agar and left to cool. Three pre-germinated seeds were placed equal distances apart on the surface of the water agar and were partially sunk to prevent dislodging. Plates were sealed with Parafilm M® film (Bemis company, Inc; USA), leaving one corner open to allow airflow. The lower half of the plate was covered with foil to provide a dark environment for root growth. Plates were placed horizontally in the growth chamber in a randomised block design generated in Genstat 20th Edition. A gap of approximately 3 cm was left between each plate to allow even access to the light source.

After four days, one root from each plant was inoculated with a 4 cm x 0.5 cm rectangular piece of inoculum cut from the leading edge of a fungal colony growing on water agar (see table 5.1 for treatment details). This enabled root infection to be accurately tracked and ruled out any potential systemic effects of infection. The low nutrient content of water agar enabled rapid root colonisation essential for the present experiment. Mock-inoculated roots were inoculated with water agar only and five replicates were set up for each treatment. Roots were sampled daily from 2-6 dpi.

Table 5.1 Summary of *in planta* treatments explored for RNA sequencing

Treatments	Time point	Replicates
Wheat -	2, 3, 4 ,5, 6 dpi	A, B, C, D, E
Wheat + Gh NZ.129.2C.17	2, 3, 4 ,5, 6 dpi	A, B, C, D, E
Wheat + Gt 17(LH)19d1	2, 3, 4 ,5, 6 dpi	A, B, C, D, E

5.2.3 *In vitro* fungal samples

In vitro fungal samples were generated to provide a control for fungal read mapping and to inform future studies into fungal gene expression. Fungal mycelium was grown up in 200 ml conical flasks containing 50 ml Potato Dextrose Broth (PDB; Formedium, UK) supplemented with 50 µg/ml kanamycin. Flasks were inoculated with 3 x mycelial plugs taken from the leading edge of a two-week old fungal colony growing on Potato Dextrose Agar (PDA; Formedium, UK) using a no.2 cork borer (5 mm). Plugs were cut up into small pieces to ensure even mycelial growth. Five flasks were set up for each fungus to provide five treatment replicates (table 5.2). Inoculated flasks were placed in a New Brunswick™ Innova® 44 orbital shaker (New Brunswick Scientific, UK) at 20 °C, 160 RPM for four days. Cultures were filtered through sterile Miracloth (Merck, USA) by vacuum filtration, followed by three washes with sterile water. Harvested mycelium was immediately snap frozen in liquid nitrogen. Several attempts were made to grow cultures in Czapek Dox liquid media to provide a low nutrient comparison. However, despite pooling samples, mycelial growth was extremely limited and RNA yield was not sufficient for sequencing.

Table 5.2 Summary of *in vitro* treatments for RNA sequencing

Treatments	Time point	Replicates
PDB + Gh NZ.129.2C.17	4 days growth	A, B, C, D, E
PDB + Gt 17(LH)19d1	4 days growth	A, B, C, D, E

5.2.4 Root sampling

Roots were sampled by removing the 4 cm inoculated root area using a sterile scalpel blade. Two 1 cm root sections were cut from the 4 cm area and placed in individual 1.5 ml Eppendorf tubes before snap freezing in liquid nitrogen. Samples were stored at -80°C prior to RNA extraction. To assess the stage of fungal colonisation in these 1 cm sections, 2x 0.5 cm root pieces were taken from the areas directly flanking each section and were stored in 50% ethanol for subsequent assessment by confocal microscopy (figure 5.1). Following confocal assessment (see section 5.2.6), 1 cm sections taken from the same plate and at the same stage of fungal colonisation were pooled together to create a single sample for RNA extraction (maximum 6 pooled root pieces per sample).

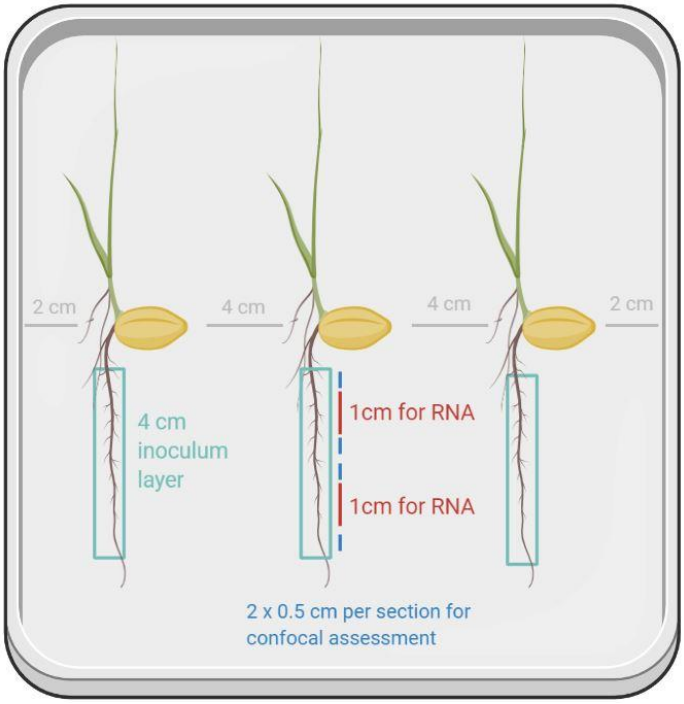


Figure 5.1 Schematic showing the root infection protocol and root areas sampled. Created in BioRender.com.

5.2.5 RNA extractions

RNA extractions were carried out as detailed in chapter 2.9. RNA concentrations were quantified using the Qubit™ RNA High Sensitivity Assay Kit (ThermoFisher Scientific, USA). RNA quality was assessed based on the RNA Integrity Number

(RIN), measured using the Bioanalyser 2100 with the corresponding RNA 6000 Nano Kit (Agilent, USA) as per manufacturer instructions.

5.2.6 Confocal microscopy of infected root pieces

To assess fungal colonisation at each time point, 2x 0.5 cm regions flanking each 1 cm section were taken for confocal analysis. Root pieces were cleared in 10% w/v potassium hydroxide (KOH) for 6 minutes at 70 °C. Cleared samples were washed in sterile distilled water, before staining with 100 µl Propidium Iodide (PI) (10 µg/ml) followed by 100 µl Wheat Germ Agglutinin, Alexa Fluor™ 488 Conjugate (WGA) (10 µg/ml) for 10 minutes each. Roots were washed three times in sterile distilled water. A ZEISS 780 Confocal Laser Scanning Microscope (ZEISS, Germany) was used for the detection of fluorescent signals from WGA and PI stained root samples. The fluorescence of WGA was excited at 495 nm and detected at 519 nm. The fluorescence of PI was excited at 535 nm and detected at 617 nm. The stage of fungal colonisation was noted and the information was used to determine the appropriate time-points for RNA sequencing.

Due to the thickness of wheat roots, visualisation of *G. tritici* in the central stele was not optimal. Hence, transversal sections were obtained to provide clear images of *G. tritici* hyphae in the stele. Transversal root sections were cut by hand using a fine edged razor blade under a dissecting microscope. Sections were transferred to a cover slip (0.17 mm thick, 22 x 50mm, 1½ thickness; Agar Scientific) and stained in situ. The cover slip was placed in a custom-made 3-D printed cover slip holder, allowing Z- stack images to be captured from the bottom facing side of each section.

5.2.7 Library preparation and sequencing

mRNA library preparation was carried out by Novogene (China) using the Novogene RNA Library Prep Set (PT042) and polyA enrichment method. Libraries were sequenced by Illumina NovaSeq to generate 150 bp paired-end reads, with a target of 40 million paired-end reads per sample.

5.2.8 Transcriptome annotation and analysis

Transcriptome annotation and analyses were carried out in collaboration with Dr Daniel Smith (Bioinformatician, Department of Computational and Analytical Sciences, Rothamsted Research, UK). Quality control of reads was performed using MultiQC (https://multiqc.info/). Sequence trimming of recognised adaptors was performed using Trimmomatic where appropriate (Bolger et al., 2014). Reads were mapped to the Chinese Spring (IWGSC RefSeq v2.1) (Zhu et al., 2021) and *G. tritici* genome (Okagaki et al., 2015) using HiSat2 (Kim et al., 2019; https://daehwankimlab.github.io/hisat2/). Count determination was performed using FeatureCounts (Liao et al., 2014; https://bioconductor.org/packages/release/bioc/html/Rsubread.html) on the R Bioconductor platform (https://bioconductor.org/).

Based on the FeatureCount data of *G. tritici* mapped reads, three samples were identified as outliers (determined from standardised residual values) and were subsequently excluded from further analyses (appendix A.7; table A.7.4). To confirm that biological replicates clustered together, Principal Component Analysis (PCA) was performed on sample differences of variance stabilising transformed (vsd) gene count data.

Library normalisation and differential expression (DE) calling was carried out using the Bioconductor package DESeq2 (Love et al., 2014; https://bioconductor.org/packages/release/bioc/html/DESeq2.html) in R studio. Gene expression levels were compared between *G. tritici* infected/*G. hyphopodioides* colonised samples and the uninoculated control samples for each time point individually. DEGs were identified by applying a log2 fold change filter of ≥ 1 or ≤ -1 and the DESeq2 implementation of Benjamini-Hochberg (Benjamini & Hochberg, 1995) was used to control for multiple testing ($q<0.05$).

Gene Ontology (GO) enrichment analysis was performed for significantly up- and down-regulated wheat genes separately via http://www.geneontology.org, using the Panther classification system. To visualise the most representative up- and down-regulated GO terms that were unique/shared across treatments at different

time-points, a stringent dispensability cut-off (<0.01) was applied using the web server REVIGO (http://revigo.irb.hr/) as per the protocol by Bonnot et al., (2019).

We also investigated the expression of several genes/gene pathways which were not identified by GO enrichment analysis, but were of interest due to their involvement in plant defence responses. DEGs in *G. hyphopodioides* colonised and *G. tritici* infected plants compared to the uninoculated control at 5 dpi were annotated using KnetMiner software (Hassani-Pak et al., 2021) (https://knetminer.com/Triticum_aestivum/). Genes of interest were cross checked by performing a nucleotide BLAST on the NCBI database (https://blast.ncbi.nlm.nih.gov/Blast.cgi).

5.2.9 Quantification of hormones from root samples

To generate sufficient root material for hormone quantifications, an experimental repeat was carried out using the method described in section 5.2.2. Roots were sampled at 5 dpi by harvesting the 4 cm inoculated root area from each plant. Samples at the same stage of fungal colonisation were pooled and lyophilised for 24 hours in a LyoDry Compact Benchtop Freeze Dryer (Mechatech systems, UK). Samples were ground to a fine powder in a Geno/Grinder ® (SPEX Europe, UK). The quantification of hormones (salicylic acid; SA, jasmonic acid; JA and gibberellic acid; GA) from lyophilised root samples (~30 mg dry weight) was performed by Dr Esther Carrera (Institute for Plant Molecular and Cell Biology, University of Valencia, Spain). Hormones were separated by UHPLC with a reverse Accucore C18 column (2.6 µm, 100 mm length; Thermo Scientific™) and an acetonitrile gradient containing 0.05% acetic acid. The hormones were analysed with a Q-Exactive mass spectrometer (Orbitrap detector; Thermo Scientific™). The concentrations of hormones in the extracts were determined using embedded calibration curves and the Xcalibur 4.0 and TraceFinder 4.1 SP1 programs. Three biological replicates per treatment (Wheat-, Wheat+Gh, Wheat+Gt) were analysed. Data were square root transformed to achieve normality prior to analysis by ANOVA in Genstat 20th edition.

5.2.10 Lignin staining of root samples

Lignin staining of root samples was carried out by Kirstie Halsey (Light Microscopist, Department of Computational and Analytical Sciences, Rothamsted Research, UK). Roots were sampled at 5 dpi as above and stored in a 50% EtOH solution at 4°C until use. Samples were embedded in glycol methacrylate resin, sectioned and stained with potassium permanganate as described in chapters 4.3.2 and 4.3.3.

5.2.11 Validation of gene expression by RT-qPCR

The transcript abundance of selected DEGs will be assessed in 5 dpi samples by RT-qPCR. DEGs were selected based on their potential role in *G. tritici* resistance. cDNA was synthesised using the SuperScript™ IV Reverse Transcriptase Kit with Oligo (dT) primers (ThermoFisher Scientific, USA), according to the manufacturer's instructions. NB: This work is still ongoing, see table 5.3 for the list of genes to be targeted in RT-qPCR validations.

Table 5.3 List of genes to be validated by RT-qPCR.

Gene IDs	Gene name
TraesCS5D02G488800 TraesCS5D02G488900	COMT-like
TraesCS2D02G377400 TraesCS2B02G398300 TraesCS2A02G380900	PAL
TraesCS3A02G478500 TraesCS3B02G522000 TraesCS3D02G473200	BAK1-like
TraesCS2A02G169300 TraesCS2D02G176800 TraesCS2B02G195600	TIFY
TraesCS7A02G509000 TraesCS7D02G497300 TraesCS7B02G418400	WRKY28-like
TraesCS5A02G548500 TraesCS4B02G383000 TraesCS4D02G358700	XTH
TraesCS3B02G120700 TraesCS3D02G105500	FLA11

TraesCS3A02G103100	
TraesCS1B02G167200 TraesCS1A02G149300 TraesCS1D02G146600	CESA7

5.3 Results

5.3.1 Control of take-all disease by *G. hyphopodioides*

To investigate take-all disease control by the closely related, non-pathogenic species *G. hyphopodioides*, a seedling co-inoculation experiment was carried out under controlled environment conditions. The data revealed a clear reduction in both take-all disease levels (GLM: d.f. 1, 21, F=29.24, p<0.001) and *G. tritici* fungal biomass (ANOVA: d.f. 1, 8, F=15.54, p=0.004) in plants pre-treated with *G. hyphopodioides* (figure 5.2, appendix A.7; table A.7.1-A.7.2). These findings are consistent with previous experiments involving a different *G. tritici* isolate and wheat cultivar (see chapter 3), demonstrating that induced plant resistance is responsible for the control of take-all disease by *G. hyphopodioides.*

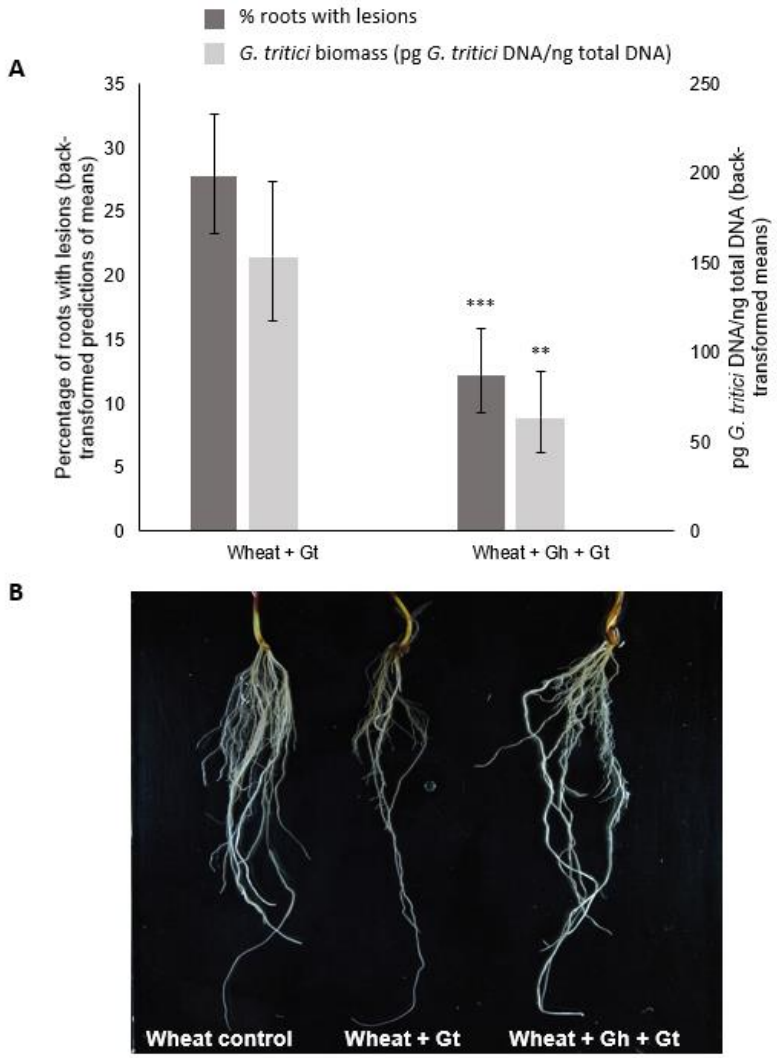


Figure 5.2 A. The percentage of roots with take-all lesions and amount of *G. tritici* fungal biomass (pg *G. tritici* DNA/ ng total DNA) with and without *G. hyphopodioides* pre-treatment. Percentage data represents back-transformed predictions of means from a LOGIT scale. Error bars represent 95 % confidence intervals. ***p<0.001, **p<0.01. B. Representative images of inoculated wheat roots.

5.3.2 Characterising fungal colonisation across time points

Three time-points (2, 4 and 5 dpi) spanning key stages of early fungal colonisation were selected for RNAseq analysis by confocal microscopy of root samples stained with PI and WGA. Due to the thickness of wheat roots, the central stele could not be easily visualised. Hence, transversal sections were also analysed in parallel. At these time-points, widescale root necrosis associated with take-all lesion development had not yet commenced, enabling the detection of key

molecular pathways induced during the early wheat response to two closely related pathogenic and non-pathogenic fungi.

At 2 dpi, small amounts of hyaline runner hyphae were detected on the surface of *G. tritici* and *G. hyphopodioides* inoculated roots (figure 5.3) though hyphae had not yet penetrated the epidermal cells (figure 5.4). By 4 dpi, hyaline runner hyphae covered a greater area of the root surface and hyphae were found inside epidermal and cortical cells of both *G. tritici* and *G. hyphopodioides* inoculated roots. Interestingly, small unknown circular structures were stained by PI and were detected in cortical cells colonised by *G. tritici* (figure 5.4). The structures were not detected in control samples but were present in both *G. tritici* and *G. hyphopodioides* infected samples at 5 dpi, suggesting that they are produced in response to infection.

At 5 dpi, hyaline runner hyphae were detected across a large area of the root surface in both fungal treatments (figure 5.3). *G. tritici* hyphae infected the stele, whereas *G. hyphopodioides* hyphal growth was arrested in the cortex (figures 5.4, 5.5). Additional samples taken at 6 dpi demonstrated that despite high colonisation levels, *G. hyphopodioides* hyphae were unable to penetrate the endodermal barrier and infect the stele (figure 5.6). Melanised macrohyphae were detected on the surface of *G. hyphopodioides* inoculated roots (figure 5.3). Interestingly, these hyphae were not always stained by WGA. Melanised macrohyphae were also found inside cortical cells, from which sub-epidermal vesicles (SEVs) were produced (figure 5.4). Newly formed SEVs were stained by WGA, whereas older melanised SEVs did not take up the stain and were only visible under transmitted light (appendix A.7; figure A.7.1). As documented in chapter 4, a small number of SEVs were observed with penetration pegs which penetrated the cell wall (chapter 4; figure 4.14). See chapter 4.5 for further discussion of this finding.

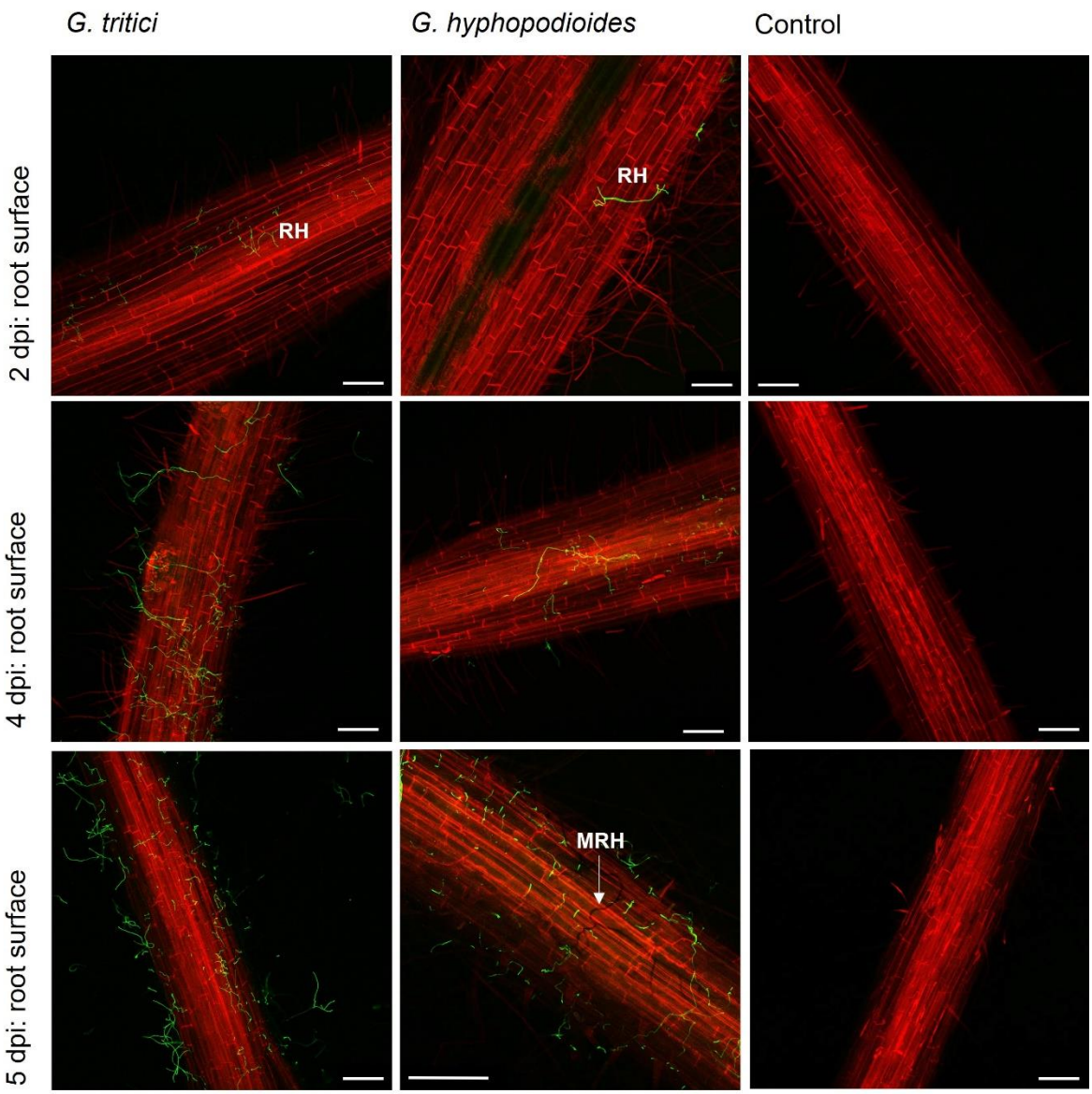


Figure 5.3 Fluorescence images obtained by confocal microscopy showing runner hyphae on the root surface at key time points selected for RNA sequencing. RH= runner hyphae, MRH=melanised runner hyphae. Scale bars represent 200 µm.

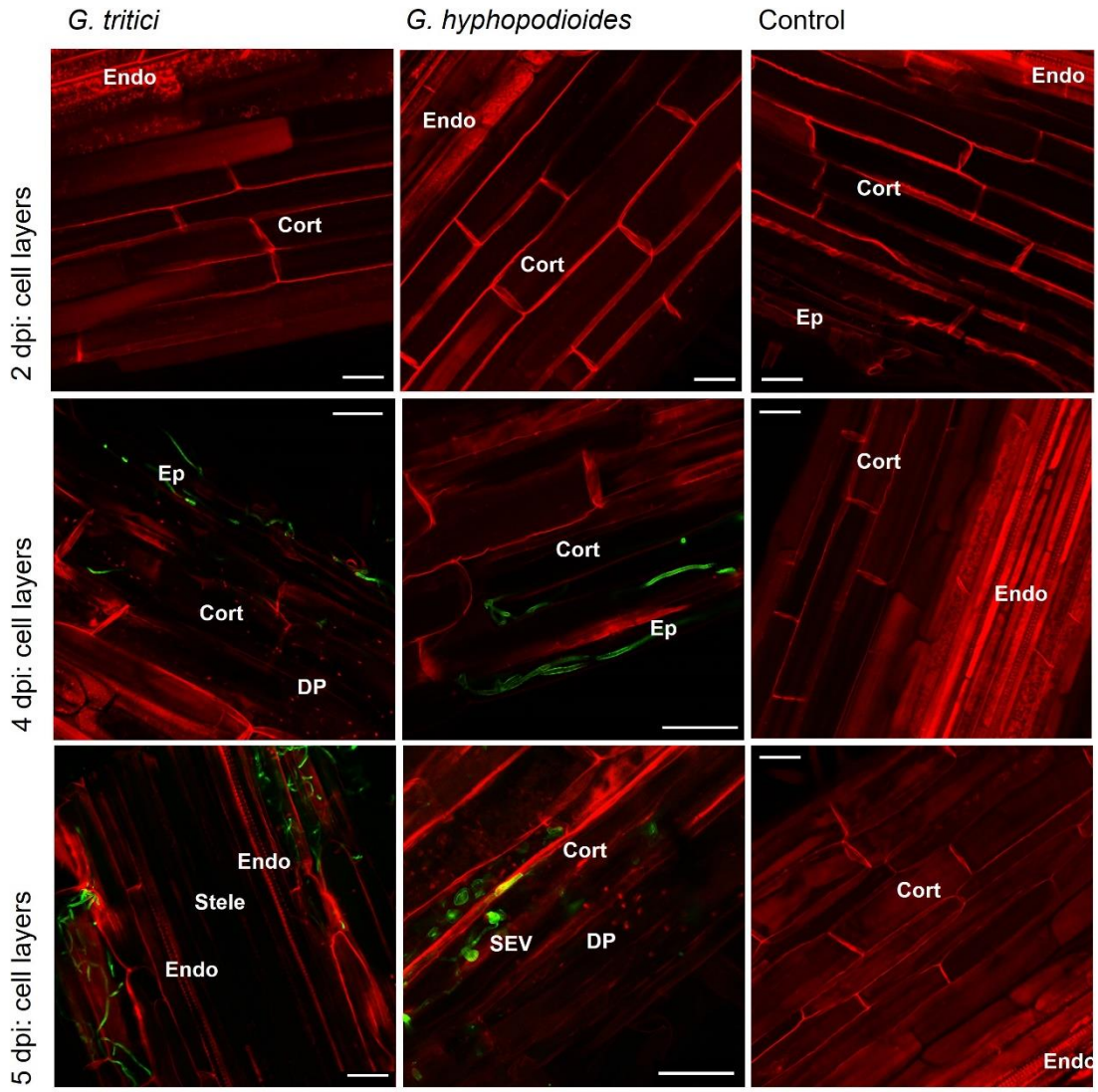


Figure 5.4 Fluorescence images obtained by confocal microscopy showing infection hyphae in different root cell layers at key time points selected for RNA sequencing. Ep=epidermal cell, Cort= cortical cell, SEV= sub-epidermal vesicle, Endo= endodermal barrier, DP= dotted PI staining. Scale bars represent 50 µm.

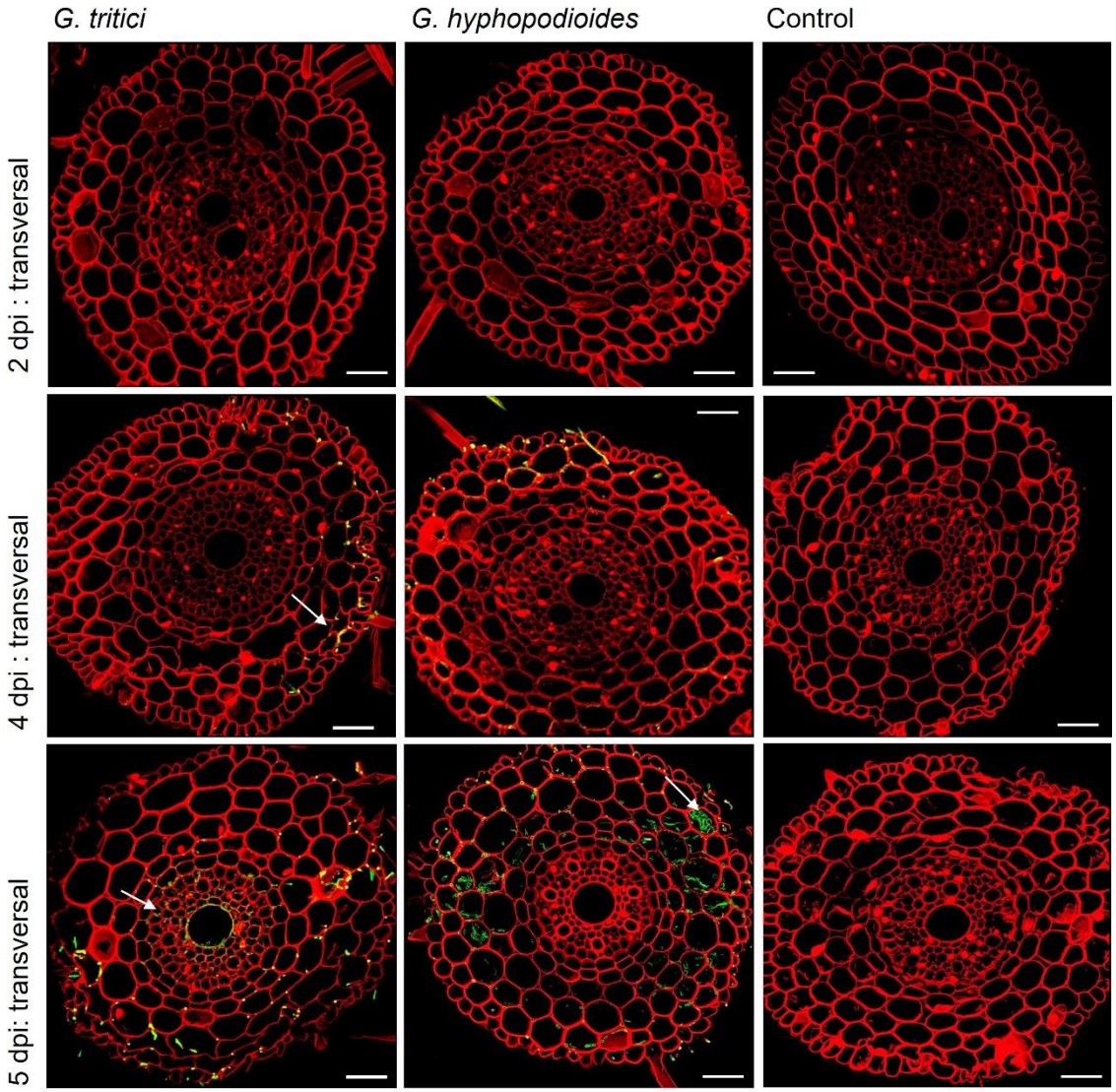


Figure 5.5 Fluorescence images obtained by confocal microscopy of transversal root sections showing the stage of fungal colonisation at key time points selected for RNA sequencing. Arrows indicate fungal hyphae. SEVs= Sub-epidermal vesicles. Scale bars represent 50 µm.

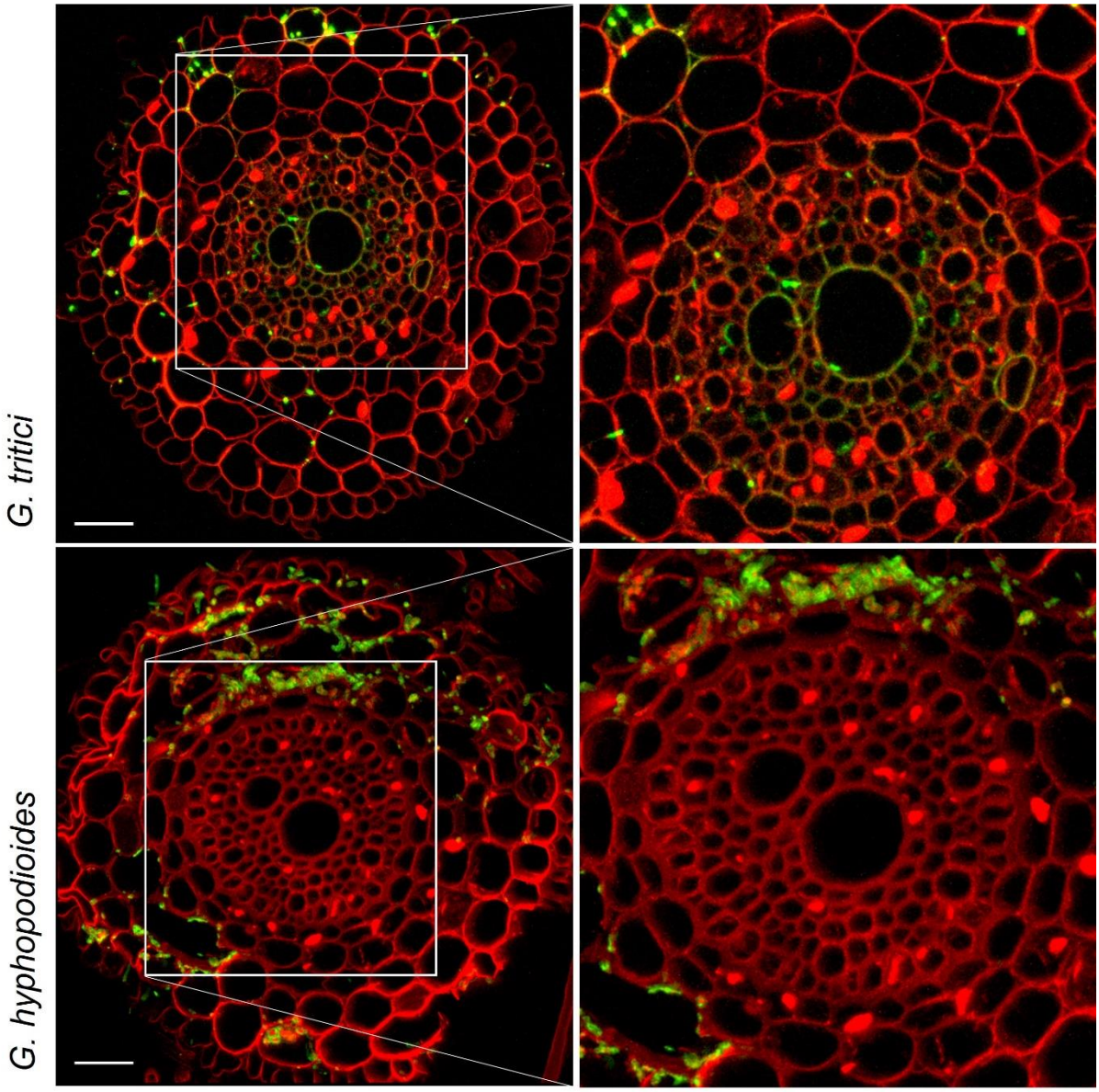


Figure 5.6 Confocal micrographs of transversal root sections at 6 dpi, demonstrating that unlike *G. tritici*, *G. hyphopodioides* does not colonise the root stele. Scale bars represent 50 µm.

5.3.3 RNA sequencing and read mapping

All samples successfully met the RNA sequencing quality measures (appendix A.7; table A.7.3) and sequencing yielded on average 42 million paired-end 150 bp reads per sample (table 5.4). Raw total reads (2,096,446,839) were mapped to the wheat genome, resulting in 1,477,788,362 total assigned reads, corresponding to 120,744 genes. To rule out genes with poor expression, we excluded genes with total counts of ≤ 1, which reduced the final number of genes to 86,308.

To investigate the progression of infection, total raw reads were also mapped to the *G. tritici* genome. However, it was not possible to map reads to *G. hyphopodioides* as a high-quality genome is not yet available. To combat this, we used the *G. tritici* mapping rates as a proxy for *G. hyphopodioides* mapping rates. As expected, the percentage of reads mapped to the *G. tritici* genome increased in *G. hyphopodioides* and *G. tritici* infected root samples from 2 to 5 dpi (table 5.4, figure 5.7). This increase was gradual for *G. tritici* infected samples, whereas mapping rates in *G. hyphopodioides* colonised roots increased drastically at 5 dpi. Based on the mapping rates of the *in vitro* fungal samples, it could be estimated that mapping rates of *G. hyphopodioides* colonised samples to the *G. hyphopodioides* genome would be approximately 4x that of the observed mapping rates to the *G. tritici* genome. This finding could explain the disparity in the percentage of reads mapped to the *T. aestivum* and *G. tritici* genomes in *G. hyphopodioides* colonised samples at 5 dpi. The mapping rates also highlight the extensive colonisation of the cortex by *G. hyphopodioides,* as observed in the confocal analyses in section 5.3.2. Having said this, there is a possibility that the core genes expressed by *G. tritici* and *G. hyphopodioides in planta* may be more similar than those expressed *in vitro*.

Table 5.4 Average read counts and percentage mapping statistics to the *T. aestivum* and *G. tritici* genome.

Treatment	Time point (dpi)	Average number of paired reads per sample	Average percentage of reads mapped to *T. aestivum* genome (%)	Average percentage of reads mapped to *G. tritici* genome (%)

Wheat -	2	41,611,165	99.03	0.00
Wheat + Gh	2	41,722,187	98.87	0.03
Wheat + Gt	2	43,906,212	98.75	0.21
Wheat -	4	41,182,744	99.03	0.00
Wheat + Gh	4	42,140,951	96.24	0.32
Wheat + Gt	4	45,673,268	95.83	2.75
Wheat -	5	43,557,205	99.09	0.01
Wheat + Gh	5	41,261,463	68.35	5.30
Wheat + Gt	5	40,703,208	93.70	3.99
PDB + Gh	NA	41,812,699	0.02	21.67
PDB + Gt	NA	41,669,207	0.01	92.76

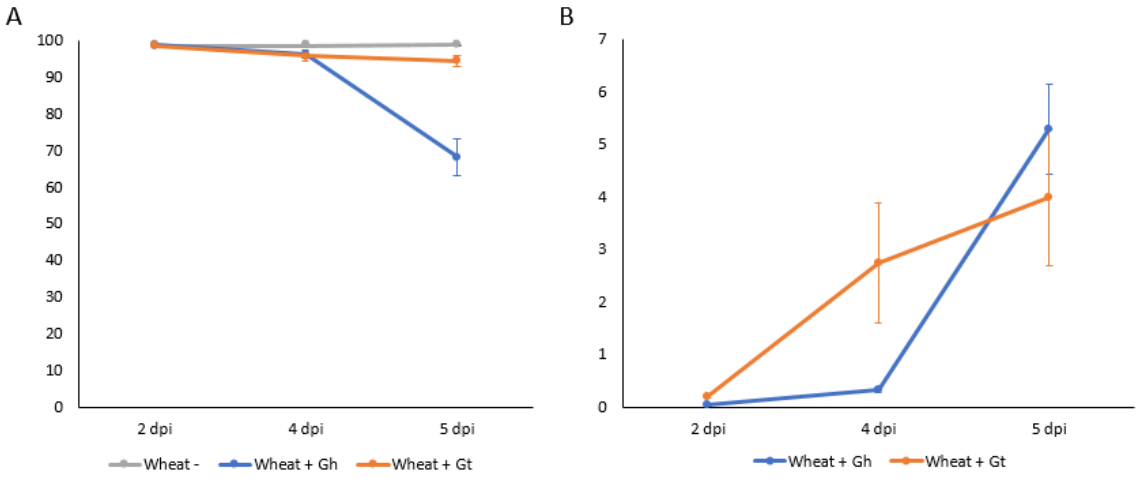


Figure 5.7 The percentage of reads mapped to the *T. aestivum* (A) and *G. tritici* (B) genome. Error bars represent standard error.

Principal Component Analysis (PCA) of sample distances demonstrated a good level of clustering between biological replicates, though *G. tritici* infected samples exhibited higher levels of variation than the other treatments (figure 5.8). The analysis also revealed that *G. hyphopodioides* colonised samples clustered together with the uninoculated control samples (Wheat-) at 2 dpi, while *G. tritici* infected samples showed a greater separation from the control. At 4 dpi, *G. hyphopodioides* colonised samples clustered within *G. tritici* infected samples, but by 5 dpi the two fungal treatments showed a good level of separation.

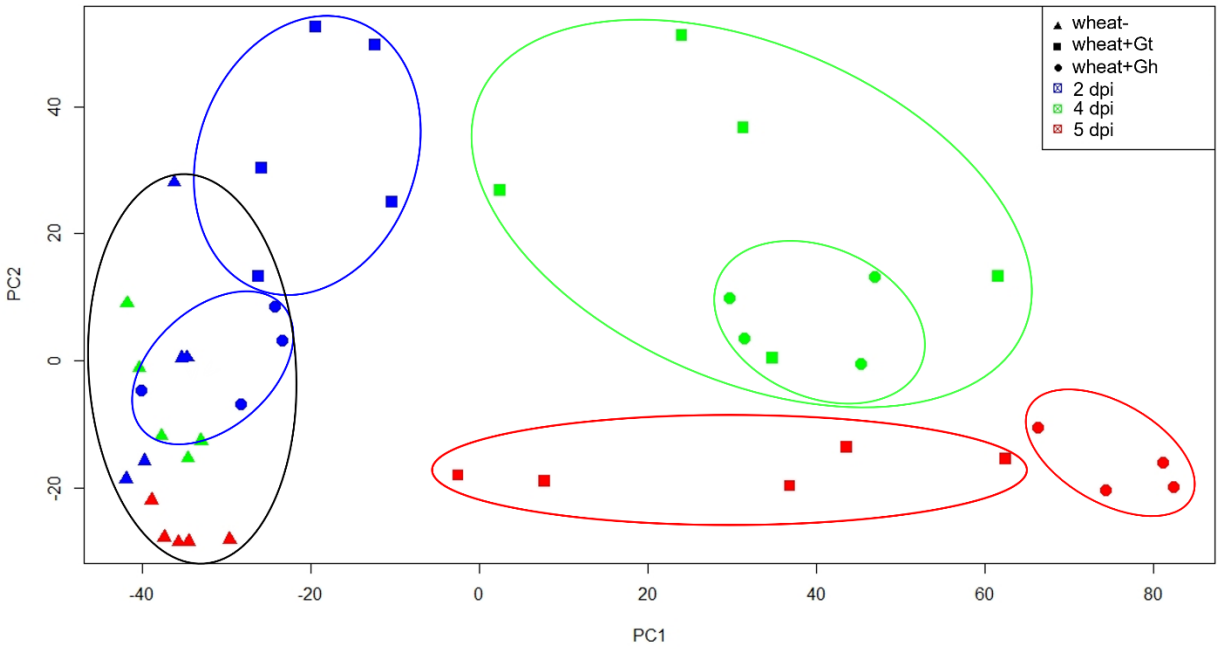


Figure 5.8 Principal Component Analysis (PCA) plot of sample distances based on vsd transformed gene count data. Generated using DeSeq2 in R studio. Data points have been categorised by shape and colour to denote treatment and timepoint, respectively. Key: triangles= wheat-, squares= wheat+*G. tritici*, circles= wheat+*G. hyphopodioides*, blue shapes= 2 dpi, green shapes= 4 dpi, red shapes= 5 dpi.

5.3.4 Identification of DEGs in wheat roots during the response to *G. tritici* infection and *G. hyphopodioides* colonisation

Gene expression levels were compared between *G. tritici* infected/ *G. hyphopodioides* colonised plants and the uninoculated control plants at each time point individually. As expected, the number of DEGs between the uninoculated control and *G. tritici* infected/ *G. hyphopodioides* colonised plants was low at 2 dpi (77 and 62 respectively). Interestingly, of these DEGs, a greater proportion were downregulated in *G. hyphopodioides* colonised wheat vs. the uninoculated control, compared to *G. tritici* infected wheat vs. the uninoculated control (figure 5.9 A). By 4 dpi, *G. tritici* and infection *G. hyphopodioides* colonisation resulted in the differential expression of 1061 and 1635 genes, respectively, with 839 genes differentially expressed (DE) in response to both fungi. At 5 dpi, a striking number of genes were DE in response to *G. hyphopodioides* colonisation (7532), whereas

the number of DEGs in response to *G. tritici* infection showed little change compared to 4 dpi. Surprisingly, 97% of the genes which were DE in response to *G. tritici* at 5 dpi were also involved in the response to *G. hyphopodioides.* Consequently, a mere 3% of DEGs were unique to *G. tritici* infection (figure 5.9 B). This finding indicates that there are a core set of genes which are DE in response to both *G. hyphopodioides* and *G. tritici*. However, this core set of genes makes up only a small proportion (14%) of all genes DE in response to *G. hyphopodioides* at 5 dpi.

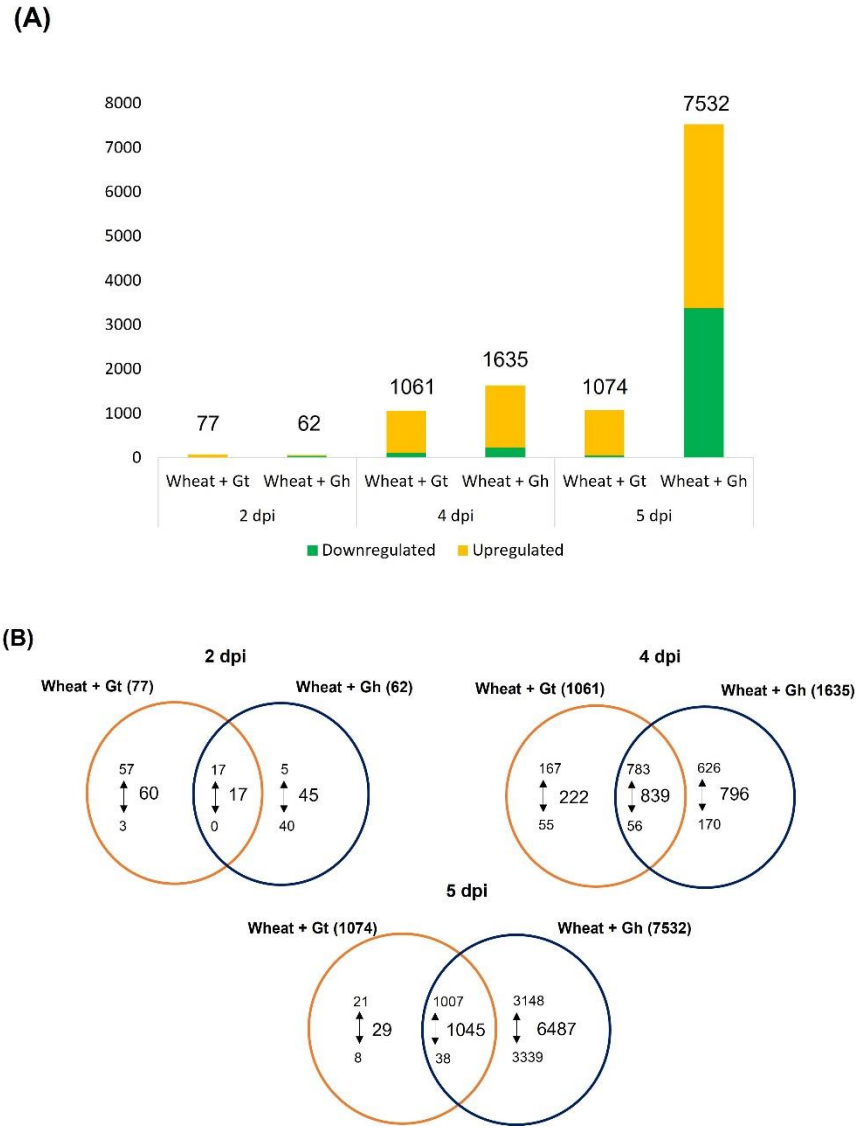


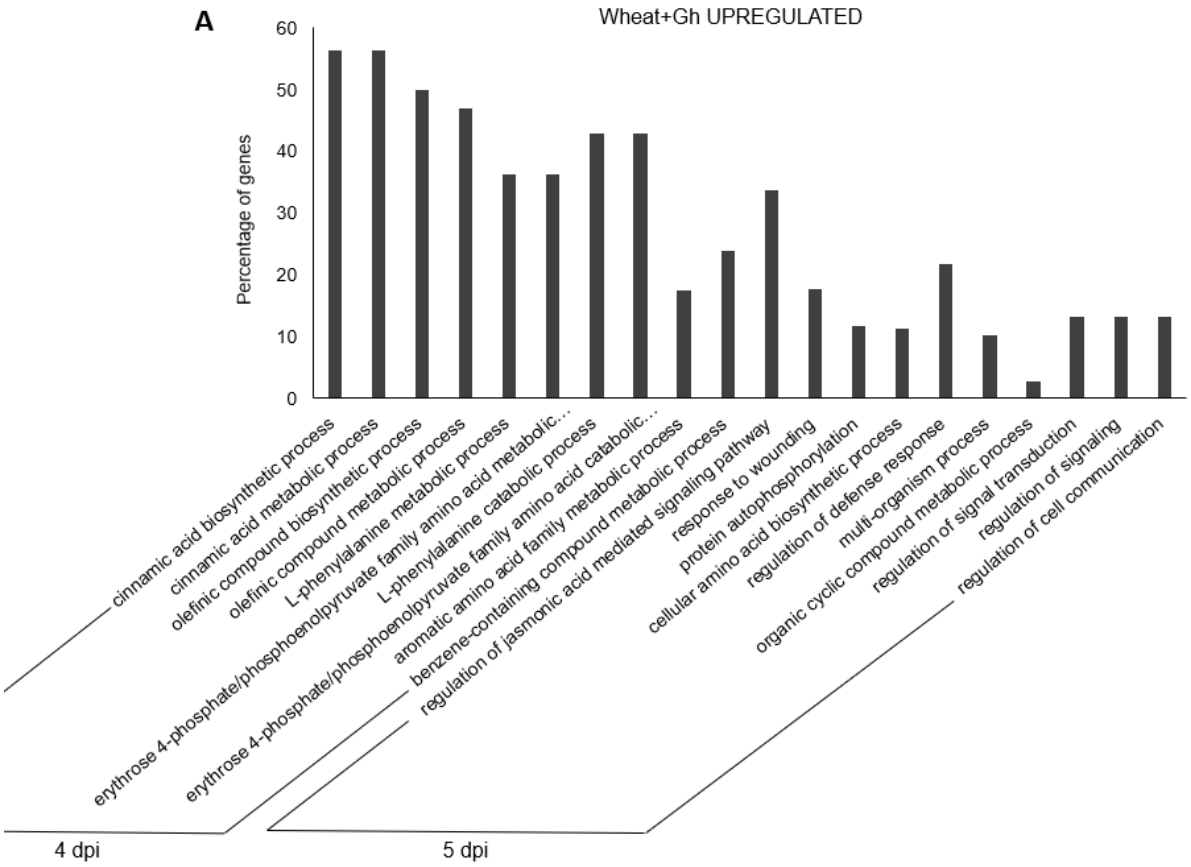
Figure 5.9 A. The number of differentially expressed genes (DEGs) in wheat colonised by *G. hyphopodioides* or *G. tritici* across three key time points. B. Venn diagram of DEGs that were unique or shared between the two fungal treatments.

5.3.5 Gene Ontology (GO) enrichment analysis

Gene Ontology (GO) enrichment analysis was carried out to compare and contrast the effect of *G. tritici* infection and *G. hyphopodioides* colonisation on wheat biological processes. The analysis was performed independently for the subsets of up and downregulated genes at 2, 4 and 5 dpi. To investigate the progression of infection, biological process GO terms were compared between each time point and the top ten new enriched terms were identified for each stage of infection (figures 5.10, 5.11).

At 2 dpi, highly enriched biological process terms for downregulated genes in *G. hyphopodioides* colonised plants included nicotianamine biosynthetic process and amine biosynthetic process. Terpenoid biosynthetic process, isoprenoid biosynthetic process, lipid biosynthetic process and gibberellin biosynthetic process were among the most enriched terms for upregulated genes in *G. tritici* infected samples, suggesting that isoprenoids play a key role in the early plant response to *G. tritici* infection. At 4 dpi, new highly enriched terms for upregulated genes in *G. hyphopodioides* colonised plants included cinnamic acid metabolic/biosynthetic process, L-phenylalanine metabolic process, phenylpropanoid metabolic process and aromatic amino acid family metabolic process, suggesting that lignin biosynthesis is important at this time point. Downregulated terms included hydrogen peroxide metabolic/catabolic process, cell wall biogenesis and response to toxic substance. For *G. tritici* infected plants, terms from upregulated genes included response to stimulus, carbohydrate derivative transport and chitin metabolic/catabolic process. Terms from downregulated genes included response to oxygen-containing compound, response to nitrate and nitrate transport, potentially indicating a role of reactive oxygen/nitrogen species in the plant defence response against *G. tritici* (Zaninotto et al., 2006).

Finally, at 5 dpi, new highly enriched terms from upregulated genes in *G. hyphopodioides* colonised plants included regulation of the jasmonic acid signalling pathway, response to wounding and regulation of defence responses. Downregulated terms included gene expression, plant-type cell wall organisation or biogenesis, RNA metabolic process and sexual reproduction. In *G. tritici* infected plants, new enriched upregulated terms included cinnamic acid metabolic/biosynthetic process, L-phenylalanine metabolic process and olefinic compound biosynthetic process, suggesting that lignin biosynthesis is also involved in the defence response to *G. tritici*, though at a later stage than *G. hyphopodioides.*



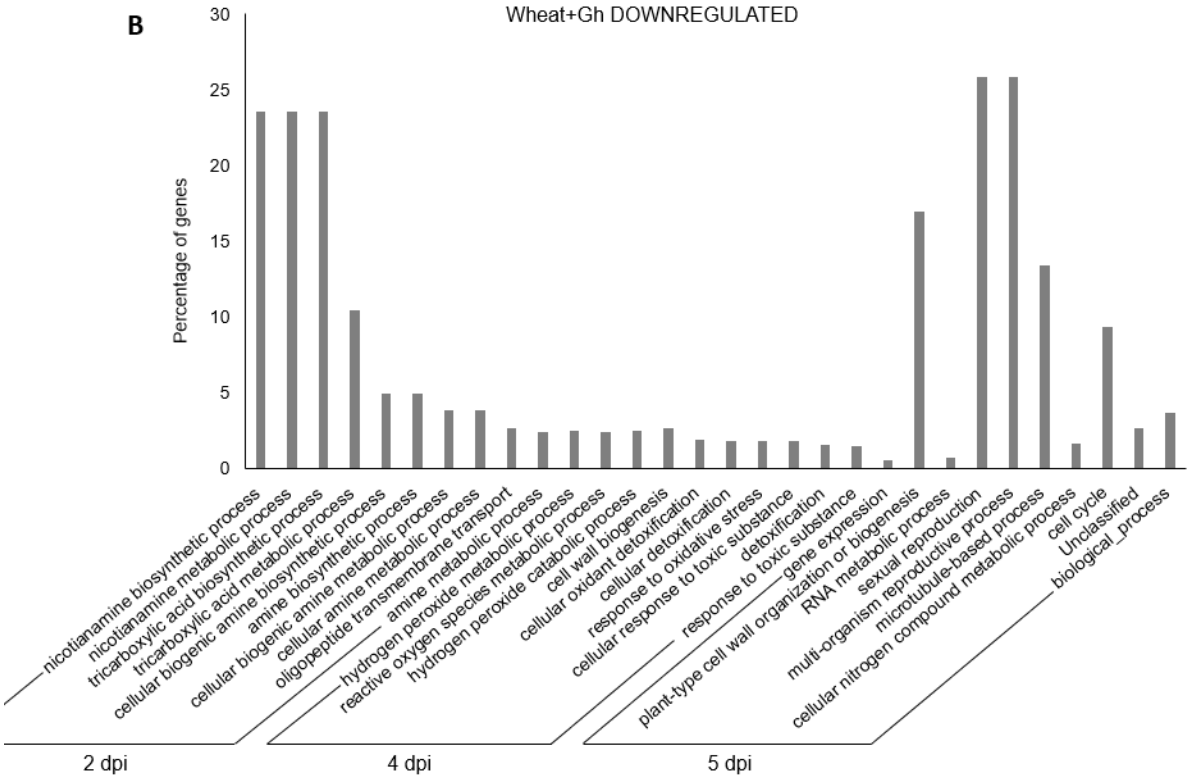
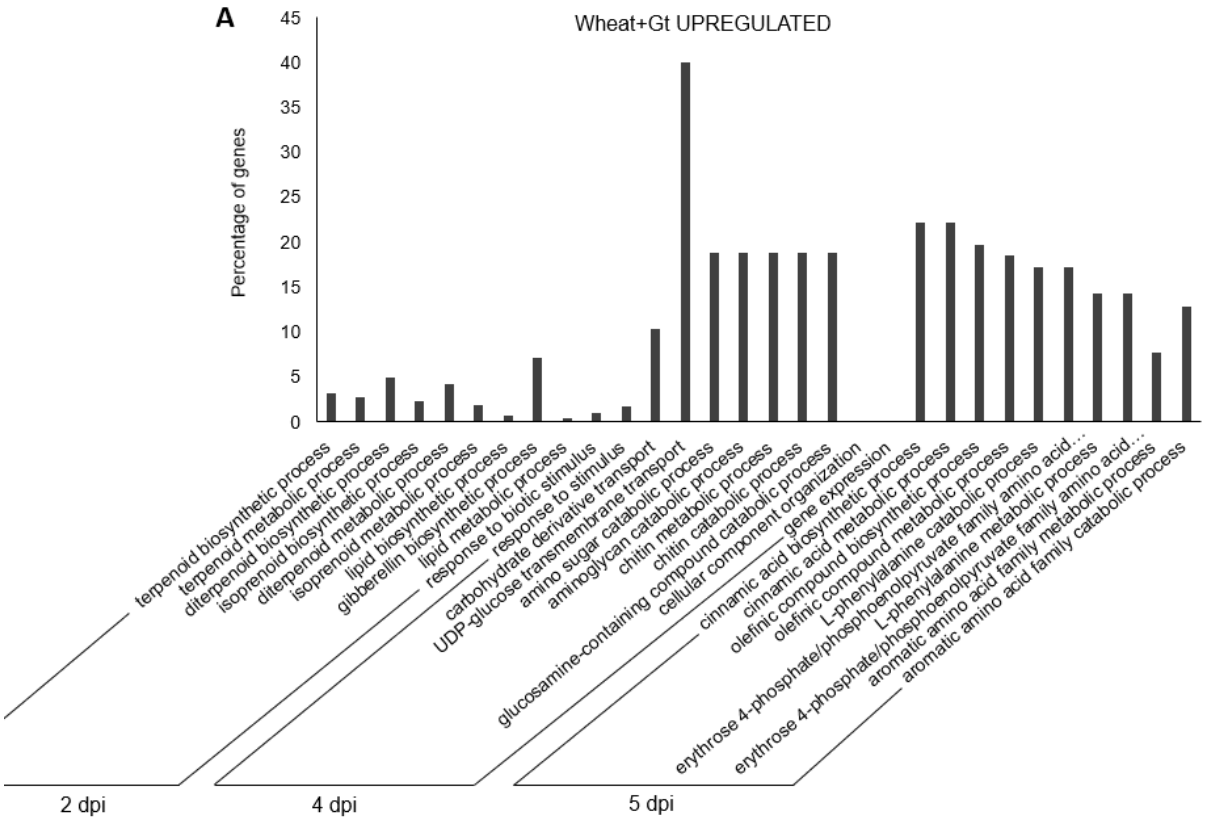


Figure 5.10 The top 10 most enriched biological process gene ontology (GO) terms unique to each time point in *G. hyphopodioides* colonised roots. A. Enriched terms among significantly upregulated genes. B. Enriched terms among significantly downregulated genes. Ordered from left to right by False Discovery Rate (FDR). Percentage of genes represents the percentage of DE genes out of the total number of known genes in that category, according to the Panther classification system.


A
Wheat+Gt UPREGULATED
Percentage of genes
45
40
35
30
25
20
15
10
5
0
terpenoid biosynthetic process
terpenoid metabolic process
diterpenoid biosynthetic process
isoprenoid biosynthetic process
diterpenoid metabolic process
isoprenoid metabolic process
lipid biosynthetic process
gibberellin biosynthetic process
lipid metabolic process
response to biotic stimulus
response to stimulus
carbohydrate derivative transport
UDP-glucose transmembrane transport
amino sugar catabolic process
aminoglycan catabolic process
chitin metabolic process
chitin catabolic process
glucosamine-containing compound catabolic process
cellular component organization
gene expression
cinnamic acid biosynthetic process
cinnamic acid metabolic process
olefinic compound biosynthetic process
olefinic compound metabolic process
L-phenylalanine catabolic process
erythrose 4-phosphate/phosphoenolpyruvate family amino acid…
L-phenylalanine metabolic process
erythrose 4-phosphate/phosphoenolpyruvate family amino acid…
aromatic amino acid family metabolic process
aromatic amino acid family catabolic process
2 dpi
4 dpi
5 dpi

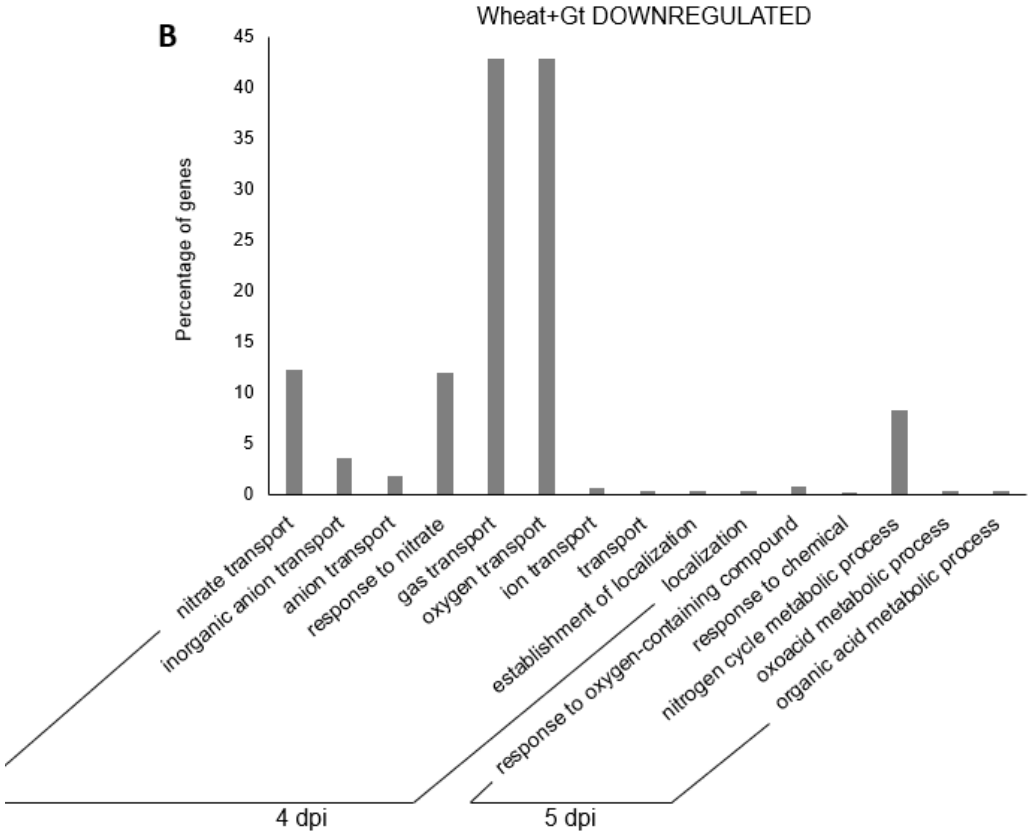
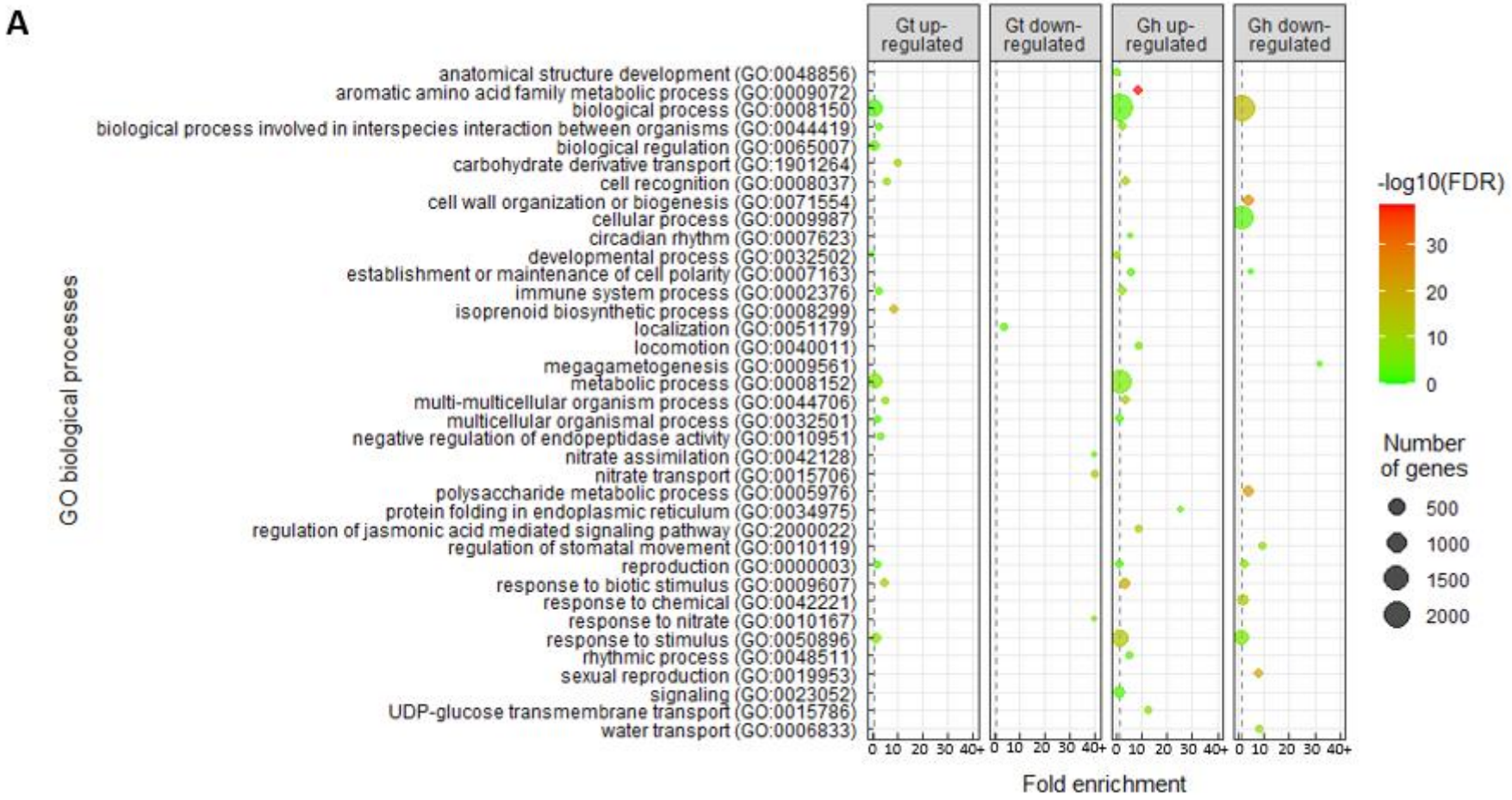

B
Wheat+Gt DOWNREGULATED
Percentage of genes
45
40
35
30
25
20
15
10
5
0
nitrate transport
inorganic anion transport
anion transport
response to nitrate
gas transport
oxygen transport
ion transport
transport
establishment of localization
localization
response to oxygen-containing compound
response to chemical
nitrogen cycle metabolic process
oxoacid metabolic process
organic acid metabolic process
4 dpi
5 dpi

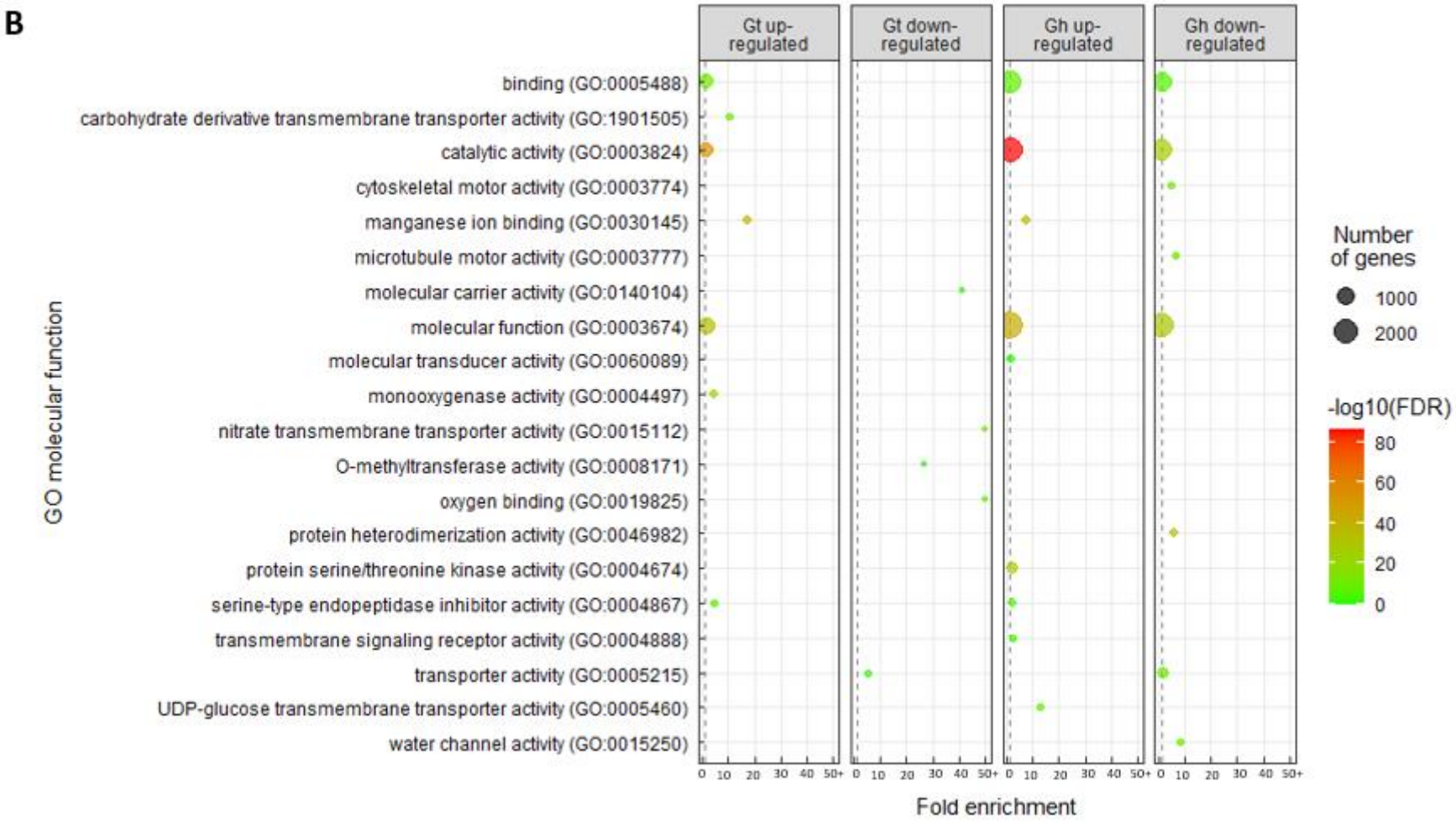
Figure 5.11 The top 10 most enriched biological process gene ontology (GO) terms unique to each time point in *G. tritici* infected roots. A. Enriched terms among significantly upregulated genes. B. Enriched terms among significantly downregulated genes. Ordered from left to right by False Discovery Rate (FDR). See previous page.

GO analysis generated a large number of similar terms, often comprising the same DE genes. To visualise the most representative biological process, molecular function and cellular component GO terms at 5 dpi and provide a broad overview of the plant responses to *G. tritici* infection and *G. hyphopodioides* colonisation at 5 dpi, redundant terms were removed using REVIGO software using a stringent dispensability cut-off of $p<0.01$. The analysis revealed that of the significantly upregulated genes in *G. hyphopodioides* colonised plants (as compared to the control), highly enriched biological process terms included protein folding in the endoplasmic reticulum, UDP glucose transmembrane transport, regulation of the jasmonic acid signalling pathway and aromatic amino acid family metabolic process. In contrast, highly enriched biological process terms in *G. tritici* infected plants included carbohydrate derivative transport, isoprenoid biosynthetic process and cell recognition. Nitrate related responses were important among the downregulated genes in *G. tritici* infected plants, while reproduction, stomatal movement, water transport and cell wall organisation or biogenesis were important in *G. hyphopodioides* colonised plants (figure 5.12 A). The subset of DE genes relating to stomatal development comprised 17 MYB transcription factors (appendix A.7; table A.7.5). Several MYB transcription factors are known to control stomatal aperture to reduce water loss, but also play a role in lignin deposition and secondary cell wall formation (Lippold et al., 2009). Hence, the data suggest that the cell wall plays a key role in the wheat response to *G. hyphopodioides*.

Catalytic activity was a significantly enriched molecular function term for both up and downregulated genes in response to *G. hyphopodioides* colonisation. Manganese ion binding was an important term among the upregulated genes in response to *G. tritici.* Though comprising only a small number of genes, oxygen binding and nitrate transmembrane transporter activity were highly enriched among the downregulated genes, again suggesting that nitrate nutrition (Mur et

al., 2017) or reactive nitrogen/oxygen species play a role in the response to *G. tritici* (Zaninotto et al., 2006) (figure 5.12 B). The apoplast and extracellular region were important cellular component terms among upregulated genes in response to *G. tritici*, while plastid stroma was the only significantly enriched cellular component term among downregulated. The apoplast was also a highly enriched term among upregulated genes in response to *G. hyphopodioides*, while cell projection and nucleosome were highly enriched terms among the downregulated genes (figure 5.12 C).


A
Gt up-regulated
Gt down-regulated
Gh up-regulated
Gh down-regulated
GO biological processes
anatomical structure development (GO:0048856)
aromatic amino acid family metabolic process (GO:0009072)
biological process (GO:0008150)
biological process involved in interspecies interaction between organisms (GO:0044419)
biological regulation (GO:0065007)
carbohydrate derivative transport (GO:1901264)
cell recognition (GO:0008037)
cell wall organization or biogenesis (GO:0071554)
cellular process (GO:0009987)
circadian rhythm (GO:0007623)
developmental process (GO:0032502)
establishment or maintenance of cell polarity (GO:0007163)
immune system process (GO:0002376)
isoprenoid biosynthetic process (GO:0008299)
localization (GO:0051179)
locomotion (GO:0040011)
megagametogenesis (GO:0009561)
metabolic process (GO:0008152)
multi-multicellular organism process (GO:0044706)
multicellular organismal process (GO:0032501)
negative regulation of endopeptidase activity (GO:0010951)
nitrate assimilation (GO:0042128)
nitrate transport (GO:0015706)
polysaccharide metabolic process (GO:0005976)
protein folding in endoplasmic reticulum (GO:0034975)
regulation of jasmonic acid mediated signaling pathway (GO:2000022)
regulation of stomatal movement (GO:0010119)
reproduction (GO:0000003)
response to biotic stimulus (GO:0009607)
response to chemical (GO:0042221)
response to nitrate (GO:0010167)
response to stimulus (GO:0050896)
rhythmic process (GO:0048511)
sexual reproduction (GO:0019953)
signaling (GO:0023052)
UDP-glucose transmembrane transport (GO:0015786)
water transport (GO:0006833)
0 10 20 30 40+
Fold enrichment
-log10(FDR)
30
20
10
0
Number of genes
500
1000
1500
2000


B
Gt up-regulated
Gt down-regulated
Gh up-regulated
Gh down-regulated
binding (GO:0005488)
carbohydrate derivative transmembrane transporter activity (GO:1901505)
catalytic activity (GO:0003824)
cytoskeletal motor activity (GO:0003774)
manganese ion binding (GO:0030145)
microtubule motor activity (GO:0003777)
molecular carrier activity (GO:0140104)
molecular function (GO:0003674)
molecular transducer activity (GO:0060089)
monooxygenase activity (GO:0004497)
nitrate transmembrane transporter activity (GO:0015112)
O-methyltransferase activity (GO:0008171)
oxygen binding (GO:0019825)
protein heterodimerization activity (GO:0046982)
protein serine/threonine kinase activity (GO:0004674)
serine-type endopeptidase inhibitor activity (GO:0004867)
transmembrane signaling receptor activity (GO:0004888)
transporter activity (GO:0005215)
UDP-glucose transmembrane transporter activity (GO:0005460)
water channel activity (GO:0015250)
GO molecular function
0 10 20 30 40 50+
Fold enrichment
Number of genes
1000
2000
-log10(FDR)
80
60
40
20
0

C

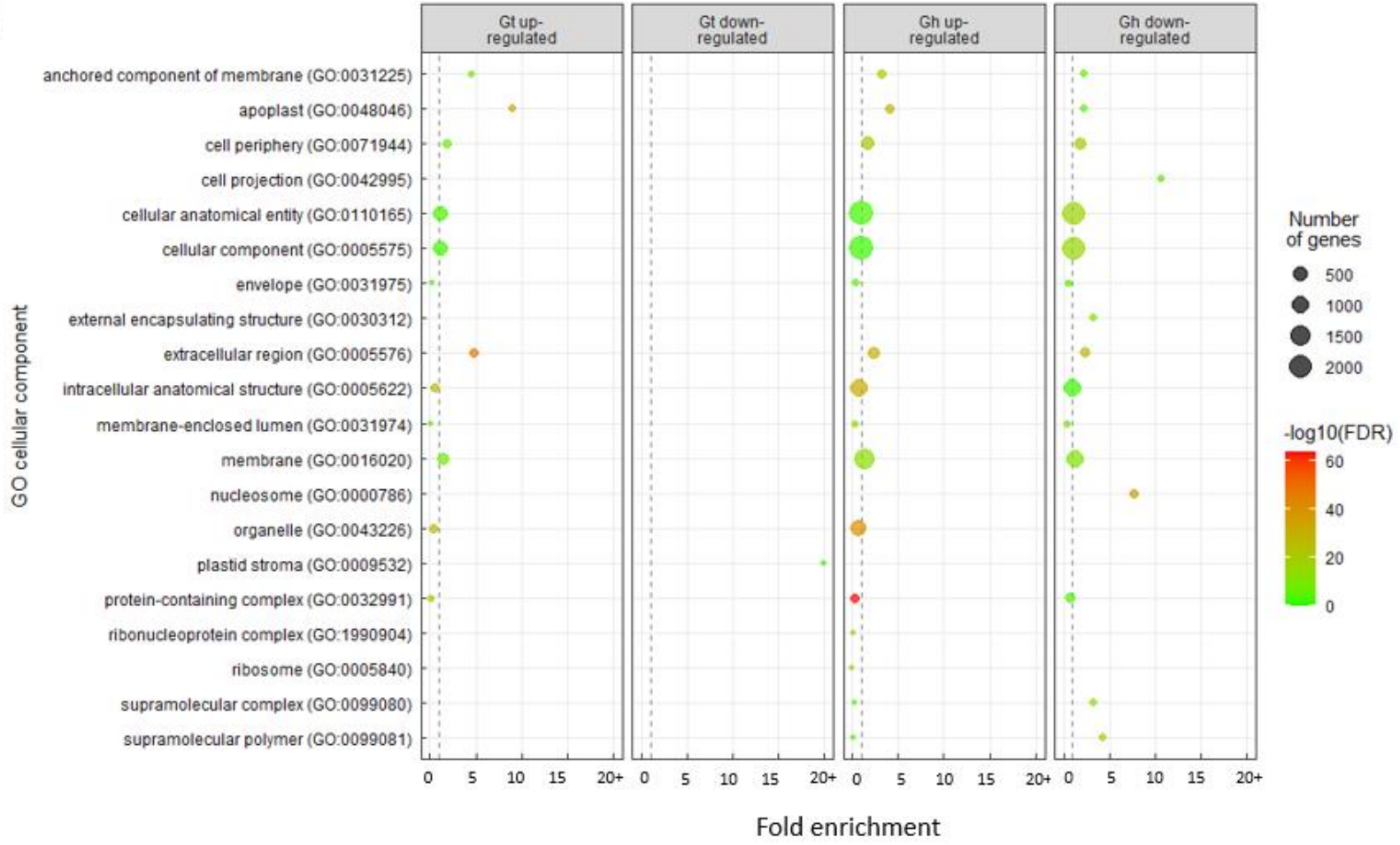

Gt up-regulated
Gt down-regulated
Gh up-regulated
Gh down-regulated
GO cellular component
anchored component of membrane (GO:0031225)
apoplast (GO:0048046)
cell periphery (GO:0071944)
cell projection (GO:0042995)
cellular anatomical entity (GO:0110165)
cellular component (GO:0005575)
envelope (GO:0031975)
external encapsulating structure (GO:0030312)
extracellular region (GO:0005576)
intracellular anatomical structure (GO:0005622)
membrane-enclosed lumen (GO:0031974)
membrane (GO:0016020)
nucleosome (GO:0000786)
organelle (GO:0043226)
plastid stroma (GO:0009532)
protein-containing complex (GO:0032991)
ribonucleoprotein complex (GO:1990904)
ribosome (GO:0005840)
supramolecular complex (GO:0099080)
supramolecular polymer (GO:0099081)
0 5 10 15 20+
Fold enrichment
Number of genes
500
1000
1500
2000
-log10(FDR)
60
40
20
0

Figure 5.12 Most representative enriched Gene Ontology (GO) terms in *G. tritici* infected and *G. hyphopodioides* colonised wheat at 5 dpi. Based on REVIGO analysis of up and downregulated GO terms related to: A. Biological processes, B. Molecular function, C. Cellular Component. See previous page.

5.3.6 Core response to *G. tritici* infection and *G. hyphopodioides* colonisation.

As mentioned in section 5.3.4, 1045 genes were DE in both *G. hyphopodioides* colonised and *G. tritici* infected plants compared to the uninoculated control at 5 dpi. To investigate the key biological functions of these core genes, we conducted GO enrichment analysis on the subset of 1045 genes. Highly enriched biological process GO terms included isoprenoid biosynthesis, plant response to biotic stimulus, phenylpropanoid metabolic process and carbohydrate derivative transport (figure 5.13). Of particular interest was the plant response to biotic stimulus term, which comprised a total of 42 DE genes, 14 of which encoded SCP-domain containing proteins, six encoded chitinases, two encoded wound induced proteins (WIN) and a further two encoded pathogenesis related PRMS proteins, thus indicating a clear defence response to both fungi (appendix A.7; table A.7.6).

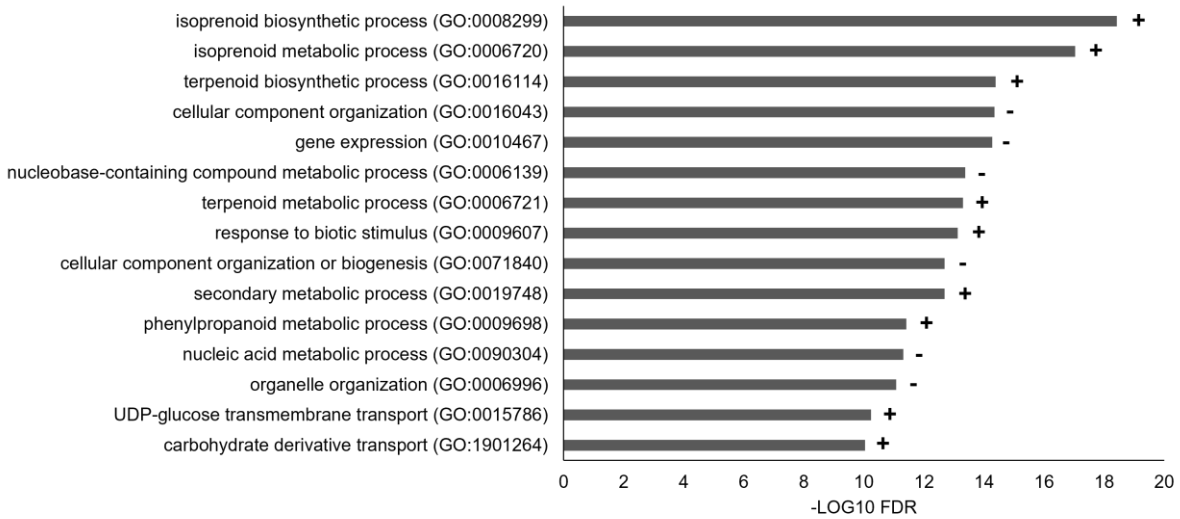
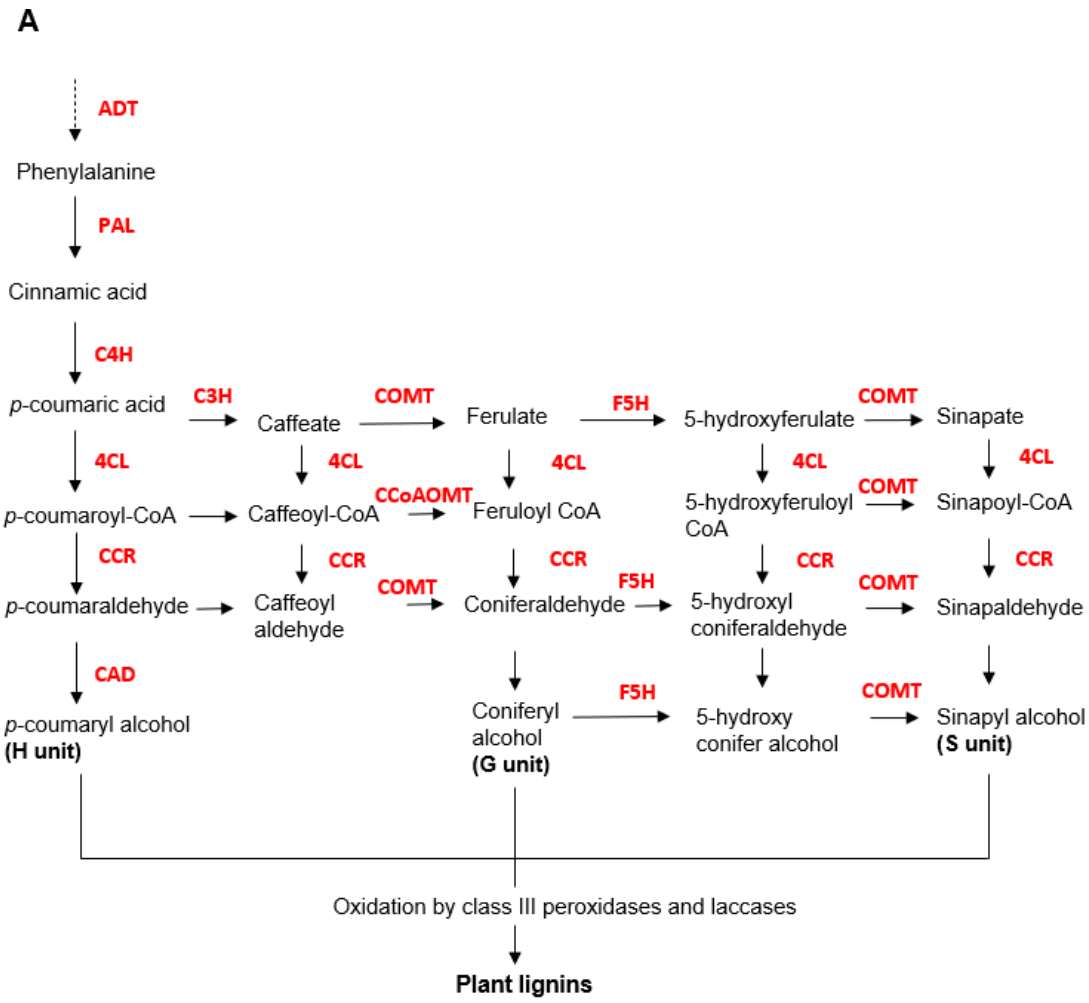


Figure 5.13 Top 10 GO enriched biological process terms among core DEGs in *G. hyphopodioides* and *G. tritici* infected plants at 5 dpi. +/- symbols indicate up/downregulated genes, respectively. See previous page.

5.3.7 Plant lignification response

Previous studies have reported higher levels of cell wall lignification in response to colonisation by several non-pathogenic *Magnaporthaceae* species compared to infection by *G. tritici* (Huang et al., 2001; Speakman & Lewis, 1978). To investigate root lignification in response to *G. hyphopodioides* and *G. tritici*, we explored the expression of key genes involved in the lignin biosynthesis pathway in wheat (figure 5.14 A). In accordance with the findings of the GO analysis (section 5.3.5), *G. hyphopodioides* colonisation resulted in the earlier upregulation of lignin biosynthesis genes compared to *G. tritici*, with key genes such as ADT, PAL, 4CL and CCR genes significantly upregulated at 4 dpi (figure 5.14 B). However, two of eight COMT genes detected were already significantly upregulated in response to *G. tritici* at 2 dpi, suggesting an early and specific response to pathogen attack. Interestingly, the remaining COMT genes were strongly downregulated in response to *G. hyphopodioides* by 5 dpi, suggesting a decrease in the proportion of S-lignin with potentially important downstream effects on pathogen interactions (Quentin et al., 2009). Most striking however, was the significant upregulation of 37 PAL genes in response to *G. hyphopodioides*, compared to the upregulation of just 12 PAL genes in response to *G. tritici* at 5 dpi. Another notable finding was the identification of 10 genes encoding tonoplast intrinsic proteins (TIP) and 15 genes encoding plasma membrane intrinsic proteins (PIP), which were significantly downregulated in response to *G. hyphopodioides* at 5 dpi. The only exceptions being three homoeologous copies of TIP3-1, which were upregulated (appendix A.7; table A.7.7). The downregulation of TIP and PIP aquaporin genes, involved in hydraulic regulation, have recently been associated with endodermal lignification in Arabidopsis (Reyt et al., 2021).


A
ADT
Phenylalanine
PAL
Cinnamic acid
C4H
p-coumaric acid
C3H
Caffeate
COMT
Ferulate
F5H
5-hydroxyferulate
COMT
Sinapate
4CL
4CL
4CL
4CL
4CL
p-coumaroyl-CoA
CCoAOMT
Caffeoyl-CoA
Feruloyl CoA
5-hydroxyferuloyl CoA
COMT
Sinapoyl-CoA
CCR
CCR
CCR
CCR
CCR
p-coumaraldehyde
COMT
Caffeoyl aldehyde
Coniferaldehyde
F5H
5-hydroxyl coniferaldehyde
COMT
Sinapaldehyde
CAD
F5H
COMT
p-coumaryl alcohol
(H unit)
Coniferyl alcohol
(G unit)
5-hydroxy conifer alcohol
Sinapyl alcohol
(S unit)
Oxidation by class III peroxidases and laccases
Plant lignins

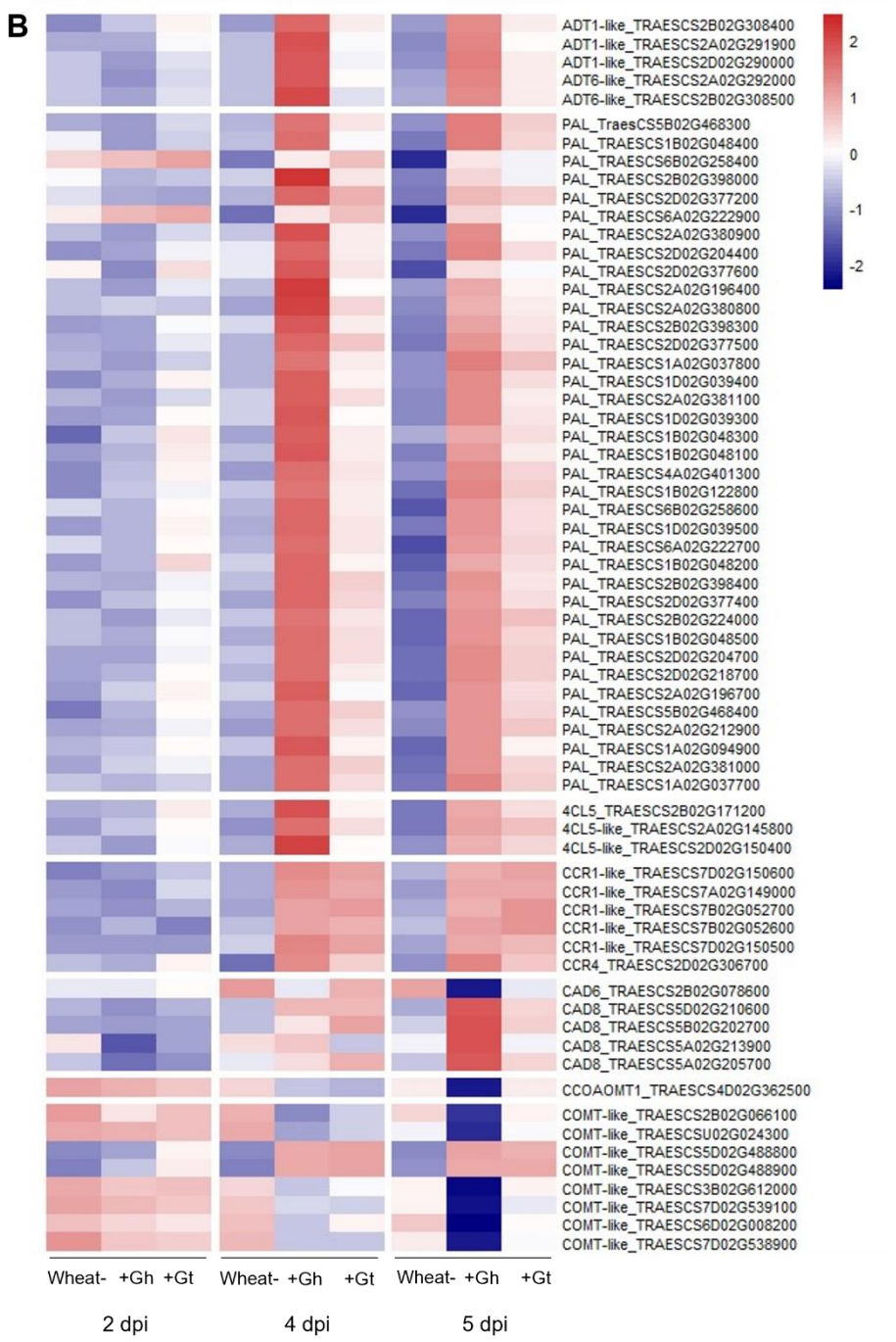


Figure 5.14 The role of lignin biosynthesis in the plant response to *G. hyphopodioides* (Gh) and *G. tritici* (Gt). A. Schematic of the lignin biosynthesis pathway in plants. B. Expression of key genes involved in the lignin biosynthesis pathway, based on LOG transformed normalised gene counts. PAL, phenylalanine ammonia-lyase; C4H, cinnamate 4-hydroxylase; 4CL, 4-coumarate: CoA ligase; HCT, quinateshikimate *p*-hydroxycinnamoyltransferase; C3′H, *p*-coumaroylshikimate 3′-hydroxylase; CCoAOMT, caffeoyl-CoA *O*-methyltransferase; CCR, cinnamoyl-CoAreductase; F5H, ferulate 5-

hydroxylase; CAD, cinnamyl alcohol dehydrogenase; COMT, caffeic acid *O*-methyltransferase

To validate the gene expression data and investigate lignin distribution in different root tissues, potassium permanganate staining of transversal root sections was performed on samples harvested at 5 dpi. Relative levels of cell wall lignification were visually determined by the intensity of the potassium permanganate stain. We found that the overall level of root lignification varied within *G. hyphopodioides* colonised and *G. tritici* infected samples, with some sections difficult to distinguish from the uninoculated control. However, heavily colonised cells exhibited cell wall thickenings and increased lignin levels when compared to uncolonised neighbouring cells. Furthermore, plant lignitubers were often detected in cells containing fungal hyphae, though these structures were more common in *G. tritici* infected samples. Despite the downregulation of TIP and PIP aquaporin genes as described above, *G. hyphopodioides* colonisation did not result in visible lignification of the stele or endodermal barrier compared to the control (figure 5.15). This finding contrasts with analyses carried out in chapter 3, and is also contrary to previously published microscopy studies into the infection mechanisms of non-pathogenic *Magnaporthaceae* species, though *G. hyphopodioides* was not among the species tested (Huang et al., 2001; Speakman & Lewis, 1978).

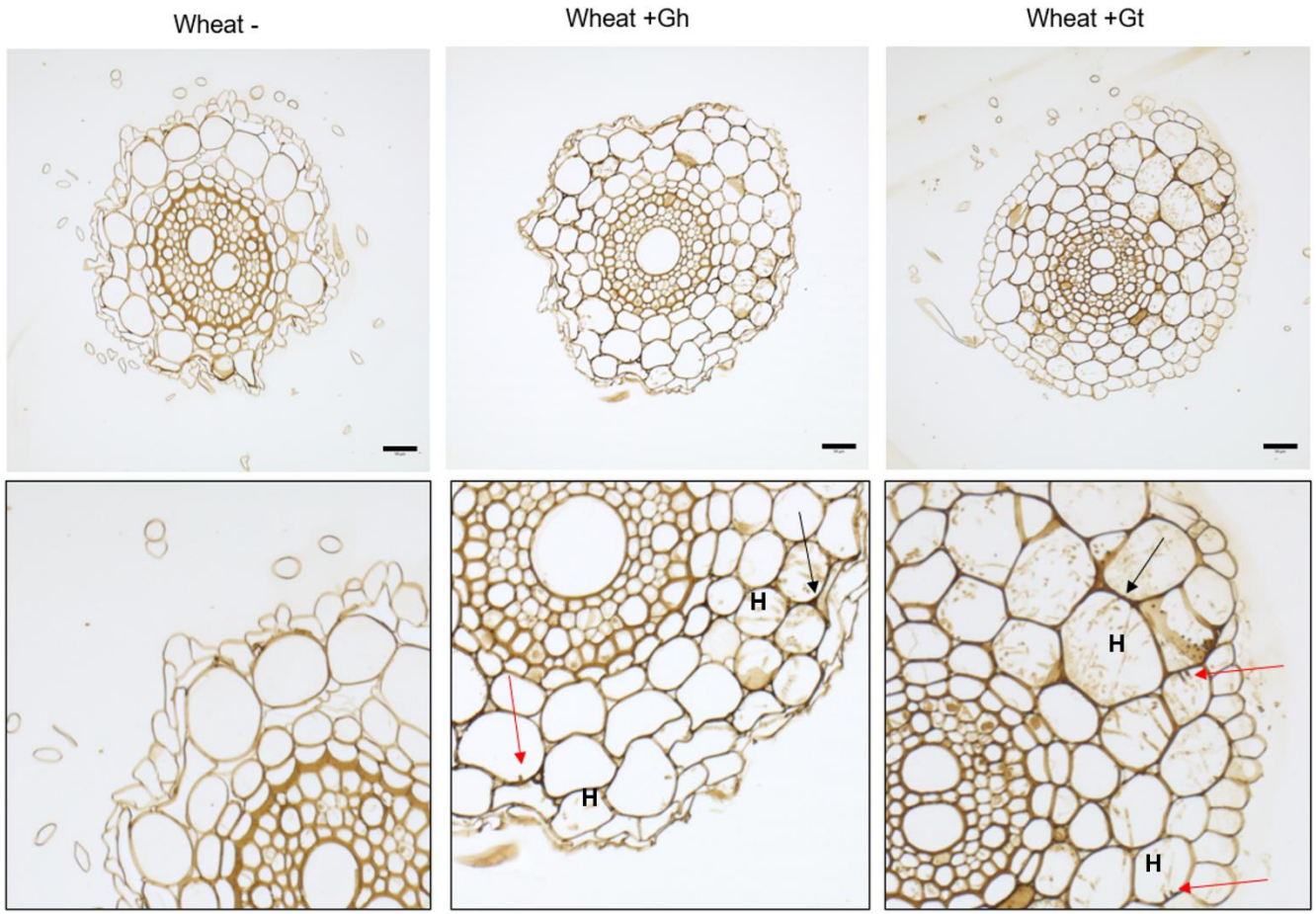


Figure 5.15 Micrographs of transversal root sections stained with potassium permanganate for the visualisation of cell wall lignification in *G. hyphopodioides* (Gh) colonised and *G. tritici* (Gt) infected roots at 5 dpi. Black arrows indicate lignified cell wall thickenings, red arrows indicate plant lignitubers. H= hyphae. Scale bars represent 50 µm.

5.3.8 Expression of genes relating to cell wall organisation and biogenesis in *G. hyphopodioides* colonised roots

As identified by GO enrichment analysis (see section 5.3.5), *G. hyphopodioides* colonisation resulted in the significant downregulation of 124 genes involved in cell wall organisation and biogenesis by 5 dpi (out of 1122 total known genes involved in cell wall organisation and biogenesis in wheat). In contrast, *G. tritici* infection did not lead to the differential expression of any genes within the cell wall organisation and biogenesis GO term. Focussing on the top 30 DE genes within this GO term in *G. hyphopodioides* colonised plants at 5 dpi, we identified six xyloglucan endotransglycosylases/hydrolases (XTH) genes, four of which were also DE at 4 dpi (table 5.5). Also ranking within the top 30 genes were three cellulose synthase-like A-like (CSLA) genes, one cellulose synthase-like F (CSLF) gene and three fasciclin-like arabinogalactan (FLA) genes. In addition, we identified a pectin methylesterase (PME), a pectin acetylesterase (PAE) and a cellulose synthase-like (CESA) gene.

Table 5.5 The top 30 most differentially expressed genes relating to cell wall organisation and biogenesis in *G. hyphopodioides* colonised plants. Ordered by significance (padj).

		4 dpi		5 dpi	
		Wheat + Gh		Wheat + Gh	
Gene ID	Gene name	Log2FC	padj	Log2FC	padj
TRAESCS5A02G548500	XTH	-2.99	2.48E-05	-5.66	4.27E-22
TRAESCS7A02G363000	XTH	-2.68	4.64E-04	-4.52	1.51E-17
TRAESCS7D02G360100	XTH	-3.75	6.68E-05	-5.10	2.71E-10
TRAESCS7D02G294300	CSLF6	-2.40	4.92E-03	-3.49	4.39E-10
TRAESCS4B02G383000	XTH	*	*	-3.39	4.97E-10
TRAESCS4D02G358700	XTH	*	*	-3.81	5.00E-10
TRAESCS7B02G265000	XTH	-4.80	2.09E-08	-6.31	5.28E-10
TRAESCS6A02G169200	CSLA1-like	*	*	-4.05	6.71E-09
TRAESCS6B02G197200	CSLA1-like	*	*	-3.61	7.97E-09
TRAESCS3B02G376800	EXPA2	*	*	-3.43	1.03E-08
TRAESCS3B02G120700	FLA11	*	*	-4.06	1.13E-08
TRAESCS2A02G082500	IRX9	*	*	-4.36	1.35E-08
TRAESCS6D02G158600	CSLA1	*	*	-3.57	5.19E-08
TRAESCS2D02G091400	Unknown	*	*	-4.14	7.54E-08
TRAESCS5D02G137300	GT3	*	*	-3.10	1.77E-07
TRAESCS3D02G105500	FLA11	*	*	-3.80	2.79E-07
TRAESCS2D02G080400	IRX9	*	*	-4.33	3.13E-07
TRAESCS2A02G153000	PAE	*	*	-2.86	3.45E-07
TRAESCS5A02G143800	GAUT7	*	*	-3.65	4.99E-07
TRAESCS1D02G404700	FLA6	*	*	-3.28	1.03E-06
TRAESCS6A02G131900	IRX15-like	*	*	-5.26	1.27E-06
TRAESCS2D02G099900	PME	*	*	-8.49	1.48E-06
TRAESCS4A02G227100	GXM-like	*	*	-7.37	1.62E-06

TRAESCS5D02G107900	COBL-5B	*	*	-3.33	2.20E-06
TRAESCS5D02G280400	CTL1	*	*	-2.22	2.68E-06
TRAESCS6D02G121700	IRX15-like	*	*	-4.45	3.22E-06
TRAESCS5A02G129800	GT3	*	*	-2.80	5.03E-06
TRAESCS1D02G111600	FLA11	*	*	-7.80	7.85E-06
TRAESCS4D02G086700	GXM1-like	*	*	-4.24	8.06E-06
TRAESCS1B02G167200	CESA7-like	*	*	-3.04	9.85E-06

5.3.9 Expression of genes associated with plant defence responses

Though not identified by GO enrichment analysis, we investigated the expression of key genes known to be involved in plant defences against fungal pathogens. We identified 51/14 probable WRKY transcription factors which were DE in response to *G. hyphopodioides* colonisation/ *G. tritici* infection at 5 dpi compared to the uninoculated control. All predicted WRKY genes were upregulated compared to the uninoculated control, with the exception of 4 WRKY genes which were downregulated in response to *G. hyphopodioides* only. In addition, we identified 12 differentially expressed PR1-like genes (7 up/ 4 down) in response to *G. hyphopodioides* colonisation, compared to just one upregulated PR1-like gene in response to *G. tritici* infection. Furthermore, we identified 29 genes encoding receptor kinases which were DE in response to *G. hyphopodioides* at 5 dpi, 6 of which were also DE in response to *G. tritici* (4 BAK1-like and 2 CERK1-like genes). Out of three FLS2 genes which were DE in response to *G. hyphopodioides* at 5 dpi, two were downregulated. Similarly, three downregulated LRR1-like genes were unique to *G. hyphopodioides* colonised plants at 5 dpi. Interestingly, a WAK3-like gene and a BIR2 gene were significantly upregulated in response to *G. tritici* at 4 dpi, but not 5 dpi (appendix A.7; table A.7.8). These findings highlight the strong defence response to *G. hyphopodioides* colonisation.

5.3.10 Role of phytohormones

In this study, the regulation of the JA mediated signalling pathway was identified as a significantly enriched GO term in *G. hyphopodioides* colonised plants compared to the uninoculated control at 5 dpi. This GO term comprised 26 DEGs (out of a total of 77 known genes in wheat), all of which were TIFY transcription factors, involved in the cross-talk between JA and other phytohormones (Singh

& Mukhopadhyay, 2021). In contrast, just three TIFY transcription factors were DE in *G. tritici* infected plants compared to the control (figure 5.16 A). Although not identified by GO enrichment analysis, we also investigated the expression of genes known to be involved in JA biosynthesis. The analysis revealed that 23 key genes predicted to be involved in the biosynthesis of jasmonic acid were DE (17 up/ 6 down) in response to *G. hyphopodioides* at 5 dpi. The list included LOX, AOS and AOS-like, OPR and OPR-like, and KAT-like genes (figure 5.15 A). Of these genes, only one was differentially expressed in response to *G. tritici (*LOX8_TraesCS7B02G145200).

Because JA and ET signalling are often closely linked, we also investigated genes involved in ET biosynthesis and signalling. The ET biosynthesis pathway comprises two key reactions. In the first reaction, the enzyme ACC-synthase (ACS) catalyses the conversion of S-adenosyl-L-methionine (SAM) into 1-aminocyclopropane-1-carboxylic acid (ACC) (Houben & Van de Poel, 2019). In the second reaction, ACC-oxidase (ACO) catalyses the conversion of ACC to ET and ACO is now thought to be the key rate-limiting enzyme in ET production *(ibid.)*. In this study, five ACO-like genes were upregulated in response to *G. hyphopodioides* by 5 dpi. In addition, 22 ethylene responsive transcription factor-like (ERF-like) genes, key integrators of downstream ET and JA signal transduction pathways (Lorenzo et al., 2003), were DE (19 up/ 3 down) in response to *G. hyphopodioides* by 5 dpi (figure 5.16 B). In contrast, four ERF-like genes were upregulated at 4 dpi and two were upregulated at 5 dpi in *G. tritici* infected roots compared to the control. The data described here suggests that JA/ET signalling is more important in the plant response to *G. hyphopodioides* colonisation than in the response to *G. tritici* infection.

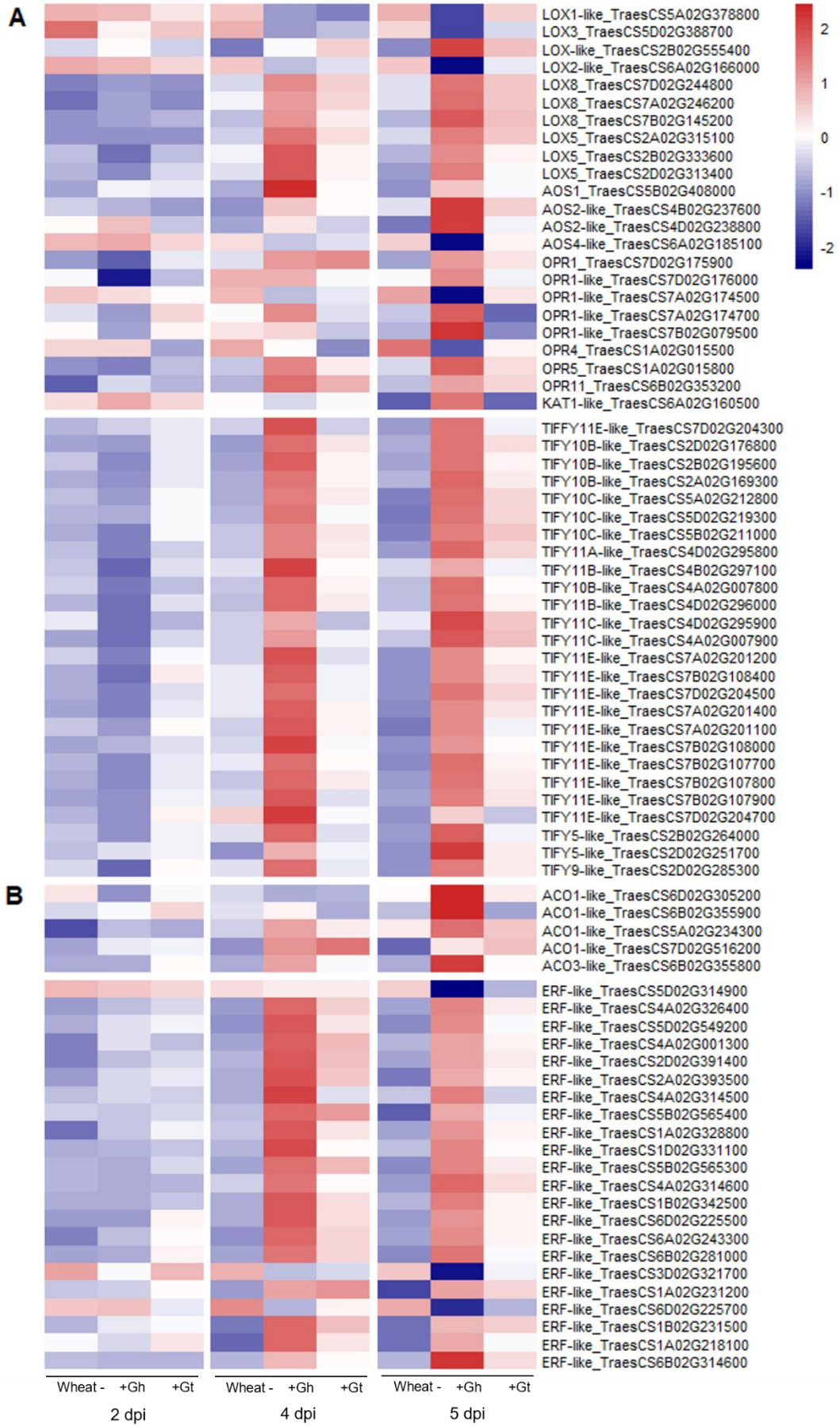

A
LOX1-like_TraesCS5A02G378800
LOX3_TraesCS5D02G388700
LOX-like_TraesCS2B02G555400
LOX2-like_TraesCS6A02G166000
LOX8_TraesCS7D02G244800
LOX8_TraesCS7A02G246200
LOX8_TraesCS7B02G145200
LOX5_TraesCS2A02G315100
LOX5_TraesCS2B02G333600
LOX5_TraesCS2D02G313400
AOS1_TraesCS5B02G408000
AOS2-like_TraesCS4B02G237600
AOS2-like_TraesCS4D02G238800
AOS4-like_TraesCS6A02G185100
OPR1_TraesCS7D02G175900
OPR1-like_TraesCS7D02G176000
OPR1-like_TraesCS7A02G174500
OPR1-like_TraesCS7A02G174700
OPR1-like_TraesCS7B02G079500
OPR4_TraesCS1A02G015500
OPR5_TraesCS1A02G015800
OPR11_TraesCS6B02G353200
KAT1-like_TraesCS6A02G160500
TIFFY11E-like_TraesCS7D02G204300
TIFY10B-like_TraesCS2D02G176800
TIFY10B-like_TraesCS2B02G195600
TIFY10B-like_TraesCS2A02G169300
TIFY10C-like_TraesCS5A02G212800
TIFY10C-like_TraesCS5D02G219300
TIFY10C-like_TraesCS5B02G211000
TIFY11A-like_TraesCS4D02G295800
TIFY11B-like_TraesCS4B02G297100
TIFY10B-like_TraesCS4A02G007800
TIFY11B-like_TraesCS4D02G296000
TIFY11C-like_TraesCS4D02G295900
TIFY11C-like_TraesCS4A02G007900
TIFY11E-like_TraesCS7A02G201200
TIFY11E-like_TraesCS7B02G108400
TIFY11E-like_TraesCS7D02G204500
TIFY11E-like_TraesCS7A02G201400
TIFY11E-like_TraesCS7A02G201100
TIFY11E-like_TraesCS7B02G108000
TIFY11E-like_TraesCS7B02G107700
TIFY11E-like_TraesCS7B02G107800
TIFY11E-like_TraesCS7B02G107900
TIFY11E-like_TraesCS7D02G204700
TIFY5-like_TraesCS2B02G264000
TIFY5-like_TraesCS2D02G251700
TIFY9-like_TraesCS2D02G285300
B
ACO1-like_TraesCS6D02G305200
ACO1-like_TraesCS6B02G355900
ACO1-like_TraesCS5A02G234300
ACO1-like_TraesCS7D02G516200
ACO3-like_TraesCS6B02G355800
ERF-like_TraesCS5D02G314900
ERF-like_TraesCS4A02G326400
ERF-like_TraesCS5D02G549200
ERF-like_TraesCS4A02G001300
ERF-like_TraesCS2D02G391400
ERF-like_TraesCS2A02G393500
ERF-like_TraesCS4A02G314500
ERF-like_TraesCS5B02G565400
ERF-like_TraesCS1A02G328800
ERF-like_TraesCS1D02G331100
ERF-like_TraesCS5B02G565300
ERF-like_TraesCS4A02G314600
ERF-like_TraesCS1B02G342500
ERF-like_TraesCS6D02G225500
ERF-like_TraesCS6A02G243300
ERF-like_TraesCS6B02G281000
ERF-like_TraesCS3D02G321700
ERF-like_TraesCS1A02G231200
ERF-like_TraesCS6D02G225700
ERF-like_TraesCS1B02G231500
ERF-like_TraesCS1A02G218100
ERF-like_TraesCS6B02G314600
2
1
0
-1
-2
Wheat -
+Gh
+Gt
2 dpi
4 dpi
5 dpi

Figure 5.16 The expression of JA and ET related genes in response to *G. hyphopodioides* (Gh) colonisation and *G. tritici* (Gt) infection. A. Expression of genes involved in the biosynthesis of JA and the regulation of JA mediated signalling pathway. B. Expression of genes involved in ET biosynthesis and downstream ET signalling pathways. Data represent LOG transformed normalised genes counts. LOX, lipoxygenase; AOS, allene oxide synthase; AOC, allene oxide cyclase; OPR, 12-oxophytodienoate reductase; KAT, 3-ketoacyl-CoA thiolase; TIFY, TIFY transcription factor; ACO, 1-aminocyclopropane-1-carboxylic acid oxidase; ERF, ethylene responsive transcription factor. See previous page.

SA can be synthesised from two independent pathways: the isochorismate synthase (ICS) and the phenylalanine ammonia-lyase (PAL) pathway. As described in section 5.3.7, *G. hyphopodioides* colonisation resulted in the strong upregulation of numerous PAL genes; PAL also being a key precursor of plant lignin. However, we identified one systemic acquired resistance deficient 1-like (SARD1-like) gene, involved in SA mediated SAR (Zhou et al., 2018), which was downregulated in response to *G. hyphopodioides*, suggesting that SA mediated SAR could be repressed. In contrast, five salicylic acid binding protein 2-like (SABP2-like) genes which catalyse the conversion of methyl salicylate (MeSA) into SA and have been implicated in SAR (Pokotylo et al., 2019), were upregulated in response to *G. hyphopodioides,* with two also upregulated in response to *G. tritici* (table 5.6). As mentioned in section 5.3.9, *G. hyphopodioides* colonisation resulted in the upregulation of several PR1-like genes. PR1 gene expression is often used as an SA marker due its strong induction during SA-mediated plant immune responses. Thus, despite some contrasting results, the data suggest that SA could be involved in plant responses to *G. hyphopodioides*, though perhaps less so for *G. tritici.*

Table 5.6 Expression of genes involved in salicylic acid (SA) biosynthesis and SA mediated signalling.

		5 dpi			
		Wheat + Gh		Wheat + Gt	
Gene ID	Gene name	Log2FC	padj	Log2FC	padj
TraesCS6B02G119900	SARD1-like	-6.05	4.66E-03	*	*
TraesCS2D02G449400	SABP2-like	4.34	1.60E-13	*	*
TraesCS4B02G296400	SABP2-like	2.86	2.23E-13	*	*
TraesCS3A02G325300	SABP2-like	3.44	2.33E-03	*	*
TraesCS4D02G295300	SABP2-like	4.26	1.14E-16	2.73	9.34E-05
TraesCS4A02G008500	SABP2-like	6.55	4.89E-12	3.95	2.33E-03

Gibberellins (GAs) are diterpenoid hormones with diverse roles in growth, development and signalling, and are produced by both plants and fungi (Chanclud & Morel, 2016). GA biosynthetic process was a significantly enriched GO term in *G. tritici* infected plants from 2 dpi onwards. Furthermore, isoprenoid biosynthetic process was a highly enriched GO term among the core subset of genes differentially expressed in both *G. tritici* infected and *G. hyphopodioides* colonised plants at 5 dpi (section 5.3.6). In accordance, the upregulation of early-stage GA biosynthesis genes such as CPS, KS and KO, generally occurred earlier and expression was higher in *G. tritici* infected plants. However, at 4 and 5 dpi, differential expression levels were highly similar in *G. hyphopodioides* colonised and *G. tritici* infected samples compared to the control. In contrast, the expression of late-stage GA biosynthesis genes such as GA20ox, GA1ox, GA2ox and GA3ox, responsible for the production of bioactive forms of GA (Huang et al., 2012), were DE in *G. hyphopodioides* colonised samples only (3 up/ 7 down) (table 5.7).

Table 5.7 Expression of key genes involved in the biosynthesis of gibberellic acid (GA). CPS, *ent*-copalyl diphosphate synthase; KS, *ent*-kaurene synthase; KO, *ent*-kaurene oxidase; KAO, *ent*-kaurenoic acid oxidase; GA20ox, GA 20-oxidase; GA1ox, GA 1-oxidase; GA2ox, GA 2-oxidase; GA3ox, GA 3-oxidase.

		2 dpi				4 dpi				5 dpi			
		Wheat + Gh		Wheat + Gt		Wheat + Gh		Wheat + Gt		Wheat + Gh		Wheat + Gt	
Gene ID	**Name**	**Log2FC**	**padj**	**Log2FC**	**padj**	**Log2FC**	**padj**	**Log2FC**	**padj**	**Log2FC**	**padj**	**Log2FC**	**padj**
TraesCS2A02G027800	CPS	6.90	6.38E-04	7.96	2.99E-06	14.33	8.66E-27	14.68	5.22E-30	12.69	2.10E-31	12.23	1.24E-30
TraesCS2B02G445500	CPS	7.80	1.68E-03	9.34	2.52E-06	16.05	1.66E-23	16.42	1.38E-26	15.19	3.79E-23	14.51	2.97E-22
TraesCS2A02G027200	CPS-like	*	*	*	*	19.25	4.03E-04	24.34	1.45E-07	29.75	3.93E-11	27.12	1.39E-09
TraesCS2D02G029600	CPS-like	*	*	6.71	2.34E-02	13.56	1.74E-16	13.41	2.02E-17	14.23	4.39E-19	13.73	2.45E-18
TraesCSU02G244600	CPS-like	*	*	16.71	1.70E-06	23.21	4.69E-16	23.05	8.61E-18	25.06	1.33E-19	25.64	2.97E-22
TraesCSU02G252000	CPS-like	*	*	*	*	22.75	2.06E-15	22.69	3.09E-17	24.83	2.76E-19	25.18	2.03E-21
TraesCS2B02G445200	KS	7.17	7.82E-03	8.33	6.62E-05	11.16	3.06E-15	11.59	2.77E-18	12.61	1.76E-18	12.14	7.60E-18
TraesCS2B02G445100	KS	*	*	*	*	8.40	2.21E-26	8.84	8.95E-34	9.06	3.29E-32	8.55	2.58E-31
TraesCSU02G008700	KS-like	*	*	5.73	6.84E-03	13.27	2.64E-19	13.89	8.24E-23	11.26	1.14E-17	11.25	2.45E-18
TraesCS2B02G445300	KO-B4-1	*	*	5.08	3.56E-03	12.68	6.78E-22	13.29	3.12E-26	12.89	1.34E-29	12.20	2.02E-28
TraesCS2B02G445400	KO-B4-2	*	*	*	*	11.94	1.74E-08	12.50	4.00E-10	13.98	1.15E-12	13.58	3.01E-12
TraesCS4A02G460100	KAO-A1	*	*	*	*	*	*	*	*	-2.38	2.75E-03	*	*
TraesCS4B02G172200	GA13ox-B2	*	*	*	*	*	*	*	*	-3.27	3.30E-02	*	*
TraesCS4A02G319100	GA20ox-A1	*	*	*	*	*	*	*	*	-3.49	2.95E-12	*	*
TraesCS5B02G560300	GA20ox-B1	*	*	*	*	*	*	*	*	-4.04	3.28E-07	*	*

TraesCS5D02G566200	GA20ox-D1	*	*	*	*	*	*	*	*	-3.91	1.04E-05	*	*
TraesCS2B02G570800	GA1ox-B1	*	*	*	*	*	*	*	*	4.57	2.27E-02	*	*
TraesCS3D02G542800	GA2ox8	*	*	*	*	*	*	*	*	-2.85	2.06E-03	*	*
TraesCS2A02G379000	GA2ox-A6-1	*	*	*	*	*	*	*	*	-4.35	3.96E-03	*	*
TraesCS1B02G145600	GA2ox-B10	*	*	*	*	*	*	*	*	4.79	2.85E-02	*	*
TraesCS3D02G149600	GA2ox-D7	*	*	*	*	2.99	3.46E-02	*	*	4.75	1.69E-08	*	*
TraesCS3B02G141800	GA3ox-B2	*	*	*	*	*	*	*	*	-4.77	3.54E-02	*	*

The differential expression of JA, ET, SA and GA related genes suggests that these phytohormones may be involved in the wheat response to *G. hyphopodioides* colonisation and/or *G. tritici* infection. To investigate whether the transcriptional changes described above result in altered hormone levels, hormone quantifications of JA, SA, GA1 and GA4 were carried out in *G. hyphopodioides* colonised, *G. tritici* infected and uninoculated control roots at 5 dpi. Due to complications with *in planta* quantification methods, ET levels were not quantified. The analysis revealed that *G. hyphopodioides* colonised roots contained significantly higher levels of GA1 (ANOVA: F=9.13, d.f. 2, 6, p=0.015) and GA4 (ANOVA: F= 46.59, d.f. 2, 6, p<0.001) as compared to the control (figure 5.17). In contrast, there was no significant difference in GA1 or GA4 levels in *G. tritici* infected roots compared to the control. Surprisingly, we found no significant difference in the levels of SA and JA between any treatments (appendix A.7; table A.7.9). Nevertheless, there was a trend for lower SA levels in *G. hyphopodioides* colonised plants and more so in *G. tritici* infected plants. Taken together, the data suggest that GA is involved in early *G. hyphopodioides* colonisation. However, the contribution of JA and SA remains inconclusive.

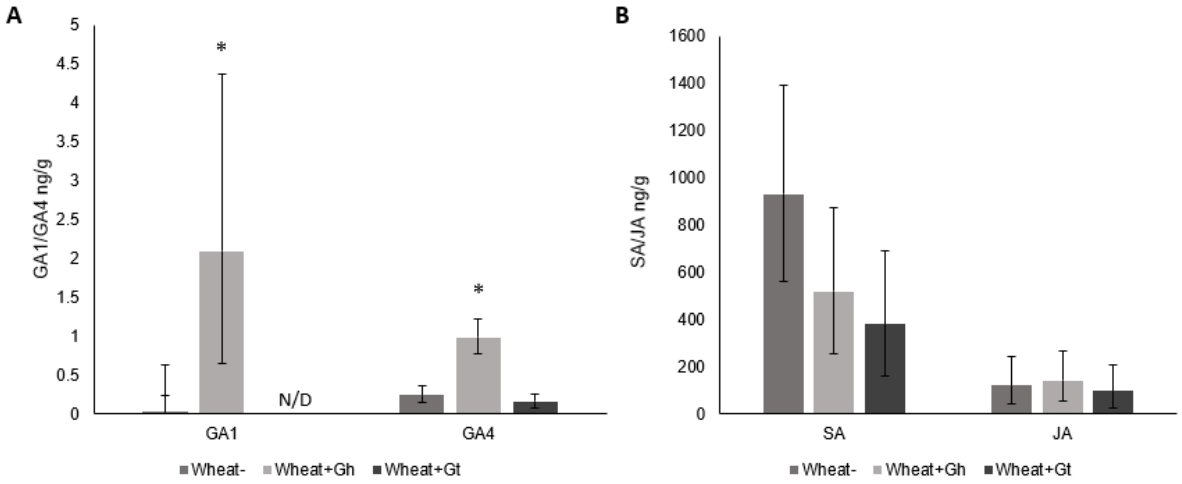


Figure 5.17 Hormone quantifications of GA1, GA4, SA and JA in roots harvested at 5 dpi. Data have been back-transformed from a square root scale. Asterisks indicate significant differences to the uninoculated control (wheat-) determined using least

significant differences of means values ($p<0.05$). Error bars represent back-transformed 95% confidence intervals. N/D= not detected.

5.4 Discussion

Using a seedling co-inoculation bioassay, we demonstrated that pre-treatment of wheat with *G. hyphopodioides* results in a significant reduction in both take-all disease levels and *G. tritici* fungal biomass. Furthermore, previous *in vitro* studies carried out in chapter 3 suggest that the direct interaction between *G. tritici* and *G. hyphopodioides* is unlikely to significantly contribute to disease reduction. Taken together, these findings suggest that *G. hyphopodioides* controls take-all by induced plant resistance. To investigate the plant responses which may be involved in *G. hyphopodioides*-induced resistance against take-all, we performed transcriptome profiling of *G. hyphopodioides* colonised and *G. tritici* infected wheat. The study has provided detailed information regarding the intricate processes which govern root immune responses to two closely related non-pathogenic and pathogenic fungi in the *Magnaporthaceae* family. In the absence of take-all resistant wheat cultivars or avirulent *G. tritici* isolates, the findings have provided several avenues of investigation for the future elucidation of take-all resistance mechanisms in wheat. Our time-resolved, dual RNA sequencing approach was made possible by detailed confocal microscopy of precision inoculated root samples, enabling comparisons of wheat responses across distinct stages of fungal infection/colonisation.

Confocal microscopy of WGA and PI stained samples enabled targeted investigations into three key stages of fungal infection; runner hyphae growth on the root surface (2 dpi), epidermal and cortical colonisation (4 dpi), and finally *G. tritici* infection of the stele or *G. hyphopodioides* production of SEVs in the cortex (5 dpi). Hence, our transcriptome data represent the early stages of fungal colonisation/infection, prior to the development of necrotic lesions by *G. tritici.* Interestingly, we found that melanised macrohyphae and mature SEVs produced by *G. hyphopodioides* were not always stained with WGA. As WGA binds to key components of fungal chitin, this finding suggests that chitin may be masked or

obstructed in these structures which may prevent plant detection (Shinya et al., 2015).

The study revealed extensive transcriptional reprogramming by 5 dpi in response to *G. hyphopodioides*, as determined by the identification of 7532 DEGs compared to the uninoculated control. In contrast, 1074 DEGs were identified in response to *G. tritici* at 5 dpi, the majority being upregulated. This finding contrasts a previous study by Zhang et al. (2020), who reported a higher proportion of downregulated genes compared to upregulated genes in response to *G. tritici* infection at 5 dpi. However, almost all of the genes which were DE in response to *G. tritici* infection were also DE in response to *G. hyphopodioides* colonisation, thus indicating a subset of common plant responses to *G. hyphopodioides* and *G. tritici.* Highly enriched GO terms within this subset of genes included isoprenoid biosynthesis, response to biotic stimulus and secondary metabolic process, indicating a very clear plant defence response to both fungi. Despite this defence response, *G. tritici* can still successfully cause disease, suggesting that the pathogen can avoid or suppress plant defences as infection progresses. Therefore, future studies should focus on elucidating candidate effectors which no doubt contribute to *G. tritici* pathogenicity. One such effector, the ortholog of the barley powdery mildew effector gene BEC1019, has already been associated with *G. tritici* virulence in wheat (Zhang et al., 2019).

Though *G. hyphopodioides* colonisation alone does not typically cause disease symptoms or adversely affect plant health (see chapter 7), the transcriptome data revealed the strong induction of a diverse range of plant defences. For instance, *G. hyphopodioides* colonisation resulted in the differential expression of 51 WRKY transcription factors (TFs) at 5 dpi, compared to 14 in response to *G. tritici.* WRKY TFs comprise a large gene family with diverse roles in growth, development, response to environmental stress and regulation of plant innate immunity (PTI and ETI) (Chen et al., 2019). In total, 14 predicted WRKY28 TFs were significantly upregulated in *G. hyphopodioides* colonised roots, compared to just four in *G. tritici* infected roots. In Arabidopsis, WRKY28 is rapidly induced by pathogen elicitors and contributes to PTI via the accumulation of SA (van Verk

et al., 2011). However, SA accumulation was not detected in the present study, suggesting that WRKY28 may operate through other pathways in wheat. Three homoeologous copies of the WRKY26 genes were DE in response to *G. hyphopodioides*, but not *G. tritici.* So far, WRKY26 has only been associated with responses to environmental stresses such as heat (Li et al., 2011), and has recently been linked to root growth during the shade avoidance response in Arabidopsis (Rosado et al., 2022). This may be the first study in which WRKY26 has been associated with plant defences, though further functional validations are required. Moreover, we noticed that *G. hyphopodioides* colonisation resulted in the strong induction of many receptor kinase genes, suggesting that *G. hyphopodioides* colonisation sensitises key components of PTI.

Various phytohormones, including JA, ET, SA and more recently GA, are known to influence and mediate plant responses to biotic stress. Notably, JA is thought to act as a core component of the phytohormone signalling network, often interacting with ET, SA and GA to regulate plant growth, stress tolerance and disease resistance (Yang et al., 2019). Though JA-dependent defences are generally considered to be important against necrotrophic pathogens and SA-dependent defences considered more important in response to biotrophic pathogens, the opposite finding has been reported for the *G. tritici*-wheat interaction (Kang et al., 2019). Indeed, this classical model may not always apply to root interactions, particularly during early stages of infection (De Coninck et al., 2015). As previously mentioned, phytohormones also play key roles in induced resistance mechanisms, with JA/ET commonly associated with induced systemic resistance (ISR) and SA usually associated with systemic acquired resistance (SAR) (Choudhary et al., 2007).

Curiously, despite the differential expression of a range of genes associated with JA/SA biosynthesis and signalling, particularly in *G. hyphopodioides* colonised plants, hormonal quantifications failed to reveal a difference in the levels of JA or SA in colonised roots compared to control roots. Therefore, the mode of *G. hyphopodioides* induced resistance remains unclear. One explanation for this discrepancy could be that as previously described for the closely related *M.*

oryzae, *G. hyphopodioides* and/or *G. tritici* may convert host and fungal derived JA to avoid triggering JA-mediated defence responses during early stages of infection (Patkar et al., 2015). Several fungi have also been reported to target the host SA pathway by preventing the formation of SA, or by targeting the expression of key regulators such as SARD (Han & Kahmann, 2019). Hence, the downregulation of SARD in response to *G. hyphopodioides* in this study (see section 5.3.10) may be significant, and future studies may wish to investigate these hypotheses.

In contrast, we detected a significant increase in GA1 and GA4 levels in *G. hyphopodioides* colonised roots, but not *G. tritici* infected roots, as compared to the control. The strong upregulation of several CPS genes by both fungi (CPS genes acting at the internode between phytoalexin and GA production) may therefore reflect the accumulation of phytoalexins, rather than GA (Hasegawa et al., 2010). If this is the case, it is tempting to suggest that *G. hyphopodioides* produces GA to favour fungal colonisation, as is the case in many mycorrhizal fungi (Liao et al., 2018) and indeed pathogenic fungi (Han & Kahmann, 2019). However, unless GA production gives *G. hyphopodioides* a competitive advantage prior to *G. tritici* infection, GA is unlikely to play a significant role in *G. hyphopodioides*-mediated resistance against take-all disease.

Plant lignins are a major component of the secondary cell wall of vascular plants and lignin biosynthesis is known to be upregulated in response to pathogen attack (Bi et al., 2011) by functioning as a physical barrier to microbial invasion (Łaźniewska et al., 2012; Miedes et al., 2014). Increased lignification has also been documented in response to colonisation by beneficial endophytes such as *Trichoderma* (Basińska-Barczak et al., 2020), potentially playing a role in induced resistance against plant pathogens. From 4 dpi onwards, *G. hyphopodioides* colonisation resulted in the upregulation of several key lignin biosynthesis genes. In agreement with previous transcriptomics studies (Kang et al., 2019; Zhang et al., 2020), *G. tritici* infection also resulted in the upregulation of key components of the lignin biosynthesis pathway. However, the response was generally slower than for *G. hyphopodioides*, with most genes significantly upregulated at 5 dpi

only, at which point *G. tritici* had already successfully infected the stele. One exception was caffeic acid O- methyltransferase (COMT), a gene involved in monolignol biosynthesis and highly upregulated in *G. tritici* infected samples from 2 dpi onwards. COMT has been associated with plant resistance to a range of pathogens (Miedes et al., 2014).

The upregulation of key lignin biosynthesis genes in response to *G. hyphopodioides* corroborates early microscopy studies into the wheat response to colonisation by non-pathogenic *Magnaporthaceae* species. Speakman & Lewis (1978) demonstrated that wheat root colonisation by *Slopeiomyces cylindrosporus* (previously *Phialophora radicicola* var. *graminicola*) and *Gaeumannomyces radicicola* (previously *Phialophora radicicola* var. *radicicola*) resulted in the lignification and suberisation of the root stele and endodermis, well in advance of the growing hyphae, which were restricted to the root cortex. However, in this study, potassium permanganate staining of samples harvested at 5 dpi did not reveal any obvious lignification of the stele. Furthermore, there was some variation in the overall level of lignification within *G. hyphopodioides* colonised and *G. tritici* infected roots, suggesting that the lignification response is likely to be very local. Indeed, individual cells containing large amounts of fungal hyphae exhibited thickened cell walls with higher levels of lignin as compared to surrounding cells which were uncolonised.

Though previous studies have suggested that root lignification is responsible for the control of *G. tritici* by non-pathogenic *Magnaporthaceae* species (Huang et al., 2001; Speakman & Lewis, 1978), the upregulation of lignin biosynthesis genes by *G. tritici* itself, and the highly localised nature of lignification suggests that lignification alone is unlikely to be sufficient for effective take-all control. Furthermore, previous studies have revealed that *G. tritici* expresses several laccase genes *in planta*, suggesting that the fungus can degrade lignin (Daval et al., 2011). Instead, we argue that take-all control by *G. hyphopodioides* is a result of numerous plant defence mechanisms, which together contribute to resistance against take-all disease.

Despite the limited role of cell wall lignification, cell wall integrity may contribute significantly to *G. hyphopodioides*-mediated resistance. The plant cell wall, once considered a passive defensive barrier, is now emerging as an important monitoring and assault system against invading pathogens (Bacete et al., 2018). Plant cells which are still expanding contain a dynamic primary cell wall consisting of cellulose, hemi-celluloses and pectins, as well as glycoproteins such as arabinogalactan proteins and extensins (Cosgrove, 2005). Cells may require additional reinforcements following cellular expansion, for example through the enrichment of xylans and lignin. These reinforcements make up the plant secondary cell wall (Sarkar et al., 2009). Apart from acting as a physical barrier to pathogen invasion, the cell wall also contains a reservoir of antimicrobial compounds which can be released upon attack to perturb pathogen invasion. As the plant cell wall is an attractive source of nutrients, the structure is a common target for a wide range of pathogens (Bacete et al., 2018). Consequently, plants have developed a cell wall integrity (CWI) maintenance mechanism. Impairment of CWI by pathogen invasion triggers the release of Damage-Associated Molecular Patterns (DAMPs), which can induce plant innate immune responses upon recognition by plant Pattern Recognition Receptors (PRRs) (Miedes et al., 2014).

In this study, *G. hyphopodioides* colonisation resulted in the significant downregulation of 124 genes, out of a total of 1122 genes known to be involved in cell wall organisation and biogenesis in wheat. Included were 13 FLA genes and 18 XTH genes. FLA proteins contain a putative cell adhesion domain which may link the cell membrane and the cell wall. FLA mutants in Arabidopsis exhibit a range of phenotypes including reduced cellulose content, altered secondary cell-wall deposition, disrupted root elongation and reduced tensile strength (Ashagre et al., 2021). Comparatively little is known about FLAs in wheat, though the downregulation of FLAs has been associated with reduced grain strength, suggesting a key role in CWI (Nirmal et al., 2017). XTH genes are also involved in the maintenance of CWI; they encode the xyloglucan modifying enzymes xyloglucan endotransglycosylase/hydrolases which cleave xyloglucan chains to enable cell wall expansion or alter cell wall strength (Cosgrove, 2005).

In addition, we detected the downregulation of several CESA genes. Mutations in the CESA4, CESA7 and CESA8 genes, required for secondary cell wall formation in Arabidopsis, conferred enhanced resistance to the necrotrophic fungus *Plectrosphaerella cucumerina* and the biotrophic bacterium *Ralstonia solanacearum* (Hernández-Blanco et al., 2007). In addition, *Fusarium oxysporum* root infection of Arabidopsis resulted in the downregulation of various CESAs, resulting in an alteration in primary cell wall cellulose and contributing to disease resistance (Menna et al., 2021). Hence, the downregulation of CESA genes in the present study could suggest a role for cellulose biosynthesis in *G. hyphopodioides*-induced take-all disease resistance. However, wheat CESAs are poorly characterised and further analysis is needed to investigate how the altered expression of different CESAs may affect primary and/or secondary cellulose biosynthesis. Therefore, we hypothesise that *G. hyphopodioides* colonisation results in the widescale disruption of CWI, likely triggering the activation of downstream defence pathways and significantly contributing to *G. hyphopodioides*-mediated resistance to take-all disease.

Due to the lack of high-quality annotated *G. tritici* and *G. hyphopodioides* genomes, comparative analysis of gene expression during *G. hyphopodioides* colonisation and *G. tritici* infection was not possible in this study. However, the genomes are expected to be ready imminently which, combined with this RNAseq dataset, will no doubt facilitate the investigation of *G. tritici* pathogenicity factors.

In summary, we reveal rapid and extensive transcriptional reprogramming in *G. hyphopodioides* wheat roots, characterised by the strong induction of diverse plant defence mechanisms. We propose that the collective effect of these defence mechanisms results in *G. hyphopodioides*-mediated take-all control. However, the transcriptional responses to *G. hyphopodioides* and *G. tritici* co-infection are yet to be elucidated.

5.5 Acknowledgement of contributions

Thank you to Dr Dan Smith for his valuable help and guidance with the bioinformatics pipeline. Thanks also to Dr Esther Carrera for carrying out the hormone quantifications, performed at the Plant Hormone Quantification Service,

IBMCP, Valencia, Spain (section 5.2.9). Thank you to Kirstie Halsey for preparing and imaging root samples for the visualisation of lignin (section 5.2.10). Thank you to Dr Andy Phillips, Dr Steve Thomas and Dr Peter Hedden for their valuable guidance interpreting hormone expression patterns and hormone quantification data.

6 A Virus-induced gene silencing (VIGS) system to study wheat interactions with root-infecting fungi

NB: The present chapter has been written in a manuscript format to facilitate future publication of this work. Hence, the introduction may contain some information which is repeated in other chapters of this thesis.

6.1 Abstract

Virus-induced gene silencing (VIGS) is a rapid alternative to stable transformation techniques. VIGS is a particularly useful technique for the study of gene function in cereal species such as wheat, which are notoriously challenging to transform. Barley stripe mosaic virus (BSMV) is a popular vector for VIGS in wheat and is already used for the study of candidate resistance genes against important foliar pathogens. However, BSMV-mediated VIGS has not yet been used for the study of cereal root-infecting pathogen interactions. Here, we describe a BSMV-VIGS protocol suitable for reverse genetics studies of genes potentially involved in the wheat interaction with *Gaeumannomyces tritici*, the causal agent of take-all disease, one of the most important root diseases of wheat worldwide. Our protocol may also be used for the study of other important wheat root interactions.

6.2 Introduction

Virus-mediated transient expression techniques enable the rapid and specific manipulation of gene expression in cereal species such as wheat, which are otherwise difficult to transform. Virus-induced gene silencing (VIGS) is one such example. In VIGS, the host plant's natural RNA-mediated antiviral defence mechanism is exploited to characterise the function of plant genes. The barley stripe mosaic virus (BSMV) has been genetically modified for this purpose and is a popular vector for VIGS in cereals. The virus contains a tripartite genome comprising RNAα, RNAβ and RNAγ. Following sequencing and cloning of these genome components in the late 1980's, we now have a detailed understanding of the molecular and biological functions of the virus, making BSMV a good vector candidate for transient expression techniques such as VIGS (Jackson et al., 2009; Jiang et al., 2021).

Indeed, BSMV-mediated VIGS has already been successfully used to study a number of wheat fungal pathogen interactions such as wheat-Septoria tritici leaf blotch (STB) (Lee et al., 2015), wheat-powdery mildew (Geng et al., 2013), wheat-leaf rust (Scofield et al., 2005), wheat-stripe rust (Wang et al., 2011) and wheat-Fusarium Head Blight (Fan et al., 2019). VIGS works by inserting a short fragment (120-300 nucleotides long) of the plant gene of interest into the cloned virus genome. The recombinant virus is then inoculated into wheat leaves, where the virus multiplies and spreads into new developing tissues, triggering post-transcriptional gene silencing. The inserted gene sequence is also targeted for silencing, as is the corresponding endogenous gene in the plant. Hence, VIGS results in the reduction or complete loss of the target gene function in newly formed plant tissues, enabling investigation of the resulting phenotype (Lee et al., 2012). Because VIGS does not require stable genetic transformation, the technique can be carried out relatively quickly, making low- to medium-throughput analysis of multiple genes possible in a wide range of cultivars. Furthermore, as BSMV infection is systemic, BSMV-VIGS can be utilised for the study of genes expressed in a range of plant tissues, including roots (Lin & Langenberg, 1984).

However, relatively few studies have attempted VIGS in cereal roots and despite the growing importance of soil-borne pathogens (Delgado-Baquerizo et al., 2020), VIGS has not yet been utilised for the study of cereal root-infecting pathogens. Unlike in foliar tissues where newly formed silenced tissues can be easily harvested, sampling of new root material produced after viral inoculation is challenging. For VIGS experiments in foliar tissues, the phytoene desaturase (PDS) gene, involved in the carotenoid biosynthesis pathway, is often targeted to provide a positive control due to the striking photobleaching symptoms produced following successful silencing. Similarly, targeting the magnesium chelatase subunit H gene (ChlH) results in a striking yellow-orange phenotype in new leaves due to a disruption in chlorophyll biosynthesis (Lee et al., 2015). However, a positive silencing control with a clear root phenotype does not exist for wheat.

Nevertheless, VIGS studies have been conducted in cereal roots. In a hydroponics system, Pacak et al., (2010) used BSMV-mediated VIGS to silence IPS1, PHR1, and PHO2 genes in barley, known to participate in inorganic phosphate uptake and reallocation in Arabidopsis. The authors noted that although the three genes were successfully silenced in barley roots using BSMV-VIGS, the instability of the viral vector prevented them from silencing other candidate genes. The authors speculate that the issue of vector instability is a bigger problem for gene silencing in roots compared to leaves, since it is more difficult to identify the optimal window for silencing in roots. More recently, He et al., (2015) reported successful silencing of the cell-wall expansin gene HvEXPB7, revealing a key role in barley root hair development and subsequent K^+ absorption.

BSMV-VIGS has also been successful in wheat roots. Bennypaul et al., (2012) reported successful silencing of the coronatine insensitive1 (COI1) gene, a root expressed gene involved in the regulation of the jasmonic acid (JA) mediated signalling pathway. Wheat leaf inoculation with the BSMV:TaCOI1 construct resulted in a 52% reduction in TaCOI1 transcript levels in wheat cv. Scarlet, with a 26% reduction in root length compared to the uninoculated control. However, inoculation with the virus-only negative control construct BSMV:MCS also resulted in a reduction in root length. Hence, the root phenotype was likely due to reduced plant vigour as a result of viral infection, rather than as a direct consequence of TaCOI1 silencing. The authors point out that silencing of root-expressed genes in wheat is extremely complex, and reproducibility depends on many factors including the host plant physiology, the degree of infection and the mobilisation of virus particles to the roots. Nevertheless, the study provides key evidence that BSMV mediated VIGS in wheat roots can be achieved by leaf inoculation.

Here, we present a system for BSMV-VIGS in wheat roots, enabling straightforward sampling of new, silenced root material. Furthermore, we present the development of the positive control construct BSMV:TaRTH3, which causes a significant reduction in TaRTH3 (*roothairless3*) transcript levels and a striking

reduction in total root length, root volume and root branching. Additionally, we demonstrate that our BSMV-VIGS system is compatible with the soil-borne pathogenic fungus *Gaeumannomyces tritici,* the causal agent of devastating take-all root disease (Palma-Guerrero et al., 2021). Together, the system will facilitate the study of candidate plant genes involved in the compatible and incompatible interactions with important and understudied root infecting pathogens such as *Gaeumannomyces tritici.*

6.3 Materials and methods

6.3.1 Gene target choice

TaRTH3 (TraesCS4A02G117100.1, TraesCS4B02G187300.1, TraesCS4D02G188600.1) and TaDGL1 (TraesCS7A02G415500.1, TraesCS7B02G315600.1, TraesCS7D02G409000.1), identified based on homology to the known genes in maize and rice respectively, were selected for construct design based on the presence of a clear mutant root phenotype in cereal species and the availability of efficient siRNAs (table 6.1). Gene fragments for cloning into the BSMV VIGS vector were selected using siRNA-Finder (si-Fi) software (Lück et al., 2019). Full details regarding selection criteria can be found in appendix A.8; table A.8.1.

Table 6.1 Root expressed genes selected for VIGS in wheat.

Gene	Function	Mutant phenotype	Reference
Roothairless3 (TaRTH3)	Encodes COBRA- like protein with GTP-binding motifs, involved in root hair formation in maize	Short root hairs in maize	(Hochholdinger et al., 2008)
Dolichyl-diphosphooligosaccharide-protein (TaDGL1)	Involved in N-glycosylation and necessary for the structure of the polysaccharide matrix of root cell walls in rice	Short roots and root cell-death in rice	(Qin et al., 2013)

6.3.2 VIGS construct preparation and *Nicotiana benthamiana* infiltration

VIGS construct preparation, transformation of electro-competent *Agrobacterium tumefaciens* cells and infiltration into *Nicotiana benthamiana* was carried out using a previously published protocol by (Lee et al., 2015). Gene fragments were inserted into the BSMV RNAy binary vector pCa-ybLIC by ligation independent cloning (see appendix A.8; figure A.8.1, for the vector map). The BSMV:mcs4D construct containing a 275-nt noncoding DNA sequence amplified from the multiple cloning site (mcs) of the pBluescript II SK vector (Agilent Technologies), was included as a negative silencing control (Saintenac et al., 2018). The BSMV:ChlH construct was included as a positive silencing control for foliar tissues due to the characteristic yellowing of leaves in silenced plants (Lee et al., 2015).

6.3.3 *G. tritici*-wheat VIGS infection protocol

The *G. tritici*-wheat VIGS protocol was developed with the goal of achieving BSMV infection (and hence gene silencing) in wheat roots prior to subsequent infection with *G. tritici.* We accomplished this by transferring BSMV-inoculated wheat plants to a larger pot containing *G. tritici* inoculum. A nylon mesh separated old and new root growth to allow easy identification and harvesting of new, silenced root material.

Wheat seeds cv. Chinese Spring were surface sterilised in 1% sodium hypochlorite for 10 mins, followed by three 1-minute washes with sterile distilled water. Seeds were pre-germinated on damp sterile filter paper in petri dishes and placed on a lit shelf (20 °C, 16 hr light cycle, humidity 60%) for 2 days. Seeds at a similar stage of germination were transplanted into small pots (W x H 4cm x 5.5cm) containing moist sterile vermiculite. Pots were placed in trays and lightly watered from above every two days. A propagation hood was used to cover the pots for the first two weeks of growth.

After 10 days, when the plants were at the second (or early third) leaf stage, the 1st and 2nd leaves were rub-inoculated with the sap from infiltrated *N.*

benthamiana plants (as described above). Leaf tissue (1 g) was ground in a pre-chilled mortar and pestle and mixed with 2.5 ml 10 mM potassium phosphate buffer (pH 7) and a small amount of Celite® 545 AW (Thermo Fisher Scientific, USA) to serve as an abrasive. Wheat leaves were rub-inoculated by dipping gloved fingers in the sap and running them along each leaf 10 times. The plants were left to absorb the virus for 10 minutes, before spraying with water to remove any residual Celite® 545 AW. Mock-inoculated plants were rub-inoculated with potassium phosphate buffer and Celite® 545 AW only.

Plants were watered with Phostrogen All Purpose Liquid Fertiliser (SolaBiol, UK; 1 scoop/4 L) and left to recover on an unlit shelf overnight. The following day, the base of each pot was cut away, replaced with a nylon mesh square (5 cm x 5 cm), and placed on top of a larger pot (W x H 5 cm x 6 cm) containing moist vermiculite. Phostrogen fertiliser was added once weekly from thereon.

For *G. tritici* treatments, the large pots were partially filled with moist vermiculite, leaving a 1 cm layer free at the top of the pot. Fungal inoculum (isolate GtLH(4)19d1) was added by taking a single plug from the leading edge of a 2-week-old *G. tritici* colony growing on potato dextrose agar (PDA) (Formedium, UK) using a no.3 cork-borer (6 mm diameter). The plug was cut into small pieces and spread on the surface of the vermiculite. A final 1 cm layer of vermiculite was added to fill the pot to the brim. Adding an inoculum layer in the larger base pot enabled *G. tritici* infection to be investigated in newly developed, silenced roots only (figure 6.1).

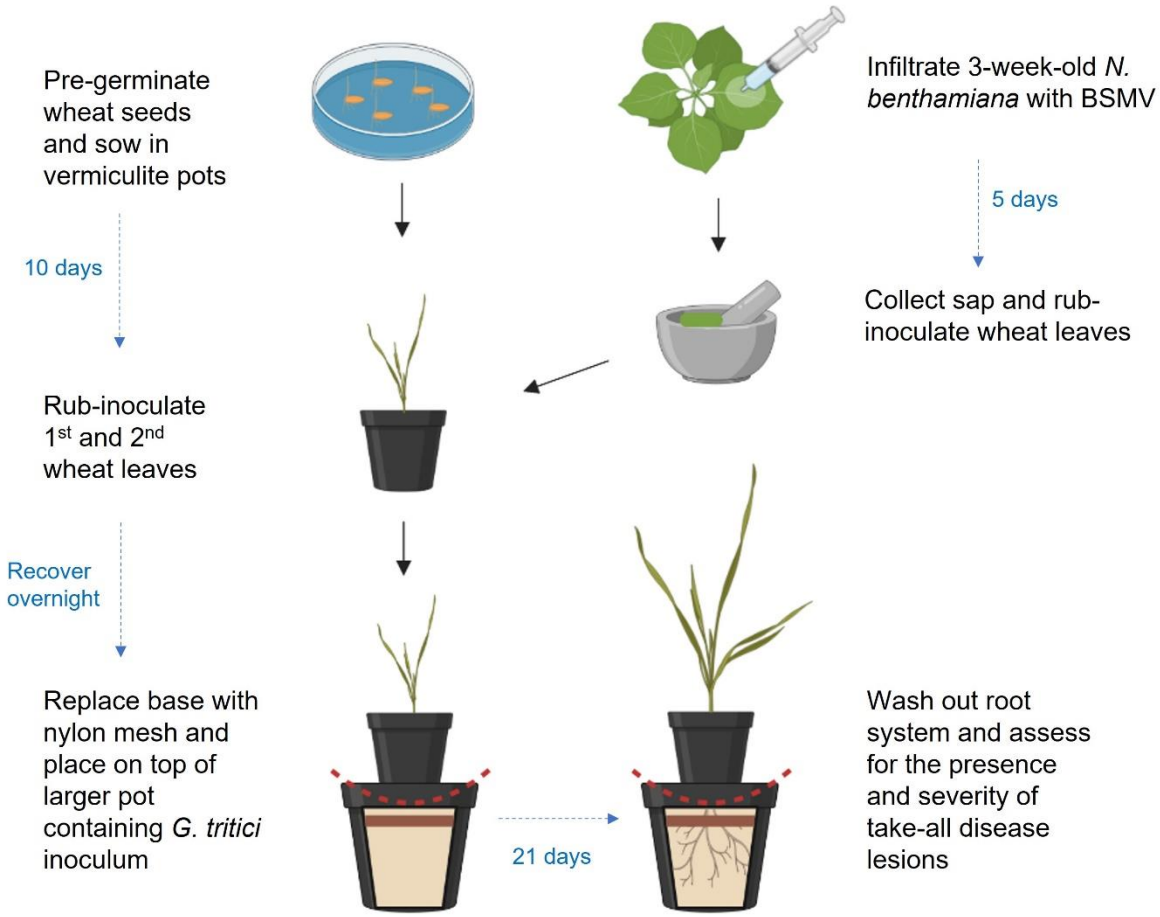


Figure 6.1 Protocol for virus-induced gene silencing (VIGS) for functional studies of candidate *G. tritici* resistance/susceptibility genes in wheat. Made in BioRender.com.

6.3.4 Harvesting and imaging root material

BSMV:ChlH inoculated plants exhibited characteristic symptoms of gene silencing in the leaves at 11 dpi. To enable the development of any silencing phenotypes in the roots, wheat plants were harvested at 21 days post BSMV inoculation. Plants exhibiting clear foliar virus symptoms (characteristic yellow stripes or yellow mottling on leaves) were taken for analysis. To sample and image the root system, plants were removed from the pots and the whole root system was placed in a shallow tray of water. Vermiculite was carefully removed from the new roots using a soft paintbrush. Clean root systems were placed in a large square petri dish (L × W × H 245 mm × 245 mm × 25 mm) containing a shallow layer of water. Roots were imaged from above using a Nikon D90 camera (Nikon, Japan) attached to a crank stand. To allow live, high-quality imaging, the

camera was linked with DigiCamControl V2 software (http://digicamcontrol.com/). Following imaging, the newly formed roots which had grown through the mesh square were cut away and immediately snap frozen in liquid nitrogen and stored at -80 °C until RNA extraction.

To aid root detection, root system images were colour inverted and converted to 32-bit grayscale format using ImageJ software (figure 6.2). Root architecture measurements were carried out using WinRHIZO Pro Arabidopsis software (Regent Instruments Inc, Canada). Data from three experimental replicates were pooled prior to analysis.

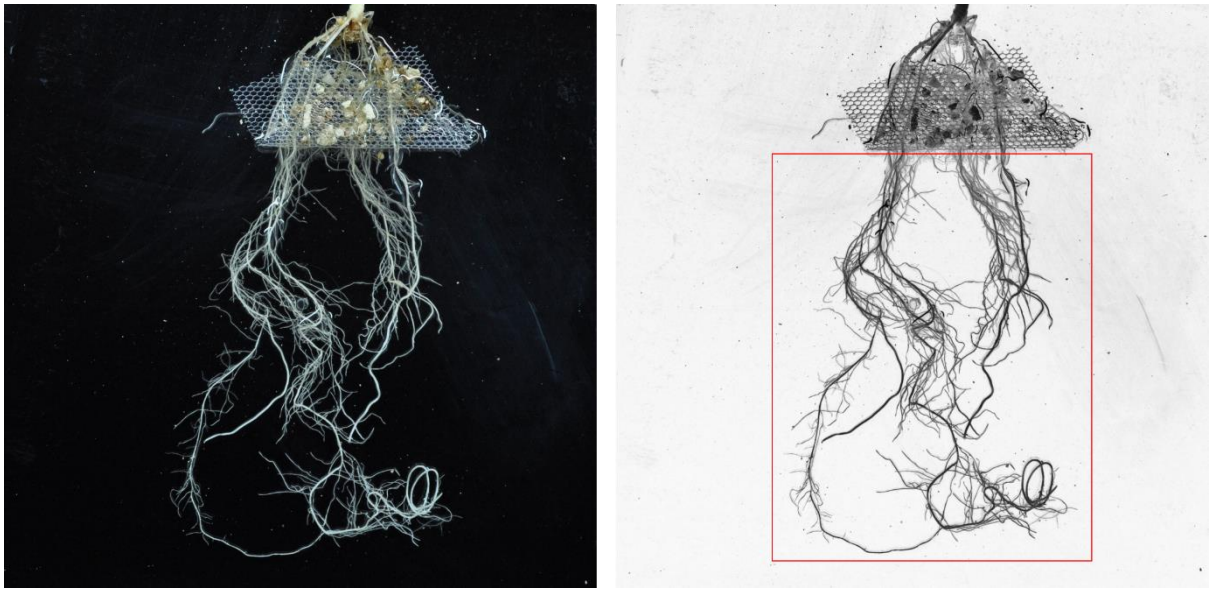


Figure 6.2 Image analysis of root architecture traits. Left: original root system image. Right: grayscale converted image for winRHIZO analysis. The red box indicates the region below the nylon mesh which was selected for analysis.

6.3.5 Take-all disease root assessments

To investigate the compatibility of BSMV-VIGS with *G. tritici* infection, two additional experiments were carried out to compare take-all disease incidence and severity with and without BSMV:mcs4D pre-inoculation. Due to a site refurbishment, the second experiment was carried out in a different growth room which was 2 °C warmer than the original conditions outlined in section 6.3.3.

Take-all disease incidence measurements were carried out as outlined in chapter 2.5, focussing only on the roots present below the nylon mesh. Take-all disease severity measurements were carried out by assessing the area of black lesion coverage on each root. Assessments were taken from the first 5 cm below the mesh and measurements were rounded to the nearest cm. The proportion of roots with lesions covering 0, 1, 2 , 3, 4 or 5 cm was then calculated. Data from the two experiments were combined prior to statistical analyses. Take-all disease incidence was analysed using a GLM, and severity data was analysed by ordinal logistic regression (see chapter 2.15).

6.3.6 RT-qPCR analysis of gene expression

RNA extractions were performed as described in chapter 2.9. RNA quality and DNA contamination was assessed by gel electrophoresis (300 ng total RNA, 1% agarose gel, 0.5 µg/ml ethidium bromide, 150 V, 20 minutes) prior to cDNA synthesis. cDNA was synthesised using the SuperScript™ IV Reverse Transcriptase Kit (ThermoFisher Scientific, USA) with Oligo (dT) primers according to the manufacturer's instructions. To confirm successful viral infection, PCR and gel electrophoresis analysis was carried out on the cDNA samples using primers BSMVα.F (5'-GTACGGCGCAACATCTCCTC-3') and BSMVα.R (5'-CACCCGCATTCACCTCACCTG-3') which amplify a 415 bp region of the BSMVα genome.

Primers for qPCR analyses were designed in Geneious software (https://www.geneious.com/) (table 6.2). Primers were selected from the 3' regions of the target gene coding sequence. An area outside of the fragment used for VIGS was targeted to avoid amplifying the viral construct. In addition, we ensured that primer annealing sites contained few/no SNPs between the three gene homoeologs and that the homoeologs had no indels located between primer annealing sites. RT-qPCR was carried out using the PowerTrack™ SYBR Green Master Mix (ThermoFisher Scientific, USA) on the QuantStudio™ 6 Pro Real-Time PCR System (Applied Biosystems™, USA). Thermal cycling conditions were as follows: 95 °C for 2 mins followed by 40 cycles at 95 °C for 5 s and 65 °C for 30 s, followed by a melt curve of 95 °C for 15 s, 60 °C for 1 min and 95 °C

for 15 s. Relative gene expression levels were calculated using the $2^{-\Delta\Delta CT}$ (Livak) method (Livak & Schmittgen, 2001), following normalisation to the cell division control 48 (CDC48) housekeeping gene (Lee et al., 2014).

Table 6.2 Primer sequences for RT-qPCR analyses. Primer annealing was performed at 65 °C.

Primer name	Primer Sequence
DGL1_qPCR_F1	ACAGGTTCCTAAAGTCTGGTGT
DGL1_qPCR_R1	AGGCTCATTTGTCTCCCCAA
RTH3_qPCR_F12	ACTTCAACAAGGGCTGGAGT
RTH3_qPCR_R10	CCGTCATACGCCTTGTCCAT
CDC48.F2	GTCCTCCTGGCTGTGGTAAAAC
CDC48.R2	AGCAGCTCAGGTCCCTTGATAC

6.4 Results and discussion

6.4.1 Development of a positive silencing control for wheat roots

BSMV-mediated VIGS experiments in wheat roots are currently hindered by the lack of a positive silencing control with a clear root phenotype. To develop a positive silencing construct, we targeted two genes (TaDGL1 and TaRTH3) with clear mutant phenotypes in rice and maize, respectively. In rice, DGL1 (UniProtKB:Q6ZLK0) is involved in N-glycosylation and root development. Rice mutants display a change of matrix polysaccharides in root cell walls, shorter root cell length, smaller root meristems, H_2O_2 accumulation and root cell death (Qin et al., 2013). TaDGL1 (UniProtKB/TrEMBL;Acc:A0A341YGZ0) transcripts in wheat were targeted by BSMV-VIGS, resulting in a significant reduction in total root length and root volume, but not root branching, across three experimental replicates (figures 6.3, 6.4). Surprisingly, RT-qPCR analysis revealed that TaDGL1 transcript levels were not significantly reduced at the point of harvest (21 days post-infection) (figure 6.4 A). We propose that TaDGL1 transcript levels may have been knocked-down at an earlier stage, but silencing was transient. A follow-up experiment involving TaDGL1 expression analysis at multiple time

points following BSMV:TaDGL1 inoculation is currently underway to test this hypothesis.

In maize, RTH3 (UniProtKB:Q5YLM2) is a COBRA-like protein involved in root hair formation. Maize mutants exhibit shorter root hairs and reduced grain yield (Hochholdinger et al., 2008). The wheat homoeologous gene copies TraesCS4A02G117100.1, TraesCS4B02G187300.1 and TraesCS4D02G188600.1 (COBRA-like 7) were identified as the putative orthologs of the maize RTH3 gene, with wheat homeologs sharing 84.1-84.7% sequence similarity with the RTH3 protein in maize. TaRTH3 transcripts were targeted in wheat using the VIGS vector BSMV:TaRTH3, resulting in a significant reduction in total root length, root volume and root branching, and on average a 46% reduction in gene expression across three experimental replicates (figures 6.3, 6.4). Though RTH3 expression was detected in emerging lateral root primordia in maize, RTH3 mutants did not display defects in lateral root formation (Hochholdinger et al., 2008). Conversely, our findings suggest that TaRTH3 could play an important role in lateral root formation in wheat, and as demonstrated by significantly shorter roots compared to the BSMV:mcs4D control, in seminal root growth. In addition, visible disruption in root hair formation was not observed in BSMV:TaRTH3 silenced plants, suggesting that RTH3 gene function is not conserved between wheat and maize. Alternatively, the level of gene silencing may not have been sufficient to cause visible disruptions in root hair formation, especially if functional redundancies exist within the COBRA gene family.

Another explanation could be that increased viral replication and viral load in BSMV:TaRTH3 plants may have resulted in the root phenotype described in this study. Initial findings revealed that despite significantly higher viral loads in BSMV:TaRTH3 inoculated plants compared to plants inoculated with BSMV:TaDGL1 and the BSMV:mcs4D control, increased viral load was not significantly correlated with reduced root volume, total root length or root branching (see appendix A.8; figure A.8.3, table A.8.4). The analyses are now being repeated with additional replicates to confirm these findings. Further studies are also required to characterise the function of RTH3 in wheat. Despite

these gaps in understanding, TaRTH3 remains a valuable marker gene for future VIGS experiments in wheat roots, enabling straightforward confirmation of successful silencing.

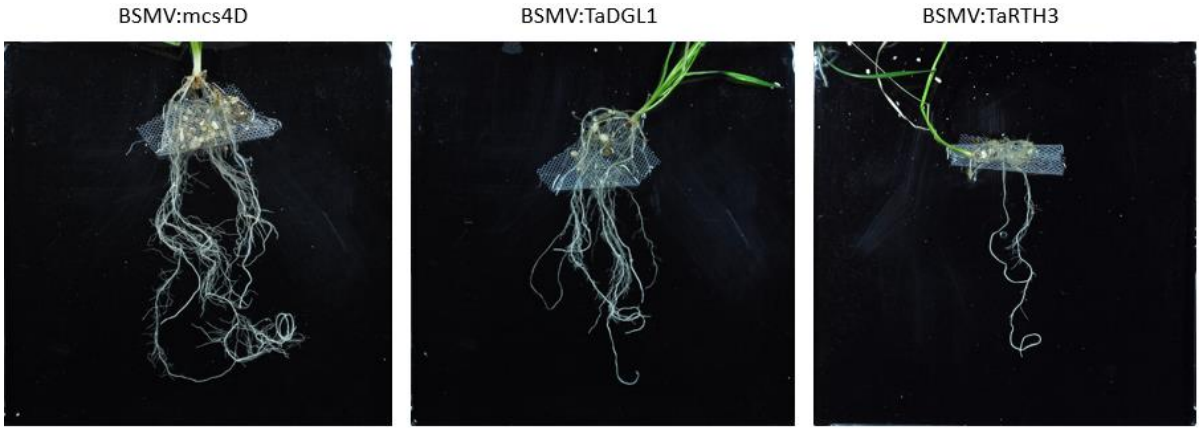


Figure 6.3 Root system images of BSMV:TaDGL1 and BSMV:TaRTH3 infected wheat plants compared to the BSMV:mcs4D control. Images taken at 21 dpi.

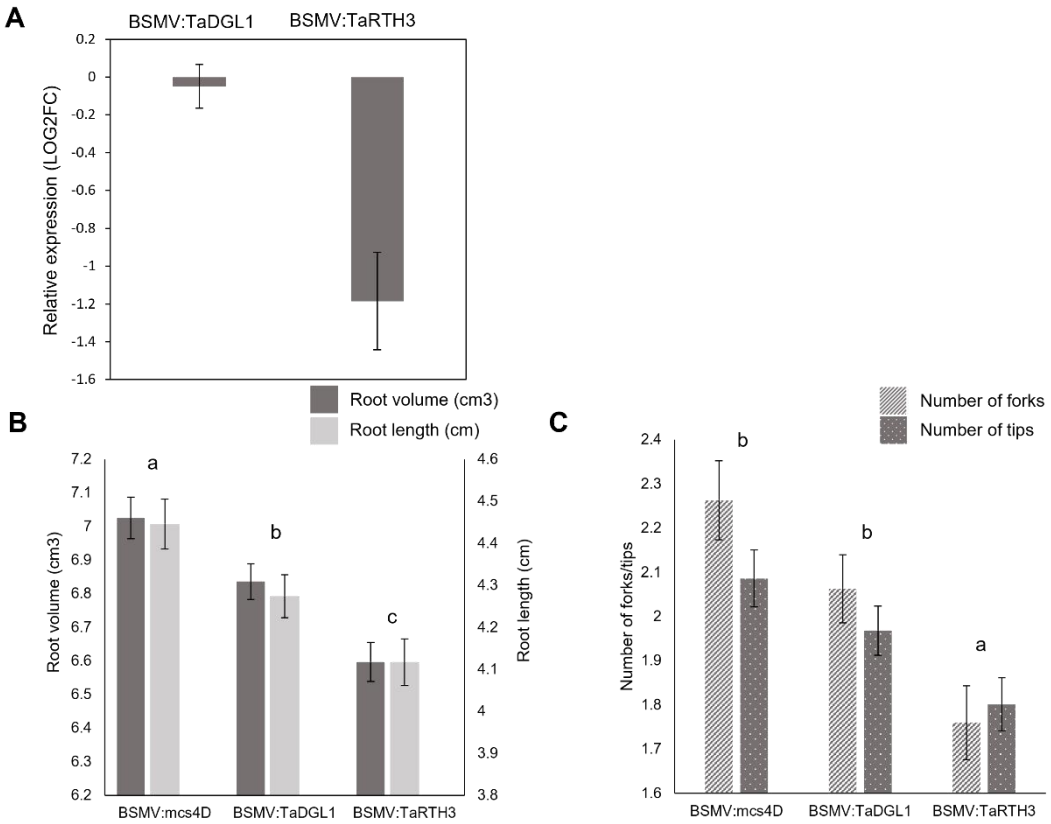


Figure 6.4 Gene expression and winRHIZO root architecture analyses. A. Relative expression of TaDGL1 and TaRTH3 (Log2FC). (TaDGL1: M= 0.99, SD= 0.25, t(8)=-0.09, p=0.93; TaRTH3: M= 0.54, SD= 0.35, t(14)=-5.05, p<.001). B, C. LOG transformed root architecture measurements. Different letters indicate significant differences based on least significant difference (LSD) values (p<0.05). Error bars represent standard error. See previous page.

6.4.2 Investigating the impact of BSMV infection on *G. tritici* virulence

BSMV-mediated VIGS provides a valuable tool for the functional validation of genes involved in wheat-pathogen interactions. An established method already exists for the investigation of genes involved in resistance to the important foliar pathogen *Zymoseptoria tritici*, responsible for Septoria tritici leaf blotch (STB) disease in wheat (Lee et al., 2015). We present a protocol for BSMV-VIGS in wheat roots, enabling studies into candidate plant genes that may play role(s) in interactions (compatible and incompatible) with root-infecting pathogens. Our protocol allows straightforward harvesting of new, “silenced” roots and prevents transcript “dilution” by avoiding old root material where target gene silencing efficiency is poor. NB: This assumption is based on previous findings in foliar studies, an experiment is currently underway to confirm this in roots.

In this study, we focus on *Gaeumannomyces tritici*, a necrotrophic fungal pathogen of wheat and the causal agent of devastating take-all disease. Though described as one of the most important root diseases of wheat worldwide (Freeman & Ward, 2004), very little is known about the molecular pathways underpinning the wheat-*G. tritici* interaction, and progress has been hindered by the lack of resistant commercial wheat cultivars and difficulties in generating stable *G. tritici* and wheat transformants (Palma-Guerrero et al., 2021). To determine if *G. tritici* is compatible with BSMV-VIGS, we studied take-all disease incidence and severity in BSMV:mcs4D-inoculated and mock-inoculated wheat plants.

Though average take-all disease levels differed significantly between the two experiments (likely due to altered conditions between the two growth rooms),

BSMV infection did not significantly affect take-all disease incidence (GLM: d.f. 1, 47, F=0.93, p=0.34) or disease severity (ordinal logistic regression: d.f. 1, 191, F= 1.38, p=0.24) (figure 6.5). These findings demonstrate that unlike the closely related fungal pathogen *Magnaporthe oryzae,* which is unable to mount an effective attack on BSMV-infected wheat (Tufan et al., 2011), *G. tritici* can effectively cause disease in a BSMV-VIGS system. However, we found that *G. tritici* hyphae can grow up the root and infect the root material in the upper pot (figure 6.6). To determine whether this could have an effect on gene silencing, a follow-up study will compare viral load, silencing efficiency, and take-all disease levels both above and below the nylon mesh.

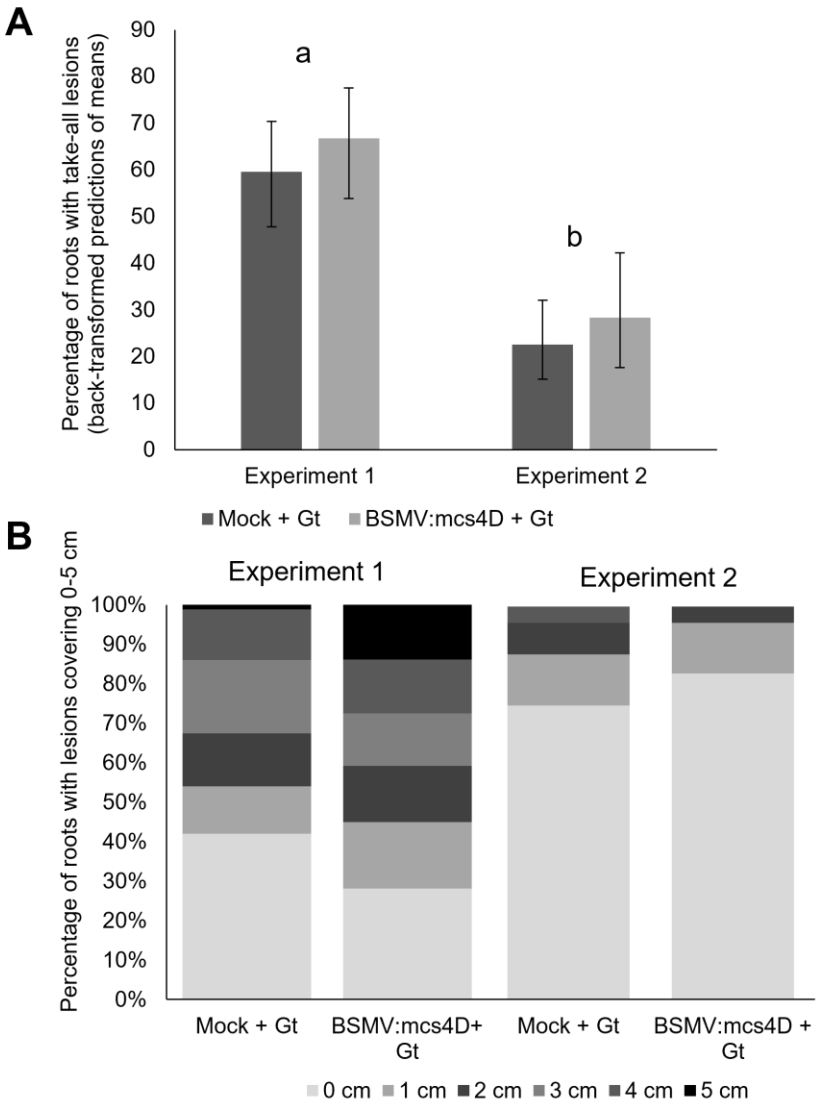


Figure 6.5 The effect of BSMV:mcs4D inoculation on take-all disease incidence and severity. A. The percentage of roots with take-all disease lesions (back-transformed predictions of means from a LOGIT scale) as calculated using a GLM. Error bars represent back-transformed 95% confidence intervals. Letters indicate significant differences ($p<0.05$). B. Take-all disease severity, indicated by the percentage of newly formed roots with take-all lesions covering 0-5 cm of each root. See previous page.

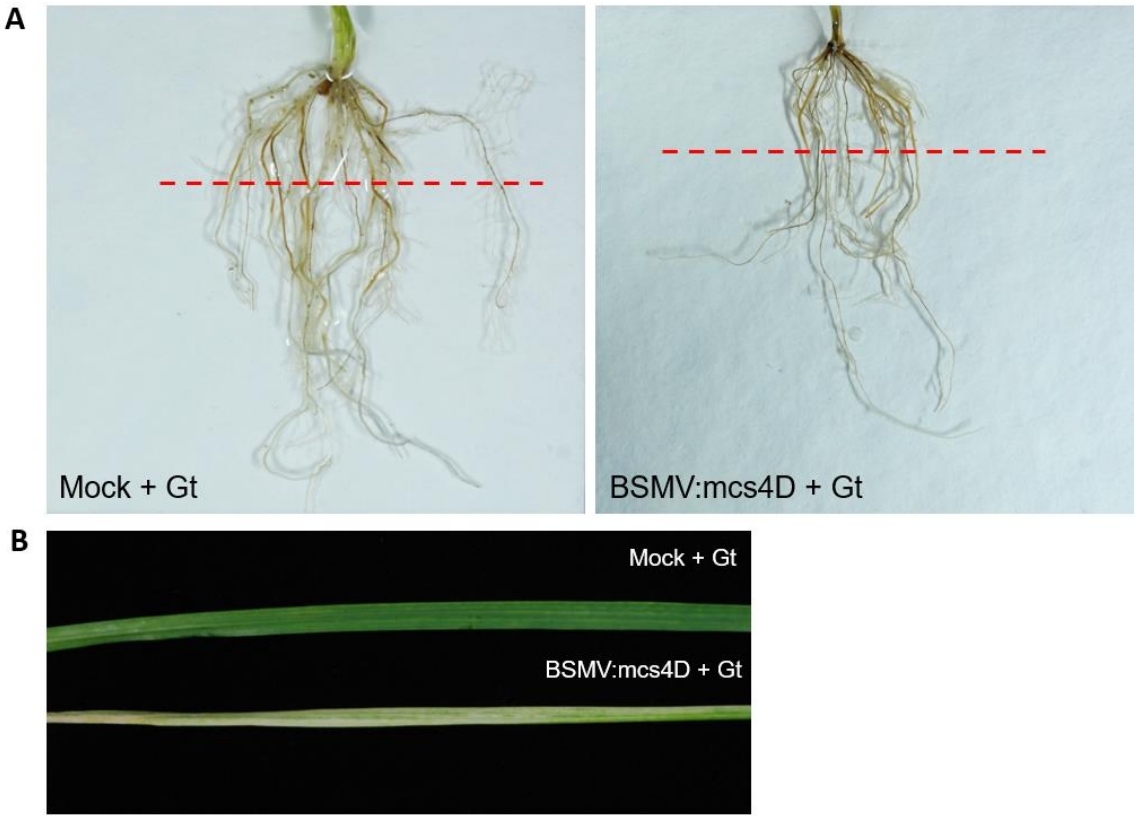


Figure 6.6 A. Root system images of *G. tritici* infected roots +/- BSMV:mcs4D. Nylon mesh was removed to allow clear visualisation of take-all disease lesions; red dashed line indicates the previous position of the nylon mesh. B. Images of leaf tissue highlighting BSMV symptoms. Gt= *G. tritici.*

6.5 Conclusions

BSMV VIGS provides a useful alternative to stable transformation methods and has already been employed in the study of various foliar pathogen interactions in wheat. However, few studies have demonstrated successful silencing in wheat roots and BSMV-VIGS has not yet been utilised for the study of root-infecting

pathogens in cereals. We have utilised existing binary VIGS vectors in a new system which allows the easy harvesting of new, silenced root material. We present the positive control for gene silencing experiments in wheat roots - the construct BSMV:TaRTH3 - which may be used by other researchers in any BSMV-VIGS experiment aiming to target gene expression in wheat roots. We confirm that *G. tritici* can successfully cause disease in this system, paving the way for future studies into the wheat-*G. tritici* interaction. Candidate resistance/susceptibility genes identified from RNA sequencing projects could be functionally validated using this new system, contributing to a better understanding of this understudied but important disease.

6.6 Acknowledgement of contributions

The plant experiments presented in this chapter were carried out with significant help from Dr Wanxin Chen, who also provided the primer sequences for the amplification of the BSMVα genome and carried out the RT-qPCR assay to assess viral load. Thank you to Dr Kostya Kanyuka for sharing his expertise and providing the binary BSMV VIGS vectors pCaBS- α, pCaBS- β, pCa- γbLIC and constructs BSMV:ChlH, BSMV:mcs4D. Thank you also to Dr Javier Palma-Guerrero for help setting up and harvesting the plant experiments. Finally, thank you to Dr Guillaume Menard for his valuable advice regarding the imaging system for wheat roots.

7 Investigating the effect of non-pathogenic *Magnaporthaceae* species on plant health and evaluating their field applicability.

7.1 Introduction

Fungal-plant interactions can range from mutualism through commensalism to parasitism in a continuous manner. Fungi may be considered parasitic or pathogenic on plants when the net cost of the symbiosis exceeds the net benefits. Thus, endophytic relationships can become pathogenic and vice versa. The mutualism-parasitism paradigm is important to consider when evaluating the

potential of the non-pathogenic *Magnaporthaceae* fungi as biocontrol agents. Indeed, the species have occasionally been described in the literature as being “weakly pathogenic”, though the discrimination between “non-pathogenic” and “weakly pathogenic” is unclear (Deacon, 1973, 1976b; Gutteridge et al., 2005).

Balis (1970) inoculated wheat with *G. radicicola* and demonstrated that colonisation did not significantly reduce grain yield or result in any visible tissue necrosis. Similarly, Wong et al., (1996) inoculated wheat plants with *G. hyphopodioides* and found that heavily colonised plants were not adversely affected and grain yield did not differ from uninoculated wheat. Similarly, Osborne et al., (2018) found no strong evidence to suggest that *G. hyphopodioides* colonisation has a detrimental effect on grain yield. Augustin et al. (1997) investigated the wheat growth when inoculated with non-pathogenic *Magnaporthaceae* species under different environmental conditions. Though the fungi were shown to improve plant growth under warm temperatures and moderate soil moisture, colonisation by certain *S. cylindrosporus* and *G. hyphopodioides* isolates resulted in reduced plant growth when conditions alternated between low and high temperatures on a weekly basis. Therefore, environmental conditions are likely to play a significant role in determining pathogenicity.

Studies into the effect of colonisation on key indicators of crop performance such as photosynthetic efficiency and root architecture are still lacking. Endophytic fungi are known to influence root development and architecture in a wide range of plants. Dark septate endophytes such as *Phialocephala fortinii* are known to increase the root biomass of colonised plants, particularly in nutrient poor environments (Sukumar et al., 2013). The colonisation of *Pinus sylvestrus* (Scots pine) by certain non-pathogenic *Rhizoctonia* species stimulates early root development and influences seedling root architecture (Grönberg et al., 2006). Root colonisation by the fungal endophyte *Piriformospora indica* triggers an auxin mediated increase in root growth and root branching; rewarding colonised plants with improved soil exploitation and plant growth promotion (Sirrenberg et al., 2007, Vadassery et al., 2008, Sukumar et al., 2013). Similarly, Martinuz et al.,

(2015) reported significantly increased root length and diameter in *Arabidopsis thaliana* plants inoculated with certain endophytic *Fusarium oxysporum* isolates.

The introduction (or promotion) of endophyte species has knock-on effects on the wider soil microbiome and hence soil health. Consequently, one of the greatest hurdles preventing the widespread use of soil-borne biocontrol agents is the highly heterogeneous nature of the soil environment, making the establishment of sufficient populations for consistent and effective control challenging. However, a study by Osborne et al., (2018) could provide a novel approach for the promotion of *G. hyphopodioides* in the field environment. A two-year field study and soil baiting experiment revealed that certain elite winter wheat cultivars can promote *G. hyphopodioides* colonisation better than others. Field sites containing natural levels of *G. hyphopodioides* were sown with 40 elite UK winter wheat cultivars in a first wheat rotation. Post-harvest soil cores were taken from plots in which the different cultivars had grown and soil cores were sown with seeds of the highTAB control cultivar Hereward (McMillan et al., 2011). Root colonisation was assessed visually after 5 weeks of growth in a controlled environment room. This method, known as baiting, provides a means to estimate the approximate viable inoculum level in the soil when molecular quantification methods such as qPCR are not possible (in this case due to the lack of species-specific primers). Because baited soil cores represent a second crop rotation, the method can also be used to assess seedling susceptibility to colonisation by *G. hyphopodioides.* Thus, soil cores were also baited with the original field plot cultivar from which the core was taken, and the resulting *G. hyphopodioides* colonisation levels were compared to the Hereward baited controls.

The study demonstrated that certain cultivars promote increased levels of *G. hyphopodioides* inoculum (determined when Hereward was used as the baiting cultivar). However, the finding was not fully consistent across the two trial years, indicating that the soil microbiome and/or wider environment plays an important role. Additionally, there was strong evidence to suggest that certain cultivars differ in their susceptibility to colonisation, demonstrated by high colonisation levels when baited with the field plot cultivar. Of these cultivars, a small number

consistently promoted high levels of colonisation regardless of the baiting method, suggesting that these genotypes can both promote *G. hyphopodioides* inoculum in the soil and are highly susceptible to colonisation. Thus, the study revealed a novel method of introducing and promoting *G. hyphopodioides* populations under field conditions, which could provide a valuable alternative to artificial inoculation or seed dressing.

Nevertheless, thorough investigation of the plant health effects of non-pathogenic *Magnaporthaceae* fungi are still vital if the species are to be considered as biocontrol agents. In addition, further investigation is required to assess the effect of current farming practices, such as the routine use of seed applied fungicides such as Latitude®, on the viability of fungal inoculum. Furthermore, the effects of introducing non-pathogenic *Magnaporthaceae* species on the wider soil microbiome requires investigation. Finally, further studies are required to validate the findings by Osborne et al., (2018) and to the unpick the genotype x environment component associated with cultivar promotion of *G. hyphopodioides* wheat root colonisation in the field environment.

7.2 Aims and hypotheses

Aim 1: To investigate the effect of root colonisation by non-pathogenic *Magnaporthaceae* species on seedling biomass and root architecture.

Hypothesis: Non-pathogenic Magnaporthaceae species have no effect on seedling biomass or root architecture.

Aim 2: To investigate the effect of *G. hyphopodioides* colonisation on key parameters of adult wheat health.

Hypothesis: G. hyphopodioides colonisation does not affect adult wheat health.

Aim 3: To determine the sensitivity of non-pathogenic *Magnaporthaceae* species to the fungicide Latitude®.

Hypothesis: Non-pathogenic Magnaporthaceae species are not sensitive to the fungicide Latitude®.

Aim 4: To investigate whether the *G. hyphopodioides* susceptibility trait is maintained under a different soil environment.

Hypothesis: Elite winter wheat cultivars differ in their susceptibility to G. hyphopodioides, regardless of the soil type.

7.3 Methods

7.3.1 Seedling health experiments

7.3.1.1 Seedling bioassays

Seedling pot test bioassays were set up using wheat cv. Hereward, as described in chapter 2.4. Fungal inoculum was prepared as described in section 2.2. Pots were inoculated with *G. hyphopodioides, S. cylindrosporus*, or an unnamed *Magnaporthaceae* species. *G. tritici* was also included for comparison purposes. Control treatments were mock- inoculated with potato dextrose agar (PDA) only (see table 7.1 for full treatment details). The experiment was carried out three times and data were combined prior to statistical analyses.

Table 7.1 Treatment details for the seedling biomass experiments 1, 2 and 3*.

Treatment	Fungal sp.	Isolate	Replicates
Hereward -	N/A	N/A	A, B, C, D, E, F*
Hereward + Gh	*G. hyphopodioides*	NZ.129.2C.17	A, B, C, D, E, F*
Hereward + Sc	*S. cylindrosporus*	H23A-SB-2b	A, B, C, D, E, F*
Hereward + Um	Unnamed *Magnaporthaceae sp.*	105C-2	A, B, C, D, E, F*
Hereward + Gt	*G. tritici*	16.NZ.1d	A, B, C, D, E, F*

An additional experiment was carried out to determine whether the pot size was masking any treatment effects on root biomass by restricting root growth. Pots were set up in the same manner as described in chapter 2.4, however at three weeks post-inoculation, the contents of each pot was carefully transferred and re-potted into larger pots (15 x 15 cm) containing sand, where they remained for a further two weeks. Root assessments and seedling biomass measurements were carried out at 5 weeks post-inoculation. There was no significant difference in

shoot or root biomass, thus indicating that pot size was not masking treatment effects on seedling biomass (data not shown here).

7.3.1.2 Seedling root assessments

Roots were assessed as outlined in chapter 2.5.

7.3.1.3 Seedling biomass measurements

Seedling dry biomass was measured as described in chapter 2.6.

7.3.1.4 Analysis of root architecture traits by WinRHIZO

Root architecture was analysed in experiment 3 only. Following root assessments, three plant samples from each pot of replicates D, E and F were individually imaged in a Perspex tray filled with water using a flatbed STD1600 scanner (Epsom, USA). Images were analysed using WinRHIZO Pro Arabidopsis software (Regent Instruments Inc, Canada) to determine root length, root volume and the number of root tips and forks.

7.3.2 Adult plant health experiment

The present experiment was carried out with the help of undergraduate summer student Jade Smith (University of Bristol). The experiment was initially planned for spring 2020. Spring wheat cv. Paragon and winter wheat cv. Hereward (artificially vernalised) were to be placed in large pots in a wheat field in May 2020 for harvest in August 2020. Experimental treatments were designed to enable bulk soil sampling for comparative analysis of the soil microbiome. However, due to COVID-19 lockdown restrictions, it was not possible to access the lab and inoculate the plants. Hence, a revised experiment was set up in autumn 2020. Due to exceptionally wet conditions, pots could not be placed in the field and were instead placed in a caged sand bed area outdoors. Unfortunately, the delays meant that analysis of the soil microbiome was not possible, though bulk soil samples were collected and stored at -80°C for future analysis.

7.3.2.1 Pilot study to determine cultivar choice

A seedling bioassay was carried out to investigate the colonisation ability of *G. hyphopodioides* on four group 1 winter milling wheats, chosen from current or

previous AHDB recommended lists (https://ahdb.org.uk/rl). Skyfall, a cultivar widely used by farmers was chosen for the main experiment (see appendix A.10 for full details).

7.3.2.2 Pot test set-up

Small pots were set up in the same manner as described in chapter 2.4 using naïve soil collected from Meadows field at Rothamsted Farm after a break crop of winter oilseed rape (see appendix A.9 for further cropping history). However, a smaller amount of inoculum was added to better represent a field scenario. A single plug was taken using a no.6 cork borer (9 mm diameter) and was macerated with soil to make a 25 g layer. Treatments A and C contained PDA only (see table 7.2 for treatment details). Two wheat seeds (cv. Skyfall) were sown per pot (treatments C and D only). After 1 week of growth, the smaller seedling was removed, leaving one seedling per pot. At 2 weeks of growth, the small pots were transferred by removing the plastic cup and placing the entire contents into a larger pot (20 cm diameter) containing a 2 cm layer of clay drainage pebbles. Three small pots were transferred to each large pot and filled in with more soil, resulting in 3 plants per pot. Inoculating the seedlings in small pots before transferring to a larger pot ensured that all three seedlings were well colonised. Eight replicates were prepared for each treatment.

A randomised block design was created in Genstat 20th Edition by Suzanne Clark (Applied Statistician, Computational and Analytical Sciences, Rothamsted Research, UK). Pots were scheduled to be placed in Great Field 4 at Rothamsted Farm (experiment code 2021_R_WW_2133) in September 2020. However, due to extremely wet conditions the farm team were unable to plough or drill the field with wheat. Instead, pots were kept in a polytunnel for 4 weeks before transferring to an outdoor caged sand bed area (see figure 7.1). Pots were weeded by hand on a weekly basis. Pots were watered twice daily using an overhead sprinkler system.

Table 7.2 Treatment details for the adult plant health experiment.

	Treatment	Fungal isolate
A	Soil only	N/A
B	Soil + *G. hyphopodioides*	NZ.129.2C.17
C	Soil + Skyfall	N/A
D	Soil + Skyfall + *G. hyphopodioides*	NZ.129.2C.17



Figure 7.1 The adult plant health experiment in a caged sand bed area. Image taken at the seedling stage in November 2020.

7.3.2.3 Chemical inputs

The following chemicals treatments were applied to each pot.

Table 7.3 Chemical inputs applied during the adult plant heath experiment

Chemical input	Date applied
Osmocote® Pro slow release fertiliser (Scotts Miracle-Gro Company, USA)	18th March 2021
Moddus Plant Growth Regulator (Syngenta, Switzerland)	26th April 2021
Application 1: Cortez® ADAMA Fungicide (Adama Agricultural Solutions, UK)	27th April 2021
Application 2: Cortez® ADAMA Fungicide (Adama Agricultural Solutions, UK)	28th May 2021

Aphox® ADAMA Aphicide (Adama Agricultural Solutions, UK)	2nd June 2021
Application 3: Cortez® ADAMA Fungicide (Adama Agricultural Solutions, UK)	15th June 2021

7.3.2.4 Measuring chlorophyll content

Chlorophyll content was measured using the Chlorophyll Content Meter-200 plus (CCM-200plus; OptiSciences, UK). Measurements were taken from the flag leaf of the leading tiller of each plant in a pot, which was marked with a waterproof label to enable easy identification. Three independent readings were taken from the centre of each flag leaf and the average was calculated. Measurements were repeated once a week, enabling comparisons across key wheat growth stages.

7.3.2.5 Measuring wheat growth progression

Wheat plants were inspected twice weekly and the date at which the leading tiller from each plant reached key principal growth stages was recorded (see table 7.4 for a description of each growth stage). The data was used to track growth progression and to calculate the number of days from booting (GS45) to anthesis (GS61).

Table 7.4 Key adult wheat growth stages as described by the Agriculture and Horticulture Development Board (AHDB) (https://ahdb.org.uk/knowledge-library/the-growth-stages-of-cereals)

Growth stage	Description
GS43	Flag leaf sheath beginning to swell (mid-boot)
GS45	Flag leaf sheath swollen (late-boot)
GS47	Flag leaf sheath opening
GS51	First spikelet of ear visible above flag leaf ligule
GS55	Half of ear emerged above ligule
GS59	Ear completely emerged above ligule
GS61	Start of flowering (first anthers emerged)

7.3.2.6 Measuring ear length and flag leaf length

Ear length and flag leaf length were measured using a 30 cm ruler at GS61, at which point plant growth had ceased.

7.3.2.7 Number of tillers

The number of tillers per plant was counted post-anthesis.

7.3.2.8 Measurements of grain parameters

Due to severe rodent damage during grain filling and ripening, grain parameters could not be measured. The following measurements had been planned:

The average grain yield per pot was to be measured. The areas, lengths and widths of mature wheat seeds were to be measured using the MARVIN- Digital Seed Analyser (MARViTECH GmbH, Germany) with associated Marvin 4.0 software. Grain hardness, individual seed weight and diameter were to be determined using the Perten Single Kernel Characterisation System (SKCS) 4100 (Perten Instruments, Calibre Control International Ltd, UK).

7.3.2.9 Root biomass measurements

Roots were washed thoroughly to remove soil and other debris. Dry biomass measurements were carried out using the method previously described in chapter 2.6.

7.3.2.10 Bulk soil sampling for future microbiome analyses

At GS45 (late-boot stage), bulk soil samples were taken at random from three different locations in each pot using a small soil corer (W X L 2 cm X 10 cm). The first 2 cm of soil was removed before taking each core to avoid sampling any moss/small weeds growing at the surface. Soil samples were placed in 50 ml falcon tubes and immediately snap frozen in liquid nitrogen before storing at -80 °C. However, due to delays caused by COVID-19, analysis of the samples was not possible.

7.3.2.11 Confirming *G. hyphopodioides* colonisation

Due to the lack of species-specific primers for *G. hyphopodioides,* fungal colonisation was confirmed by visual root assessment and ITS sequencing, as in Osborne et al. (2018). *G. hyphopodioides* colonisation was confirmed by the presence of characteristic sub-epidermal vesicles (SEVs). The percentage of roots with runner hyphae was not assessed, due to the large and matted adult root system. Three 2-5 cm root pieces from each plant (9 root pieces per pot) thought to contain SEVs were taken at random for further confirmation using a stereomicroscope (see chapter 2.7). Fungal isolations were performed on root pieces confirmed to contain SEVs and species identification was determined by ITS sequencing as outlined in chapter 2.3, 2.8, and 2.10-2.13. One replicate was harvested in May for the early confirmation of *G. hyphopodioides* colonisation. The remaining replicates were processed post-harvest in July.

7.3.3 Latitude® sensitivity experiments

7.3.3.1 *In vitro* sensitivity test

Three agar plugs were taken with a no.3 cork borer from the leading edge of a fungal colony (growth conditions as described in chapter 2.2) and placed at equal distances on a PDA plate supplemented with 1 µg/ml Latitude® (Certis, UK), as previously described by Freeman et al. (2005). Control treatments contained PDA only (see table 7.5 for full treatment details). Fungal colonies were left to grow in the dark at 21 °C for 5 days, except for *S. cylindrosporus* which was left for 14 days due to the slow growth rate of this species. The colony diameter of each colony on a plate was measured using a ruler and the average diameter per plate was calculated. Three plates were set up for each treatment and the experiment was carried out twice. Data from the two experiments were combined prior to statistical analysis.

Table 7.5 Treatment details for the *in vitro* Latitude® sensitivity tests. Lat= Latitude®.

Treatment	Fungal sp.	Isolate
PDA+ Gh	*G. hyphopodioides*	NZ.129.2C.17
PDA + Sc	*S. cylindrosporus*	H23A-SB-2b
PDA + Um	Unnamed *Magnaporthaceae Sp.*	105C-2
PDA+ Gt	*G. tritici*	16.NZ.1d
PDA + Lat + Gh	*G. hyphopodioides*	NZ.129.2C.17
PDA + Lat + Sc	*S. cylindrosporus*	H23A-SB-2b
PDA + Lat + Um	Unnamed *Magnaporthaceae Sp.*	105C-2
PDA + Lat + Gt	*G. tritici*	16.NZ.1d

7.3.3.2 *In planta* sensitivity test

An *in planta* sensitivity test was required to validate the results of the *in vitro* sensitivity test. Seedling bioassays were set up in the same manner as for the seedling biomass experiments described above. For fungicide treatments (see table 7.6), wheat seeds (cv. Hereward) were treated with Latitude® (Certis, UK) at an application rate of 200 ml per 100 kg seed, as per manufacturer instructions. Seeds were coated by applying the treatment and shaking together in a 50 ml falcon tube until even coverage was achieved. Six replicates were set up for each treatment and pots were placed in the growth room using a randomised block design generated in Genstat 20th Edition. Fungal colonisation and colonisation severity were assessed after 5 weeks growth based on the presence of runner hyphae as described in chapter 2.5.

Table 7.6 Treatment details for *in planta* Latitude® sensitivity tests. Lat= Latitude®.

Treatment	Fungal sp.	Isolate
Hereward -	N/A	N/A
Hereward + Gh	*G. hyphopodioides*	NZ.129.2C.17
Hereward + Sc	*S. cylindrosporus*	H23A-SB-2b
Hereward + Um	Unnamed *Magnaporthaceae Sp.*	105C-2
Hereward + Gt	*G. tritici*	16.NZ.1d

Hereward + Lat	N/A	N/A
Hereward + Lat + Gh	*G. hyphopodioides*	NZ.129.2C.17
Hereward + Lat + Sc	*S. cylindrosporus*	H23A-SB-2b
Hereward + Lat + Um	Unnamed *Magnaporthaceae Sp.*	105C-2
Hereward + Lat + Gt	*G. tritici*	16.NZ.1d

7.3.4 Seedling bioassay to assess the susceptibility of elite winter wheat varieties to colonisation by *G. hyphopodioides*

Seedling pot test bioassays were prepared as described in section 2.4, with the exception that naïve field soil collected from Rothamsted Farm field site Webb's (after a break crop of winter oats) was used rather than sand (see appendix A.9 for further cropping history). Field soil was used rather than sand to determine whether the cultivar susceptibility trait held up under different soil environments. The cultivar susceptibility trait was discovered by Osborne et al., (2018) using soil cores sampled from two sites on New Zealand field at the Rothamsted Farm. The preceding crop was oilseed rape (2014 trial) or oilseed rape followed by oats (2015 trial).

Pots were sown with ten seeds of different elite winter wheat cultivars which were chosen based on their ability to support *G. hyphopodioides* in the original study by Osborne et al., (2018). Two additional cultivars (Player and Hereford) and a cultivar with a low take-all build-up (lowTAB) trait (Avalon) were included. The existence of mapping populations, generated within the Wheat Genomic Improvement Network (WGIN), which could be used to investigate the genetic basis of *G. hyphopodioides* promotion, was also considered.

The experiment was subsequently repeated with a selection of cultivars from the first experiment. The cultivars which most consistently supported low/high *G. hyphopodioides* levels (Alchemy and Conqueror, KWS Kielder and Scout, respectively), the low/highTAB cultivars Cadenza and Avalon, and the highTAB control cultivar Hereward were chosen. The repeat experiment was carried out using a lower inoculum level (single plug taken using a no.4 cork borer) with the

aim of better replicating the colonisation levels in the study by Osborne et al., (2018) (table 7.7). In both experiments, a negative control treatment (mock-inoculated wheat cv. Hereward) was set-up to confirm that the field soil did not contain natural populations of *Magnaporthaceae* species which could have skewed root assessments. Five replicates were established per cultivar and seedlings were harvested after 5 weeks of growth. The percentage of roots with runner hyphae was determined as described in chapter 2.5

Table 7.7 UK winter wheat cultivars chosen for inclusion in a *G. hyphopodioides* susceptibility experiment. Asterisks indicate cultivars also tested in a repeat experiment with lower inoculum levels.

Wheat cultivar	Low/Medium/High *G. hyphopodioides* builder (Osborne et al., 2018)	Mapping populations generated within the Wheat Genetic Improvement Network (WGIN)
Gallant	High	Gallant x Invicta (F2)
Einstein	High	Einstein x KWS Santiago (F2)
Cordiale	High	Cordialle x Alchemy, Cordialle x Revelation (F4), Cordiale x Crusoe (F3)
KWS Kielder*	High	N/A (KWS Kielder x Gallant, but these are both High) (F2)
Scout*	High	Conqueror x Scout (F2)
Hereward*	High	N/A
Denman	Low	Scout x Denman (F2)
KWS Croft	Low	KWS Croft x Scout (F2)
Invicta	Low	Gallant x Invicta (F2)
KWS Santiago	Low	Einstein x KWS Santiago (F2)
Alchemy*	Low	Cordialle x Alchemy (F2)
Conqueror*	Low	Conqueror x Scout (F2)
Cadenza*	Medium	Avalon x Cadenza (F6)
Avalon*	Unknown	Avalon x Cadenza (F6)
Hereford	Unknown	N/A
Player	Unknown	N/A

7.4 Results

7.4.1 The effect of non-pathogenic *Magnaporthaceae* species on seedling health

Early plant development is a key determinant of future plant productivity. To investigate the effect of colonisation by non-pathogenic *Magnaporthaceae* species, seedling pot bioassays were conducted under controlled growth conditions. Wheat seedlings (cv. Hereward) were inoculated with non-pathogenic *G. hyphopodioides*, *S. cylindrosporus* or an unnamed *Magnaporthaceae* species. Seedling health was assessed by measuring the dry biomass of plants after 5-weeks growth, as compared to an uninoculated negative control (Hereward-) and a *G. tritici* inoculated positive control (Hereward + Gt). The experiment was carried out three times and additional root architecture measurements were taken in the final experimental repetition.

Visual root assessments revealed significant differences in the level of root colonisation (represented by the percentage of roots with runner hyphae) by the different *Magnaporthaceae* species (ANOVA: $F=45.27$, d.f. 3, 53, $p<0.001$; appendix A.10, table A.10.1). *G. tritici* colonisation levels were significantly greater than the colonisation levels of the non-pathogenic *Magnaporthaceae* species. *S. cylindrosporus* and the unnamed *Magnaporthaceae* species had similar levels of colonisation, while *G. hyphopodioides* had the lowest levels of colonisation (figure 7.2).

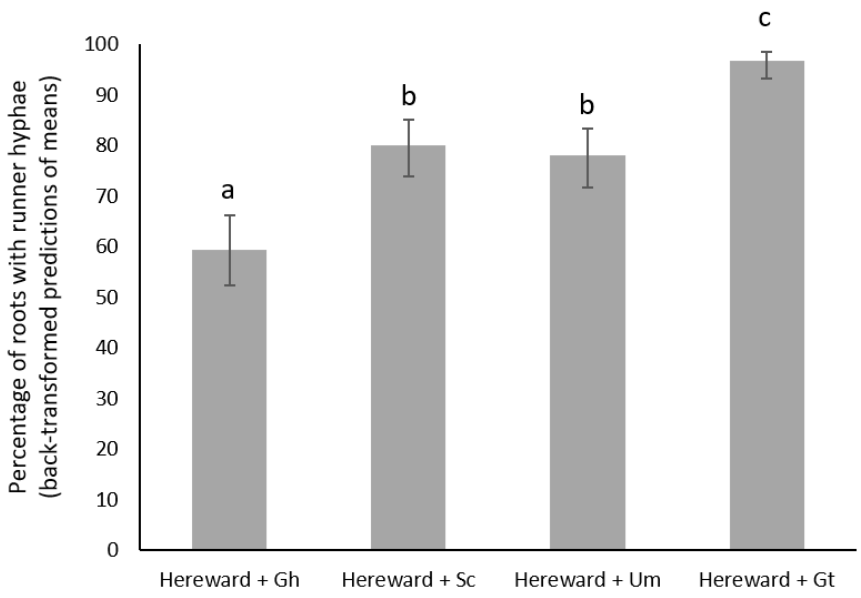


Figure 7.2 The percentage of roots with fungal runner hyphae. Data represent back-transformed predictions of means calculated using a GLM. Error bars represent 95% confidence intervals. Gt = *G. tritici*, Gh = *G. hyphopodioides*, Sc = *S. cylindrosporus,* Um = Unnamed *Magnaporthaceae* sp. Different letters indicate significant differences as calculated by Tukey's multiple-comparisons test ($p<0.05$).

As hypothesised, colonisation by the non-pathogenic *Magnaporthaceae* species did not significantly alter seedling dry biomass, neither for shoot nor root measurements across three experimental replicates. In contrast, seedling biomass was significantly reduced in *G. tritici* infected plants, with average shoot and root biomass reduced by 50% and 71% respectively, as compared to the uninoculated control (figure 7.3, appendix A.10; table A.10.2).

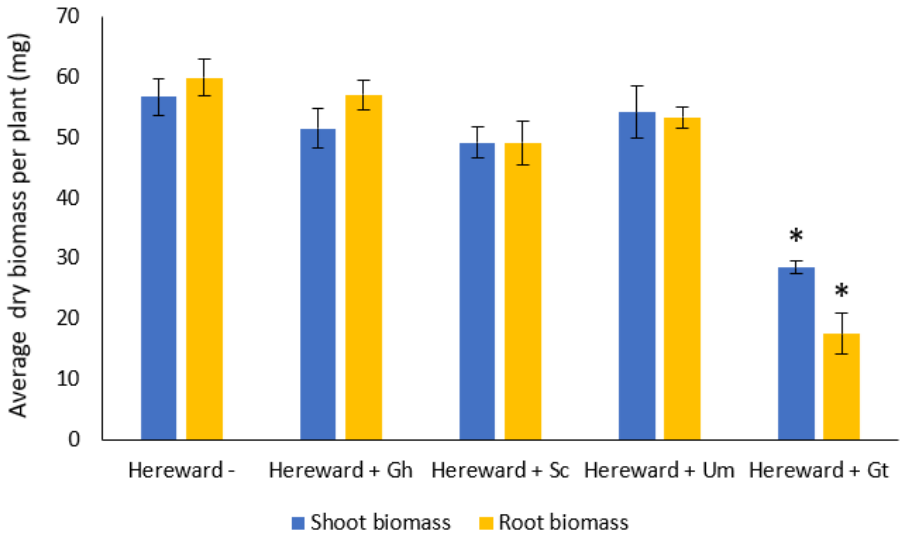


Figure 7.3 The average shoot and root biomass per plant (mg) in the seedling health experiments. Error bars indicate standard error. Gt = *G. tritici*, Gh = *G. hyphopodioides*, Sc = *S. cylindrosporus,* Um = Unnamed *Magnaporthaceae* sp. Asterisks indicate significant differences to the uninoculated control (Hereward-) as calculated by Dunnett's post-hoc test.

To investigate the effect of *Magnaporthaceae* species on root architecture, individual plants were imaged using a flatbed scanner (figure 7.4) and images were analysed using WinRHIZO software. As expected, *G. tritici* infection had a striking effect on all root architecture traits investigated (figure 7.5 A, B). Interestingly, the analysis revealed a small but significant increase in the total root length, but not root volume, of *G. hyphopodioides* colonised seedlings (figure 7.5 A, appendix A.10; table A.10.3). Furthermore, significantly more root tips were detected in *G. hyphopodioides* colonised plants compared to uninoculated control plants, suggesting an increase in the number of seminal and/or lateral roots. Conversely, the number of root forks, another indicator of root branching, was not significantly affected by *G. hyphopodioides* colonisation, though there was an upwards trend (figure 7.5 B; appendix A.10; table A.10.4). Taken together, the findings demonstrate that *G. hyphopodioides* colonisation results in small, though potentially important alterations in key root architecture traits. The subtle nature of these changes may explain why the differences were not picked up in root

biomass measurements; hence experimental repetition is required to better characterise this phenotype.

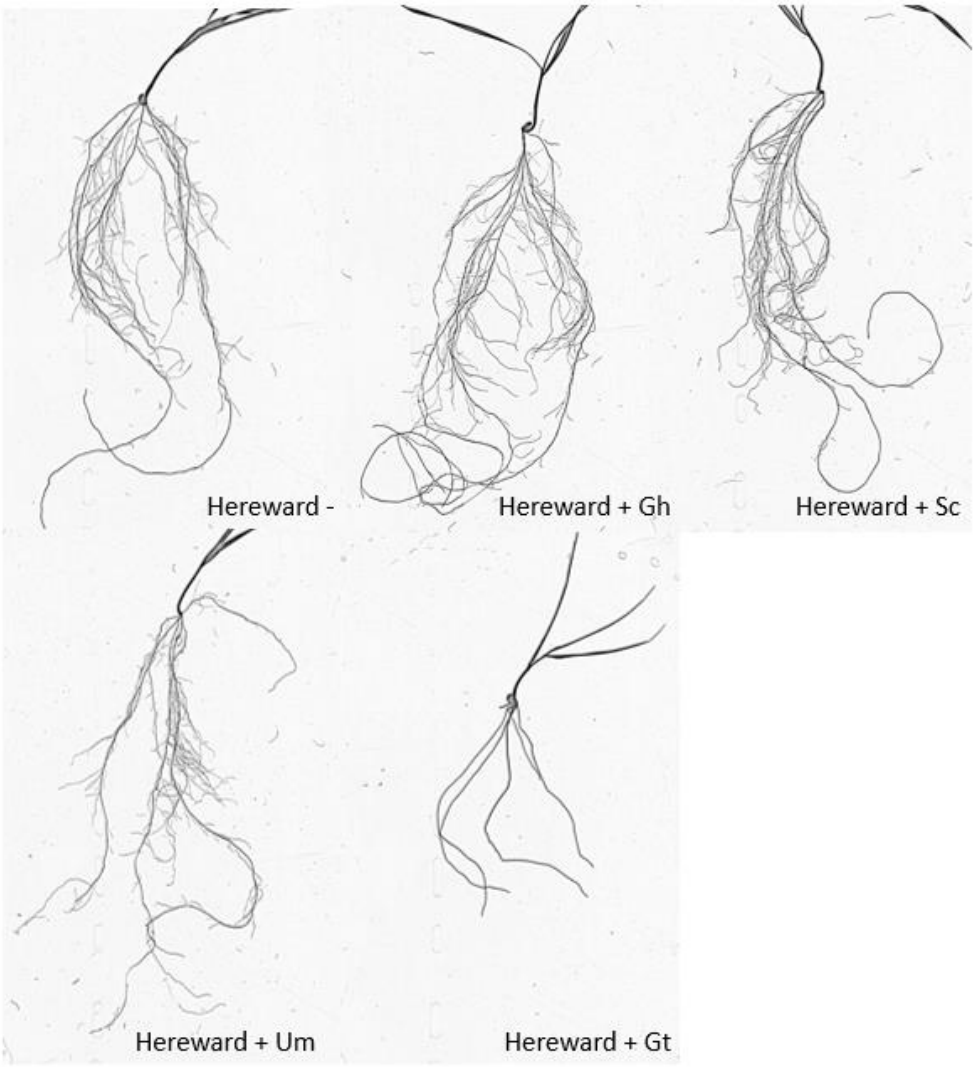


Figure 7.4 Representative images of wheat seedlings cv. Hereward colonised by different *Magnaporthaceae* species. Gt = *G. tritici*, Gh = *G. hyphopodioides*, Sc = *S. cylindrosporus,* Um = Unnamed *Magnaporthaceae* sp. Images taken using a flatbed scanner.

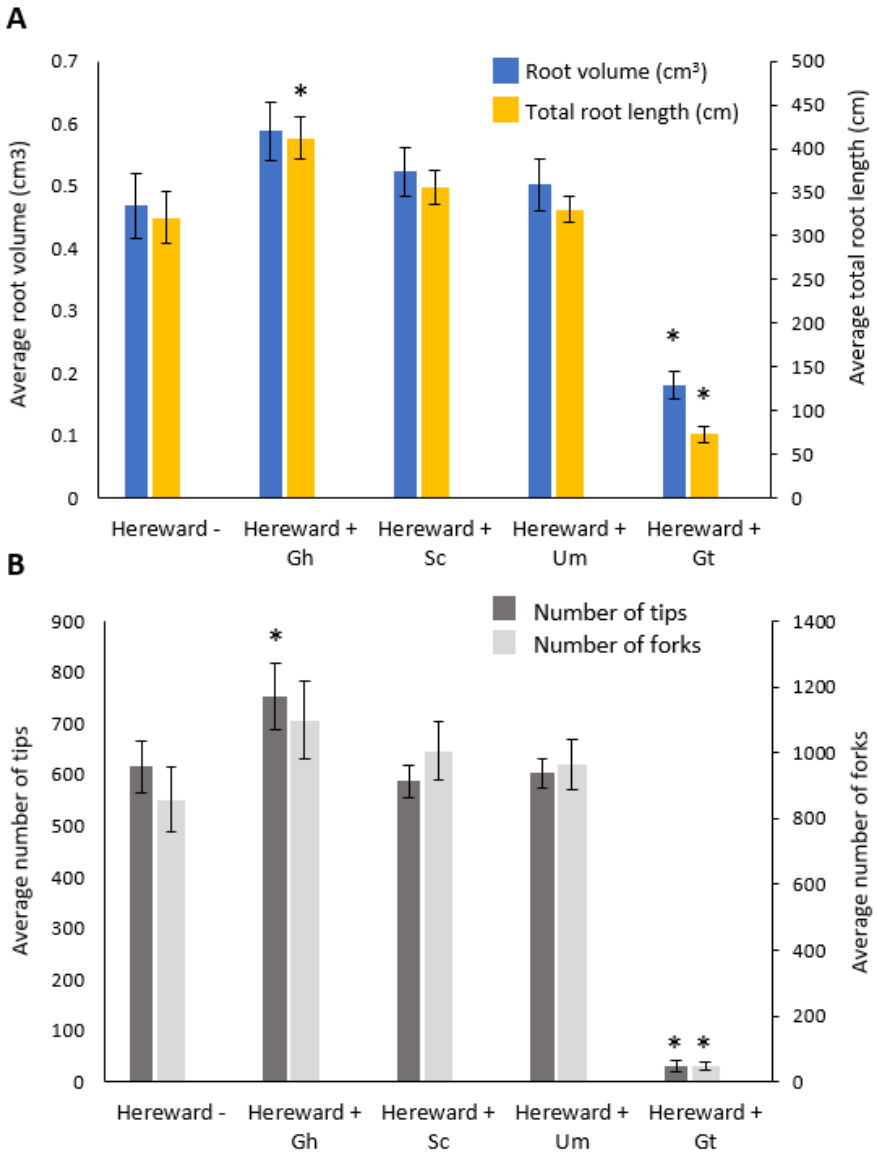


Figure 7.5 The average root volume (cm^3), total root length (cm) (A) and number of tips and forks (B) as determined by WinRHIZO software. Error bars represent standard error. Asterisks indicate significant differences from the uninoculated control (Hereward -) as calculated by Dunnett's post-hoc test ($p<.05$).

7.4.2 The effect of *G. hyphopodioides* on adult health

G. hyphopodioides has been identified as a promising candidate for the biocontrol of take-all disease (see chapter 3) and as outlined above, the species causes subtle alterations in root architecture traits at the seedling stage. To further investigate the effects of *G. hyphopodioides* on plant health and therefore

evaluate its biocontrol applicability, a large-pot experiment was carried out which enabled detailed investigation into the effects of *G. hyphopodioides* colonisation on key traits of agronomic importance during adult growth stages. Seeds of the commercial winter wheat cv. Skyfall were grown in small pots containing *G. hyphopodioides* inoculum, before being transferred into larger pots outdoors. Due to delays caused by the COVID-19 pandemic, the experiment could only be carried out once (Sept 2020-July 2021).

7.4.2.1 Foliar measurements

There was no significant difference between the average plant height, ear length or number of tillers in *G. hyphopodioides* inoculated and uninoculated plants (figure 7.6-7.7). Furthermore, the speed of plant development, represented by the number of days from booting (GS45) to anthesis (GS61) was unaffected by *G. hyphopodioides* colonisation (figure 7.7, appendix A.11; table A.11.2).

The average Chlorophyll Content Index (CCI) of each flag leaf was measured across three key adult growth stages. Statistical analysis by ANOVA revealed a significant effect of growth stage ($F=4.89$, d.f. 2, 67, $p=0.01$), but not of *G. hyphopodioides* inoculation ($F=2.07$, d.f. 1, 67, $p=0.2$) (appendix A.11; table A.11.3). Hence, *G. hyphopodioides* did not significantly alter the chlorophyll content of the flag leaf at any growth stage. Furthermore, there was no significant difference ($t(40)=0.56$, $p=0.58$) between the average flag leaf length in *G. hyphopodioides* inoculated ($M=13.72$, $SD=2.46$) and uninoculated plants ($M=14.09$, $SD=1.77$).

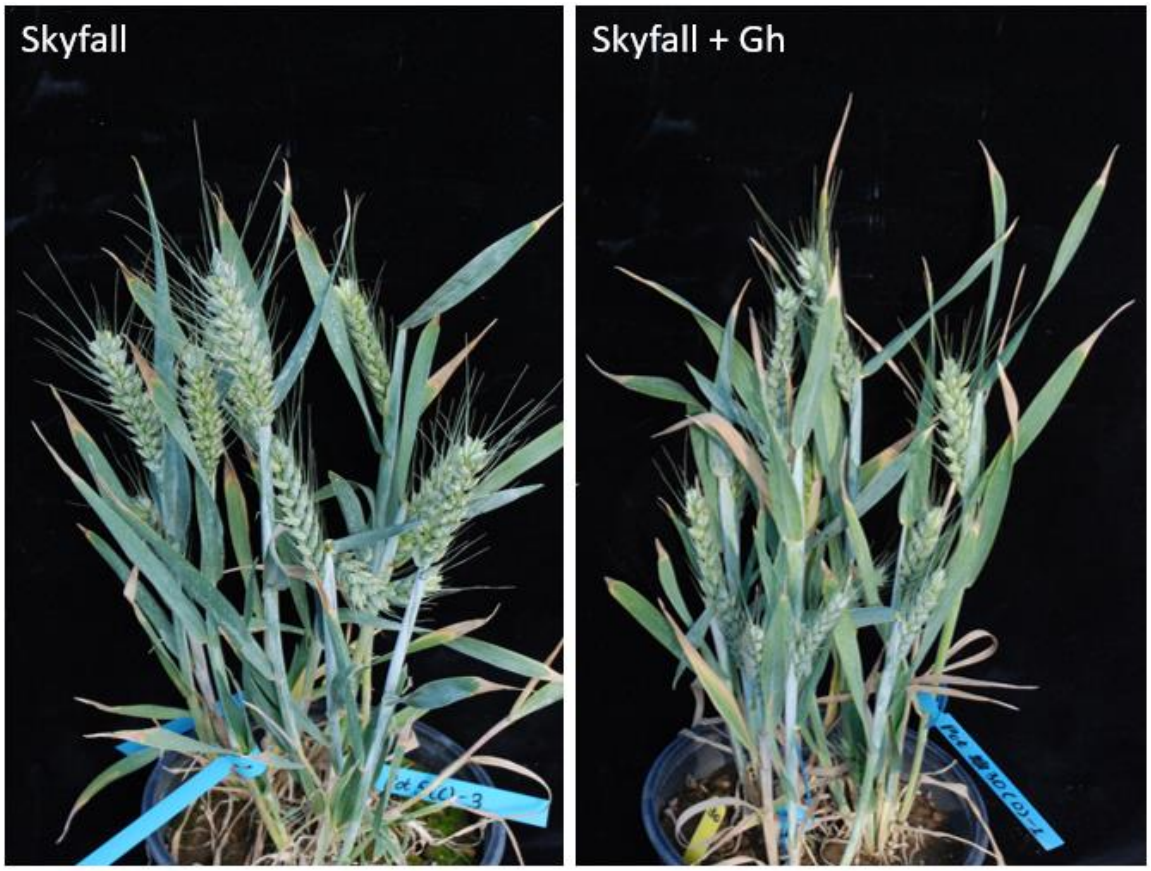


Figure 7.6 Representative images of *G. hyphopodioides*-inoculated and uninoculated wheat plants. Images taken post-anthesis using a Nikon D80 digital camera.

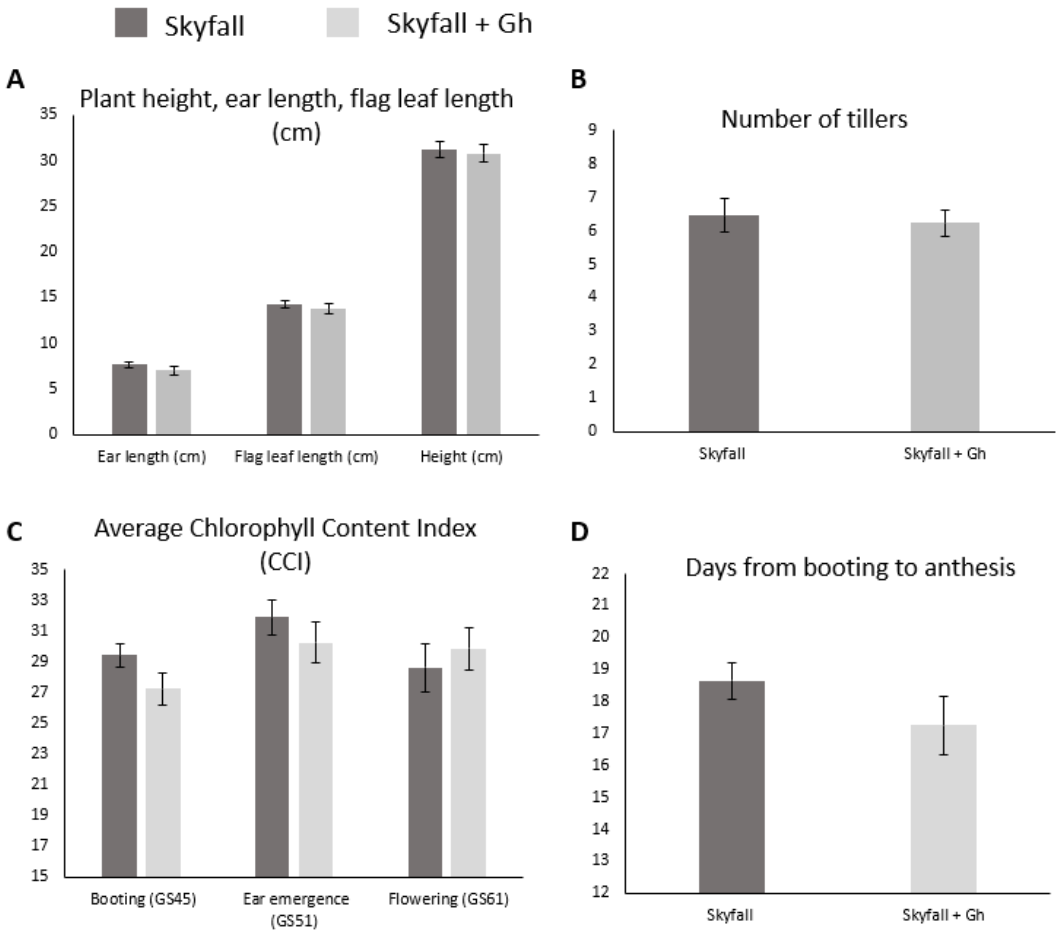


Figure 7.7 Foliar measurements of *G. hyphopodioides* inoculated and uninoculated adult wheat plants. Error bars represent standard error. For full summary statistics see appendix A.11.

7.4.2.2 Root biomass

There was no significant difference (t(12)=-0.15, p=0.86) in the average dry biomass of roots inoculated with *G. hyphopodioides* (M=5.05, SD=0.70) compared to the uninoculated control (M=4.99, SD=0.70) (figure 7.8). Due to the nature of the extensive adult root system (see figure 7.9), root architecture traits could not be accurately analysed using WinRHIZO software.

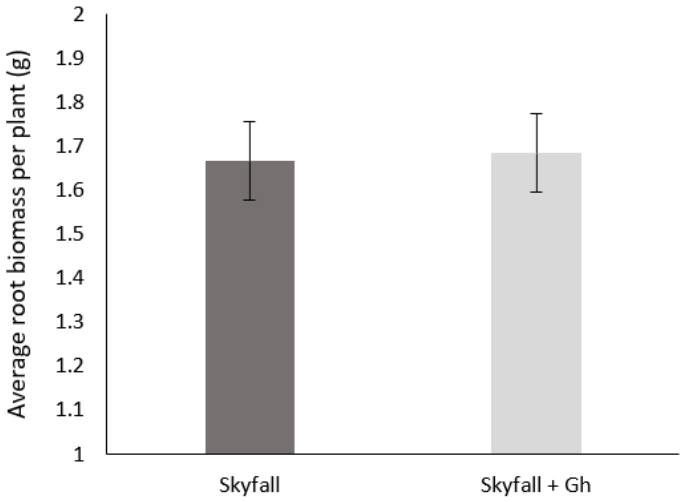


Figure 7.8 The average root biomass (g) of *G. hyphopodioides*-inoculated and uninoculated plants. Error bars represent standard error.



Figure 7.9 Representative images of *G. hyphopodioides*-inoculated and uninoculated wheat roots. Images taken post-harvest using a Nikon D80 digital camera.

7.4.2.3 ITS sequence confirmation of *G. hyphopodioides* colonisation

Currently, species-specific primers for the non-pathogenic *Magnaporthaceae* fungi are not available as unique genomic regions could not be identified from the publicly available draft genome sequences. To confirm that colonisation by *G.*

hyphopodioides was successful, roots were assessed for the presence of characteristic sub-epidermal vesicles. One pot was sampled in May and the remaining pots were sampled in July. Root pieces containing sub-epidermal vesicles consistent with those previously reported for *G. hyphopodioides* (large, singular vesicles) were subject to fungal isolation and ITS sequencing for species identification. However, root pieces with sub-epidermal vesicles characteristic of *S. cylindrosporus/* the unnamed *Magnaporthaceae* species (small and clustered) were also occasionally detected and were subsequently sampled for species identification. It should also be noted that due to the nature of fungal root isolations, which represent only a very small sample of each root system and may be further biased by surface sterilising procedures (fungi which colonise the outer root tissues are more likely to be killed during surface sterilisation), the quantification of root colonisation by individual species is not possible.

Unexpectedly, sub-epidermal vesicles were detected in both *G. hyphopodioides* inoculated and uninoculated pots, revealing that the naïve soil used for the pot bioassay contained natural levels of non-pathogenic *Magnaporthaceae* species (figure 7.10). The soil was collected from Meadows field at the Rothamsted Farm after a break crop of winter oilseed rape. Non-pathogenic *Magnaporthaceae* species had not previously been isolated from this field, but may have been introduced through the spread of grass volunteer species. Nevertheless, sub-epidermal vesicles consistent with *G. hyphopodioides* were found far more frequently in the inoculated treatment compared to the uninoculated treatment. Therefore, the present experiment explores the effects of artificially increasing *G. hyphopodioides* levels in the soil, on wheat health and productivity.



Figure 7.10 Micrographs of adult wheat roots exhibiting characteristic sub-epidermal vesicles (SEVs) of the non-pathogenic *Magnaporthaceae* species. Imaged using a stereomicroscope. White arrows indicate SEVs.

The NCBI Basic Local Alignment Search Tool (BLAST) was used to identify regions of similarity between ITS sequences, enabling species identification. As expected, *G. hyphopodioides* and the unnamed *Magnaporthaceae* species were found in both inoculated and uninoculated pots. Interestingly, despite the lack of take-all lesions in the sampled roots, *G. tritici* was also identified, suggesting that *G. tritici* and *G. hyphopodioides*/the unnamed *Magnaporthaceae* sp. may exist in close quarters in the root. Furthermore, several unexpected root-infecting fungi (uncultured *Podospora* sp., *Periconia* sp., *Eppicoccum* spp.) were detected, again implying intimate associations with the non-pathogenic *Magnaporthaceae* species (table 7.8).

Table 7.8 Fungal species isolated from root pieces containing sub-epidermal vesicles. For full details of ITS species identification see appendix A.11, table A.11.4.

Sample time	Skyfall	Skyfall + Gh
May	*G. hyphopodioides*	*G. hyphopodioides*
	Unnamed *Magnaporthaceae* sp.	*G. tritici*
		Uncultured *Podospora* sp.
July	*G. tritici*	*G. hyphopodioides*
	Unnamed *Magnaporthaceae* species	Unnamed *Magnaporthaceae* species
	Periconia sp.	*Periconia macrospinosa*
	Epicoccum nigrum	*Epicoccum layuense*

7.4.3 Sensitivity of non-pathogenic *Magnaporthaceae* species to Latitude® fungicide

The fungicide Latitude® is described in the literature as being *G. tritici* specific (Bateman et al., 2008; Freeman et al., 2005). However, studies into the sensitivity of closely related non-pathogenic *Magnaporthaceae* species are not publicly available. In this section, the sensitivity of closely related species within the *Magnaporthaceae* family was investigated both *in vitro* and *in planta.* The *in vitro* growth of *G. hyphopodioides*, *S. cylindrosporus*, an unnamed *Magnaporthaceae* sp. and *G. tritici* was measured in the presence and absence of Latitude® (figure 7.11). ANOVA analysis of the average colony diameter after 5 days growth (14 days in the case of *S. cylindrosporus*) revealed that the radial growth of the three non-pathogenic *Magnaporthaceae* species was unaffected by the presence of the fungicide. As expected, this was not the case for *G. tritici,* which exhibited a significant growth reduction when grown on PDA supplemented with Latitude® (figure 7.12). Further studies are required to investigate whether the growth response/hyphal integrity of non-pathogenic *Magnaporthaceae* species is altered at higher concentrations of Latitude®.

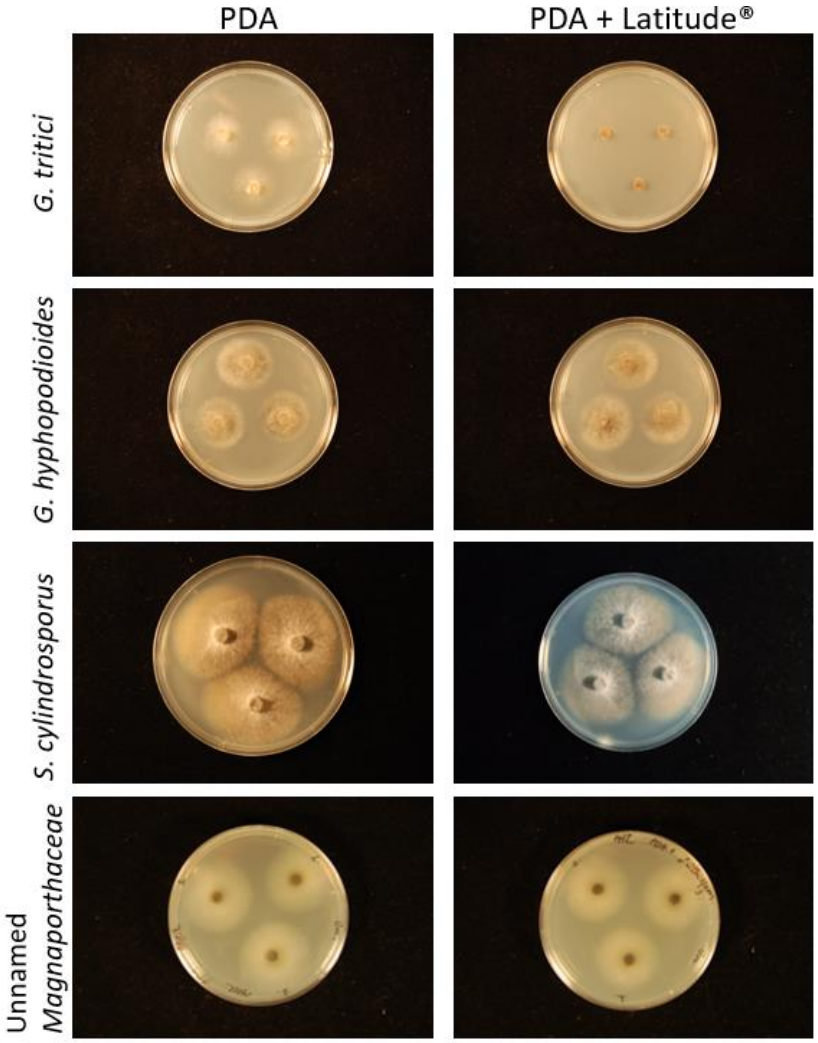


Figure 7.11 Representative images of *Magnaporthaceae* colonies growing in an *in vitro* fungicide sensitivity test. Colonies were imaged after 5 days of growth except for *S. cylindrosporus* colonies, which were imaged at 14 days of growth.

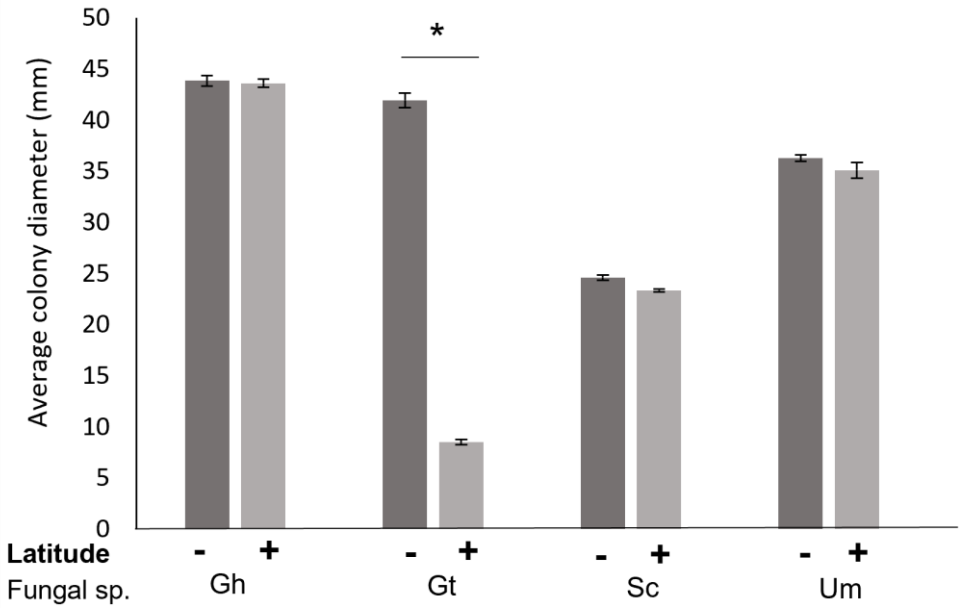


Figure 7.12 The average colony diameter of *Magnaporthaceae* species grown on PDA in the presence and absence of the fungicide Latitude®. Error bars represent standard error. Asterisks indicate significant differences as calculated by Tukey's multiple-comparisons test ($p<0.05$). See appendix A.12 (table A.12.1) for full summary statistics.

Consistent with the findings of the *in vitro* experiment, a seedling pot bioassay revealed that both the colonisation incidence (figure 7.13, appendix A.12; table A.12.2) and severity (figure 7.14, appendix A.12; table A.12.3) of plants inoculated with non-pathogenic *Magnaporthaceae* species were not significantly altered when wheat seeds (cv. Hereward) were treated with Latitude® at agriculturally relevant application rates. However, there was a slight trend for less extreme and more moderate *G. hyphopodioides* colonisation in Latitude® treated plants (figure 7.14). As expected, the incidence and severity of *G. tritici* disease was significantly altered by fungicide treatment.

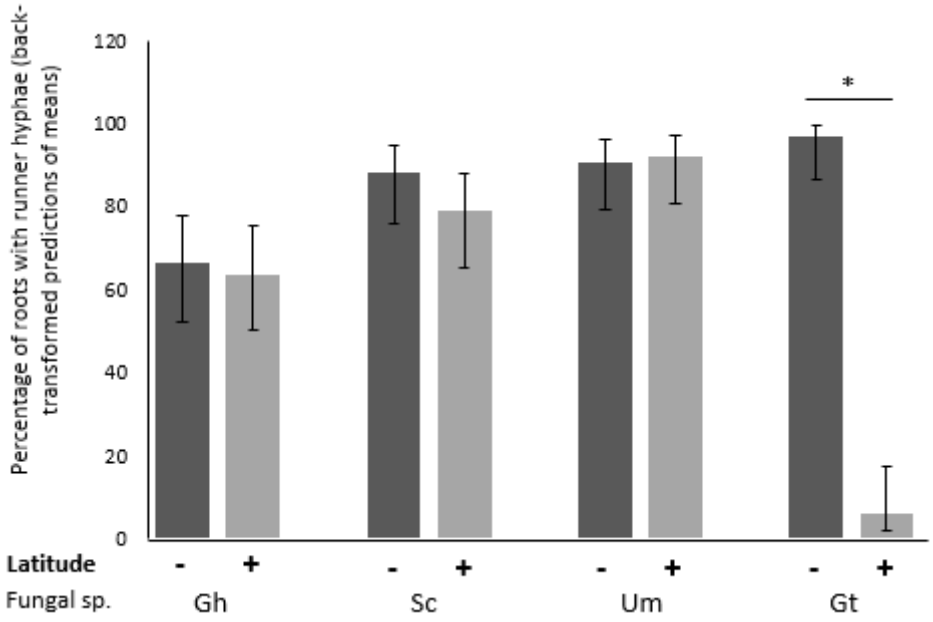


Figure 7.13 The percentage of roots with runner hyphae in the presence and absence of the fungicide Latitude®. Error bars represent back-transformed predictions of means calculated using a GLM. Error bars represent 95% confidence intervals. Gt = *G. tritici*, Gh = *G. hyphopodioides*, Sc = *S. cylindrosporus,* Um = Unnamed *Magnaporthaceae* sp. Asterisk indicates a significant differences as calculated by Tukey's multiple comparisons test ($p<0.05$).

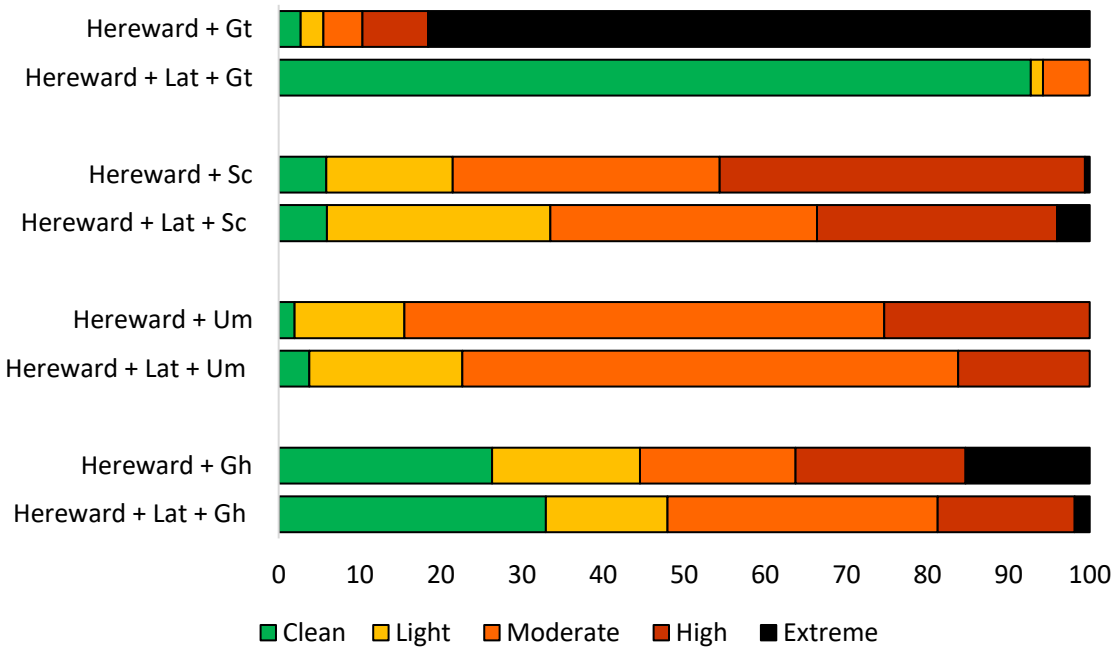


Figure 7.14 Colonisation severity in the *in planta* Latitude® sensitivity test. Severity is represented by the percentage of roots classified as having no colonisation (0% runner hyphae coverage), light colonisation (1-25% runner hyphae coverage), moderate colonisation (26-50% runner hyphae coverage), high colonisation (51-75% runner hyphae coverage) or extreme colonisation (76-100% runner hyphae coverage). Data analysed by ordinal logistic regression of original count data. See previous page.

7.4.4 Susceptibility of elite winter wheat cultivars to colonisation by *G. hyphopodioides*

As mentioned previously, a soil-core baiting study carried out by Osborne et al., (2018) demonstrated that certain elite winter wheat cultivars differ in their susceptibility to *G. hyphopodioides* colonisation. The aim of the present study was to further characterise the *G. hyphopodioides* susceptibility trait by determining whether the trait was consistent under a different soil environment. A seedling bioassay was carried out using naïve soil collected from Webb's field at Rothamsted Farm, an arable site which had previously been sown with winter oats. A selection of cultivars which consistently demonstrated either high or low susceptibility to *G. hyphopodioides* were selected from the original study (see table 7.7 for full details) and the controlled environment growth conditions were replicated.

Contrary to previous findings by Osborne et al., (2018) (figure 7.15 A, B), elite winter wheat varieties did not significantly differ in their susceptibility to *G. hyphopodioides* (GLM: F= 1.36, d.f. 15, 64, p= 0.194) (figure 7.15, C). However, the present study relied on artificial inoculation, resulting in far higher levels of colonisation compared to the original study. The experiment was subsequently repeated with a reduced level of inoculum to better replicate a field scenario. In this case, a smaller selection of cultivars was chosen (see section 7.3.4 for full details). Despite achieving lower levels of colonisation, there was no significant difference among the different cultivars in the percentage of roots colonised by *G. hyphopodioides* (GLM: F=0.93, d.f. 6, 21, p=0.492) (figure 7.15 D), suggesting that the soil environment and/or the mode of original colonisation within the soil plays a significant role in the *G. hyphopodioides* susceptibility trait.

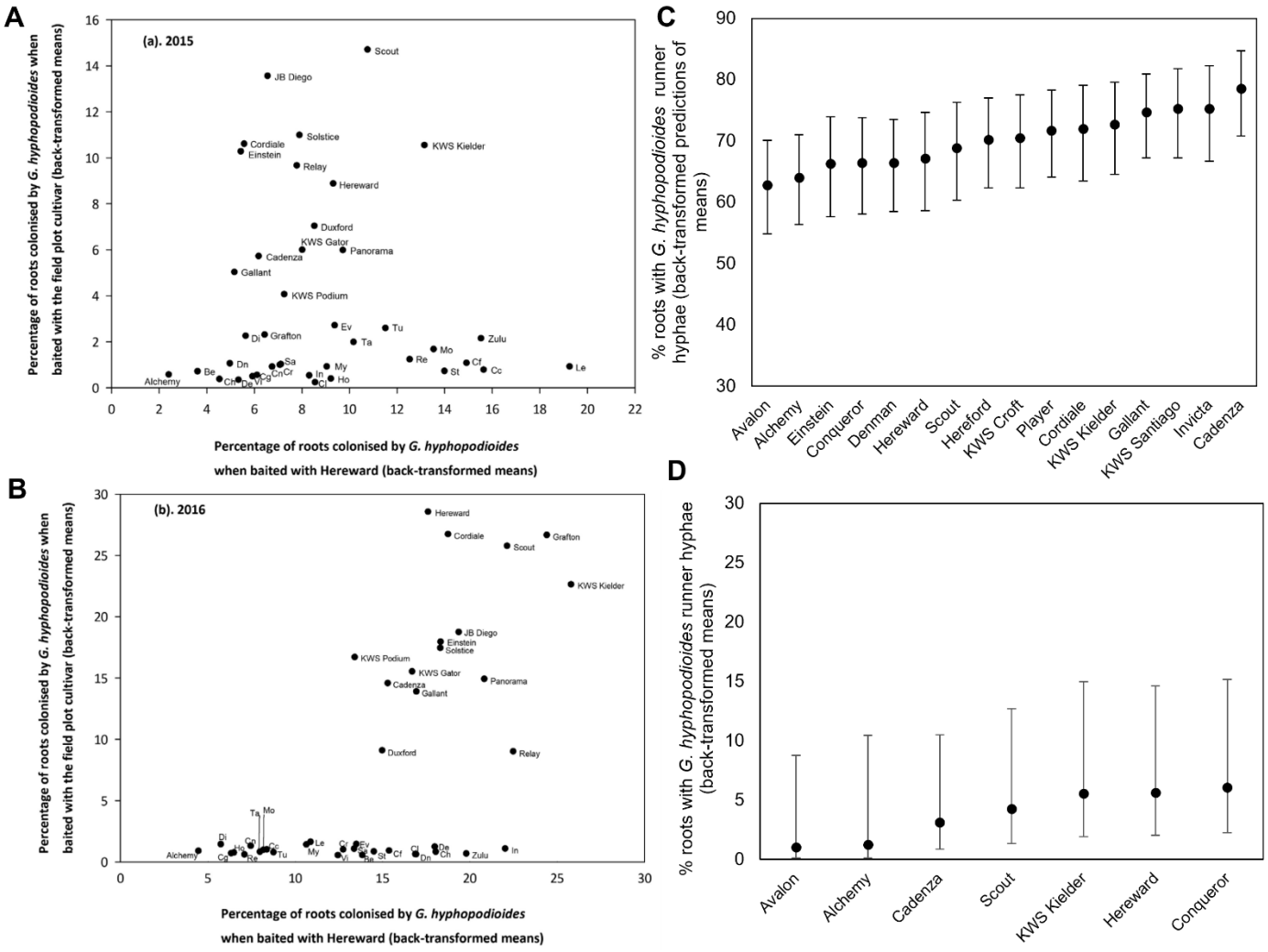

A
(a). 2015
Percentage of roots colonised by G. hyphopodioides when baited with the field plot cultivar (back-transformed means)
Percentage of roots colonised by G. hyphopodioides when baited with Hereward (back-transformed means)
Scout
JB Diego
Solstice
Cordiale
Einstein
KWS Kielder
Relay
Hereward
Duxford
KWS Gator
Panorama
Cadenza
Gallant
KWS Podium
Ev
Tu
Di
Grafton
Ta
Zulu
Mo
Re
Cf
Dn
Sa
My
St
Cc
Be
Ch
Cr
Ir
Ho
Cl
Le
Alchemy
B
(b). 2016
Percentage of roots colonised by G. hyphopodioides when baited with the field plot cultivar (back-transformed means)
Percentage of roots colonised by G. hyphopodioides when baited with Hereward (back-transformed means)
Hereward
Cordiale
Scout
Grafton
KWS Kielder
JB Diego
Einstein
Solstice
KWS Podium
KWS Gator
Cadenza
Panorama
Gallant
Duxford
Relay
Ta
Mo
Di
Le
My
Ev
Cf
Cl
De
In
Zulu
Alchemy
Tu
Re
St
Dn
Ch
C
% roots with G. hyphopodioides runner hyphae (back-transformed predictions of means)
Avalon
Alchemy
Einstein
Conqueror
Denman
Hereward
Scout
Hereford
KWS Croft
Player
Cordiale
KWS Kielder
Galliant
KWS Santiago
Invicta
Cadenza
D
% roots with G. hyphopodioides runner hyphae (back-transformed means)
Avalon
Alchemy
Cadenza
Scout
KWS Kielder
Hereward
Conqueror

Figure 7.15 The percentage of roots colonised with *G. hyphopodioides* in a two-year soil-core baiting study by Osborne et al., (2018) (A, B) and in follow-up seedling susceptibility studies (C, D). See appendix A.13 for full summary statistics. Parts A and B have been reproduced from Osborne et al., (2018) under the Creative Commons Attribution License (https://creativecommons.org/licenses/by/4.0/). See previous page.

7.5 Discussion

The effect of non-pathogenic *Magnaporthaceae* species on wheat health is a major consideration when evaluating their potential as biocontrol agents against take-all disease. Seedling bioassays revealed that as hypothesised, neither plant root nor shoot biomass was significantly altered when plants were inoculated with *G. hyphopodioides*, *S. cylindrosporus* or an unnamed *Magnaporthaceae* species. Hence, unlike pathogenic *G. tritici*, non-pathogenic *Magnaporthaceae* species have no overall negative effect on plant growth at the seedling stage. Though this finding is promising in the context of biocontrol and especially considering the high colonisation rates, total root/shoot biomass offers only a snapshot of plant health, which is determined by a multitude of factors and is exhibited in a number of phenotypes. Furthermore, total biomass measurements are unlikely to be precise enough to reveal small phenotypic differences which may have important implications for overall health. This is evidenced by the subtle but statistically significant increase in the total root length and the number of root tips in *G. hyphopodioides* colonised plants, detected using WinRHIZO software. Other root architecture traits such as total root volume and the number of root forks were not significantly altered in *G. hyphopodioides* colonised plants, though a clear upwards trend was found. This unexpected finding suggests that *G. hyphopodioides* colonisation results in either increased root length (of seminal and/or lateral roots), increased root branching, or both. However, further experimental repetitions are required before drawing solid conclusions.

As mentioned previously, a range of fungal endophytes are known to alter root architecture, often giving colonised plants a competitive advantage in nutrient deprived or water limited environments. This is particularly true of dark septate endophytes (DSEs) in forest habitats, though fewer studies have reported root

architecture changes in cereal crops, possibly due to the addition of artificial fertilisers (Li et al., 2019). As plant nutrient status is likely to influence endophyte driven changes in root architecture, future studies should investigate whether the subtle changes presented in this study are altered under different nutrient regimes.

To further investigate the effect of *G. hyphopodioides* colonisation on adult wheat health, a large pot experiment was conducted in an outdoor area. To do this, a new inoculation protocol was established. This study revealed that artificially inoculating wheat plants with *G. hyphopodioides* did not significantly alter key parameters of plant health, including plant height, ear length and the number of tillers per plant. Furthermore, the speed of plant development, represented by the number of days from booting (GS45) to anthesis (GS61), was not significantly altered by *G. hyphopodioides* colonisation. In addition, the chlorophyll content of the flag leaf did not significantly differ between uninoculated and inoculated plants. This was true across three principal wheat growth stages (booting (GS45), ear emergence (GS51) and flowering (GS61)). Flag leaf photosynthetic traits are key determinants of grain yield (Carmo-Silva et al., 2017). Therefore, despite being unable to generate yield data in the present experiment (see section 7.3.2.8), we can infer that based on flag leaf data, significant yield differences between *G. hyphopodioides* inoculated and uninoculated plants would be unlikely.

Endophyte inoculants are known to alter the soil microbiome. Therefore, the successful introduction of an endophyte biocontrol agent also requires a detailed understanding of its effects on the soil environment. Using the Denaturing Gradient Gel Electrophoresis (DGGE) technique, Rabiey et al., (2017) demonstrated that wheat inoculation with *Pirisformospora indica*, an endophyte species widely studied for its potential as a biocontrol agent, resulted in a substantial increase in the diversity of microbes detected in root and bulk soil samples. Though not investigated in the study, the authors acknowledge that the observed changes in microbial soil communities could have downstream effects on plant productivity, ecosystem processes and soil function. Furthermore, such

changes could have significant implications for key microbe-microbe interactions, which may indirectly affect the disease control ability of the biocontrol agent.

Therefore, a key aim of the present study was to generate bulk soil samples, enabling the comparison of soil microbial communities in *G. hyphopodioides* inoculated and uninoculated pots. In an ideal scenario, rhizosphere samples would also be taken, however generating this material would require destructive sampling before the onset of senescence and hence a time-course experiment would be necessary. Bulk soil samples were stored at -80 °C for future analysis of microbial composition, which could offer key information regarding *G. hyphopodioides* interactions in the soil. Indeed, recent evidence suggests that fungal endophytes and bacteria can work synergistically with the plant host to limit fungal disease (Mahdi et al., 2021). Understanding these interactions could help us to exploit the synergistic relationships between bacteria and fungi for improved disease control, potentially by developing combined inoculants or seed dressings. Furthermore, this understanding may help us to identify field sites where biocontrol by *G. hyphopodioides* could be highly successful, or where its effect may be negligible or even deleterious.

Biocontrol efficacy is also governed by compatibility with current and well adopted commercial farming practices. The fungicide Latitude® (active ingredient silthiofam; previously Mon65500) is widely applied as a seed dressing, though delivers only partial take-all control in the field environment (Freeman et al., 2005). Although Latitude® is reported to be specific to *G. tritici*, evidence regarding the sensitivity of closely related species is not available. In this chapter, *in vitro* and *in planta* Latitude® sensitivity tests revealed that hyphal growth and root colonisation by several non-pathogenic *Magnaporthaceae* species is not significantly altered by Latitude® treatments. This is promising for the potential of *G. hyphopodioides* as a biocontrol agent, as seed dressings containing a mixture of Latitude® and *G. hyphopodioides* inoculum could be developed for increased take-all control.

However, the promotion of natural populations of *G. hyphopodioides* could provide a sustainable alternative to artificial inoculation methods. Mauchline et

al., (2015) reported that the growth of different wheat cultivars has a strong and long-lasting effect on the bacterial community. Indeed, a field trial and soil-core baiting study carried out by Osborne et al., (2018) demonstrated that certain elite winter wheat cultivars differ in their ability to promote *G. hyphopodioides*, both by building inoculum in the soil, and by exhibiting high susceptibility to colonisation. In this study, seedling bioassays using naïve soil sampled from Rothamsted Farm were carried out to determine whether cultivar susceptibility to *G. hyphopodioides* is consistent across different soil types. A selection of cultivars which consistently demonstrated either high or low susceptibility to *G. hyphopodioides* were tested. Contrary to the findings by Osborne et al., (2018), elite winter wheat cultivars did not significantly differ in their susceptibility to *G. hyphopodioides* under high or low inoculum pressures, suggesting that the soil environment may play a major role in cultivar susceptibility. Alternatively, the artificial inoculation technique used in this experiment may not adequately represent colonisation processes in fields containing natural populations of *G. hyphopodioides*. Therefore, to better study the effect of the soil environment on *G. hyphopodioides* susceptibility and build-up, the original field trial and soil-core baiting study should be repeated across a range of different soil types. Nevertheless, the findings presented in this study highlight the complexities of plant-microbe interactions and demonstrate the need for robust testing before new disease management strategies are recommended.

7.6 Future work

The studies presented in this chapter have provided key information regarding the applicability of *G. hyphopodioides* as a biocontrol agent. However, several questions remain unanswered. A seedling pot bioassay provided some evidence to suggest that *G. hyphopodioides* colonisation results in fine-scale alterations in root architecture traits, but what benefits (if any) do these give the plant, and are these traits altered across different environmental conditions? Seedling co-inoculation assays carried out in chapter 3 revealed that pre-treatment with *G. hyphopodioides* resulted in significant take-all disease reductions when plants were subsequently infected with *G. tritici*. However, despite the disease reduction, plant biomass levels never fully recovered to uninoculated levels.

Thus, co-inoculation studies should be extended to the adult plant stages to determine whether the root phenotypes are still observed, and more importantly, whether *G. hyphopodioides*-induced control offers significant yield benefits.

Furthermore, does the promotion or introduction of *G. hyphopodioides* result in changes in the community composition of microbes, and if so, what are the downstream effects of these changes? The analysis of bulk soil samples from the adult plant health experiment may help to answer these questions. Denaturing Gradient Gel Electrophoresis (DGGE) would be a rapid and affordable method of comparing the microbial diversity in *G. hyphopodioides* inoculated and uninoculated soils. For a more in-depth approach, amplicon sequencing of the 16S rRNA gene in bacteria and the nuclear ribosomal internal transcribed spacer (ITS) region in fungi could be appropriate (Hao et al., 2016). Using this approach, it may be possible to investigate interactions between *G. hyphopodioides* and *Pseudomonas* species, as well as other abundant soil microbes, to evaluate their potential role in the take-all decline (TAD) phenomenon.

In addition, further information is needed regarding the survival of *G. hyphopodioides* under different environmental conditions and in response to current farming practices such as no till, tilling, complete inversion or crop undersowing. Finally, the wheat-*G. hyphopodioides* interaction should be studied under a range of different climate change scenarios; how will warmer and wetter winters influence *G. hyphopodioides* colonisation and plant health effects, and could *G. hyphopodioides* confer additional benefits to the plant under temporary or extended drought and/or high temperature conditions?

7.7 Summary

Pot bioassays demonstrated that colonisation by non-pathogenic *G. hyphopodioides*, *S. cylindrosporus* and an unnamed *Magnaporthaceae* species does not affect the overall shoot or root biomass of wheat seedlings. However, root architecture analysis by WinRHIZO software revealed a small increase in the total root length and the number of root tips of plants colonised by *G. hyphopodioides*. The effect of *G. hyphopodioides* on a range of adult plant health parameters was investigated across key principal wheat growth stages. The

results confirmed that artificially increasing the level of *G. hyphopodioides* inoculum in field soils does not detrimentally affect wheat health. *In vitro* and *in planta* experiments revealed that non-pathogenic *Magnaporthaceae* species are insensitive to Latitude®, a fungicide commonly used for the control of take-all disease. Taken together, these findings highlight the potential of *G. hyphopodioides* as a biocontrol agent against take-all disease of wheat. However, further investigations are required to assess the health benefits (if any) conferred by *G. hyphopodioides* when plants are co-infected with *G. tritici* under different environmental conditions.

7.8 Acknowledgement of contributions

The adult plant health experiment would not have been possible without the hard work of undergraduate summer student Jade Smith. The summer project bursary funding was provided by the Department for Environment, Food and Rural Affairs (DEFRA) funded Wheat Genetic Improvement Network (WGIN). Thank you to Gail Canning for guidance with the various measurements and for helping with the bulk soil sampling.

8 General discussion

8.1 Summary and main findings

Take-all disease is one of the most important root infecting diseases of wheat worldwide (Freeman & Ward, 2004). However, effective control methods do not yet exist. The biocontrol potential of several non-pathogenic *Magnaporthaceae* species has been reported as early as the 1970s (Deacon, 1973, 1976b; Wong & Southwell, 1980), however the precise mechanism(s) of control, the molecular pathways underpinning these interactions, and the applicability of these potential biocontrol agents within modern farming systems has remained unexplored. The main aim of this project was to assess the potential of non-pathogenic *Magnaporthaceae* species for the biocontrol of take-all disease of wheat, with a particular emphasis on the wheat-*G. hyphopodioides* interaction. To achieve this, a multifaceted approach ranging from gene expression studies to plant bioassay experiments was required.

This project has contributed a range of novel findings and generated useful tools for future studies. *In vitro* experiments have shown that the non-pathogenic species investigated are unlikely to control take-all disease by direct hyphal interaction with *G. tritici.* Co-inoculation bioassays revealed that *G. hyphopodioides* was the most promising biocontrol candidate but must infect the root system first in order to provide effective control. Importantly, adding inoculum to plants already infected with *G. tritici* may even result in increased disease levels (see chapter 3). Microscopy studies revealed that enigmatic structures produced by several *Magnaporthaceae* species and previously described in the literature as “sub-epidermal vesicles” are chlamydospore-like structures with thick multi-layer cell walls, which may also play a role in infection (see chapter 4). A dual RNAseq experiment revealed that *G. hyphopodioides* colonisation results in the induction of a range of plant defence mechanisms, which may trigger the formation of these fungal resistance structures. The same defences are also likely to be involved in the control of take-all disease (see chapter 5). Together, the data generated in this project demonstrates that induced plant resistance plays a major role in the control of take-all by *G. hyphopodioides.* However, despite extensive transcriptional reprogramming, *G. hyphopodioides* colonisation alone does not negatively affect wheat health (see chapter 7). Finally, a

new delivery system for VIGS in wheat roots was developed, providing a valuable tool for future take-all research and for the wider research community (see chapter 6).

8.2 How does *G. hyphopodioides* control take-all disease?

Co-inoculation bioassays carried out in chapter 3 revealed that take all levels are reduced when seedlings are pre-treated with *G. hyphopodioides* inoculum. This finding corroborates data from early field studies (Balis, 1970; Deacon, 1976b; Wong & Southwell, 1980), confirming that *G. hyphopodioides* mediated take-all control is a result of induced plant resistance. Having said this, we cannot rule out the potential role of direct hyphal inhibition *in planta,* which may also contribute to take-all control, though is unlikely to play a significant role (see chapter 3). Microscopy studies in chapter 4 revealed that cortical and endodermal cell walls were heavily lignified in response to *G. hyphopodioides* colonisation, as were the stelar compartments. Conversely, an experiment using an alternative infection protocol (see chapter 5) failed to reveal lignification of the stele or endodermal barrier in response to *G. hyphopodioides* colonisation, perhaps due to differences in inoculum levels between the two experiments. Nevertheless, both studies demonstrated a local plant lignification response to *G. hyphopodioides*. Though previous studies have suggested that cell wall lignification is responsible for take-all control (Speakman & Lewis, 1978), the data presented in this PhD project suggests that this is unlikely to be the case, given that *G. tritici* infection also induces significant cell wall lignification, and as mentioned previously, *G. tritici* is capable of producing lignin degrading enzymes *in planta* (Daval et al., 2011). Therefore, other resistance mechanisms must be responsible.

As discussed in chapter 5, the two main forms of induced resistance, induced systemic resistance (ISR) and systemic acquired resistance (SAR), can be distinguished by the crucial involvement of different phytohormones. SAR generally relies on the induction of SA mediated signalling pathways, whereas ISR generally relies of the induction of JA/ET mediated signalling pathways (Choudhary et al., 2007; Pieterse et al., 2014). However, the transcriptomic study carried out in chapter 5 could not conclusively demonstrate ISR or SAR. Although gene expression data suggested that JA and ET signalling was involved in the plant response to *G. hyphopodioides* colonisation, indicating an ISR mechanism, hormone quantifications failed to identify any significant

differences in the levels of JA between uninoculated roots, *G. hyphopodioides* colonised roots, or *G. tritici* infected roots. The same was true for SA, though there was a trend for SA suppression in *G. tritici* infected and *G. hyphopodioides* colonised roots. As discussed in chapter 5, the ability of some fungi to target phytohormone pathways or convert phytohormones to prevent detection by the plant, may provide an explanation for the discrepancies (Han & Kahmann, 2019). When available, the fungal genomes could be analysed to determine whether either species contain genes encoding enzymes which are known to target phytohormone pathways, such as the antibiotic biosynthesis monooxygenase (Abm) that converts endogenous JA into 12OH-JA in *Magnaporthe oryzae,* enabling the pathogen to avoid detection and attenuate plant immunity (Patkar et al., 2015). Alternatively, and as in *Fusarium oxysporum*-induced resistance in tomato, *G. hyphopodioides*-induced resistance may be independent of ISR or SAR (Constantin et al., 2019), meaning that JA, ET or SA are not required for resistance. However, the latter scenario is difficult to rationalise given the clear induction of JA and ET related genes.

Surprisingly, the transcriptomic study revealed that plant cell wall-mediated immunity could play an important role in take-all control by *G. hyphopodioides.* As mentioned in chapter 5, impairment of CWI by pathogen invasion triggers the release of antimicrobial compounds and DAMPs which induce plant innate immune responses upon recognition by PRRs (Bacete et al., 2018; Miedes et al., 2014). In accordance, *G. hyphopodioides* colonisation resulted in the differential expression of 29 predicted receptor kinase genes, compared to just six in response to *G. tritici* infection. Perhaps as a consequence of DAMP recognition, *G. hyphopodioides* colonisation resulted in the induction of a wide range of defence related genes and pathways, which together may lead to induced take-all resistance. Further studies are now underway to test this hypothesis by targeting highly downregulated cell wall biogenesis genes identified in the RNAseq dataset, using the VIGS system developed in chapter 6.

This defence induction may also be responsible for the formation of *G. hyphopodioides* SEVs in the cortex. TEM analysis (see chapter 4) revealed that the structures shared striking similarities with fungal chlamydospores; most notably by having a multi-layer, thickened cell wall. However, penetration pegs were observed emerging from some SEVs and penetrating the plant cell wall, suggesting a role in fungal infection rather than fungal resistance. As discussed in chapter 4, SEVs also share characteristics

with infection structures produced by *M. oryzae,* which are known as appressoria. Appressoria contain a thick cell wall comprising a characteristic layer of fungal melanin which is crucial for turgor generation within the appressorium (Wang et al., 2007). SEV-like structures have been reported in a diverse range of ascomycete DSE fungi, though the structures are referred to as “microsclerotia” in the literature (Ban et al., 2012; Knapp et al., 2018; Su et al., 2013). Detailed microscopy studies are now required to compare the structures of “microsclerotia” and SEVs in different species and investigate their potential role in fungal infection. Further investigation is also required to determine the molecular pathways involved in fungal SEV production, both in the host plant and in the fungus. Though purely speculative at this point, comparative genomics studies could provide novel and exciting insights into the evolution of what could be conserved, intracellular, root-specific infection structures.

The finding that *G. hyphopodioides*-induced resistance provides both local and systemic control is mentioned briefly in chapter 3. However, follow up studies are required to confirm these initial findings. Furthermore, future studies could investigate whether root colonisation by *G. hyphopodioides* also confers resistance against foliar pathogens. The findings of such studies may have important implications for the overall potential of *G. hyphopodioides* as a biocontrol agent.

8.3 Should *G. hyphopodioides* be applied as a commercial biocontrol agent?

The use of microbial biocontrol agents for disease management is an attractive alternative to chemical control. However, there are a number of hurdles which have prevented the widespread adoption of biocontrol agents. Possibly the greatest hurdle is the highly heterogeneous nature of the soil environment, making it challenging to establish sufficient microbial populations for consistent and effective control, particularly if the microbial agent is not usually associated with the soil environment into which it is deployed. Although *G. hyphopodioides* has been isolated from several sites in the UK and globally (Wong et al., 1996), almost no information is available regarding the microbial associations that *G. hyphopodioides* forms in the soil. As discussed in chapter 7, endophyte inoculants can change the diversity of root-associated microbes, which may have downstream effects on plant productivity, ecosystem processes, soil function and the efficacy of disease control (Rabiey et al.,

2017). Furthermore, we do not know how a changing climate will affect the survival of *G. hyphopodioides* in the soil or what potential impacts colonisation could have on plant health under changing conditions. However, answering these questions could prove an enormous task, requiring a multi-level approach and necessitating both laboratory and field scale experiments.

Further studies are also required to assess how well *G. hyphopodioides* can control take-all under field conditions. However, a lot can be learnt from other endophytes which are capable of inducing plant resistance. For instance, several species of *Trichoderma* are known to trigger induced resistance and colonised roots are often primed against future pathogen attack (Walters et al., 2013). As a result, *Trichoderma* species represent the majority of biocontrol agents currently available commercially (Woo et al., 2007). However, ISR induction is often strongly determined by host genotype, as demonstrated by the defence induction and subsequent control against *Botrytis cinerea* in some, but not all tomato lines tested by Tucci et al. (2011). Furthermore, though induced resistance mechanisms can be long-lasting, disease control is rarely complete, and can be affected by the environment, crop nutrition, and the extent to which crops are already induced in the field (Walters et al., 2013). Nevertheless, given that *G. tritici* populations exhibit limited sensitivity to the fungicide Latitude® (Freeman et al., 2005), and given the unique ability to combine Latitude® and *G. hyphopodioides* treatments, induced resistance mechanisms could still provide an advantageous level of disease reduction. In this study, *G. hyphopodioides*-induced resistance against take-all disease was demonstrated in two wheat cultivars (cv. Hereward in chapter 3 and cv. Chinese Spring in chapter 5). To understand whether *G. hyphopodioides* can provide comprehensive control against take-all disease, the biocontrol ability of *G. hyphopodioides* should be tested in a range of different commercial wheat cultivars.

Another important risk to consider is the potential for *G. hyphopodioides* to develop increased virulence in wheat. Microscopy studies carried out in chapter 3 confirmed previous reports that *G. hyphopodioides* is able to penetrate further into the cortex than other non-pathogenic *Magnaporthaceae* species, though is still unable to penetrate the endodermal barrier (Speakman & Lewis, 1978). However, are there scenarios in which *G. hyphopodioides* could infect the stele, and how would this affect plant health? Indeed, the high inoculum pressures generated in the seedling infection

assay carried out in chapter 3 resulted in the production of superficial lesions on the root surface, and though such levels of inoculum are unlikely to be achieved even via artificial inoculation in the field environment, this finding should be taken into consideration.

Co-inoculation bioassays revealed that adding *G. hyphopodioides* inoculum to plants already infected with *G. tritici* may worsen take-all disease levels. Microscopy studies carried out in chapter 4 revealed that *G. tritici* hyphae can directly penetrate plant cell walls without the formation of cell wall appositions, likely by exuding a range of cell-wall degrading enzymes (Dori et al., 1995). Therefore, extensive cell-wall damage as a result of *G. tritici* infection may favour *G. hyphopodioides* colonisation by enabling hyphae to penetrate the cell wall with greater ease and make use of the various carbohydrates, sugars and nutrients released following *G. tritici* infection. Future studies should investigate whether pre-infection with *G. tritici* can enable *G. hyphopodioides* to infect the stele and therefore become pathogenic.

Despite the risks outlined in this section, *G. hyphopodioides* could provide desirable reductions in take-all disease. However, significant knowledge gaps still exist, requiring both lab and field-based experiments before *G. hyphopodioides* mediated control strategies can be deployed safely. Collaborations with industry partners would be highly beneficial for the next phase of investigations. Regardless of the outcome of these experiments, the wheat-*G. hyphopodioides*/*G. tritici* system remains a useful model for fungal pathogenicity and plant resistance studies, and this is an exciting prospect in itself.

G. hyphopodioides inoculum could be applied as a seed coating in combination with the *G. tritici* specific fungicide Latitude®. Alternatively, *G. hyphopodioides* inoculum could be combined with other biocontrol agents with different modes of action to increase the breadth of protection and prevent the evolution of pathogen resistance. To improve survival rates during seed storage, seed coatings may be applied with an appropriate binding agent such as sodium alginate (Ma, 2019). Otherwise, inoculum may be directly introduced in seed rows at drilling. The introduction of *G. hyphopodioides* could be followed with the careful deployment of crop genetics (Osborne et al., 2018) to promote the long-term survival of *G. hyphopodioides* populations and provide a more sustainable approach for biocontrol deployment.

8.4 The importance of investigating fungal endophytes in arable settings

There is a global need to increase crop resilience in a changing climate. One way to achieve this is by exploiting natural relationships with fungal endophytes. However, despite the growing wealth of research, the ecological significance of fungal endophytes, particularly in arable settings, remains poorly characterised (Rodriguez et al., 2009). Thus, investigating endophyte relationships with crop plants such as wheat will help to provide a better understanding of the services that endophytes provide, helping to unlock their full potential in agroecosystems.

As explored in the present study, many fungal endophytes offer great potential as biocontrol agents due to their ability to protect colonised plants against disease via induced plant resistance, direct competition or a combination of both. The discovery of new biocontrol agents is particularly pertinent given the increasing incidence of fungicide resistance in key fungal pathogens and thus the need for alternative methods of disease control (Fisher et al., 2018). Furthermore, the long-term use of fungicides has been associated with decreasing soil health, water pollution and damage to non-target organisms (Zubrod et al., 2019). Tougher EU restrictions have resulted in several fungicides being banned. Indeed, the new UK government sustainable farming incentive strategy places an important emphasis on maintaining and regenerating soil health (DEFRA, 2021). It will be interesting to see if/how biocontrol strategies will be incorporated within the new UK standard of integrated pest management (IPM), which is set to launch in 2023. In any case, bioprospecting of soil microbes will be an important step toward developing new biocontrol methods but ultimately, the success of new agents will rely on a detailed understanding of the complex microbial interactions in the soil.

Unlike in mycorrhizal relationships, where plant derived carbon is exchanged for fungus derived phosphate and nitrogen, thus conferring a clear benefit to both species, the direct and indirect benefits/costs of endophyte colonisation are less well defined. Therefore, endophyte research can also help us to understand the fine balance between endophytic/pathogenic relationships. As mentioned previously, comparative genetic and transcriptomic studies of pathogenic and non-pathogenic endophytic fungal relationships could help to determine whether there is a conserved

genetic/molecular fingerprint which could help to predict if a species has the propensity to become pathogenic, or rather, if key determinants of pathogenicity are species and/or host specific. Based on comparative studies between endophytic and pathogenic *Fusarium oxysporum* isolates, we would expect non-pathogenic species such as *G. hyphopodioides* to contain fewer effector genes compared to pathogenic strains which contain a host-specific effector repertoire (de Lamo & Takken, 2020). Comparative genomics studies could provide insights into the evolutionary relationship between *G. hyphopodioides* and *G. tritici*, and may determine whether *G. hyphopodioides* evolved from a pathogenic ancestor, as is true for *H. oryzae* (Xu et al., 2014).

8.5 Potential implications of this work for the wider research and farming communities

Due to the nature of the disease, take-all research has primarily been undertaken at the field scale. In order to characterise wheat-*Magnaporthaceae* interactions at a fine-scale and investigate the molecular pathways underpinning these interactions, a range of new systems and protocols were required. For instance, a co-inoculation seedling bioassay in semi-sterile conditions was designed to investigate the biocontrol effect of different non-pathogenic *Magnaporthaceae* species (see chapter 3). This protocol is now being used to investigate new candidate biocontrol agents against take-all disease. A precise root infection and root staining protocol enabling accurate tracking of fungal colonisation across distinct stages of colonisation/infection was developed in chapter 5. The same study also revealed that *G. tritici* and *G. hyphopodioides* produce hyaline hyphae before melanised macrohyphae (see appendix A.6). Visual assessments of root colonisation have previously been carried out based on the presence of melanised macrohyphae, hence these assessments are likely to be an underestimate of the true levels of colonisation. Thus, the data and protocols developed in this study will help to inform future take-all research.

New protocols developed in this study also have implications for the wider research community. The VIGS system developed in chapter 6 may be applied to investigate interactions with other root-infecting pathogens. Root expressed resistance mechanisms are poorly defined compared to those above ground and this is particularly true for cereal species. The prospect of characterising

resistance/susceptibility genes against a variety of different root-infecting pathogens, be they biotrophic or necrotrophic, without the need for stable transformation is particularly exciting. The identification of key resistance genes against important pathogens such as *G. tritici* will contribute not only to our understanding of the molecular basis of these interactions but could also enable the identification of novel targets for crop improvement. In addition, the development of a positive silencing control construct (BSMV:TaRTH3) with a clear root phenotype may also be utilised by plant biology research groups investigating the function of key wheat root expressed genes for improved crop resilience, for example those involved in root architecture, nutrient uptake or drought stress.

A key element of this project was the generation of a dual RNAseq dataset to investigate the wheat-*G. tritici/G. hyphopodioides* interaction. Though investigating gene expression in *G. tritici/G. hyphopodioides* was beyond the scope of this project, the study has provided a wealth of data which will be analysed in a future project following successful genome sequencing of the two fungal species. Despite the lack of avirulent *G. tritici* isolates, comparative transcriptomic analysis with closely related non-pathogenic *G. hyphopodioides* could enable the detection of *G. tritici* pathogenicity factors. As pathogenicity factors are often conserved between species (Ortoneda et al., 2004; Turrà et al., 2014), the data may not only progress take-all research, but may also be applicable to other pathosystems.

Finally, this study has provided key information regarding the control mechanisms of *G. hyphopodioides*, which should guide future strategies for biocontrol deployment (see section 8.3). Another key finding was that cultivar susceptibility to *G. hyphopodioides* could be heavily influenced by the soil environment (see chapter 7). Thus, further investigation is required to fully characterise the *G. hyphopodioides* susceptibility/build-up trait described by Osborne et al., (2018), before advising farmers of potential management strategies.

In conclusion, this PhD project has contributed to our overall understanding of an important root-infecting pathogen of wheat, a closely related non-pathogenic endophyte species and the wheat defence responses triggered following infection by either species. The data generated in this project will not only help to inform future

take-all research, but also has important implications for wider research and farming communities.

Appendices

A.1 *In vitro* studies

Confrontation assays

Table A.1.1 Summary statistics and ANOVA analysis of the average colony diameter of *G. hyphopodioides* and *G. tritici* after 4 days of growth when plated as single or dual colonies compared to *G. hyphopodioides* vs. *G. tritici* confrontation assays. Based on a single experiment with four biological replicates per treatment. d.f.=degrees of freedom, s.s.=sums of squares, m.s. = mean squares.

Colony type	Mean colony diameter (mm)	Standard deviation		Standard error	
Gh single	38.75	0.96		0.48	
Gt single	39.25	2.63		1.32	
Gh dual	38.00	2.16		1.08	
Gt dual	38.25	2.22		1.11	
Gh confrontation	39.50	1.29		0.65	
Gt confrontation	38.75	0.96		0.48	
Source of variation	d.f.	s.s.	m.s.	F value	p value
Colony type	5	6.50	1.30	0.39	0.85
Residual	18	60.00	3.33		
Total	23	66.50			

"Sandwich" plate assays

Sandwich plate assays were carried out to determine whether *G. hyphopodioides* fungal volatiles contribute to the inhibition of *G. tritici*. The centre of each PDA plate was inoculated with a single plug (6 mm diameter) taken from the leading edge of a *G. tritici* (16.NZ.1d) colony, a *G. hyphopodioides* (NZ.129.2C.17) colony, or an agar plug taken from the edge of an uninoculated PDA plate. Plates inoculated with *G. tritici* were inverted and placed on top of a base plate containing *G. hyphopodioides* or a *G. tritici* or PDA control (figure A.1.1). Units were sealed with parafilm and left to grow in the dark for 6 days at 21 °C, after which the average colony area of the top plate containing *G. tritici* was measured. Three replicates were set up for each treatment and the experiment was carried out twice. Growth measurements were taken from the *G. tritici* colony in the top plate after 6 days of growth. There was no significant difference in the average colony diameter of *G. tritici* between treatments, nor was

fungal melanisation observed in any colony, suggesting that *G. hyphopodioides* fungal volatiles, at least *in vitro*, are not capable of inhibiting *G. tritici* (table A.1.2). Furthermore, the assay confirmed that direct hyphal contact is required for the melanisation response between *G. hyphopodioides* and *G. tritici.*

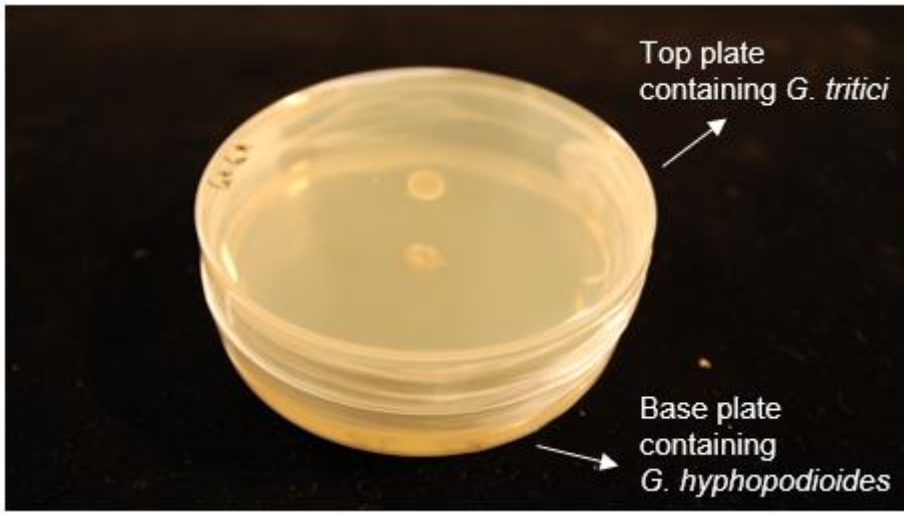


Figure A.1.1 Image of sandwich plate bioassay set-up.

Table A.1.2 Summary statistics and ANOVA analysis of the average colony diameter of *G. tritici* (mm) after 6 days of growth in a sandwich plate bioassay. Based on two experimental replicates with three biological replicates per treatment. Data were combined prior to analysis. d.f.=degrees of freedom, s.s.=sums of squares, m.s. = mean squares.

Treatment					
Bottom	Top	Mean	Standard deviation	Standard error	
Control	*G. tritici*	54.38	1.56	0.64	
G. tritici	*G. tritici*	55.36	1.98	0.81	
G. hyphopodioides	*G. tritici*	54.96	1.33	0.54	
ANOVA: Average colony diameter of *G. tritici* (mm)					
Source of variation	d.f.	s.s.	m.s.	F value	p value
Experiment	1	13.87	13.87	7.31	
Treatment	2	2.88	1.44	0.76	0.48
Residual	14	26.54	1.90		
Total	17	43.30			

A.2 Co-inoculation bioassays

Table A.2.1 Predicted mean proportions of roots with take-all lesions and accumulated analysis of deviance in co-inoculation experiment 1. Calculated using a Generalised Linear Regression Model (GLM). Significant differences to the *G. tritici* mean were calculated by Dunnett's post-hoc test (critical value 2.79). *Gt = G. tritici,* Gh = *G. hyphopodioides*, Sc = *S. cylindrosporus*, Um = Unnamed *Magnaporthaceae* sp. d.f.=degrees of freedom.

Treatment	LOGIT prediction of mean (back-transformed)	Lower 95% confidence limit (back-transformed)	Upper 95% confidence limit (back-transformed)	Dunnett's test
Gt Control	-1.53 (0.18)	-2.02 (0.12)	-1.04 (0.26)	
Gh 2-weeks prior to Gt	-4.75 (0.01)	-6.65 (0.00)	-2.85 (0.05)	p<0.05
Gh + Gt Co-inoculation	-3.19 (0.04)	-4.16 (0.02)	-2.22 (0.10)	p<0.05
Gh 2-weeks after Gt	-2.16 (0.10)	-2.78 (0.06)	-1.53 (0.18)	
Sc 2-weeks prior to Gt	-1.95 (0.12)	-2.52 (0.07)	-1.38 (0.20)	
Sc + Gt Co-inoculation	-1.85 (0.14)	-2.40 (0.08)	-1.30 (0.21)	
Sc 2-weeks after Gt	-2.2 (0.10)	-2.84 (0.06)	-1.56 (0.17)	
Um 2-weeks prior to Gt	-2.96 (0.05)	-3.81 (0.02)	-2.11 (0.11)	p<0.05
Um + Gt Co-inoculation	-1.77 (0.15)	-2.29 (0.09)	-1.25 (0.22)	
Um 2-weeks after Gt	-1.59 (0.17)	-2.19 (0.10)	-0.1 (0.27)	

Table of accumulated analysis of deviance

Change	d.f.	Deviance	Mean deviance	F value	p value
+/- fungi	1	24.208	24.208	6.47	0.015
+/- fungi x species	2	52.462	26.231	7.01	0.003
+/- fungi x timing	2	32.613	16.306	4.36	0.02
+/- fungi x species x timing	4	48.421	12.105	3.24	0.022
Residual	39	145.883	3.741		
Total	48	303.587	6.325		

Table A.2.2 Summary statistics and ANOVA analysis of the average shoot and root biomass per plant (mg) in co-inoculation experiment 1. Asterisks indicate significant differences to the *G. tritici* control ($p<0.05$) as calculated by Tukey's multiple comparisons test. d.f.=degrees of freedom, s.s.=sums of squares, m.s. = mean squares, m.v.= missing values.

	Shoot biomass per plant (mg)						Root biomass per plant (mg)					
Treatment	Mean	Standard deviation	Standard error	Tukey's test			Mean	Standard deviation	Standard error	Tukey's test		
PDB Control	149.50	20.35	9.10	e			63.92	5.34	2.39	d		
Gt Control	121.40	16.15	7.22	de			42.91	8.30	3.71	bc		
Gh 2-weeks prior to Gt	116.40	13.78	6.16	cd			45.90	4.90	2.19	c		
Gh + Gt Co-inoculation	88.20	14.50	6.49	abc*			37.90	5.39	2.41	abc		
Gh 2-weeks after Gt	82.40	13.31	5.95	ab*			30.92	9.74	4.35	ab		
Sc 2-weeks prior to Gt	114.80	29.51	13.20	cd			44.27	9.55	4.27	bc		
Sc + Gt Co-inoculation	112.00	6.79	3.04	cd			43.90	3.92	1.75	bc		
Sc 2-weeks after Gt	77.50	3.34	1.50	a*			29.70	2.07	0.93	ab		
Um 2-weeks prior to Gt	112.40	26.64	11.91	cd			46.75	12.14	5.43	c		
Um + Gt Co-inoculation	111.70	5.91	2.65	bcd			44.20	2.53	1.13	bc		
Um 2-weeks after Gt	81.10	26.03	11.64	a*			31.83	9.71	4.34	a*		
Source of variation	d.f.	m.v.	s.s.	m.s.	F	p	d.f.	m.v.	s.s.	m.s.	F	p
+/- fungi	4		4928	1232	6.58		4		291.85	72.96	1.56	
+/- fungi x species	2		13518	6759	36.13	<.001	2		2810.67	1405.33	30.08	<.001
+/- fungi x timing	2		284.8	142.4	0.76	0.474	2		12.02	6.01	0.13	0.88
+/- fungi x species x timing	2		12377.1	6188.6	33.08	<.001	2		2217.64	1108.82	23.74	<.001
+/- fungi	4		2337.2	584.3	3.12	0.025	4		166.71	41.68	0.89	0.478
Residual	39	-1	7296.7	187.1			39	-1	1821.89	46.72		
Total	53	-1	37690.9				53	-1	7019.61			

Table A.2.3 Predicted mean proportions of roots with take-all lesions and accumulated analysis of deviance in co-inoculation experiment 2. Calculated using a GLM. Significant differences to the *G. tritici* mean were calculated by Dunnett's post-hoc test (critical value 2.81).

Treatment	LOGIT prediction of mean (back-transformed)	Lower 95 % confidence limit (back-transformed)	Upper 95 % confidence limit (back-transformed)	Dunnett's test
G. tritici control	-0.87 (0.29)	-1.37 (0.20)	-0.37 (0.41)	
Gh 2-weeks prior to Gt	-2.68 (0.06)	-3.63 (0.03)	-1.73 (0.15)	p<.05
Gh 1-week prior to Gt	-11.84 (0.00)	-68.33 (0.00)	44.65 (0.00)	p<.05
Gh + Gt Co-inoculation	-1.02 (0.26)	-1.55 (0.18)	-0.5 (0.38)	
Gh 2-weeks after Gt	0.76 (0.68)	0.25 (0.56)	1.26 (0.78)	p<.05
Um 2-weeks prior to Gt	-3.73 (0.02)	-5.22 (0.01)	-2.25 (0.10)	p<.05
Um 1-week prior to Gt	-2.95 (0.05)	-4.04 (0.02)	-1.85 (0.14)	p<.05
Um +Gt Co-inoculation	-0.41 (0.40)	-0.88 (0.29)	0.07 (0.52)	
Um 2-weeks after Gt	0.62 (0.65)	0.13 (0.53)	1.12 (0.75)	p<.05

Table of accumulated analysis of deviance

Change	d.f.	Mean deviance	Deviance ratio	F value	p value
+/- fungi	1	1.256	1.256	0.25	0.621
+/- fungi x species	1	0.937	0.937	0.19	0.669
+/- fungi x timing	3	1043.261	347.754	68.85	<.001
+/- fungi x species x timing	3	41.408	13.803	2.73	0.058
Residual	36	181.841	5.051		
Total	44	1268.703	28.834		

Table A.2.4 Summary statistics and ANOVA analysis of the average shoot and root biomass per plant (mg) in co-inoculation experiment 2. Asterisks indicate significant differences to the *G. tritici* control ($p<0.05$) as calculated by Tukey's multiple comparisons test.

	Shoot biomass per plant (mg)					Root biomass per plant (mg)				
Treatment	Mean	Standard deviation	Standard error	Tukey's test		Mean	Standard deviation	Standard error	Tukey's test	
PDB Control	96.76	7.37	3.30	d		85.04	11.07	4.95	c	
G. tritici control	89.09	6.27	2.80	cd		70.53	7.28	3.25	bc	
Gh 2-weeks prior to Gt	86.16	9.87	4.41	cd		70.01	4.74	2.12	bc	
Gh 1-week prior to Gt	73.26	6.01	2.69	abc		72.93	3.75	1.68	bc	
Gh + Gt Co-inoculation	80.07	10.92	4.88	bcd		58.96	13.43	6.00	b	
Gh 2-weeks after Gt	61.92	8.06	3.60	ab*		33.57	2.10	0.94	a*	
Um 2-weeks prior to Gt	85.12	16.63	7.44	cd		68.70	10.59	4.73	bc	
Um 1-week prior to Gt	73.10	9.69	4.33	abc		71.11	5.79	2.59	bc	
Um +Gt Co-inoculation	82.22	11.98	5.36	cd		66.18	13.52	6.05	b	
Um 2-weeks after Gt	59.15	8.70	3.89	a*		33.57	2.81	1.26	a*	
ANOVA: Shoot biomass per plant (mg)						ANOVA: Root biomass per plant (mg)				
Source of variation	d.f.	s.s.	m.s.	F value	p value	d.f.	s.s.	m.s.	F value	p value
Replicate	4	817.54	204.39	2.31		4	795.33	198.83	3.35	
+/- fungi	2	2680.97	1340.49	15.15	<.001	2	3238.2	1619.1	27.29	<.001
+/- fungi x species	1	2.07	2.07	0.02	0.879	1	10.45	10.45	0.18	0.677
+/- fungi x timing	3	3633.7	1211.23	13.69	<.001	3	9354.41	3118.14	52.55	<.001
+/- fungi x species x timing	3	31.61	10.54	0.12	0.948	3	132.49	44.16	0.74	0.533
Residual	36	3184.69	88.46			36	2135.95	59.33		
Total	49	10350.58				49	15666.82			

Table A.2.5 Predicted mean proportions of roots with take-all lesions and accumulated analysis of deviance in co-inoculation experiment 3. Calculated using a GLM. Significant differences to the *G. tritici* mean were calculated by Dunnett's post-hoc test (critical value 2.77).

Treatment	LOGIT prediction of mean (back-transformed)	Lower 95 % confidence limit (back-transformed)	Upper 95 % confidence limit (back-transformed)	Dunnett's post-hoc test
G. tritici control	0.43 (0.61)	-0.20 (0.45)	1.10 (0.74)	
Gh 2-weeks prior to *Gt*	-2.21 (0.10)	-3.21 (0.04)	-1.21 (0.23)	p<.05
Gh 1-week prior to *Gt*	-1.89 (0.13)	-2.78 (0.06)	-1.00 (0.27)	p<.05
Gh + *Gt* Co-inoculation	0.15 (0.54)	-0.46 (0.39)	0.75 (0.68)	
Gh 2-weeks after *Gt*	0.57 (0.64)	-0.07 (0.48)	1.21 (0.77)	
Um 2-weeks prior to *Gt*	-0.91 (0.29)	-1.58 (0.17)	-0.24 (0.44)	p<.05
Um 1-week prior to *Gt*	-0.65 (0.34)	-1.32 (0.21)	0.02 (0.50)	p<.05
Um + *Gt* co-inoculation	-0.94 (0.28)	-1.62 (0.17)	-0.27 (0.43)	p<.05
Um 2-weeks after *Gt*	0.32 (0.58)	-0.32 (0.42)	0.95 (0.72)	

Table of accumulated analysis of deviance

Change	d.f.	Deviance	Mean deviance	F value	p value
+/- fungi	1	78.60	78.60	9.04	0.00
+/- fungi x species	1	1.47	1.47	0.17	0.68
+/- fungi x timing	3	339.40	113.13	13.01	<.001
+/- fungi x species x timing	3	140.63	46.88	5.39	0.003
Residual	45	391.25	8.69		
Total	53	951.35	17.95		

Table A.2.6 Summary statistics and ANOVA analysis of the mean *G. tritici* fungal biomass (indicated by pg *G. tritici*/ng total DNA) in root samples from co-inoculation experiment 3. Significant differences to the *G. tritici* mean were calculated by Dunnett's post-hoc test (two-sided confidence interval 7.75, 18.80).

	Square root transformed mean (back-transformed)	Lower 95 % confidence limit (back-transformed)	Upper 95 % confidence limit (back-transformed)	Dunnett's post-hoc test	
PDB Control	1.41 (1.99)	-1.20 (1.44)	4.02 (16.16)		
G. tritici control	13.28 (176.25)	10.67 (113.74)	15.89 (252.49)		
Gh 2-weeks prior to Gt	3.54 (12.56)	2.75 (7.58)	7.97 (63.52)	p<.05	
Gh 1-week prior to Gt	5.36 (28.77)	0.93 (0.87)	6.15 (37.82)	p<.05	
Gh + Gt Co-inoculation	11.12 (123.70)	8.51 (72.45)	13.73 (188.51)		
Gh 2-weeks after Gt	18.75 (351.53)	16.14 (260.47)	21.36 (456.25)		
Um 2-weeks prior to Gt	11.72 (137.41)	8.37 (70.06)	13.59 (184.69)		
Um 1-week prior to Gt	10.98 (120.56)	9.11 (83.03)	14.33 (205.35)		
Um + Gt Co-inoculation	6.72 (45.14)	4.11 (16.88)	9.33 (87.05)	p<.05	
Um 2-weeks after Gt	12.03 (144.72)	9.42 (88.74)	14.64 (214.33)		
ANOVA: Square root transformed pg Gt DNA/ng total DNA					
Source of variation	d.f.	s.s.	m.s.	F value	p value
Replicate/block	2	12.72	6.36	0.46	
+/- fungi	2	737.11	368.55	26.53	<.001
+/- fungi x species	1	8.03	8.025	0.58	0.457
+/- fungi x timing	3	704.77	234.92	16.91	<.001
+/- fungi x species x timing	3	725.24	241.75	17.4	<.001
Residual	18	250.06	13.89	50.68	
Replicate/block x pot x technical rep	60	16.45	0.27		
Total	89	2454.37			

Table A.2.7 Summary statistics and ANOVA analysis of the average shoot and root biomass per plant (mg) in co-inoculation experiment 3.

	Shoot biomass per plant (mg)				Root biomass per plant (mg)			
	Mean	Standard deviation	Standard error	Tukey's test	Mean	Standard deviation	Standard error	Tukey's test
PDB Control	70.20	1.18	0.68	a	76.77	6.09	3.52	c
G. tritici control	69.61	6.98	4.03	a	53.53	7.64	4.41	ab
Gh 2-weeks prior to Gt	58.57	7.10	4.10	a	51.79	8.88	5.13	ab
Gh 1-week prior to Gt	71.04	4.18	2.41	a	56.91	1.35	0.78	ab
Gh + Gt Co-inoculation	57.33	3.37	1.94	a	60.37	1.47	0.85	bc
Gh 2-weeks after Gt	66.56	1.90	1.10	a	43.80	5.89	3.40	a
Um 2-weeks prior to Gt	70.53	13.98	8.07	a	60.90	8.53	4.92	bc
Um 1-week prior to Gt	67.70	7.61	4.39	a	55.80	3.90	2.25	ab
Um + Gt Co-inoculation	66.73	3.00	1.73	a	61.67	1.40	0.81	bc
Um 2-weeks after Gt	56.33	6.39	3.69	a	43.47	5.65	3.26	a

ANOVA: Shoot biomass per plant (mg)						ANOVA: Root biomass per plant (mg)				
Source of variation	d.f.	s.s.	m.s.	F value	p value	d.f.	s.s.	m.s.	F value	p value
Replicate/block	2	154.66	77.33	1.94		2	94.2	47.1	1.47	
+/- fungi	2	148.62	74.31	1.86	0.18	2	1370.89	685.44	21.44	<.001
+/- fungi x species	1	22.73	22.73	0.57	0.46	1	30.15	30.15	0.94	0.344
+/- fungi x timing	3	234.09	78.03	1.96	0.16	3	1003.55	334.52	10.46	<.001
+/- fungi x species x timing	3	498.09	166.03	4.17	0.02	3	99.03	33.01	1.03	0.402
Residual	18	717.47	39.86			18	575.51	31.97		
Total	29	1775.66				29	3173.32			

Table A.2.8 Statistical analysis of take-all severity in co-inoculation experiment 3. Estimates of parameters and accumulated analysis of deviance as calculated by ordinal logistic regression analysis. p values are differences compared with the reference level: *G. tritici* control.

Parameter	Parameter estimate	Inverse logit of estimate	Standard error	T value	p value
Cut-point 0/1	-1.44	19.20	0.23	-6.36	<.001
Cut-point 1/2	1.31	78.75	0.22	5.86	<.001
Cut-point 2/3	4.32	98.69	0.50	8.63	<.001
Gh 2-weeks prior to *Gt*	-3.24	3.77	0.42	-7.72	<.001
Gh 1-week prior to *Gt*	-3.04	4.59	0.36	-8.44	<.001
Gh + *Gt* Co-inoculation	-0.36	41.14	0.30	-1.20	0.23
Gh 2-weeks after *Gt*	-0.12	46.90	0.31	-0.41	0.69
Um 2-weeks prior to *Gt*	-1.88	13.23	0.31	-6.13	<.001
Um 1-week prior to *Gt*	-1.72	15.20	0.31	-5.51	<.001
Um + *Gt* co-inoculation	-1.99	12.02	0.31	-6.52	<.001
Um 2-weeks after *Gt*	0.12	53.10	0.31	0.40	0.69

Source of variation	d.f.	Deviance	Mean deviance	F value	p value
Regression	8	446.7	55.837	28.79	<.001
Residual	67	129.9	1.939		
Total	75	576.6	7.689		
Change	-8	-446.7	55.837	28.79	<.001

A.3 Pilot experiments to investigate *G. hyphopodioides*-induced local and systemic protection against take-all disease

Several attempts were made to design a split-pot experiment in sand using liquid inoculum (figure A.3.1). However, take-all disease levels were high and infection of the stem base often occurred, resulting in contamination between the split-pots. Thus, a new methodology was developed using a hydroponics system, with the aim of better tracking and therefore controlling take-all disease levels to prevent cross-contamination. The water agar system used in chapter 5 was not appropriate as plants cannot be grown for long enough to allow mature lesion development.

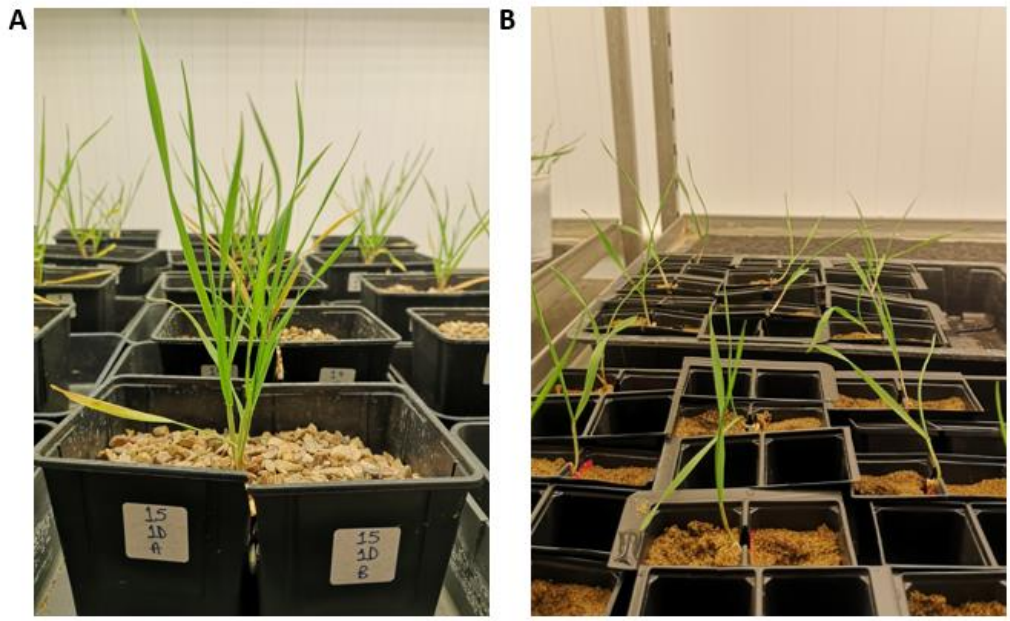


Figure A.3.1 Split-pot assays in sand using liquid inoculum. A. Growth room images of plants in a 4 week split-pot bioassay. B. Growth room images of plants in a 2 week split-pot bioassay.

Methods

A new hydroponics system was set up as follows. Chinese Spring seeds were surface sterilised with 1% sodium hypochlorite for 10 mins, followed by 3 x 1-minute washes with sterile distilled water. Seeds were pre-germinated on sterile filter paper in a growth chamber for 3 days (20 °C, 16hr light cycle, light intensity 5) until the radicle had emerged and the first roots had developed. Growth tubes were set up by filling 15 ml falcon tubes with nutrient solution to the 13 ml mark. Plastic mesh was placed inside the top of each tube and a single pre-germinated seed was placed on the mesh such that the roots were oriented toward the nutrient solution. Tubes were wrapped in foil and placed in the growth chamber for 4 days until the plants were large enough to handle and at least four roots had developed.

Plants were removed from the mesh and roots from the same plant were separated evenly into two 15 ml tubes (held together with tape) containing fresh nutrient solution, again filled to the 13 ml mark. Parafilm was wrapped around the neck of the tubes and sealed around the stem base to provide stability and maintain a semi-sterile environment. Tubes were wrapped in foil and placed in the growth chamber for 3 days to allow the roots to establish.

Roots were inoculated by adding two fungal plugs of *G. hyphopodioides* isolate NZ.129.2C.17 (using no.3 cork borer) to the roots of one tube, in the 2 cm area between the nutrient solution and the seed. Inoculated plants were left for one week before removing the plugs and adding two plugs of *G. tritici* isolate Gt 17LH(4)19d1 to the same roots (local effect) or the uninoculated

roots in the neighbouring tube (systemic effect). Root assessments were conducted 1 week after the final inoculum addition. Disease severity was scored by assessing the number of roots with lesions measuring 0-5 cm (figure A.3.2.).

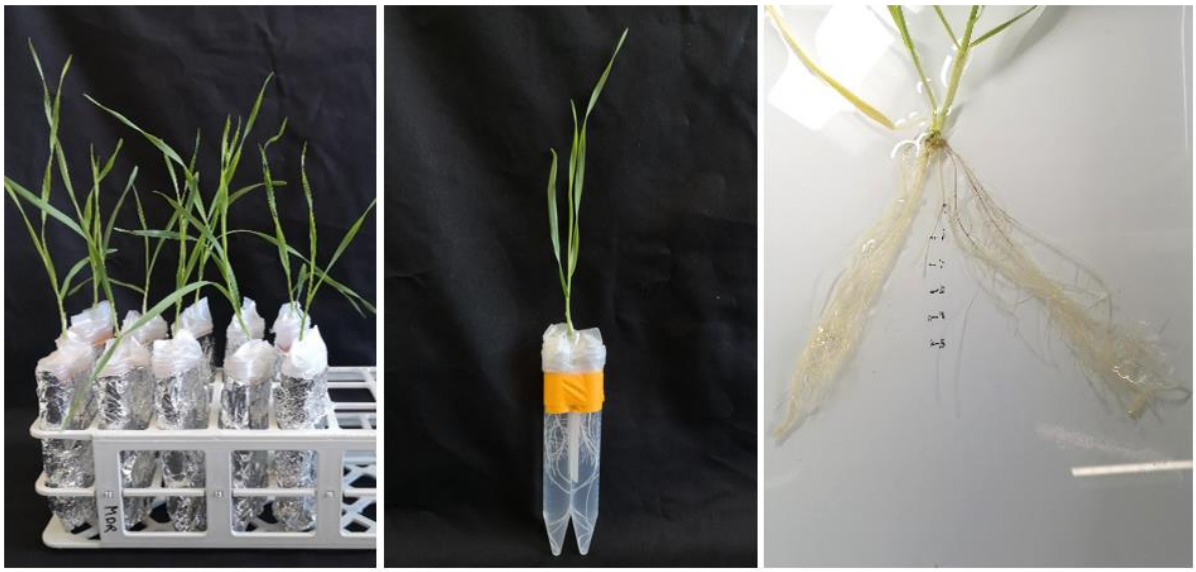


Figure A.3.2 Split-root hydroponics set-up

Results

Based on the limited data available (3 replicates per treatment), *G. hyphopodioides*-induced resistance seems to provide both local and systemic protection against take-all disease (figure A.3.3). However, additional replications are required before statistical testing can be carried out. Further optimisation of the protocol is needed to reduce plant stress and allow a higher-throughput.

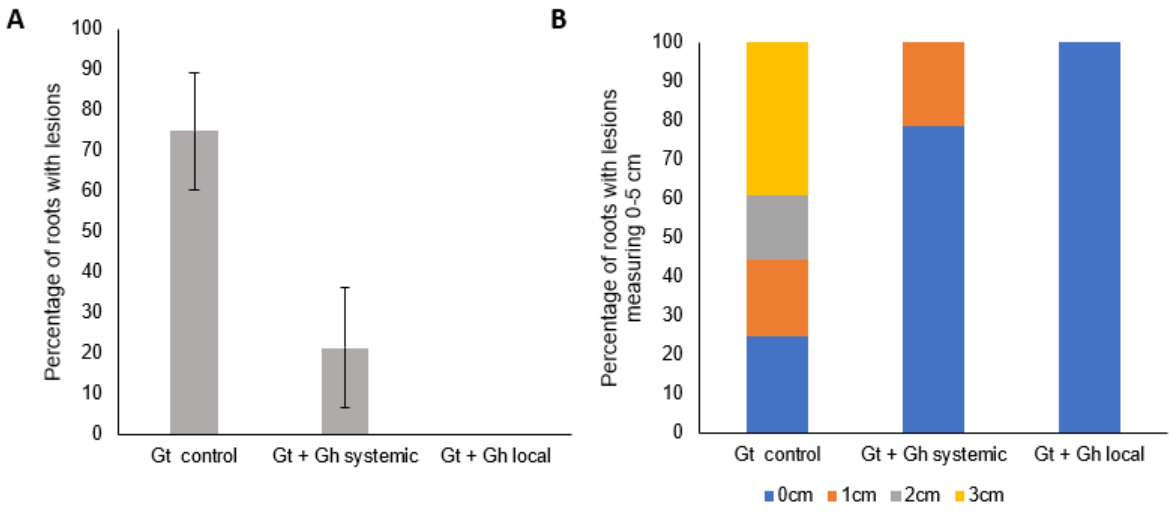


Figure A.3.3 Take-all disease incidence (A) and severity (B) in a split root hydroponics pilot study. Error bars represent standard error. See previous page.

A.4 Pilot experiments for the Eppendorf seedling infection assay

Table A.4.1 Summary of pilot experiments for the optimisation of root infection and sample preparation

Experiment	Methods	Results	Implications
Petri dish infection assay	A surface sterilised seed was placed in a petri dish containing moist sterile filter paper. Seedlings were grown for 4 days before inoculating one root per plant with a fungal plug (5 mm) taken from a colony growing on PDA. Plugs were placed on the surface of the root. Three replicates per treatment were set-up, with control treatments containing PDA plugs only. Petri dishes were placed in a growth chamber (20 °C day, 16 °C night, 16 hr light cycle, light intensity 5) and sampled daily for a week.	Fungal plugs were frequently dislodged by the growing roots and as a result there were very poor levels of colonisation. Fungal runner hyphae were not observed until day 6 and take-all disease symptoms were not observed until day 7 for *G. tritici* treatments.	Alternative growth media was required.
Eppendorf sand infection assay (1)	2 ml Eppendorf tubes were filled to the 0.5 ml mark with surface sterilised sand. A fungal plug (as above) was added followed by sand to the 1.5 ml mark. A surface sterilised seed was placed on the sand surface and lightly covered with sand. Replication as above. Placed in a growth chamber and sampled as above.	Colonisation levels were improved, though fungal runner hyphae were not detected until day 4.	Increased humidity was needed to encourage fungal colonisation.
Eppendorf sand infection assay (2)	As above, with the exception that an 8 mm fungal plug was added at the 1.5 ml mark, and parafilm was used to cover the Eppendorf tube to increase humidity. Replication as above. Plants were sampled at 3, 6 and 9 days growth.	Colonisation levels were improved, with fungal runner hyphae visible from day 3.	This infection protocol was taken forward for the main experiment.
Optimisation of sample preparation (1)	Roots were fixed in a 2.5 % glutaraldehyde/ 4% paraformaldehyde solution, dehydrated in a graded ethanol series and embedded in LR White Resin (medium hardness). Resin blocks were sectioned using a rotary microtome to 1 µm thickness.	Despite repeated attempts to section the blocks, section quality was affected by sample tearing, possibly linked to root structural alterations in response to fungal colonisation.	An alternative embedding method was needed.

Optimisation of sample preparation (2)	Roots were fixed as above. Based on findings by Marques et al., (2013), glycol methacrylate resin (Agar Scientific) was tested as an alternative to LR White Resin.	Intact sections containing plant and fungal material were successfully obtained.	This method was taken forward for the main experiment.

Table A.4.2 Summary of histochemical stains tested.

Stains tested	Target	Staining time	Results	Implications
1% Safranin (aq)	Plant cell wall	4 mins	Stains plant cells well but interacts with other fungal stains	
1 % Pontamine fast scarlet (aq)	Plant cell wall	4 mins	Poor staining and interactions with other fungal stains	Dual staining of plant and fungi will not be carried out
1% Phloroglucinol (in 20% HCL)	Plant lignin	10 mins	Poor staining	
1% Potassium permanganate (aq)	Plant lignin	10 mins	Stains lignin well	To be taken forward for final experiment
0.5% Trypan blue (in 45% acetic acid)	Fungal chitin	20 mins	Weak staining of fungal hyphae	
1 % Trypan blue (in lactophenol)	Fungal chitin	30 secs	Poor distinction between plant and fungus	
1 % Toluidine blue (in phosphate-citrate buffer)	Fungal infection structures (callose deposition)	10 mins	Poor distinction between plant and fungus	
1 % Aniline blue (aq)	Hyaline fungal hyphae	20 mins	Poor staining	
1 % Aniline blue (in lactophenol)	Hyaline fungal hyphae	30 secs	Stains fungal hyphae well	To be taken forward for final experiment

A.5 Analysis of SEVs and infection hyphae

Table A.5.1 ANOVA analysis of the cell wall width of sub-epidermal vesicles (SEVs) and infection hyphae in TEM micrographs.

	Mean (µm)		s.e.	s.d.	
SEVs	0.66		0.02	0.16	
Hyphae	0.09		0.01	0.04	
Source of variation	d.f.	s.s.	m.s.	F value	p value

Technical rep stratum	2	0.13	0.07	0.45	
Technical rep x plant samples stratum	6	0.87	0.15	17.82	
Fungal structure	1	14.71	14.71	1798.54	<.001
Residual	170	1.39	0.01		
Total	179	17.11			

A.6 RNAseq pilot experiments

Several pilot studies were carried out prior to the main experiment to:

1. Determine whether *G. tritici* and *G. hyphopodioides* can effectively colonise wheat cv. Chinese Spring
2. Investigate the progression of colonisation/infection across different time points in a vermiculite system
3. Test and optimise fluorescent staining of colonised samples with WGA and PI
4. Investigate the growth of wheat in a water agar system
5. Test different RNA extraction kits

Study 1: Investigating the progression of colonisation/infection in a vermiculite system

Methods

Plants were grown in 50 ml falcon tubes filled with 30 ml sterile vermiculite followed by four mycelial plugs taken from the leading edge of a fungal colony using a no.2 cork borer. A further 5 ml of vermiculite was added, followed by a surface sterilised, pre-germinated Chinese Spring seed and a final 5 ml layer of vermiculite. Seeds were sterilised by washing in 1 % sodium hypochlorite for 10 minutes with occasional shaking, followed by 3 x 1-minute washes in sterile distilled water. Tubes were watered with 20 ml sterile distilled water and placed in a growth chamber (20 °C day, 16 °C night, 16h light cycle). The experiment was carried out twice, the second time with the additional of a parafilm layer covering the tubes, with the aim of promoting fungal colonisation.

Plants were carefully washed out in a tray of water. Clean roots were placed in a petri dish filled with water and colonisation was assessed using a stereomicroscope. Notes were taken on the abundance of runner hyphae and take-all lesions. One root piece per plant was taken for further analysis by confocal microscopy. Root pieces approximately 1 cm in length were co-stained with 200 µl 10 µg/ml Wheat Germ Agglutinin, Alexa Fluor™ 488 Conjugate (WGA) and 10 µg/ml Propidium Iodide for 10 minutes in a 1.5 ml Eppendorf tube in the dark to visualise fungal structures and plant cell walls, respectively.

Table A.6.1 Treatments details for RNAseq pilot study 1

Treatment	Isolate	Time Points	Replicates
Wheat + Gt	Gt17LH(4)19d1	2, 3, 4, 5, 9, 12, 14 dpi	A, B, C
Wheat + Gh	NZ.129.2C.17	2, 3, 4, 5, 9, 12, 14 dpi	A, B, C
Wheat -	N/A	2, 3, 4, 5, 9, 12, 14 dpi	A, B, C

Results and conclusions

Light microscopy failed to identify *G. tritici* runner hyphae, and only very small amounts of *G. hyphopodioides* runner hyphae were detected during the early stages of colonisation. These findings suggested that multiple root samples must be collected and pooled to yield sufficient RNA for sequencing. In addition, fungal colonisation was not homogenous, with some plants exhibiting multiple *G. tritici* root lesions at 14 dpi while others did not exhibit any infection symptoms.

The initial fluorescent staining protocol resulted in poor visualisation of the WGA stain and a large amount of nuclear staining by PI. To improve the strength of the WGA signal, roots were instead stained with PI first, followed by WGA. In addition, roots were cleared in 10% KOH (w/v) solution at 70 °C prior to staining to reduce the level of nuclear staining by PI.

Surprisingly, comparative assessments by light microscopy and confocal microscopy of the same root samples revealed that fungal runner hyphae were not always visible by light microscopy, resulting in inaccurate estimates of fungal colonisation. The study revealed that hyaline hyphae, which are produced during the early stages of colonisation in this system, are not visible without staining. Only the thicker, melanised runner hyphae could be detected by light microscopy. Though, like the SEVs, they did not take up the fluorescent WGA stain. The melanised hyphae were produced earlier and in larger amounts by *G. hyphopodioides*. Therefore, initial root assessments using light microscopy are not a viable method for selecting colonised root pieces, especially during the early stages of colonisation.

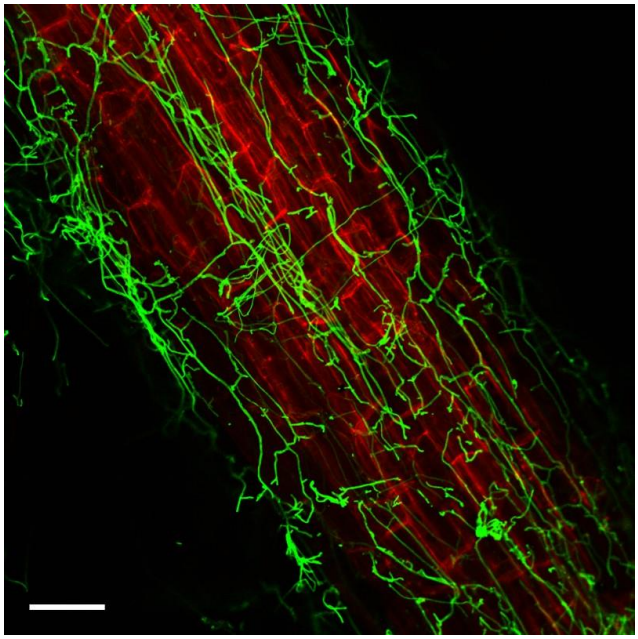


Figure A.6.1 Wheat root stained with WGA and PI, demonstrating severe infection with *G. tritici* hyaline hyphae despite hyphae being invisible by eye. Image obtained by confocal microscopy. Scale bar represents 200 µm.

Conclusions:

A new infection protocol was required to provide a more targeted infection approach which would allow the easy identification of colonised areas for sampling without requiring light microscopy. This approach would also drastically reduce the time needed for follow-on confocal assessments, allowing the stage of fungal colonisation in each sample to be identified more quickly. In addition, a more controlled infection method would reduce the potential of other infection sites on the same root (potentially all at a different stages of fungal colonisation) from influencing the plant transcriptome. Valuable feedback from Dr Daniel Smith (Bioinformatician, Department of Computational and Analytical Sciences, Rothamsted Research, UK) also highlighted the need for an infection method which prevents the potential systemic effects of colonisation in other roots of the same plant from impacting the plant transcriptome.

Study 2: Investigating the growth of wheat on water agar

Method outline:

Wheat seeds cv. Chinese Spring were surface sterilised and pre-germinated for 2 days as in study 1. Five pre-germinated seeds were either placed in individual 50 ml falcon tubes containing moist vermiculite, or on water agar plates (1.5 % w/v) sealed with parafilm and partially covered in foil to create a dark environment for the roots. Plates were placed vertically

on the growth shelf. The growth conditions were as in study 1. All seedlings were harvested after 5 days of growth. Shoot lengths were measured using a ruler, while root lengths and root volumes were measured using WinRHIZO Pro Arabidopsis software (Regent Instruments Inc, Canada).

Results and conclusions:

There was no significant different in the average shoot length (ANOVA: F=4.25, d.f. 1, 8, p=0.073), root length (ANOVA: F=0.09, d.f. 1,8, p=0.771) or root volume (ANOVA: F= 1.15, d.f. 1, 8, p=0.314) of seedlings grown on water agar plates compared to vermiculite tubes. Therefore, the water agar infection protocol was carried forward for the final experiment.

Study 3: Testing different RNA extraction kits

Methods:

Root pieces 1-2 cm in length were sampled from infected plants generated in study 1. Samples were placed in a 1.5 ml Eppendorf tube and flash frozen in liquid nitrogen. Samples were ground to a fine powder using an RNAse free disposable pestle by dipping the tube in liquid nitrogen. RNA was extracted using the Qiagen RNeasy® Plant Mini Kit (Qiagen, Germany), the PicoPure™ RNA Isolation Kit (ThermoFisher Scientific, USA) (following protocol by Siles et al., 2020) or the E.Z.N.A® Plant RNA Kit (Omega-Biotek, USA) according to manufacturer instructions. RNA quality was assessed by Nanodrop and bleach gel (Aranda et al, 2012).

Results:

Nanodrop and bleach gel analysis revealed that RNA extractions carried out using the E.Z.N.A plant RNA extraction kit resulted in superior RNA quality and yield as compared to the PicoPure™ and Qiagen RNeasy® kits. Further analysis revealed that by pooling at least 3 cm of root material, RNA yields met the requirement for sequencing by Novogene (minimum 400 ng total RNA).

Table A.6.2 Nanodrop analysis of RNA extracted using the PicoPure™, RNeasy® or E.Z.N.A kits.

Sample no.	Quantity root material	Kit	Nucleic acid conc. (ng/ul)	260/280	260/230
1	1-2 cm	Picopure	10	1.98	0.86
2	1-2 cm	Picopure	8.6	1.76	0.24
3	1-2 cm	RNeasy	7.5	1.96	0.67
4	1-2 cm	RNeasy	8.2	1.84	0.32
5	1-2 cm	E.Z.N.A	15.4	2.16	1.76
6	1-2 cm	E.Z.N.A	12	2.17	2.01
7	3 cm	E.Z.N.A	18.8	1.86	2.13

8	6 cm	E.Z.N.A	33.3		2.09	2.35

A.7 RNAseq supplementary materials

Table A.7.1 Predicted mean proportions of roots with take-all lesions and accumulated analysis of deviance calculated using a Generalised Linear Regression Model (GLM).

Treatment	LOGIT prediction of mean (back-transformed)	Lower 95% confidence limit (back-transformed)	Upper 95% confidence limit (back-transformed)		
Wheat + Gt	-0.957 (0.27)	-1.19 (0.23)	-0.73 (0.33)		
Wheat +Gh +Gt	-1.975 (0.12)	-2.28 (0.09)	-1.67 (0.16)		
Table of accumulated analysis of deviance					
Change	d.f.	Mean deviance	Deviance ratio	F value	p value
Experiment	1	14.00	14.00	7.24	0.01
+/- Gh	1	56.52	56.52	29.24	<.001
Residual	21	40.59	1.93		
Total	23	111.11	4.83		

Table A.7.2 ANOVA analysis of *G. tritici* fungal biomass as measured in a TaqMan qPCR assay. *G. tritici* biomass is represented by pg *G. tritici* DNA/ ng total DNA.

Treatment	SQRT transformed mean (back-transformed	Lower 95% confidence limit (back-transformed)	Upper 95% confidence limit (back-transformed)		
Wheat + Gt	10.55 (111.30)	8.72 (76.02)	12.38 (153.26)		
Wheat +Gh +Gt	6.13 (37.52)	2.30 (18.45)	7.96 (63.36)		
Analysis of Variance (ANOVA)					
Source of variation	d.f.	s.s.	m.s.	F value	p value
Experiment	1	25.08	25.08	1.51	
Experiment x block	7	115.94	16.56	0.97	
Experiment x block x pot x technical rep					
	36	1.26	0.04		
+/-Gh	1	264.25	264.25	15.54	0.004
Residual	8	136.05	17.01	484.95	
Total	53	542.59			

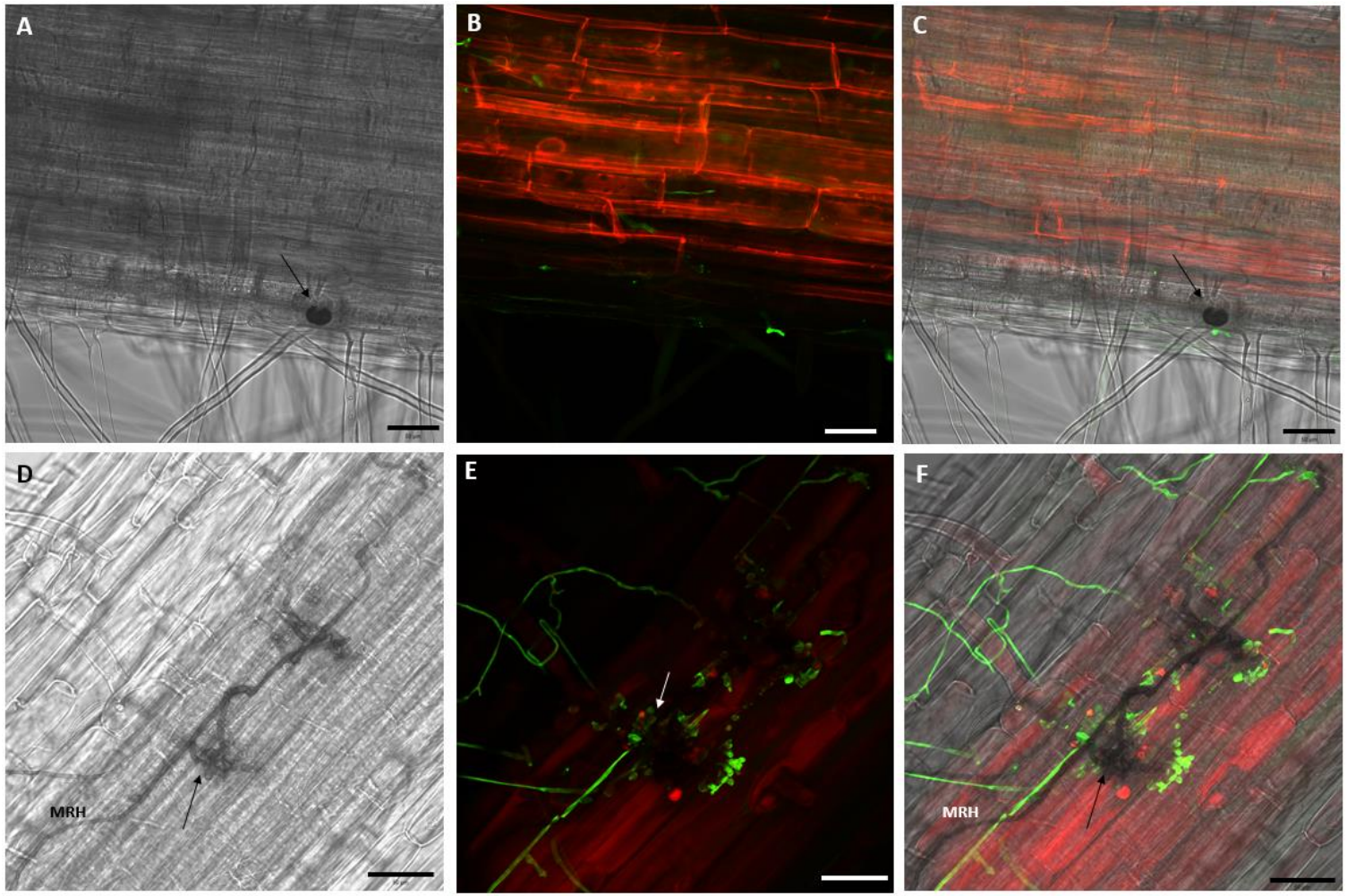


Figure A.7.1 Confocal and transmitted light overlays showing SEVs and melanised runner hyphae with and without WGA staining. Black arrows indicate unstained SEVs. White arrows indicate SEVs with WGA staining. MRH=melanised runner hyphae. Scale bars represent 50 µm.

Table A.7.3 RNA and RNA sequencing quality control measures.

Sample	Treatment	Time point (dpi)	Replicate	RIN value	Effective(%)	Error(%)	Q20(%)	Q30(%)	GC(%)
P5	Wheat -	2	A	8.9	98.43	0.02	98.17	94.83	56.41
P26	Wheat -	2	B	8.7	98.35	0.02	98.24	95.01	56.72
P42	Wheat -	2	C	9.3	98.93	0.02	98.06	94.54	56.14
P54	Wheat -	2	D	8.8	98.81	0.02	98.04	94.5	56.14
P64	Wheat -	2	E	8.5	98.57	0.02	98.1	94.66	56.23
P15	Wheat -	4	A	9.5	99.26	0.02	98.01	94.37	55.76
P17	Wheat -	4	B	9.3	99.18	0.03	97.52	93.39	55.58
P38	Wheat -	4	C	9.4	98.82	0.02	98.2	94.88	55.98
P51	Wheat -	4	D	9.5	99.3	0.02	98	94.37	56.08
P68	Wheat -	4	E	9.2	97.89	0.03	97.54	93.49	56.61
P14	Wheat -	5	A	9.7	98.11	0.02	98.01	94.44	56.19
P21	Wheat -	5	B	9.3	97.3	0.02	98.03	94.49	56.18
P35	Wheat -	5	C	9.9	98.2	0.02	98.1	94.67	56.29
P49	Wheat -	5	D	9.6	98.34	0.03	97.47	93.33	56.00
P65	Wheat -	5	E	9.9	98.8	0.02	98.09	94.67	56.66
P13	Wheat + Gh	2	A	8	98.91	0.02	98.02	94.49	56.02
P25	Wheat + Gh	2	B	9.2	99.16	0.02	98.14	94.77	56.14
P39	Wheat + Gh	2	C	8.7	98.77	0.02	98.02	94.43	56.11
P47	Wheat + Gh	2	D	8.5	99.01	0.02	98.1	94.64	56.81
P69	Wheat + Gh	2	E	8.5	99.14	0.02	98.23	94.97	56.30
P11	Wheat + Gh	4	A	9.3	98.87	0.02	98.09	94.65	55.81
P23	Wheat + Gh	4	B	9.6	99.1	0.03	97.82	94.12	56.15
P43	Wheat + Gh	4	C	9.2	99.04	0.02	98.06	94.55	57.17
P57	Wheat + Gh	4	D	9.5	98.92	0.02	98.16	94.81	56.20
P61	Wheat + Gh	4	E	9.7	99.06	0.02	98.08	94.61	56.15
P9	Wheat + Gh	5	A	8.7	98.26	0.03	97.5	93.45	58.28
P30	Wheat + Gh	5	B	8.9	97.42	0.03	97.59	93.67	58.79
P44	Wheat + Gh	5	C	9.3	97.37	0.03	97.55	93.47	56.60
P48	Wheat + Gh	5	D	8.5	97.9	0.03	97.62	93.68	58.20
P67	Wheat + Gh	5	E	9.5	98.82	0.03	97.59	93.63	57.72
P4	Wheat + Gt	2	A	8.6	98.86	0.02	98.1	94.68	56.27
P19	Wheat + Gt	2	B	7.5	98.98	0.02	98.11	94.63	56.72
P37	Wheat + Gt	2	C	8.9	98.96	0.02	98.12	94.69	56.73
P58	Wheat + Gt	2	D	8.6	99.05	0.02	98.11	94.68	56.41

P73	Wheat + Gt	2	E	8.9	98.83	0.02	98.13	94.76	56.36
P3	Wheat + Gt	4	A	9	98.93	0.03	97.94	94.24	56.00
P16	Wheat + Gt	4	B	9.1	98.74	0.02	98.13	94.78	56.64
P31	Wheat + Gt	4	C	8.9	99.12	0.02	98.17	94.8	56.29
P46	Wheat + Gt	4	D	9.5	99.1	0.02	98.02	94.47	56.63
P74	Wheat + Gt	4	E	9.6	99.11	0.02	98.11	94.74	56.2
P2	Wheat + Gt	5	A	9.8	98.73	0.03	97.41	93.19	55.83
P27	Wheat + Gt	5	B	9.7	98.34	0.02	98.21	94.92	56.99
P34	Wheat + Gt	5	C	9.6	98.58	0.02	98.11	94.73	56.59
P50	Wheat + Gt	5	D	9.5	97.58	0.02	98.14	94.76	56.70
P63	Wheat + Gt	5	E	9.5	98.21	0.02	98.08	94.64	56.29
Gh_PDB_A	PDB + Gh	NA	A	7.8	98.55	0.03	97.83	94.14	61.03
Gh_PDB_B	PDB + Gh	NA	B	8.6	98.23	0.02	97.99	94.5	60.79
Gh_PDB_C	PDB + Gh	NA	C	7.8	97.78	0.03	97.87	94.06	60.85
Gh_PDB_D	PDB + Gh	NA	D	8.5	98.16	0.03	97.81	94.15	60.55
Gh_PDB_E	PDB + Gh	NA	E	6.3	98.4	0.02	97.91	94.37	60.71
Gt_PDB_A	PDB + Gt	NA	A	6.9	97.43	0.03	97.82	94.21	61.21
Gt_PDB_B	PDB + Gt	NA	B	7.5	98.22	0.03	97.8	94.21	61.30
Gt_PDB_C	PDB + Gt	NA	C	7.3	98.24	0.03	97.85	94.3	61.13
Gt_PDB_D	PDB + Gt	NA	D	8.2	98.33	0.03	97.81	94.19	61.23
Gt_PDB_E	PDB + Gt	NA	E	6.7	98.4	0.02	97.89	94.39	61.21

Table A.7.4 Mapping statistics for all RNA sequencing samples. Samples highlighted in grey were identified as outliers and were subsequently excluded.

Sample	Treatment	Time point (dpi)	Replicate	Total no. reads	No. reads mapped to *T. aestivum* genome	% reads mapped to *T. aestivum* genome	No. reads mapped to *G. tritici* genome	% reads mapped to *G. tritici* genome
P5	Wheat -	2	A	90134088	89244719	99.01	3237	0.00
P26	Wheat -	2	B	78184760	77408857	99.01	2522	0.00
P42	Wheat -	2	C	76324856	75593740	99.04	2420	0.00
P54	Wheat -	2	D	79527852	78745226	99.02	2686	0.00
P64	Wheat -	2	E	91940094	91072384	99.06	3059	0.00
P13	Wheat + Gh	2	A	76708182	75577837	98.53	63528	0.08

P25	Wheat + Gh	2	B	78082532	77206072	98.88	16037	0.02
P39	Wheat + Gh	2	C	81908220	81098677	99.01	19953	0.02
P47	Wheat + Gh	2	D	81154030	79023983	97.38	258321	0.32
P69	Wheat + Gh	2	E	97078558	96170974	99.07	4998	0.01
P4	Wheat + Gt	2	A	76774180	75968881	98.95	142236	0.19
P19	Wheat + Gt	2	B	100010994	98390995	98.38	284279	0.28
P37	Wheat + Gt	2	C	94369430	93365860	98.94	100804	0.11
P58	Wheat + Gt	2	D	78119068	77141753	98.75	155906	0.20
P73	Wheat + Gt	2	E	89788446	88651702	98.73	224790	0.25
P15	Wheat -	4	A	80947798	80164034	99.03	2745	0.00
P17	Wheat -	4	B	81038642	80193572	98.96	2492	0.00
P38	Wheat -	4	C	80456670	79679281	99.03	2666	0.00
P51	Wheat -	4	D	79188898	78430059	99.04	2287	0.00
P68	Wheat -	4	E	90195434	89366947	99.08	3356	0.00
P11	Wheat + Gh	4	A	88059970	86207234	97.90	201186	0.23
P23	Wheat + Gh	4	B	81678704	78797038	96.47	344067	0.42
P43	Wheat + Gh	4	C	91115724	74723998	82.01	2511177	2.76
P57	Wheat + Gh	4	D	78329942	72700758	92.81	331341	0.42
P61	Wheat + Gh	4	E	89058988	87090618	97.79	199541	0.22
P3	Wheat + Gt	4	A	90613712	88893356	98.10	652716	0.72
P16	Wheat + Gt	4	B	88185896	80083814	90.81	6346851	7.20
P31	Wheat + Gt	4	C	87450538	84161888	96.24	2162007	2.47
P46	Wheat + Gt	4	D	88129834	85565533	97.09	1444340	1.64
P74	Wheat + Gt	4	E	102352696	99197253	96.92	1766474	1.73
P14	Wheat -	5	A	82959136	82167423	99.05	3944	0.00
P21	Wheat -	5	B	83867052	83087307	99.07	4881	0.01
P35	Wheat -	5	C	82471624	81743367	99.12	3949	0.00
P49	Wheat -	5	D	105040974	104122425	99.13	6574	0.01
P65	Wheat -	5	E	81233264	80509020	99.11	8176	0.01
P9	Wheat + Gh	5	A	88050582	57835301	65.68	4845288	5.50
P30	Wheat + Gh	5	B	79433014	44938543	56.57	5860524	7.38
P44	Wheat + Gh	5	C	76670472	68422160	89.24	469008	0.61
P48	Wheat + Gh	5	D	81440060	57256739	70.31	4192853	5.15
P67	Wheat + Gh	5	E	81168048	65609362	80.83	2560048	3.15
P2	Wheat + Gt	5	A	80581548	78961801	97.99	723543	0.90
P27	Wheat + Gt	5	B	80934872	73390667	90.68	6096905	7.53
P34	Wheat + Gt	5	C	81661188	75736175	92.74	4551008	5.57
P50	Wheat + Gt	5	D	80537328	75326305	93.53	3933420	4.88
P63	Wheat + Gt	5	E	83317146	81514854	97.84	902834	1.08

Gh_PDB_A	PDB + Gh	NA	A	88709756	18831	0.02	20291154	22.87
Gh_PDB_B	PDB + Gh	NA	B	76224766	12980	0.02	16264789	21.34
Gh_PDB_C	PDB + Gh	NA	C	89811792	15723	0.02	19748234	21.99
Gh_PDB_D	PDB + Gh	NA	D	81126370	20791	0.03	16853367	20.77
Gh_PDB_E	PDB + Gh	NA	E	82254310	24134	0.03	17571613	21.36
Gt_PDB_A	PDB + Gt	NA	A	73113822	8155	0.01	67671112	92.56
Gt_PDB_B	PDB + Gt	NA	B	74697276	11185	0.01	69182205	92.62
Gt_PDB_C	PDB + Gt	NA	C	77542878	8988	0.01	72019297	92.88
Gt_PDB_D	PDB + Gt	NA	D	97194650	11154	0.01	90536809	93.15
Gt_PDB_E	PDB + Gt	NA	E	94143440	12157	0.01	87181518	92.60

Table A.7.5 Full list of genes involved in the GO term “stomatal movement”, which was significantly enriched among downregulated genes in response to *G. hyphopodioides* colonisation at 5 dpi.

		Wheat + Gh 5 dpi	
Gene ID	**PANTHER protein family**	**LOG2FC**	**padj**
TraesCS1B02G383700	MYB-RELATED PROTEIN (PTHR47997:SF79)	-2.83	1.61E-03
TraesCS1D02G371800	MYB-RELATED PROTEIN (PTHR47997:SF79)	-2.30	2.48E-02
TraesCS1B02G383900	MYB-RELATED PROTEIN (PTHR47997:SF79)	-6.17	8.25E-05
TraesCS1D02G371700	MYB-RELATED PROTEIN (PTHR47997:SF79)	-3.29	7.48E-08
TraesCS1A02G366300	MYB-RELATED PROTEIN (PTHR47997:SF79)	-4.40	4.35E-02
TraesCS1D02G371500	MYB-RELATED PROTEIN (PTHR47997:SF79)	-4.22	1.20E-05
TraesCS1D02G084400	MYB DOMAIN PROTEIN 55 (PTHR47997:SF75)	-2.31	4.12E-02
TraesCS1B02G383800	MYB-RELATED PROTEIN (PTHR47997:SF79)	-3.38	7.19E-03
TraesCS3A02G254500	OS01G0702700 PROTEIN (PTHR47997:SF1)	-3.79	7.57E-05
TraesCS1D02G371400	MYB-RELATED PROTEIN (PTHR47997:SF79)	-2.39	7.09E-04
TraesCS1A02G366100	MYB-RELATED PROTEIN (PTHR47997:SF79)	-2.99	2.72E-05
TraesCS3B02G286500	OS01G0702700 PROTEIN (PTHR47997:SF1)	-2.79	2.50E-02
TraesCS1B02G383600	MYB-RELATED PROTEIN (PTHR47997:SF79)	-2.61	2.39E-03
TraesCS2B02G177900	TRANSCRIPTION FACTOR MYB46 (PTHR47997:SF19)	-2.67	5.74E-05
TraesCS3D02G255400	OS01G0702700 PROTEIN (PTHR47997:SF1)	-4.47	2.35E-05
TraesCS2A02G152700	TRANSCRIPTION FACTOR MYB46 (PTHR47997:SF19)	-2.12	1.35E-02
TraesCS1A02G366200	MYB-RELATED PROTEIN (PTHR47997:SF79)	-2.31	2.70E-02

Table A.7.6 Full list of genes involved in the GO term “response to biotic stimulus”, which was significantly enriched among the core set of genes differentially expressed in both *G. hyphopodioides* colonised and *G. tritici* infected plants at 5 dpi.

		Wheat + Gh 5 dpi		Wheat + Gt 5 dpi	
Gene ID	**PANTHER Protein Family**	**LOG2FC**	**padj**	**LOG2FC**	**padj**
TraesCS1A02G355300	BARWIN DOMAIN-CONTAINING PROTEIN (PTHR46351:SF15)	7.37	4.95E-05	5.48	3.07E-02
TraesCS6A02G403200	BARWIN DOMAIN-CONTAINING PROTEIN (PTHR46351:SF15)	9.17	6.42E-18	7.87	1.70E-13
TraesCS7D02G164700	BET_V_1 DOMAIN-CONTAINING PROTEIN (PTHR31213:SF152)	6.92	3.26E-04	5.81	1.74E-02
TraesCS1D02G232700	BETA-GLUCOSIDASE 22 (PTHR10353:SF61)	9.69	6.18E-10	7.88	6.10E-06
TraesCS6D02G403200	CHITIN ELICITOR RECEPTOR KINASE 1 (PTHR46204:SF2)	9.47	6.75E-09	6.73	9.30E-04
TraesCS6A02G417900	CHITIN ELICITOR RECEPTOR KINASE 1 (PTHR46204:SF2)	9.73	2.87E-09	7.20	2.16E-04
TraesCS3B02G293200	CHITINASE 12 (PTHR22595:SF79)	8.50	1.25E-09	6.25	9.96E-05
TraesCS3D02G260300	CHITINASE 12 (PTHR22595:SF79)	7.03	1.32E-19	4.53	4.55E-07
TraesCS3A02G260100	CHITINASE 12 (PTHR22595:SF79)	13.09	2.70E-12	11.86	4.58E-10
TraesCS3D02G260500	CHITINASE 12 (PTHR22595:SF79)	6.51	1.41E-06	4.58	1.25E-02
TraesCS1B02G260600	CHITINASE 2 (PTHR22595:SF140)	3.11	1.93E-04	2.78	6.34E-03
TraesCS1A02G203600	CHITINASE 8 (PTHR22595:SF169)	4.44	1.43E-08	3.26	1.29E-03
TraesCS5B02G410900	L-TYPE LECTIN-DOMAIN CONTAINING RECEPTOR KINASE IV.1 (PTHR27007:SF325)	7.60	2.73E-09	6.18	2.08E-05
TraesCS7A02G021600	MLO-LIKE PROTEIN (PTHR31942:SF102)	7.67	5.22E-07	6.05	1.10E-03
TraesCS2B02G097800	OS02G0562600 PROTEIN (PTHR31942:SF83)	5.40	2.03E-18	4.25	1.08E-10
TraesCS5D02G446900	OS07G0128800 PROTEIN (PTHR10334:SF492)	28.45	1.69E-46	25.32	2.44E-39
TraesCS5B02G442700	OS07G0128800 PROTEIN (PTHR10334:SF492)	12.00	8.47E-18	10.30	8.91E-13
TraesCS5A02G439800	OS07G0128800 PROTEIN (PTHR10334:SF492)	8.20	1.82E-07	6.22	8.39E-04
TraesCS2D02G129100	OS07G0575750 PROTEIN (PTHR27007:SF215)	5.39	2.71E-08	3.86	2.41E-03
TraesCS5A02G183300	PATHOGENESIS-RELATED PROTEIN PRMS (PTHR10334:SF314)	8.89	1.45E-09	6.98	1.48E-05
TraesCS5B02G181500	PATHOGENESIS-RELATED PROTEIN PRMS (PTHR10334:SF314)	7.24	4.49E-08	5.10	2.06E-03
TraesCS3A02G477300	PROTEIN KINASE DOMAIN-CONTAINING PROTEIN (PTHR27002:SF513)	7.10	6.84E-07	5.37	3.79E-03
TraesCS3B02G338800	PROTEIN KINASE DOMAIN-CONTAINING PROTEIN (PTHR27007:SF150)	5.32	1.04E-02	5.22	4.30E-02

TraesCS7B02G415600	PROTEIN KINASE DOMAIN-CONTAINING PROTEIN (PTHR27007:SF320)	7.71	9.20E-12	5.31	1.28E-04
TraesCS4B02G041300	PROTEIN KINASE DOMAIN-CONTAINING PROTEIN (PTHR27007:SF320)	6.77	1.72E-05	6.02	1.07E-03
TraesCS7D02G161200	SCP DOMAIN-CONTAINING PROTEIN (PTHR10334:SF394)	5.95	3.94E-07	4.02	1.58E-02
TraesCS7B02G105200	SCP DOMAIN-CONTAINING PROTEIN (PTHR10334:SF420)	7.78	8.47E-04	8.11	1.02E-03
TraesCS7B02G105100	SCP DOMAIN-CONTAINING PROTEIN (PTHR10334:SF420)	6.86	9.22E-05	6.91	1.47E-04
TraesCS5B02G442900	SCP DOMAIN-CONTAINING PROTEIN (PTHR10334:SF467)	9.10	2.53E-10	8.08	3.93E-08
TraesCS5D02G447000	SCP DOMAIN-CONTAINING PROTEIN (PTHR10334:SF467)	10.67	2.04E-15	9.38	2.15E-12
TraesCS5B02G442800	SCP DOMAIN-CONTAINING PROTEIN (PTHR10334:SF467)	12.56	5.46E-09	11.57	1.93E-07
TraesCSU02G226400	SCP DOMAIN-CONTAINING PROTEIN (PTHR10334:SF467)	15.62	8.54E-13	14.62	1.56E-11
TraesCSU02G076600	SCP DOMAIN-CONTAINING PROTEIN (PTHR10334:SF467)	26.33	7.04E-20	26.03	5.56E-21
TraesCS5B02G443700	SCP DOMAIN-CONTAINING PROTEIN (PTHR10334:SF467)	7.68	2.14E-03	6.92	2.94E-02
TraesCS5B02G442600	SCP DOMAIN-CONTAINING PROTEIN (PTHR10334:SF467)	12.20	5.43E-18	10.66	7.98E-14
TraesCS5B02G443100	SCP DOMAIN-CONTAINING PROTEIN (PTHR10334:SF467)	10.53	3.25E-12	9.62	1.62E-10
TraesCS5B02G443800	SCP DOMAIN-CONTAINING PROTEIN (PTHR10334:SF467)	6.96	9.82E-07	6.00	1.14E-04
TraesCS5D02G446800	SCP DOMAIN-CONTAINING PROTEIN (PTHR10334:SF533)	14.97	9.73E-16	13.37	9.18E-13
TraesCS5A02G439700	SCP DOMAIN-CONTAINING PROTEIN (PTHR10334:SF533)	15.65	4.81E-21	13.34	1.26E-15
TraesCS5D02G061400	SUBFAMILY NOT NAMED (PTHR27007:SF356)	4.41	6.07E-06	3.66	1.89E-03
TraesCS3A02G517100	WOUND-INDUCED PROTEIN WIN2 (PTHR46351:SF3)	9.47	1.06E-14	7.61	2.06E-09
TraesCS3D02G524700	WOUND-INDUCED PROTEIN WIN2 (PTHR46351:SF3)	5.32	4.94E-10	3.54	1.97E-03

Table A.7.7 Differential expression of TIP and PIP aquaporin genes in *G. hyphopodioides* colonised roots compared to the uninoculated control.

		5 dpi Wheat + Gh	
Gene ID	Gene name	Log2FC	padj
TraesCS2A02G407700	PIP1-3-like	-2.11	1.35E-02
TraesCS5A02G181000	PIP1-5	-3.42	6.83E-11
TraesCS6B02G450200	PIP1-5-like	-2.83	4.57E-04
TraesCS5B02G178700	PIP1-5-like	-2.42	4.37E-04
TraesCS6A02G405700	PIP1-5-like	-2.41	4.40E-03
TraesCS7B02G002000	PIP2-1	-5.33	1.12E-02
TraesCS6B02G259000	PIP2-2	-4.46	2.57E-07
TraesCS6A02G222100	PIP2-2	-3.95	5.31E-05
TraesCS6D02G212900	PIP2-2	-3.76	2.27E-05
TraesCS2B02G396800	PIP2-5	-2.95	5.97E-05
TraesCS2A02G379800	PIP2-5	-1.98	3.00E-02
TraesCS6A02G082900	PIP2-5-like	-5.16	1.19E-02
TraesCS2A02G379900	PIP2-5-like	-3.88	6.90E-06
TraesCS2D02G376100	PIP2-5-like	-2.97	2.90E-05
TraesCS5D02G112500	PIP2-6-like	-3.36	1.40E-03
TraesCS3B02G608500	TIP1-3	-3.66	6.90E-09
TraesCS3A02G535300	TIP1-3	-2.66	2.16E-04
TraesCS6A02G250300	TIP2-1	-8.58	2.13E-07
TraesCS6D02G232100	TIP2-1	-5.87	4.48E-12
TraesCS6B02G275100	TIP2-1	-4.69	2.26E-14
TraesCS7B02G243000	TIP2-2	-2.78	2.51E-04
TraesCS2A02G414100	TIP2-2-like	-7.34	5.71E-06
TraesCS2D02G411400	TIP2-3	-4.39	7.31E-05
TraesCS2B02G433200	TIP2-3-like	-9.22	6.70E-11
TraesCS7D02G339600	TIP2-4	-2.29	4.94E-05
TraesCS1D02G175200	TIP3-1	4.57	3.51E-04
TraesCS1B02G182200	TIP3-1	4.79	3.87E-03
TraesCS1A02G165400	TIP3-1	9.64	3.22E-04

Table A.7.8 Genes of interest associated with plant defence responses against fungal pathogens

		4 dpi				5 dpi			
		Wheat + Gh		Wheat + Gt		Wheat + Gh		Wheat + Gt	
Gene ID	**Gene name**	**Log2FC**	**padj**	**Log2FC**	**padj**	**Log2FC**	**padj**	**Log2FC**	**padj**
WRKY Transcription Factors									
TraesCS3B02G129900	WRKY24	3.93	1.39E-05	*	*	4.43	2.96E-08	*	*
TraesCS1A02G298600	WRKY24-like	3.67	3.13E-09	2.79	2.17E-04	4.19	3.68E-14	2.57	2.20E-03
TraesCS1B02G308200	WRKY24-like	4.03	2.31E-09	3.22	2.08E-05	4.43	7.54E-13	2.95	3.87E-04
TraesCS1D02G292700	WRKY24-like	3.47	1.02E-09	2.43	2.07E-03	3.78	3.96E-13	*	*
TraesCS3A02G347500	WRKY24-like	2.59	1.22E-05	*	*	2.91	1.01E-08	*	*
TraesCS3B02G379200	WRKY24-like	2.43	7.13E-05	*	*	2.67	2.90E-07	*	*
TraesCS3D02G113200	WRKY24-like	3.07	7.88E-03	*	*	3.34	3.64E-04	*	*
TraesCS1B02G088900	WRKY26	3.08	1.78E-04	*	*	3.65	6.38E-08	*	*
TraesCS1D02G072900	WRKY26	2.28	4.74E-03	*	*	2.66	8.94E-06	*	*
TraesCS1A02G070400	WRKY26	2.51	1.50E-03	*	*	2.77	1.58E-05	*	*
TraesCS7A02G508800	WRKY28	3.76	7.32E-03	*	*	5.35	1.32E-07	*	*
TraesCS7B02G418500	WRKY28-like	3.49	3.96E-03	*	*	6.16	3.11E-13	3.10	4.71E-02
TraesCS7D02G497700	WRKY28-like	9.73	3.62E-07	7.20	1.14E-03	10.59	2.65E-09	6.36	1.14E-02
TraesCS7A02G509000	WRKY28-like	6.93	1.02E-07	5.52	1.06E-04	9.81	1.84E-13	6.89	7.32E-06
TraesCS7D02G497400	WRKY28-like	3.59	2.20E-05	*	*	5.38	6.07E-16	*	*
TraesCS7D02G497300	WRKY28-like	2.92	1.04E-02	*	*	5.41	9.96E-15	*	*
TraesCS7D02G497800	WRKY28-like	5.23	7.85E-07	*	*	7.02	3.74E-14	*	*
TraesCS7B02G419400	WRKY28-like	4.02	3.68E-07	*	*	4.73	9.13E-12	*	*
TraesCS7B02G418400	WRKY28-like	4.49	4.35E-05	*	*	5.68	1.53E-09	*	*
TraesCS3D02G341100	WRKY28-like	2.78	1.00E-06	*	*	2.98	5.11E-09	*	*
TraesCS1A02G121500	WRKY28-like	3.76	2.47E-08	2.62	6.11E-03	3.71	5.23E-09	*	*
TraesCS7B02G418600	WRKY28-like	3.98	4.08E-03	*	*	5.84	7.70E-09	*	*
TraesCS7A02G508700	WRKY28-like	*	*	*	*	7.09	2.21E-06	*	*
TraesCS1D02G430000	WRKY28-like	*	*	*	*	2.37	4.34E-03	*	*
TraesCS6D02G136200	WRKY33	*	*	*	*	2.36	2.23E-04	*	*
TraesCS2D02G332300	WRKY34	*	*	*	*	2.72	9.11E-03	*	*
TraesCS1D02G363300	WRKY51	5.60	1.61E-12	3.52	5.72E-04	5.17	3.31E-11	3.05	1.27E-02
TraesCS1D02G362900	WRKY51	8.18	2.45E-14	5.79	1.01E-06	5.89	3.03E-09	3.96	2.72E-03
TraesCS1B02G374700	WRKY51	7.91	8.99E-09	4.95	7.41E-03	9.89	3.56E-11	7.44	1.47E-05
TraesCS1A02G358100	WRKY51	11.15	1.21E-13	8.35	2.51E-07	9.99	3.13E-14	7.50	2.37E-07
TraesCS3A02G111200	WRKY51	3.16	1.03E-04	*	*	2.80	8.33E-04	*	*
TraesCS3D02G212700	WRKY51	*	*	*	*	4.94	2.75E-03	*	*
TraesCS6A02G080500	WRKY55	6.37	3.51E-04	6.30	4.02E-04	6.76	1.78E-05	4.86	4.63E-02
TraesCS6B02G108000	WRKY55	*	*	*	*	7.08	2.24E-04	*	*

TraesCS6D02G074200	WRKY55-like	7.13	1.22E-04	6.33	1.60E-03	6.71	1.03E-05	*	*
TraesCS3B02G240200	WRKY56	*	*	*	*	3.37	3.46E-02	*	*
TraesCS3A02G248700	WRKY57	10.09	2.28E-08	6.03	1.70E-02	11.12	4.47E-11	6.99	1.22E-03
TraesCS2D02G262100	WRKY57	*	*	*	*	-2.99	2.51E-05	*	*
TraesCS2B02G280300	WRKY57	*	*	*	*	-2.42	1.87E-02	*	*
TraesCS1B02G374900	WRKY57-like	5.91	3.26E-11	3.28	1.80E-02	6.20	1.95E-13	3.51	4.32E-03
TraesCS3B02G277300	WRKY59	7.90	1.76E-02	*	*	8.43	1.84E-03	*	*
TraesCS1A02G300900	WRKY70	*	*	*	*	-3.99	5.51E-03	*	*
TraesCS4B02G170100	WRKY70-like	*	*	*	*	-6.57	9.39E-03	*	*
TraesCS6B02G175100	WRKY71	*	*	*	*	2.69	1.38E-05	*	*
TraesCS3B02G130000	WRKY72	*	*	*	*	2.35	3.35E-05	*	*
TraesCS3D02G113300	WRKY72	*	*	*	*	2.11	8.57E-04	*	*
TraesCS2A02G011000	WRKY75	3.66	3.38E-06	2.61	2.74E-02	4.63	1.55E-12	2.94	1.62E-03
TraesCS1A02G358400	WRKY75	5.56	1.61E-12	3.45	8.43E-04	5.39	1.59E-12	3.01	1.45E-02
TraesCS2B02G010500	WRKY75	3.42	2.28E-06	2.51	1.47E-02	3.95	2.45E-10	*	*
TraesCS2D02G011700	WRKY75	*	*	*	*	3.59	1.80E-06	*	*
TraesCS6A02G146900	WRKY80	*	*	*	*	2.28	1.55E-04	*	*
Pathogenesis Related (PR) Proteins									
TraesCS7D02G164700	PR1-like	*	*	*	*	6.92	3.26E-04	5.81	1.74E-02
TraesCS7D02G164500	PR1-like	*	*	*	*	4.74	2.19E-02	*	*
TraesCS7B02G068400	PR1-like	*	*	*	*	5.29	1.87E-03	*	*
TraesCS7A02G162700	PR1-like	*	*	*	*	2.03	2.08E-03	*	*
TraesCS7A02G162600	PR1-like	*	*	*	*	4.37	1.89E-03	*	*
TraesCS6D02G327600	PR1-like	*	*	*	*	-4.30	3.40E-03	*	*
TraesCS6A02G346300	PR1-like	*	*	*	*	-3.17	2.92E-02	*	*
TraesCS6A02G345100	PR1-like	*	*	*	*	-4.59	3.64E-02	*	*
TraesCS6A02G345000	PR1-like	*	*	*	*	-4.21	2.26E-03	*	*
TraesCS5A02G013500	PR1-like	*	*	*	*	-2.22	5.47E-03	*	*
TraesCS4A02G116400	PR1-like	*	*	*	*	3.03	5.23E-03	*	*
TraesCS2D02G420900	PR1-like	*	*	*	*	2.99	2.34E-03	*	*
Receptor kinases									
TraesCS3A02G536900	At1g06840	*	*	*	*	2.47	6.87E-04	*	*
TraesCS7D02G542600	At1g35710	*	*	*	*	4.04	3.90E-02	*	*
TraesCS3A02G423600	At1g56140	*	*	*	*	2.49	2.20E-05	*	*
TraesCS2D02G248200	At3g03770	*	*	*	*	-2.45	5.07E-07	*	*
TraesCS4A02G330100	At3g47570	3.59	6.32E-04	*	*	3.69	7.49E-05	*	*
TraesCS4A02G446600	At3g47570	*	*	*	*	2.78	1.55E-03	*	*
TraesCS2D02G491600	At3g47570	*	*	*	*	1.86	1.62E-02	*	*
TraesCS5D02G548000	At3g47570	*	*	*	*	-3.25	1.32E-04	*	*
TraesCS2B02G121100	At5g58300	*	*	*	*	-2.32	3.22E-05	*	*
TraesCS3D02G364000	ATCSA-1-like	*	*	*	*	-4.34	2.59E-02	*	*

TraesCS3A02G478500	BAK1-like	9.61	3.99E-11	10.56	1.63E-14	10.21	1.95E-13	9.23	1.50E-10
TraesCS3B02G522000	BAK1-like	6.35	1.59E-10	7.04	3.34E-15	6.30	2.47E-11	5.43	3.29E-08
TraesCS3D02G473200	BAK1-like	4.17	9.76E-05	4.47	3.18E-06	5.06	1.57E-08	4.05	8.58E-05
TraesCS3A02G478700	BAK1-like	3.59	4.92E-03	4.58	1.87E-06	3.69	7.01E-04	3.71	1.31E-03
TraesCS2D02G344600	BIR2	2.83	3.93E-04	2.70	7.47E-04	2.90	4.16E-05	*	*
TraesCS6B02G280300	CERK	*	*	*	*	1.83	9.58E-03	*	*
TraesCS6D02G226300	CERK	*	*	*	*	1.62	1.70E-02	*	*
TraesCS6A02G417900	CERK1-like	7.54	8.95E-05	7.10	2.99E-04	9.73	2.87E-09	7.20	2.16E-04
TraesCS6D02G403200	CERK1-like	7.81	2.78E-05	7.10	2.48E-04	9.47	6.75E-09	6.73	9.30E-04
TraesCS2A02G461800	FLS2	*	*	*	*	-3.07	9.20E-04	*	*
TraesCS6D02G396900	FLS2	*	*	*	*	2.82	1.90E-02	*	*
TraesCS2D02G462000	FLS2	*	*	*	*	-4.71	2.62E-02	*	*
TraesCS2B02G011200	LRR1-like	*	*	*	*	-4.56	5.73E-04	*	*
TraesCS2A02G010500	LRR1-like	*	*	*	*	-7.58	7.55E-04	*	*
TraesCS2B02G011300	LRR1-like	*	*	*	*	-6.33	2.06E-02	*	*
TraesCS7A02G058800	SIK1	2.62	3.39E-02	*	*	3.37	2.64E-05	*	*
TraesCS7D02G053300	SIK1	*	*	*	*	3.53	9.86E-05	*	*
TraesCS7D02G053900	WAK3-like	6.45	2.66E-03	6.63	1.25E-03	5.03	1.74E-02	*	*
TraesCS6B02G441800	Xa21	*	*	*	*	-2.27	4.65E-03	*	*

Table A.7.9 ANOVA analysis of SA, JA, GA1, GA4 levels (ng/g) in wheat roots at 5 dpi. N/D= not detected.

Variate: SA	SQRT transformed mean	(Back-transformed)	Lower 95% confidence limit	(Back-transformed)	Upper 95% confidence limit	(Back-transformed)
Wheat-	30.51	930.86	23.72	562.64	37.29	1390.54
Wheat+Gh	22.76	518.02	15.98	255.36	29.55	873.20
Wheat+Gt	19.46	378.69	12.68	160.78	26.24	688.54
Source of variation	d.f.	s.s.	m.s.	F value	p value	
Treatment	2.00	192.89	96.44	4.19	0.07	
Residual	6.00	138.27	23.05			
Total	8.00	331.16				

Variate: JA	SQRT transformed mean	(Back-transformed)	Lower 95% confidence limit	(Back-transformed)	Upper 95% confidence limit	(Back-transformed)
Wheat-	10.96	120.12	6.41	41.02	15.51	240.56
Wheat+Gh	11.82	139.71	7.27	52.79	16.37	267.98
Wheat+Gt	9.78	95.65	5.23	27.35	14.33	205.35
Source of variation	d.f.	s.s.	m.s.	F value	p value	
Treatment	2.00	6.27	3.14	0.30	0.75	
Residual	6.00	62.24	10.37			
Total	8.00	68.51				

Variate: GA1	SQRT transformed mean	(Back-transformed)	Lower 95% confidence limit	(Back-transformed)	Upper 95% confidence limit	(Back-transformed)
Wheat-	0.15	0.02	-0.49	0.24	0.80	0.64
Wheat+Gh	1.45	2.09	0.80	0.65	2.09	4.36
Wheat+Gt	N/D	N/D	N/D	N/D	N/D	N/D
Source of variation	d.f.	s.s.	m.s.	F value	p value	
Treatment	2.00	3.78	1.89	9.13	0.02	
Residual	6.00	1.24	0.21			
Total	8.00	5.03				

l.s.d. (SQRT scale)=0.909

Variate: GA4	SQRT transformed mean	(Back-transformed)	Lower 95% confidence limit	(Back-transformed)	Upper 95% confidence limit	(Back-transformed)
Wheat-	0.49	0.24	0.38	0.14	0.61	0.37
Wheat+Gh	0.99	0.98	0.88	0.77	1.11	1.22
Wheat+Gt	0.40	0.16	0.28	0.08	0.51	0.26
Source of variation	d.f.	s.s.	m.s.	F value	p value	
Treatment	2.00	0.61	0.31	46.59	<.001	
Residual	6.00	0.04	0.01			
Total	8.00	0.65				

l.s.d. (SQRT scale)=0.1622

A.8 VIGS supplementary materials

To investigate the efficacy of BSMV-VIGS in roots, a list of candidate genes for silencing was produced (table A.8.1). Candidate genes were chosen based on previous VIGS success in the literature, or the presence of a visible silencing phenotype in roots. Due to the limited understanding of gene function in wheat roots, genes known to function in root development in other cereal species were also investigated. The expression of all candidate genes was analysed using the wheat expression atlas (http://www.wheat-expression.com/). Genes with sufficient levels of root expression were further analysed using siRNA-Finder software to predict the efficiency of the resulting RNAi construct.

Table A.8.1 Candidate genes for virus-induced gene silencing (VIGS) in wheat roots.

Gene ID	Gene name	Interest	Function	Selected?	Reason for choice	References
TraesCS4A02G117100.1, TraesCS4B02G187300.1, TraesCS4D02G188600.1	Root hairless 3 (TaRTH3)	Characteristic mutant phenotype in roots (short root hairs)	COBRA protein with putative GTP-binding motifs	YES	Visible silencing phenotype, high expression level in roots, plenty of siRNAs available and no off-target silencing predicted.	(Hochholdinger et al., 2008)
TraesCS7A02G415500.1, TraesCS7B02G315600.1, TraesCS7D02G409000.1	Dolichyl-diphosphooligosaccharide--protein (TaDGL1)	Characteristic mutant phenotype in rice roots (shorter roots, cell death)	DGL-protein glycosyltransferase 8 kDa subunit precursor; necessary for the proper structuration of the polysaccharide matrix of root cell walls in rice	YES	Visible silencing phenotype, high expression level in roots, plenty of siRNAs available and no off-target silencing predicted.	(Qin et al., 2013)
TraesCS2A02G317000, TraesCS2B02G335400, TraesCS2D02G314900	Wheat zeaxanthin epoxidase (TaZEP)	Previous VIGS silencing in the literature	Plays important role in the xanthophyll cycle and abscisic acid (ABA) biosynthesis.	NO	Despite previous silencing success, has low expression in roots and no clear phenotype	(Kang et al., 2019)
TraesCS3A02G397500, TraesCS3B02G429400, TraesCS3D02G391300	Short postembryonic roots 1 (TaSPR1)	Characteristic mutant phenotype in rice roots (shorter roots)	Mitochondrial protein in rice. Precise molecular function uncharacterised. Involved in root development and Fe homeostasis in rice.	NO	Low expression in wheat roots.	(Jia et al., 2011)

Table A.8.2 Primer sequences for the amplification of TaDGL1 and TaRTH3 gene fragments. 5’ extensions permitting ligation independent cloning (LIC) into the RNAγ vector are indicated in bold.

Gene		Primer Sequence	Annealing temp (°C)	Fragment size
TaRTH3	FWD	**AACCACCACCACCGT**CCCGGTACAATGACACACAGAT		
	REV	**AAGGAAGTTTAA**AACCGCCAGCGTTGTAGAGT	65	281 bp
TaDGL1	FWD	**AACCACCACCACCGT**GAAGCCATATGTTGCTGATGATG		
	REV	**AAGGAAGTTTAA**TATGAAGAAGGCTCCCATTGTTG	66	292 bp

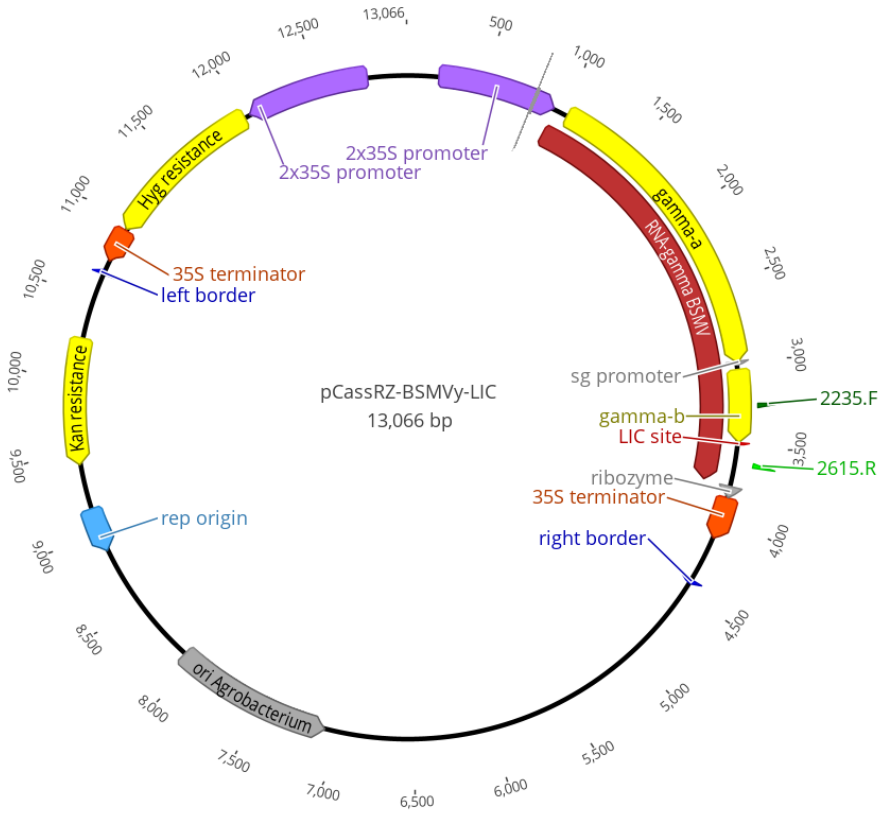


Figure A.8.1 Vector map of pCa- γbLIC.

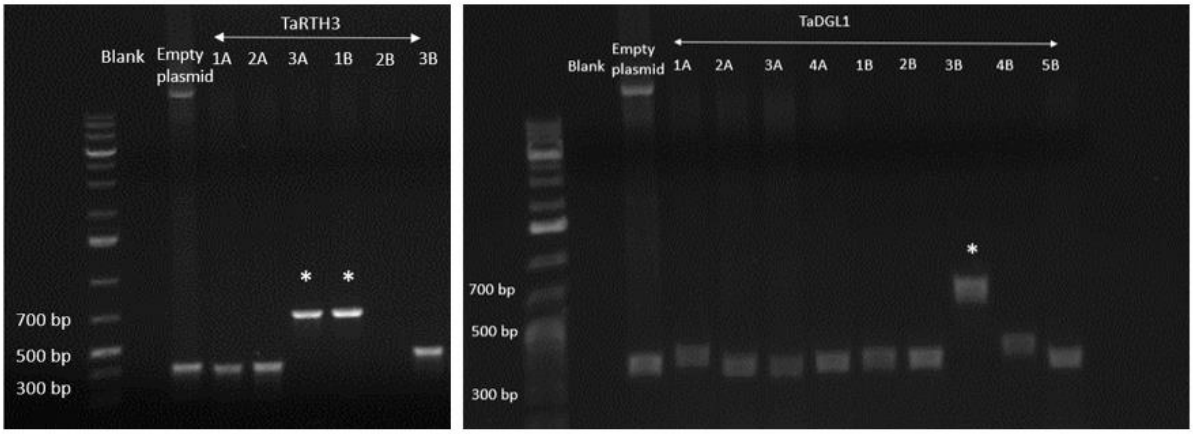


Figure A.8.2 Colony PCR to screen colonies for the presence of TaRTH3 or TaDGL1 gene fragments. Positive transformants are marked with an asterisk.

Table A.8.3 Summary statistics and unbalanced ANOVA analysis of LOG transformed root architecture data. Different letters represent significant differences as calculated by Fisher's l.s.d. test.

Log transformed root volume (cm3)					
Treatment	Mean	Standard error	Fisher's l.s.d		
BSMV:mcs4D	7.03	0.06	c		
BSMV:TaDGL1	6.84	0.05	b		
BSMV:TaRTH3	6.60	0.06	a		
Accumulated analysis of deviance					
Change	d.f.	s.s.	m.s.	F value	p value
+ Experiment	2	1.97	0.99	12.9	<.001
+ Treatment	2	1.96	0.98	12.83	<.001
Residual	65	4.96	0.08		
Total	69	8.89	0.13		
Log transformed total root length (cm)					
Treatment	Mean	Standard error	Fisher's l.s.d		
BSMV:mcs4D	4.446	0.0592	c		
BSMV:TaDGL1	4.274	0.05093	b		
BSMV:TaRTH3	4.117	0.05535	a		
Accumulated analysis of deviance					
Change	d.f.	s.s.	m.s.	F value	p value
+ Experiment	2	1.99	1.00	14.26	<.001
+ Treatment	2	1.15	0.57	8.21	<.001
Residual	65	4.54	0.07		
Total	69	7.69	0.11		
Log transformed number of root forks					
Treatment	Mean	Standard error	Fisher's l.s.d		
BSMV:mcs4D	2.263	0.08941	b		

BSMV:TaDGL1	2.063	0.07691	b		
BSMV:TaRTH3	1.76	0.08359	a		
Accumulated analysis of deviance					
Change	d.f.	s.s.	m.s.	F value	p value
+ Experiment	2	3.91	1.95	12.26	<.001
+ Treatment	2	2.76	1.38	8.64	<.001
Residual	65	10.37	0.16		
Total	69	17.03	0.25		
Log transformed number of root tips					
Treatment	Mean	Standard error	Fisher's l.s.d		
BSMV:mcs4D	2.086	0.06422	b		
BSMV:TaDGL1	1.968	0.05524	b		
BSMV:TaRTH3	1.801	0.06004	a		
Accumulated analysis of deviance					
Change	d.f.	s.s.	m.s.	F value	p value
+ Experiment	2	1.44	0.72	8.74	<.001
+ Treatment	2	0.88	0.44	5.33	0.007
Residual	65	5.35	0.08		
Total	69	7.66	0.11		

Investigating the effect of BSMV viral load on root phenotype

Methods:

To investigate whether viral load has an effect on root phenotype, RT-qPCR analysis was performed by targeting the BSMVα genome using primers as described in chapter 6.3.6. cDNA was prepared as outlined in chapter 6.3.6 and RT-qPCR was carried out using the PowerTrack™ SYBR Green Master Mix (ThermoFisher Scientific, USA) on the QuantStudio™ 6 Pro Real-Time PCR System (Applied Biosystems™, USA). Thermal cycling conditions were as follows: 95 °C for 2 mins followed by 35 cycles at 95 °C for 5 s and 60 °C for 45 s. Viral load was calculated relative to the reference sample BSMV:mcs4D-1-1 containing an unknown amount of viral cDNA. Data was square root transformed to achieve a normal distribution prior to statistical analysis.

Results and conclusions:

RT-qPCR analysis revealed that the relative viral load was significantly higher in BSMV:TaRTH3 inoculated plants compared to BSMV:TaDGL1 and BSMV:mcs4D inoculated plants (figure A.8.3 A). However, Pearson's correlation analysis revealed that relative viral load was not negatively correlated with any of the root architecture traits analysed in this experiment, suggesting that the small root phenotype is not a result of increased viral load

(figure A.8.3 B-D, table A.8.4). In fact, a positive correlation was found between relative viral load and wheat root volume in BSMV:TaRTH3 inoculated plants. The analyses are now being repeated with additional replicates and a known quantity of viral cDNA to confirm these initial findings.

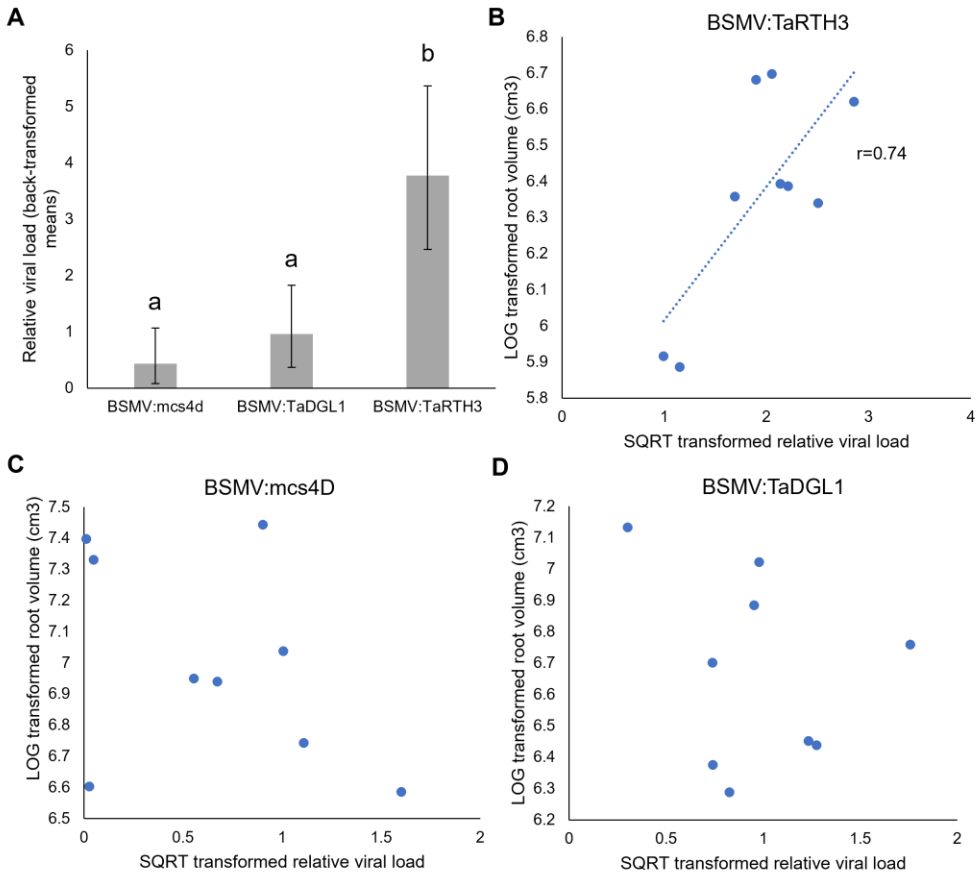


Figure A.8.3 Investigation of BSMV viral load and wheat root volume. A. Relative viral load of BSMVα in plants inoculated with BSMV:mcs4D, BSMV:TaDGL1 and BSMV:RTH3. Error bars represent back-transformed 95% confidence intervals. B-D. Correlation between relative viral load and root volume (cm^3).

Table A.8.4 Pearson's correlation coefficient analysis of BSMV viral load and root architecture traits.

Correlation	Pearson's correlation coefficient (r)	p value
BSMV:TaRTH3, n=9		
Relative viral load and root volume (cm^3)	0.74	0.02
Relative viral load and total root length (cm)	0.66	0.06
Relative viral load and number of root tips	0.55	0.13
Relative viral load and number of root forks	0.31	0.41
BSMV:TaDGL1, n=9		
Relative viral load and root volume (cm^3)	-0.25	0.51
Relative viral load and total root length (cm)	-0.27	0.48
Relative viral load and number of root tips	-0.24	0.53
Relative viral load and number of root forks	-0.30	0.43
BSMV:mcs4D, n=9		
Relative viral load and root volume (cm^3)	-0.40	0.28
Relative viral load and total root length (cm)	-0.27	0.48
Relative viral load and number of root tips	-0.24	0.53
Relative viral load and number of root forks	-0.30	0.43

Table A.8.5 Predicted mean proportions of roots with take-all lesions and accumulated analysis of deviance calculated using a GLM.

	LOGIT prediction of mean	back-transformed	Lower 95% confidence limit	back-transformed	Upper 95% confidence limit	back-transformed
Experiment 1						
Mock+ Gt	0.39	0.60	-0.09	0.48	0.87	0.70
BSMV:Mcs4+ Gt	0.70	0.67	0.15	0.54	1.24	0.78
Experiment 2						
Mock+ Gt	-1.24	0.22	-1.72	0.15	-0.75	0.32
BSMV:Mcs4+ Gt	-0.93	0.28	-1.55	0.18	-0.32	0.42

Change	d.f.	Deviance	Mean deviance	F value	p value
Experiment	1	42.87	42.87	32.54	<.001
+/- BSMV:mcs4d	1	1.23	1.23	0.93	0.34
Residual	47	61.92	1.32		
Total	49	106.01	2.16		

Table A.8.6 Ordinal regression analysis of take-all disease severity, represented by the percentage of roots with take-all lesions covering 0, 1, 2, 3, 4, or 5 cm.

Parameter	Estimate	s.e.	t(191)	t pr.	Antilog of estimate
Cut-point 0/1	-0.85	0.24	-3.57	<.001	0.43
Cut-point 1/2	-0.17	0.23	-0.75	0.45	0.84
Cut-point 2/3	0.50	0.23	2.15	0.03	1.65
Cut-point 3/4	1.39	0.27	5.23	<.001	4.00
Cut-point 4/5	2.62	0.39	6.80	<.001	13.77
Experiment 2	-1.84	0.27	-6.75	<.001	0.16
Treatment Wheat+Gt	-0.31	0.26	-1.19	0.24	0.73

Accumulated analysis of deviance

Change	d.f.	Deviance	Mean deviance	F value	p value
Experiment	1	58.30	58.30	53.57	<.001
+/- BSMV:mcs4D	1	1.51	1.51	1.38	0.24
Residual	191	207.89	1.09		
Total	193	267.69	1.39		

A.9 Cropping histories for field soils

Table A.9.1 Cropping history details for field soils used in experiments in chapter 7. Highlighted rows indicate the final crop prior to soil collection or field experimentation. Soils were collected the following September, before the next crop was drilled.

Rothamsted Farm field name	Sowing year	Crop species
Webb's	2013	Winter wheat
	2014	Winter wheat
	2015	Winter wheat
	2016	Winter oats
Meadows	2016	Winter oats
	2017	Winter wheat
	2018	Winter wheat
	2019	Winter oilseed rape

A.10 Seedling plant health experiments

Table A.10.1 Predicted mean proportions of roots with runner hyphae in the seedling health experiments. Accumulated analysis of deviance calculated using a GLM. Different letters represent significant differences as calculated by Tukey's multiple comparisons test.

Treatment	LOGIT prediction of mean (back-transformed)	Lower 95 % confidence limit (back-transformed)	Upper 95 % confidence limit (back-transformed)	Tukey's test (p<0.05)
Hereward + Gh	0.38 (0.59)	0.09 (0.52)	0.67 (0.66)	a
Hereward + Sc	1.39 (0.80)	1.04 (0.74)	1.74 (0.85)	b
Hereward + Um	1.27 (0.78)	0.93 (0.72)	1.61 (0.83)	b
Hereward + Gt	3.4 (0.97)	2.63 (0.93)	4.17 (0.98)	c

Table of accumulated analysis of deviance

Change	d.f.	Mean deviance	Deviance ratio	F value	p value
Experiment	2	60.111	30.055	9.89	<.001
Block	5	18.62	3.724	1.23	0.31
Fungal species	3	412.552	137.517	45.27	<.001
Residual	53	161.001	3.038		
Total	63	652.284	10.354		

Table A.10.2 Summary statistics and ANOVA analysis of the average shoot and root biomass per plant (mg) in the seedling health experiments. Different letters represent significant differences as calculated by Tukey's multiple comparisons test ($p<0.05$).

	Shoot biomass per plant (mg)					Root biomass per plant (mg)				
Treatment	Mean	Standard deviation	Standard error	Tukey's test		Mean	Standard deviation	Standard error	Tukey's test	
Hereward -	56.66	11.10	3.08	b		59.82	11.07	3.07	c	
Hereward + Gh	51.47	11.63	3.23	b		56.96	9.02	2.50	bc	
Hereward + Sc	49.1	9.36	2.60	b		49.06	12.91	3.58	b	
Hereward + Um	54.15	15.38	4.27	b		53.29	6.46	1.79	bc	
Hereward + Gt	28.49	3.83	1.06	a		17.54	12.35	3.43	a	
ANOVA: Shoot biomass per plant (mg)						ANOVA: Root biomass per plant (mg)				
Source of variation	d.f.	s.s.	m.s.	F value	p value	d.f.	s.s.	m.s.	F value	p value
Experiment	2	4461.14	2230.57	87.87		2	1236.97	618.48	5.55	
Experiment x block	10	253.86	25.39	0.5		10	1115.31	111.53	1.21	
Fungal species	4	6586.77	1646.69	32.21	<.001	4	15274.16	3818.54	41.39	<.001
Residual	48	2453.97	51.12			48	4427.89	92.25		
Total	64	13755.74				64	22054.33			

Table A.10.3 Summary statistics and ANOVA analysis of the total root length (cm) and root volume (cm^3) in seedling health experiment 3. Significant differences to the Hereward- control were calculated by Dunnett's post-hoc test. Dunnett's 95% confidence intervals: 259.9, 381.4 and 0.321, 0.616, respectively.

	Total root length (cm)					Root volume (cm^3)				
Treatment	Mean	Standard deviation	Standard error	Dunnett's post-hoc test		Mean	Standard deviation	Standard error	Dunnett's post-hoc test	
Hereward -	320.6	88.68	29.56	Reference level		0.4687	0.16	0.05	Reference level	
Hereward + Gh	411.9	71.10	23.70	p<0.05		0.5877	0.14	0.05		
Hereward + Sc	355.3	59.01	19.67			0.5228	0.12	0.04		
Hereward + Um	330.1	45.46	15.15			0.5027	0.12	0.04		
Hereward + Gt	72.5	28.26	9.99	p<0.05		0.1815	0.06	0.02	p<0.05	
ANOVA table										
Source of variation	d.f.	s.s.	m.s.	F value	p value	d.f.	s.s.	m.s.	F value	p value
Block	2	10284	5142	2.83		2	0.04686	0.02343	2.18	
Fungal species	4	624741	156185	85.95	<.001	4	0.91422	0.22855	21.24	<.001
Residual	8	14537	1817	0.41		8	0.08607	0.01076	0.63	
Block x Pot x Sample	29	128718	4439			29	0.49293	0.017		
Total	43	719013				43	1.4444			

Table A.10.4 Summary statistics and ANOVA analysis of the number of roots tips and forks in the seedling health experiment 3. Significant differences to the Hereward- control were calculated by Dunnett's post-hoc test. Dunnett's 95% confidence intervals: 484.0, 746.7 and 574, 1139, respectively.

	Number of root tips					Number of root forks				
Treatment	Mean	Standard deviation	Standard error	Dunnett's post-hoc test		Mean	Standard deviation	Standard error	Dunnett's post-hoc test	
Hereward -	615.3	151.40	50.46	Reference level		856.6	296.80	98.94	Reference level	
Hereward + Gh	753.1	196.00	65.32	p<0.05		1099.8	352.60	117.54		
Hereward + Sc	587.4	97.90	32.62			1004.4	266.90	88.95		
Hereward + Um	602.7	82.80	27.60			965.3	232.60	77.53		
Hereward + Gt	29.8	32.60	11.53	p<0.05		47.9	40.80	14.42	p<0.05	
ANOVA table						ANOVA table				
Source of variation	d.f.	s.s.	m.s.	F value	p value	d.f.	s.s.	m.s.	F value	p value
Block	2	19522	9761	1.15		2	82533	41267	1.05	
Fungal species	4	2828608	707152	83.26	<.001	4	6562308	1640577	41.69	<.001
Residual	8	67949	8494	0.45		8	314804	39350	0.49	
Block x Pot x Sample	29	542015	18690			29	2316506	79880		
Total	43	3222130				43	8693000			

A.11 Adult plant health experiments

A pilot experiment was carried out to investigate the colonisation ability of *G. hyphopodioides* on four group 1 winter milling wheats, chosen from current or recent AHDB recommended lists (https://ahdb.org.uk/rl) (table A.10.1). The winter wheat cultivar Hereward, known to support high levels of *G. tritici* and *G. hyphopodioides* was included as a control. Cultivars were tested in a 5-week seedling bioassay using sand, following the method described in chapter 2.4. There was no significant difference in *G. hyphopodioides* colonisation between any of the cultivars tested (GLM: F= 0.38, d.f. 4, 12, p=0.82). Therefore, Skyfall was chosen for the final experiment due to its current widespread use by UK farmers, thereby increasing the impact of the study.

Table A.11.1 List of winter wheat cultivars investigated for their ability to host *G. hyphopodioides*

Cultivar	Supplier	Years in AHDB list	Ability to promote *G. hyphopodioides* (Osborne et al. 2018)
Gallant	Syngenta	2010-2017	Medium
RGT Skyfall	RAGT	2015-2022	Unknown
Crusoe	Lima Grain (LG)	2015-2022	Low
RGT Illustrious	RAGT	2016-2022	Unknown
Hereward	Lima Grain (LG)	1991-2011	High

Table A.11.2 Summary of two-sample t-tests for the analysis of plant health parameters in *G. hyphopodioides* inoculated (Skyfall + Gh) and uninoculated plants (Skyfall).

	Plant height (cm)		Ear length (cm)		Flag leaf length (cm)	
Treatment	Skyfall	Skyfall + Gh	Skyfall	Skyfall + Gh	Skyfall	Skyfall + Gh
Mean	31.65	30.79	7.74	7.03	14.09	13.72
Standard deviation	4.32	3.89	7.512	2.105	1.77	2.46
Standard error	0.94	0.917	0.33	0.49	0.39	0.54
d.f.	37		37		40	
t value	0.65		1.21		0.56	
p value	0.519		0.233		0.579	
	Number of tillers		Days from booting to anthesis		Root biomass per plant (g)	
Treatment	Skyfall	Skyfall + Gh	Skyfall	Skyfall + Gh	Skyfall	Skyfall + Gh
Mean	6.44	6.22	18.9	17.25	4.99	5.05
Standard deviation	1.51	1.2	2.85	3.62	0.7	0.7
Standard error	0.5	0.4	0.64	0.9	0.27	0.27

d.f.	16	34	12
t value	0.35	1.53	-0.15
p value	0.734	0.135	0.885

Table A.11.3 Summary statistics and ANOVA analysis of the average Chlorophyll Content Index (CCI) of the main flag leaf at different stages of adult plant growth.

Growth stage	Treatment	Mean	Standard deviation	Standard error	
Booting (GS45)	Skyfall	29.43	3.236	0.742	
	Skyfall + Gh	27.24	4.286	1.04	
Ear Emergence (GS51)	Skyfall	31.92	5.075	1.135	
	Skyfall + Gh	30.24	5.585	1.316	
Flowering (GS61)	Skyfall	28.61	7.1	1.549	
	Skyfall + Gh	29.85	5.942	1.401	
ANOVA table					
Source of variation	d.f.	s.s.	m.s.	F value	p value
Block stratum					
	6	1072.45	178.74	5.8	
Block x pot stratum					
+/- Gh	1	63.82	63.82	2.07	0.2
Residual	6	184.99	30.83	0.52	
Block x pot x plant stratum					
	28	1650.91	58.96	5.38	
Block x pot x plant x growth stage stratum					
Growth stage	2	107.17	53.59	4.89	0.01
Growth stage x +/-Gh	2	49.65	24.83	2.26	0.112
Residual	67	734.93	10.97		
Total	112	3345.31			

Table A.11.4 ITS sequencing and species identification of fungal colonies isolated from wheat roots in the adult health experiment

Pot	Treatment	Sample time	Species identification	NCBI BLAST match	Percentage identity (%)	Query cover (%)
9	Skyfall	May	*G. hyphopodioides*	*Gaeumannomyces hyphopodioides* strain CPC 26267 18S ribosomal RNA gene, partial sequence; internal transcribed spacer 1, 5.8S ribosomal RNA gene, and internal transcribed spacer 2, complete sequence; and 28S ribosomal RNA gene, partial sequence	100	100
9	Skyfall	May	*G. hyphopodioides*	*Gaeumannomyces hyphopodioides* strain CPC 26267 18S ribosomal RNA gene, partial sequence; internal transcribed spacer 1, 5.8S ribosomal RNA gene, and internal transcribed spacer 2, complete sequence; and 28S ribosomal RNA gene, partial sequence	99.61	100
9	Skyfall	May	*G. hyphopodioides*	*Gaeumannomyces hyphopodioides* strain CPC 26267 18S ribosomal RNA gene, partial sequence; internal transcribed spacer 1, 5.8S ribosomal RNA gene, and internal transcribed spacer 2, complete sequence; and 28S ribosomal RNA gene, partial sequence	99.61	100
9	Skyfall	May	*Magnaporthaceae sp.*	*Magnaporthaceae* sp. CPC 26284 18S ribosomal RNA gene, partial sequence; internal transcribed spacer 1, 5.8S ribosomal RNA gene, and internal transcribed spacer 2, complete sequence; and 28S ribosomal RNA gene, partial sequence	100	99
11	Skyfall + Gh	May	*G. hyphopodioides*	*Gaeumannomyces hyphopodioides* strain CPC 26267 18S ribosomal RNA gene, partial sequence; internal transcribed spacer 1, 5.8S ribosomal RNA gene, and internal transcribed spacer 2, complete sequence; and 28S ribosomal RNA gene, partial sequence	99.61	100

11	Skyfall + Gh	May	*G. tritici*	*Gaeumannomyces tritici* strain CPC 26280 18S ribosomal RNA gene, partial sequence; internal transcribed spacer 1, 5.8S ribosomal RNA gene, and internal transcribed spacer 2, complete sequence; and 28S ribosomal RNA gene, partial sequence	99.8	100
11	Skyfall + Gh	May	*G. tritici*	*Gaeumannomyces tritici* strain CPC 26280 18S ribosomal RNA gene, partial sequence; internal transcribed spacer 1, 5.8S ribosomal RNA gene, and internal transcribed spacer 2, complete sequence; and 28S ribosomal RNA gene, partial sequence	100	100
11	Skyfall + Gh	May	*G. tritici*	*Gaeumannomyces tritici* strain CPC 26280 18S ribosomal RNA gene, partial sequence; internal transcribed spacer 1, 5.8S ribosomal RNA gene, and internal transcribed spacer 2, complete sequence; and 28S ribosomal RNA gene, partial sequence	100	100
11	Skyfall + Gh	May	*Uncultured Podospora*	Uncultured *Podospora* genomic DNA containing 18S rRNA gene, ITS1, 5.8S rRNA gene, ITS2 and 28S rRNA gene, clone 09J70C37 (MOTU114)	99.8	100
31	Skyfall	July	*Epicoccum nigrum*	*Epicoccum nigrum* isolate 18 small subunit ribosomal RNA gene, partial sequence; internal transcribed spacer 1, 5.8S ribosomal RNA gene, and internal transcribed spacer 2, complete sequence; and large subunit ribosomal RNA gene, partial sequence	100	100
31	Skyfall	July	*G. tritici*	*Gaeumannomyces tritici* strain CPC 26280 18S ribosomal RNA gene, partial sequence; internal transcribed spacer 1, 5.8S ribosomal RNA gene, and internal transcribed spacer 2, complete sequence; and 28S ribosomal RNA gene, partial sequence	100	100

31	Skyfall	July	*G. tritici*	*Gaeumannomyces tritici* strain CPC 26280 18S ribosomal RNA gene, partial sequence; internal transcribed spacer 1, 5.8S ribosomal RNA gene, and internal transcribed spacer 2, complete sequence; and 28S ribosomal RNA gene, partial sequence	100	100
4	Skyfall	July	*Magnaporthaceae sp.*	*Magnaporthaceae* sp. CPC 26284 18S ribosomal RNA gene, partial sequence; internal transcribed spacer 1, 5.8S ribosomal RNA gene, and internal transcribed spacer 2, complete sequence; and 28S ribosomal RNA gene, partial sequence	100	99
4	Skyfall	July	*Periconia sp.*	*Periconia* sp. isolate EW_ITS1F_131 internal transcribed spacer 1, partial sequence; 5.8S ribosomal RNA gene and internal transcribed spacer 2, complete sequence; and large subunit ribosomal RNA gene, partial sequence	100	100
18	Skyfall + Gh	July	*Epicoccum layuense*	*Epicoccum layuense* isolate 17 small subunit ribosomal RNA gene, partial sequence; internal transcribed spacer 1, 5.8S ribosomal RNA gene, and internal transcribed spacer 2, complete sequence; and large subunit ribosomal RNA gene, partial sequence	100	100
18	Skyfall + Gh	July	*G. hyphopodioides*	*Gaeumannomyces hyphopodioides* strain CPC 26267 18S ribosomal RNA gene, partial sequence; internal transcribed spacer 1, 5.8S ribosomal RNA gene, and internal transcribed spacer 2, complete sequence; and 28S ribosomal RNA gene, partial sequence	99.61	100
18	Skyfall + Gh	July	*G. hyphopodioides*	*Gaeumannomyces hyphopodioides* strain CPC 26267 18S ribosomal RNA gene, partial sequence; internal transcribed spacer 1, 5.8S ribosomal RNA gene, and internal transcribed spacer 2, complete sequence; and 28S ribosomal RNA gene, partial sequence	99.61	100

30	Skyfall + Gh	July	*Magnaporthaceae sp.*	*Magnaporthaceae* sp. CPC 26284 18S ribosomal RNA gene, partial sequence; internal transcribed spacer 1, 5.8S ribosomal RNA gene, and internal transcribed spacer 2, complete sequence; and 28S ribosomal RNA gene, partial sequence	100	99
18	Skyfall + Gh	July	*Periconia macrospinoa*	*Periconia macrospinosa* strain ZMXR37 small subunit ribosomal RNA gene, partial sequence; internal transcribed spacer 1, 5.8S ribosomal RNA gene, and internal transcribed spacer 2, complete sequence; and large subunit ribosomal RNA gene, partial sequence	100	100
18	Skyfall + Gh	July	*Periconia macrospinosa*	*Periconia macrospinosa* strain ZMXR37 small subunit ribosomal RNA gene, partial sequence; internal transcribed spacer 1, 5.8S ribosomal RNA gene, and internal transcribed spacer 2, complete sequence; and large subunit ribosomal RNA gene, partial sequence	100	100

A.12 Latitude® sensitivity experiments

Table A.12.1 Average colony diameter of *Magnaporthaceae* fungi in the presence and absence of Latitude®. Different letters represent significant differences as calculated by Tukey's multiple comparisons test ($p<0.05$).

Treatment	Mean	Standard deviation	Standard error	Tukey's test	
PDA + Gh	43.83	1.211	0.4944	d	
PDA + Lat + Gh	43.58	0.97	0.3962	d	
PDA+ Um	36.25	0.758	0.3096	c	
PDA + Lat + Um	35.08	1.882	0.7683	c	
PDA + Sc	24.58	0.585	0.2386	b	
PDA + Lat + Sc	23.33	0.408	0.1667	b	
PDA+ Gt	41.92	1.772	0.7236	d	
PDA + Lat + Gt	8.5	0.632	0.2582	a	
ANOVA table					
Source of variation	d.f.	s.s.	m.s.	F value	p value
Experiment stratum					
	1	1.505	1.505	1.91	
Experiment x block stratum					
	4	3.146	0.786	0.57	
Experiment x block x plate stratum					
Treatment	1	976.505	976.505	708.73	<.001
Species	3	3135.016	1045.005	758.44	<.001
Treatment x Species	3	2382.474	794.158	576.38	<.001
Residual	35	48.224	1.378		
Total	47	6546.87			

Table A.12.2 Proportion of roots with runner hyphae in an *in planta* Latitude® sensitivity test. Accumulated analysis of deviance calculated using a GLM. Different letters represent significant differences as calculated by Tukey's multiple comparisons test ($p<0.05$). *Gt = G. tritici,* Gh = *G. hyphopodioides*, Sc= *S. cylindrosporus*, Um = Unnamed *Magnaporthaceae* sp., d.f.=degrees of freedom.

Treatment	LOGIT prediction of mean (back-transformed)	Lower 95 % confidence limit (back-transformed)	Upper 95 % confidence limit (back-transformed)	Tukey's test
Hereward +Gh	0.67 (0.66)	0.08 (0.52)	1.27 (0.78)	bc
Hereward +Gh +Lat	0.55 (0.63)	0 (0.5)	1.11 (0.75)	b
Hereward +Sc	1.99 (0.88)	1.14 (0.76)	2.84 (0.94)	cd
Hereward +Sc +Lat	1.32 (0.79)	0.62 (0.65)	2.01 (0.88)	bcd
Hereward +Um	2.29 (0.91)	1.33 (0.79)	3.24 (0.96)	d
Hereward +Um +Lat	2.47 (0.92)	1.43 (0.81)	3.52 (0.97)	d
Hereward +Gt	3.44 (0.97)	1.86 (0.87)	5.02 (0.99)	d
Hereward +Gt +Lat	-2.75 (0.06)	-3.94 (0.02)	-1.57 (0.17)	a

Table of accumulated analysis of deviance					
Change	d.f.	Mean deviance	Deviance ratio	F value	p value
Fungal sp.	3	294.74	98.25	16.92	<.001
+/- Latitude	1	217.74	217.74	37.50	<.001
Fungal sp. x Latitude	3	377.66	125.89	21.68	<.001
Residual	40	232.27	5.81		
Total	47	1122.41	23.88		

Table A.12.3 Ordinal logistic regression analysis of colonisation severity in the *in planta* Latitude® sensitivity test. p values are differences compared with the reference level: Fungal_sp Gh- Fungicide. Gh = *G. hyphopodioides*, Sc= *S. cylindrosporus*, Um = Unnamed *Magnaporthaceae* sp., d.f.=degrees of freedom.

Parameter	Estimate	s.e.	t(85)	p value	Antilog of estimate
Cut-point 0/1	-1.77	0.35	-5.07	<.001	0.17
Cut-point 1/2	-0.66	0.32	-2.05	0.04	0.52
Cut-point 2/3	1.07	0.33	3.26	0.00	2.91
Cut-point 3/4	3.19	0.43	7.43	<.001	24.21
Fungal_sp Sc	0.39	0.44	0.88	0.38	1.47
Fungal_sp Um	0.71	0.44	1.62	0.11	2.04
Fungal_sp Gt	4.54	0.60	7.53	<.001	93.38
+Fungicide	-0.72	0.43	-1.67	0.10	0.49
Fungal_sp Sc.+Fungicide	0.44	0.62	0.70	0.48	1.55
Fungal_sp Um.+Fungicide	0.24	0.61	0.40	0.69	1.27
Fungal_sp Gt.+Fungicide	-8.12	0.96	-8.43	<.001	0.00

Accumulated analysis of deviance					
Change	d.f.	Deviance	Mean deviance	Deviance ratio	p value
Fungal species	3	23.31	7.77	1.78	0.16
Fungicide	1	194.37	194.37	44.58	<.001
Fungal species x fungicide	3	643.82	214.61	49.22	<.001
Residual	85	370.64	4.36		
Total	92	1232.14	13.39		

A.13 Susceptibility of elite winter wheat varieties to *G. hyphopodioides* colonisation

Table A.13.1 The proportion of roots with *G. hyphopodioides* runner hyphae in the first cultivar susceptibility test. Accumulated analysis of deviance calculated using a GLM.

Treatment	LOGIT prediction of mean (back-transformed)	Lower 95 % confidence limit (back-transformed)	Upper 95 % confidence limit (back-transformed)		
Avalon	0.52 (0.63)	0.2 (0.55)	0.85 (0.7)		
Alchemy	0.58 (0.64)	0.26 (0.56)	0.9 (0.71)		
Einstein	0.68 (0.66)	0.31 (0.58)	1.04 (0.74)		
Conqueror	0.68 (0.66)	0.33 (0.58)	1.04 (0.74)		
Denman	0.68 (0.66)	0.34 (0.59)	1.02 (0.74)		
Hereward	0.72 (0.67)	0.35 (0.59)	1.08 (0.75)		
Scout	0.79 (0.69)	0.42 (0.6)	1.17 (0.76)		
Hereford	0.86 (0.7)	0.5 (0.62)	1.21 (0.77)		
KWS Croft	0.87 (0.7)	0.5 (0.62)	1.24 (0.78)		
Player	0.93 (0.72)	0.58 (0.64)	1.28 (0.78)		
Cordiale	0.94 (0.72)	0.55 (0.64)	1.33 (0.79)		
KWS Kielder	0.98 (0.73)	0.6 (0.65)	1.36 (0.8)		
Gallant	1.08 (0.75)	0.72 (0.67)	1.45 (0.81)		
KWS Santiago	1.11 (0.75)	0.72 (0.67)	1.5 (0.82)		
Invicta	1.11 (0.75)	0.7 (0.67)	1.53 (0.82)		
Cadenza	1.3 (0.79)	0.89 (0.71)	1.71 (0.85)		
Table of accumulated analysis of deviance					
Change	d.f.	Mean deviance	Deviance ratio	F value	p value
Cultivar	15	42.86	2.86	1.36	0.19
Residual	64	134.32	2.10		
Total	79	177.18	2.24		

Table A.13.2 The proportion of roots with *G. hyphopodioides* runner hyphae in a repeat cultivar susceptibility test with reduced inoculum levels. Accumulated analysis of deviance calculated using a GLM.

Treatment	LOGIT prediction of mean (back-transformed)	Lower 95 % confidence limit (back-transformed)	Upper 95 % confidence limit (back-transformed)
Alchemy	-4.37 (0.01)	-6.59 (0)	-2.15 (0.1)
Avalon	-4.57 (0.01)	-6.8 (0)	-2.34 (0.09)
Cadenza	-3.44 (0.03)	-4.74 (0.01)	-2.14 (0.11)
Conqueror	-2.74 (0.06)	-3.77 (0.02)	-1.72 (0.15)
Hereward	-2.82 (0.06)	-3.88 (0.02)	-1.76 (0.15)
Kielder	-2.83 (0.06)	-3.93 (0.02)	-1.74 (0.15)
Scout	-3.11 (0.04)	-4.3 (0.01)	-1.93 (0.13)

Table of accumulated analysis of deviance

Change	d.f.	Mean deviance	Deviance ratio	F value	p value
Cultivar	6	21.544	3.591	0.93	0.492
Residual	21	80.792	3.847		
Total	27	102.336	3.79		

References

Aberra, M. B., Seah, S., & Sivasithamparam, K. (1998). Suppression of the take-all fungus (Gaeumannomyces graminis var. tritici) by a sterile red fungus through induced resistance in wheat (Triticum aestivum) seedling roots. *Soil Biology and Biochemistry*, *30*(10–11), 1457–1461. https://doi.org/10.1016/S0038-0717(97)00225-3

Ajaz, S., Benbow, H. R., Christodoulou, T., Uauy, C., & Doohan, F. M. (2021). Evaluation of the susceptibility of modern, wild, ancestral, and mutational wheat lines to Septoria tritici blotch disease. *Plant Pathology*, *70*(5), 1123–1137. https://doi.org/10.1111/PPA.13369

Allen, A. M., Winfield, M. O., Burridge, A. J., Downie, R. C., Benbow, H. R., Barker, G. L. A., Wilkinson, P. A., Coghill, J., Waterfall, C., Davassi, A., Scopes, G., Pirani, A., Webster, T., Brew, F., Bloor, C., Griffiths, S., Bentley, A. R., Alda, M., Jack, P., … Edwards, K. J. (2017). Characterization of a Wheat Breeders' Array suitable for high-throughput SNP genotyping of global accessions of hexaploid bread wheat (Triticum aestivum). *Plant Biotechnology Journal*, *15*(3), 390–401. https://doi.org/10.1111/pbi.12635

Ambawat, S., Sharma, P., Yadav, N. R., & Yadav, R. C. (2013). MYB transcription factor genes as regulators for plant responses: an overview. *Physiology and Molecular Biology of Plants*, *19*(3), 307–321. https://doi.org/10.1007/S12298-013-0179-1

Anderson, N. A. (1982). The Genetics and Pathology of Rhizoctonia Solani. *Annual Review of Phytopathology*, *20*(1), 329–347. https://doi.org/10.1146/annurev.py.20.090182.001553

Appels, R., Eversole, K., Feuillet, C., Keller, B., Rogers, J., Stein, N., Pozniak, C. J., Choulet, F., Distelfeld, A., Poland, J., Ronen, G., Barad, O., Baruch, K., Keeble-Gagnère, G., Mascher, M., Ben-Zvi, G., Josselin, A. A., Himmelbach, A., Balfourier, F., … Wang, L. (2018). Shifting the limits in wheat research and breeding using a fully annotated reference genome. *Science*, *361*(6403). https://doi.org/10.1126/science.aar7191

Aranda, P. S., Lajoie, D. M., & Jorcyk, C. L. (2012). Bleach gel: A simple agarose gel for analyzing RNA quality. *Electrophoresis*, *33*(2), 366–369. https://doi.org/10.1002/elps.201100335

Asari, S., Matzén, S., Petersen, M. A., Bejai, S., & Meijer, J. (2016). Multiple effects of Bacillus amyloliquefaciens volatile compounds: Plant growth promotion and growth inhibition of phytopathogens. *FEMS Microbiology Ecology*, *92*(6), 1–11. https://doi.org/10.1093/femsec/fiw070

Ashagre, H., Zaltzman, D., Idan-Molakandov, A., Romano, H., Tzfadia, O., & Harpaz-Saad,

S. (2021). FASCICLIN-LIKE 18 Is a New Player Regulating Root Elongation in Arabidopsis thaliana. *Frontiers in Plant Science*, *12*, 391. https://doi.org/10.3389/FPLS.2021.645286/BIBTEX

Asher, M. J. C., & Shipton, P. J. (1981). *Biology and control of take-all* (M. J. C. Asher & P. J. Shipton (eds.)). London Academic Press.

Asseng, S., Ewert, F., Martre, P., Rötter, R. P., Lobell, D. B., Cammarano, D., Kimball, B. A., Ottman, M. J., Wall, G. W., White, J. W., Reynolds, M. P., Alderman, P. D., Prasad, P. V. V., Aggarwal, P. K., Anothai, J., Basso, B., Biernath, C., Challinor, A. J., De Sanctis, G., … Zhu, Y. (2015). Rising temperatures reduce global wheat production. *Nature Climate Change*, *5*(2), 143–147. https://doi.org/10.1038/nclimate2470

Augustin, C., Jacob, H. J., & Werner, A. (1997). Effects on growth of wheat plants of isolates of Gaeumannomyces / Phialophora -complex fungi in different conditions of soil moisture, temperature, and photoperiod. *European Journal of Plant Pathology*, *103*, 417–426. https://doi.org/10.1023/A:1008621018486

Avery, S. V., Singleton, I., Magan, N., & Goldman, G. H. (2019). The fungal threat to global food security. *Fungal Biology*, *123*(8), 555–557. https://doi.org/10.1016/j.funbio.2019.03.006

Bacete, L., Mélida, H., Miedes, E., & Molina, A. (2018). Plant cell wall-mediated immunity: cell wall changes trigger disease resistance responses. *Plant Journal*, *93*(4), 614–636. https://doi.org/10.1111/tpj.13807

Bailey, D. J., Paveley, N., Pillinger, C., Foulkes, J., Spink, J., & Gilligan, C. A. (2005). Epidemiology and Chemical Control of Take-All on Seminal and Adventitious Roots of Wheat. *Phytopathology*, *95*(1), 62–68. https://doi.org/10.1094/PHYTO-95-0062

Balis, C. (1970). A comparative study of Phialophora radicicola, an avirulent fungal root parasite of grasses and cereals. *Annals of Applied Biology*, *66*(1), 59–73. https://doi.org/10.1111/j.1744-7348.1970.tb04603.x

Ban, Y., Tang, M., Chen, H., Xu, Z., Zhang, H., & Yang, Y. (2012). The Response of Dark Septate Endophytes (DSE) to Heavy Metals in Pure Culture. *PLoS ONE*, *7*(10). https://doi.org/10.1371/journal.pone.0047968

Barnett, S. J., Ballard, R. A., & Franco, C. M. M. (2019). Field assessment of microbial inoculants to control Rhizoctonia root rot on wheat. *Biological Control*, *132*, 152–160. https://doi.org/10.1016/j.biocontrol.2019.02.019

Basińska-Barczak, A., Błaszczyk, L., & Szentner, K. (2020). Plant Cell Wall Changes in Common Wheat Roots as a Result of Their Interaction with Beneficial Fungi of Trichoderma. *Cells*, *9*(10). https://doi.org/10.3390/cells9102319

Bateman, G., Gutteridge, R., & John Jenkyn. (2006). *Take-all in winter wheat- management guidelines (HGCA)*. http://adlib.everysite.co.uk/adlib/defra/content.aspx?id=000HK277ZX.0FCGEHKLWPS4KF

Bateman, G. L., Gutteridge, R. J., Jenkyn, J. F., & Self, M. M. (2008). Effects of fluquinconazole and silthiofam, applied as seed treatments to single or consecutive crops of wheat, on take-all epidemic development and grain yields. *Annals of Applied Biology*, *152*(2), 243–254. https://doi.org/10.1111/j.1744-7348.2007.00204.x

Bateman, G. L., Ward, E., Hornby, D., & Gutteridge, R. J. (1997). Comparisons of isolates of the take-all fungus, Gaeumannomyces graminis var. tritici, from different cereal sequences using DNA probes and non-molecular methods. *Soil Biology and Biochemistry*, *29*(8), 1225–1232. https://doi.org/10.1016/S0038-0717(97)00025-4

Bemena, L. D., Min, K., Konopka, J. B., & Neiman, A. M. (2021). A conserved machinery underlies the synthesis of a chitosan layer in the Candida chlamydospore cell wall. *BioRxiv*, 2021.01.19.427374. https://doi.org/10.1101/2021.01.19.427374

Benjamini, Y., & Hochberg, Y. (1995). Controlling the False Discovery Rate: A Practical and Powerful Approach to Multiple Testing. *Journal of the Royal Statistical Society: Series B (Methodological)*, *57*(1), 289–300. https://doi.org/10.1111/J.2517-6161.1995.TB02031.X

Bennypaul, H. S., Mutti, J. S., Rustgi, S., Kumar, N., Okubara, P. A., & Gill, K. S. (2012). Virus-induced gene silencing (VIGS) of genes expressed in root, leaf, and meiotic tissues of wheat. *Functional and Integrative Genomics*, *12*(1), 143–156. https://doi.org/10.1007/s10142-011-0245-0

Bi, C., Chen, F., Jackson, L., Gill, B. S., & Li, W. (2011). Expression of Lignin Biosynthetic Genes in Wheat during Development and upon Infection by Fungal Pathogens. *Plant Molecular Biology Reporter*, *29*(1), 149–161. https://doi.org/10.1007/s11105-010-0219-8

Bithell, S. L., McKay, A., Butler, R. C., Herdina, Ophel-Keller, K., Hartley, D., & Cromey, M. G. (2012). Predicting Take-All Severity in Second-Year Wheat Using Soil DNA Concentrations of *Gaeumannomyces graminis* var. *tritici* Determined with qPCR. *Plant Disease*, *96*(3), 443–451. https://doi.org/10.1094/PDIS-05-11-0445

Bolger, A. M., Lohse, M., & Usadel, B. (2014). Trimmomatic: A flexible trimmer for Illumina sequence data. *Bioinformatics*, *30*(15), 2114–2120. https://doi.org/10.1093/bioinformatics/btu170

Boller, T., & Felix, G. (2009). A Renaissance of Elicitors: Perception of Microbe-Associated Molecular Patterns and Danger Signals by Pattern-Recognition Receptors. *Annual Review of Plant Biology*, *60*(1), 379–406. https://doi.org/10.1146/annurev.arplant.57.032905.105346

Bonnot, T., Gillard, M., & Nagel, D. (2019). A Simple Protocol for Informative Visualization of Enriched Gene Ontology Terms. *BIO-PROTOCOL*, *9*(22). https://doi.org/10.21769/BIOPROTOC.3429

Bouton, C., King, R. C., Chen, H., Azhakanandam, K., Bieri, S., Hammond-Kosack, K. E., & Kanyuka, K. (2018). Foxtail mosaic virus: A Viral Vector for Protein Expression in Cereals. *Plant Physiology*, *177*(4), 1352–1367. https://doi.org/10.1104/PP.17.01679

Bowyer, P., Clarke, B. R., Lunness, P., Daniels, M. J., & Osbourn, A. E. (1995). Host range of a plant pathogenic fungus determined by a saponin detoxifying enzyme. *Science*, *267*(5196), 371–374. https://doi.org/10.1126/science.7824933

Bowyer, P., Musker, R., Osbourn, A. E., Clarke, B., Caten, C., & Daniels, M. J. (1992). Production of mutants of Gaeumannomyces graminis var. tritici and var. avenae by 4-nitroquinolene-oxide treatment of protoplasts. *Fungal Genetics Reports*, *39*, 3. https://doi.org/10.4148/1941-4765.1429

Brennan, C. J., Benbow, H. R., Mullins, E., & Doohan, F. M. (2019). A review of the known unknowns in the early stages of septoria tritici blotch disease of wheat. *Plant Pathology*, *68*(8), 1427–1438. https://doi.org/10.1111/ppa.13077

Brilli, F., Loreto, F., & Baccelli, I. (2019). Exploiting plant volatile organic compounds (VOCS) in agriculture to improve sustainable defense strategies and productivity of crops. *Frontiers in Plant Science*, *10*, 1–8. https://doi.org/10.3389/fpls.2019.00264

Bryan, G. T., Daniels, M. J., & Osbourn, A. E. (1995). Comparison of fungi within the Gaeumannomyces-Phialophora complex by analysis of ribosomal DNA sequences. *Applied and Environmental Microbiology*, *61*(2), 681–689. https://doi.org/10.1128/aem.61.2.681-689.1995

Cabral, A., Groenewald, J. Z., Rego, C., Oliveira, H., & Crous, P. W. (2012). Cylindrocarpon root rot: Multi-gene analysis reveals novel species within the Ilyonectria radicicola

species complex. *Mycological Progress*, *11*(3), 655–688. https://doi.org/10.1007/s11557-011-0777-7

Cai, Q., He, B., Wang, S., Fletcher, S., Niu, D., Mitter, N., Birch, P. R. J., & Jin, H. (2021). Message in a Bubble: Shuttling Small RNAs and Proteins Between Cells and Interacting Organisms Using Extracellular Vesicles. *Annual Review of Plant Biology*, *72*, 497–524. https://doi.org/10.1146/ANNUREV-ARPLANT-081720-010616

Cai, Q., Qiao, L., Wang, M., He, B., Lin, F.-M., Palmquist, J., Huang, S.-D., & Jin, H. (2018). Plants send small RNAs in extracellular vesicles to fungal pathogen to silence virulence genes. *Science*, *360*, 1126–1129. https://doi.org/10.1126/science.aar4142

Cambaza, E. (2018). Comprehensive Description of Fusarium graminearum Pigments and Related Compounds. *Foods*, *7*(10), 165. https://doi.org/10.3390/FOODS7100165

Canarini, A., Kaiser, C., Merchant, A., Richter, A., & Wanek, W. (2019). Root exudation of primary metabolites: Mechanisms and their roles in plant responses to environmental stimuli. *Frontiers in Plant Science*, *10*(157). https://doi.org/10.3389/fpls.2019.00157

Carmo-Silva, E., Andralojc, P. J., Scales, J. C., Driever, S. M., Mead, A., Lawson, T., Raines, C. A., & Parry, M. A. J. (2017). Phenotyping of field-grown wheat in the UK highlights contribution of light response of photosynthesis and flag leaf longevity to grain yield. *Journal of Experimental Botany*, *68*(13), 3473–3486. https://doi.org/10.1093/JXB/ERX169

Carrión, V. J., Perez-Jaramillo, J., Cordovez, V., Tracanna, V., De Hollander, M., Ruiz-Buck, D., Mendes, L. W., van Ijcken, W. F. J., Gomez-Exposito, R., Elsayed, S. S., Mohanraju, P., Arifah, A., van der Oost, J., Paulson, J. N., Mendes, R., van Wezel, G. P., Medema, M. H., & Raaijmakers, J. M. (2019). Pathogen-induced activation of disease-suppressive functions in the endophytic root microbiome. *Science*, *366*(6465), 606–612. https://doi.org/10.1126/science.aaw9285

Carvajal-Yepes, M., Cardwell, K., Nelson, A. K., Garrett, A., Giovani, B., Saunders, D. G. O., Kamoun, S., Legg, J. P., Verdier, V., Lessel, J., Neher, R. A., Day, R., Pardey, P., Gullino, M. L., Records, A. R., Bextine, B., Leach, J. E., Staiger, S., & Tohme, J. (2020). A global surveillance system for crop diseases. *Science*, *364*(6447), 1237–1240. https://science.sciencemag.org/content/364/6447/1237.long

Chakraborty, S., & Newton, A. C. (2011). Climate change, plant diseases and food security: an overview. *Plant Pathology*, *60*(1), 2–14. https://doi.org/10.1111/j.1365-3059.2010.02411.x

Chakraborty, Sukumar, & Datta, S. (2003). How will plant pathogens adapt to host plant resistance at elevated CO2 under a changing climate? *New Phytologist*, *159*(3), 733–742. https://doi.org/10.1046/j.1469-8137.2003.00842.x

Chanclud, E., & Morel, J. B. (2016). Plant hormones: a fungal point of view. *Molecular Plant Pathology*, *17*(8), 1289–1297. https://doi.org/10.1111/MPP.12393

Chareesri, A., De Deyn, G. B., Sergeeva, L., Polthanee, A., & Kuyper, T. W. (2020). Increased arbuscular mycorrhizal fungal colonization reduces yield loss of rice (Oryza sativa L.) under drought. *Mycorrhiza*, *30*(2–3), 315–328. https://doi.org/10.1007/S00572-020-00953-Z/FIGURES/5

Chen, J., Upadhyaya, N. M., Ortiz, D., Sperschneider, J., Li, F., Bouton, C., Breen, S., Dong, C., Xu, B., Zhang, X., Mago, R., Newell, K., Xia, X., Bernoux, M., Taylor, J. M., Steffenson, B., Jin, Y., Zhang, P., Kanyuka, K., … Dodds, P. N. (2017). Loss of AvrSr50 by somatic exchange in stem rust leads to virulence for Sr50 resistance in wheat. *Science*, *358*(6370), 1607–1610. https://doi.org/10.1126/science.aao4810

Chen, X., Li, C., Wang, H., & Guo, Z. (2019). WRKY transcription factors: evolution, binding, and action. *Phytopathology Research 2019 1:1*, *1*(1), 1–15. https://doi.org/10.1186/S42483-019-0022-X

Chitarra, W., Siciliano, I., Ferrocino, I., Gullino, M. L., & Garibaldi, A. (2015). Effect of elevated atmospheric CO2 and temperature on the disease severity of rocket plants caused by fusarium wilt under phytotron conditions. *PLoS ONE*, *10*(10). https://doi.org/10.1371/journal.pone.0140769

Choudhary, D. K., Prakash, A., & Johri, B. N. (2007). Induced systemic resistance (ISR) in plants: Mechanism of action. *Indian Journal of Microbiology*, *47*(4), 289–297. https://doi.org/10.1007/s12088-007-0054-2

Choulet, F., Alberti, A., Theil, S., Glover, N., Barbe, V., Daron, J., Pingault, L., Sourdille, P., Couloux, A., Paux, E., Leroy, P., Mangenot, S., Guilhot, N., Le Gouis, J., Balfourier, F., Alaux, M., Jamilloux, V., Poulain, J., Durand, C., … Feuillet, C. (2014). Structural and functional partitioning of bread wheat chromosome 3B. *Science*, *345*(6194). https://doi.org/10.1126/science.1249721

Chudinova, E., Platonov, V., Elansky, S., Alexandrova, A., Kokaeva, L., & Krutyakov, Y. (2019). First report of Ilyonectria crassa on potato. *Journal of Plant Pathology*, *101*(4), 1293–1294. https://doi.org/10.1007/s42161-019-00355-x

Compant, S., Samad, A., Faist, H., & Sessitsch, A. (2019). A review on the plant microbiome: Ecology, functions, and emerging trends in microbial application. *Journal of Advanced Research*, *19*, 29–37. https://doi.org/10.1016/j.jare.2019.03.004

Constantin, M. E., de Lamo, F. J., Vlieger, B. V., Rep, M., & Takken, F. L. W. (2019). Endophyte-Mediated Resistance in Tomato to Fusarium oxysporum Is Independent of ET, JA, and SA. *Frontiers in Plant Science*, *10*, 979. https://doi.org/10.3389/fpls.2019.00979

Cook, R. J. (2003). Take-all of wheat. *Physiological and Molecular Plant Pathology*, *62*(2), 73–86. https://doi.org/10.1016/S0885-5765(03)00042-0

Cooney, J. M., Lauren, D. R., & Di Menna, M. E. (2001). Impact of competitive fungi on trichothecene production by Fusarium graminearum. *Journal of Agricultural and Food Chemistry*, *49*(1), 522–526. https://doi.org/10.1021/jf0006372

Cordero, R. J. B., & Casadevall, A. (2017). Functions of fungal melanin beyond virulence. *Fungal Biology Reviews*, *31*(2), 99–112. https://doi.org/10.1016/j.fbr.2016.12.003

Cosgrove, D. J. (2005). Growth of the plant cell wall. *Nature Reviews Molecular Cell Biology 2005 6:11*, *6*(11), 850–861. https://doi.org/10.1038/nrm1746

Couteaudier, Y., & Alabouvette, C. (1990). Survival and inoculum potential of conidia and chlamydospores of Fusarium oxysporum f.sp. lini in soil. *Canadian Journal of Microbiology*, *36*(8), 551–556. https://doi.org/10.1139/m90-096

Daval, S., Lebreton, L., Gazengel, K., Boutin, M., Guillerm-Erckelboudt, A.-Y., & Sarniguet, A. (2011). The biocontrol bacterium Pseudomonas fluorescens Pf29Arp strain affects the pathogenesis-related gene expression of the take-all fungus Gaeumannomyces graminis var. tritici on wheat roots. *Molecular Plant Pathology*, *12*(9), 839–854. https://doi.org/10.1111/j.1364-3703.2011.00715.x

Daval, S., Lebreton, L., Gazengel, K., Guillerm-Erckelboudt, A.-Y., & Sarniguet, A. (2010). Genetic evidence for differentiation of Gaeumannomyces graminis var. tritici into two major groups. *Plant Pathology*, *59*, 165–178. https://doi.org/10.1111/j.1365-3059.2009.02158.x

De Coninck, B., Timmermans, P., Vos, C., Cammue, B. P. A., & Kazan, K. (2015). What lies beneath: Belowground defense strategies in plants. *Trends in Plant Science*, *20*(2), 91–101. https://doi.org/10.1016/j.tplants.2014.09.007

de la Fuente Cantó, C., Simonin, M., King, E., Moulin, L., Bennett, M. J., Castrillo, G., &

Laplaze, L. (2020). An extended root phenotype: the rhizosphere, its formation and impacts on plant fitness. *The Plant Journal*, *103*(3), 951–964. https://doi.org/10.1111/TPJ.14781

de Lamo, F. J., & Takken, F. L. W. (2020). Biocontrol by Fusarium oxysporum Using Endophyte-Mediated Resistance. *Frontiers in Plant Science*, *11*, 1. https://doi.org/10.3389/fpls.2020.00037

De Silva, N. I., Brooks, S., Lumyong, S., & Hyde, K. D. (2019). Use of endophytes as biocontrol agents. *Fungal Biology Reviews*, *33*(2), 133–148. https://doi.org/10.1016/J.FBR.2018.10.001

De Souza Cabral, A., De Carvalho, P. M. B., Pinotti, T., Hagler, A. N., Leda, C. S. M. H., & Macrae, A. (2009). Killer yeasts inhibit the growth of the phytopathogen moniliophthora perniciosa, the causal agent of witches' broom disease. *Brazilian Journal of Microbiology*, *40*(1), 108–110. https://doi.org/10.1590/s1517-83822009000100018

Deacon, J. W. (1973). Phialophora radicicola and Gaeumannomyces graminis on roots of grasses and cereals. *Transactions of the British Mycological Society*, *61*(3), 471–485. https://doi.org/10.1016/s0007-1536(73)80117-2

Deacon, J. W. (1974a). Interactions between Varieties of Gaeumannomyces graminis and Phialophora radicicola on Roots, Stem Bases and Rhizomes of the Gramineae. *Plant Pathology*, *23*, 85–92. https://doi.org/10.1111/j.1365-3059.1974.tb02914.x

Deacon, J. W. (1974b). Further studies on Phialophora radicicola and Gaeumannomyces graminis on roots and stem bases of grasses and cereals. *Transactions of the British Mycological Society*, *63*(2), 307–327. https://doi.org/10.1016/S0007-1536(74)80177-4

Deacon, J. W. (1976a). Biology of the Gaeumannomyces graminis Arx & Olivier/Phialophora radicicola Cain Complex on Roots of the Gramineae. *EPPO Bulletin*, *6*(5), 349–363. https://doi.org/10.1111/j.1365-2338.1976.tb02033.x

Deacon, J. W. (1976b). Biological control of the take-all fungus, Gaeumannomyces graminis, by Phialophora radicicola and similar fungi. *Soil Biology and Biochemistry*, *8*(4), 275–283. https://doi.org/10.1016/0038-0717(76)90057-2

Deacon, J. W., & Henry, C. M. (1981). Death of the root cortex of winter wheat in field conditions; effects of break crops and possible implications for the take-all fungus and its biological control agent, Phialophora radicicola var. graminicola. *The Journal of Agricultural Science*, *96*(3), 579–585. https://doi.org/10.1017/S0021859600034547

DEFRA. (2021). *Sustainable Farming Incentive: how the scheme will work in 2022 - GOV.UK*. https://www.gov.uk/government/publications/sustainable-farming-incentive-how-the-scheme-will-work-in-2022/sustainable-farming-incentive-how-the-scheme-will-work-in-2022

Delgado-Baquerizo, M., Guerra, C. A., Cano-Díaz, C., Egidi, E., Wang, J. T., Eisenhauer, N., Singh, B. K., & Maestre, F. T. (2020). The proportion of soil-borne pathogens increases with warming at the global scale. *Nature Climate Change*, *10*(6), 550–554. https://doi.org/10.1038/s41558-020-0759-3

Ding, Y., Gardiner, D. M., & Kazan, K. (2022). Transcriptome analysis reveals infection strategies employed by Fusarium graminearum as a root pathogen. *Microbiological Research*, *256*. https://doi.org/10.1016/J.MICRES.2021.126951

Dolan, L. (2017). Root hair development in grasses and cereals (Poaceae). *Current Opinion in Genetics and Development*, *45*, 76–81. https://doi.org/10.1016/j.gde.2017.03.009

Dooley, H., Shaw, M. W., Mehenni-Ciz, J., Spink, J., & Kildea, S. (2016). Detection of *Zymoseptoria tritici* SDHI-insensitive field isolates carrying the *SdhC* -H152R and *SdhD* -R47W substitutions. *Pest Management Science*, *72*(12), 2203–2207. https://doi.org/10.1002/ps.4269

Dori, S., Solel, Z., & Barash, I. (1995). Cell wall-degrading enzymes produced by Gaeumannomyces graminis var. tritici in vitro and in vivo. *Physiological and Molecular Plant Pathology*, *46*(3), 189–198. https://doi.org/10.1006/pmpp.1995.1015

Dreisigacker, S., Kishii, M., Lage, J., & Warburton, M. (2008). Use of synthetic hexaploid wheat to increase diversity for CIMMYT bread wheat improvement. *Australian Journal of Agricultural Research*, *59*(5), 413–420. https://doi.org/10.1071/AR07225

Duffy, B. K. Weller, D. M. (1994). A semiselective and Diagnostic Medium for Gaeumannomyces graminis var. tritici. *Techniques*, *84*(12), 1407–1415. https://doi.org/10.1094/Phyto-84-1407

Dufresne, M., & Osbourn, A. E. (2001). Definition of Tissue-Specific and General Requirements for Plant Infection in a Phytopathogenic Fungus. *Molecular Plant-Microbe Interactions*, *14*(3), 300–307. https://doi.org/10.1094/MPMI.2001.14.3.300

Dunken, N., Widmer, H., Balcke, G. U., Straube, H., Langen, G., Charura, N. M., Saake, P., Leson, L., Rövenich, H., Wawra, S., Djamei, A., Tissier, A., Witte, C.-P., & Zuccaro, A. (2022). A fungal endophyte-generated nucleoside signal regulates host cell death and

promotes root colonization. *BioRxiv*, 2022.03.11.483938. https://doi.org/10.1101/2022.03.11.483938

Dunnett, C. W. (1955). A Multiple Comparison Procedure for Comparing Several Treatments with a Control. *Journal of the American Statistical Association*, *50*(272), 1096–1121. https://doi.org/10.1080/01621459.1955.10501294

Duplessis, S., Cuomo, C. A., Lin, Y. C., Aerts, A., Tisserant, E., Veneault-Fourrey, C., Joly, D. L., Hacquard, S., Amselem, J., Cantarel, B. L., Chiu, R., Coutinho, P. M., Feaue, N., Field, M., Frey, P., Gelhaye, E., Goldberg, J., Grabherr, M. G., Kodira, C. D., … Martin, F. (2011). Obligate biotrophy features unraveled by the genomic analysis of rust fungi. *Proceedings of the National Academy of Sciences of the United States of America*, *108*(22), 9166–9171. https://doi.org/10.1073/pnas.1019315108

Durán, P., Tortella, G., Viscardi, S., Barra, P. J., Carrión, V. J., Mora, M. de la L., & Pozo, M. J. (2018). Microbial Community Composition in Take-All Suppressive Soils. *Frontiers in Microbiology*, *9*, 2198. https://doi.org/10.3389/fmicb.2018.02198

Eichmann, R., & Schäfer, P. (2015). Growth versus immunity-a redirection of the cell cycle? *Current Opinion in Plant Biology*, *26*, 106–112. https://doi.org/10.1016/j.pbi.2015.06.006

Eisenman, H. C., & Casadevall, A. (2012). Synthesis and assembly of fungal melanin. *Applied Microbiology and Biotechnology*, *93*(3), 931–940. https://doi.org/10.1007/s00253-011-3777-2

Elshafie, H., Camele, I., Racioppi, R., Scrano, L., Iacobellis, N., & Bufo, S. (2012). In Vitro Antifungal Activity of Burkholderia gladioli pv. agaricicola against Some Phytopathogenic Fungi. *International Journal of Molecular Sciences*, *13*(12), 16291–16302. https://doi.org/10.3390/ijms131216291

Fan, Y. hui, Qian, H. B., Su, P. sen, Wu, H. yan, Wang, G. ping, Kong, L. rang, Ma, X., & Wang, H. wei. (2019). Application of virus-induced gene silencing for identification of FHB resistant genes. *Journal of Integrative Agriculture*, *18*(10), 2183–2192. https://doi.org/10.1016/S2095-3119(18)62118-5

FAO. (2009). How to Feed the World in 2050. In *Insights from an expert meeting at FAO* (Vol. 2050, Issue 1). https://doi.org/10.1111/j.1728-4457.2009.00312.x

FAO, IFAD, UNICEF, WFP, & WHO. (2021). The State of Food Security and Nutrition in the World 2021. *The State of Food Security and Nutrition in the World 2021. Transforming Food Systems for Food Security, Improved Nutrition and Affordable Healthy Diets for All.*

https://doi.org/10.4060/cb4474en

FAOSTAT. (2018). *Food and Agriculture Organization of the United Nations (FAO), FAOSTAT*. https://www.fao.org/faostat/en/#data/QCL

Fathima Mirza, N., Motamarry, S., Bhadra, P., & Mishra, B. (2018). Antifungal peptides: Biosynthesis, production and applications. *Biotechnological Communication*, *11*(3), 376–386. https://doi.org/10.21786/bbrc/11.3/5

Ferraz, P., Cássio, F., & Lucas, C. (2019). Potential of Yeasts as Biocontrol Agents of the Phytopathogen Causing Cacao Witches' Broom Disease: Is Microbial Warfare a Solution? *Frontiers in Microbiology*, *10*, 1766. https://doi.org/10.3389/fmicb.2019.01766

Figueroa, M., Hammond-Kosack, K. E., & Solomon, P. S. (2018). A review of wheat diseases-a field perspective. *Molecular Plant Pathology*, *19*(6), 1523–1536. https://doi.org/10.1111/mpp.12618

Fira, D., Dimkić, I., Berić, T., Lozo, J., & Stanković, S. (2018). Biological control of plant pathogens by Bacillus species. *Journal of Biotechnology*, *285*, 44–55. https://doi.org/10.1016/j.jbiotec.2018.07.044

Fisher, M. C., Hawkins, N. J., Sanglard, D., & Gurr, S. J. (2018). Worldwide emergence of resistance to antifungal drugs challenges human health and food security. *Science*, *360*(6390), 739–742. https://doi.org/10.1126/science.aap7999

Fisher, M. C., Henk, D. A., Briggs, C. J., Brownstein, J. S., Madoff, L. C., McCraw, S. L., & Gurr, S. J. (2012). Emerging fungal threats to animal, plant and ecosystem health. *Nature*, *484*(7393), 186–194. https://doi.org/10.1038/nature10947

Fones, H. N., Bebber, D. P., Chaloner, T. M., Kay, W. T., Steinberg, G., & Gurr, S. J. (2020). Threats to global food security from emerging fungal and oomycete crop pathogens. *Nature Food 2020 1:6*, *1*(6), 332–342. https://doi.org/10.1038/s43016-020-0075-0

Francisco, C. S., Ma, X., Zwyssig, M. M., McDonald, B. A., & Palma-Guerrero, J. (2019). Morphological changes in response to environmental stresses in the fungal plant pathogen Zymoseptoria tritici. *Scientific Reports*, *9*(1), 1–18. https://doi.org/10.1038/s41598-019-45994-3

Frederick, B. A., Caesar-Tonthat, T.-C., Wheeler, M. H., Sheehan, K. B., Edens, W. A., & Henson, J. M. (1999). Isolation and characterisation of *Gaeumannomyces graminis* var. *graminis* melanin mutants. *Mycological Research*, *103*(1), 99–110. https://doi.org/10.1017/S0953756298006959

Freeman, J., Ward, E., Gutteridge, R. J., & Bateman, G. L. (2005). Methods for studying population structure, including sensitivity to the fungicide silthiofam, of the cereal take-all fungus, Gaeumannomyces graminis var. tritici. *Plant Pathology*, *54*(5), 686–698. https://doi.org/10.1111/j.1365-3059.2005.01252.x

Freeman, Jacqueline, & Ward, E. (2004). Gaeumannomyces graminis, the take-all fungus and its relatives. *Molecular Plant Pathology*, *5*(4), 235–252. https://doi.org/10.1111/j.1364-3703.2004.00226.x

Gao, Z., Zhang, B., Liu, H., Han, J., & Zhang, Y. (2017). Identification of endophytic Bacillus velezensis ZSY-1 strain and antifungal activity of its volatile compounds against Alternaria solani and Botrytis cinerea. *Biological Control*, *105*, 27–39. https://doi.org/10.1016/j.biocontrol.2016.11.007

Garrett, S. D. (1936). Soil conditions and the take-all disease of wheat. *Annals of Applied Biology*, *23*(4), 667–699. https://doi.org/10.1111/J.1744-7348.1936.TB06120.X

Geng, S., Li, A., Tang, L., Yin, L., Wu, L., Lei, C., Guo, X., Zhang, X., Jiang, G., Zhai, W., Wei, Y., Zheng, Y., Lan, X., & Mao, L. (2013). TaCPK2-A, a calcium-dependent protein kinase gene that is required for wheat powdery mildew resistance enhances bacterial blight resistance in transgenic rice. *Journal of Experimental Botany*, *64*(11), 3125–3136. https://doi.org/10.1093/jxb/ert146

Ghahfarokhi, R. M., & Goltapeh, M. E. (2010). Potential of the root endophytic fungus Piriformospora indica; Sebacina vermifera and Trichoderma species in biocontrol of take-all disease of wheat Gaeumannomyces graminis var. tritici in vitro. *Journal of Agricultural Technology*, *6*(1), 11–18. http://www.ijat-rmutto.com

Ghanbari, L., & Mohammadi, S. (2015). In vitro Antagonistic Mechanisms of Trichoderma spp. and Talaromyces flavus to Control Gaeumannomyces graminis var. tritici the Causal Agent of Wheat Take-all Disease. *Turkish Journal of Agriculture - Food Science and Technology*, *3*(8), 629–634. https://doi.org/10.24925/turjaf.v3i8.629-634.271

Gholami, M., Amini, J., Abdollahzadeh, J., & Ashengroph, M. (2019). Basidiomycetes fungi as biocontrol agents against take-all disease of wheat. *Biological Control*, *130*, 34–43. https://doi.org/10.1016/j.biocontrol.2018.12.012

Goellner, K., & Conrath, U. (2008). Priming: It's all the world to induced disease resistance. *European Journal of Plant Pathology*, *121*(3), 233–242. https://doi.org/10.1007/s10658-007-9251-4

Goodwin, S. B., M'Barek, S. Ben, Dhillon, B., Wittenberg, A. H. J., Crane, C. F., Hane, J. K., Foster, A. J., van der Lee, T. A. J., Grimwood, J., Aerts, A., Antoniw, J., Bailey, A., Bluhm, B., Bowler, J., Bristow, J., van der Burgt, A., Canto-Canché, B., Churchill, A. C. L., Conde-Ferràez, L., … Kema, G. H. J. (2011). Finished genome of the fungal wheat pathogen Mycosphaerella graminicola reveals dispensome structure, chromosome plasticity, and stealth pathogenesis. *PLoS Genetics*, *7*(6). https://doi.org/10.1371/journal.pgen.1002070

Goyal, R. K., Schmidt, M. A., & Hynes, M. F. (2021). Molecular Biology in the Improvement of Biological Nitrogen Fixation by Rhizobia and Extending the Scope to Cereals. *Microorganisms*, *9*(1), 125. https://doi.org/10.3390/MICROORGANISMS9010125

Graeff, S., Link, J., & Claupein, W. (2006). Identification of powdery mildew (Erysiphe graminis sp. tritici) and take-all disease (Gaeumannomyces graminis sp. tritici) in wheat (Triticum aestivum L.) by means of leaf reflectance measurements. *Central European Journal of Biology*, *1*(2), 275–288. https://doi.org/10.2478/s11535-006-0020-8

Grönberg, H., Kaparakis, G., & Sen, R. (2006). Binucleate Rhizoctonia (Ceratorhiza spp.) as non-mycorrhizal endophytes alter Pinus sylvestris L. seedling root architecture and affect growth of rooted cuttings. *Scandinavian Journal of Forest Research*, *21*(6), 450–457. https://doi.org/10.1080/02827580601019662

Guilleroux, M., & Osbourn, A. (2004). Gene expression during infection of wheat roots by the "take-all" fungus Gaeumannomyces graminis. *Molecular Plant Pathology*, *5*(3), 203–216. https://doi.org/10.1111/j.1364-3703.2004.00219.x

Gupta, O. P., Pandey, V., Gopalareddy, K., Sharma, P., & Singh, G. P. (2019). Genomic Intervention in Wheat Improvement. In *Plant Biotechnology: Progress in Genomic Era* (pp. 77–90). Springer Singapore. https://doi.org/10.1007/978-981-13-8499-8_3

Gutteridge, R., & Hammond-Kosack, K. E. (2008). Strategies for the control of take-all. In G. Jellis & C. Edwards (Eds.), *Cereal Pathosystems Papers from BSPP Presidential Meeting, Queen Mary, University of London* (pp. 75–86).

Gutteridge, R. J., Jenkyn, J. F., & Bateman, G. L. (2007). The potential of non-pathogenic Gaeumannomyces spp., occurring naturally or introduced into wheat crops or preceding crops, for controlling take-all in wheat: Research article. *Annals of Applied Biology*, *150*(1), 53–64. https://doi.org/10.1111/j.1744-7348.2006.00107.x

Gutteridge, R. J., Zhang, J. P., Jenkyn, J. F., & Bateman, G. L. (2005). Survival and multiplication of Gaeumannomyces graminis var. tritici (the wheat take-all fungus) and

related fungi on different wild and cultivated grasses. *Applied Soil Ecology*, *29*(2), 143–154. https://doi.org/10.1016/j.apsoil.2004.11.003

Han, X., & Kahmann, R. (2019). Manipulation of phytohormone pathways by effectors of filamentous plant pathogens. *Frontiers in Plant Science*, *10*, 822. https://doi.org/10.3389/FPLS.2019.00822/BIBTEX

Hao, D. C., Song, S. M., Mu, J., Hu, W. L., & Xiao, P. G. (2016). Unearthing microbial diversity of Taxus rhizosphere via MiSeq high-throughput amplicon sequencing and isolate characterization. *Scientific Reports* , *6*(1). https://doi.org/10.1038/srep22006

Hasegawa, M., Seo, I. M. S., Lmai, T., Koga, J., Okada, K., Yamane, H., & Ohashi, Y. (2010). Phytoalexin Accumulation in the Interaction Between Rice and the Blast Fungus. *Molecular Plant-Microbe Interactions*, *23*(8), 1000–1011. https://doi.org/10.1094/MPMI-23-8-1000

Hassani-Pak, K., Singh, A., Brandizi, M., Hearnshaw, J., Parsons, J. D., Amberkar, S., Phillips, A. L., Doonan, J. H., & Rawlings, C. (2021). KnetMiner: a comprehensive approach for supporting evidence-based gene discovery and complex trait analysis across species. *Plant Biotechnology Journal*, *19*(8), 1670–1678. https://doi.org/10.1111/PBI.13583

He, X., Zeng, J., Cao, F., Ahmed, I. M., Zhang, G., Vincze, E., & Wu, F. (2015). HvEXPB7, a novel β-expansin gene revealed by the root hair transcriptome of Tibetan wild barley, improves root hair growth under drought stress. *Journal of Experimental Botany*, *66*(22), 7405–7419. https://doi.org/10.1093/JXB/ERV436

Henson, J. M., Blake, N. K., & Pilgeram, A. L. (1988). Transformation of Gaeumannomyces graminis to benomyl resistance. *Current Genetics*, *14*(2), 113–117. https://doi.org/10.1007/BF00569334

Hernández-Blanco, C., Feng, D. X., Hu, J., Sánchez-Vallet, A., Deslandes, L., Llorente, F., Berrocal-Lobo, M., Keller, H., Barlet, X., Sánchez-Rodríguez, C., Anderson, L. K., Somerville, S., Marco, Y., & Molinaa, A. (2007). Impairment of cellulose synthases required for Arabidopsis secondary cell wall formation enhances disease resistance. *Plant Cell*, *19*(3), 890–903. https://doi.org/10.1105/tpc.106.048058

Hernández-Restrepo, M., Groenewald, J. Z., Elliott, M. L., Canning, G., McMillan, V. E., & Crous, P. W. (2016). Take-all or nothing. *Studies in Mycology*, *83*, 19–48. https://doi.org/10.1016/j.simyco.2016.06.002

Hochholdinger, F., Wen, T. J., Zimmermann, R., Chimot-Marolle, P., Da Costa E Silva, O.,

Bruce, W., Lamkey, K. R., Wienand, U., & Schnable, P. S. (2008). The maize (Zea mays L.) roothairless3 gene encodes a putative GPI-anchored, monocot-specific, COBRA-like protein that significantly affects grain yield. *Plant Journal*, *54*(5), 888–898. https://doi.org/10.1111/j.1365-313X.2008.03459.x

Hochholdinger, F., & Zimmermann, R. (2018). Molecular and Genetic Dissection of Cereal Root System Development. In *Annual Plant Reviews online* (pp. 175–191). John Wiley & Sons, Ltd. https://doi.org/10.1002/9781119312994.apr0402

Holden, J. (1976). Infection of wheat seminal roots by varieties of Phialophora radicicola and Gaeumannomyces graminis. *Soil Biology and Biochemistry*, *8*(2), 109–119. https://doi.org/10.1016/0038-0717(76)90074-2

Hornby, D. (1988). Diseases caused by soilborne pathogens. In D. G. Jones (Ed.), *The Epidemiology of Plant Diseases* (2nd ed., Vol. 99, pp. 308–322). Springer, Dordrecht. https://doi.org/10.1007/978-94-017-3302-1_15

Hornby, D. (1998). Take-all disease of cereals: a regional perspective. In D. Hornby (Ed.), *Take-all disease of cereals: a regional perspective.* CAB INTERNATIONAL. https://www.cabdirect.org/cabdirect/abstract/19981005789

Hou, L., Gao, W., van der Bom, F., Weng, Z., Doolette, C. L., Maksimenko, A., Hausermann, D., Zheng, Y., Tang, C., Lombi, E., & Kopittke, P. M. (2022). Use of X-ray tomography for examining root architecture in soils. *Geoderma*, *405*. https://doi.org/10.1016/J.GEODERMA.2021.115405

Houben, M., & Van de Poel, B. (2019). 1-aminocyclopropane-1-carboxylic acid oxidase (ACO): The enzyme that makes the plant hormone ethylene. *Frontiers in Plant Science*, *10*(695). https://doi.org/10.3389/fpls.2019.00695

Huang, C. Y., Wang, H., Hu, P., Hamby, R., & Jin, H. (2019). Small RNAs – Big Players in Plant-Microbe Interactions. *Cell Host & Microbe*, *26*(2), 173–182. https://doi.org/10.1016/J.CHOM.2019.07.021

Huang, L, Kang, Z., & Buchenauer, H. (2001). Comparison of infection of wheat roots by Phialophora graminicola and Gaeumannomyces graminis var. tritici by ultrastructural and cytochemical studies. *Journal of Plant Diseases and Protection*, *108*(6), 593–607.

Huang, LiLi, Kang, Z., Heppner, C., & Buchenauer, H. (2001). Ultrastructural and immunocytochemical studies on effects of the fungicide Mon65500 (Latitude ®) on colonization of roots of wheat seedlings by Gaeumannomyces graminis var. tritici.

Journal of Plant Diseases and Protection, *108*(2), 188–203.

Huang, Y., Yang, W., Pei, Z., Guo, X., Liu, D., Sun, J., & Zhang, A. (2012). The genes for gibberellin biosynthesis in wheat. *Functional and Integrative Genomics*, *12*(1), 199–206. https://doi.org/10.1007/S10142-011-0243-2/FIGURES/2

Hughes, D. J., West, J. S., Atkins, S. D., Gladders, P., Jeger, M. J., & Fitt, B. D. (2011). Effects of disease control by fungicides on greenhouse gas emissions by UK arable crop production. *Pest Management Science*, *67*(9), 1082–1092. https://doi.org/10.1002/ps.2151

Illana, A., Rodriguez-Romero, J., & Sesma, A. (2013). Major Plant Pathogens of the Magnaporthaceae Family. In B. Horwitz, P. Mukherjee, M. Mukherjee, & C. Kubicek (Eds.), *Soil Biology, vol 36* (pp. 45–88). Springer, Berlin, Heidelberg. https://doi.org/10.1007/978-3-642-39339-6_4

Impa, S. M., Vennapusa, A. R., Bheemanahalli, R., Sabela, D., Boyle, D., Walia, H., & Jagadish, S. V. K. (2020). High night temperature induced changes in grain starch metabolism alters starch, protein, and lipid accumulation in winter wheat. *Plant Cell and Environment*, *43*(2), 431–447. https://doi.org/10.1111/pce.13671

IPCC. (2021). Climate Change 2021: The Physical Science Basis. Contribution of Working Group I to the Sixth Assessment Report of the Intergovernmental Panel on Climate Change. In V. Masson-Delmotte, P. Zhai, A. Pirani, S. . Connors, C. Péan, S. Berger, N. Caud, Y. Chen, L. Goldfarb, M. . Gomis, M. Huang, K. Leitzell, J. B. . Matthews, T. . Maycock, T. Waterfield, O. Yelekçi, R. Yu, & B. Zhou (Eds.), *Cambridge University Press*. https://www.ipcc.ch/report/ar6/wg1/downloads/report/IPCC_AR6_WGI_Full_Report.pdf

Ireland, K. B., & Kriticos, D. J. (2019). Why are plant pathogens under-represented in eco-climatic niche modelling? *International Journal of Pest Management*, *65*(3), 207–216. https://doi.org/10.1080/09670874.2018.1543910

Islam, M. T., Croll, D., Gladieux, P., Soanes, D. M., Persoons, A., Bhattacharjee, P., Hossain, M. S., Gupta, D. R., Rahman, M. M., Mahboob, M. G., Cook, N., Salam, M. U., Surovy, M. Z., Sancho, V. B., Maciel, J. L. N., NhaniJúnior, A., Castroagudín, V. L., Reges, J. T. d. A., Ceresini, P. C., … Kamoun, S. (2016). Emergence of wheat blast in Bangladesh was caused by a South American lineage of Magnaporthe oryzae. *BMC Biology*, *14*(84), 1–11. https://doi.org/10.1186/s12915-016-0309-7

Islam, M. T., Kim, K. H., & Choi, J. (2019). Wheat blast in Bangladesh: The current situation and future impacts. *Plant Pathology Journal*, *35*(1), 1–10.

https://doi.org/10.5423/PPJ.RW.08.2018.0168

Jackson, A. O., Lim, H. S., Bragg, J., Ganesan, U., & Lee, M. Y. (2009). Hordeivirus Replication, Movement, and Pathogenesis. *Annual Reviews*, *47*, 385–422. https://doi.org/10.1146/ANNUREV-PHYTO-080508-081733

Jasem, A. M., Sharifi, R., & Abbasi, S. (2018). Induced systemic resistance to wheat take-all disease by probiotic bacteria. *Journal of Plant Protection Research*, *58*(3), 304–310. https://doi.org/10.24425/jppr.2018.124639

Jenkyn, J. F., Bateman, G. L., Gutteridge, R. J., & Edwards, S. G. (2000). Effects of foliar sprays of azoxystrobin on take-all in wheat. *Annals of Applied Biology*, *137*(2), 99–106. https://doi.org/10.1111/j.1744-7348.2000.tb00041.x

Jia, L. J., Tang, H. Y., Wang, W. Q., Yuan, T. L., Wei, W. Q., Pang, B., Gong, X. M., Wang, S. F., Li, Y. J., Zhang, D., Liu, W., & Tang, W. H. (2019). A linear nonribosomal octapeptide from Fusarium graminearum facilitates cell-to-cell invasion of wheat. *Nature Communications*, *10*(1), 1–20. https://doi.org/10.1038/s41467-019-08726-9

Jia, L., Wu, Z., Hao, X., Carrie, C., Zheng, L., Whelan, J., Wu, Y., Wang, S., Wu, P., & Mao, C. (2011). Identification of a novel mitochondrial protein, short postembryonic roots 1 (SPR1), involved in root development and iron homeostasis in Oryza sativa. *New Phytologist*, *189*(3), 843–855. https://doi.org/10.1111/j.1469-8137.2010.03513.x

Jiang, F., Zhang, L., Zhou, J., George, T. S., & Feng, G. (2021). Arbuscular mycorrhizal fungi enhance mineralisation of organic phosphorus by carrying bacteria along their extraradical hyphae. *New Phytologist*, *230*(1), 304–315. https://doi.org/10.1111/NPH.17081

Jiang, Z., Yang, M., Zhang, Y., Jackson, A. O., & Li, D. (2021). Hordeiviruses (Virgaviridae). *Encyclopedia of Virology*, 420–429. https://doi.org/10.1016/B978-0-12-809633-8.21250-8

Jiao, Y., Peluso, P., Shi, J., Liang, T., Stitzer, M. C., Wang, B., Campbell, M. S., Stein, J. C., Wei, X., Chin, C. S., Guill, K., Regulski, M., Kumari, S., Olson, A., Gent, J., Schneider, K. L., Wolfgruber, T. K., May, M. R., Springer, N. M., … Ware, D. (2017). Improved maize reference genome with single-molecule technologies. *Nature*, *546*(7659), 524–527. https://doi.org/10.1038/nature22971

Jones, J. D. G., & Dangl, J. L. (2006). The plant immune system. *Nature*, *444*(7117), 323–329. https://doi.org/10.1038/nature05286

Jordan, T., Seeholzer, S., Schwizer, S., Töller, A., Somssich, I. E., & Keller, B. (2011). The wheat Mla homologue TmMla1 exhibits an evolutionarily conserved function against powdery mildew in both wheat and barley. *The Plant Journal*, *65*(4), 610–621. https://doi.org/10.1111/j.1365-313X.2010.04445.x

Joseph-Horne, T., Heppner, C., Headrick, J., & Hollomon, D. W. (2000). Identification and characterization of the mode of action of MON 65500: A novel inhibitor of ATP export from mitochondria of the wheat “take-all” fungus, Gaeumannomyces graminis var. tritici. *Pesticide Biochemistry and Physiology*, *67*(3), 168–186. https://doi.org/10.1006/pest.2000.2483

Joshi, D. C., Singh, V., Hunt, C., Mace, E., van Oosterom, E., Sulman, R., Jordan, D., & Hammer, G. (2017). Development of a phenotyping platform for high throughput screening of nodal root angle in sorghum. *Plant Methods*, *13*(1), 56. https://doi.org/10.1186/s13007-017-0206-2

Kang, G., Wu, Y., Li, G., Wang, P., Han, Q., Wang, Y., Xie, Y., Feng, W., Ma, D., Wang, C., & Guo, T. (2019). Proteomics combined with BSMV-VIGS methods identified some N deficiency-responsive protein species and ABA role in wheat seedling. *Plant and Soil*, *444*(1–2), 177–191. https://doi.org/10.1007/s11104-019-04260-1

Kang, X., Guo, Y., Leng, S., Xiao, L., Wang, L., Xue, Y., & Liu, C. (2019). Comparative Transcriptome Profiling of Gaeumannomyces graminis var. tritici in Wheat Roots in the Absence and Presence of Biocontrol Bacillus velezensis CC09. *Frontiers in Microbiology*, *10*(1474). https://doi.org/10.3389/fmicb.2019.01474

Kang, X., Wang, L., Guo, Y., Zain Ul Arifeen, M., Cai, X., Xue, Y., Bu, Y., Wang, G., & Liu, C. (2019). A Comparative Transcriptomic and Proteomic Analysis of Hexaploid Wheat’s Responses to Colonization by Bacillus velezensis and Gaeumannomyces graminis, Both Separately and Combined. *Molecular Plant-Microbe Interactions*, *32*(10). https://doi.org/10.1094/MPMI-03-19-0066-R

Kang, X., Zhang, W., Cai, X., Zhu, T., Xue, Y., & Liu, C. (2018). Bacillus velezensis CC09: A potential ‘Vaccine’ for controlling wheat diseases. *Molecular Plant-Microbe Interactions*, *31*(6), 623–632. https://doi.org/10.1094/MPMI-09-17-0227-R

Karlsson, M., Atanasova, L., Jensen, D. F., & Zeilinger, S. (2017). Necrotrophic Mycoparasites and Their Genomes. *Microbiology Spectrum*, *5*(2). https://doi.org/10.1128/microbiolspec.funk-0016-2016

Keenan, S., Cromey, M. G., Harrow, S. A., Bithell, S. L., Butler, R. C., Beard, S. S., & Pitman,

A. R. (2015). Quantitative PCR to detect Gaeumannomyces graminis var. tritici in symptomatic and non-symptomatic wheat roots. *Australasian Plant Pathology*, *44*(6), 591–597. https://doi.org/10.1007/s13313-015-0379-y

Keller, B., Wicker, T., & Krattinger, S. G. (2018). Advances in Wheat and Pathogen Genomics: Implications for Disease Control. *Annual Review of Phytopathology*, *56*(1), 67–87. https://doi.org/10.1146/annurev-phyto-080516-035419

Khaosaad, T., García-Garrido, J. M., Steinkellner, S., & Vierheilig, H. (2007). Take-all disease is systemically reduced in roots of mycorrhizal barley plants. *Soil Biology and Biochemistry*, *39*(3), 727–734. https://doi.org/10.1016/j.soilbio.2006.09.014

Kim, D., Paggi, J. M., Park, C., Bennett, C., & Salzberg, S. L. (2019). Graph-based genome alignment and genotyping with HISAT2 and HISAT-genotype. *Nature Biotechnology*, *37*(8), 907–915. https://doi.org/10.1038/s41587-019-0201-4

Kim, D. W., Kim, G. Y., Kim, H. K., Kim, J., Jeon, S. J., Lee, C. W., Lee, H. B., & Yun, S. H. (2016). Characterization of nivalenol-producing Fusarium culmorum isolates obtained from the air at a rice paddy field in Korea. *Plant Pathology Journal*, *32*(3), 182–189. https://doi.org/10.5423/PPJ.OA.12.2015.0268

Kiran, K., Rawal, H. C., Dubey, H., Jaswal, R., Devanna, B. N., Gupta, D. K., Bhardwaj, S. C., Prasad, P., Pal, D., Chhuneja, P., Balasubramanian, P., Kumar, J., Swami, M., Solanke, A. U., Gaikwad, K., Singh, N. K., & Sharma, T. R. (2016). Draft genome of the wheat rust pathogen (Puccinia triticina) unravels genome-wide structural variations during evolution. *Genome Biology and Evolution*, *8*(9), 2702–2721. https://doi.org/10.1093/gbe/evw197

Kitomi, Y., Nakao, E., Kawai, S., Kanno, N., Ando, T., Fukuoka, S., Irie, K., & Uga, Y. (2018). Fine mapping of QUICK ROOTING 1 and 2, quantitative trait loci increasing root length in rice. *G3: Genes, Genomes, Genetics*, *8*(2), 727–735. https://doi.org/10.1534/g3.117.300147

Kloepper, J. W., Ryu, C. M., & Zhang, S. (2004). Induced systemic resistance and promotion of plant growth by Bacillus spp. *Phytopathology*, *94*(11), 1259–1266. https://doi.org/10.1094/PHYTO.2004.94.11.1259

Knapp, D. G., Németh, J. B., Barry, K., Hainaut, M., Henrissat, B., Johnson, J., Kuo, A., Lim, J. H. P., Lipzen, A., Nolan, M., Ohm, R. A., Tamás, L., Grigoriev, I. V., Spatafora, J. W., Nagy, L. G., & Kovács, G. M. (2018). Comparative genomics provides insights into the lifestyle and reveals functional heterogeneity of dark septate endophytic fungi. *Scientific Reports*, *8*(1), 1–13. https://doi.org/10.1038/s41598-018-24686-4

Kogel, K. H., Franken, P., & Hückelhoven, R. (2006). Endophyte or parasite - what decides? *Current Opinion in Plant Biology*, *9*(4), 358–363. https://doi.org/10.1016/j.pbi.2006.05.001

Kumar, A., Prakash, A., & Johri, B. N. (2011). Bacillus as PGPR in Crop Ecosystem. In *Bacteria in Agrobiology: Crop Ecosystems*. https://doi.org/10.1007/978-3-642-18357-7_2

Kwak, Y.-S., & Weller, D. M. (2013). Take-all of Wheat and Natural Disease Suppression: A Review. *The Plant Pathology Journal*, *29*(2), 125–135. https://doi.org/10.5423/PPJ.SI.07.2012.0112

Kwak, Y. S., Bakker, P. A. H. M., Glandorf, D. C. M., Rice, J. T., Paulitz, T. C., & Weller, D. M. (2009). Diversity, Virulence, and 2,4-Diacetylphloroglucinol Sensitivity of Gaeumannomyces graminis var. Tritici Isolates from Washington State. *Phytopathology*, *99*(5), 472–479. https://doi.org/10.1094/PHYTO-99-5-0472

Kwak, Y. S., Bonsall, R. F., Okubara, P. A., Paulitz, T. C., Thomashow, L. S., & Weller, D. M. (2012). Factors impacting the activity of 2,4-diacetylphloroglucinol-producing Pseudomonas fluorescens against take-all of wheat. *Soil Biology and Biochemistry*, *54*, 48–56. https://doi.org/10.1016/j.soilbio.2012.05.012

Kwon, Y. S., Jeon, C. W., Bae, D. W., Seo, J. S., Thomashow, L. S., Weller, D. M., & Kwak, Y. S. (2018). Construction of a proteome reference map and response of Gaeumannomyces graminis var. tritici to 2,4-diacetylphloroglucinol. *Fungal Biology*, *122*(11), 1098–1108. https://doi.org/10.1016/j.funbio.2018.09.001

Lareen, A., Burton, F., & Schäfer, P. (2016). Plant root-microbe communication in shaping root microbiomes. *Plant Molecular Biology*, *90*(6), 575–587. https://doi.org/10.1007/s11103-015-0417-8

Łaźniewska, J., Macioszek, V. K., & Kononowicz, A. K. (2012). Plant-fungus interface: The role of surface structures in plant resistance and susceptibility to pathogenic fungi. *Physiological and Molecular Plant Pathology*, *78*, 24–30. https://doi.org/10.1016/j.pmpp.2012.01.004

Lebreton, L., Lucas, P., Dugas, F., Guillerm, A. Y., Schoeny, A., & Sarniguet, A. (2004). Changes in population structure of the soilborne fungus Gaeumannomyces graminis var. tritici during continuous wheat cropping. *Environmental Microbiology*, *6*(11), 1174–1185. https://doi.org/10.1111/j.1462-2920.2004.00637.x

Lee, W.-S., Hammond-Kosack, K. E., & Kanyuka, K. (2012). Barley stripe mosaic virus-

mediated tools for investigating gene function in cereal plants and their pathogens: virus-induced gene silencing, host-mediated gene silencing, and virus-mediated overexpression of heterologous protein. *Plant Physiology*, *160*(2), 582–590. https://doi.org/10.1104/pp.112.203489

Lee, W.-S., Rudd, J. J., Hammond-Kosack, K. E., & Kanyuka, K. (2014). Mycosphaerella graminicola LysM Effector-Mediated Stealth Pathogenesis Subverts Recognition Through Both CERK1 and CEBiP Homologues in Wheat. *C*, *27*(3), 236–243. https://doi.org/10.1094/MPMI-07-13-0201-R

Lee, W. S., Rudd, J. J., & Kanyuka, K. (2015). Virus induced gene silencing (VIGS) for functional analysis of wheat genes involved in Zymoseptoria tritici susceptibility and resistance. *Fungal Genetics and Biology*, *79*, 84–88. https://doi.org/10.1016/j.fgb.2015.04.006

Leveau, A., Reed, J., Qiao, X., Stephenson, M. J., Mugford, S. T., Melton, R. E., Rant, J. C., Vickerstaff, R., Langdon, T., & Osbourn, A. (2018). Towards take-all control: a C-21β oxidase required for acylation of triterpene defence compounds in oat. *New Phytologist*. https://doi.org/10.1111/nph.15456

Li, J., Mu, W., Veluchamy, S., Liu, Y., Zhang, Y., Pan, H., & Rollins, J. A. (2018). The GATA-type IVb zinc-finger transcription factor SsNsd1 regulates asexual–sexual development and appressoria formation in Sclerotinia sclerotiorum. *Molecular Plant Pathology*, *19*(7), 1679–1689. https://doi.org/10.1111/MPP.12651

Li, Q., Wang, C., & Mou, Z. (2020). Perception of Damaged Self in Plants. *Plant Physiology*, *182*(4), 1545–1565. https://doi.org/10.1104/pp.19.01242

Li, S., Fu, Q., Chen, L., Huang, W., & Yu, D. (2011). Arabidopsis thaliana WRKY25, WRKY26, and WRKY33 coordinate induction of plant thermotolerance. *Planta*, *233*(6), 1237–1252. https://doi.org/10.1007/S00425-011-1375-2/FIGURES/8

Li, W., Feng, Y., Sun, H., Deng, Y., Hanshou, ·, & Chen, Y. · H. (2014). Analysis of simple sequence repeats in the Gaeumannomyces graminis var. tritici genome and the development of microsatellite markers. *Curr Genet*, *60*, 237–245. https://doi.org/10.1007/s00294-014-0428-z

Li, X., He, C., He, X., Su, F., Hou, L., Ren, Y., & Hou, Y. (2019). Dark septate endophytes improve the growth of host and non-host plants under drought stress through altered root development. *Plant and Soil*, *439*(1–2), 259–272. https://doi.org/10.1007/s11104-019-04057-2

Li, Y., Leveau, A., Zhao, Q., Feng, Q., Lu, H., Miao, J., Xue, Z., Martin, A. C., Wegel, E., Wang, J., Orme, A., Rey, M. D., Karafiátová, M., Vrána, J., Steuernagel, B., Joynson, R., Owen, C., Reed, J., Louveau, T., … Osbourn, A. (2021). Subtelomeric assembly of a multi-gene pathway for antimicrobial defense compounds in cereals. *Nature Communications 2021 12:1*, *12*(1), 1–13. https://doi.org/10.1038/s41467-021-22920-8

Liao, D., Wang, S., Cui, M., Liu, J., Chen, A., & Xu, G. (2018). Phytohormones Regulate the Development of Arbuscular Mycorrhizal Symbiosis. *International Journal of Molecular Sciences 2018, Vol. 19, Page 3146*, *19*(10), 3146. https://doi.org/10.3390/IJMS19103146

Liao, Y., Smyth, G. K., & Shi, W. (2014). FeatureCounts: An efficient general purpose program for assigning sequence reads to genomic features. *Bioinformatics*, *30*(7), 923–930. https://doi.org/10.1093/bioinformatics/btt656

Lim, S. M., Yoon, M. Y., Choi, G. J., Choi, Y. H., Jang, K. S., Shin, T. S., Park, H. W., Yu, N. H., Kim, Y. H., & Kim, J. C. (2017). Diffusible and volatile antifungal compounds produced by an antagonistic bacillus velezensis G341 against various phytopathogenic fungi. *Plant Pathology Journal*, *33*(5), 488–498. https://doi.org/10.5423/PPJ.OA.04.2017.0073

Lin, N. S., & Langenberg, W. G. (1984). Distribution of Barley Stripe Mosaic Virus Protein in Infected Wheat Root and Shoot Tips. *Journal of General Virology*, *65*(12), 2217–2224. https://doi.org/10.1099/0022-1317-65-12-2217

Lippold, F., Sanchez, D. H., Musialak, M., Schlereth, A., Scheible, W. R., Hincha, D. K., & Udvardi, M. K. (2009). AtMyb41 Regulates Transcriptional and Metabolic Responses to Osmotic Stress in Arabidopsis. *Plant Physiology*, *149*(4), 1761–1772. https://doi.org/10.1104/PP.108.134874

Liu, B., Qiao, H., Huang, L., Buchenauer, H., Han, Q., Kang, Z., & Gong, Y. (2009). Biological control of take-all in wheat by endophytic Bacillus subtilis E1R-j and potential mode of action. *Biological Control*, *49*(3), 277–285. https://doi.org/10.1016/j.biocontrol.2009.02.007

Liu, X., Yang, L., Zhou, X., Zhou, M., Lu, Y., Ma, L., Ma, H., & Zhang, Z. (2013). Transgenic wheat expressing Thinopyrum intermedium MYB transcription factor TiMYB2R. *Journal of Experimental Botany*, *64*(8), 2243–2253. https://doi.org/10.1093/jxb/ert084

Livak, K. J., & Schmittgen, T. D. (2001). Analysis of Relative Gene Expression Data Using Real-Time Quantitative PCR and the 2−ΔΔCT Method. *Methods*, *25*(4), 402–408. https://doi.org/10.1006/METH.2001.1262

Lo Presti, L., Lanver, D., Schweizer, G., Tanaka, S., Liang, L., Tollot, M., Zuccaro, A., Reissmann, S., & Kahmann, R. (2015). Fungal Effectors and Plant Susceptibility. *Annu. Rev. Plant Biol*, *66*, 513–545. https://doi.org/10.1146/annurev-arplant-043014-114623

Long, S. P., Ainsworth, E. A., & Long, S. P. (2004). What have we learned from 15 years of free-air CO2 enrichment (FACE)? A meta-analytic review of the responses of photosynthesis, canopy properties and plant production to rising CO2. *New Phytologist*, *165*, 351–372. https://doi.org/10.1111/j.1469-8137.2004.01224.x

Lorenzo, O., Piqueras, R., Sánchez-Serrano, J. J., & Solano, R. (2003). ETHYLENE RESPONSE FACTOR1 Integrates Signals from Ethylene and Jasmonate Pathways in Plant Defense. *The Plant Cell*, *15*(1), 165–178. https://doi.org/10.1105/TPC.007468

Love, M. I., Huber, W., & Anders, S. (2014). Moderated estimation of fold change and dispersion for RNA-seq data with DESeq2. *Genome Biology*, *15*(12), 550. https://doi.org/10.1186/s13059-014-0550-8

Lu, X., Kracher, B., Saur, I. M. L., Bauer, S., Ellwood, S. R., Wise, R., Yaeno, T., Maekawa, T., & Schulze-Lefert, P. (2016). Allelic barley MLA immune receptors recognize sequence-unrelated avirulence effectors of the powdery mildew pathogen. *Proceedings of the National Academy of Sciences of the United States of America*, *113*(42). https://doi.org/10.1073/pnas.1612947113

Lück, S., Kreszies, T., Strickert, M., Schweizer, P., Kuhlmann, M., & Douchkov, D. (2019). siRNA-Finder (si-Fi) Software for RNAi-Target Design and Off-Target Prediction. *Frontiers in Plant Science*, *10*(1023), 1–12. https://doi.org/10.3389/fpls.2019.01023

Lugtenberg, B. (2014). *Principles of Plant-Microbe Interactions: Microbes for Sustainable Agriculture* (Issue 1). Springer. https://doi.org/10.1007/s13398-014-0173-7.2

Lupoi, J. S., Singh, S., Parthasarathi, R., Simmons, B. A., & Henry, R. J. (2015). Recent innovations in analytical methods for the qualitative and quantitative assessment of lignin. *Renewable and Sustainable Energy Reviews*, *49*, 871–906. https://doi.org/10.1016/J.RSER.2015.04.091

Ma, Y. (2019). Seed coating with beneficial microorganisms for precision agriculture. *Biotechnology Advances*, *37*(7). https://doi.org/10.1016/j.biotechadv.2019.107423

Macdonald, A. J., & Gutteridge, R. J. (2012). Effects of take-all (Gaeumannomyces graminis var. tritici) on crop N uptake and residual mineral N in soil at harvest of winter wheat. *Plant and Soil*, *350*(1–2), 253–260. https://doi.org/10.1007/s11104-011-0900-1

Mahdi, L. K., Miyauchi, S., Uhlmann, C., Garrido-Oter, R., Langen, G., Wawra, S., Niu, Y., Guan, R., Robertson-Albertyn, S., Bulgarelli, D., Parker, J. E., & Zuccaro, A. (2021). The fungal root endophyte Serendipita vermifera displays inter-kingdom synergistic beneficial effects with the microbiota in Arabidopsis thaliana and barley. *ISME Journal*, *September*. https://doi.org/10.1038/s41396-021-01138-y

Marcussen, T., Sandve, S. R., Heier, L., Spannagl, M., Pfeifer, M., Jakobsen, K. S., Wulff, B. B. H., Steuernagel, B., Mayer, K. F. X., Olsen, O. A., Rogers, J., Doležel, J., Pozniak, C., Eversole, K., Feuillet, C., Gill, B., Friebe, B., Lukaszewski, A. J., Sourdille, P., … Praud, S. (2014). Ancient hybridizations among the ancestral genomes of bread wheat. *Science*, *345*(6194). https://doi.org/10.1126/science.1250092

Marques, J. P. R., Soares, M. K. M., & Appezzato-Da-Gloria, B. (2013). New staining technique for fungal-infected plant tissues. *Turkish Journal of Botany*, *37*(4), 784–787. https://doi.org/10.3906/bot-1204-9

Martínez-Medina, A., Van Wees, S. C. M., & Pieterse, C. M. J. (2017). Airborne signals from *Trichoderma* fungi stimulate iron uptake responses in roots resulting in priming of jasmonic acid-dependent defences in shoots of *Arabidopsis thaliana* and *Solanum lycopersicum*. *Plant, Cell & Environment*, *40*(11), 2691–2705. https://doi.org/10.1111/pce.13016

Martinuz, A., Zewdu, G., Ludwig, N., Grundler, F., Sikora, R. A., & Schouten, A. (2015). The application of Arabidopsis thaliana in studying tripartite interactions among plants, beneficial fungal endophytes and biotrophic plant-parasitic nematodes. *Planta*, *241*(4), 1015–1025. https://doi.org/10.1007/S00425-014-2237-5/FIGURES/7

Mascher, M., Gundlach, H., Himmelbach, A., Beier, S., Twardziok, S. O., Wicker, T., Radchuk, V., Dockter, C., Hedley, P. E., Russell, J., Bayer, M., Ramsay, L., Liu, H., Haberer, G., Zhang, X. Q., Zhang, Q., Barrero, R. A., Li, L., Taudien, S., … Stein, N. (2017). A chromosome conformation capture ordered sequence of the barley genome. *Nature*, *544*(7651), 427–433. https://doi.org/10.1038/nature22043

MATHRE, D. E., JOHNSTON, R. H., & GREY, W. E. (1998). Biological Control of Take-all Disease of Wheat Caused by Gaeumannomyces graminis var. tritici Under Field Conditions Using a Phialophora sp. *Biocontrol Science and Technology*, *8*(3), 449–457. https://doi.org/10.1080/09583159830243

Mauch-Mani, B., Mauch, F., Luna Diez, E., Ciancio, A., Pieterse, C. M. J., & Mercado-Blanco, J. (2019). Editorial: Harnessing Useful Rhizosphere Microorganisms for Pathogen and

Pest Biocontrol - Second Edition. *Frontiers in Microbiology*, *10*(1935). https://doi.org/10.3389/fmicb.2019.01935

Mauchline, T. H., Chedom-Fotso, D., Chandra, G., Samuels, T., Greenaway, N., Backhaus, A., Mcmillan, V., Canning, G., Powers, S. J., Hammond-Kosack, K. E., Hirsch, P. R., Clark, I. M., Mehrabi, Z., Roworth, J., Burnell, J., & Malone, J. G. (2015). An analysis of Pseudomonas genomic diversity in take-all infected wheat fields reveals the lasting impact of wheat cultivars on the soil microbiota. *Environmental Microbiology*, *17*(11), 4764–4778. https://doi.org/10.1111/1462-2920.13038

Mauchline, Tim H., & Malone, J. G. (2017). Life in earth – the root microbiome to the rescue? *Current Opinion in Microbiology*, *37*, 23–28. https://doi.org/10.1016/j.mib.2017.03.005

Mavrodi, O. V., Walter, N., Elateek, S., Taylor, C. G., & Okubara, P. A. (2012). Suppression of Rhizoctonia and Pythium root rot of wheat by new strains of Pseudomonas. *Biological Control*, *62*(2), 93–102. https://doi.org/10.1016/j.biocontrol.2012.03.013

Mazzola, M. (2002). Mechanisms of natural soil suppressiveness to soilborne diseases. *Antonie van Leeuwenhoek, International Journal of General and Molecular Microbiology*, *81*(1–4), 557–564. https://doi.org/10.1023/A:1020557523557

Mc Carthy, U., Uysal, I., Badia-Melis, R., Mercier, S., O'Donnell, C., & Ktenioudaki, A. (2018). Global food security – Issues, challenges and technological solutions. *Trends in Food Science & Technology*, *77*, 11–20. https://doi.org/10.1016/J.TIFS.2018.05.002

McCartney, H. A., Foster, S. J., Fraaije, B. A., & Ward, E. (2003). Molecular diagnostics for fungal plant pathogens. *Pest Management Science*, *59*(2), 129–142. https://doi.org/10.1002/ps.575

Mckenney, P. T., Driks, A., & Eichenberger, P. (2013). The Bacillus subtilis endospore: Assembly and functions of the multilayered coat. *Nature Reviews Microbiology*, *11*(1), 33–44. https://doi.org/10.1038/nrmicro2921

McMillan, V. E., Canning, G., Moughan, J., White, R. P., Gutteridge, R. J., & Hammond-Kosack, K. E. (2018). Exploring the resilience of wheat crops grown in short rotations through minimising the build-up of an important soil-borne fungal pathogen. *Scientific Reports*, *8*(1), 1–13. https://doi.org/10.1038/s41598-018-25511-8

McMillan, V. E., Hammond-Kosack, K. E., & Gutteridge, R. J. (2011). Evidence that wheat cultivars differ in their ability to build up inoculum of the take-all fungus, Gaeumannomyces graminis var. tritici, under a first wheat crop. *Plant Pathology*.

https://doi.org/10.1111/j.1365-3059.2010.02375.x

McMillan, Vanessa E., Gutteridge, R. J., & Hammond-Kosack, K. E. (2014). Identifying variation in resistance to the take-all fungus, Gaeumannomyces graminis var. tritici, between different ancestral and modern wheat species. *BMC Plant Biology*. https://doi.org/10.1186/s12870-014-0212-8

Mehrabi, Z., McMillan, V. E., Clark, I. M., Canning, G., Hammond-Kosack, K. E., Preston, G., Hirsch, P. R., & Mauchline, T. H. (2016). Pseudomonas spp. diversity is negatively associated with suppression of the wheat take-all pathogen. *Scientific Reports*, *6*(August), 1–9. https://doi.org/10.1038/srep29905

Menna, A., Dora, S., Sancho-Andrés, G., Kashyap, A., Meena, M. K., Sklodowski, K., Gasperini, D., Coll, N. S., & Sánchez-Rodríguez, C. (2021). A primary cell wall cellulose-dependent defense mechanism against vascular pathogens revealed by time-resolved dual transcriptomics. *BMC Biology*, *19*(1), 1–20. https://doi.org/10.1186/s12915-021-01100-6

Micali, C. O., & Smith, M. L. (2003). On the independence of barrage formation and heterokaryon incompatibility in Neurospora crassa. *Fungal Genetics and Biology*, *38*(2), 209–219. https://doi.org/10.1016/S1087-1845(02)00533-9

Miedes, E., Vanholme, R., Boerjan, W., & Molina, A. (2014). The role of the secondary cell wall in plant resistance to pathogens. *Frontiers in Plant Science*, *5*(358). https://doi.org/10.3389/fpls.2014.00358

Mishra, J., Singh, R., & Arora, N. K. (2017). Plant growth-promoting microbes: Diverse roles in agriculture and environmental sustainability. In *Probiotics and Plant Health* (pp. 71–111). Springer Singapore. https://doi.org/10.1007/978-981-10-3473-2_4

Mur, L. A. J., Simpson, C., Kumari, A., Gupta, A. K., & Gupta, K. J. (2017). Moving nitrogen to the centre of plant defence against pathogens. *Annals of Botany*, *119*(5), 703–709. https://doi.org/10.1093/AOB/MCW179

Newbery, F., Qi, A., & Fitt, B. D. (2016). Modelling impacts of climate change on arable crop diseases: progress, challenges and applications. In *Current Opinion in Plant Biology* (Vol. 32, pp. 101–109). Elsevier Ltd. https://doi.org/10.1016/j.pbi.2016.07.002

Nirmal, R. C., Furtado, A., Rangan, P., & Henry, R. J. (2017). Fasciclin-like arabinogalactan protein gene expression is associated with yield of flour in the milling of wheat. *Scientific Reports 2017 7:1*, *7*(1), 1–11. https://doi.org/10.1038/s41598-017-12845-y

Niu, D., Hamby, R., Sanchez, J. N., Cai, Q., Yan, Q., & Jin, H. (2021). RNAs — a new frontier in crop protection. *Current Opinion in Biotechnology*, *70*, 204–212. https://doi.org/10.1016/J.COPBIO.2021.06.005

Novotný, J. (1979). Beziehungen Zwischen Den Pilzen Gaeumannomyces Graminis Und Phialophora Radicicola Bei Gemeinsamem Wachstum AußErhalb Der Wirtspflanze. *Zentralblatt Für Bakteriologie, Parasitenkunde, Infektionskrankheiten Und Hygiene. Zweite Naturwissenschaftliche Abteilung: Mikrobiologie Der Landwirtschaft, Der Technologie Und Des Umweltschutzes*, *134*(5), 419–422. https://doi.org/10.1016/S0323-6056(79)80094-4

Okagaki, L. H., Nunes, C. C., Sailsbery, J., Clay, B., Brown, D., John, T., Oh, Y., Young, N., Fitzgerald, M., Haas, B. J., Zeng, Q., Young, S., Adiconis, X., Fan, L., Levin, J. Z., Mitchell, T. K., Okubara, P. A., Farman, M. L., Kohn, L. M., … Dean, R. A. (2015). *Genome Sequences of Three Phytopathogenic Species of the Magnaporthaceae Family of Fungi*. https://doi.org/10.1534/g3.115.020057

Okubara, P. A., & Bonsall, R. F. (2008). Accumulation of Pseudomonas-derived 2,4-diacetylphloroglucinol on wheat seedling roots is influenced by host cultivar. *Biological Control*, *46*(3), 322–331. https://doi.org/10.1016/j.biocontrol.2008.03.013

Okubara, P. A., Kornoely, J. P., & Landa, B. B. (2004). Rhizosphere colonization of hexaploid wheat by Pseudomonas fluorescens strains Q8r1-96 and Q2-87 is cultivar-variable and associated with changes in gross root morphology. *Biological Control*, *30*(2), 392–403. https://doi.org/10.1016/j.biocontrol.2003.11.003

Oldroyd, G. E. D. (2013). Speak, friend, and enter: Signalling systems that promote beneficial symbiotic associations in plants. *Nature Reviews Microbiology*, *11*(4), 252–263. https://doi.org/10.1038/nrmicro2990

Ortoneda, M., Guarro, J., Madrid, M. P., Caracuel, Z., Roncero, M. I. G., Mayayo, E., & Di Pietro, A. (2004). Fusarium oxysporum as a Multihost Model for the Genetic Dissection of Fungal Virulence in Plants and Mammals. *Infection and Immunity*, *72*(3), 1760–1766. https://doi.org/10.1128/IAI.72.3.1760–1766.2004

Osborne, S.-J. (2016). Exploring the genetic and mechanistic basis of resistance to take-all disease in wheat. *PhD Thesis, University of Nottingham*.

Osborne, S. J., McMillan, V. E., White, R., & Hammond-Kosack, K. E. (2018). Elite UK winter wheat cultivars differ in their ability to support the colonization of beneficial root-infecting fungi. *Journal of Experimental Botany*, *69*(12), 3103–3115.

https://doi.org/10.1093/jxb/ery136

Pacak, A., Geisler, K., Jørgensen, B., Barciszewska-Pacak, M., Nilsson, L., Nielsen, T., Johansen, E., Grønlund, M., Jakobsen, I., & Albrechtsen, M. (2010). Investigations of barley stripe mosaic virus as a gene silencing vector in barley roots and in Brachypodium distachyon and oat. *Plant Methods*, *6*(1), 26. https://doi.org/10.1186/1746-4811-6-26

Palma-Guerrero, J., Chancellor, T., Spong, J., Canning, G., Hammond, J., McMillan, V. E., & Hammond-Kosack, K. E. (2021). Take-All Disease: New Insights into an Important Wheat Root Pathogen. *Trends in Plant Science*, *26*(8), 836–848. https://doi.org/10.1016/j.tplants.2021.02.009

Panda, S., Busatto, N., Hussain, K., & Kamble, A. (2019). Piriformospora indica-primed transcriptional reprogramming induces defense response against early blight in tomato. *Scientia Horticulturae*, *255*, 209–219. https://doi.org/10.1016/j.scienta.2019.05.031

Paoletti, M. (2016). Vegetative incompatibility in fungi: From recognition to cell death, whatever does the trick. *Fungal Biology Reviews*, *30*(4), 152–162. https://doi.org/10.1016/j.fbr.2016.08.002

Papadopoulou, K., Melton, R. E., Leggett, M., Daniels, M. J., & Osbourn, A. E. (1999). Compromised disease resistance in saponin-deficient plants. *Proceedings of the National Academy of Sciences of the United States of America*, *96*(22), 12923–12928. https://doi.org/10.1073/PNAS.96.22.12923

Patkar, R. N., Benke, P. I., Qu, Z., Chen, Y. Y. C., Yang, F., Swarup, S., & Naqvi, N. I. (2015). A fungal monooxygenase-derived jasmonate attenuates host innate immunity. *Nature Chemical Biology 2015 11:9*, *11*(9), 733–740. https://doi.org/10.1038/nchembio.1885

Paulitz, T. C., & Adams, K. (2003). Composition and distribution of Pythium communities in wheat fields in eastern Washington State. *Phytopathology*, *93*(7), 867–873. https://doi.org/10.1094/PHYTO.2003.93.7.867

Paulitz, T. C., Smiley, R. W., & Cook, R. J. (2002). Insights into the prevalence and management of soilborne cereal pathogens under direct seeding in the Pacific Northwest, U.S.A. *Canadian Journal of Plant Pathology*, *24*(4), 416–428. https://doi.org/10.1080/07060660209507029

Peng, S. (1983). Biological Control- One of The Fine Traditions of Ancient Chinese Agricultural Techniques. *Scientia Agricultura Sinica*, *1*, 92–98.

Pérez-Jaramillo, J. E., Mendes, R., & Raaijmakers, J. M. (2016). Impact of plant domestication

on rhizosphere microbiome assembly and functions. *Plant Molecular Biology*, *90*(6), 635–644. https://doi.org/10.1007/s11103-015-0337-7

Periyannan, S., Moore, J., Ayliffe, M., Bansal, U., Wang, X., Huang, L., Deal, K., Luo, M., Kong, X., Bariana, H., Mago, R., McIntosh, R., Dodds, P., Dvorak, J., & Lagudah, E. (2013). The gene Sr33, an ortholog of barley Mla genes, encodes resistance to wheat stem rust race Ug99. *Science*, *341*(6147), 786–788. https://doi.org/10.1126/science.1239028

Pescador, L., Fernandez, I., Pozo, M. J., Romero-Puertas, M. C., Pieterse, C. M. J., & Martínez-Medina, A. (2022). Nitric oxide signalling in roots is required for MYB72-dependent systemic resistance induced by Trichoderma volatile compounds in Arabidopsis . *Journal of Experimental Botany*, *73*(2), 584–595. https://doi.org/10.1093/jxb/erab294

Peškan-Berghöfer, T., Shahollari, B., Pham, H. G., Hehl, S., Markert, C., Blanke, V., Kost, G., Varma, A., & Oelmüller, R. (2004). Association of Piriformospora indica with Arabidopsis thaliana roots represents a novel system to study beneficial plant-microbe interactions and involves early plant protein modifications in the endoplasmic reticulum and at the plasma membrane. *Physiologia Plantarum*, *122*(4), 465–477. https://doi.org/10.1111/j.1399-3054.2004.00424.x

Pieterse, C., Zamioudis, C., Berendsen, R., Weller, D., Van Wees, S., & Bakker, P. (2014). Induced Systemic Resistance by Beneficial Microbes. *Annual Review of Phytopathology*, *52*, 347–375. https://doi.org/10.1146/annurev-phyto-082712-102340

Pilgeram, A. L, & Henson, J. M. (1990). Transformation and Cotransformation of Gaeumannomyces graminis to Phleomycin resistance. *The American Phytopathological Society*, *80*(10), 1124–1129.

Pilgeram, Alice L., & Henson, J. M. (1992). Sexual crosses of the homothallic fungusGaeumannomyces graminis var.tritici based on use of an auxotroph obtained by transformation. *Experimental Mycology*, *16*(1), 35–43. https://doi.org/10.1016/0147-5975(92)90039-T

Placido, D. F., Sandhu, J., Sato, S. J., Nersesian, N., Quach, T., Clemente, T. E., Staswick, P. E., & Walia, H. (2020). The LATERAL ROOT DENSITY gene regulates root growth during water stress in wheat. *Plant Biotechnology Journal*. https://doi.org/10.1111/pbi.13355

Plett, J. M., Plett, K. L., Bithell, S. L., Mitchell, C., Moore, K., Powell, J. R., & Anderson, I. C.

(2016). Improved Phytophthora resistance in commercial chickpea (Cicer arietinum) varieties negatively impacts symbiotic gene signalling and symbiotic potential in some varieties. *Plant Cell and Environment*, *39*(8), 1858–1869. https://doi.org/10.1111/pce.12757

Pokotylo, I., Kravets, V., & Ruelland, E. (2019). Salicylic Acid Binding Proteins (SABPs): The Hidden Forefront of Salicylic Acid Signalling. *International Journal of Molecular Sciences 2019, Vol. 20, Page 4377*, *20*(18), 4377. https://doi.org/10.3390/IJMS20184377

Pollard, M., Beisson, F., Li, Y., & Ohlrogge, J. B. (2008). Building lipid barriers: biosynthesis of cutin and suberin. *Trends in Plant Science*, *13*(5), 236–246. https://doi.org/10.1016/j.tplants.2008.03.003

Pour-Aboughadareh, A., Kianersi, F., Poczai, P., & Moradkhani, H. (2021). Potential of Wild Relatives of Wheat: Ideal Genetic Resources for Future Breeding Programs. *Agronomy 2021, Vol. 11, Page 1656*, *11*(8), 1656. https://doi.org/10.3390/AGRONOMY11081656

Puga-Freitas, R., Belkacem, L., Barot, S., Bertrand, M., Roger-Estrade, J., & Blouin, M. (2016). Transcriptional profiling of wheat in response to take-all disease and mechanisms involved in earthworm's biocontrol effect. *European Journal of Plant Pathology*, *144*(1), 155–165. https://doi.org/10.1007/s10658-015-0759-8

Qin, C., Li, Y., Gan, J., Wang, W., Zhang, H., Liu, Y., & Wu, P. (2013). OsDGL1, a homolog of an oligosaccharyltransferase complex subunit, is involved in N-glycosylation and root development in rice. *Plant and Cell Physiology*, *54*(1), 129–137. https://doi.org/10.1093/pcp/pcs159

Quentin, M., Allasia, V., Pegard, A., Allais, F., Ducrot, P. H., Favery, B., Levis, C., Martinet, S., Masur, C., Ponchet, M., Roby, D., Schlaich, N. L., Jouanin, L., & Keller, H. (2009). Imbalanced lignin biosynthesis promotes the sexual reproduction of homothallic oomycete pathogens. *PLoS Pathogens*, *5*(1), 1–9. https://doi.org/10.1371/journal.ppat.1000264

Raaijmakers, J. M., Paulitz, T. C., Steinberg, C., Alabouvette, C., & Moënne-Loccoz, Y. (2009). The rhizosphere: A playground and battlefield for soilborne pathogens and beneficial microorganisms. *Plant and Soil*, *321*(1–2), 341–361. https://doi.org/10.1007/s11104-008-9568-6

Rabiey, M., Ullah, I., Shaw, L. J., & Shaw, M. W. (2017). Potential ecological effects of Piriformospora indica, a possible biocontrol agent, in UK agricultural systems. *Biological Control*, *104*, 1–9. https://doi.org/10.1016/j.biocontrol.2016.10.005

Rajani, P., Rajasekaran, C., Vasanthakumari, M. M., Olsson, S. B., Ravikanth, G., & Uma Shaanker, R. (2021). Inhibition of plant pathogenic fungi by endophytic Trichoderma spp. through mycoparasitism and volatile organic compounds. *Microbiological Research*, *242*, 126595. https://doi.org/10.1016/j.micres.2020.126595

Ravensberg, W. J. (2015). Commercialisation of microbes: Present situation and future prospects. In *Principles of Plant-Microbe Interactions: Microbes for Sustainable Agriculture* (pp. 309–317). Springer International Publishing. https://doi.org/10.1007/978-3-319-08575-3_32

Ren, Z., Qi, D., Pugh, N., Li, K., Wen, B., Zhou, R., Xu, S., Liu, S., & Jones, A. R. (2019). Improvements to the rice genome annotation through large-scale analysis of RNA-seq and proteomics data sets. *Molecular and Cellular Proteomics*, *18*(1), 86–98. https://doi.org/10.1074/mcp.RA118.000832

Rengel, Z., Graham, R. D., & Pedler, J. F. (1993). Manganese nutrition and accumulation of phenolics and lignin as related to differential resistance of wheat genotypes to the take-all fungus. *Plant and Soil*, *151*(2), 255–263. https://doi.org/10.1007/BF00016291

Reynolds, E. S. (1963). The use of lead citrate at high pH as an electron-opaque stain in electron microscopy. *The Journal of Cell Biology*, *17*(1), 208. https://doi.org/10.1083/JCB.17.1.208

Reyt, G., Ramakrishna, P., Salas-González, I., Fujita, S., Love, A., Tiemessen, D., Lapierre, C., Morreel, K., Calvo-Polanco, M., Flis, P., Geldner, N., Boursiac, Y., Boerjan, W., George, M. W., Castrillo, G., & Salt, D. E. (2021). Two chemically distinct root lignin barriers control solute and water balance. *Nature Communications 2021 12:1*, *12*(1), 1–15. https://doi.org/10.1038/s41467-021-22550-0

Rocha, I., Ma, Y., Souza-alonso, P., Vosátka, M., Freitas, H., & Oliveira, R. S. (2019). Seed Coating : A Tool for Delivering Beneficial Microbes to Agricultural Crops. *Frontiers in Plant Science*, *10*(November). https://doi.org/10.3389/fpls.2019.01357

Rodriguez, R. J., White, J. F., Arnold, a E., & Redman, R. S. (2009). Fungal endophytes: diversity and functional roles. *The New Phytologist*, *182*(2), 314–330. https://doi.org/10.1111/j.1469-8137.2009.02773.x

Rolfe, S. A., Griffiths, J., & Ton, J. (2019). Crying out for help with root exudates: adaptive mechanisms by which stressed plants assemble health-promoting soil microbiomes. *Current Opinion in Microbiology*, *49*, 73–82. https://doi.org/10.1016/j.mib.2019.10.003

Rong, W., Qi, L., Wang, J., Du, L., Xu, H., Wang, A., & Zhang, Z. (2013). Expression of a potato antimicrobial peptide SN1 increases resistance to take-all pathogen Gaeumannomyces graminis var. tritici in transgenic wheat. *Functional and Integrative Genomics*, *13*(3), 403–409. https://doi.org/10.1007/s10142-013-0332-5

Rosado, D., Ackermann, A., Spassibojko, O., Rossi, M., & Pedmale, U. V. (2022). WRKY transcription factors and ethylene signaling modify root growth during the shade-avoidance response. *Plant Physiology*, *188*(2), 1294–1311. https://doi.org/10.1093/PLPHYS/KIAB493

Roth, R., Hillmer, S., Funaya, C., Chiapello, M., Schumacher, K., Lo Presti, L., Kahmann, R., & Paszkowski, U. (2019). Arbuscular cell invasion coincides with extracellular vesicles and membrane tubules. *Nature Plants*, *5*(2), 204–211. https://doi.org/10.1038/s41477-019-0365-4

Roux, B., Rodde, N., Jardinaud, M. F., Timmers, T., Sauviac, L., Cottret, L., Carrère, S., Sallet, E., Courcelle, E., Moreau, S., Debellé, F., Capela, D., De Carvalho-Niebel, F., Gouzy, J., Bruand, C., & Gamas, P. (2014). An integrated analysis of plant and bacterial gene expression in symbiotic root nodules using laser-capture microdissection coupled to RNA sequencing. *Plant Journal*, *77*(6), 817–837. https://doi.org/10.1111/tpj.12442

Rudrappa, T., Czymmek, K. J., Paré, P. W., & Bais, H. P. (2008). Root-secreted malic acid recruits beneficial soil bacteria. *Plant Physiology*, *148*(3), 1547–1556. https://doi.org/10.1104/pp.108.127613

Sadat, M. A., & Choi, J. (2017). Wheat blast: A new fungal inhabitant to Bangladesh threatening world wheat production. *Plant Pathology Journal*, *33*(2), 103–108. https://doi.org/10.5423/PPJ.RW.09.2016.0179

Saintenac, C., Lee, W. S., Cambon, F., Rudd, J. J., King, R. C., Marande, W., Powers, S. J., Bergès, H., Phillips, A. L., Uauy, C., Hammond-Kosack, K. E., Langin, T., & Kanyuka, K. (2018). Wheat receptor-kinase-like protein Stb6 controls gene-for-gene resistance to fungal pathogen Zymoseptoria tritici. *Nature Genetics*, *50*(3), 368–374. https://doi.org/10.1038/s41588-018-0051-x

Sakulkoo, W., Osés-Ruiz, M., Garcia, E. O., Soanes, D. M., Littlejohn, G. R., Hacker, C., Correia, A., Valent, B., & Talbot, N. J. (2018). A single fungal MAP kinase controls plant cell-to-cell invasion by the rice blast fungus. *Science*, *359*(6382), 1399–1403. https://doi.org/10.1126/science.aaq0892

Salcedo, A., Rutter, W., Wang, S., Akhunova, A., Bolus, S., Chao, S., Anderson, N., De Soto,

M. F., Rouse, M., Szabo, L., Bowden, R. L., Dubcovsky, J., & Akhunov, E. (2017). Variation in the AvrSr35 gene determines Sr35 resistance against wheat stem rust race Ug99. *Science*, *358*(6370), 1604–1606. https://doi.org/10.1126/science.aao7294

Saleem, M., Law, A. D., Sahib, M. R., Pervaiz, Z. H., & Zhang, Q. (2018). Impact of root system architecture on rhizosphere and root microbiome. *Rhizosphere*, *6*, 47–51. https://doi.org/10.1016/j.rhisph.2018.02.003

Sánchez-Martín, J., & Keller, B. (2019). Contribution of recent technological advances to future resistance breeding. *Theoretical and Applied Genetics*, *132*(3), 713–732. https://doi.org/10.1007/s00122-019-03297-1

Sankaran, S., Mishra, A., Ehsani, R., & Davis, C. (2010). A review of advanced techniques for detecting plant diseases. *Computers and Electronics in Agriculture*, *72*(1), 1–13. https://doi.org/10.1016/j.compag.2010.02.007

Sarkar, D., Rovenich, H., Jeena, G., Nizam, S., Tissier, A., Balcke, G. U., Mahdi, L. K., Bonkowski, M., Langen, G., & Zuccaro, A. (2019). The inconspicuous gatekeeper: endophytic Serendipita vermifera acts as extended plant protection barrier in the rhizosphere. *New Phytologist*, *224*(2), 886–901. https://doi.org/10.1111/nph.15904

Sarkar, P., Bosneaga, E., & Auer, M. (2009). Plant cell walls throughout evolution: towards a molecular understanding of their design principles. *Journal of Experimental Botany*, *60*(13), 3615–3635. https://doi.org/10.1093/JXB/ERP245

Sasse, J., Martinoia, E., & Northen, T. (2018). Feature Review Feed Your Friends: Do Plant Exudates Shape the Root Microbiome? *Trends in Plant Science*, *23*(1). https://doi.org/10.1016/j.tplants.2017.09.003

Savary, S., Willocquet, L., Pethybridge, S. J., Esker, P., McRoberts, N., & Nelson, A. (2019). The global burden of pathogens and pests on major food crops. *Nature Ecology & Evolution*, *3*(3), 430–439. https://doi.org/10.1038/s41559-018-0793-y

Scherm, B., Balmas, V., Spanu, F., Pani, G., Delogu, G., Pasquali, M., & Migheli, Q. (2013). *Fusarium culmorum*: causal agent of foot and root rot and head blight on wheat. *Molecular Plant Pathology*, *14*(4), 323–341. https://doi.org/10.1111/mpp.12011

Schillinger, W. F., & Paulitz, T. C. (2006). Reduction of Rhizoctonia bare patch in wheat with barley rotations. *Plant Disease*, *90*(3), 302–306. https://doi.org/10.1094/PD-90-0302

Scofield, S. R., Huang, L., Brandt, A. S., & Gill, B. S. (2005). Development of a Virus-Induced Gene-Silencing System for Hexaploid Wheat and Its Use in Functional Analysis of the

Lr21 -Mediated Leaf Rust Resistance Pathway 1. *Plant Physiology*, *138*, 2165–2173. https://doi.org/10.1104/pp.105.061861.1

Segarra, G., Van der Ent, S., Trillas, I., & Pieterse, C. M. J. (2009). MYB72, a node of convergence in induced systemic resistance triggered by a fungal and a bacterial beneficial microbe. *Plant Biology*, *11*(1), 90–96. https://doi.org/10.1111/j.1438-8677.2008.00162.x

Senapati, N., & Semenov, M. A. (2020). Large genetic yield potential and genetic yield gap estimated for wheat in Europe. *Global Food Security*, *24*, 100340. https://doi.org/10.1016/j.gfs.2019.100340

Sesma, A., & Osbourn, A. E. (2004). The rice leaf blast pathogen undergoes developmental processes typical of root-infecting fungi. *Nature*, *431*(7008), 582–586. https://doi.org/10.1038/nature02880

Shewry, W. P. R. (2009). Wheat. *Journal of Experimental Botany*, *60*(6), 1537–1553. https://doi.org/10.1093/jxb/erp058

Shiferaw, B., Smale, M., Braun, H. J., Duveiller, E., Reynolds, M., & Muricho, G. (2013). Crops that feed the world 10. Past successes and future challenges to the role played by wheat in global food security. *Food Security*, *5*(3), 291–317. https://doi.org/10.1007/s12571-013-0263-y

Shinya, T., Nakagawa, T., Kaku, H., & Shibuya, N. (2015). Chitin-mediated plant–fungal interactions: catching, hiding and handshaking. *Current Opinion in Plant Biology*, *26*, 64–71. https://doi.org/10.1016/J.PBI.2015.05.032

Siles, L., Eastmond, P., & Kurup, S. (2020). Big data from small tissues: Extraction of high-quality RNA for RNA-sequencing from different oilseed Brassica seed tissues during seed development. *Plant Methods*, *16*(1), 80. https://doi.org/10.1186/s13007-020-00626-0

Singh, P., & Mukhopadhyay, K. (2021). Comprehensive molecular dissection of TIFY Transcription factors reveal their dynamic responses to biotic and abiotic stress in wheat (Triticum aestivum L.). *Scientific Reports*, *11*(1), 1–17. https://doi.org/10.1038/s41598-021-87722-w

Sirrenberg, A., Göbel, C., Grond, S., Czempinski, N., Ratzinger, A., Karlovsky, P., Santos, P., Feussner, I., & Pawlowski, K. (2007). Piriformospora indica affects plant growth by auxin production. *Physiologia Plantarum*, *131*(4), 581–589. https://doi.org/10.1111/j.1399-

3054.2007.00983.x

Son, H., Lee, J., & Lee, Y. W. (2012). Mannitol induces the conversion of conidia to chlamydospore-like structures that confer enhanced tolerance to heat, drought, and UV in Gibberella zeae. *Microbiological Research*, *167*(10), 608–615. https://doi.org/10.1016/j.micres.2012.04.001

Speakman, J. B., & Lewis, B. G. (1978). Limitation of Gaeumannomyces graminis by wheat root responses to Phialophora radicicola. *New Phytologist*, *80*(2), 373–380. https://doi.org/10.1111/j.1469-8137.1978.tb01571.x

Stein, T. (2005). Bacillus subtilis antibiotics: structures, syntheses and specific functions. *Molecular Microbiology*, *56*(4), 845–857. https://doi.org/10.1111/j.1365-2958.2005.04587.x

Steuernagel, B., Periyannan, S. K., Hernández-Pinzón, I., Witek, K., Rouse, M. N., Yu, G., Hatta, A., Ayliffe, M., Bariana, H., Jones, J. D. G., Lagudah, E. S., & Wulff, B. B. H. (2016). Rapid cloning of disease-resistance genes in plants using mutagenesis and sequence capture. *Nature Biotechnology*, *34*(6), 652–655. https://doi.org/10.1038/nbt.3543

Steuernagel, B., Witek, K., Jones, J. D. G., & Wulff, B. B. H. (2017). MutRenSeq: A method for rapid cloning of plant disease resistance genes. In S Periyannan (Ed.), *Wheat Rust Diseases. Methods in Molecular Biology* (Vol. 1659, pp. 215–229). Humana Press, New York, NY. https://doi.org/10.1007/978-1-4939-7249-4_19

Stracquadanio, C., Quiles, J. M., Meca, G., & Cacciola, S. O. (2020). Antifungal Activity of Bioactive Metabolites Produced by Trichoderma asperellum and Trichoderma atroviride in Liquid Medium. *Journal of Fungi*, *6*(4), 263. https://doi.org/10.3390/jof6040263

Studholme, D. J., Harris, B., Le Cocq, K., Winsbury, R., Perera, V., Ryder, L., Ward, J. L., Beale, M. H., Thornton, C. R., & Grant, M. (2013). Investigating the beneficial traits of Trichoderma hamatum GD12 for sustainable agriculture—insights from genomics. *Frontiers in Plant Science*, *4*(JUL), 258. https://doi.org/10.3389/fpls.2013.00258

Su, Z. Z., Mao, L. J., Li, N., Feng, X. X., Yuan, Z. L., Wang, L. W., Lin, F. C., & Zhang, C. L. (2013). Evidence for Biotrophic Lifestyle and Biocontrol Potential of Dark Septate Endophyte Harpophora oryzae to Rice Blast Disease. *PLOS ONE*, *8*(4), 61332. https://doi.org/10.1371/JOURNAL.PONE.0061332

Sukumar, P., Legué, V., Vayssières, A., Martin, F., Tuskan, G. A., & Kalluri, U. C. (2013). Involvement of auxin pathways in modulating root architecture during beneficial plant-

microorganism interactions. *Plant, Cell and Environment*, *36*(5), 909–919. https://doi.org/10.1111/pce.12036

Tadesse, W., Sanches-Garcia, M., Assefa, S., Amri, A., Bishaw, Z., Ogbonnaya, F., & Baum, M. (2019). Genetic Gains in Wheat Breeding and Its Role in Feeding the World. *Crop Breeding, Genetics and Genomics*. https://doi.org/10.20900/cbgg20190005

Tian, B., Xie, J., Fu, Y., Cheng, J., Li, B., Chen, T., Zhao, Y., Gao, Z., Yang, P., Barbetti, M. J., Tyler, B. M., & Jiang, D. (2020). A cosmopolitan fungal pathogen of dicots adopts an endophytic lifestyle on cereal crops and protects them from major fungal diseases. *ISME Journal*, *14*(12), 3120–3135. https://doi.org/10.1038/s41396-020-00744-6

Tilocca, B., Cao, A., & Migheli, Q. (2020). Scent of a Killer: Microbial Volatilome and Its Role in the Biological Control of Plant Pathogens. *Frontiers in Microbiology*, *11*(41). https://doi.org/10.3389/fmicb.2020.00041

Tong, S., Li, M., Keyhani, N. O., Liu, Y., Yuan, M., Lin, D., Jin, D., Li, X., Pei, Y., & Fan, Y. (2020). Characterization of a fungal competition factor: Production of a conidial cell-wall associated antifungal peptide. *PLoS Pathogens*, *16*(4). https://doi.org/10.1371/journal.ppat.1008518

Tracy, S. R., Nagel, K. A., Postma, J. A., Fassbender, H., Wasson, A., & Watt, M. (2020). Crop Improvement from Phenotyping Roots: Highlights Reveal Expanding Opportunities. *Trends in Plant Science*, *25*(1), 105–118. https://doi.org/10.1016/J.TPLANTS.2019.10.015

Troppens, D. M., Dmitriev, R. I., Papkovsky, D. B., O'Gara, F., & Morrissey, J. P. (2013). Genome-wide investigation of cellular targets and mode of action of the antifungal bacterial metabolite 2,4-diacetylphloroglucinol in Saccharomyces cerevisiae. *FEMS Yeast Research*, *13*(3), 322–334. https://doi.org/10.1111/1567-1364.12037

Tucci, M., Ruocco, M., De Masi, L., De Palma, M., & Lorito, M. (2011). The beneficial effect of Trichoderma spp. on tomato is modulated by the plant genotype. *Molecular Plant Pathology*, *12*(4), 341–354. https://doi.org/10.1111/J.1364-3703.2010.00674.X

Tufan, H. A., Stefanato, F. L., McGrann, G. R. D., MacCormack, R., & Boyd, L. A. (2011). The Barley stripe mosaic virus system used for virus-induced gene silencing in cereals differentially affects susceptibility to fungal pathogens in wheat. *Journal of Plant Physiology*, *168*(9), 990–994. https://doi.org/10.1016/J.JPLPH.2010.11.019

Turrà, D., Segorbe, D., & Di Pietro, A. (2014). Protein Kinases in Plant-Pathogenic Fungi:

Conserved Regulators of Infection. *Annual Review of Phytopathology*, *52*, 267–288. https://doi.org/10.1146/ANNUREV-PHYTO-102313-050143

Tzelepis, G., & Karlsson, M. (2019). Killer toxin-like chitinases in filamentous fungi: Structure, regulation and potential roles in fungal biology. *Fungal Biology Reviews*, *33*(2), 123–132. https://doi.org/10.1016/j.fbr.2018.11.001

Ulrich, K., Augustin, C., & Werner, A. (2000). Identification and characterization of a new group of root-colonizing fungi within the Gaeumannomyces-Phialophora complex. *New Phytologist*, *145*(1), 127–135. https://doi.org/10.1046/j.1469-8137.2000.00553.x

Umar, A., Kandula, D. R. W., Hampton, J. G., Phil Rolston, M., & Chng, S. F. (2019). Potential biological control of take-all disease in perennial ryegrass. *New Zealand Plant Protection*, *72*, 213–220. https://doi.org/10.30843/nzpp.2019.72.271

Vadassery, J., Ritter, C., Venus, Y., Camehl, I., Varma, A., Shahollari, B., Novák, O., Strnad, M., Ludwig-Müller, J., & Oelmüller, R. (2008). The Role of Auxins and Cytokinins in the Mutualistic Interaction Between *Arabidopsis* and *Piriformospora indica*. *Molecular Plant-Microbe Interactions*, *21*(10), 1371–1383. https://doi.org/10.1094/MPMI-21-10-1371

van Dusschoten, D., Metzner, R., Kochs, J., Postma, J. A., Pflugfelder, D., Bühler, J., Schurr, U., & Jahnke, S. (2016). Quantitative 3D analysis of plant roots growing in soil using magnetic resonance imaging. *Plant Physiology*, *170*(3), 1176–1188. https://doi.org/10.1104/pp.15.01388

van Verk, M. C., Bol, J. F., & Linthorst, H. J. M. (2011). WRKY Transcription Factors Involved in Activation of SA Biosynthesis Genes. *BMC Plant Biology*, *11*(1), 1–12. https://doi.org/10.1186/1471-2229-11-89/TABLES/1

Vera Palma, C. A., Madariaga Burrows, R. P., González, M. G., Sepúlveda, B. R., & Moya-Elizondo, E. A. (2019). Integration between Pseudomonas protegens strains and fluquinconazole for the control of take-all in wheat. *Crop Protection*, *121*, 163–172. https://doi.org/10.1016/j.cropro.2019.03.020

Voigt, C. A. (2014). Callose-mediated resistance to pathogenic intruders in plant defense-related papillae. *Frontiers in Plant Science*, *5*, 168. https://doi.org/10.3389/fpls.2014.00168

Voss-Fels, K. P., Robinson, H., Mudge, S. R., Richard, C., Newman, S., Wittkop, B., Stahl, A., Friedt, W., Frisch, M., Gabur, I., Miller-Cooper, A., Campbell, B. C., Kelly, A., Fox, G., Christopher, J., Christopher, M., Chenu, K., Franckowiak, J., Mace, E. S., … Hickey, L.

T. (2018). VERNALIZATION1 Modulates Root System Architecture in Wheat and Barley. *Molecular Plant*, *11*(1), 226–229. https://doi.org/10.1016/j.molp.2017.10.005

Voss-Fels, K. P., Snowdon, R. J., & Hickey, L. T. (2018). Designer Roots for Future Crops. *Trends in Plant Science*, *23*(11), 957–960. https://doi.org/10.1016/j.tplants.2018.08.004

Wagacha, J. M., & Muthomi, J. W. (2007). Fusarium culmorum: Infection process, mechanisms of mycotoxin production and their role in pathogenesis in wheat. *Crop Protection*, *26*(7), 877–885. https://doi.org/10.1016/j.cropro.2006.09.003

Walker, J. L. (1981). Taxonomy of take-all fungi and related genera and species. In *Asher, M., Shipton, PJ (ed.) Biology and Control of Take-all.* London: Academic Press.

Walters, D. R., Ratsep, J., & Havis, N. D. (2013). Controlling crop diseases using induced resistance: Challenges for the future. *Journal of Experimental Botany*, *64*(5), 1263–1280. https://doi.org/10.1093/jxb/ert026

Wang, A., Wei, X., Rong, W., Dang, L., Du, L. P., Qi, L., Xu, H. J., Shao, Y., & Zhang, Z. (2015). GmPGIP3 enhanced resistance to both take-all and common root rot diseases in transgenic wheat. *Functional and Integrative Genomics*, *15*(3), 375–381. https://doi.org/10.1007/s10142-014-0428-6

Wang, G.-F., Wei, X., Fan, R., Zhou, H., Wang, X., Yu, C., Dong, L., Dong, Z., Wang, X., Kang, Z., Ling, H., Shen, Q.-H., Wang, D., & Zhang, X. (2011). Molecular analysis of common wheat genes encoding three types of cytosolic heat shock protein 90 (Hsp90): functional involvement of cytosolic Hsp90s in the control of wheat seedling growth and disease resistance. *New Phytologist*, *191*(2), 418–431. https://doi.org/10.1111/j.1469-8137.2011.03715.x

Wang, M., Zhang, J., Wang, L., Han, L., Zhang, X., & Feng, J. (2018). Optimization of Production Conditions for Protoplasts and Polyethylene Glycol-Mediated Transformation of Gaeumannomyces tritici. *Molecules*, *23*(6), 1253. https://doi.org/10.3390/molecules23061253

Wang, Z. Y., Soanes, D. M., Kershaw, M. J., & Talbot, N. J. (2007). Functional analysis of lipid metabolism in Magnaporthe grisea reveals a requirement for peroxisomal fatty acid β-oxidation during appressorium-mediated plant infection. *Molecular Plant-Microbe Interactions*, *20*(5), 475–491. https://doi.org/10.1094/MPMI-20-5-0475

Ward, E., & Bateman, G. L. (1999). Comparison of Gaeumannomyces- and Phialophora-like fungal pathogens from maize and other plants using DNA methods. *New Phytologist*,

141(2), 323–331. https://doi.org/10.1046/j.1469-8137.1999.00346.x

Wasson, A., Bischof, L., Zwart, A., & Watt, M. (2016). A portable fluorescence spectroscopy imaging system for automated root phenotyping in soil cores in the field. *Journal of Experimental Botany*, *67*(4), 1033–1043. https://doi.org/10.1093/JXB/ERV570

Weller, D. M., Raaijmakers, J. M., Gardener, B. B. M., & Thomashow, L. S. (2002). Microbial populations responsible for specific soil suppressiveness to plant pathogens. *Annual Review of Phytopathology*, *40*(1), 309–348. https://doi.org/10.1146/annurev.phyto.40.030402.110010

Wicker, T., Oberhaensli, S., Parlange, F., Buchmann, J. P., Shatalina, M., Roffler, S., Ben-David, R., Doležel, J., Šimková, H., Schulze-Lefert, P., Spanu, P. D., Bruggmann, R., Amselem, J., Quesneville, H., Ver Loren Van Themaat, E., Paape, T., Shimizu, K. K., & Keller, B. (2013). The wheat powdery mildew genome shows the unique evolution of an obligate biotroph. *Nature Genetics*, *45*(9), 1092–1096. https://doi.org/10.1038/ng.2704

Wong, J. W. H., & Plett, J. M. (2019). Root renovation: How an improved understanding of basic root biology could inform the development of elite crops that foster sustainable soil health. *Functional Plant Biology*, *46*(7), 597–612. https://doi.org/10.1071/FP18200

Wong, P. (1995). *GB2286123A - Biocontrol of take-all using Phialophora sp. (lobed hyphopodia) - Google Patents*. https://patents.google.com/patent/GB2286123A/en

Wong, P. T. W., Mead, J. A., & Holley, M. P. (1996). Enhanced field control of wheat take-all using cold tolerant isolates of Gaeumannomyces graminis var. graminis and Phialophora sp. (lobed hyphopodia). *Plant Pathology*, *45*(2), 285–293. https://doi.org/10.1046/j.1365-3059.1996.d01-132.x

Wong, P. T. W., & Southwell, R. J. (1980). Field control of take-all of wheat by avirulent fungi. *Annals of Applied Biology*, *94*(1), 41–49. https://doi.org/10.1111/j.1744-7348.1980.tb03894.x

Woo, S. L., Scala, F., Ruocco, M., & Lorito, M. (2007). The Molecular Biology of the Interactions Between Trichoderma spp., Phytopathogenic Fungi, and Plants. *Http://Dx.Doi.Org/10.1094/PHYTO-96-0181*, *96*(2), 181–185. https://doi.org/10.1094/PHYTO-96-0181

Xu, X. H., Su, Z. Z., Wang, C., Kubicek, C. P., Feng, X. X., Mao, L. J., Wang, J. Y., Chen, C., Lin, F. C., & Zhang, C. L. (2014). The rice endophyte Harpophora oryzae genome reveals evolution from a pathogen to a mutualistic endophyte. *Scientific Reports*, *4*, 1–9.

https://doi.org/10.1038/srep05783

Yang, J., Duan, G., Li, C., Liu, L., Han, G., Zhang, Y., & Wang, C. (2019). The Crosstalks Between Jasmonic Acid and Other Plant Hormone Signaling Highlight the Involvement of Jasmonic Acid as a Core Component in Plant Response to Biotic and Abiotic Stresses. *Frontiers in Plant Science*, *0*, 1349. https://doi.org/10.3389/FPLS.2019.01349

Yang, L., Han, X., Zhang, F., Goodwin, P. H., Yang, Y., Li, J., Xia, M., Sun, R., Jia, B., Zhang, J., Quan, X., Wu, C., Xue, B., & Lu, C. (2018). Screening Bacillus species as biological control agents of Gaeumannomyces graminis var. tritici on wheat. *Biological Control*, *118*, 1–9. https://doi.org/10.1016/J.BIOCONTROL.2017.11.004

Yang, L., Quan, X., Xue, B., Goodwin, P. H., Lu, S., Wang, J., Du, W., & Wu, C. (2015). Isolation and identification of bacillus subtilis strain YB-05 and its antifungal substances showing antagonism against Gaeumannomyces graminis var. tritici. *Biological Control*, *85*, 52–58. https://doi.org/10.1016/j.biocontrol.2014.12.010

Yang, L., Xie, L., Xue, B., Goodwin, P. H., Quan, X., Zheng, C., Liu, T., Lei, Z., Yang, X., Chao, Y., & Wu, C. (2015). Comparative Transcriptome Profiling of the Early Infection of Wheat Roots by Gaeumannomyces graminis var. tritici. *PLOS ONE*, *10*(4), e0120691. https://doi.org/10.1371/journal.pone.0120691

Yang, M., Mavrodi, D. V., Thomashow, L. S., & Weller, D. M. (2018). Differential response of wheat cultivars to pseudomonas brassicacearum and take-all decline soil. *Phytopathology*, *108*(12), 1363–1372. https://doi.org/10.1094/PHYTO-01-18-0024-R

You, M. P., Rensing, K., Renton, M., & Barbetti, M. J. (2017). Modeling Effects of Temperature, Soil, Moisture, Nutrition and Variety As Determinants of Severity of Pythium Damping-Off and Root Disease in Subterranean Clover. *Frontiers in Microbiology*, *8*(NOV), 2223. https://doi.org/10.3389/fmicb.2017.02223

Yu, Y., Kang, Z., Han, Q., Buchenauer, H., & Huang, L. (2010). Immunolocalization of 1,3-β-Glucanases Secreted by Gaeumannomyces graminis var. tritici in Infected Wheat Roots. *Journal of Phytopathology*, *158*(5), 344–350. https://doi.org/10.1111/j.1439-0434.2009.01614.x

Yun, Y., Yu, F., Wang, N., Chen, H., Yin, Y., & Ma, Z. (2012). Sensitivity to silthiofam, tebuconazole and difenoconazole of Gaeumannomyces graminis var. tritici isolates from China. *Pest Management Science*, *68*(8), 1156–1163. https://doi.org/10.1002/ps.3277

Zaninotto, F., Camera, S. La, Polverari, A., & Delledonne, M. (2006). Cross Talk between

Reactive Nitrogen and Oxygen Species during the Hypersensitive Disease Resistance Response. *Plant Physiology*, *141*(2), 379–383. https://doi.org/10.1104/PP.106.078857

Zhang, D. D., Guo, X. J., Wang, Y. J., Gao, T. G., & Zhu, B. C. (2017). Novel screening strategy reveals a potent Bacillus antagonist capable of mitigating wheat take-all disease caused by Gaeumannomyces graminis var. tritici. *Letters in Applied Microbiology*, *65*(6), 512–519. https://doi.org/10.1111/lam.12809

Zhang, J., Yan, H., Xia, M., Han, X., Xie, L., Goodwin, P. H., Quan, X., Sun, R., Wu, C., & Yang, L. (2020). Wheat root transcriptional responses against Gaeumannomyces graminis var . tritici. *Phytopathology Research*, *2*(23). https://doi.org/https://doi.org/10.1186/s42483-020-00066-7

Zhang, Y., Xu, K., Yu, D., Liu, Z., Peng, C., Li, X., Zhang, J., Dong, Y., Zhang, Y., Tian, P., Guo, T., & Li, C. (2019). The highly conserved barley powdery mildew effector BEC1019 confers susceptibility to biotrophic and necrotrophic pathogens in wheat. *International Journal of Molecular Sciences*, *20*(18), 1–16. https://doi.org/10.3390/ijms20184376

Zhang, Z., Hua, L., Gupta, A., Tricoli, D., Edwards, K. J., Yang, B., & Li, W. (2019). Development of an *Agrobacterium* -delivered CRISPR/Cas9 system for wheat genome editing. *Plant Biotechnology Journal*, *17*(8), 1623–1635. https://doi.org/10.1111/pbi.13088

Zhong, Z., Marcel, T. C., Hartmann, F. E., Ma, X., Plissonneau, C., Zala, M., Ducasse, A., Confais, J., Compain, J., Lapalu, N., Amselem, J., McDonald, B. A., Croll, D., & Palma-Guerrero, J. (2017). A small secreted protein in *Zymoseptoria tritici* is responsible for avirulence on wheat cultivars carrying the *Stb6* resistance gene. *New Phytologist*, *214*(2), 619–631. https://doi.org/10.1111/nph.14434

Zhou, F., Emonet, A., Dénervaud Tendon, V., Marhavy, P., Wu, D., Lahaye, T., & Geldner, N. (2020). Co-incidence of Damage and Microbial Patterns Controls Localized Immune Responses in Roots. *Cell*, *180*(3), 440–453. https://doi.org/10.1016/j.cell.2020.01.013

Zhou, M., Lu, Y., Bethke, G., Harrison, B. T., Hatsugai, N., Katagiri, F., & Glazebrook, J. (2018). WRKY70 prevents axenic activation of plant immunity by direct repression of SARD1. *New Phytologist*, *217*(2), 700–712. https://doi.org/10.1111/NPH.14846

Zhou, Y., Van Leeuwen, S. K., Pieterse, C. M. J., Bakker, P. A. H. M., & Van Wees, S. C. M. (2019). Effect of atmospheric CO2 on plant defense against leaf and root pathogens of Arabidopsis. *European Journal of Plant Pathology*, *154*(1), 31–42. https://doi.org/10.1007/s10658-019-01706-1

Zhu, T., Wang, L., Rimbert, H., Rodriguez, J. C., Deal, K. R., De Oliveira, R., Choulet, F., Keeble-Gagnère, G., Tibbits, J., Rogers, J., Eversole, K., Appels, R., Gu, Y. Q., Mascher, M., Dvorak, J., & Luo, M. C. (2021). Optical maps refine the bread wheat Triticum aestivum cv. Chinese Spring genome assembly. *The Plant Journal*, *107*(1), 303–314. https://doi.org/10.1111/TPJ.15289

Zipfel, C., & Oldroyd, G. E. D. (2017). Plant signalling in symbiosis and immunity. *Nature*, *543*(7645), 328–336. https://doi.org/10.1038/nature22009

Zubrod, J. P., Bundschuh, M., Arts, G., Brühl, C. A., Imfeld, G., Knäbel, A., Payraudeau, S., Rasmussen, J. J., Rohr, J., Scharmüller, A., Smalling, K., Stehle, S., Schulz, R., & Schäfer, R. B. (2019). Fungicides: An Overlooked Pesticide Class? *Environmental Science and Technology*, *53*(7), 3347–3365. https://doi.org/10.1021/acs.est.8b04392